Power Systems

A. Penin

Analysis of Electrical Circuits with Variable Load Regime Parameters

Projective Geometry Method

Second Edition

Springer

Power Systems

More information about this series at http://www.springer.com/series/4622

A. Penin

Analysis of Electrical Circuits with Variable Load Regime Parameters

Projective Geometry Method

Second Edition

Springer

A. Penin
"D. Ghitu" Institute of Electronic
Engineering and Nanotechnologies
Academy of Sciences of Moldova
Chişinău
Moldova

ISSN 1612-1287 ISSN 1860-4676 (electronic)
Power Systems
ISBN 978-3-319-28450-7 ISBN 978-3-319-28451-4 (eBook)
DOI 10.1007/978-3-319-28451-4

Library of Congress Control Number: 2015935416

Printed on acid-free paper

This Springer imprint is published by SpringerNature
The registered company is Springer International Publishing AG Switzerland

To my wife Lyudmila for many years of hope of success

Foreword

The classical electric circuit theory is widely presented in modern educational and scientific publications. The properties of circuits, which allow simplifying the analysis of complex networks in the case of change of one (or several) resistance or load, are known. These properties make appropriate sections in the circuit theory books. The problems of application and development of basic properties of circuits in an analytical view draw the attention of researchers at present times, despite opportunities of simulation computer systems.

It occurs in science that someone looks at traditional problems from another viewpoint and a whole new direction with a new mathematical apparatus appears in this traditional area of science and engineering. The book, written by A. Penin, is an example of such a new approach in circuit theory or methods of their analysis.

This book includes the author's main publications, results of more than 30-year searches, reflections, and doubts. All this determine a new, unusual approach to the solution of a number of tasks of circuit theory.

The combination of such concepts as circuit theory and projective geometry (in general, non-Euclidean geometry), is a new representation in electrical engineering and circuit theory. There are almost no modern publications of other authors using such a geometrical approach for circuit analysis. At the same time, similar geometrical methods are widely used in other areas of science. For a wide audience, it is necessary to explain that geometry is a much deeper concept than a simple graphical representation of studied dependences.

In the foreword, there is no opportunity and no need to speak about the content of the author's main results, but one important circumstance should be noted. The used mathematical apparatus gives a successful interpretation for observed dependences, validation of used definitions and concepts, removes a tradition, and their formal introduction. Therefore, the book supplements and develops basic methods of circuit analysis, makes them evidential, and simplifies understanding of the complicated interconnected processes happening in electric circuits.

The author restricts his analysis by direct current circuits (as models of power supply systems with one, two, and more loads), which gives the possibility to show

in the simplest way the new things or results that geometry can propose for circuit analysis.

The theorem of the generalized equivalent circuit is such a result. The author determines the parameters of this equivalent for a network with changeable parameters and load.

Another result is that mutual changes of resistance and current are set not in the form of generally used increments (typical for mathematical analysis and a concept of the derivative) but as well-founded fractionally linear expression. On this basis, convenient formulas of recalculation of currents turn out. It is possible to carry out the normalization of running regime parameters and to prove a technique for comparison of regimes for circuits similar to each other.

Using own scientific and practical experience in power electronics, the author applies new representations to a number of traditional problems in this area. It is natural that the author uses idealized models of considered power electronics appliances and therefore does not give the finished practical decisions. Also, the possible directions of development of this approach are shown in this book.

As a whole, the book represents a theoretical, methodological, and methodical interest for those who study circuit theory or work in this area directly. It is possible to hope that the presented geometrical approach to known tasks and arising new problems will cause the active permanent interest of experts in various areas of electrical engineering and radio electronics.

Prof. Anatolie Sidorenko

Preface

The circuit regime analysis is one of the main problems for electric circuit theory. The finding of the actual (absolute) value of regime parameters (voltage, current, power, and transformation ratio for different parts of a circuit) is the simplest analysis task. If a circuit has variable elements (loads and voltage regulators), additional analysis tasks appear.

The interest in such circuits is defined, in particular, by the state and tendencies of development of power electronics, modular power supply, or distributed power supply systems with renewable power sources. Similar devices, in general, represent the complex multiple inputs and multiple outputs systems and their loads can change from the short circuit to open circuit and further give energy. In turn, the loads can be subdivided into high priority and additional (ballast) loads. For definiteness, it is possible to accept that such systems, for circuit theory, present linear mesh circuits of a direct current or multi-port networks.

We will consider some of the arising additional tasks of analysis. For example, it is important to confront operating regime parameters with characteristic values; that is, to represent these parameters in the normalized or relative form. In this case, the informational content of these parameters is increasing; it is possible to appreciate qualitative characteristics of an operating regime or its effectiveness, to compare regimes of different circuits, and to set a necessary regime.

The other task of analysis is the determination of the dependence of the regime parameter changes on the respective change of element's parameters (for example, the problem of the recalculation of load currents). Thus, it is necessary to set the form of these changes reasonably; that is, to determine whether these changes are increments or any other expressions.

Another task of analysis is the definition of the view or character of such an active circuit with a changeable element (as a power source concerning load); that is, this circuit shows more property of a voltage source or current source.

In the electric circuit theory, a range of circuit's properties, theorems, and methods is well known, and their use simplifies the decision of these problems.

However, the known approaches do not completely disclose the properties of such circuits, which reduces the effectiveness of analysis.

The method of analysis for a circuit with variable element parameters is developed by the author. For interpretation of changes or "kinematics" of circuit regimes, projective geometry is used. For example, the known expression has the typical fractionally linear view for functional dependence of current (or voltage) via resistance. It gives the grounds for considering this expression as a projective transformation. The projective transformations preserve an invariant; there is a cross ratio of four points (a ratio of two proportions) or four values of current and resistance. The value of this invariant is preserved for all the variables (as a current, voltage, and resistance) and for parts or sections of a circuit. Thus, this invariant is accepted as the determination of the regime in the relative form. Therefore, obvious changes in regime parameters in the form of increments are formal and do not reflect the substantial aspect of the mutual influences: resistance → current.

In general, this geometrical approach grounds the introduction and determination of required concepts.

The book has an introduction (Chap. 1) and four parts. The disadvantages of known methods are considered in Chap. 1.

Part I (Chaps. 2–5) considers electrical circuits with one load. The application of projective geometry to analysis of an active two-pole is shown in Chap. 2. The concept of generalized equivalent circuits is introduced in Chap. 3. The invariant relationships of cascaded two-ports are considered in Chap. 4. In Chap. 5, the paralleling voltage sources are presented.

Part II (Chaps. 6–9) considers multi-port circuits. The application of projective geometry to analysis of an active two-port and three-port is shown in Chap. 6. The concept of generalized equivalent circuits of multi-port is introduced in Chap. 7. The recalculation formulas of load currents are obtained in Chap. 8. The invariant relationships of cascaded four-ports are considered in Chap. 9.

Part III (Chaps. 10–12) considers circuits with nonlinear regulation curves. The voltage regulator regimes are studied in Chap. 10. The load voltage stabilization is shown in Chap. 11. The pulse-width modulation converters are considered in Chap. 12.

Part IV (Chaps. 13 and 14) discusses circuits with nonlinear load characteristics. The concepts of power-source and power-load elements with two-valued characteristics are shown in Chap. 13. Quasi-resonant voltage converters with self-limitation of current are considered in Chap. 14. The attention to similarity of characteristics of this converter and some electronic devices is paid.

The book may be useful to those who are interested in the foundations of the electric circuit theory and also for a professional circle of experts in various areas of electrical engineering and radio electronics.

The author thanks Prof. A. Scherba (Ukraine) for the attention shown and recommendations to the publication of the first results. He also thanks Prof. P. Butyrin (Russia) for long-term constructive criticism and recommendations to the publication of series of papers. He also thanks Prof. V. Mazin (Russia), who shares his

area of researches, and appreciates scientific editor B. Makarshin (Russia) for a 20-year hard effort on the preparation of paper manuscripts for publication.

The author is grateful to academician D. Ghitu, the founder of Institute of Electronic Engineering and Nanotechnologies (Moldova), for the given opportunity to work according to the individual plan of researches. He appreciates Prof. A. Sidorenko, the director of "D. Ghitu" Institute of Electronic Engineering and Nanotechnologies, for permanent interest to the direction of research, support for this direction and the book publication.

Moldova Republic A. Penin
October 2015

Contents

About the Author

A. Penin has engineering interests related to power electronics. He worked (1980–2006) on the design office of solid-state electronics of Academy of Sciences of Moldova; elaboration of power supply systems. From 2006 to the present, he works in "D. Ghitu" Institute of Electronic Engineering and Nanotechnologies of Academy of Sciences of Moldova; he continues the early begun independent theoretical researches in the electric circuit theory with variable regimes. He is a senior research assistant, Ph.D. (2011). The author has to his credit more than 60 publications, 40 patents of Moldova, and one European patent.

About the Book

This book introduces electric circuits with variable loads and voltage regulators. It allows to define invariant relationships for various parameters of regime and circuit sections and to prove the concepts characterizing these circuits. Generalized equivalent circuits are introduced. Projective geometry is used for the interpretation of changes of operating regime parameters. Expressions of normalized regime parameters and their changes are presented. Convenient formulas for the calculation of currents are given. Parallel voltage sources and the cascade connection of multi-port networks are described. The two-value voltage regulation characteristics of loads with limited power of voltage source is considered. The book presents the fundamentals of electric circuits and develops circuit theorems.

The second edition was extended and contains additional chapters to circuits with nonlinear regulation curves, circuits with nonlinear load characteristics, concepts of power-source and power-load elements with two-valued characteristics, quasi-resonant voltage converters with self-limitation of current as well as the similarity of characteristics of converters and electronic devices.

This book is useful to engineers, researchers, and graduate students who are interested in the basic electric circuit theory and the regulation and monitoring of power supply systems.

Chapter 1
Introduction

1.1 Typical Structure and Equivalent Circuits of Power Supply Systems. Features of Circuits with Variable Operating Regime Parameters

The circuit regime analysis is one of the main problems for the electric circuit theory [1, 7]. The finding of the actual (absolute) value of regime parameters (voltage, current, voltage transformation ratio, and so on), is the simplest analysis task. In turn, the determination of the maximum load power and maximum efficiency is an essential energy problem [6, 14], including distributed power supply systems. Such systems, shown in Fig. 1.1, contain multiple power sources, energy storages, direct current *DC*/*DC* voltage converters, charge/discharge units, point-of-load *POL* regulators, and loads [4, 13].

Usually, the static characteristics of all the incoming units are used for energy analysis [9, 12] and analog computation of power systems [11]. Therefore, this power supply system is the complex *DC* circuit with a given number of input and output terminals. For example, such a circuit is shown in Fig. 1.2. The voltage *DC*/*DC* converters are simply *DC* transformers. The resistive network determines losses of all the converters and supply lines.

Let us consider the feature of the show circuit. The interaction both between power sources and loads is the main feature of this system. The regime of the loads and energy storages may change from the energy consumption to return of energy. The loads may be also subdivided into basic (priority) and additional (buffer) loads.

Therefore, additional analysis tasks appear for these circuits with variable elements (loads, voltage regulators). For example, it is important to confront operating regime parameters with the characteristic values; that is, to represent these parameters in the normalized or relative form. In this case, the informational content of these parameters is increasing; it is possible to appreciate the qualitative characteristics of an operating regime or its effectiveness, to compare regimes of different circuits, to set a necessary regime in the sense of similarity theory.

A. Penin, *Analysis of Electrical Circuits with Variable Load Regime Parameters*,
Power Systems, DOI 10.1007/978-3-319-28451-4_1

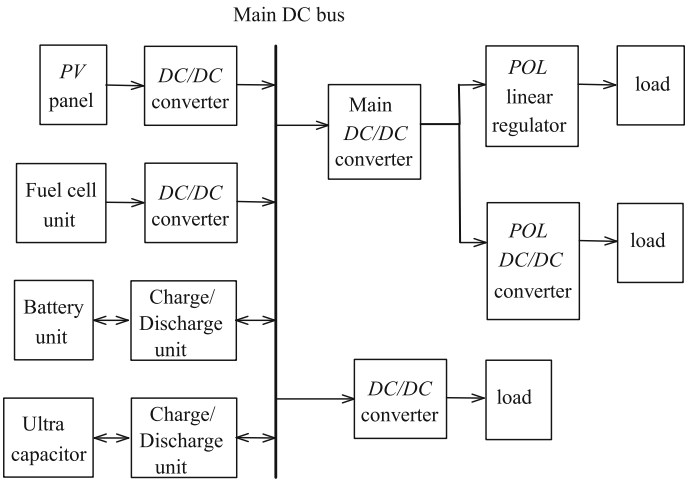

Fig. 1.1 Typical distributed power supply system

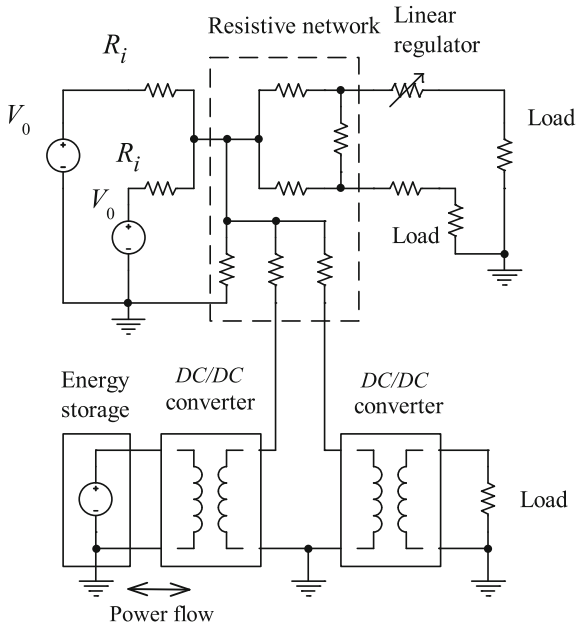

Fig. 1.2 Simplified equivalent circuit of distributed power supply system

Usually, relative expressions are constituted by using of the characteristic values (as scales) for the corresponding regime parameter [19]. Similarly, the regime change is defined by the difference or ratio of subsequent and initial regime parameters; there are changes in the form of "times" or "percents." For example, the open-circuit *OC* voltage and short circuit *SC* current will be the corresponding scales for the load

voltage and current of the simplest circuit. In the same way, the maximum load power or maximum source power will be the scales for the running load power.

The other task of analysis is the determination of the regime parameter changes via respective changes of element parameters (for example, the problem of the recalculation of load currents). Thus, it is necessary to set the form of these changes reasonably; that is, if these changes are increments or the other expressions.

Also, we have the next task. The change of the load parameters or parameters of circuit defines the corresponding regime change and its effectiveness. Therefore, a deeper analysis and introduction of changes in the valid form of both regime parameters and effectiveness indicators are necessary.

In the electric circuit theory a range of properties, theorems, and methods are well-known, and their use can simplify the solution of these problems.

However, the known approaches do not completely disclose the properties of the circuits with variable elements that reduce the efficiency of analysis.

Using the equivalent circuit in Fig. 1.2, we will choose the simplest and important circuits. The analysis of such simple networks shows the disadvantages of the known methods.

1.2 Disadvantages of the Well-Known Calculation Methods of Regime Parameters in the Relative Form for Active Two-Poles

1.2.1 Volt–Ampere Characteristics of an Active Two-Pole

The simplest circuit of an active two-pole is shown in Fig. 1.3a. At change of a load resistance R_L from the short circuit SC to open circuit OC, a load straight line or volt–ampere characteristic in Fig. 1.3b is given by a linear expression

$$I_L = \frac{V_0}{R_i} - \frac{V_L}{R_i} = I_L^{SC} - \frac{V_L}{R_i}, \tag{1.1}$$

where R_i is an internal resistance and I_L^{SC} is the SC current.

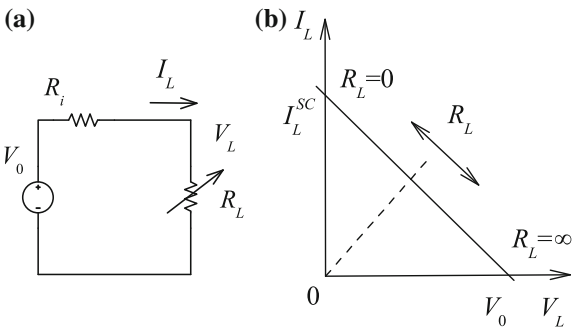

Fig. 1.3 **a** Simplest circuit. **b** Load straight line

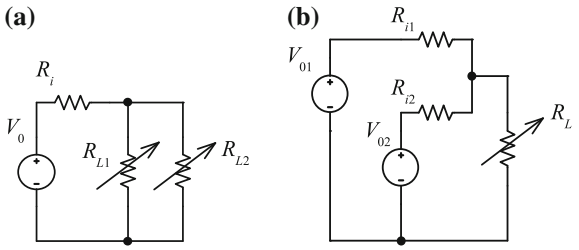

Fig. 1.4 **a** Influence of loads to each other. **b** Influence of voltages sources to each other

In turn, an internal resistance R_i in Fig. 1.4a determines the influence of the load resistances R_{L1}, R_{L2} to each other. Similarly, the influence between the paralleling voltage sources V_{01}, V_{02} takes place in Fig. 1.4b.

Let us consider the straight lines of the initial circuit and a similar circuit with the other values $\tilde{V}_0$, $\tilde{R}_i$ in Fig. 1.5. The regimes of these circuits will be similar or equivalent if the correspondence of the characteristic and running regime parameters takes place. For the given case, this conformity is specified by arrows.

1.2.2 Regime Parameters in the Relative Form

Let us constitute the relative expression of the load straight line for our simplest circuit in Fig. 1.3. For that, it is possible to use the values I_L^{SC}, V_0 as the scales.

We may rewrite Eq. (1.1) in the form

$$\frac{I_L}{I_L^{SC}} = 1 - \frac{V_L}{V_0}. \tag{1.2}$$

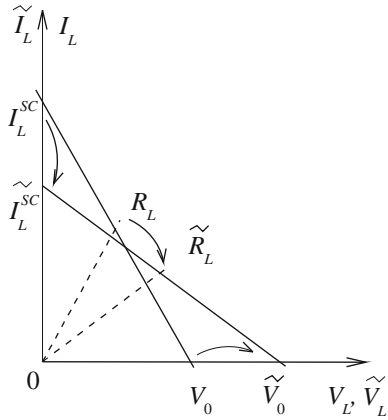

Fig. 1.5 Straight lines of comparable circuits

Similarly, for the other circuit

$$\frac{\tilde{I}_L}{\tilde{I}_L^{SC}} = 1 - \frac{\tilde{V}_L}{\tilde{V}_0}.$$

From this, the equality of the relative or normalized values for currents and voltages determines the similarity of regimes

$$\overline{I}_L = \frac{I_L}{I_L^{SC}} = \frac{\tilde{I}_L}{\tilde{I}_L^{SC}}, \quad \overline{V}_L = \frac{V_L}{V_0} = \frac{\tilde{V}_L}{\tilde{V}_0}. \tag{1.3}$$

Then, Eq. (1.2) obtains the relative view

$$\overline{I}_L = 1 - \overline{V}_L. \tag{1.4}$$

Therefore, the relative values $\overline{I}_L$, $\overline{V}_L$ allow evaluating the use of the voltage source for current and voltage of the running regime.

From (1.3), the recalculation formulas of the actual regime parameters are as follows:

$$m_I = \frac{I_L}{\tilde{I}_L} = \frac{I_{LM}}{\tilde{I}_{LM}}, \quad m_V = \frac{V_L}{\tilde{V}_L} = \frac{V_0}{\tilde{V}_0}, \tag{1.5}$$

where m_I, m_V are the scales.

If $m_I = m_V$, a geometrical similarity or, more precisely, the Euclidean equivalence in sense of Euclidean geometry is obtained.

If $m_I \neq m_V$, an affine similarity in sense of affine geometry is fulfilled.

The load-power dependence

$$\overline{P}_L = \overline{V}_L \overline{I}_L = \overline{V}_L(1 - \overline{V}_L) \tag{1.6}$$

determines a parabola in Fig. 1.6.

In turn, the power transfer ratio K_P or efficiency η of the running regime

$$K_P = \eta = \frac{P_L}{P_0} = \overline{V}_L \tag{1.7}$$

is a linear function shown in Fig. 1.6.

Let us consider the analogous relationships for the load resistance.

From (1.1), we get the corresponding expression

$$V_L = V_0 \frac{R_L}{R_i + R_L}. \tag{1.8}$$

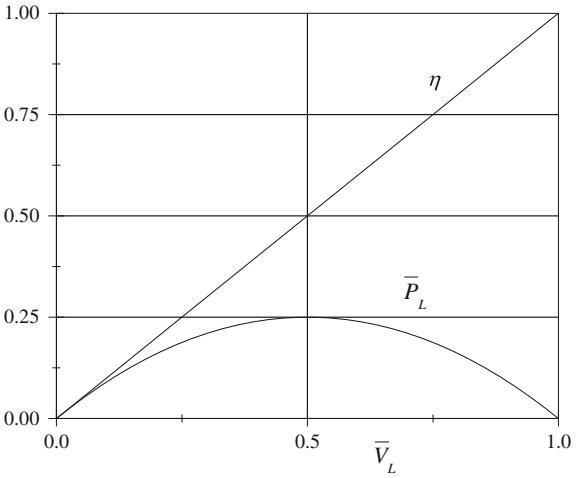

Fig. 1.6 Load power and efficiency via the load voltage

It is possible to express the relative load resistance by the internal resistance

$$\overline{R}_L = \frac{R_L}{R_i} = \frac{\tilde{R}_L}{\tilde{R}_i}. \tag{1.9}$$

Then, we have the relative expression

$$\overline{V}_L = \frac{\overline{R}_L}{1 + \overline{R}_L}. \tag{1.10}$$

From (1.9), the recalculation formula is as follows:

$$m_R = \frac{R_L}{\tilde{R}_L} = \frac{R_i}{\tilde{R}_i}, \tag{1.11}$$

where m_R is the scale.

Hence, we have obtained relative values (1.3), (1.9) and relative expressions (1.4), (1.10), which coincide for different circuits. It shows as though we do not have the problem. But, it is possible to remark that relative regime parameters (1.3), (1.9) have the different quantities. For example, the maximum load power regime corresponds to the values $\overline{R}_L = 1, \overline{V}_{LM} = 0.5$. That is, inconvenient for the more complex circuits with a large number of parameters. If the internal resistance $R_i = 0$, the circuit has not scales for the load current and resistance.

The examples of circuits, which have two characteristic values of regime parameters, will be shown later. Then, the problem of scales and relative expressions arises.

1.2.3 Regime Change in the Relative Form

Let an initial (the first) regime correspond to values R_L^1, V_L^1, I_L^1. In turn, a subsequent (the second) regime corresponds to R_L^2, V_L^2, I_L^2. For convenience, we consider $V_0 = 10, R_i = 1$. Using (1.1), (1.8), we get the concrete or absolute values of all the regime parameters shown in Fig. 1.7.

Let us obtain these changes of regime parameters in the absolute and relative form. In the given case, we use the difference of values that corresponds to the known variation theorem of resistance and current into a circuit.

Then, we get the relative changes for the currents and voltages

$$\begin{aligned} \frac{I_L^2}{I_L^{SC}} - \frac{I_L^1}{I_L^{SC}} &= \frac{\Delta I_L^{21}}{I_L^{SC}} = \frac{-1}{10} = \overline{I}_L^{21} = -0.1. \\ \frac{V_L^2}{V_0} - \frac{V_L^1}{V_0} &= \frac{\Delta V_L^{21}}{V_0} = \frac{1}{10} = \overline{V}_L^{21} = 0.1. \end{aligned} \tag{1.12}$$

Using (1.9), we constitute the following relative changes for the resistances:

$$\frac{R_L^2}{R_i} - \frac{R_L^1}{R_i} = \frac{\Delta R_L^{21}}{R_i} = \frac{0.5}{1} = 0.5. \tag{1.13}$$

In turn, corresponding to the known variation theorem of resistance and current [2], we have the dependence $\Delta I_L^{21}(\Delta R_L^{21})$ in the form

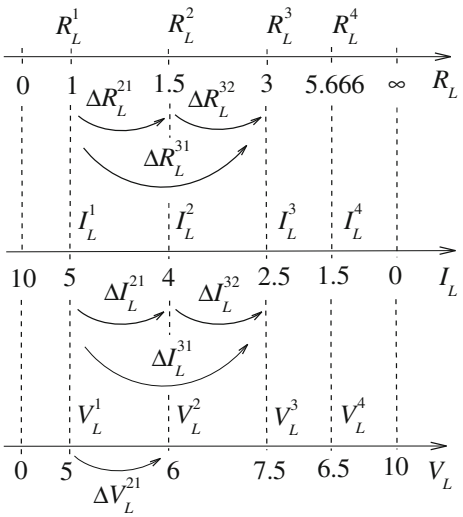

Fig. 1.7 Correspondence of the regime parameters at change of the load resistance

$$\Delta I_L^{21} = -\frac{\Delta R_L^{21}/R_{\text{IN}}^1}{1+\Delta R_L^{21}/R_{\text{IN}}^1} I_L^1 = -\frac{0.5/2}{1+0.5/2} \cdot 5 = -1, \tag{1.14}$$

where $R_{\text{IN}}^1 = R_i + R_L^1 = 2$ is the input resistance of our circuit for the subsequent load.

It is possible to rewrite expression (1.14) in the relative view

$$\frac{\Delta I_L^{21}}{I_L^1} = -\frac{\Delta R_L^{21}/R_{\text{IN}}^1}{1+\Delta R_L^{21}/R_{\text{IN}}^1}.$$

Therefore, we get the other determination of the relative changes

$$\frac{\Delta R_L^{21}}{R_{\text{IN}}^1} = 0.25, \quad \frac{\Delta I_L^{21}}{I_L^1} = -0.2. \tag{1.15}$$

Hence, the practical question arises, which expressions may we use? Because both initial expressions (1.12), (1.13), and complementary expression (1.15) have a clear physical sense.

Group Properties of Regime Changes

Let the next regime correspond to the values R_L^3, V_L^3, I_L^3 shown in Fig. 1.7. Then, corresponding to (1.15), we get the changes relatively to the first regime

$$\frac{\Delta R_L^{31}}{R_{\text{IN}}^1} = 1, \quad \frac{\Delta I_L^{31}}{I_L^1} = -0.5.$$

Let us obtain the changes relatively to the second regime. To do this, we must calculate $R_{\text{IN}}^2 = R_i + R_L^2 = 2.5$. Then,

$$\frac{\Delta R_L^{32}}{R_{\text{IN}}^2} = 0.6, \quad \frac{\Delta I_L^{32}}{I_L^2} = -0.375.$$

We note that the resultant regime change $\Delta I_L^{31}/I_L^1 = -0.5$ is not expressed through the initial change $\Delta I_L^{21}/I_L^1 = -0.2$ and intermediate change $\Delta I_L^{32}/I_L^2 = -0.375$ by the group operation (addition or multiplication). In this sense, regime changes (1.12), (1.13) hold the group properties that are convenient for analysis.

Anyway, the next regime changes will lead to the increase of a number of the relative values for various parameters and determinations of changes that complicates analysis.

Equal Regime Changes for Different Initial Regimes

Let the initial regime correspond to R_L^1, V_L^1, I_L^1, and subsequent regime corresponds to R_L^2, V_L^2, I_L^2. Then, we have some regime changes. Similarly, let the same regime change correspond to the other initial R_L^3, V_L^3, I_L^3 and subsequent R_L^4, V_L^4, I_L^4 values. We obtain even more the relative values for various parameters and determinations of changes.

1.2.4 Active Two-Port with Changeable Resistance

Let an active two-pole A with a load resistance R_{L1} contain a changeable resistance R_{L2} shown in Fig. 1.8a.

Therefore, values R_{L2}^1, R_{L2}^2 and so on determine a family of load straight lines with the various values of SC currents and OC voltages in Fig. 1.8b. Then, we have the set of the base or characteristic values as the parameters of the Thévenin equivalent circuit. Also, the corresponding variations of scales (1.3) complicate analysis.

Hence, it is necessary to obtain such base values which do not depend on the variation of an additional load. Also, we may get the relative values and relative changes of this additional load for comparing regimes for different circuits.

1.2.5 Scales of Regime Parameters for Cascaded Two-Ports

Let us consider a cascade connection of two two-ports $TP1$, $TP2$ with a variable load conductivity Y_{L2} in Fig. 1.9a. At change of load conductivity, we get a family of load straight lines for various sections; that is, we have some correspondence between these load lines by dash–dot lines shown in Fig. 1.9b.

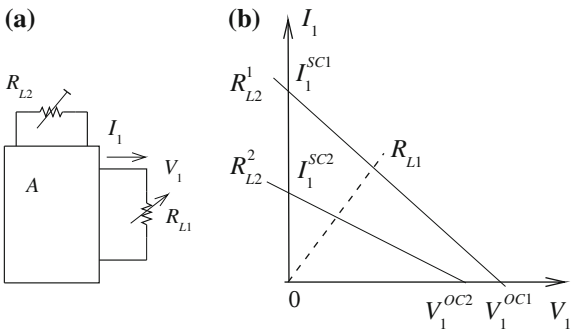

Fig. 1.8 **a** Active two-pole with a changeable resistance R_{L2}. **b** Family of load straight lines

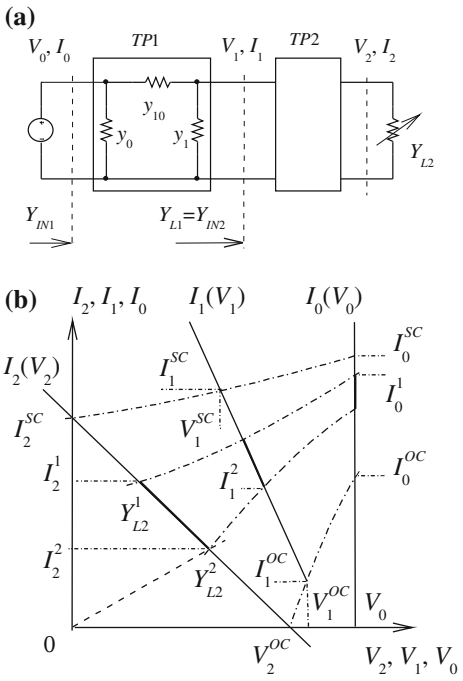

Fig. 1.9 **a** Cascade connection of two two-ports. **b** Correspondence of load straight lines

Our cascaded circuit, relatively to the load Y_{L2}, is similar to the simplest circuit in Fig. 1.3. Then, the characteristic values V_2^{OC}, I_2^{SC} are the scales or base values. Therefore, the relative values of the load current and voltage are determined by (1.3)

$$\overline{I}_2 = \frac{I_2}{I_2^{SC}}, \quad \overline{V}_2 = \frac{V_2}{V_2^{OC}}.$$

We must remark that the other characteristic values $V_2^{SC} = 0$, $I_2^{OC} = 0$. In turn, the internal resistance or conductivity $R_{i2} = 1/Y_{i2} = V_2^{OC}/I_2^{SC}$. Therefore, the relative load is determined by (1.9)

$$\overline{R}_{L2} = \frac{R_{L2}}{R_{i2}}.$$

So, we have the following base values for the load section V_2, I_2

$$V_2^{OC}, I_2^{SC}, V_2^{SC} = 0, I_2^{OC} = 0. \tag{1.16}$$

These values determine the corresponding base values for the other section of the cascaded circuit. For the section V_1, I_1, we get

$$V_1^{OC}, I_1^{SC}, V_1^{SC}, I_1^{OC}. \tag{1.17}$$

In turn, for the section V_0, I_0, the base values are

$$I_0^{SC}, I_0^{OC}. \tag{1.18}$$

The two nonzero base values turn out for all the regime parameters.

Then, there is a problem, how reasonably we may express these parameters for the initial regime Y_{L2}^1, subsequent Y_{L2}^2 and regime changes in the relative form.

It is possible to note that regime changes, as the length of segments on all the load straight lines have different lengths for usually used Euclidean geometry.

1.3 Analysis of the Traditional Approach to Normalizing of Regime Parameters for the Voltage Linear Stabilization

For the illustration of the assigned task, we consider two simple active two-poles with a load conductivity Y_{L1} in Fig. 1.10. The equation of the load straight line of the first active two-pole in Fig. 1.10a is given by

$$I_1 = (V_0 - V_1)y_{01} = y_{01}V_0 - y_{01}V_1,$$

where the conductivity y_{01} corresponds to the internal resistance of the voltage source V_0 and SC current $I_1^{SC} = y_{01}V_0$.

Then, we use normalized expression (1.2) which contains the two normalized values

$$\frac{I_1}{I_1^{SC}}, \frac{V_1}{V_0}.$$

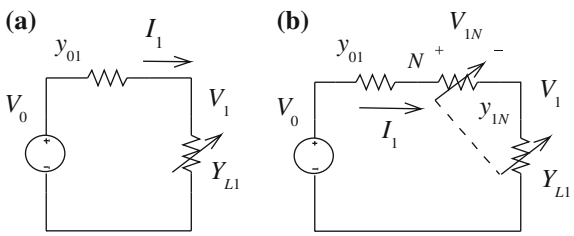

Fig. 1.10 **a** Active two-pole without a voltage stabilization. **b** Stabilization of a load voltage

The regimes of two similar circuits with running values of currents I_1, $\tilde{I}_1$ and voltages V_1, $\tilde{V}_1$ will be equivalent or equal to each other if the normalized values of currents and voltages (1.3) take place; that is,

$$\frac{I_1}{I_1^{SC}} = \frac{\tilde{I}_1}{\tilde{I}_1^{SC}}, \quad \frac{V_1}{V_0} = \frac{\tilde{V}_1}{\tilde{V}_0}.$$

The equation of the load straight line of the second active two-pole in Fig. 1.10b is given by

$$I_1 = \frac{y_{0N} y_{1N}}{y_{0N} + y_{1N}} (V_0 - V_1),$$

where conductivity y_{1N} corresponds to the conductivity of voltage regulator.

It is possible to carry out the normalization by the *SC* current I_1^{SC} if there is an access to this source at an experimental investigation. Then,

$$\frac{I_1}{I_1^{SC}} = \frac{y_{1N}/y_{0N}}{1 + y_{1N}/y_{0N}} \left(1 - \frac{V_1}{V_0}\right). \tag{1.19}$$

This expression contains the three normalized values. Therefore, a possible condition of equal regimes corresponds to the equalities

$$\frac{I_1}{I_1^{SC}} = \frac{\tilde{I}_1}{\tilde{I}_1^{SC}}, \quad \frac{V_1}{V_0} = \frac{\tilde{V}_1}{\tilde{V}_0}, \quad \frac{y_{1N}}{y_{0N}} = \frac{\tilde{y}_{1N}}{\tilde{y}_{0N}}. \tag{1.20}$$

If regimes differ, how may we express this difference in the convenient view? It is not clear, how may we work with the set of these six different values. It would be convenient to work with one value which characterizes this difference.

If the access to the voltage source is missing, what then must we choose as the normalizing value? It is possible to normalize by the maximum load current $I_{1M} = y_{0N}(V_0 - V_1)$, when the linear regulator is completely closed. Then, we have

$$\frac{I_1}{I_{1M}} = \frac{y_{1N}/y_{0N}}{1 + y_{1N}/y_{0N}}. \tag{1.21}$$

Therefore, the possible condition of the equal regimes corresponds to the equalities

$$\frac{I_1}{I_{1M}} = \frac{\tilde{I}_1}{\tilde{I}_{1M}}, \quad \frac{y_{1N}}{y_{0N}} = \frac{\tilde{y}_{1N}}{\tilde{y}_{0N}}.$$

We again obtain the two normalized values. But there is a contradiction with condition (1.20) for currents.

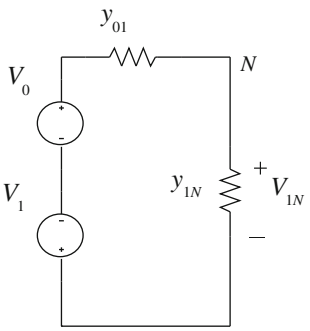

Fig. 1.11 Equivalent circuit of the active two-pole with the voltage stabilization

In Eq. (1.21) we pass from the value y_{1N} to the voltage V_{1N} of the linear regulator. Then, we obtain the normalized expression of the regulator

$$\frac{I_1}{I_{1M}} = 1 - \frac{V_{1N}}{V_0 - V_1}.$$

The equivalent circuit in Fig. 1.11 corresponds to this expression.

Even for such a simple circuit there is an uncertainty, how correctly or reasonably we may represent the normalized expression of regime?

The problem becomes complicated even more for a case of two and more loads with the voltage stabilization. For this, we consider Fig. 1.12.

In the case of two loads (without conductivity y_N), the two equations turns out to be

$$I_1 \frac{y_{0N} + y_{1N}}{y_{1N}} = (V_0 - V_1) y_{0N} - I_2,$$
$$I_2 \frac{y_{0N} + y_{2N}}{y_{2N}} = (V_0 - V_2) y_{0N} - I_1.$$

It is possible to carry out the normalization by the *SC* current of the voltage source. These expressions contain six normalized values. If regimes differ, we have the set of 12 different values.

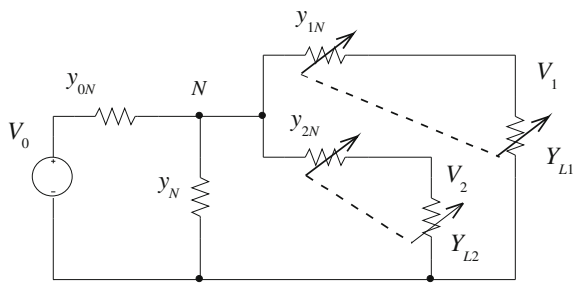

Fig. 1.12 Active circuit with the voltage stabilization of two loads

On the other hand, the normalization by the maximum load currents $I_{1M} = y_{0N}(V_0 - V_1), I_{2M} = y_{0N}(V_0 - V_2)$ leads to the reciprocal components $I_2/I_{1M}, I_1/I_{2M}$. These components raise a number of normalized values.

Therefore, the shown examples of the formal normalization do not allow comparing the regimes of different systems.

1.4 Active Two-Port

1.4.1 Volt Characteristics of an Active Two-Port

Let us consider the features of an active two-port with two load conductivities Y_{L1}, Y_{L2} in Fig. 1.13a. The interaction between load voltages is observed at change of loads. Therefore, the variable slope of the load volt characteristics or load straight lines $V_2(V_1, Y_{L1})$, $V_2(V_1, Y_{L2})$ takes place in Fig. 1.13b; the values Y_{L1}, Y_{L2} are parameters.

Therefore, such base values as the load *SC* currents and *OC* voltages are changed. In turn, the corresponding variations of scales (1.3) complicate analysis.

Hence, similar to Sect. 1.2.4, it is necessary to obtain such base values that do not depend on variable loads.

1.4.2 Traditional Recalculation of the Load Currents

Let us lead the base statements of the traditional approach to the recalculation of the load currents [3]. Expression for the currents I_1, I_2 of Fig. 1.14a has the view

$$\begin{bmatrix} I_1 \\ I_2 \end{bmatrix} = \begin{bmatrix} -Y_{11} & Y_{12} \\ Y_{12} & -Y_{22} \end{bmatrix} \cdot \begin{bmatrix} V_1 \\ V_2 \end{bmatrix} + \begin{bmatrix} I_1^{SC} \\ I_2^{SC} \end{bmatrix}. \tag{1.22}$$

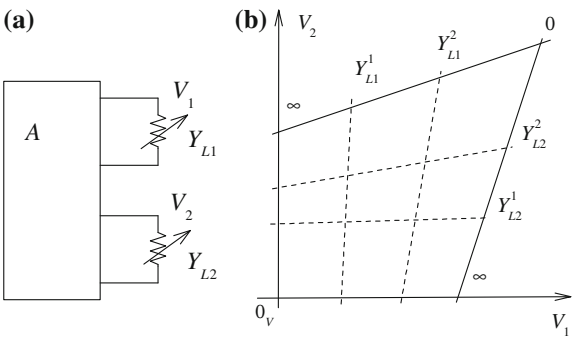

Fig. 1.13 **a** Active two-ports. **b** Family of load volt characteristics

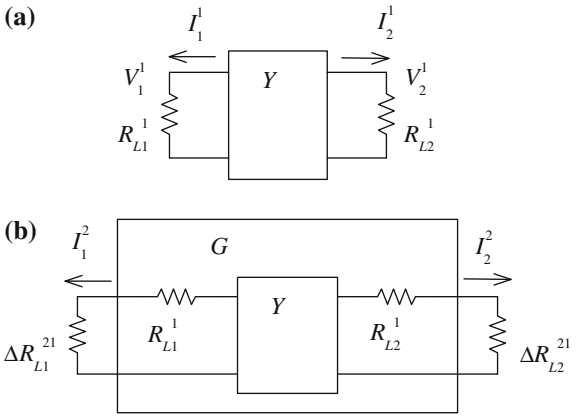

Fig. 1.14 **a** Initial values of loads. **b** Increments of loads concerning to the initial values

SC currents I_1^{SC}, I_2^{SC} are considered as the initial values I_1^0, I_2^0 of the load currents for the zero load resistances $R_{L1}^0 = 0$, $R_{L2}^0 = 0$.

Now, we introduce the first load resistances R_{L1}^1, R_{L2}^1 as the first increments $\Delta R_{L1}^{10}, \Delta R_{L2}^{10}$ concerning the initial zero values; that is,

$$R_{L1}^1 = \Delta R_{L1}^{10} + R_{L1}^0 = \Delta R_{L1}^{10}, \quad R_{L2}^1 = \Delta R_{L2}^{10} + R_{L2}^0 = \Delta R_{L2}^{10}.$$

Therefore, the relationships take place for these subsequent or the first values of currents and voltages

$$V_1^1 = \Delta R_{L1}^{10} I_1^1, \quad V_2^2 = \Delta R_{L2}^{10} I_2^1.$$

We rewrite expression (1.22) as

$$\begin{cases} I_1^1 = -Y_{11}\Delta R_{L1}^{10} I_1^1 + Y_{12}\Delta R_{L2}^{10} I_2^1 + I_1^0 \\ I_2^1 = Y_{12}\Delta R_{L1}^{10} I_1^1 - Y_{22}\Delta R_{L2}^{10} I_2^1 + I_2^0. \end{cases}$$

Then, we get

$$\begin{cases} (1 + Y_{11}\Delta R_{L1}^{10}) I_1^1 - Y_{12}\Delta R_{L2}^{10} I_2^1 = I_1^0 \\ -Y_{12}\Delta R_{L1}^{10} I_1^1 + (1 + Y_{22}\Delta R_{L2}^{10}) I_2^1 = I_2^0. \end{cases} \tag{1.23}$$

The solution of Eq. (1.23) gives the subsequent currents

$$\begin{aligned} I_1^1 &= \frac{I_1^0 + \Delta R_{L2}^{10}(Y_{22} I_1^0 + Y_{12} I_2^0)}{D^{10}}, \\ I_2^1 &= \frac{I_2^0 + \Delta R_{L1}^{10}(Y_{11} I_2^0 + Y_{12} I_1^0)}{D^{10}}, \end{aligned} \tag{1.24}$$

where the determinant is

$$D^{10} = (1 + Y_{11}\Delta R_{L1}^{10})(1 + Y_{22}\Delta R_{L2}^{10}) - (Y_{12})^2 \Delta R_{L1}^{10}\Delta R_{L2}^{10}.$$

Let us carry out the analysis of these relationships. Let the second load resistances R_{L1}^2, R_{L2}^2 be given as the second increments ΔR_{L1}^{20}, ΔR_{L2}^{20} concerning the initial zero values; that is,

$$R_{L1}^2 = \Delta R_{L1}^{20} + R_{L1}^0 = \Delta R_{L1}^{20}, \quad R_{L2}^2 = \Delta R_{L2}^{20} + R_{L2}^0 = \Delta R_{L2}^{20}.$$

Then,

$$I_1^2 = \frac{I_1^0 + \Delta R_{L2}^{20}(Y_{22}I_1^0 + Y_{12}I_2^0)}{D^{20}},$$
$$I_2^2 = \frac{I_2^0 + \Delta R_{L1}^{20}(Y_{11}I_2^0 + Y_{12}I_1^0)}{D^{20}},$$

where the determinant is

$$D^{20} = (1 + Y_{11}\Delta R_{L1}^{20})(1 + Y_{22}\Delta R_{L2}^{20}) - (Y_{12})^2 \Delta R_{L1}^{20}\Delta R_{L2}^{20}. \tag{1.25}$$

We try to introduce the intermediate changes ΔR_{L1}^{21}, ΔR_{L2}^{21} thus

$$R_{L1}^2 = \Delta R_{L1}^{21} + R_{L1}^1 = \Delta R_{L1}^{21} + \Delta R_{L1}^{10} = \Delta R_{L1}^{20},$$
$$R_{L2}^2 = \Delta R_{L2}^{21} + R_{L2}^1 = \Delta R_{L2}^{21} + \Delta R_{L2}^{10} = \Delta R_{L2}^{20}.$$

Therefore, the denominator D^{20} will contain both intermediate changes ΔR_{L1}^{21}, ΔR_{L2}^{21}, and the first values of resistances R_{L1}^1, R_{L2}^1. Thus, the structure of denominator (1.25) shows that group properties are not carried out for intermediate changes of load resistances. Therefore, subsequent changes must be counted concerning initial zero values. However, if we want to use the changes ΔR_{L1}^{21}, ΔR_{L2}^{21} concerning the values R_{L1}^1, R_{L2}^1, the two-port with conductivity parameters G is obtained in Fig. 1.14b. Thus, the recalculation of parameters of a new two-port is required.

Let us introduce variations of currents as increments $\Delta I_1^{10}, \Delta I_2^{10}$ concerning the initial values; that is,

$$I_1^1 = -\Delta I_1^{10} + I_1^0, \quad I_2^1 = -\Delta I_2^{10} + I_2^0.$$

From (1.23), we get

$$\begin{cases} -(1 + Y_{11}\Delta R_{L1}^{10})\Delta I_1^{10} + Y_{12}\Delta R_{L2}^{10}\Delta I_2^{10} = -Y_{11}\Delta R_{L1}^{10}I_1^0 + Y_{12}\Delta R_{L2}^{10}I_2^0 \\ Y_{12}\Delta R_{L1}^{10}\Delta I_1^{10} - (1 + Y_{22}\Delta R_{L2}^{10})\Delta I_2^{10} = Y_{12}\Delta R_{L1}^{10}I_1^0 - Y_{22}\Delta R_{L2}^{10}I_2^0. \end{cases}$$

The solution of this system gives the increments of currents via the increments of load resistances

$$\begin{aligned}\Delta I_1^{10} &= \frac{Y_{11}\Delta R_{L1}^{10} + [Y_{11}Y_{22} - (Y_{12})^2]\Delta R_{L1}^{10}\Delta R_{L2}^{10}}{D^{10}} I_1^0 - \frac{Y_{12}\Delta R_{L2}^{10}}{D^{10}} I_2^0, \\ \Delta I_2^{10} &= \frac{Y_{22}\Delta R_{L2}^{10} + [Y_{11}Y_{22} - (Y_{12})^2]\Delta R_{L1}^{10}\Delta R_{L2}^{10}}{D^{10}} I_2^0 - \frac{Y_{12}\Delta R_{L1}^{10}}{D^{10}} I_1^0,\end{aligned} \tag{1.26}$$

Let us compare these expressions with expression (1.14). We cannot already directly introduce the relative changes of type (1.15).

It is possible to draw the conclusion that it is necessary to carry out a deeper research of such circuits to obtain the relative expressions of regimes and its changes.

1.5 Nonlinear Characteristics

Besides the considered linear volt–ampere characteristics of linear circuits, nonlinear characteristics represent a practical interest too. The above-mentioned dependence of power via load voltage (1.6) is such nonlinear characteristic. For a passive two-port network, the dependence of efficiency via load voltage is also a nonlinear function.

Besides linear active two-pole networks, a wide class of active nonlinear two-poles is known. Solar cells, quasi-resonant voltage converters possess a typical convex characteristic. Power-source and power-load elements with a concave characteristic are also known. Further, we will consider features of such nonlinear characteristics.

1.5.1 Efficiency of Two-Ports with Different Losses

Let us consider a two-port in Fig. 1.15. In this case, the power transfer ratio K_P or efficiency η is a nonlinear function.

As it is known, the system of equation of this circuit has the view

$$\begin{bmatrix} I_0 \\ I_1 \end{bmatrix} = \begin{bmatrix} Y_{00} - Y_{10} \\ Y_{10} - Y_{11} \end{bmatrix} \cdot \begin{bmatrix} V_0 \\ V_1 \end{bmatrix}, \tag{1.27}$$

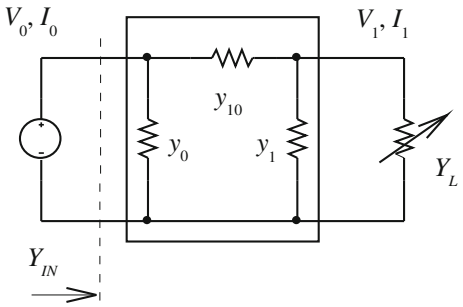

Fig. 1.15 Two-port with loss and a variable load conductivity

where Y parameters

$$Y_{00} = y_{10} + y_0, \quad Y_{11} = y_{10} + y_1, \quad Y_{10} = y_{10}.$$

The matrix determinant is

$$\Delta_Y = Y_{00}Y_{11} - (Y_{10})^2.$$

The characteristic admittance at the input and output or load is

$$Y_{IN.C} = \sqrt{\frac{Y_{00}}{Y_{11}}\Delta_Y}, \quad Y_{L.C} = \sqrt{\frac{Y_{11}}{Y_{00}}\Delta_Y}. \tag{1.28}$$

Next, we use the transmission a parameters. Then,

$$\begin{bmatrix} V_0 \\ I_0 \end{bmatrix} = \begin{bmatrix} a_{11}a_{12} \\ a_{21}a_{22} \end{bmatrix} \cdot \begin{bmatrix} V_1 \\ I_1 \end{bmatrix} = \begin{bmatrix} \frac{Y_{11}}{Y_{10}} & \frac{1}{Y_{10}} \\ \frac{\Delta_Y}{Y_{10}} & \frac{Y_{00}}{Y_{10}} \end{bmatrix} \cdot \begin{bmatrix} V_1 \\ I_1 \end{bmatrix}. \tag{1.29}$$

Using the attenuation coefficient γ [2], we may rewrite Eq. (1.29) as

$$\begin{bmatrix} V_0 \\ \frac{I_0}{Y_{IN.C}} \end{bmatrix} = \begin{bmatrix} ch\gamma & sh\gamma \\ sh\gamma & ch\gamma \end{bmatrix} \cdot \begin{bmatrix} V_1 \frac{Y_{L.C}}{\sqrt{\Delta_Y}} \\ \frac{I_1}{\sqrt{\Delta_Y}} \end{bmatrix}. \tag{1.30}$$

In turn, the admittance transformation has the view

$$\frac{Y_{IN}}{Y_{IN.C}} = \frac{\frac{Y_L}{Y_{L.C}} + th\gamma}{1 + \frac{Y_L}{Y_{L.C}}th\gamma}. \tag{1.31}$$

We have the relative values $Y_{IN}/Y_{IN.C}, Y_L/Y_{L.C}$. However, expression (1.31) is not a pure relative because contains the value $th\gamma$. This value is diverse for two-ports with different losses.

In turn, the power transfer ratio has the following forms:

$$\begin{cases} K_P = \frac{P_1}{P_0} = ch^2\gamma + sh^2\gamma - ch\gamma \cdot sh\gamma \cdot \left(\frac{Y_{IN}}{Y_{IN.C}} + \frac{Y_{IN.C}}{Y_{IN}}\right) \\ K_P = \left[ch^2\gamma + sh^2\gamma + ch\gamma \cdot sh\gamma \cdot \left(\frac{Y_L}{Y_{L.C}} + \frac{Y_{L.C}}{Y_L}\right)\right]^{-1}. \end{cases} \tag{1.32}$$

Sequentially, the maximum value K_{PM} corresponds to the admittance matching

$$K_{PM} = ch^2\gamma + sh^2\gamma - 2\, ch\gamma \cdot sh\gamma = (ch\gamma - sh\gamma)^2. \tag{1.33}$$

So, the relative values $Y_{IN}/Y_{IN.C}, Y_L/Y_{L.C}$ determine the deviation from the admittance matching by some way. However, expressions (1.32) are not pure relative because they contain the value $th\gamma$. If we try to use the value K_{PM}, as the scale value, we cannot obtain the pure relative form of expression (1.32).

Let us use the following voltage transfer ratio:

$$K_G = \frac{V_1}{V_1^{OC}} = \frac{Y_{11}}{Y_{10}}\frac{V_1}{V_0},$$

which corresponds to the voltage ratio of the Thévenin equivalent circuit. Using (1.30), we get

$$K_P(K_G) = K_G \frac{1 - K_G}{A - K_G}, \quad A = ch^2\gamma. \tag{1.34}$$

An example of efficiency (1.34) is shown in Fig. 1.16 for the various values A. The maximum values of K_{PM} correspond to the various values K_G.

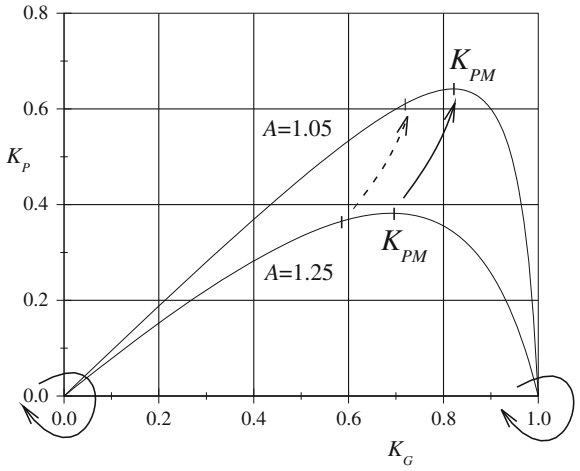

Fig. 1.16 Efficiency of two-ports for different losses

The solid arrows demonstrate the correspondence of the characteristic points. So, we have the three characteristic regimes. Then, the problem of scales, relative expressions, and correspondence of running points (dash arrow) arises.

1.5.2 Characteristic Regimes of Solar Cells

Let us consider volt–ampere and power-volt characteristics of two different solar cells in Fig. 1.17a. These characteristics have the maximum power points $P_M, \tilde{P}_M$ with the different currents $I_M, \tilde{I}_M$ and voltages $V_M, \tilde{V}_M$ [8]. There are also such characteristic values as SC currents $I^{SC}, \tilde{I}^{SC}$ and OC voltages V^{OC}, $\tilde{V}^{OC}$.

The solid arrows show the correspondence of the characteristic points. So, we have the three characteristic regimes. Similar to Sect. 1.5.1, the problem of scales, relative expressions, correspondence of running points (dash arrow), and approximation arises [15, 16].

1.5.3 Quasi-resonant Voltage Converter

It is known the load resonant converters, for example, with the zero-current switching [17]. These converters regulate their output by changing the switching period T_S. Simulation of *ORCAD* model shows that its load curve is almost

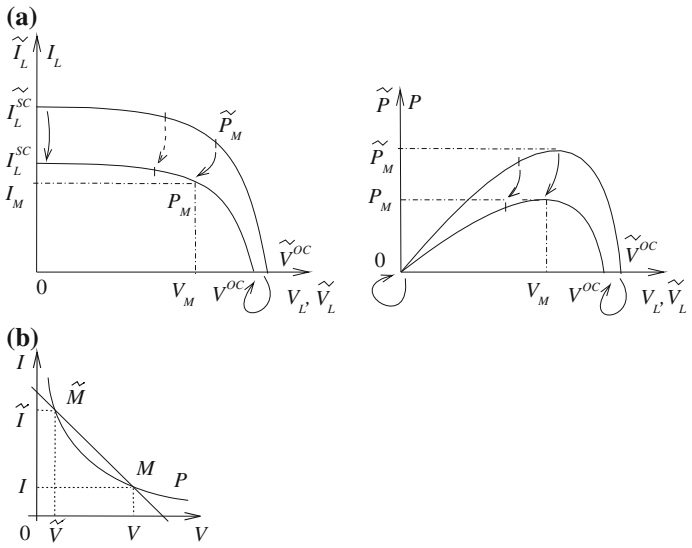

Fig. 1.17 **a** Volt–ampere characteristic and power-volt characteristic of solar cells. **b** Volt–ampere characteristic of power-load element

rectangular with maximum load power point P_M and similar to Fig. 1.17a. So, we have the same problems to determine the regime parameters.

1.5.4 Power-Source and Power-Load Elements

The power-source and power-load elements are known from [4, 18]. Their load characteristics have the typical form as shown in Fig. 1.17b. Analysis of the power-load element shows the two-valued voltage of a limited capacity voltage source; that is, points $M, \tilde{M}$. But for all that, the volt–ampere characteristic of this power-load element has one-valued representation.

On the other hand, taking into account the losses of real power-source and power-load elements, we get the two-valued volt–ampere characteristic of these elements. So, we have some characteristic regimes, and the same problems to determine the regime parameters.

1.6 Regulated Voltage Converters

1.6.1 Voltage Regulator with a Limited Capacity Voltage Source

In power supply systems with limited capacity voltage sources, the limitation of load power appears. An independent power supply system with a solar array and rechargeable battery may be the example of one.

We consider *DC* transformer with switched tapped secondary windings as a voltage regulator *VR*1 connected to a limited capacity voltage source V_0 in Fig. 1.18a. The regulator defines a transformation ratio

$$n_1 = \frac{V_1}{V}. \tag{1.35}$$

The regulation characteristic $V_1(n_1)$, by an internal resistance R_i, is a nonlinear and two-valued function shown in Fig. 1.18b. In this case, the upslope direction or forward branch of its regulation characteristic is used and the down movement of an operating point on the back branch is restrained.

Let R_i be equal to the load R_1. Then, the expression of $V_1(n_1)$ has the view

$$\frac{V_1}{V_0} = \overline{V}_1 = \frac{n_1}{1 + (n_1)^2}. \tag{1.36}$$

We get the relative expression which coincides with different circuits. But, similar to Sect. 1.2.2, the relative regime parameters $\overline{V}_1, n_1$ have the different quantities. For example, the maximum value $\overline{V}_{1M} = 0.5$ corresponds to $n_{1M} = 1$.

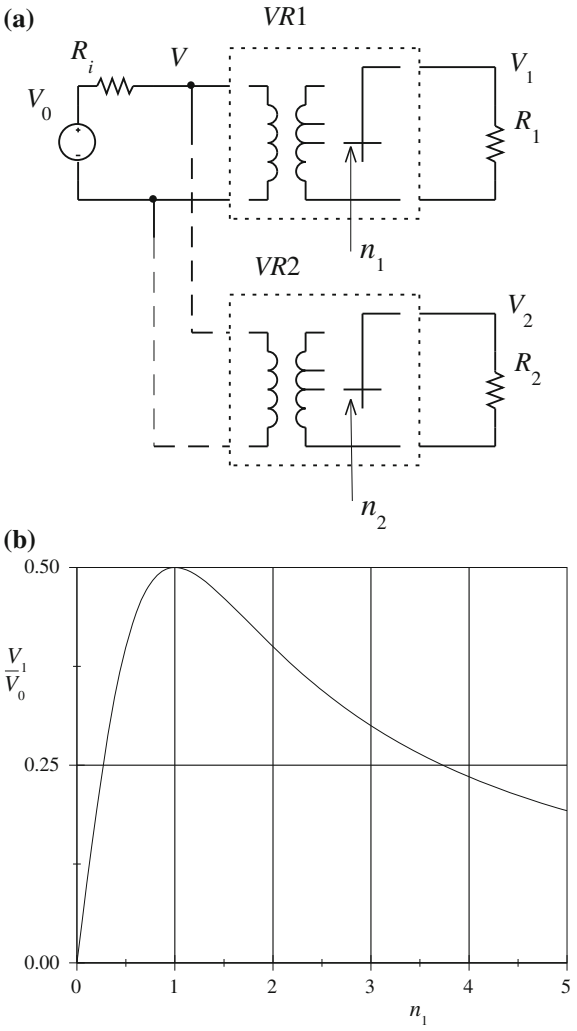

Fig. 1.18 **a** Power supply system with limited capacity voltage sources. **b** Example of its regulation characteristic

Therefore, it is necessary to stipulate the parameter to set the regime value in the form of a number.

Also, there is a question of the next switching step for the secondary winding; whether the regular or irregular step will be for the load voltage or for transformation ratio relatively to maximum permissible values. It is determined by how to set the value changes; that is, by increments, ratio and so on. The situation becomes complicated even more, if such a power supply system contains two loads with individual voltage regulators shown by dash lines in Fig. 1.18a; the interference of these loads takes place.

1.6.2 Buck Converter

Let us consider a buck converter in Fig. 1.19.

The expression of the static regulation characteristic for the continuous current mode of a choke L with a loss resistance R has the known view [5, 10]

$$V_L = \frac{V_0}{1 + \frac{R}{R_L}} D = \frac{V_0}{1 + (\sigma)^2} D, \tag{1.37}$$

where D is the relative pulse width and $(\sigma)^2$ is the relative loss.

Let us express (1.37) in the relative form. There are some variants.

First, it is possible to introduce the value $\overline{V}_L = V_L / V_0$. Then

$$\overline{V}_L = \frac{1}{1 + (\sigma)^2} D. \tag{1.38}$$

This expression is not a pure relative because it contains the value $(\sigma)^2$.

Let D be changed, $D^1 \rightarrow D^2$, and a subsequent value $D^2 = D^1 + D^{21}$. Then, the voltage change $\overline{V}_L^{21}$, by (1.38), depends on the parameter $(\sigma)^2$.

Let us consider the ratio of the initial and subsequent values

$$\frac{\overline{V}_L^2}{\overline{V}_L^1} = \frac{D^2}{D^1}.$$

This determination of regime change does not depend on parameter $(\sigma)^2$.

Second, we may introduce the value

$$\hat{V}_L = \frac{V_L}{V_{LM}} = D, \tag{1.39}$$

where the maximum load voltage is

$$V_{LM} = \frac{V_0}{1 + (\sigma)^2}.$$

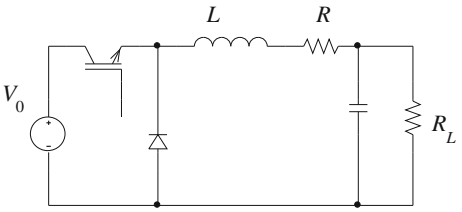

Fig. 1.19 Buck converter

Therefore, we obtain the following equalities for regimes of different converters:

$$D_1 = D_2, \quad \hat{V}_{L1} = \hat{V}_{L2}.$$

In turn, the regime changes are expressed by the ratio or increment of values $\hat{V}_{L1}$, $\hat{V}_{L2}$.

If an initial expression of type (1.37) is more complex, it will be also difficult to constitute relative expression (1.39) directly and reasonably. This case is considered in the next section.

1.6.3 Boost Converter

Let us consider a boost converter in Fig. 1.20a. Similar to (1.37), we offer an equation of the known static regulation characteristic

$$\frac{V_L}{V_0} = \frac{n}{1 + (\sigma)^2 (n)^2}, \tag{1.40}$$

where $n = \frac{1}{1-D} \geq 1$ is the inverse relative pause width.

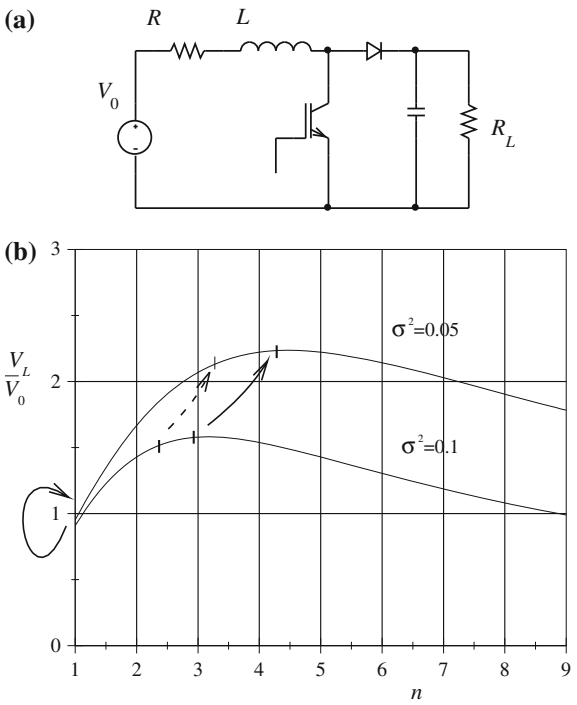

Fig. 1.20 **a** Boost converter. **b** Its regulation characteristics for different losses

This expression is analogous to (1.36). The regulation characteristics for various values $(\sigma)^2$ are shown in Fig. 1.20b. It is obvious that the maximum values V_L correspond to the various values n. The characteristic value is also $n = 1$.

The solid arrows show the correspondence of the characteristic points and dash arrow shows running points.

Let us attempt to express (1.40) in the relative form. We may introduce the new values

$$\hat{V}_L = \frac{\sigma}{V_0} V_L, \quad \hat{n} = \sigma n.$$

Then

$$\hat{V}_L = \frac{\hat{n}}{1 + (\hat{n})^2}.$$

Although the relative expression turns out, for the characteristic value $n = 1$ (the transistor is switched off) the new value $\hat{n} = \sigma$ depends on the parameter of the converter.

References

1. Alexander, C.K., Sadiku, M.N.O.: Fundamentals of Electric Circuits, 5th edn. McGraw–Hill, New York (2009)
2. Bessonov L.A.: Teoreticheskie Osnovy Elektrotekhniki. Elektricheskie tsepi, Izd.9. (Basic electrical engineering theory: Electric circuits, 9th edn.). Vyshaia shkola, Moskva (1996)
3. Bogatyrev, O.M.: General method of solving of problems for linear circuit at changeable resistances of branches. Elektrichestvo. **9**, 67–69 (1955)
4. Emadi, A., Khaligh, A., Rivetta, C.H., Williamson, G.A.: Constant power loads and negative impedance instability in automotive systems: definition, modeling, stability, and control of power electronic converters and motor drives. IEEE Trans. Veh. Technol. **55**(4), 1112–1125 (2006)
5. Erickson, R.W., Maksimovic, D.: Fundamentals of power electronics. Springer, Berlin (2001)
6. Glisson, T.H.: Introduction to circuit analysis and design. Springer, Berlin (2011)
7. Irwin, J.D., Nelms, R.M.: Basic Engineering Circuit Analysis, 10th edn. Wiley, Hoboken (2011)
8. Ishibashi, K., Kimura, Y., Nivano, M.: An extensively valid and stable method for derivation of all parameters of a solar cell from a single current-voltage characteristic. J. Appl. Phys. **103** (9), 094507/1–094507/6 (2008)
9. Ivanov–Tsyganov, A,I.: Electropreobrazovatel'nye ustroistva RES. (Electro-converting equipments of radio-electronic systems RES). Vyshaia shkola, Moskva (1991)
10. Kazimierczuk, M.K.: Pulse–width Modulated DC–DC Power Converters. Wiley, New York (2008)
11. Leger, A.S., Nwankpa, C.O.: Analog and hybrid computation approaches for static power flow. Paper presented at the 40th Annual Hawaii international conference on system sciences (2007)

12. Levron, Y., Shmilovitz, D.: On the maximum efficiency of systems containing multiple sources. IEEE Trans. Circuits Syst. I Regul. Pap. **57**(8), 2232–2241 (2010)
13. Liu, X., Wang, P., Loh, P.C.: A hybrid AC/DC microgrid and its coordination control. IEEE Trans. Smart Grid **2**(2), 278–286 (2011)
14. Nelatury, S.R.: Didactic uses of maximum power transfer theorem and guided problem solving. Int. J. Electr. Eng. Educ. **51**(3), 244–260 (2014)
15. Penin, A., Sidorenko, A.: A convenient model for *I-V* characteristic of a solar cell generator as an active two–pole with self–limitation of current. World Acad. Sci. Eng. Technol. **3**(4), 905-909 (2009). http://www.waset.org/publications/9926. Accessed 30Nov 2014
16. Penin, A., Sidorenko, A.: Determination of deviation from the maximum power regime of a photovoltaic module. Moldavian J. Phys. Sci. **9**(2), 191–198 (2010). http://sfm.asm.md/moldphys/2010/vol9/n2/index.html. Accessed 30 Nov 2014
17. Penin, A.: A quasi-resonance voltage converter with improved parameters. Elektrichestvo. **2**, 58–64 (2009)
18. Singer, S., Erickson, R.W.: Power–source element and its properties. IEEE Proc. Circ. Devices Syst. **141**(3), 220–226 (1994)
19. Venikov, V.A.: Theory of similarity and simulation: with applications to problems in electrical power engineering. Macdonald, London (1969)

Part I
Electrical Circuits with one Load. Projective Coordinates of a Straight Line Point

Chapter 2
Operating Regimes of an Active Two-Pole. Display of Projective Geometry

2.1 Volt–Ampere Characteristics of an Active Two-Pole. Affine and Projective Transformations of Regime Parameters

2.1.1 Affine Transformations

It is known that any linear circuit (an active two-pole A) relative to load terminals is replaced by a voltage source V_0 in series with an internal resistance R_i [1, 6]. Let us consider two cases of the load.

Case 1

A variable voltage source V_L is the load of an active two-pole A in Fig. 2.1. The voltage V_L (independent quantity) and load current I_L are the parameters of operating or running regime.

At change of the load voltage from the short circuit SC $(V_L = 0)$ to open circuit OC $(V_L^{OC} = V_0)$, a load straight line is given by (1.1)

$$I_L = \frac{V_0}{R_i} - \frac{V_L}{R_i} = I_L^{SC} - \frac{V_L}{R_i}, \tag{2.1}$$

where I_L^{SC} is the SC current. This straight line is shown in Fig. 2.2.

The characteristic regime parameters I_L^{SC}, V_0 determine the different scales for the axes of coordinates.

We want to represent a running regime parameter of the load by a certain quantity, which would have an identical value for various actual regime parameters such as voltage and current. To do this, we use a geometrical interpretation of change or "kinematics" of a circuit regime.

As the load characteristic is defined by linear expression (2.1), a similar expression in geometry defines an affine transformation, conformity, or mapping of

A. Penin, *Analysis of Electrical Circuits with Variable Load Regime Parameters*, Power Systems, DOI 10.1007/978-3-319-28451-4_2

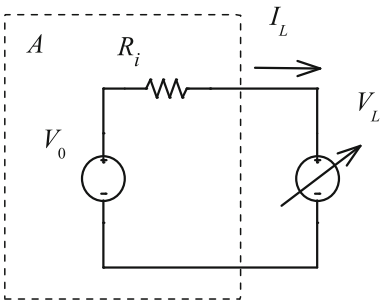

Fig. 2.1 Active two-pole with a load voltage source

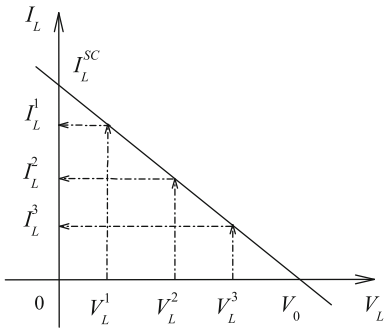

Fig. 2.2 Load straight line of an active two-pole

the voltage axis to current axis $V_L \rightarrow I_L$ [7]. The values I_L^{SC}, R_i are parameters of this affine transformation. The mechanism of this mapping is shown by parallel lines with arrows for three voltage values or points $V_L^1,\ V_L^2,\ V_L^3$.

An affine transformation is characterized by an invariant of three points

$$\varphi(V_L^1, V_L^2, V_L^3) = \varphi(I_L^1, I_L^2, I_L^3).$$

The invariant represents a certain expression, which only contains the chosen values of voltage or corresponding values of current; the parameters of the affine transformation do not enter in this expression.

To obtain the invariant expression, it is necessary to exclude the two parameters from Eq. (2.1) by means of three equations. For arbitrary three voltage values $V_L^1,\ V_L^2,\ V_L^3$ we have the system of equations

$$\left\{ I_L^1 = I_L^{SC} - \frac{V_L^1}{R_i}, \quad I_L^2 = I_L^{SC} - \frac{V_L^2}{R_i}, \quad I_L^3 = I_L^{SC} - \frac{V_L^3}{R_i}. \right. \tag{2.2}$$

Using the first and second equations, we exclude I_L^{SC}

$$I_L^1 - I_L^2 = + \frac{V_L^2}{R_i} - \frac{V_L^1}{R_i}. \tag{2.3}$$

Similarly, we have

$$I_L^1 - I_L^3 = + \frac{V_L^3}{R_i} - \frac{V_L^1}{R_i}. \tag{2.4}$$

$$I_L^2 - I_L^3 = + \frac{V_L^3}{R_i} - \frac{V_L^2}{R_i}. \tag{2.5}$$

Let us exclude the parameter R_i. To do this, we use expressions (2.3) and (2.5). Then, the required invariant or affine ratio is obtained as follows:

$$\frac{I_L^1 - I_L^2}{I_L^2 - I_L^3} = \frac{V_L^2 - V_L^1}{V_L^3 - V_L^2}. \tag{2.6}$$

If we use expressions (2.3) and (2.4), we get the other invariant

$$\frac{I_L^1 - I_L^3}{I_L^1 - I_L^2} = \frac{V_L^3 - V_L^1}{V_L^2 - V_L^1}. \tag{2.7}$$

Application of the concrete invariant is determined by a physical sense of a parameter of running regime, as it will be shown later.

Let us consider expression (2.6). We accept values $I_L^1,\ V_L^1$ corresponding to the running regime. In turn, values $I_L^2,\ V_L^2$ correspond to the open-circuit regime, $I_L^2 = 0,\ V_L^2 = V_0$; values $I_L^3,\ V_L^3$ correspond to the short circuit regime, $I_L^3 = I_L^{\mathrm{SC}}, V_L^3 = 0$. The pairs of the respective points $I_L^2,\ V_L^2$ and $I_L^3,\ V_L^3$ are the base or extreme points; the points $I_L^1,\ V_L^1$ are the dividing points.

Then, expression (2.6) takes the form

$$\begin{aligned} \frac{I_L^1 - 0}{0 - I_L^{SC}} &= \frac{V_0 - V_L^1}{0 - V_0}, \\ \frac{I_L^1 - 0}{I_L^{SC} - 0} &= \frac{V_0 - V_L^1}{V_0 - 0}. \end{aligned} \tag{2.8}$$

The affine ratio n^1 can be represented by the formal view

$$n^1 = (I_L^1\ 0\ I_L^{SC}) = (V_L^1\ V_0\ 0),$$

where

$$(I_L^1\ 0\ I_L^{SC}) = \frac{0 - I_L^1}{0 - I_L^{SC}} = \frac{I_L^1}{I_L^{SC}}, \tag{2.9}$$

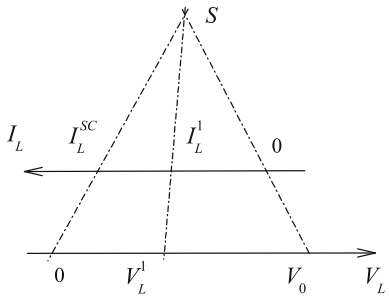

Fig. 2.3 Affine transformation $V_L \rightarrow I_L$

$$(V_L^1 \;\; V_0 \;\; 0) = \frac{V_0 - V_L^1}{V_0 - 0}. \tag{2.10}$$

Further, we consider the sense of the value n^1. We obtain the quantity that has an identical value for current and voltage. For the current, this value n^1 is simply the normalized value (at the expense of a particular choice of the base points).

Therefore, expression (2.8) coincides with Eq. (2.1) for the normalized values

$$\frac{I_L^1}{I_L^{SC}} = 1 - \frac{V_L^1}{V_0}. \tag{2.11}$$

The more convenient representation of affine transformation (2.1) is given in Fig. 2.3 for the actual values of the current and voltage. There is a projection center S and straight lines V_L, I_L are parallel. The affine conformity is also given by two pairs of respective base points.

As it was already shown, as the respective base points, it is convenient to use the points of characteristic regimes, which can be easily determined at a qualitative level; that is, the short circuit and open-circuit regimes. The sense of this affine transformation is visible in Fig. 2.3. The projection center S has a final coordinate because of different scales or base points of the current and voltage lines.

If the projection center is $S \rightarrow \infty$, the projection is carried out by parallel lines. This mapping corresponds to the Euclidean transformation; that is, the parallel translation of a segment in Fig. 2.4. Such a case conforms to Eq. (2.11).

Now, we consider changes of regime; that is, how to set this change in the invariant form too. Let an initial regime be given by values I_L^1, V_L^1 and subsequent regime be set by I_L^2, V_L^2. Let us express the subsequent value of current through the initial value. Using Eq. (2.3), we get

$$I_L^2 = I_L^1 + \frac{V_L^1}{R_i} - \frac{V_L^2}{R_i} = I_L^1 + I_L^{21}. \tag{2.12}$$

The obtained transformation with a parameter I_L^{21} translates the initial regime I_L^1 point into the subsequent regime I_L^2 point; that is, $I_L^1 \rightarrow I_L^2$ shown in Fig. 2.5.

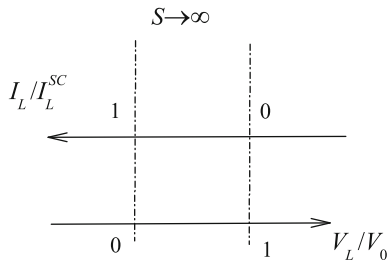

Fig. 2.4 Euclidean transformation $V_L \rightarrow I_L$

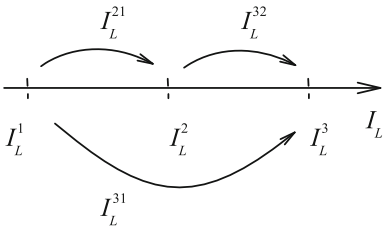

Fig. 2.5 Translation of point $I_L^1 \rightarrow I_L^2 \rightarrow I_L^3$ along a line

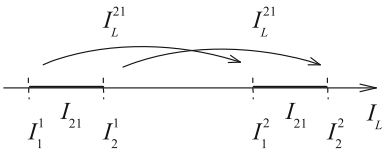

Fig. 2.6 Movement of a segment I_{21}

Further, transformation (2.12) with a parameter I_L^{32} translates the point $I_L^2 \rightarrow I_L^3$; that is,

$$I_L^3 = I_L^2 + I_L^{32}.$$

For example, let I_L^{32} be equal I_L^{21}, as it is shown in Fig. 2.5. It now follows that

$$I_L^3 = I_L^1 + I_L^{21} + I_L^{32} = I_L^1 + I_L^{31}.$$

Therefore, we have the resultant transformation $I_L^1 \rightarrow I_L^3$ with a parameter I_L^{31}.

Thus, a set of transformations (2.12) is a group.

Let an initial regime be given by two values I_1^1, I_2^1. These values correspond to a segment I_{21} in Fig. 2.6.

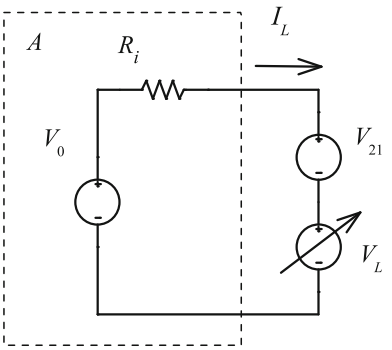

Fig. 2.7 Signal V_{21} and bias V_L voltage is the load of an active two-pole

For example, this segment or increment of current I_{21} corresponds to a signal voltage V_{21} in series with a variable bias voltage V_L in Fig. 2.7.

If we apply transformation (2.12) to the initial points I_1^1, I_2^1, we obtain the subsequent points

$$I_1^2 = I_1^1 + I^{21}, \quad I_2^2 = I_2^1 + I^{21}. \tag{2.13}$$

Obviously, translation (2.12) or (2.13) is characterized by the invariant of two points $\varphi(I_1^1, I_2^1) = I_2^1 - I_1^1$, because

$$I_2^2 - I_1^2 = I_2^1 - I_1^1. \tag{2.14}$$

Thus, this invariant is the Euclidean distance between two points. Therefore, geometry of this transformation group is geometry of a Euclidean straight line.

Also, we can consider the dual variant of segment and its movement in Fig. 2.8.

Let an initial regime be given by two values I_1^1, I_1^2 or segment $I_1^2 I_1^1$. We use the translation with a parameter I_{21}. Then, the subsequent points

$$I_2^1 = I_1^1 + I_{21}, \quad I_2^2 = I_2^1 + I_{21}.$$

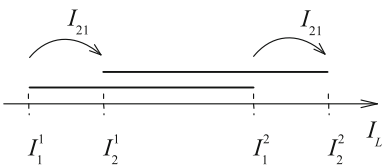

Fig. 2.8 Movement of segment $I_1^2 I_1^1 \rightarrow I_2^2 I_2^1$

Obviously, there is an invariant of two points

$$I_1^2 - I_1^1 = I_2^2 - I_2^1.$$

Using (2.11), we get the similar invariant for the normalized voltage and current values

$$\frac{I_L^2}{I_L^{SC}} - \frac{I_L^1}{I_L^{SC}} = \frac{V_L^1}{V_0} - \frac{V_L^2}{V_0} = n^{21}. \tag{2.15}$$

This regime change corresponds to a relative change in "percent". Note that the invariants of transformation (2.12) coincide with the known principle of superposition for linear circuits.

Remark Let us introduce a regime change by ratio of currents. Using expression (2.11), we get

$$\frac{I_L^2}{I_L^{SC}} \div \frac{I_L^1}{I_L^{SC}} = \frac{I_L^2}{I_L^1} = \frac{V_0 - V_L^2}{V_0 - V_L^1}.$$

We can note that the ratio of currents does not contain a transformation parameter. But, this ratio of voltages contains the transformation parameter V_0. Hence, the condition of invariant is not executed.

Case 2

A variable conductivity Y_L is a load of the simplest circuit in Fig. 2.9; an internal resistance of this active two-pole $R_i = 0$.The equation of this circuit

$$I_L = V_0 Y_L. \tag{2.16}$$

The conductivity Y_L (independent quantity) and load current are the parameters of a running regime.

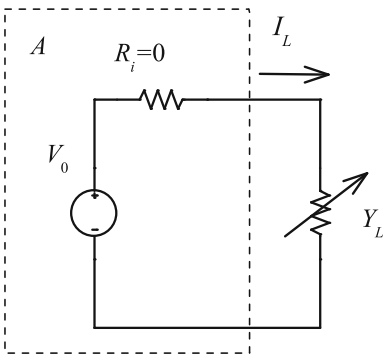

Fig. 2.9 Active two-pole with $R_i = 0$

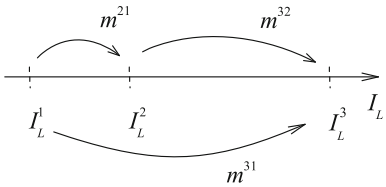

Fig. 2.10 Transformation of a point $I_L^1 \to I_L^2 \to I_L^3$

For this circuit, the regime has only an absolute value; it is impossible to state a relative expression in view of the absence of a scale.

Now, we consider changes of regime. The initial conductivity value equals Y_L^1 and subsequent one equals Y_L^2. Then, we have the two values of currents

$$I_L^1 = V_0 Y_L^1, \quad I_L^2 = V_0 Y_L^2. \tag{2.17}$$

Using the ratio of these equations, we get

$$\frac{I_L^2}{I_L^1} = \frac{Y_L^2}{Y_L^1} = m^{21}. \tag{2.18}$$

Then, the subsequent current is obtained as

$$I_L^2 = m^{21} I_L^1. \tag{2.19}$$

This transformation with a parameter m^{21} translates a point of an initial regime I_L^1 to a point of a subsequent regime I_L^2; that is, $I_L^1 \to I_L^2$. The transformation is a group transformation because

$$I_L^3 = m^{32} I_L^2 = m^{32} m^{21} I_L^1 = m^{31} I_L^1.$$

This group is the dilation group. For example, let m^{32} be equal m^{21}, as shown in Fig. 2.10; a usual distance between currents is increased.

Let an initial regime be given by two values I_1^1, I_2^1. These values correspond to segment $I_1 I_2$ in Fig. 2.11. If we apply transformation (2.19) to the initial points I_1^1, I_2^1 or to the segment, we obtain the subsequent points

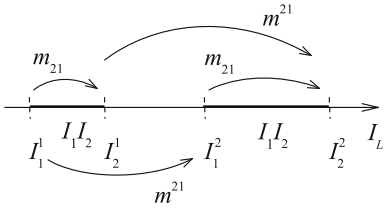

Fig. 2.11 Movement of segment $I_1 I_2$

$$I_1^2 = m^{21} I_1^1, \quad I_2^2 = m^{21} I_2^1.$$

Obviously, transformation (2.19) has the invariant of two points

$$\varphi(I_2^2, I_1^2) = \frac{I_2^2}{I_1^2} = \frac{m^{21} I_2^1}{m^{21} I_1^1} = \frac{I_2^1}{I_1^1} = m_{21} = \varphi(I_2^1, I_1^1). \tag{2.20}$$

This invariant m_{21} is the invariable "length" of segment $I_1 I_2$. Therefore, we obtain the segment end

$$I_2^1 = m_{21} I_1^1.$$

These two examined cases correspond to the known similarity property.

And so, the consideration of regime changes as geometrical transformations gives a methodical foundation for the valid introduction of regime changes for more complex cases.

2.1.2 Projective Transformations

Let us consider a circuit with a variable load resistance in Fig. 2.12.

The load straight line is also given by expression (2.1)

$$I_L = \frac{V_0}{R_i} - \frac{V_L}{R_i} = I_L^{SC} - \frac{V_L}{R_i}. \tag{2.21}$$

This straight line is shown in Fig. 2.13.

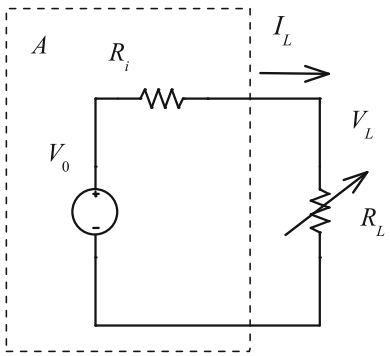

Fig. 2.12 Circuit with a load resistance

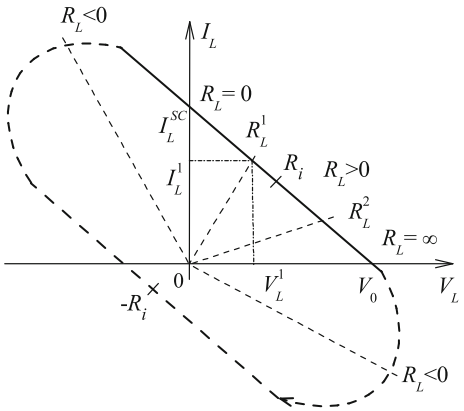

Fig. 2.13 Load straight line of a circuit with a load resistance

The bunch of straight lines with a parameter R_L corresponds to this straight line. The bunch center is the point 0. The equation of this bunch is given as

$$I_L = \frac{1}{R_L} V_L. \tag{2.22}$$

Further, it is possible to calibrate the load straight line in the load resistance values [10, 13, 15]. The internal area $R_L > 0$ at the load change corresponds to regime of energy consumption by the load. If to continue the calibration for the negative values $R_L < 0$, the regime passes into the external area, which physically means return of energy to the voltage source V_0.

Therefore, at the infinitely remote point $R_L = -R_i$, the calibrations of the load straight line will coincide for the areas $V_L > V_0, V_L < 0$. So, this straight line is closed; that is typical property of projective geometry.

The load resistance value determines the nonhomogeneous coordinate for a point of load straight line. In turn, the two values V_L, I_L are the homogeneous coordinates because $R_L = \rho V_L \div \rho I_L$, where ρ is any nonzero real number. Homogeneous coordinates have finite values. Further, the equation $V_L(R_L)$ has the characteristic fractionally linear view

$$V_L = V_0 \frac{R_L}{R_i + R_L}. \tag{2.23}$$

Of course, similar expressions take place for currents and resistances for different branches of active circuits and are used for measurement of circuit parameters [2].

That gives the solid grounds for considering the map $R_L \to V_L$ as a projective transformation of projective geometry [4, 5, 7]. In general, a projective transformation of points of one straight line into points of another line is set by a center S of projection or three pairs of respective points in Fig. 2.14. Therefore, the infinitely remote point $R_L = \infty$ corresponds to the finite point $V_L = V_0$. Also, fractionally linear expressions of type (2.23) as projective transformations are used for

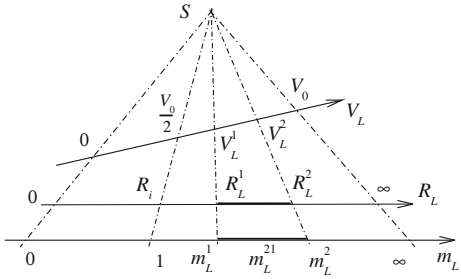

Fig. 2.14 Projective transformation of points $R_L \to V_L$

measuring instruments [8, 9]. In addition, a class of infinite "ideal" points of projective geometry is introduced to represent infinite resistances [3].

As the pairs of respective points, it is convenient to use the points of the characteristic regimes, which can be easily determined at a qualitative level; that is, the short circuit, open circuit, and maximum load power. In turn, the point of a running regime is the fourth point.

We want to represent the running regime of load in the relative form regarding to these three characteristic or base points. To do this, we may use a cross-ratio of four points.

The projective transformations preserve a cross-ratio of four points. For values R_L^1, V_L^1, I_L^1 of initial or running regime, the cross-ratio m_L has the view

$$m_L^1 = (0\ R_L^1\ R_i\ \infty) = \frac{R_L^1 - 0}{R_L^1 - \infty} : \frac{R_i - 0}{R_i - \infty} = \frac{R_L^1}{R_i}, \tag{2.24}$$

$$m_L^1 = (0\ V_L^1\ \frac{V_0}{2}\ V_0) = \frac{V_L^1 - 0}{V_L^1 - V_0} \div \frac{\frac{V_0}{2} - 0}{\frac{V_0}{2} - V_0} = \frac{V_L^1}{V_0 - V_L^1}, \tag{2.25}$$

$$m_L^1 = (I_L^{SC}\ I_L^1\ \frac{I_L^{SC}}{2}\ 0) = \frac{I_L^1 - I_L^{SC}}{I_L^1 - 0} \div \frac{\frac{I_L^{SC}}{2} - I_L^{SC}}{\frac{I_L^{SC}}{2} - 0} = \frac{I_L^{SC} - I_L^1}{I_L^1}. \tag{2.26}$$

We note that expression (2.26) corresponds to (2.7).

The cross-ratio in geometry underlies the definition of the "distance" between points $R_L^1, R_L = R_i$ concerning the extreme or base values $0, \infty$. The point R_i is a scale or a unit point. Similarly, we have the base points $0, V_0$, and a unit point $V_0/2$ of voltage. Thus, a projective coordinate of running regime point is set by the value m_L, which is defined in an identical (invariant) manner through various regime parameters as R_L, V_L, I_L.

In turn, a regime change $R_L^1 \to R_L^2$ (respectively $V_L^1 \to V_L^2$, $I_L^1 \to I_L^2$) can be expressed similarly

$$m_L^{21} = (0\ R_L^2\ R_L^1\ \infty) = \frac{R_L^2}{R_L^1}, \tag{2.27}$$

$$m_L^{21} = (0\ V_L^2\ V_L^1\ V_0) = \frac{V_L^2}{V_0 - V_L^2} \div \frac{V_L^1}{V_0 - V_L^1}, \tag{2.28}$$

$$m_L^{21} = (I_L^{SC}\ I_L^2\ I_L^1\ 0) = \frac{I_L^{SC} - I_L^2}{I_L^2} \div \frac{I_L^{SC} - I_L^1}{I_L^1}. \tag{2.29}$$

The cross-ratio has the next quality

$$m_L^{12} = (0\ R_L^1\ R_L^2\ \infty) = \frac{R_L^1}{R_L^2} = \frac{1}{m_L^{21}}.$$

A group property of the cross-ratio realizes

$$m_L^2 = m_L^{21} m_L^1. \tag{2.30}$$

For the next regime change $R_L^2 \to R_L^3$, the group property is given by

$$m_L^3 = m_L^{32} m_L^2 = m_L^{32} m_L^{21} m_L^1 = m_L^{31} m_L^1.$$

Let us express the subsequent voltage value V_L^2 by the initial value V_L^1 and regime change value m_L^{21}. Using (2.28), we get the recalculation formula

$$\frac{V_L^2}{V_0} = \frac{\frac{V_L^1}{V_0} m_L^{21}}{\frac{V_L^1}{V_0}(m_L^{21} - 1) + 1}. \tag{2.31}$$

This formula allows finding a subsequent voltage value by an initial voltage and transformation parameter m_L^{21}. Also, this expression can be obtained from (2.23). For an initial R_L^1 and subsequent R_L^2 value, we get the following system of the equations:

$$\begin{cases} V_L^1 = V_0 \frac{R_L^1}{R_i + R_L^1} \\ V_L^2 = V_0 \frac{R_L^2}{R_i + R_L^2} \end{cases}.$$

Excepting R_i, we get expression (2.31).

In general, transformation (2.31) translates an initial point V_L^1 to subsequent point V_L^2. Therefore, we can set the identical regime changes for the different initial regimes shown in Fig. 2.15 for the straight line V_L as a closed projective straight line.

The identical transformation parameter m_L^{21} forms a segment of invariable "length" (in sense of projective geometry) and we observe the movement of this segment. Here, the change of the Euclidean (usual) length is visible. For the base points, the Euclidean length is decreasing to zero.

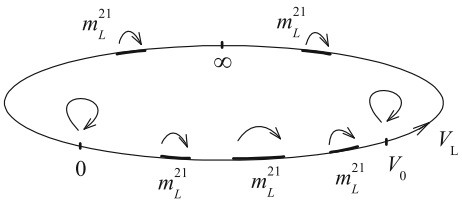

Fig. 2.15 Identical regime changes for the different initial regimes

In the theory of the projective transformations, the fixed points play an important role. For their finding, Eq. (2.31) is solved as $V_L^1 = V_L^2$. It turns out the two real roots, $V_L = 0, V_L = V_0$, which define the hyperbolic transformation of hyperbolic (Lobachevski) geometry. Physically, the fixed point means such a regime when a variable V_L does not depend on the initial or subsequent value R_L. It is evident for SC, OC regimes.

If the roots of equation coincide, the fixed point defines the parabolic transformation and, respectively, parabolic (Euclidean) geometry. If the roots are imaginary, geometry is elliptic (Riemannian).

In geometry, it is established that these three kinds of transformations (projective, affine, and Euclidean) exhaust possible variants of group transformations, which underlie the definition of the metrics of a straight line. Thus, the geometrical approach allows validating regimes determination, and both definitions of a regime and its change are coordinated by structure of expressions and ensure the performance of group properties.

Reasoning from such a geometrical interpretation, it is possible to give the following definition [12, 13]:

- a circuit regime is a coordinate of point on load straight lines and axes of coordinates;
- a regime change is a movement of point on all the straight lines, which defines a segment of corresponding length.

In this connection, it is possible to accept the following requirement (likewise to metric space axioms):

- independence or invariance of regimes and their changes from variables (regime parameters) as type R, V, I;
- the additive postulate of regimes changes;
- assignment of equal regime change for various initial regimes.

2.2 Volt–Ampere Characteristics of an Active Two-Pole with a Variable Element

2.2.1 *Thévenin Equivalent Circuit with the Variable Internal Resistance*

Let us consider the Thévenin equivalent circuit with the variable internal resistance R_i in Fig. 2.16.

In this case, a bunch of load straight lines with a parameter R_i is obtained at a center G in Fig. 2.17. The unified equation of this bunch is given by

$$I_L = \frac{1}{R_i}(-V_L + V_0). \tag{2.32}$$

The coordinate of the center G corresponding to V_0 does not depend on R_i.

Physically, it means that the current across this element is equal to zero. The element R_i can accept the two base or characteristic values, as $0, \infty$. The third characteristic value is not present for R_i.

Also, the bunch of straight lines with a parameter R_L corresponds to these load straight lines. The point 0 is the bunch center. Therefore, R_L can accept the two base or characteristic values, as $0, \infty$. Hereafter, we say about the two bunches with the parameter R_i and R_L correspondingly.

Let relative regimes be considered for this circuit.

Case 1

Let the internal resistance R_i be equal to R_i^1 and the load resistance varies from R_L^1 to R_L^2. In this case, a point of initial regime is $C_1 \rightarrow C_2$. If R_i is equal to R_i^2, a point of initial regime $B_1 \rightarrow B_2$. Therefore, the regime change, which is determined by the load change (an own change), is expressed similar to (2.27)

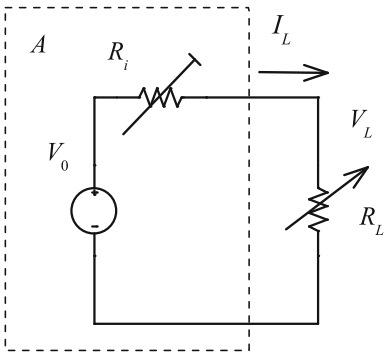

Fig. 2.16 Thévenin equivalent with the variable internal resistance

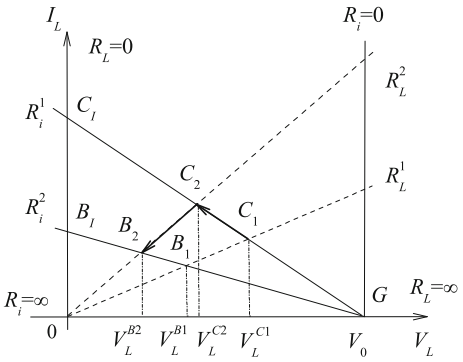

Fig. 2.17 Bunch of load straight lines for a voltage source

$$m_L^{21} = (C_I\ C_2\ C_1\ G) = (B_I\ B_2\ B_1\ G) = (0\ R_L^2\ R_L^1\ \infty) = \frac{R_L^2}{R_L^1}. \tag{2.33}$$

This determination of a regime change does not depend on R_i. Therefore, we must use only the load voltage for this calculation, as (2.28)

$$m_L^{21} = (0\ V_L^{C2}\ V_L^{C1}\ V_0) = \frac{V_L^{C2} - 0}{V_L^{C2} - V_0} \div \frac{V_L^{C1} - 0}{V_L^{C1} - V_0}. \tag{2.34}$$

In this case, the base points C_I, B_I correspond to the common value $V_L = 0$.

Case 2

Similarly, the regime change, which is determined by R_i change (a mutual change), is given by

$$m_i^{21} = (0\ B_2\ C_2\ A_2) = (0\ B_1\ C_1\ A_1) = (\infty\ R_i^2\ R_i^1\ 0) = \frac{R_i^1}{R_i^2}. \tag{2.35}$$

This determination of a regime change does not depend on R_L. Therefore, we must use only load voltage for calculation, as (2.34)

$$m_i^{21} = (0\ V_L^{B2}\ V_L^{C2}\ V_0) = \frac{V_L^{B2} - 0}{V_L^{B2} - V_0} \div \frac{V_L^{C2} - 0}{V_L^{C2} - V_0}. \tag{2.36}$$

In expressions (2.34) and (2.36) the identical base points, which are the centers of the two bunches of straight lines R_L,R_i, are used.

Case 3

If the regime is changed as point $C_1 \rightarrow C_2 \rightarrow B_2$, it is possible to speak about the general or compound change

$$m^{21} = m_i^{21} m_L^{21} = \frac{R_i^1}{R_i^2} \frac{R_L^2}{R_L^1}. \tag{2.37}$$

Then

$$m^{21} = \left(\frac{V_L^{B2} - 0}{V_L^{B2} - V_0} \div \frac{V_L^{C2} - 0}{V_L^{C2} - V_0} \right) \cdot \left(\frac{V_L^{C2} - 0}{V_L^{C2} - V_0} \div \frac{V_L^{C1} - 0}{V_L^{C1} - V_0} \right).$$

Finally, we obtain

$$m^{21} = \frac{V_L^{B2} - 0}{V_L^{B2} - V_0} \div \frac{V_L^{C1} - 0}{V_L^{C1} - V_0} = (0 \; V_L^{B2} \; V_L^{C1} \; V_0). \tag{2.38}$$

Analogous to (2.31), we get the recalculation formula

$$\frac{V_L^{B2}}{V_0} = \frac{\frac{V_L^{C1}}{V_0} m^{21}}{\frac{V_L^{C1}}{V_0} (m^{21} - 1) + 1}. \tag{2.39}$$

The compound regime and voltage changes, as point moving, are shown in Fig. 2.18.

We may note that values R_L, R_i have not any scales.

2.2.2 *Norton Equivalent Circuit with the Variable Internal Conductivity*

Let us consider the Norton equivalent circuit with the variable internal resistance or conductance Y_i and load conductance Y_L in Fig. 2.19.

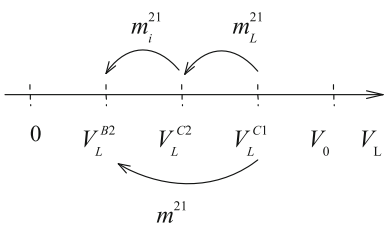

Fig. 2.18 Compound voltage changes

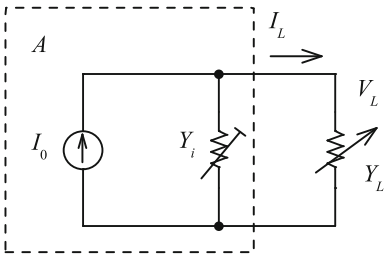

Fig. 2.19 Norton equivalent with the variable internal conductance

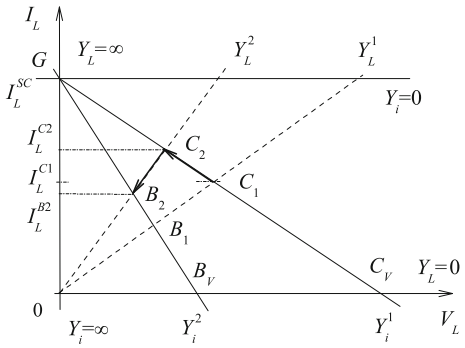

Fig. 2.20 Bunch of load straight lines for a current source

In this case, a bunch of load straight lines Y_i is obtained at the center G in Fig. 2.20.

The unified equation of this bunch is given as

$$I_L - I_0 = -Y_i V_L. \tag{2.40}$$

The coordinate of the center G corresponding to $I_0 = I_L^{SC}$ does not depend on the value Y_i. Physically, it means that the current across this element is equal to zero. The element Y_i can accept the two base or characteristic values, as $0, \infty$. The third characteristic value is not present for Y_i.

Let the relative regimes be considered for this case.

Case 1

Let the internal conductance Y_i be equal to Y_i^1 and the load conductance varies from Y_L^1 to Y_L^2. In this case, a point of initial regime $C_1 \rightarrow C_2$. If Y_i is equal to Y_i^2, a point of initial regime $B_1 \rightarrow B_2$. Therefore, the regime change, which is determined by the load change (an own change), is expressed similarly to (2.33)

$$\begin{aligned} m_L^{21} &= (C_V\ C_2\ C_1\ G) = (B_V\ B_2\ B_1\ G) \\ &= (0\ Y_L^2\ Y_L^1\ \infty) = \frac{Y_L^2}{Y_L^1}. \end{aligned} \tag{2.41}$$

This determination of a regime change does not depend on Y_i. Therefore, we must use only the load current for calculation; that is,

$$m_L^{21} = (0\ I_L^{C2}\ I_L^{C1}\ I_0) = \frac{I_L^{C2} - 0}{I_L^{C2} - V_0} \div \frac{I_L^{C1} - 0}{I_L^{C1} - I_0}. \tag{2.42}$$

In this case, the base points C_V, B_V correspond to the common value $I_L = 0$

Case 2

Similarly, the regime change, which is determined by Y_i change (a mutual change), is given as

$$\begin{aligned} m_i^{21} &= (0\ B_2\ C_2\ F_2) = (0\ B_1\ C_1\ F_1) \\ &= (\infty\ Y_i^2\ Y_i^1\ 0) = \frac{Y_i^1}{Y_i^2}. \end{aligned} \tag{2.43}$$

This determination of a regime change does not depend on Y_L. Therefore, we must use only the load current for calculation

$$m_i^{21} = (0\ I_L^{B2}\ I_L^{C2}\ I_0) = \frac{I_L^{B2} - 0}{I_L^{B2} - I_0} \div \frac{I_L^{C2} - 0}{I_L^{C2} - I_0}. \tag{2.44}$$

Case 3

If regime is changed as $C_1 \to C_2 \to B_2$, the compound change is

$$m^{21} = m_i^{21} m_L^{21} = \frac{Y_i^1}{Y_i^2} \frac{Y_L^2}{Y_L^1}. \tag{2.45}$$

Then

$$m^{21} = \frac{I_L^{B2} - 0}{I_L^{B2} - I_0} \div \frac{I_L^{C1} - 0}{I_L^{C1} - I_0} = (0\ I_L^{B2}\ I_L^{C1}\ I_0). \tag{2.46}$$

The recalculation formula

$$\frac{I_L^{B2}}{I_0} = \frac{\frac{I_L^{C1}}{I_0} m^{21}}{\frac{I_L^{C1}}{I_0}(m^{21} - 1) + 1}. \tag{2.47}$$

The compound regime and current changes are shown in Fig. 2.21.

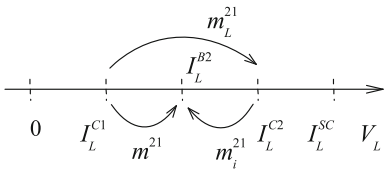

Fig. 2.21 Compound current changes

We may note that values Y_L, Y_i have not any scales also.

The above-mentioned arguments make it possible to confront regimes of compared circuits and give the basis for analysis of the general case of circuit.

2.3 Regime Symmetry for a Load-Power

In the above Sect. 2.1, the examined regime parameters of the type V, I, R are expressed among themselves by linear and fractionally linear expressions (2.1), (2.23) and have projective properties. In turn, such an important energy characteristic, as a load-power, represents quadratic expression (1.6) and determines a parabola in Fig. 1.6. This quadratic curve has similar projective properties that permit to compare the regime of different circuits, to determine the deviation from the power matching [11, 12, 14]. Let us consider these properties in detail.

To do this, we use the circuit in Fig. 2.12 and rewrite Eq. (2.21) of load straight line in the following relative form

$$\frac{I_L}{I_L^{SC}} = I = 1 - \frac{V_L}{V_0} = 1 - K_V, \tag{2.48}$$

where K_V is the voltage transfer ratio. Also, we rewrite Eq. (1.6) of load power in the similar relative form

$$P = \frac{P_L}{P_0^{SC}} = K_V - (K_V)^2, \tag{2.49}$$

where P_0^{SC} is the maximum power of the voltage source V_0 for SC regime.

Therefore, the task of equal regimes does not cause a problem; that is simply corresponding equality of values K_V, I, P. But a deeper analysis will be useful, which allows generalizing the justification of the equality of regimes and will be used for considering a more complex case, the efficiency of two-ports.

2.3.1 Symmetry of Consumption and Return of Power

Let us consider load straight line (2.48) in Fig. 2.22.

In the first quadrant, a positive load consumes energy; there is the maximum load power point P_{LM}^{+} for $R_L = R_i$. At SC and OC regime points, $R_L = 0, \infty$, load power (2.49) is equal to zero, as shown in Fig. 2.23.

We remind if a negative load returns energy into the voltage source V_0, then the load voltage $V_L < 0$ and $V_L > V_0$. In this case, the load resistance $R_L < 0$; the load power increases. In the final analysis, the load power $P_{LM}^{-} = \infty$ for the resistance $R_L = -R_i$. Therefore, the load straight line is closed and the parabola is a closed oval curve too, which concerns the infinitely remote straight line TP_{LM}^{-} at the point P_{LM}^{-}.

Let us use expression (2.24) of the cross-ratio

$$m_L^1 = (0\ R_L^1\ R_i\ \infty) = \frac{R_L^1}{R_i}. \tag{2.50}$$

For the point $R_L = -R_i$, cross-ratio (2.50)

$$m_L(-R_i) = \frac{-R_i}{R_i} = -1.$$

This special case of the fourth point $-R_i$ determines the property of the harmonic conjugacy of four points, which determines the symmetry of points $-R_i$, R_i relatively to base points 0, ∞.

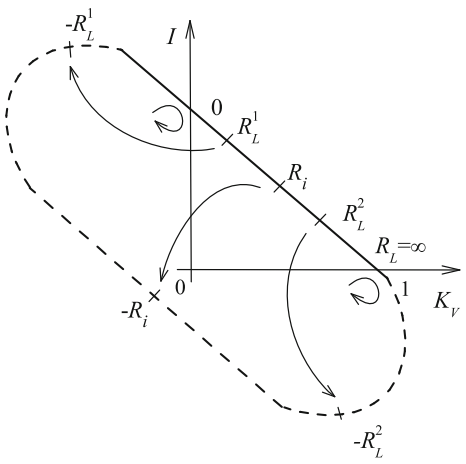

Fig. 2.22 Conformity of points for positive and negative load

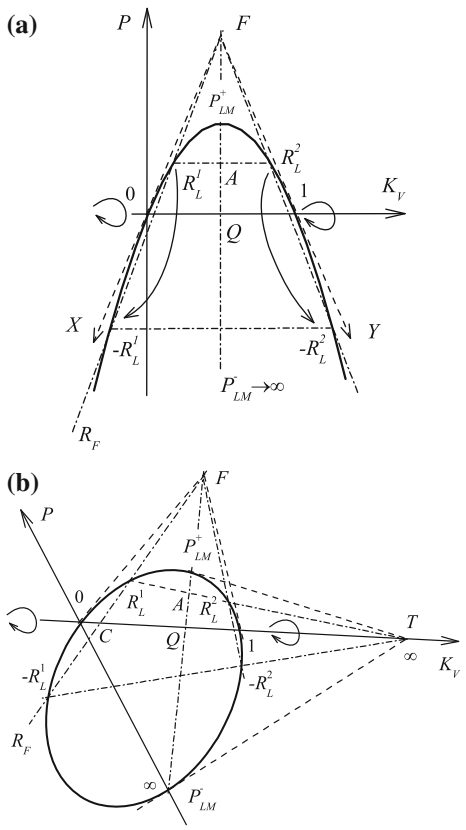

Fig. 2.23 **a** Parabola of power for the Cartesian coordinates, **b** this parabola into the projective coordinates is as a closed curve

For an arbitrary running load R_L, we obtain, at once, the corresponding conjugate load resistance equals $-R_L$ because cross-ratio (2.50)

$$(0\ -R_L\ R_L\ \infty) = -1. \tag{2.51}$$

So, we have the symmetry of points $-R_L$, R_L relatively to the base points 0, ∞ too. The points R_i, $-R_i$; R^1_L, $-R^1_L$ and so on pass into each other, as it is shown by arrows. Physically, this symmetry corresponds to mapping of the region of power consumption by a load on the region of return. Then, the mapping of points of parabola of the region $P > 0$ onto the region $P < 0$ is realized from a point F. In this case, the points 0, 1 of the axis K_V are fixed. Therefore, we obtain the following condition:

$$(0\ K_V(-R_L)\ K_V(R_L)\ 1) = \frac{K_V(-R_L) - 0}{K_V(-R_L) - 1} \div \frac{K_V(R_L) - 0}{K_V(R_L) - 1} = -1. \tag{2.52}$$

From here, we get

$$\frac{K_V(R_L)\cdot K_V(-R_L)}{K_V(R_L)+K_V(-R_L)}=0.5. \tag{2.53}$$

The point F is formed due to the intersection of the tangential FX, FY at the fixed points. This point F is called a pole, and a straight line, passing through the fixed points 0, 1 is a polar $0T$. The indicated symmetry is obtained relatively to the polar.

We may pass to the projective system of coordinates YFX. In this coordinate system, a polar is considered as the infinitely remote straight line. Therefore, our initial parabola will be already a hyperbola, and the coordinate axes FX, FY are asymptotes in Fig. 2.24. The point P_{LM}^{-} has a finite value.

In this case, a point on hyperbola is assigned as the rotation of radius-vector $R_F F$ from the initial position at the point P_{LM}^{+}.

The non-Euclidean distance $R_1 P_M^{-}$ is determined by a hyperbolic arc length of a hyperbola; it will be later on shown in Sect. 4.4.

2.3.2 Symmetry Relatively to the Maximum Power Point

Also, the symmetry of points R_L^1, R_L^2, as the points of equal power, is manifested by arrows relatively to the point R_i or relatively to the straight line $P_{LM}^{+}P_{LM}^{-}$ in Figs. 2.25 and 2.26. The points $+R_i, -R_i$ are the fixed points. This symmetry corresponds to points K_V^1, K_V^2 also.

Using (2.49), we get the following condition:

$$K_V^1 + K_V^2 = 1. \tag{2.54}$$

Also, the mapping of points $R_L^1 \rightarrow R_L^2$, relatively to the straight P_M^{-}, P_M^{+} of the parabola, leads to an additional system of pole and polar; the point T is a pole, and the straight line $P_M^{-}\, P_M^{+}$ is a polar. Similarly, the regime or the point of the parabola,

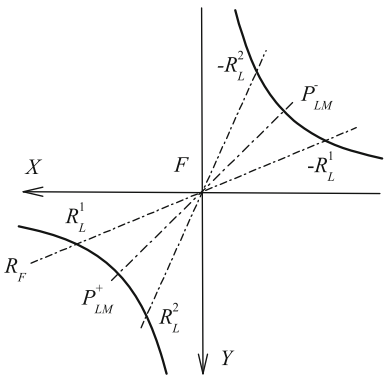

Fig. 2.24 Rotation of a radius-vector $R_F F$

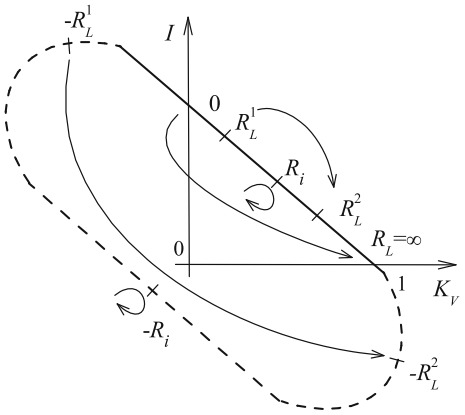

Fig. 2.25 Mapping of points relatively to the maximum load power point

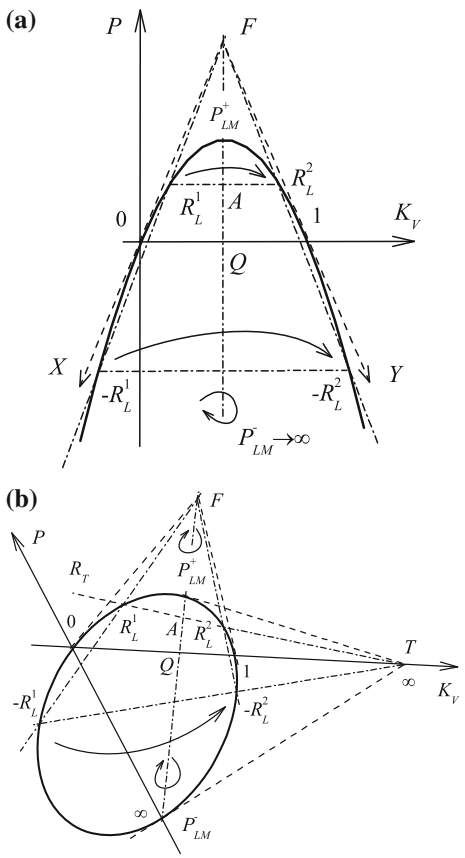

Fig. 2.26 Mapping of a parabola relatively to the maximum load power line. **a** Cartesian coordinates, **b** projective coordinates

is assigned as the rotation of radius-vector $R_T T$ from the initial position at the point 0 or point 1. In the Cartesian coordinate system, this radius-vector $R_T T$ is the parallel line to the axis K_V.

Similar to (2.50), we introduce the other value of running regime

$$m_L^1 = (R_i\ R_L^1\ 0\ -R_i) = \frac{R_L^1 - R_i}{R_L^1 + R_i} \div \frac{0 - R_i}{0 + R_i} = \frac{-R_L^1 + R_i}{R_L^1 + R_i}. \tag{2.55}$$

The point $R_L = 0$ is a unit point.

Similar to (2.51), we obtain the harmonic conjugate point using the condition

$$(R_i\ R_L^1\ R_L^2\ -R_i) = \frac{R_L^1 - R_i}{R_L^1 + R_i} \div \frac{R_L^2 - R_i}{R_L^2 + R_i} = -1.$$

From that, we get

$$R_L^1 R_L^2 = (R_i)^2. \tag{2.56}$$

2.3.3 Two Systems of Characteristic Points

Thus, we have obtained a "kinematics" diagram of the regime deviations relatively to the selected base points and initial point. Also, we get two conjugate systems of pole and polar. For example, there are four harmonic conjugate points $0, Q, 1, T$ onto the polar $0T$ of the pole F. Reciprocally, there are four harmonic conjugate points $P_M^-, Q,\ P_M^+, F$ onto the polar $P_M^-\ P_M^+$ of the pole T. Let us consider this harmonic conjugacy in detail.

For the pole T, the following correspondences take place. We believe the harmonic conjugate points $0,\ 1$ relatively to the base points Q, T of the polar $0T$. Then, these points correspond to four points $0, 1, K_V(Q) = 0.5, K_V(T) = \infty$ of the axis K_V. The mutual mapping of the points $0, 1$ relatively to fixed points $K_V(T), K_V(Q)$ is shown by arrows in Fig. 2.27.

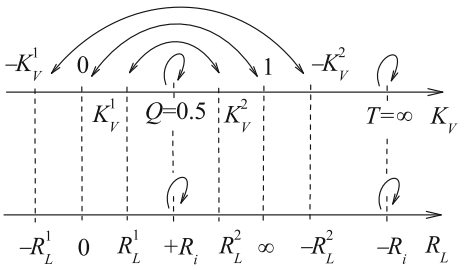

Fig. 2.27 Mutual mapping of points relatively to the fixed points onto the straight line TR_1

In turn, there are such harmonic conjugate points R_L^1, R_L^2 relatively to the base points A, T of running straight line TR_1. The harmonic conjugate points $K_V^1, K_V^2, 0.5, \infty$ of the axis K_V correspond to these points of the line TR_1.

The mutual mapping of points K_V^1, K_V^2 relatively to the fixed or base points $\infty, 0.5$ is shown by arrows in Fig. 2.27 too. Therefore, we can constitute the cross-ratio

$$(0.5\ K_V^1\ K_V^2\ \infty) = \frac{K_V^1 - 0.5}{K_V^1 - \infty} \div \frac{K_V^2 - 0.5}{K_V^2 - \infty} = \frac{K_V^1 - 0.5}{K_V^2 - 0.5} = -1.$$

From this, we get expression (2.54) that confirms the accepted geometrical model.

Similarly, for the pole F, the following correspondences take place. We believe the harmonic conjugate points P_{LM}^+, P_{LM}^- relatively to the base points F, Q of the polar $P_{LM}^+ P_{LM}^-$. In turn, there are such harmonic conjugate points $R_L^1, -R_L^1$ relatively to the base points F, C of running straight line FR_1. The harmonic conjugate points $K_V(C), K_V(R_1), 0.5, K_V(-R_1)$ of the axis K_V correspond to these points of the line FR_1.

The mutual mapping of points $K_V(R_L^1), K_V(-R_L^1)$ relatively to the points $K_V(C), 0.5$ is shown by arrows in Fig. 2.28.

Now, it is necessary to find the common fixed or base points for these two systems of harmonic conjugate points.

We note at once that points $K_V(R_L^1), K_V(-R_L^1)$ are the harmonic conjugate points relatively to the points 0, 1 in accordance with (2.52). Obviously, the points T, Q are the harmonic conjugate points relatively to the points 0, 1 too. These correspondences are shown by dash arrows in Fig. 2.29. Therefore, we may choose the points 0, 1 as the base points.

Thus, the suggested geometrical approach allows to reunite all the points of characteristic regimes into one system and to prove the choice of base points and a unit point. Therefore, it is possible to express any running regime point by a cross-ratio of type (2.50). All the values of cross-ratios for the characteristic and running points are shown on the axis m in Fig. 2.29.

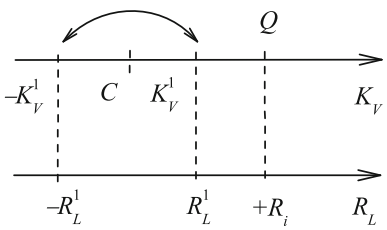

Fig. 2.28 Mutual mapping of points of the straight line FR_1

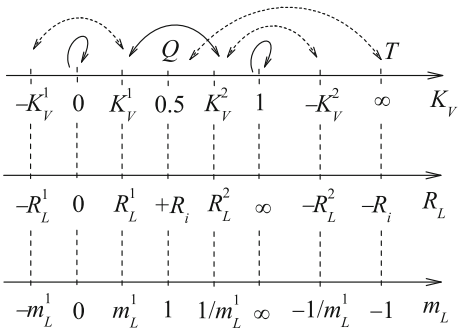

Fig. 2.29 Mutual mapping of points relative to the fixed points and correspondence of the different values

References

1. Alexander, C.K., Sadiku, M.N.O.: Fundamentals of Electric Circuits, 5th edn. McGraw-Hill, New York (2009)
2. Bhattacharyya, S.P., Keel, L.H., Mohsenizadeh, D.N.: Linear Systems: A Measurement Based Approach. Springer, India (2014)
3. Bryant, R.E., Tygar, J.D., Huang, L.P.: Geometric characterization of series-parallel variable resistor networks. Circ. Syst. I Fundam. Theory Appl. IEEE Trans. **41**(11), 686–698 (1994)
4. Frank, J.A.: Schaum's Outline of Theory and Problems of Projective Geometry. McGraw-Hill, New York (1967)
5. Glagolev, N.A.: Proektivnaia geometria (Projective Geometry). Nauka, Moskva (1963)
6. Irwin, J.D., Nelms, R.M.: Basic Engineering Circuit Analysis, 10th edn. Wiley, Hoboken (2011)
7. Kagan, V.F.: Osnovania geometrii, Chasti II (Geometry Basics. Part II). Gostekhizdat, Moskva (1956)
8. Mazin, V.D.: Method for raising the precision of measuring instruments and transducers. Meas. Tech. **23**(6), 479–480 (1980)
9. Mazin, V.D.: Error of measurement in the compound-ratio method. Meas. Tech. **26**(8), 628–629 (1983)
10. Penin, A.: Projectively-affine properties of resistive two-ports with a variable load. Tehnicheskaia elektrodinamika **2**, 38–42 (1991)
11. Penin, A.: Definition of deviation from the matching regime for two-port circuit. Electrichestvo **4**, 32–40 (1994)
12. Penin, A.: Fractionally linear relations in the problems of analysis of resistive circuits with variable parameters. Electrichestvo **11**, 32–44 (1999)
13. Penin, A.: Determination of regimes of the equivalent generator based on projective geometry: the generalized equivalent generator. World Acad. Sci. Eng. Technol. **2**(10), 703–711 (2008). http://www.waset.org/publications/10252. Accessed 30 Nov 2014
14. Penin, A.: Projective geometry method in the theory of electric circuits with variable parameters of elements. Int. J. Electron. Commun. Electr. Eng. **3**(2), 18–34 (2013). https://sites.google.com/site/ijeceejournal/volume-3-issue-2. Accessed 30 November 2014
15. Penin, A., Sidorenko, A.: Determination of deviation from the maximum power regime of a photovoltaic module. Moldavian J. Phys. Sci. **9**(2), 191–198 (2010). http://sfm.asm.md/moldphys/2010/vol9/n2/index.html. Accessed 30 November 2014

Chapter 3
Generalized Equivalent Circuit of an Active Two-Pole with a Variable Element

3.1 Introduction

To simplify the calculation of circuits with variable parameters of elements, Thévenin/Helmholtz and Norton/Mayer theorems are used [1, 6–8]. In practice, it can be DC power supply systems with variable loads.

According to these theorems, the fixed part of a circuit, concerning terminals of the specified load, is replaced by an equivalent circuit or equivalent generator. The open circuit voltage (or short current) and internal resistance are the parameters of this equivalent generator. These parameters can be used as scales for the normalized values of load parameters or load regimes. Such a definition of the relative regimes allows comparing or setting the regimes of different systems.

Considering importance of ideas of the equivalent generator, the attention is given to the respective theorems in education [2, 14]. Also, these theorems attract the attention of researchers [3–5].

However, this known equivalent generator does not completely disclose the property of a circuit, for example, power supply systems with a base (priority) load and a variable auxiliary (buffer) load or voltage regulator. In this case, the change of the auxiliary load leads to change of the open circuit voltage and short circuit current, as the parameters of the equivalent generator. Thus, the problem of the calculation of this circuit and finding of the equivalent generator parameters again arises.

In this chapter, the generalized equivalent generator, which develops Thévenin/Helmholtz and Norton/Mayer theorems, is proposed. It appears that the load straight line at various values of anyone changeable resistance passes into a bunch of these lines. Since the bunch center coordinates do not depend on this changeable element, then these coordinates can be accepted as the parameters of the generalized equivalent generator [9–11]. Also, the approach based on projective geometry of Chap. 2 for interpretation of changes (kinematics) of regimes is developed [12]. That allows revealing the invariant properties of a circuit; that is, such expressions,

A. Penin, *Analysis of Electrical Circuits with Variable Load Regime Parameters*,
Power Systems, DOI 10.1007/978-3-319-28451-4_3

which turn out identical to the load and element changes. Such invariant expressions permit to obtain convenient formulas of recalculation of the load current.

3.2 Circuit with a Series Variable Resistance

3.2.1 Disadvantage of the Known Equivalent Circuit

Let us consider an active two-pole circuit with a variable series resistance r_{0N} and base load resistance R_L in Fig. 3.1. This circuit has a practical importance for a voltage regulation.

At change of the load resistance from the short circuit *SC* to open circuit *OC* for the specified series resistance r_{0N}, a load straight line is given by

$$I_L = \frac{V_L^{OC}}{R_i} - \frac{V_L}{R_i} = I_L^{SC} - \frac{V_L}{R_i}, \tag{3.1}$$

where I_L^{SC} is the *SC* current; the *OC* voltage V_L^{OC} and the internal resistance R_i are the parameters of the Thévenin equivalent circuit in Fig. 3.2.

For our two-pole circuit, we have

$$V_L^{OC} = V_0 \frac{r_N}{r_N + r_{0N}}, \tag{3.2}$$

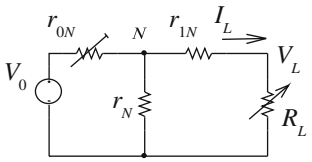

Fig. 3.1 Electric circuit with a variable series resistance

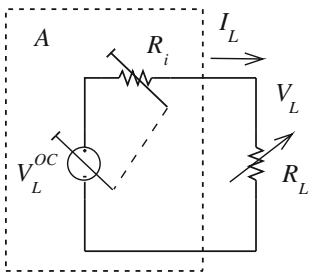

Fig. 3.2 Thévenin equivalent circuit with a variable internal resistance and voltage source

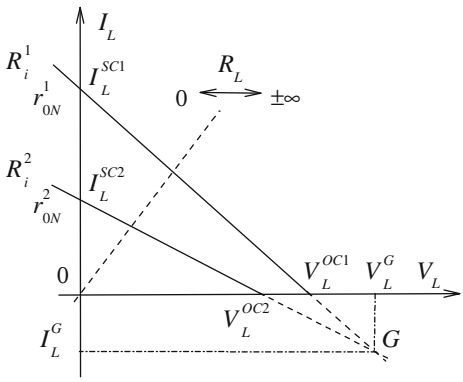

Fig. 3.3 Two load straight lines with the parameters r_{0N}^1, r_{0N}^2

$$R_i = r_{1N} + \frac{r_{0N} r_N}{r_{0N} + r_N}, \tag{3.3}$$

$$I_L^{SC} = \frac{V_L^{OC}}{R_i} = \frac{V_0}{r_{0N}\left(1 + \frac{r_{1N}}{r_N}\right) + r_{1N}}. \tag{3.4}$$

Let the resistance r_{0N} vary from r_{0N}^1 to r_{0N}^2. Then, we get the two load straight lines in Fig. 3.3 with the following parameters of the Thévenin equivalent circuit

$$V_L^{OC1}, V_L^{OC2}; \quad R_i^1, R_i^2; \quad I_L^{SC1}, I_L^{SC2}.$$

Expression (3.1) allows calculating the load current for the given load resistance. But, the recalculation of all the parameters of the equivalent circuit is necessary that defines the disadvantage of this known Thévenin equivalent circuit.

3.2.2 *Generalized Equivalent Circuit*

According to Fig. 3.3, these load straight lines intersect into a point G. Physically, it means that regime parameters do not depend on the value r_{0N}; that is, the current across this element is equal to zero at the expense of the load value.

In this case, the point G will be a bunch center of the load straight lines with the parameter r_{0N}.

Let us define this bunch center. At once, it is obvious that the current across the resistance r_{0N} will be equal to zero if the voltage $V_N = V_0$. Then, we get a circuit in Fig. 3.4 for the calculation of the load parameters.

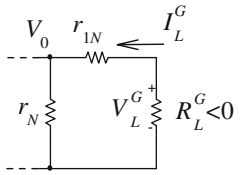

Fig. 3.4 Part of the circuit with zero current across the variable resistance r_{0N}

Then, the load current and voltage

$$-I_L^G = \frac{V_0}{r_N}, \tag{3.5}$$

$$V_L^G = V_0 + r_{1N} I_L^G = \frac{r_{1N} + r_N}{r_N} V_0 > V_0. \tag{3.6}$$

The load resistance is a negative value

$$R_L^G = \frac{V_L^G}{I_L^G} = -(r_{1N} + r_N). \tag{3.7}$$

Thus, an equation of straight line, passing through a point $I_1^G,\ V_1^G$, has the form

$$I_L + I_L^G = \frac{V_L^G}{R_i} - \frac{V_L}{R_i}. \tag{3.8}$$

So, the values I_1^G, V_1^G, and R_i are the parameters of the generalized Thévenin/Helmholtz equivalent generator in Fig. 3.5.

We note that *besides a base energy source of one kind (a voltage source V_L^G) there is an additional energy source of another kind (a current source I_L^G) that it is possible to consider as a corresponding theorem.*

It is natural, when the value $I_L^G = 0$, we obtain the known Thévenin/Helmholtz equivalent generator. In this case $V_L^G = V_L^{OC}$. Using the generalized generator, we must recalculate the internal resistance only. It is the advantage of the offered generator.

Let us show how the internal resistance R_i and changeable resistance $r_{0N,}$ respectively influence on properties of the generalized equivalent generator in Fig. 3.5. The corresponding family of the load straight lines is shown in Fig. 3.6.

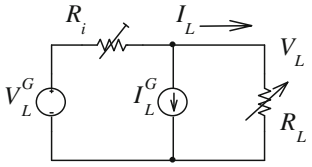

Fig. 3.5 Generalized Thévenin/Helmholtz equivalent generator

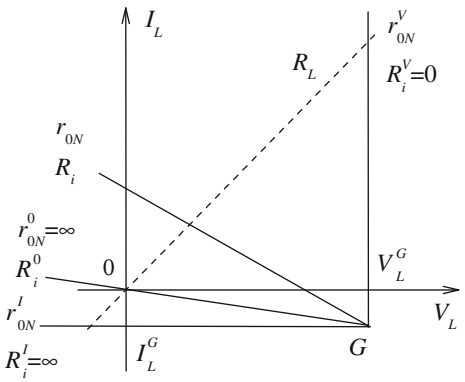

Fig. 3.6 Family of the load straight lines with the characteristic values R_i and r_{0N}

Further, we use the inverse expression to (3.3); that is,

$$r_{0N} = \frac{r_N(R_i - r_{1N})}{r_N - (R_i - r_{1N})}. \tag{3.9}$$

The resistances R_i, r_{0N} have the following characteristic values:

$$R_i^V = 0, \quad r_{0N}^V = -\frac{r_N r_{1N}}{r_N + r_{1N}}, \tag{3.10}$$

which defines the generalized equivalent generator as an ideal voltage source;

$$R_i^I = \infty, \quad r_{0N}^I = -r_N, \tag{3.11}$$

which defines the generalized equivalent generator as an ideal current source;

$$R_i^0 = -R_L^G = r_{1N} + r_N, \quad r_{0N}^0 = \infty, \tag{3.12}$$

which corresponds to the beam $G0$ and defines the "zero-order" source when the current and voltage of the load are always equal to zero for all the load values.

The generalized equivalent generator that displays the "zero-order" generator is presented in Fig. 3.7. $V_L = 0$ because the internal resistance voltage $V_i^0 = -V_L^G$.

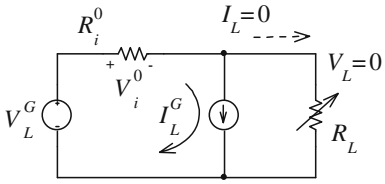

Fig. 3.7 "Zero-order" generator

So, a variable element and internal resistance can have these three specified characteristic values. These values are defined at a qualitative level. This brings up the problem of determination in the relative or normalized form of the value r_{0N} regarding of these characteristic values. In this case, it is possibly to define a kind of active two-pole as an energy source and to compare the different circuits. Therefore, the obvious value $r_{0N} = 0$ is not characteristic one concerning the load.

Let us view the possible load characteristic values. Both the traditional values $R_L = 0$, $R_L = \infty$, and R_L^G will be the characteristic values according to Fig. 3.6. Physical sense of these values is clear.

3.2.3 *Relative Operative Regimes. Recalculation of the Load Current*

Let us consider a common change of load R_L and variable resistance r_{0N} of the circuit in Fig. 3.1. The corresponding load straight lines are shown in Fig. 3.8.

In this figure, we get the two bunches with parameters R_L and r_{0N}. Let an initial value of the variable element be r_{0N}^1 and subsequent value is r_{0N}^2. Similarly, an initial value of the load equals R_L^1 and subsequent one is R_L^2.

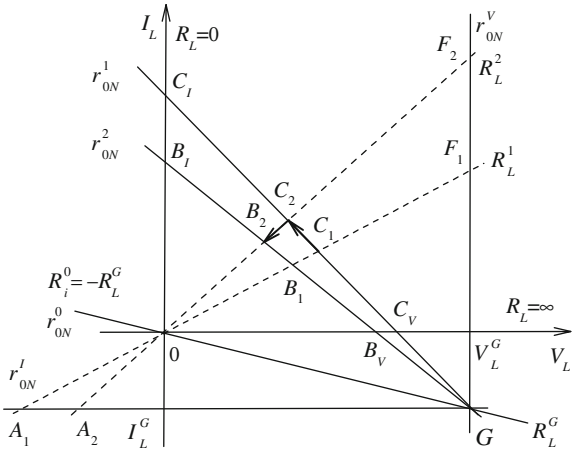

Fig. 3.8 Common change of load R_L and variable resistance r_{0N}

Let us consider the straight line of the initial load R_L^1. The three straight lines with the characteristic values r_{0N}^I, r_{0N}^0, r_{0N}^V and the two lines with the parameters r_{0N}^1, r_{0N}^2 intersect this line R_L^1. The points A_1, 0, B_1, C_1, F_1 are points of this intersection. In turn, the points A_2, 0, B_2, C_2, F_2 are points of intersection of the line R_L^2. Therefore, a projective map (conformity) of one line R_L^1 on the other line R_L^2 takes place. This conformity is set by a projection center G.

Similarly, we consider the straight line r_{0N}^1. The three straight lines with the characteristic values of load R_L and two lines with parameters R_L^1, R_L^2 intersect this line r_{0N}^1. The points G, C_V, C_1, C_2, C_I are points of this intersection.

In turn, the points G, B_V, B_1, B_2, B_I are points of intersection of the line r_{0N}^2.

Therefore, a projective map (conformity) of one line r_{0N}^1 on the other line r_{0N}^2 takes place. This conformity is set by the projection center 0.

The above conformities of straight line points represent projective geometry transformations. As shown earlier, it is convenient to use projective geometry for analysis of circuits with variable elements. The projective transformation is also set by three pairs of respective points. As pairs of these points, it is convenient to use the points corresponding to the characteristic values of the load and variable element. The projective transformations preserve a cross ratio of four points; otherwise, a cross ratio is an invariant of these transformations. Further, we will show the use of such invariants.

Case 1 Definition of the relative operating regime at the load change

Let the series resistance r_{0N} be equal r_{0N}^1 and the load resistance varies from R_L^1 to R_L^2. In this case, a point of initial regime $C_1 \rightarrow C_2$, as it is shown in Fig. 3.8. If the series resistor is equal to r_{0N}^2, a point of initial regime $B_1 \rightarrow B_2$. The given points C_I, C_2, C_1, C_V, G correspond to the points B_I, B_2, B_1, B_V, G.

Using (2.24), we may constitute the cross ratio for the initial regime in the form

$$\begin{aligned} m_L^1 &= (C_I\, C_1\, C_V\, G) = (B_I\, B_1\, B_V\, G) \\ &= (0\, R_L^1 \infty R_L^G) = \frac{R_L^1}{R_L^1 - R_L^G}. \end{aligned} \tag{3.13}$$

The points C_I, G (and B_I, G) are the base points, and C_V (and B_V) is a unit one. Likewise, we have the base values $R_L = 0$, R_L^G, and a unit $R_L = \infty$.

This determination of relative regime does not depend on r_{0N}. Therefore, we must use the load voltage for the cross ratio calculation. In this case, the base points C_I, B_I give the common base point $V_L = 0$.

Similarly to (2.23), the equation $V_L(R_L)$ from (3.8) has the fractionally linear view; it is possible by formalized method to express the cross ratio right now

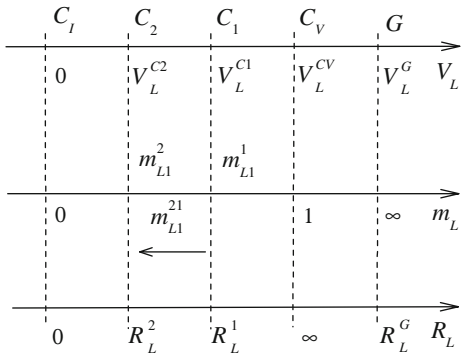

Fig. 3.9 Mutual conformity of the load voltage, resistance, and cross ratio

$$\begin{aligned} m_L^1 &= (0\ V_L^{C1}\ V_L^{CV}\ V_L^G) = \frac{V_L^{C1}-0}{V_L^{C1}-V_L^G} \div \frac{V_L^{CV}-0}{V_L^{CV}-V_L^G} \\ &= (0\ V_L^{B1}\ V_L^{BV}\ V_L^G) = \frac{V_L^{B1}-0}{V_L^{B1}-V_L^G} \div \frac{V_L^{BV}-0}{V_L^{BV}-V_L^G}. \end{aligned} \tag{3.14}$$

In this case, we have the base values $V_L = 0,\ V_L^G$, and a unit value V_L^{CV}.

The corresponding values of this cross ratio are shown in Fig. 3.9.

So, it is possible to consider cross ratio (3.13) and (3.14) as a projective coordinate of the initial or running regime points V_L^{C1}, R_L^1. This coordinate is expressed by invariant (identical) manner by various regime parameters.

The cross ratio for the subsequent regime

$$\begin{aligned} m_L^2 &= (C_I\ C_2\ C_V\ G) = (B_I\ B_2\ B_V\ G) \\ &= (0\ R_L^2\ \infty\ R_L^G) = \frac{R_L^2}{R_L^2 - R_L^G}. \end{aligned} \tag{3.15}$$

$$\begin{aligned} m_L^2 &= (0\ V_L^{C2}\ V_L^{CV}\ V_L^G) = \frac{V_L^{C2}-0}{V_L^{C2}-V_L^G} \div \frac{V_L^{CV}-0}{V_L^{CV}-V_L^G} \\ &= (0\ V_L^{B2}\ V_L^{BV}\ V_L^G) = \frac{V_L^{B2}-0}{V_L^{B2}-V_L^G} \div \frac{V_L^{BV}-0}{V_L^{BV}-V_L^G}. \end{aligned} \tag{3.16}$$

Similarly to (2.33) and (2.34), the regime change has the view

$$\begin{aligned} m_L^{21} &= (C_I\ C_2\ C_1\ G) = (B_I\ B_2\ B_1\ G) \\ &= (0\ R_L^2\ R_L^1\ R_L^G) = \frac{R_L^2}{R_L^2 - R_L^G} \div \frac{R_L^1}{R_L^1 - R_L^G} = m_L^2 \div m_L^1, \end{aligned} \tag{3.17}$$

$$m_L^{21} = (0\ V_L^{C2}\ V_L^{C1}\ V_L^G) = \frac{V_L^{C2}}{V_L^{C2} - V_L^G} \div \frac{V_L^{C1}}{V_L^{C1} - V_L^G}$$
$$= (0\ V_L^{B2}\ V_L^{B1}\ V_L^G) = \frac{V_L^{B2} - 0}{V_L^{B2} - V_L^G} \div \frac{V_L^{B1} - 0}{V_L^{B1} - V_L^G}. \tag{3.18}$$

This change is expressed by invariant manner through various regime parameters. Therefore, usually used regime changes by increments (as formal) are eliminated.

In turn, the values V_L^G, R_L^G are the scales for normalizing the voltage and resistance values. Then, expressions (3.17) and (3.18) represent the relative regimes. It permits to compare or set the regime of different circuits with various parameters.

Let us remind properties of a cross ratio. If the components V_L^{C1}, V_L^{C2} of expression (3.18) are interchanged, we get

$$m_L^{12} = \frac{1}{m_L^{21}}. \tag{3.19}$$

Also, the group property takes place

$$m_L^3 = m_L^{32} m_L^2 = m_L^{32} m_L^{21} m_L^1 = m_L^{31} m_L^1. \tag{3.20}$$

Let us obtain the subsequent voltage value from expression (3.18). Then, we have

$$V_L^{C2} = \frac{V_L^G V_L^{C1} m_L^{21}}{V_L^{C1}(m_L^{21} - 1) + V_L^G}. \tag{3.21}$$

The obtained transformation with a parameter m_L^{21} allows realizing the direct recalculation of load voltage at load change. This expression is especially convenient for the set of the load changes on account of group property (3.20).

Case 2 Definition of the relative operating regime at the change of the series resistance r_{0N} or internal resistance R_i

The cross ratio m_i^1 of four points, three of these are the characteristic 0, A_1, F_1 of the line R_L^1, and the fourth point C_1 of the initial regime r_{0N}^1 or R_i^1, has the view

$$m_i^1 = (0\ C_1\ A_1\ F_1) = \frac{C_1 - 0}{C_1 - F_1} \div \frac{A_1 - 0}{A_1 - F_1}. \tag{3.22}$$

The points 0, F_1 are chosen as the base points; that will be explained later. In turn, A_1 is a unit point.

The cross ratio for the points 0, C_2, A_2, F_2 of the line R_L^2 has the same value

$$m_i^1 = (0\ C_2\ A_2\ F_2) = \frac{C_2 - 0}{C_2 - F_2} \div \frac{A_2 - 0}{A_2 - F_2}. \tag{3.23}$$

Cross ratio (3.22) is expressed by voltage components

$$m_i^1 = (0\ V_L^{C1}\ V_L^{A1}\ V_L^G) = \frac{V_L^{C1} - 0}{V_L^{C1} - V_L^G} \div \frac{V_L^{A1} - 0}{V_L^{A1} - V_L^G}. \tag{3.24}$$

Similarly, the cross ratio for the subsequent regime

$$m_i^2 = (0\ V_L^{B1}\ V_L^{A1}\ V_L^G) = \frac{V_L^{B1} - 0}{V_L^{B1} - V_L^G} \div \frac{V_L^{A1} - 0}{V_L^{A1} - V_L^G}. \tag{3.25}$$

The "distance" between the points of the initial and subsequent regimes on the straight line R_L^1

$$m_i^{21} = m_i^2 \div m_i^1 = \frac{V_L^{B1} - 0}{V_L^{B1} - V_L^G} \div \frac{V_L^{C1} - 0}{V_L^{C1} - V_L^G} = (0\ V_L^{B1}\ V_L^{C1}\ V_L^G). \tag{3.26}$$

The same "distance" of the points on the line R_L^2

$$m_i^{21} = (0\ V_L^{B2}\ V_L^{C2}\ V_L^G) = \frac{V_L^{B2} - 0}{V_L^{B2} - V_L^G} \div \frac{V_L^{C2} - 0}{V_L^{C2} - V_L^G}. \tag{3.27}$$

For a given load, the equation $V_L(R_i) = V_L(r_{0N})$ from expression (3.8) has fractionally linear view; it is possible, by the formalized method, to express cross ratio (3.24) and (3.26) for the resistance R_i and r_{0N}

$$\begin{aligned} m_i^1 &= (0\ V_L^{C1}\ V_L^{A1}\ V_L^G) = (R_i^0\ R_i^1\ R_i^I\ R_i^V) \\ &= (-R_L^G\ R_i^1\ \infty\ 0) = \frac{R_i^1 + R_L^G}{R_i^1 - 0} \div \frac{\infty + R_L^G}{\infty - 0} = \frac{R_i^1 + R_L^G}{R_i^1}, \end{aligned} \tag{3.28}$$

$$\begin{aligned} m_i^1 &= (0\ V_L^{C1}\ V_L^{A1}\ V_L^G) = (r_{0N}^0\ r_{0N}^1\ r_{0N}^I\ r_{0N}^V) \\ &= (\infty\ r_{0N}^1\ r_{0N}^I\ r_{0N}^V) = \frac{r_{0N}^1 - \infty}{r_{0N}^1 - r_{0N}^V} \div \frac{r_{0N}^I - \infty}{r_{0N}^I - r_{0N}^V} = \frac{r_{0N}^I - r_{0N}^V}{r_{0N}^1 - r_{0N}^V}. \end{aligned} \tag{3.29}$$

$$\begin{aligned} m_i^{21} &= (0\ V_L^{B1}\ V_L^{C1}\ V_L^G) = (R_i^0\ R_i^2\ R_i^1\ R_i^V) \\ &= (-R_L^G\ R_i^2\ R_i^1 0) = \frac{R_i^2 + R_L^G}{R_i^2} \div \frac{R_i^1 + R_L^G}{R_i^1}, \end{aligned} \tag{3.30}$$

$$m_i^{21} = (0\ V_L^{B1}\ V_L^{C1}\ V_L^G) = (r_{0N}^0\ r_{0N}^2\ r_{0N}^1\ r_{0N}^V)$$
$$= (\infty\ r_{0N}^2\ r_{0N}^1 r_{0N}^V) = \frac{r_{0N}^2 - \infty}{r_{0N}^2 - r_{0N}^V} \div \frac{r_{0N}^1 - \infty}{r_{0N}^1 - r_{0N}^V} = \frac{r_{0N}^1 - r_{0N}^V}{r_{0N}^2 - r_{0N}^V}. \tag{3.31}$$

The subsequent voltage value from expression (3.26) is obtained

$$V_L^{B1} = \frac{V_L^G V_L^{C1} m_i^{21}}{V_L^{C1}(m_i^{21} - 1) + V_L^G}. \tag{3.32}$$

This transformation with a parameter m_i^{21} allows realizing the direct recalculation of load voltage.

Case 3 Definition of the relative operating regime at the common change of the load R_L and resistance r_{0N}

Let a common or compound change of regime be given as $C_1 \rightarrow C_2 \rightarrow B_2$.

Then, the view of expressions (3.27) and (3.18) shows that it is possible to use the multiplication of these cross ratios as the compound regime change

$$m^{21} = m_i^{21} m_L^{21} = \frac{V_L^{B2} - 0}{V_L^{B2} - V_L^G} \div \frac{V_L^{C1} - 0}{V_L^{C1} - V_L^G} = (0\ V_L^{B2}\ V_L^{C1}\ V_L^G). \tag{3.33}$$

In this resultant expression, intermediate components are reduced at the expense of the identical base points. Therefore, we obtain the resultant voltage value for the point B_2

$$V_L^{B2} = \frac{V_L^G V_L^{C1} m^{21}}{V_L^{C1}(m^{21} - 1) + V_L^G}. \tag{3.34}$$

3.2.4 Example

Let us consider a circuit with given values in Fig. 3.10. Dimensions of these values are not indicated for simplifying.

Let the initial value of the resistance r_{0N} be equal to $r_{0N}^1 = 0.5$.

Parameters (3.2)–(3.4) of the Thévenin equivalent circuit

$$V_L^{OC1} = V_0 \frac{r_N}{r_N + r_{0N}^1} = 10 \frac{5}{5 + 0.5} = 9.0909,$$
$$R_i^1 = r_{1N} + \frac{r_{0N}^1 r_N}{r_{0N}^1 + r_N} = 1 + \frac{0.5 \cdot 5}{0.5 + 5} = 1.4545,$$
$$I_L^{SC1} = \frac{V_L^{OC1}}{R_i^1} = 6.25.$$

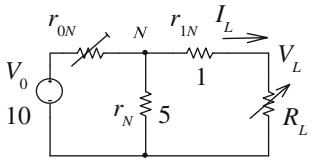

Fig. 3.10 Example of a circuit with given elements

Let the subsequent value of the resistance r_{0N} be equal to $r_{0N}^2 = 1$.
The corresponding parameters of the Thévenin equivalent circuit

$$V_L^{OC2} = 10\frac{5}{5+1} = 8.3333, \quad R_i^2 = 1 + \frac{1 \cdot 5}{1+5} = 1.8333, \quad I_L^{SC2} = 4.5454.$$

The corresponding load straight lines are shown in Fig. 3.11.
The parameters of the known equivalent generator correspond to points C_V, C_I, and points B_V, B_I; that is,

$$V_L^{CV} = 9.0909, \quad I_L^{CI} = 6.25;$$
$$V_L^{BV} = 8.3333, \quad I_L^{BI} = 4.5454.$$

Bunch center coordinates (3.5), and (3.6)

$$-I_L^G = \frac{V_0}{r_N} = \frac{10}{5} = 2, \quad V_L^G = \frac{r_{1N} + r_N}{r_N} V_0 = \frac{1+5}{5} 10 = 12.$$

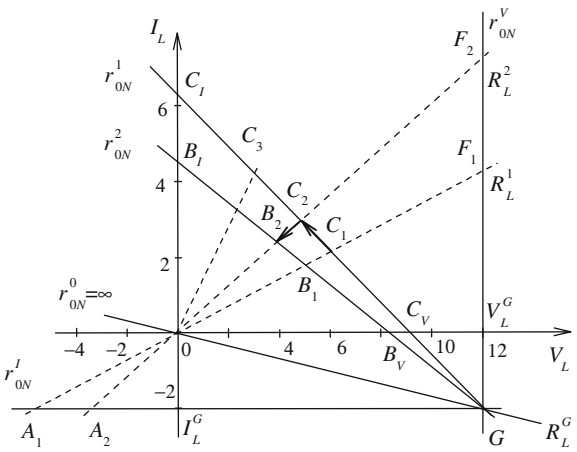

Fig. 3.11 Example of load straight lines of a circuit with the variable series resistance

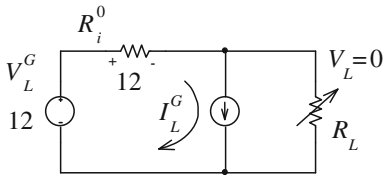

Fig. 3.12 Example of the "zero-order" generator

Corresponding negative load resistance (3.7)

$$R_L^G = \frac{V_L^G}{I_L^G} = -6.$$

Characteristic values (3.10)–(3.12) of variable element and internal resistance

$$R_i^V = 0, \quad r_{0N}^V = -\frac{5 \cdot 1}{5+1} = -0.8333,$$
$$R_i^I = \infty, \quad r_{0N}^I = -r_N = -5,$$
$$R_i^0 = -R_L^G = 6, \quad r_{0N}^0 = \infty.$$

Figure 3.12 demonstrates the "zero-order" generator.

Case 1 Recalculation of the load voltage at the load change

Let the series resistance r_{0N} be equal to r_{0N}^1 and the load resistance varies from R_L^1 to R_L^2. In this case, the initial regime point $C_1 \rightarrow C_2$.

We consider the load voltage of the initial regime $V_L^{C1} = 6$. Using expression (3.8) of the generalized equivalent generator, we get the load current

$$I_L^{C1} = -I_L^G + \frac{V_L^G - V_L^{C1}}{R_i^1} = -2 + \frac{12-6}{1.4545} = 2.1251.$$

Then, the load resistance

$$R_L^1 = \frac{V_L^{C1}}{I_L^{C1}} = \frac{6}{2.1251} = 2.8233.$$

We consider the load voltage of the subsequent regime $V_L^{C2} = 4.5$. We get the load current and resistance

$$I_L^{C2} = 3.1564, \quad R_L^2 = 1.4256.$$

If the series resistor is equal to r_{0N}^2, the initial regime point $B_1 \rightarrow B_2$. Then,

$$V_L^{B1} = 5.0524, \quad V_L^{B2} = 3.6455.$$

Initial regime cross ratio (3.13)

$$m_L^1 = (C_I\ C_1\ C_V\ G) = (B_I\ B_1\ B_V\ G) = \frac{R_L^1}{R_L^1 - R_L^G} = \frac{2.8233}{2.8233 + 6} = 0.32.$$

We check cross ratio (3.14)

$$m_L^1 = \frac{V_L^{C1} - 0}{V_L^{C1} - V_L^G} \div \frac{V_L^{CV} - 0}{V_L^{CV} - V_L^G} = \frac{6 - 0}{6 - 12} \div \frac{9.0909 - 0}{9.0909 - 12} = -1 \div (-3.1249) = 0.32,$$

$$m_L^1 = \frac{V_L^{B1} - 0}{V_L^{B1} - V_L^G} \div \frac{V_L^{BV} - 0}{V_L^{BV} - V_L^G} = \frac{5.0524 - 0}{5.0524 - 12} \div \frac{8.3333 - 0}{8.3333 - 12} = -0.7272 \div (-2.2726) = 0.32.$$

Subsequent regime cross ratio (3.15)

$$m_L^2 = (C_I\ C_2\ C_V\ G) = (B_I\ B_2\ B_V\ G) = \frac{R_L^2}{R_L^2 - R_L^G} = \frac{1.4256}{1.4256 + 6} = 0.192.$$

Regime change (3.17)

$$m_L^{21} = \frac{R_L^2}{R_L^2 - R_L^G} \div \frac{R_L^1}{R_L^1 - R_L^G} = 0.192 \div 0.32 = 0.6.$$

We may check subsequent value (3.18) of load voltage

$$V_L^{C2} = \frac{V_L^G V_L^{C1} m_L^{21}}{V_L^{C1}(m_L^{21} - 1) + V_L^G} = \frac{12 \cdot 6 \cdot 0.6}{6 \cdot (0.6 - 1) + 12} = \frac{43.2}{9.6} = 4.5.$$

We consider the load resistance $R_L^3 = 0.7163$ that corresponds to the point C_3 and cross ratio

$$m_L^3 = (C_I\ C_3\ C_V\ G) = \frac{R_L}{R_L^3 - R_L^G} = \frac{0.7163}{0.7163 + 6} = 0.1066.$$

Regime change (3.20)

$$m_L^{32} = 0.1066 \div 0.192 = 0.5555.$$

Using group property (3.20), we may directly calculate the load voltage

$$V_L^{C3} = \frac{V_L^G V_L^{C2} m_L^{32}}{V_L^{C2}(m_L^{32} - 1) + V_L^G} = \frac{12 \cdot 4.5 \cdot 0.5555}{4.5 \cdot (0.5555 - 1) + 12} = \frac{30}{10} = 3.0.$$

Case 2 Recalculation of the load voltage at the series resistance r_{0N} change

Let the load resistance be equal to R_L^1 and the series resistance $r_{0N}^1 \rightarrow r_{0N}^2$. In this case, the initial regime point $C_1 \rightarrow B_1$.

Regime change (3.31)

$$m_i^{21} = (\infty\ r_{0N}^2\ r_{0N}^1\ r_{0N}^V) = \frac{r_{0N}^1 - r_{0N}^V}{r_{0N}^2 - r_{0N}^V} = \frac{0.5 + 0.8333}{1 + 0.8333} = 0.7272.$$

We consider the load voltage of the initial regime $V_L^{C1} = 6$. Then, subsequent voltage value (3.32)

$$V_L^{B1} = \frac{V_L^G V_L^{C1} m_i^{21}}{V_L^{C1}(m_i^{21} - 1) + V_L^G} = \frac{12 \cdot 6 \cdot 0.7272}{6 \cdot (0.7272 - 1) + 12} = 5.0523.$$

Similarly, let the load resistance be equal to R_L^2; the point of the initial regime $C_2 \rightarrow B_2$. We consider the load voltage of the initial regime $V_L^{C2} = 4.5$. Then, the subsequent voltage value

$$V_L^{B2} = \frac{V_L^G V_L^{C2} m_i^{21}}{V_L^{C2}(m_i^{21} - 1) + V_L^G} = \frac{12 \cdot 4.5 \cdot 0.7272}{4.5 \cdot (0.7272 - 1) + 12} = 3.6453.$$

Case 3 Recalculation of the load voltage at the common change of the load R_L and resistance r_{0N}

Let the regime change be given as $C_1 \rightarrow C_2 \rightarrow B_2$.

Common regime change (3.33)

$$m^{21} = m_i^{21} m_L^{21} = 0.7272 \cdot 0.6 = 0.4363.$$

Resultant voltage value (3.34) for the point B_2

$$V_L^{B2} = \frac{V_L^G V_L^{C1} m^{21}}{V_L^{C1}(m^{21} - 1) + V_L^G} = \frac{12 \cdot 6 \cdot 0.4363}{6 \cdot (0.4363 - 1) + 12} = 3.6453.$$

3.3 Circuit with a Shunt Variable Conductivity

3.3.1 Disadvantage of the Known Equivalent Circuit

Let us consider an active two-pole circuit with a base load conductivity Y_L and variable auxiliary load or shunt regulating conductivity y_N in Fig. 3.13. This circuit has a practical importance for a current regulation.

At change of the load conductivity from the short circuit *SC* to open circuit *OC* for the specified shunt conductivity y_N, a load straight line is given by expression (3.1)

$$I_L = Y_i V_L^{OC} - Y_i V_L = I_L^{SC} - Y_i V_L, \tag{3.35}$$

where V_L^{OC} is the *OC* voltage; the internal conductivity Y_i and *SC* current I_L^{SC} are the parameters of the Norton equivalent circuit in Fig. 3.14.

For our two-pole circuit we have

$$V_L^{OC} = V_0 \frac{y_{0N}}{y_N + y_{0N}}, \tag{3.36}$$

$$Y_i = \frac{y_{0N} + y_N}{y_{0N} + y_N + y_{1N}} y_{1N}, \tag{3.37}$$

$$I_L^{SC} = Y_i V_L^{OC} = V_0 \frac{y_{0N} y_{1N}}{y_{1N} + y_{0N} + y_N}. \tag{3.38}$$

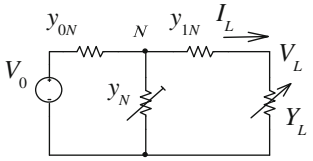

Fig. 3.13 Electric circuit with a variable shunt conductivity

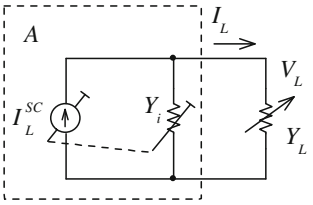

Fig. 3.14 Norton equivalent circuit with the variable internal conductivity and current source

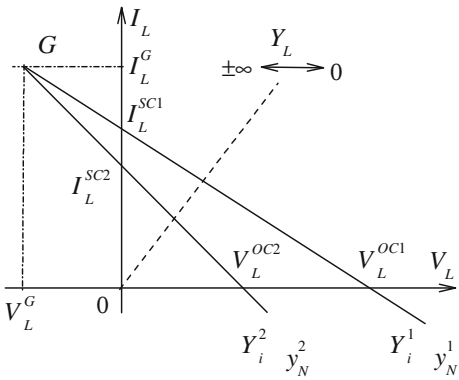

Fig. 3.15 Two load straight lines with parameters y_N^1, y_N^2

Let the conductivity y_N varies from y_N^1 to y_N^2. Then, we get the two load straight lines in Fig. 3.15 with the following parameter of the Norton equivalent circuit

$$V_L^{OC1}, V_L^{OC2}; \quad Y_i^1, Y_i^2; \quad I_L^{SC1}, I_L^{SC2}.$$

Expression (3.35) allows calculating the load current for the given load resistance. But, the recalculation of all parameters of the equivalent circuit is necessary that defines the disadvantage of this known Norton equivalent circuit.

3.3.2 *Generalized Equivalent Circuit*

According to Fig. 3.15, these load straight lines intersect into a point G. Physically, it means that regime parameters do not depend on the value y_N; that is, the current through this element is equal to zero at the expense of the load value.

In this case, the point G will be a bunch center of load straight lines with the parameter y_N.

Let us define this bunch center. At once, it is visible that the current across y_N will be equal to zero if the voltage $V_N = 0$. Then, we get a circuit in Fig. 3.16 for the calculation of the load parameters.

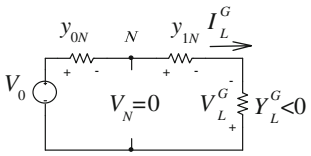

Fig. 3.16 Circuit with the zero voltage of the variable conductance y_N

Then, the current across the conductivity y_{0N} is

$$I_L^G = y_{0N} V_0. \tag{3.39}$$

The voltage through the conductivity y_{1N} is

$$V_{1N} = \frac{I_L^G}{y_{1N}}.$$

On the other hand,

$$V_L^G + V_{1N} = V_N = 0.$$

Therefore

$$-V_L^G = V_{1N} = \frac{y_{0N}}{y_{1N}} V_0. \tag{3.40}$$

In turn, the load conductivity is a negative value

$$Y_L^G = \frac{I_L^G}{V_L^G} = -y_{1N}. \tag{3.41}$$

Thus, an equation of a straight line, passing through a point $I_1^G,\ V_1^G$, has the form

$$I_L - I_L^G = -Y_i (V_L^G + V_L). \tag{3.42}$$

So, the values I_L^G, V_L^G, and Y_i are the parameters of the generalized Norton/Mayer equivalent generator in Fig. 3.17.

We note that *besides a base energy source of one kind (a current source I_L^G) there is an additional energy source of another kind (a voltage source V_L^G) that it is possible to consider as a corresponding theorem.*

It is natural, when the value $V_L^G = 0$, we obtain the known Norton/Mayer equivalent generator. In this case $I_L^G = I_L^{SC}$. Using the generalized generator, we must

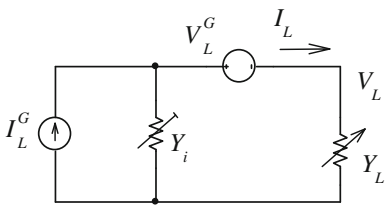

Fig. 3.17 Generalized Norton/Mayer equivalent generator

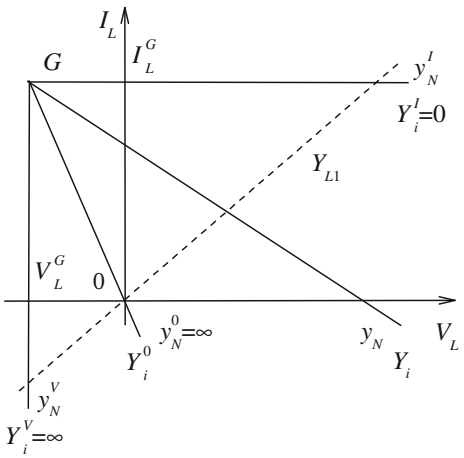

Fig. 3.18 Family of the load straight lines with the characteristic values Y_i and y_N

recalculate the internal conductivity value only. It is the advantage of the offered generator.

Let us demonstrate how the internal conductivity Y_i and respectively the changeable conductivity y_N influence on properties of the generalized equivalent generator in Fig. 3.17. The corresponding family of the load straight lines is shown in Fig. 3.18.

Further, we use expression (3.37).

The conductivities Y_i, y_N have the following characteristic values:

$$Y_i^I = 0, \quad y_N^I = -y_{0N}, \tag{3.43}$$

which defines the generalized equivalent generator as an ideal current source;

$$Y_i^V = \infty, \quad y_N^V = -(y_{0N} + y_{1N}), \tag{3.44}$$

which defines the generalized equivalent generator as an ideal voltage source;

$$Y_i^0 = y_{1N} = -Y_L^G, \quad y_N^0 = \infty, \tag{3.45}$$

which corresponds to the beam $G0$ and defines the "zero-order" source when the current and voltage of the load are always equal to zero for all load values.

The generalized equivalent generator that exhibits the "zero-order" generator is presented in Fig. 3.19. The load voltage $V_L = 0$ because $V_i^0 = -V_L^G$.

So, a variable element and internal conductivity can have these three specified characteristic values. This brings up the problem of determination in the relative or normalized form of the conductivity value y_N regarding of these characteristic values. Therefore, the obvious value $y_N = 0$ is not characteristic ones concerning the load.

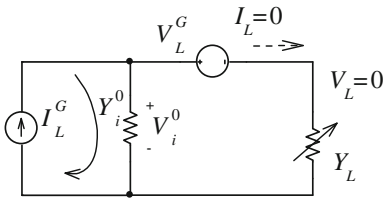

Fig. 3.19 "Zero-order" generator

Let us view the load characteristic values. Both the traditional values $Y_L = 0$, $Y_L = \infty$, and Y_L^G will be the characteristic values according to Fig. 3.18.

3.3.3 *Relative Operative Regimes. Recalculation of the Load Current*

Let us consider a common change of load Y_L and variable shunt conductivity y_N of the circuit in Fig. 3.13. The corresponding load straight lines are shown in Fig. 3.20.

In this figure, we get the two bunches with parameters Y_L and y_N. Let an initial value of the variable element be y_N^1 and subsequent value is y_N^2. Similarly, an initial value of the load equals Y_L^1 and subsequent one is Y_L^2.

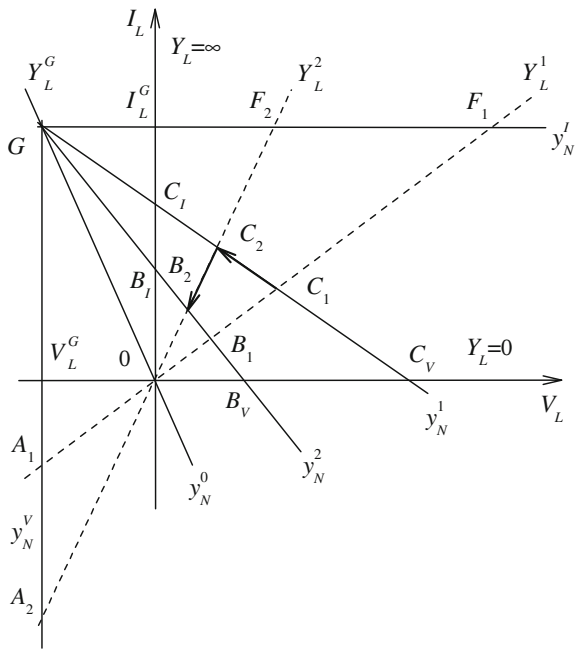

Fig. 3.20 Common change of load Y_L and variable conductivity y_N

Case 1 Definition of the relative operating regime at the load change

The cross ratio m_L^1 of the four point, three of these are the characteristic points C_V, C_I, G of the line y_N^1, and the fourth C_1 is the point of the initial regime $Y_L{}^1$, has the view

$$\begin{aligned} m_L^1 &= (C_V\ C_1\ C_I\ G) = \frac{C_1 - C_V}{C_1 - G} \div \frac{C_I - C_V}{C_I - G} \\ &= (0\ Y_L^1 \infty\ Y_L^G) = \frac{Y_L^1}{Y_L^1 - Y_L^G}. \end{aligned} \tag{3.46}$$

The cross ratio for the points B_V, B_1, B_I, G of the line y_N^2 has the same value

$$m_L^1 = (B_V\ B_1\ B_I\ G) = \frac{B_1 - B_V}{B_1 - G} \div \frac{B_I - B_V}{B_I - G}. \tag{3.47}$$

The points C_V, G (and B_V, G) are the base points, and C_I (and B_I) is a unit one. Correspondingly, we have the base values $y_L = 0$, y_L^G, and a unit $y_L = \infty$. This determination of relative regime does not depend on Y_N. Therefore, we must use the load current for the cross ratio calculation. In this case, the base points C_V, B_V give the common base point $I_L = 0$.

Then, the cross ratio is expressed by current components

$$m_L^1 = (0\ I_L^{C1}\ I_L^{CI}\ I_L^G) = \frac{I_L^{C1} - 0}{I_L^{C1} - I_L^G} \div \frac{I_L^{CI} - 0}{I_L^{CI} - I_L^G}. \tag{3.48}$$

The corresponding values of this cross ratio are shown in Fig. 3.21.

Similarly, the subsequent regime cross ratio

$$m_L^2 = (0\ I_L^{C2}\ I_L^{CI}\ I_L^G) = \frac{I_L^{C2} - 0}{I_L^{C2} - I_L^G} \div \frac{I_L^{CI} - 0}{I_L^{CI} - I_L^G}. \tag{3.49}$$

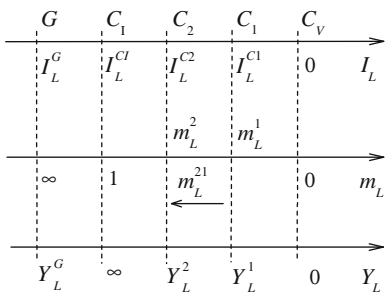

Fig. 3.21 Mutual conformity of the load current, conductivity, and cross ratio

The regime change has the view

$$m_L^{21} = (C_V\ C_2\ C_1\ G) = (B_V\ B_2\ B_1\ G)$$
$$= (0\ Y_L^2\ Y_L^1\ Y_L^G) = \frac{Y_L^2}{Y_L^2 - Y_L^G} \div \frac{Y_L^1 - 0}{Y_L^1 - Y_L^G}. \tag{3.50}$$

$$m_L^{21} = (0\ I_L^{C2}\ I_L^{C1}\ I_L^G) = \frac{I_L^{C2} - 0}{I_L^{C2} - I_L^G} \div \frac{I_L^{C1} - 0}{I_L^{C1} - I_L^G}. \tag{3.51}$$

This change is expressed by invariant manner through various regime parameters. Therefore, usually used regime changes by increments (as formal), are eliminated.

In turn, the values I_L^G, Y_L^G are the scales for normalizing the current and conductivity values. Then, expressions (3.50) and (3.51) represent the relative regimes. It permits to compare or set the regime of the different circuits with various parameters.

Also, the group property takes place

$$m_L^3 = m_L^{32} m_L^2 = m_L^{32} m_L^{21} m_L^1 = m_L^{31} m_L^1. \tag{3.52}$$

Let us obtain the subsequent current value from expression (3.51). Then, we have

$$I_L^{C2} = \frac{I_L^G I_L^{C1} m_L^{21}}{I_L^{C1}(m_L^{21} - 1) + I_L^G}. \tag{3.53}$$

The obtained transformation with a parameter m_L^{21} allows realizing the direct recalculation of a load current at a load change. This expression is especially convenient for the set of the load changes on account of group property (3.52).

Case 2 Definition of the relative operating regime at the change of the shunt conductivity y_N or internal conductivity Y_i

The cross ratio m_i^1 of the four points, three of these are the characteristic 0, A_1, F_1 of the line Y_L^1, and the fourth point C_1 of the initial regime y_N^1 or Y_i^1, has the view

$$m_i^1 = (0\ C_1\ A_1\ F_1) = \frac{C_1 - 0}{C_1 - F_1} \div \frac{A_1 - 0}{A_1 - F_1}. \tag{3.54}$$

The points 0, F_1 are chosen as the base points; that will be explained later. In turn, the point A_1 is a unit point.

The cross ratio for the points 0, C_2, A_2, F_2 of the line Y_L^2 has the same value

$$m_i^1 = (0\ C_2\ A_2\ F_2) = \frac{C_2 - 0}{C_2 - F_2} \div \frac{A_2 - 0}{A_2 - F_2}. \tag{3.55}$$

Cross ratio (3.54) is expressed by current components

$$m_i^1 = (0\ I_L^{C1}\ I_L^{A1}\ I_L^G) = \frac{I_L^{C1} - 0}{I_L^{C1} - I_L^G} \div \frac{I_L^{A1} - 0}{I_L^{A1} - I_L^G}. \tag{3.56}$$

Similarly, the cross ratio of the subsequent regime

$$m_i^2 = (0\ I_L^{B1}\ I_L^{A1}\ I_L^G) = \frac{I_L^{B1} - 0}{I_L^{B1} - I_L^G} \div \frac{I_L^{A1} - 0}{I_L^{A1} - I_L^G}. \tag{3.57}$$

The "distance" between the points of the initial and subsequent regimes on the straight line Y_L^1

$$m_i^{21} = m_i^2 \div m_i^1 = \frac{I_L^{B1} - 0}{I_L^{B1} - I_L^G} \div \frac{I_L^{C1} - 0}{I_L^{C1} - I_L^G} = (0\ I_L^{B1}\ I_L^{C1}\ I_L^G). \tag{3.58}$$

The same "distance" of the points on the line Y_L^2

$$m_i^{21} = (0\ I_L^{B2}\ I_L^{C2}\ I_L^G) = \frac{I_L^{B2} - 0}{I_L^{B2} - I_L^G} \div \frac{I_L^{C2} - 0}{I_L^{C2} - I_L^G}. \tag{3.59}$$

For a given load, the expression $I_L = (Y_i) = I_L = (y_N)$ has fractionally linear view; it is possible, by the formalized method, to express cross ratio (3.56) and (3.58) for the conductivity Y_i and y_N

$$\begin{aligned} m_i^1 &= (0\ I_L^{C1}\ I_L^{A1}\ I_L^G) = (Y_i^0\ Y_i^1\ Y_i^V\ Y_i^I) \\ &= (-Y_L^G\ Y_i^1\ \infty\ 0) = \frac{Y_i^1 + Y_L^G}{Y_i^1 - 0} \div \frac{\infty + Y_L^G}{\infty - 0} = \frac{Y_i^1 + Y_L^G}{Y_i^1}. \end{aligned} \tag{3.60}$$

$$\begin{aligned} m_i^1 &= (0\ I_L^{C1}\ I_L^{A1}\ I_L^G) = (y_N^0\ y_N^1\ y_N^V\ y_N^I) \\ &= (\infty\ y_N^1\ y_N^V\ y_N^I) = \frac{y_N^1 - \infty}{y_N^1 - y_N^I} \div \frac{y_N^V - \infty}{y_N^V - y_N^I} = \frac{y_N^V - y_N^I}{y_N^1 - y_N^I}. \end{aligned} \tag{3.61}$$

$$\begin{aligned} m_i^{21} &= (0\ I_1^{B1}\ I_1^{C1}\ I_1^G) = (0\ Y_i^2\ Y_i^1\ Y_i^I) \\ &= (-Y_L^G\ Y_i^2\ Y_i^1\ 0) = \frac{Y_i^2 + Y_L^G}{Y_i^2 - 0} \div \frac{Y_i^1 + Y_L^G}{Y_i^1 - 0}. \end{aligned} \tag{3.62}$$

$$\begin{aligned} m_i^{21} &= (0\ I_L^{B1}\ I_L^{C1}\ I_L^G) = (y_N^0\ y_N^2\ y_N^1\ y_N^I) \\ &= (\infty\ y_N^2\ y_N^1\ y_N^I) = \frac{y_N^2 - \infty}{y_N^2 - y_N^I} \div \frac{y_N^1 - \infty}{y_N^1 - y_N^I} = \frac{y_N^1 - y_N^I}{y_N^2 - y_N^I}. \end{aligned} \tag{3.63}$$

The subsequent current value from expression (3.58) is obtained

$$I_1^{B1} = \frac{I_L^G I_L^{C1} m_i^{21}}{I_1^{C1}(m_i^{21} - 1) + I_L^G}. \tag{3.64}$$

This transformation with a parameter m_i^{21} allows realizing the direct recalculation of load current.

Case 3 Definition of the relative operating regime at the common change of the load Y_L and conductivity y_N

Let a common change of regime be given as $C_1 \rightarrow C_2 \rightarrow B_2$.

Then, the view of expressions (3.58) and (3.49) shows that it is possible to use the multiplication of these cross ratios as the common regime change

$$m^{21} = m_i^{21} m_L^{21} = \frac{I_L^{B2} - 0}{I_L^{B2} - I_L^G} \div \frac{I_L^{C1} - 0}{I_L^{C1} - I_L^G} = (0\ I_L^{B2}\ I_L^{C1}\ I_L^G). \tag{3.65}$$

In this resultant expression, intermediate components are reduced at the expense of the identical base points. Therefore, we obtain the resultant current value for the point B_2

$$I_L^{B2} = \frac{I_L^G I_L^{C1} m^{21}}{I_L^{C1}(m^{21} - 1) + I_L^G}. \tag{3.66}$$

3.3.4 Example

Let us consider a circuit with given values in Fig. 3.22.

Let the initial value of the conductivity y_N be equal to $y_N^1 = 0.1$. Parameters (3.36)–(3.38) of the Norton equivalent circuit

$$V_L^{OC1} = V_0 \frac{y_{0N}}{y_N^1 + y_{0N}} = 10 \frac{1}{0.1 + 1} = 9.0909,$$

$$Y_i^1 = \frac{y_N^1 + y_{0N}}{y_N^1 + y_{0N} + y_{1N}} y_{1N} = \frac{0.1 + 1}{0.1 + 1 + 2} 2 = 0.7096,$$

$$I_L^{SC1} = Y_i^1 V_L^{OC1} = 0.7096 \cdot 9.0909 = 6.4516.$$

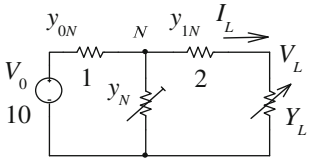

Fig. 3.22 Example of a circuit with given elements

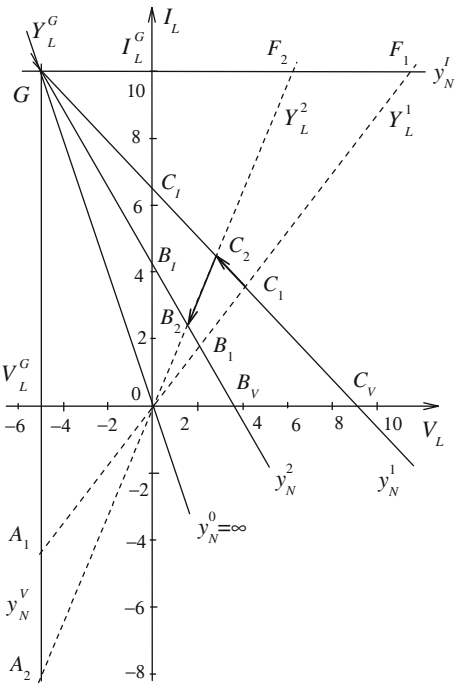

Fig. 3.23 Example of load straight lines of a circuit with the variable shunt conductivity

Let the subsequent value of the conductivity y_N be equal to $y_N^2 = 1.6987$. The corresponding parameters of the Norton equivalent circuit

$$V_L^{OC2} = 10\frac{1}{1.6987+1} = 3.7055,$$
$$Y_i^2 = \frac{1.6987+1}{1.6987+1+2}2 = 1.1486, \quad I_L^{SC2} = 4.2561.$$

The corresponding load straight lines are shown in Fig. 3.23.

The parameters of the known equivalent generator correspond to points C_V, C_I, and points B_V, B_I; that is,

$$V_L^{CV} = 9.0909, \quad I_L^{CI} = 6.4516;$$
$$V_L^{BV} = 3.7055, \quad I_L^{BI} = 4.2561.$$

Bunch center coordinates (3.39) and (3.40)

$$I_L^G = y_{0N}V_0 = 1 \cdot 10 = 10, \quad -V_L^G = \frac{y_{0N}}{y_{1N}}V_0 = \frac{1}{2}10 = 5.$$

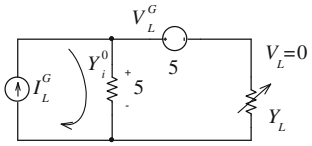

Fig. 3.24 Example of the "zero-order" generator

Corresponding negative load conductivity (3.41)

$$Y_L^G = \frac{I_L^G}{V_L^G} = -2.$$

Characteristic values (3.43)–(3.45) of the variable element and internal conductivity

$$\begin{aligned} Y_i^I &= 0, \qquad y_N^I = -y_{0N} = -1, \\ Y_i^V &= \infty, \qquad y_N^V = -(y_{0N} + y_{1N}) = -3, \\ Y_i^0 &= -Y_L^G = 2, \quad y_N^0 = \infty. \end{aligned}$$

Figure 3.24 demonstrates the "zero-order" generator.

Case 1 Recalculation of the load current at the load change

Let the shunt conductivity y_N be equal to y_N^1 and the load conductivity varies from Y_L^1 to Y_L^2. In this case, the initial regime point $C_1 \rightarrow C_2$.

We consider the load current of the initial regime $I_L^{C1} = 3.5$. Using expression (3.42) of the generalized equivalent generator, we get the load voltage

$$V_L^{C1} = -V_L^G + \frac{I_L^G - I_L^{C1}}{Y_i^1} = -5 + \frac{10 - 3.5}{0.7096} = 4.160.$$

Then, the load conductivity is

$$Y_L^1 = \frac{I_L^{C1}}{V_L^{C1}} = \frac{3.5}{4.16} = 0.8413.$$

We consider the load current of the subsequent regime $I_L^{C2} = 4.5$. We get the load voltage and conductivity

$$V_L^{C2} = 2.75, \quad Y_L^2 = 1.635.$$

If the shunt conductivity is equal to $y_N^2 = 1.6987$, the initial regime point $B_1 \rightarrow B_2$. Then, we obtain

$$I_L^{B1} = 1.8, \quad I_L^{B2} = 2.5.$$

Cross ratio (3.46) for the initial regime

$$\begin{aligned} m_L^1 &= (C_V\ C_1\ C_I\ G) = (B_V\ B_1\ B_I\ G) \\ &= \frac{Y_L^1}{Y_L^1 - Y_L^G} = \frac{0.8413}{0.8413 + 2} = 0.296. \end{aligned}$$

We check cross ratio (3.48)

$$\begin{aligned} m_L^1 &= \frac{I_L^{C1} - 0}{I_L^{C1} - I_L^G} \div \frac{I_L^{CI} - 0}{I_L^{CI} - I_L^G} \\ &= \frac{3.5 - 0}{3.5 - 10} \div \frac{6.4516 - 0}{6.4516 - 10} \\ &= -0.5384 \div (-1.8181) = 0.296. \end{aligned}$$

Subsequent regime cross ratio (3.49)

$$\begin{aligned} m_L^2 &= \frac{I_L^{C2} - 0}{I_L^{C2} - I_L^G} \div \frac{I_L^{CI} - 0}{I_L^{CI} - I_L^G} \\ &= -0.8181 \div (-1.8181) = 0.45. \end{aligned}$$

Regime change (3.50)

$$m_L^{21} = \frac{Y_L^2}{Y_L^2 - Y_L^G} \div \frac{Y_L^1}{Y_L^1 - Y_L^G} = 0.45 \div 0.296 = 1.5202.$$

We may check subsequent value (3.53) of load current

$$I_L^{C2} = \frac{I_L^G I_L^{C1} m_L^{21}}{I_L^{C1}(m_L^{21} - 1) + I_L^G} = \frac{10 \cdot 3.5 \cdot 1.5207}{3.5 \cdot 0.5207 + 10} = 4.5.$$

Case 2 Recalculation of the load current at the shunt conductivity y_N change

Let the load conductivity be equal to Y_L^1 and the shunt conductivity varies from y_N^1 to y_N^2. In this case, the initial regime point $C_1 \rightarrow B_1$.

Regime change (3.63)

$$m_i^{21} = (\infty\ y_N^2\ y_N^1\ y_N^I) = \frac{y_N^1 - y_N^I}{y_N^2 - y_N^I} = \frac{0.1 + 1}{1.6987 + 1} = 0.407.$$

We consider the load current of the initial regime $I_L^{C1} = 3.5$. Then, subsequent current (3.64)

$$I_L^{B1} = \frac{I_L^G I_L^{C1} m_i^{21}}{I_L^{C1}(m_i^{21} - 1) + I_L^G} = \frac{10 \cdot 3.5 \cdot 0.407}{3.5 \cdot (0.407 - 1) + 10} = 1.8.$$

Case 3 Recalculation of the load current at the common change of the load Y_L and conductivity y_N

Let the common change of regime be given as $C_1 \rightarrow C_2 \rightarrow B_2$.

Common regime change (3.65)

$$m^{21} = m_i^{21} m_L^{21} = 0.407 \cdot 1.5207 = 0.6187.$$

Resultant current (3.66) for the point B_2

$$I_L^{B2} = \frac{I_L^G I_L^{C1} m^{21}}{I_L^{C1}(m^{21} - 1) + I_L^G} = \frac{10 \cdot 3.5 \cdot 0.6187}{3.5 \cdot (0.6187 - 1) + 10} = 2.5.$$

3.4 General Case of an Active Two-Pole with a Variable Conductivity

Let us consider an active two-pole A with a load conductivity Y_{L1} and variable auxiliary conductivity Y_{L2} in Fig. 3.25. For convenience of a mathematical description, the variable element Y_{L2} is taken out from the two-pole contour.

This circuit (as a two-port network) is described by the following system of the Y parameter equations

$$\begin{bmatrix} I_1 \\ I_2 \end{bmatrix} = \begin{bmatrix} -Y_{11} & Y_{12} \\ Y_{12} & -Y_{22} \end{bmatrix} \cdot \begin{bmatrix} V_1 \\ V_2 \end{bmatrix} + \begin{bmatrix} I_1^{SC,SC} \\ I_2^{SC,SC} \end{bmatrix}. \tag{3.67}$$

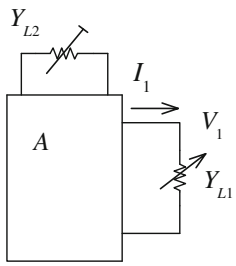

Fig. 3.25 Active two-pole with a load conductivity Y_{L1} and variable element Y_{L2}

The short circuit *SC* currents of all the loads

$$I_1^{SC,SC} = Y_{10}V_0, \quad I_2^{SC,SC} = Y_{20}V_0,$$

where V_0 is a resultant value of sources entering into this active two-pole.

3.4.1 Known Equivalent Generator

Taking into account the current

$$I_2 = Y_{L2}V_2, \tag{3.68}$$

we obtain an expression of a load straight line

$$I_1 = -\left(Y_{11} - \frac{Y_{12}^2}{Y_{L2} + Y_{22}}\right)V_1 + \left(Y_{10} + \frac{Y_{12}Y_{20}}{Y_{L2} + Y_{22}}\right)V_0. \tag{3.69}$$

The load straight line with the parameter Y_{L2} is shown in Fig. 3.26.
Let us consider the short circuit current I_1^{SC}. In this case $V_1 = 0$ and

$$I_1^{SC} = \left(Y_{10} + \frac{Y_{12}Y_{20}}{Y_{L2} + Y_{22}}\right)V_0. \tag{3.70}$$

Similarly, we consider the open circuit voltage V_1^{OC}. In this case $I_1 = 0$ and

$$V_1^{OC} = \frac{1}{Y_i}I_1^{SC}, \tag{3.71}$$

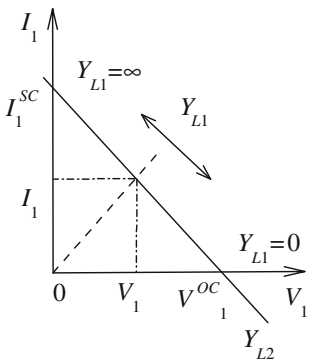

Fig. 3.26 Load straight lines with the parameter Y_{L2}

where the value

$$Y_i = Y_{11} - \frac{Y_{12}^2}{Y_{L2} + Y_{22}} = \frac{Y_{L2}Y_{11} + \Delta_Y}{Y_{L2} + Y_{22}} = \frac{1}{R_i} \tag{3.72}$$

is the internal conductivity (internal resistance R_i) of the circuit relatively to the load Y_{L1}; Δ_Y is the determinate of the matrix Y parameters.

Taking into account the entered parameters, Eq. (3.69) becomes as

$$I_1 = -Y_i V_1 + I_1^{SC}. \tag{3.73}$$

This expression we represent as

$$I_1 - I_1^{SC} = -Y_i V_1. \tag{3.74}$$

Thus, we obtain an equation of a straight line passing through a point I_1^{SC}. In turn, conductivity Y_i defines a slope angle of this line.

So, the values I_1^{SC}, Y_i are the parameters of the Norton equivalent circuit.

By analogy to (3.74) and taking into account (3.71), we obtain an equation of a straight line passing through a point V_1^{OC}

$$I_1 = (V_1^{OC} - V_1)Y_i\,. \tag{3.75}$$

So, the values V_1^{OC}, $Y_i = 1/R_i$ are the parameters of known Thévenin equivalent circuit. We note that the parameters I_1^{SC}, V_1^{OC} depend on the changeable conductivity Y_{L2}.

3.4.2 Generalized Equivalent Circuit

Let us study features of load straight line (3.69). This expression represents a bunch of the load straight lines with the parameter Y_{L2}. To find the coordinates V_1^G, I_1^G of the bunch center G of these lines, it is convenient to use the extreme parameter values; that is, $Y_{L2} = 0$, $Y_{L2} = \infty$. These lines are shown in Fig. 3.27.

In this case, expression (3.69) gives the following system of equations

$$\begin{cases} I_1(0) = -\left(Y_{11} - \frac{Y_{12}^2}{Y_{22}}\right)V_1 + \left(Y_{10} + \frac{Y_{12}Y_{20}}{Y_{22}}\right)V_0 \\ I_1(\infty) = -Y_{11}V_1 + Y_{10}V_0. \end{cases} \tag{3.76}$$

At the point of intersection we have that

$$I_1^G = I_1(0) = I_1(\infty).$$

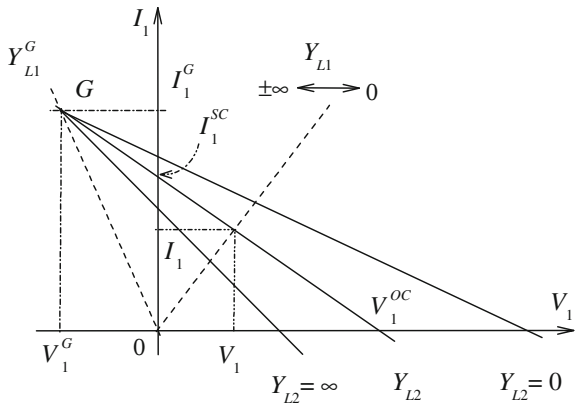

Fig. 3.27 Bunch of load straight lines with the parameters Y_{L2}

The solving of the system gives the following values

$$V_1^G = -\frac{Y_{20}}{Y_{12}} V_0, \tag{3.77}$$

$$I_1^G = \left(Y_{10} + \frac{Y_{11}Y_{20}}{Y_{12}}\right) V_0. \tag{3.78}$$

The obtained values V_1^G, I_1^G, and the internal conductivity Y_i allow to represent Eq. (3.69) or (3.74) in the other kind

$$I_1 - I_1^G = -Y_i (V_1 + V_1^G). \tag{3.79}$$

Thus, we obtain an equation of a straight line passing through a point I_1^G, V_1^G. So, the values I_1^G, V_1^G, and Y_i are the parameters of the generalized Norton/Mayer equivalent circuit in Fig. 3.17 of Sect. 3.2. In turn, this equation corresponds to expression (3.42).

Let us note the bunch center G corresponds to such a voltage V_1^G and current I_1^G of the load $Y_{L1} = Y_{L1}^G$ when the current of the element Y_{L2} is equal to zero. According to this condition, from (3.67), it is also possible to find values (3.77) and (3.78) of V_1^G, I_1^G. Then, the corresponding negative load conductivity

$$Y_{L1}^G = \frac{I_1^G}{V_1^G} = -\frac{Y_{11}Y_{20} + Y_{10}Y_{21}}{Y_{20}}. \tag{3.80}$$

In the above case, the bunch center G is in the second quadrant of the coordinate system and so $V_1^G < 0$, $I_1^G > 0$. It is natural to consider a case when the bunch center G is in the fourth quadrant shown in Fig. 3.28.

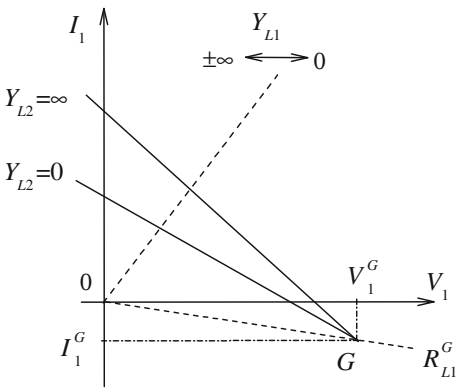

Fig. 3.28 Bunch center is in the fourth quadrant

To do this, we may consider expression (3.80) as follows

$$Y_{L1}^G = \frac{-I_1^G}{-V_1^G}. \tag{3.81}$$

Then, expressions (3.77) and (3.78) become as

$$V_1^G = \frac{Y_{20}}{Y_{12}} V_0. \tag{3.82}$$

$$I_1^G = -\left(Y_{10} + \frac{Y_{11}Y_{20}}{Y_{12}}\right) V_0. \tag{3.83}$$

Thus, Eq. (3.79) has the form

$$I_1 + I_1^G = -\frac{1}{R_i}(V_1 - V_1^G). \tag{3.84}$$

So, the values I_1^G, V_1^G, and R_i are the parameters of the generalized Thévenin/Helmholtz equivalent generator in Fig. 3.5 of Sect. 3.1. In turn, Eq. (3.84) corresponds to expression (3.8).

The position of center G (in the second or fourth quadrant) is defined by the kind or type of an active two-pole as an energy source. If an active two-pole shows more properties of current source, the case of Fig. 3.27 takes place. If it shows more properties of voltage source, we have the case of Fig. 3.28.

Let us demonstrate how the internal conductivity Y_i and respectively the conductivity Y_{L2} influence on properties of the generalized equivalent generator.

Further, we use the inverse expression to (3.72)

$$Y_{L2} = \frac{Y_{22}Y_i - \Delta_Y}{Y_{11} - Y_i}. \tag{3.85}$$

The conductivities have the following characteristic values:

$$Y_i^I = 0, \quad Y_{L2}^I = -\frac{\Delta_Y}{Y_{11}}, \tag{3.86}$$

which defines the generalized equivalent generator as an ideal current source;

$$Y_i^V = \infty, \quad Y_{L2}^V = -Y_{22}, \tag{3.87}$$

which defines the generalized equivalent generator as an ideal voltage source;

$$\begin{aligned} Y_i^0 &= -\frac{I_1^G}{V_1^G} = -Y_{L1}^G = \frac{Y_{11}Y_{20} + Y_{10}Y_{21}}{Y_{20}}, \\ Y_{L2}^0 &= -Y_{22} - \frac{Y_{20}Y_{12}}{Y_{10}}, \end{aligned} \tag{3.88}$$

which defines a "zero-order" source.

3.4.3 *Example of a Circuit. Recalculation of the Load Current*

Let us consider the electric circuit with the base load conductivity Y_{L1} and auxiliary load conductivity Y_{L2} in Fig. 3.29.

This circuit may be considered as an active two-port A network relatively to the specified loads in Fig. 3.30.

Taking into account the specified directions of currents, this network is described by (3.67)

$$\begin{aligned} \begin{bmatrix} I_1 \\ I_2 \end{bmatrix} &= \begin{bmatrix} -Y_{11} & Y_{12} \\ Y_{12} & -Y_{22} \end{bmatrix} \cdot \begin{bmatrix} V_1 \\ V_2 \end{bmatrix} + \begin{bmatrix} I_1^{SC,SC} \\ I_2^{SC,SC} \end{bmatrix} \\ &= \begin{bmatrix} -1.2 & 0.2 \\ 0.2 & -0.95 \end{bmatrix} \cdot \begin{bmatrix} V_1 \\ V_2 \end{bmatrix} + \begin{bmatrix} 3 \\ 2 \end{bmatrix}. \end{aligned}$$

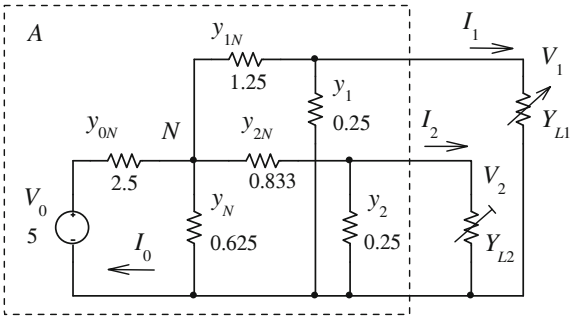

Fig. 3.29 Active two-pole with the load conductivity Y_{L1} and variable element Y_{L2}

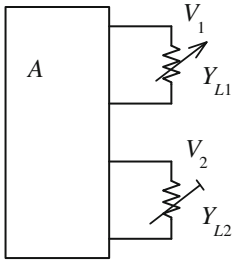

Fig. 3.30 Active two-port *A* network with the specified loads

In turn, *Y* parameters are

$$Y_{11} = y_1 + y_{1N} - \frac{y_{1N}^2}{y_\Sigma} = 0.25 + 1.25 - \frac{1.5625}{5.2083} = 1.2,$$

$$y_\Sigma = y_{0N} + y_N + y_{1N} + y_{2N} = 2.5 + 0.625 + 1.25 + 0.8333 = 5.2083,$$

$$Y_{12} = y_{2N}\frac{y_{1N}}{y_\Sigma} = 0.8333\frac{1.25}{5.2083} = 0.2,$$

$$Y_{22} = y_2 + y_{2N} - \frac{y_{2N}^2}{y_\Sigma} = 0.25 + 0.8333 - \frac{0.6944}{5.2083} = 0.95.$$

The short circuit *SC* currents

$$I_1^{SC,SC} = Y_{10}V_0 = y_{0N}\frac{y_{1N}}{y_\Sigma}V_0 = 2.5\frac{1.25}{5.2083}5 = 0.6 \cdot 5 = 3,$$

$$I_2^{SC,SC} = Y_{20}V_0 = y_{0N}\frac{y_{2N}}{y_\Sigma}V_0 = 2.5\frac{0.8333}{5.2083}5 = 0.4 \cdot 5 = 2.$$

Let the initial value of the conductivity Y_{L2} be equal to $Y_{L2}^1 = 0.5$. Parameters (3.70)–(3.72) of the Norton equivalent circuit

$$I_1^{SC1} = I_1^{CI} = \left(Y_{10} + \frac{Y_{12}Y_{20}}{Y_{L2}^1 + Y_{22}}\right)V_0 = \left(0.6 + \frac{0.2 \cdot 0.4}{0.5 + 0.95}\right) \cdot 5 = 3.2758.$$

$$Y_i^1 = \frac{Y_{L2}^1 Y_{11} + \Delta_Y}{Y_{L2}^1 + Y_{22}} = \frac{0.5 \cdot 1.2 + 1.1}{0.5 + 0.95} = 1.1724,$$

$$V_1^{OC1} = V_1^{CV} = \frac{1}{Y_i^1} I_1^{SC1} = 2.7941.$$

Let the subsequent value of the conductivity Y_{L2} be equal to $Y_{L2}^2 = 2$. The corresponding parameters of the Norton equivalent circuit

$$I_1^{SC2} = I_1^{BI} = 3.1355, \quad Y_i^2 = 1.1864, \quad V_1^{OC2} = V_1^{BV} = 2.6428.$$

The bunch of the load straight lines is shown in Fig. 3.31.
Bunch center coordinates (3.77) and (3.78)

$$V_1^G = -\frac{Y_{20}}{Y_{12}} V_0 = -2 \cdot 5 = -10,$$

$$I_1^G = \left(Y_{10} + \frac{Y_{11}Y_{20}}{Y_{12}}\right)V_0 = \left(0.6 + \frac{1.2 \cdot 0.4}{0.2}\right) \cdot 5 = 15.$$

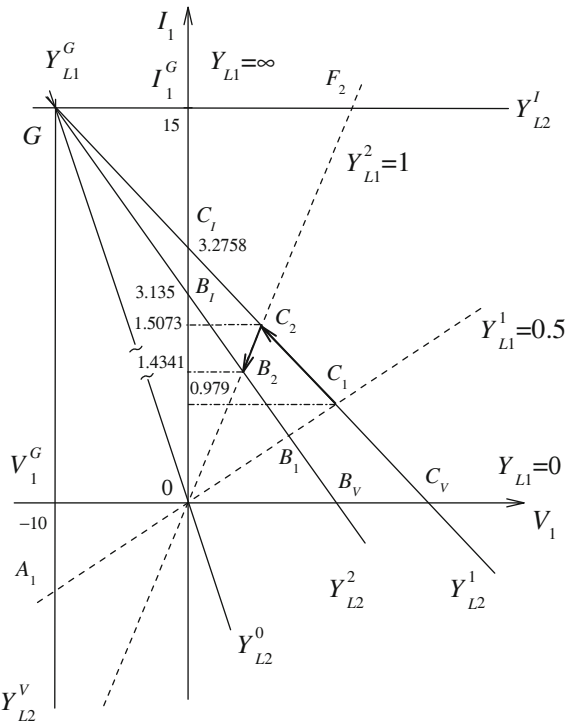

Fig. 3.31 Example of load straight lines of a circuit with the variable conductivity Y_{L2}

The corresponding negative load conductivity

$$Y_{L1}^G = \frac{I_1^G}{I_1^G} = -\frac{Y_{11}Y_{20} + Y_{10}Y_{21}}{Y_{20}} = -(y_{1N} + y_1) = -1.5.$$

Characteristic values (3.86)–(3.88)

$$Y_i^I = 0, \quad Y_{L2}^I = -\frac{\Delta_Y}{Y_{11}} = -\frac{1.1}{1.2} = -0.9166,$$
$$Y_i^V = \infty, \quad Y_{L2}^V = -Y_{22} = -0.95,$$
$$Y_i^0 = -Y_{L1}^G = 1.5, \quad Y_{L2}^0 = -Y_{22} - \frac{Y_{12}Y_{20}}{Y_{10}} = -(y_{2N} + y_2) = -1.0833.$$

So, the case of the generalized Norton/Mayer equivalent generator takes place. Therefore, we will use the corresponding relationships of Sect. 3.2.

Case 1 Recalculation of the load current at the load change

Let the conductivity Y_{L2} be equal to Y_{L2}^1 and load conductivity varies from $Y_{L1}^1 = 0.5$ to $Y_{L1}^2 = 1$. In this case, the initial regime point $C_1 \rightarrow C_2$; the load current of the initial regime $I_1^{C1} = 0.979$.

Cross ratio (3.46) for the initial regime

$$m_L^1 = (C_V\ C_1\ C_I\ G) = \frac{Y_{L1}^1}{Y_{L1}^1 - Y_L^G} = \frac{0.5}{0.5 + 1.5} = 0.25.$$

Subsequent regime cross ratio (3.49)

$$m_L^2 = \frac{Y_{L1}^2}{Y_{L1}^2 - Y_L^G} = \frac{1}{1 + 1.5} = 0.4.$$

Regime change (3.50)

$$m_L^{21} = 0.4 \div 0.25 = 1.6.$$

Subsequent value (3.53) of load current

$$I_1^{C2} = \frac{I_L^G I_1^{C1} m_L^{21}}{I_1^{C1}(m_L^{21} - 1) + I_L^G} = \frac{15 \cdot 0.979 \cdot 1.6}{0.979 \cdot 0.6 + 15} = 1.5073.$$

Case 2 Recalculation of the load current at the conductivity Y_{L2} change

Let the load conductivity be equal to $Y_{L1}^2 = 1$ and conductivity Y_{L2} varies from $Y_{L2}^1 = 0.5$ to $Y_{L2}^2 = 2$. In this case, the initial regime point $C_2 \rightarrow B_2$.

Cross ratio (3.55) and (3.61) for the initial regime

$$m_i^1 = (0\ C_2\ A_2\ F_2) = (Y_{L2}^0\ Y_{L2}^1\ Y_{L2}^V\ Y_{L2}^I) = \frac{Y_{L2}^1 - Y_{L2}^0}{Y_{L2}^1 - Y_{L2}^I} \div \frac{Y_{L2}^V - Y_{L2}^0}{Y_{L2}^V - Y_{L2}^I}$$
$$= \frac{0.5 + 1.0833}{0.5 + 0.9166} \div \frac{-0.95 + 1.0833}{-0.95 + 0.9166} = 1.1176 \div (-4) = -0.2794.$$

Subsequent regime cross ratio

$$m_i^2 = (0\ B_2\ A_2\ F_2) = (Y_{L2}^0\ Y_{L2}^2\ Y_{L2}^V\ Y_{L2}^I) = \frac{Y_{L2}^2 - Y_{L2}^0}{Y_{L2}^2 - Y_{L2}^I} \div \frac{Y_{L2}^V - Y_{L2}^0}{Y_{L2}^V - Y_{L2}^I}$$
$$= \frac{2 + 1.0833}{2 + 0.9166} \div (-4) = 1.0571 \div (-4) = -0.2642.$$

The regime change

$$m_i^{21} = m_i^2 \div m_i^1 = 0.2642 \div 0.2794 = 0.9459.$$

Then, subsequent value (3.64) of current for the point B_2

$$I_1^{B2} = \frac{I_1^G I_1^{C2} m_i^{21}}{I_1^{C2}(m_i^{21} - 1) + I_1^G} = \frac{15 \cdot 1.5073 \cdot 0.9459}{1.5073 \cdot (0.9459 - 1) + 15} = 1.434.$$

Case 3 Recalculation of the load current at the common change of the load Y_{L1} and conductivity Y_{L2}

Let the common change of regime be given as $C_1 \rightarrow C_2 \rightarrow B_2$.

The common regime change

$$m^{21} = m_i^{21} m_L^{21} = 0.9459 \cdot 1.6 = 1.5134.$$

Resultant current (3.66) for the point B_2

$$I_1^{B2} = \frac{I_1^G I_1^{C1} m^{21}}{I_1^{C1}(m^{21} - 1) + I_1^G} = \frac{15 \cdot 0.979 \cdot 1.5134}{0.979 \cdot (1.5134 - 1) + 15} = 1.434.$$

3.5 Stabilization of the Load Current

The influence of the conductivity Y_{L2} on properties of the generalized equivalent generator can be used in practice, for example, for a parametric stabilization of load current. In this case, the conductivity value Y_{L2} is determined by expression (3.86). Figure 3.32 schematically shows a structure of the appliance designed to stabilization of the adjustable load current [13]. Power supply voltage source 1 are connected to the input of line 2 with longitudinal 3 and lateral 4 resistances (loss resistances). The load 5 is connected to the output of line 2. Negative resistance 6

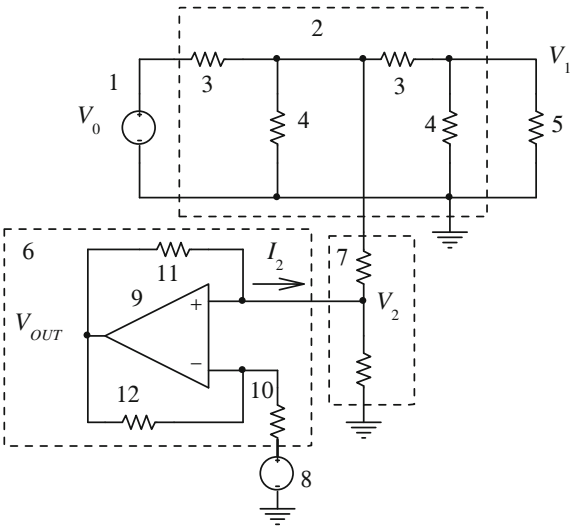

Fig. 3.32 Appliance for stabilization of the load current

through a match circuit 7 (general case) and a bias voltage source 8 are connected to one of the lateral resistance 4.

In turn, the negative resistance 6 is determined by a negative-impedance converter with an operation amplifier 9. Resistor 10 is an initial positive resistance, corresponding to the negative resistance 6; resistances 11, 12 are a feedback circuit.

The appliance in Fig. 3.32 work as follows. Let the bias voltage 8 be equal to zero at first. The power supply voltage source 1 sets the load current I_1 and voltage V_2. The operation amplifier 9 gains this voltage V_2; the output voltage V_{OUT} specifies the current I_2. The voltage for the inverse input of the amplifier 9 is equal to V_2 and the same current, as I_2, flows across the resistor 10. Therefore, the operation amplifier 9 with the resistor 10 is an energy source. This energy source, as the negative resistance 6, sets the voltage V_2, current I_2; the ratio V_2/I_2 is equal to the resistance 10 value. If the resistance 10 is chosen by necessary way, the load current will be constant. In turn, the voltage V_0 determines the value of the load current.

For convenience of use of expression (3.86), we may consider a three-port in Fig. 3.33, which is equivalent to the structure in Fig. 3.32 and the circuit in Fig. 3.29. In particular, conductivities y_{0N}, y_{1N} correspond to the longitudinal resistances; conductivities y_N, y_1 correspond to the lateral resistances of the line. Also, we have the load conductivity Y_{L1}, negative conductivity Y_{L2}, and bias voltage V_{BS}.

For example, let us consider a circuit of *ORCAD* model in Fig. 3.34. The negative resistance, by expression (3.86), is equal to −6.63488 kΩ.

The results of modeling for various values of the load resistance R_{L1} and voltages V_0, V_{BS} are given in Tables 3.1 and 3.2.

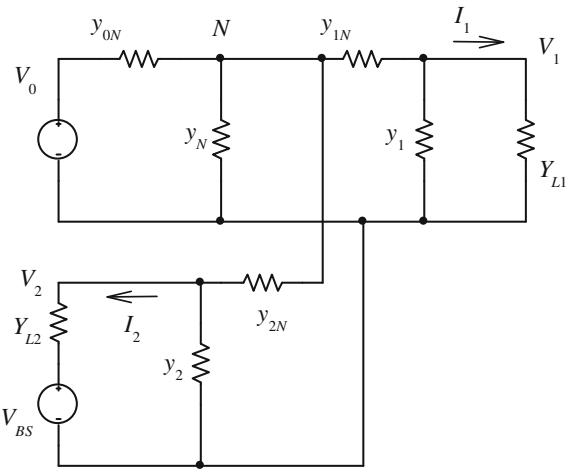

Fig. 3.33 Equivalent circuit to the structure of stabilization of the load current

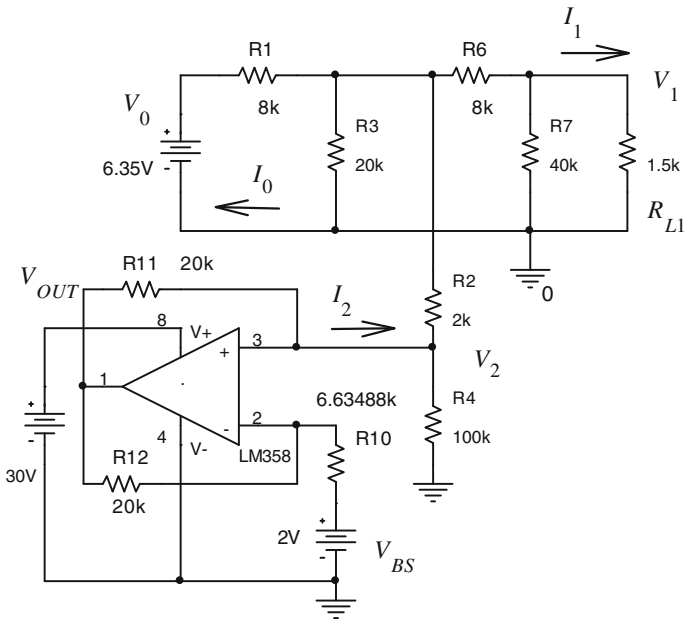

Fig. 3.34 *ORCAD* model of stabilization of the load current

We consider Table 3.1. It is visible, that the output voltage V_{OUT} of the operational amplifier reaches the maximum value at the load resistance of 3.0 kΩ.

Also, we note that the voltage source 1 does not give but consumes energy in the given load values because the negative current I_0.

Table 3.1 $V_0 = 3$ V, $V_{BS} = 0$ V

R_{L1} (kΩ)	0.001	1.5	3.0
I_1 (mA)	0.451	0.4508	0.4506
I_0 (mA)	−0.076	−0.177	−0.2784
V_2 (V)	5.022	6.15	7.276
I_2 (mA)	0.757	0.9273	1.097
V_{OUT} (V)	20.17	24.7	29.21

Table 3.2 $V_0 = 6.35$ V, $V_{BS} = 2$ V

R_{L1} (kΩ)	0.001	1.5	6.1
I_1 (mA)	0.4502	0.450	0.4496
I_0 (mA)	0.345	0.242	−0.0067
V_2 (V)	4.175	5.3	8.749
I_2 (mA)	0.328	0.497	1.017
V_{OUT} (V)	10.75	15.26	29.1

Let us consider Table 3.2. The output voltage V_{OUT} of the operational amplifier reaches the maximum value at the load resistance of 6.1 kΩ. It is the advantage of utilization of a bias voltage source. Also, the voltage source 1 gives energy practically for all load values. Therefore, the use of a bias voltage source improves an energy effectiveness of power supply voltage source.

References

1. Alexander, C.K., Sadiku, M.N.O.: Fundamentals of Electric Circuits, 5th edn. McGraw–Hill, New York (2009)
2. Chatzarakis, G.E.: A new method for finding the Thévenin and Norton equivalent circuits. Engineering **2**(05), 328–336 (2010)
3. Gluskin, E., Patlakh, A.: An ideal independent source as an equivalent 1-port. arXiv preprint arXiv:1108.4592 (2011)
4. Hashemian, R.: Hybrid equivalent circuit, and alternative to Thévenin and Norton equivalents, its properties and application. In: Midwest Symposium on Circuits and Systems, MWSCAS (2009)
5. Hosoya, M.: Derivation of the equivalent circuit of a multi-terminal network given by generalization of Helmholtz-Thevenin's theorem. Bull. Coll. Sci. Univ. Ryukyus. **84**, 1–3 (2007)
6. Irwin, J.D., Nelms, R.M.: Basic Engineering Circuit Analysis, 10th edn. Wiley, Hoboken (2011)
7. Johnson, D.: Origins of the equivalent circuit concept: the voltage-source equivalent. Proc. IEEE **91**(4), 636–640 (2003)
8. Karris, S.T.: Circuit Analysis I with MATLAB Computing and Simulink/SimPower Systems Modeling. Orchard Publications, Fremont (2004)
9. Penin, A.: Utilization of the projective coordinates in the linear electrical network with the variable regimes. Buletinul Academiei de Stiinte a Republicii Moldova, Fizica si tehnica. **2**, 64–71 (1992)

10. Penin, A.: Characteristics of modified equivalent generator of active two-terminal network with variable resistor. Electrichestvo **4**, 55–59 (1995)
11. Penin, A.: Linear-fractional relations in the problems of analysis of resistive circuits with variable parameters. Electrichestvo **11**, 32–44 (1999)
12. Penin, A.: Generalized Thévenin/Helmholtz and Norton/Mayer theorems of electric circuits with variable resistances. WSEAS Trans. Circ. Syst. **13**, 104–116 (2014). http://www.wseas.org/cms.action?id=7648. Accessed 30 Nov 2014
13. Penin, A., Sidorenko, A.: Transmission of measuring signals and power supply of remote sensors. In: Bonca, J., Kruchinin, S. (eds.) Nanotechnology in the Security Systems. NATO Science for Peace and Security Series C: Environmental Security, pp. 267–281. Springer, Dordrecht (2014)
14. Vandewalle, J.: Shortcuts in circuits and systems education with a case study of the Thévenin/Helmholtz and Norton/Mayer equivalents. In: International Symposium on the Circuits and Systems (ISCAS), IEEE (2012)

Chapter 4
Two-Port Circuits

4.1 Input-Output Conformity of Two-Ports as Affine Transformations

4.1.1 Conformity of a Two-Port

Let us consider a two-port *TP1* circuit in Fig. 4.1. A variable voltage source V_1 is the load of this two-port. The voltage V_1 (independent quantity) and current I_1 are the parameters of operating or running load regime. Therefore, we use the approach of Sect. 2.1.1.

As it is known [1, 2], the system of equation of this two-port has the view

$$\begin{cases} I_0 = Y_{00}V_0 - Y_{10}V_1 \\ I_1 = Y_{10}V_0 - Y_{11}V_1. \end{cases} \tag{4.1}$$

where Y parameters are

$$Y_{00} = y_{10} + y_0, \quad Y_{11} = y_{10} + y_1, \quad Y_{10} = y_{10}.$$

We determine the characteristic value of regime parameters for the short circuit *SC* ($V_1^{SC} = 0$) and open circuit *OC* ($I_1^{OC} = 0$). Then,

$$V_1^{SC} = 0, \quad I_1^{SC} = Y_{10}V_0, \quad I_0^{SC} = Y_{00}V_0, \tag{4.2}$$

$$V_1^{OC} = \frac{Y_{10}}{Y_{11}}V_0, \quad I_1^{OC} = 0, \quad I_0^{OC} = \frac{\Delta_Y}{Y_{11}}V_0. \tag{4.3}$$

A. Penin, *Analysis of Electrical Circuits with Variable Load Regime Parameters*, Power Systems, DOI 10.1007/978-3-319-28451-4_4

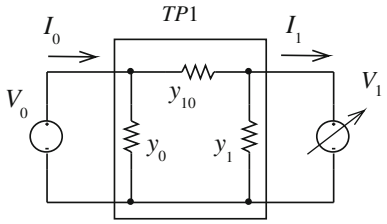

Fig. 4.1 Two-port with a load voltage source

For these parameters, system (4.1) becomes

$$\begin{cases} I_0 = I_0^{SC} - \frac{I_1^{SC}}{V_0} V_1 \\ I_1 = I_1^{SC} - \frac{I_1^{SC}}{V_1^{OC}} V_1. \end{cases} \tag{4.4}$$

Equation (4.4) gives the following input and output load straight lines in Fig. 4.2.

Our circuit represents an active two-pole relatively to load. By definition, the internal conductivity of the active two-pole is $Y_i = I_1^{SC}/V_1^{OC}$. Therefore, the second equation of system (4.4) corresponds to Eq. (2.1) of Chap. 2. Then, we may use the results of this chapter and determine the running regime parameter by an identical value for the various actual regime parameters (voltages, currents) and for different sections of circuit (input and output).

As the load characteristics are defined by linear expression (4.4), an affine transformation or mapping $V_1 \to I_1, V_1 \to I_0, I_1 \to I_0$ takes place [3, 9].

Let an initial regime be given by values V_1^1, I_1^1, I_0^1. Then, affine ratio (2.6) or (2.8) has the form

$$n_1^1 = \frac{V_1^{OC} - V_1^1}{V_1^{OC} - V_1^{SC}} = \frac{I_1^1 - I_1^{OC}}{I_1^{SC} - I_1^{OC}} = \frac{I_0^1 - I_0^{OC}}{I_0^{SC} - I_0^{OC}} \tag{4.5}$$

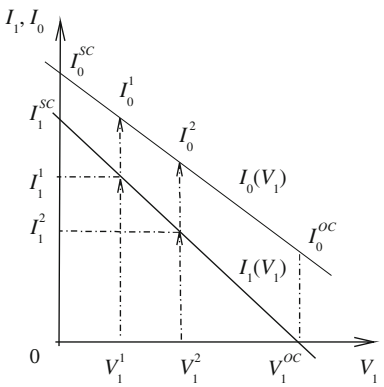

Fig. 4.2 Conformity of the input and output load straight lines of a two-port

This affine ratio can be represented by the formal view

$$n^1 = (I_1^1\ I_1^{OC}\ I_1^{SC}) = (V_1^1\ V_1^{OC}\ V_1^{SC}) = (I_0^1\ I_0^{OC}\ I_0^{SC}). \tag{4.6}$$

Let a subsequent regime be set by values V_1^2, I_1^2, I_0^2. Then, the affine ratio is

$$n_1^2 = \frac{V_1^{OC} - V_1^2}{V_1^{OC} - V_1^{SC}} = \frac{I_1^2 - I_1^{OC}}{I_1^{SC} - I_1^{OC}} = \frac{I_0^2 - I_0^{OC}}{I_0^{SC} - I_0^{OC}} \tag{4.7}$$

Now, we use regime change (2.15)

$$n_1^{21} = n_1^2 - n_1^1 = \frac{V_1^1 - V_1^2}{V_1^{OC} - V_1^{SC}} = \frac{I_1^2 - I_1^1}{I_1^{SC} - I_1^{OC}} = \frac{I_0^2 - I_0^1}{I_0^{SC} - I_0^{OC}}. \tag{4.8}$$

So, we obtain the identical values for the voltage and currents at the output and input.

Using (4.8), we get the recalculation formulas

$$I_1^2 = I_1^1 + n_1^{21}(I_1^{SC} - I_1^{OC}), \quad I_0^2 = I_0^1 + n_1^{21}(I_0^{SC} - I_0^{OC}). \tag{4.9}$$

Let us consider the practical case. Let the voltage V_1 be changed once again. We get regime change (4.8) and currents (4.9). The structure of expression (4.8) shows that errors of voltage measurement are reduced. Therefore, recalculation formula (4.9) gives a more great accuracy, than primary Eq. (4.4), which contains the actual voltage value V_1. Also, the invariant value n_1 can represent the interest for remote voltage measurement that will be shown in this chapter further.

4.1.2 Conformity of Cascaded Two-Ports

Let us now consider the cascade connection of two-ports *TP1* and *TP2* in Fig. 4.3. A variable voltage source V_2 is the load of this connection.

At change of the load voltage V_2, we get the family of load straight lines in Fig. 4.4.

Similarly, we have affine transformations or mapping of regime parameters for various sections; that is,

$$V_2 \to I_2, \quad V_2 \to I_1, \quad V_2 \to V_1, \quad V_2 \to I_0, \quad I_2 \to I_1 \to I_0.$$

Therefore, it is possible to constitute the affine ratio, as an invariant of these transformations, for initial parameters of all the sections relatively to the load. Using (4.5), we get

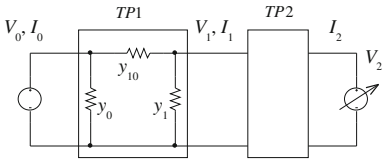

Fig. 4.3 Cascade connection of two-ports

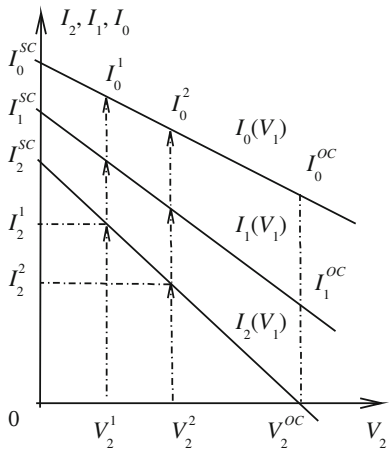

Fig. 4.4 Family of load straight lines for sections of cascaded two-ports

$$
\begin{aligned}
n_2^1 &= \frac{V_2^{OC} - V_2^1}{V_2^{OC} - V_2^{SC}} = \frac{I_2^1 - I_2^{OC}}{I_2^{SC} - I_2^{OC}} \\
&= \frac{V_1^{OC} - V_1^1}{V_1^{OC} - V_1^{SC}} = \frac{I_1^1 - I_1^{OC}}{I_1^{SC} - I_1^{OC}} \\
&= \frac{I_0^1 - I_0^{OC}}{I_0^{SC} - I_0^{OC}}.
\end{aligned}
\tag{4.10}
$$

Also, we may obtain the other affine ratio likewise to (2.7). Similarly to (4.8), the regime change has the form

$$
\begin{aligned}
n_2^{21} &= \frac{V_2^1 - V_2^2}{V_2^{OC} - V_2^{SC}} = \frac{I_2^2 - I_2^1}{I_2^{SC} - I_2^{OC}} \\
&= \frac{V_1^1 - V_1^2}{V_1^{OC} - V_1^{SC}} = \frac{I_1^2 - I_1^1}{I_1^{SC} - I_1^{OC}} \\
&= \frac{I_0^2 - I_0^1}{I_0^{SC} - I_0^{OC}}.
\end{aligned}
\tag{4.11}
$$

So, we obtain the identical values for the voltages and currents of different sections. From here, we get the voltage recalculation formula

$$V_1^2 = V_1^1 - n_2^{21}(V_1^{OC} - V_1^{SC}) \tag{4.12}$$

Example Let us consider a circuit with given values in Fig. 4.5a. The initial and subsequent regimes correspond to the load voltages $V_2^1 = 1$, $V_2^2 = 3$. The calculated currents, voltages of all the sections and their conformity are shown by the diagram in Fig. 4.5b.

Affine ratio (4.10) for the initial regime

$$n_2^1 = \frac{V_2^{OC} - V_2^1}{V_2^{OC} - V_2^{SC}} = \frac{3.902 - 1}{3.902 - 0} = 0.743,$$
$$n_2^1 = \frac{I_2^1 - I_2^{OC}}{I_2^{SC} - I_2^{OC}} = \frac{10.43 - 0}{14.03 - 0} = 0.743,$$
$$n_2^1 = \frac{V_1^{OC} - V_1^1}{V_1^{OC} - V_1^{SC}} = \frac{4.878 - 3.86}{4.878 - 3.509} = 0.743,$$
$$n_2^1 = \frac{I_1^1 - I_1^{OC}}{I_1^{SC} - I_1^{OC}} = \frac{15.3 - 8.78}{17.55 - 8.78} = 0.743,$$
$$n_2^1 = \frac{I_0^1 - I_0^{OC}}{I_0^{SC} - I_0^{OC}} = \frac{34.56 - 30.49}{35.97 - 30.49} = 0.743.$$

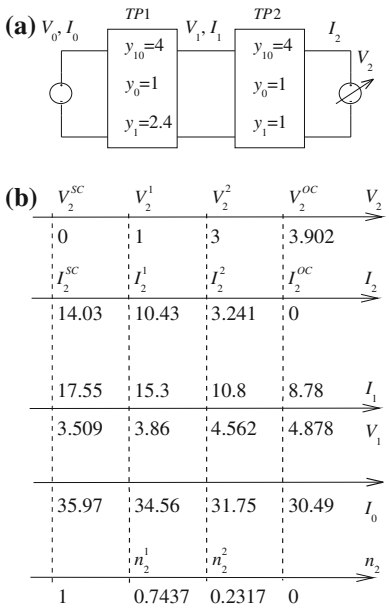

Fig. 4.5 **a** Example of the cascaded circuit, **b** conformity of the regime parameters

Regime change (4.11)

$$n_2^{21} = \frac{V_2^1 - V_2^2}{V_2^{OC} - V_2^{SC}} = \frac{1-3}{3.9-0} = -0.513.$$

Subsequent voltage (4.12)

$$V_1^2 = V_1^1 - n_2^{21}(V_1^{OC} - V_1^{SC}) = 3.86 + 0.513(4.878 - 3.509) = 4.562.$$

4.2 Input-Output Conformity of Two-Ports as Projective Transformations

4.2.1 Conformity of a Two-Port

Let us consider an asymmetrical two-port *TP1* in Fig. 4.6. A variable conductivity Y_{L1} is the load of this two-port. Therefore, we use the approach of Sect. 2.1.2.

System of Eq. (4.1) has the matrix form

$$\begin{bmatrix} I_0 \\ I_1 \end{bmatrix} = \begin{bmatrix} Y_{00} & -Y_{10} \\ Y_{10} & -Y_{11} \end{bmatrix} \cdot \begin{bmatrix} V_0 \\ V_1 \end{bmatrix} \tag{4.13}$$

At change of the load conductivity Y_{L1}, we get the load straight lines in Fig. 4.7.

In turn, bunches of straight lines with parameters Y_{L1}, Y_{IN1} correspond to these load lines. It is also possible to calibrate the load straight lines in the conductivity values. The point of maximum load power corresponds to values $V_1^i = 0.5V_1^{OC}$, $Y_{L1}^i = Y_i$. The value Y_i is the internal conductivity of circuit relatively to load Y_{L1}.

In previous Sect. 4.1.1 it was shown that the conformity of load straight lines is an affine transformation for voltage and current. Now, we consider the conformity $Y_{L1} \rightarrow Y_{IN1}$ [5, 9]. For this purpose, we demonstrate the relationship $Y_{IN1}(Y_{L1})$ by the transmission a parameters.

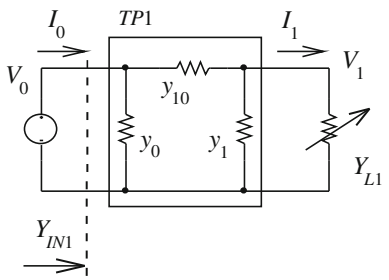

Fig. 4.6 Two-port with a load conductivity

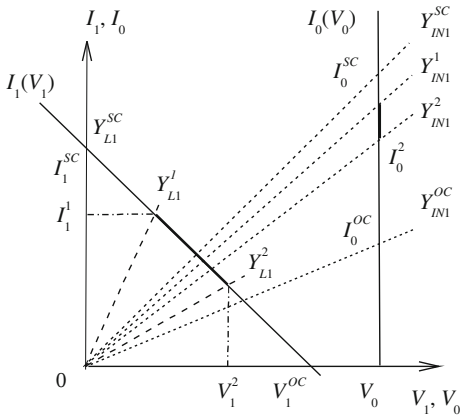

Fig. 4.7 Input and output load straight lines

In this case, the equation of two-port has a view

$$\begin{bmatrix} V_0 \\ I_0 \end{bmatrix} = \begin{bmatrix} a_{11} & a_{12} \\ a_{21} & a_{22} \end{bmatrix} \cdot \begin{bmatrix} V_1 \\ I_1 \end{bmatrix} = \begin{bmatrix} \frac{Y_{11}}{Y_{10}} & \frac{1}{Y_{10}} \\ \frac{\Delta_Y}{Y_{10}} & \frac{Y_{00}}{Y_{10}} \end{bmatrix} \cdot \begin{bmatrix} V_1 \\ I_1 \end{bmatrix}. \tag{4.14}$$

The inverse expression

$$\begin{bmatrix} V_1 \\ I_1 \end{bmatrix} = \begin{bmatrix} a_{22} & -a_{12} \\ -a_{21} & a_{11} \end{bmatrix} \cdot \begin{bmatrix} V_0 \\ I_0 \end{bmatrix} \tag{4.15}$$

The determinant of a matrix

$$\Delta_A = a_{11}a_{22} - a_{12}a_{21} = 1.$$

This feature of a parameters allows introducing the hyperbolic functions

$$\Delta_A = ch^2\gamma - sh^2\gamma = 1,$$

where γ is an attenuation coefficient.

Then, Eq. (4.14) is given by

$$\begin{bmatrix} V_0 \\ \frac{I_0}{Y_{IN1.C}} \end{bmatrix} = \begin{bmatrix} ch\gamma & sh\gamma \\ sh\gamma & ch\gamma \end{bmatrix} \cdot \begin{bmatrix} V_1 \frac{Y_{L1.C}}{\sqrt{\Delta_Y}} \\ \frac{I_1}{\sqrt{\Delta_Y}} \end{bmatrix} \tag{4.16}$$

where characteristic admittance at the input and output are

$$Y_{IN1.C} = \sqrt{\frac{Y_{00}}{Y_{11}}\Delta_Y}, \quad Y_{L1.C} = \sqrt{\frac{Y_{11}}{Y_{00}}\Delta_Y}. \tag{4.17}$$

In turn, the relation $Y_{IN1}(Y_{L1})$ or admittance transformation has the fractionally linear view by (4.14)

$$Y_{IN1} = \frac{I_0}{V_0} = \frac{a_{22}Y_{L1} + a_{21}}{a_{12}Y_{L1} + a_{11}}. \tag{4.18}$$

Using (4.16), we get the normalized form of this expression

$$\frac{Y_{IN1}}{Y_{IN1.C}} = \frac{\frac{Y_{L1}}{Y_{L1.C}} + th\gamma}{1 + \frac{Y_{L1}}{Y_{L1.C}} th\gamma}. \tag{4.19}$$

Similarly to (2.23) this conformity $Y_{L1} \rightarrow Y_{IN1}$ is a projective transformation. The projective transformations preserve a cross ratio of four points. Therefore, analogously to (2.24), the cross ratio m^1_{L1} for initial values Y^1_{L1} has the view

$$\begin{aligned} m^1_{L1} &= (Y^{SC}_{L1}\ Y^1_{L1}\ Y^i_{L1}\ Y^{OC}_{L1}) = (\infty Y^1_{L1}\ Y_i 0) \\ &= \frac{Y^1_{L1} - \infty}{Y^1_{L1} - 0} \div \frac{Y_i - \infty}{Y_i - 0} = \frac{Y_i}{Y^1_{L1}}. \end{aligned} \tag{4.20}$$

The conformity of all the parameters is given by the diagram in Fig. 4.8. Then, we can constitute the cross ratio for these parameters.

For the input conductivity

$$\begin{aligned} m^1_{L1} &= (Y^{SC}_{IN1}\ Y^1_{IN1}\ Y^i_{IN1}\ Y^{OC}_{IN1}) \\ &= \frac{Y^1_{IN1} - Y^{SC}_{IN1}}{Y^1_{IN1} - Y^{OC}_{IN1}} \div \frac{Y^i_{IN1} - Y^{SC}_{IN1}}{Y^i_{IN1} - Y^{OC}_{IN1}} = \frac{Y^{SC}_{IN1} - Y^1_{IN1}}{Y^1_{IN1} - Y^{OC}_{IN1}}, \end{aligned} \tag{4.21}$$

where the point Y^i_{IN1} is the center of segment $Y^{SC}_{IN1}\ Y^{OC}_{IN1}$; that is,

$$Y^i_{IN1} = Y^{OC}_{IN1} + \frac{Y^{SC}_{IN1} - Y^{OC}_{IN1}}{2}.$$

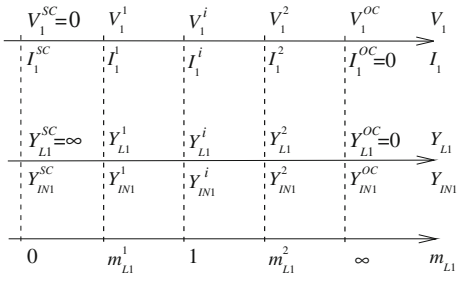

Fig. 4.8 Conformity of the regime parameters

Also, we have

$$m_{L1}^{1} = (0\ V_1^1\ \frac{V_1^{OC}}{2}\ V_1^{OC}) = \frac{V_1^1}{V_1^{OC} - V_1^1}, \tag{4.22}$$

$$m_{L1}^{1} = (I_1^{SC}\ I_1^1\ \frac{I_1^{SC}}{2}\ 0) = \frac{I_1^{SC} - I_1^1}{I_1^1}, \tag{4.23}$$

$$\begin{aligned} m_{L1}^{1} &= (I_0^{SC}\ I_0^1\ I_0^i\ I_0^{OC}) \\ &= \frac{I_0^1 - I_0^{SC}}{I_0^1 - I_0^{OC}} \div \frac{I_0^i - I_0^{SC}}{I_0^i - I_0^{OC}} = \frac{I_0^{SC} - I_0^1}{I_0^1 - I_0^{OC}}, \end{aligned} \tag{4.24}$$

where the input current I_0^i is the center of segment $I_0^{SC} I_0^{OC}$; that is,

$$I_0^i = I_0^{OC} + \frac{I_0^{SC} - I_0^{OC}}{2}.$$

We consider the load change $Y_{L1}^1 \to Y_{L1}^2$. This change defines the segment $Y_{L1}^2\ Y_{L1}^1$ and segment $Y_{IN1}^2\ Y_{IN1}^1$ on the line $I_0(V_0)$. It may be noted that length of segments is different for usually used Euclidean geometry. However, if the mapping is viewed as a projective transformation, an invariant or cross ratio is performed, which defines the same "length" of segments.

Similar to (2.27)–(2.29), this cross ratio has the forms

$$m_{L1}^{21} = (\infty\ Y_{L1}^2\ Y_{L1}^1\ 0) = \frac{Y_{L1}^1}{Y_{L1}^2}, \tag{4.25}$$

$$\begin{aligned} m_{L1}^{21} &= (Y_{IN1}^{SC}\ Y_{IN1}^2\ Y_{IN1}^1\ Y_{IN1}^{OC}) \\ &= \frac{Y_{IN1}^2 - Y_{IN1}^{SC}}{Y_{IN1}^2 - Y_{IN1}^{OC}} \div \frac{Y_{IN1}^1 - Y_{IN1}^{SC}}{Y_{IN1}^1 - Y_{IN1}^{OC}} = m_{L1}^2 \div m_{L1}^1, \end{aligned} \tag{4.26}$$

$$m_{L1}^{21} = (0\ V_1^2\ V_1^1\ V_1^{OC}) = \frac{V_1^2 - 0}{V_1^2 - V_1^{OC}} \div \frac{V_1^1 - 0}{V_1^1 - V_1^{OC}}, \tag{4.27}$$

$$m_{L1}^{21} = (I_1^{SC}\ I_1^2\ I_1^1\ 0) = \frac{I_1^2 - I_1^{SC}}{I_1^2 - 0} \div \frac{I_1^1 - I_1^{SC}}{I_1^1 - 0}, \tag{4.28}$$

$$m_{L1}^{21} = (I_0^{SC}\ I_0^2\ I_0^1\ I_0^{OC}) = \frac{I_0^2 - I_0^{SC}}{I_0^2 - I_0^{OC}} \div \frac{I_0^1 - I_0^{SC}}{I_0^1 - I_0^{OC}} \tag{4.29}$$

Using (4.26), we get the subsequent input conductivity

$$Y_{IN1}^2 = \frac{Y_{IN1}^{SC} + Y_{IN1}^{OC} m_{L1}^{21} m_{L1}^1}{1 + m_{L1}^{21} m_{L1}^1}. \tag{4.30}$$

Similarly, the subsequent values

$$V_1^2 = \frac{V_1^1 V_1^{OC} m_{L1}^{21}}{V_1^1 (m_{L1}^{21} - 1) + V_1^{OC}}, \tag{4.31}$$

$$I_1^2 = \frac{I_1^{SC} I_1^1}{I_1^1 (1 - m_{L1}^{21}) + I_1^{SC} m_{L1}^{21}}. \tag{4.32}$$

$$I_0^2 = \frac{I_0^{SC} + I_0^{OC} m_{L1}^{21} m_{L1}^1}{1 + m_{L1}^{21} m_{L1}^1}. \tag{4.33}$$

4.2.2 Versions of Conformities, Invariants, and Cross Ratios

There are different versions or variants of cross ratio depending on the choice of the base points and a unit point. Let us consider expression (4.19). This expression sets the conformity $Y_{L1} \to Y_{IN1}$, including negative values, as it is shown in Fig. 4.9 for the values $Y_{L1.C} = Y_{IN1.C} = \pm 1$.

Version 1

If the base points are $Y_{L1}^{OC} = 0, Y_{L1}^{SC} = \infty$ and a unit point is $Y_{L1} = Y_{L1.C} = 1$, the cross ratio

$$\tilde{m}_{L1}^1 = (\infty \;\; Y_{L1}^1 \;\; 1 \;\; 0) = \frac{1}{Y_{L1}^1}.$$

Then, for the input conductivity,

$$\tilde{m}_{L1}^1 = \left(\frac{1}{th\gamma} \;\; Y_{IN1}^1 \;\; 1 \;\; th\gamma\right) = \frac{Y_{IN1}^1 - \frac{1}{th\gamma}}{Y_{IN1}^1 - th\gamma} \div \frac{1 - \frac{1}{th\gamma}}{1 - th\gamma} = \frac{1 - Y_{IN1}^1 th\gamma}{Y_{IN1}^1 - th\gamma}.$$

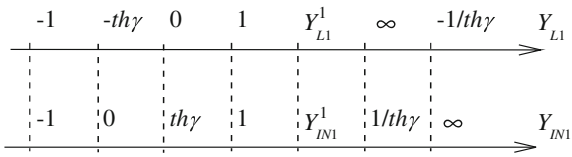

Fig. 4.9 Conformity of points of the line Y_{L1} and Y_{IN1}

We express the regime change for $Y^1_{L1} \to Y^2_{L1}$ and $Y^1_{IN1} \to Y^2_{IN1}$ as follows

$$m^{21}_{L1} = \tilde{m}^2_{L1} \div \tilde{m}^1_{L1} = (\frac{1}{th\gamma}\ Y^2_{IN1}\ Y^1_{IN1}\ th\gamma)$$
$$= \frac{1 - Y^2_{IN1} th\gamma}{Y^2_{IN1} - th\gamma} \div \frac{1 - Y^1_{IN1} th\gamma}{Y^1_{IN1} - th\gamma} = \frac{Y^1_{L1}}{Y^2_{L1}}.$$

It may be noted that the expression for the regime change and the expressions for the conductivity changes at the input and output are expressed analytically in different ways, but their numerical values are equal. In this matter, we can choose the base points and a unit point in such a way as to these expressions are the same view. This case is presented by the following version 2.

Version 2

We use the characteristic values $-1, 1$ as the base points. Then, the regime change

$$m^{21} = (-1\ \ Y^2_{L1}\ \ Y^1_{L1}\ \ 1) = \frac{Y^2_{L1} + 1}{Y^2_{L1} - 1} \div \frac{Y^1_{L1} + 1}{Y^1_{L1} - 1} = \frac{1 + \frac{Y^2_{L1} - Y^1_{L1}}{1 - Y^2_{L1} Y^1_{L1}}}{1 - \frac{Y^2_{L1} - Y^1_{L1}}{1 - Y^2_{L1} Y^1_{L1}}}.$$

The obtained expression shows that *there is a solid argumentation to introduce the value of the load change in the form*

$$Y^{21}_{L1} = \frac{Y^2_{L1} - Y^1_{L1}}{1 - Y^2_{L1} Y^1_{L1}}. \tag{4.34}$$

Then, the regime change

$$m^{21} = \frac{1 + Y^{21}_{L1}}{1 - Y^{21}_{L1}}. \tag{4.35}$$

Similarly, the same regime change and the conductivity change are resulted at the input

$$m^{21} = (-1\ \ Y^2_{IN1}\ \ Y^1_{IN1}\ \ 1) = \frac{1 + Y^2_{IN1}}{1 - Y^2_{IN1}}, \tag{4.36}$$

$$Y^{21}_{IN1} = \frac{Y^2_{IN1} - Y^1_{IN1}}{1 - Y^2_{IN1} Y^1_{IN1}}. \tag{4.37}$$

Now, we constitute the cross ratio for the initial regime. It is possible to use the point $Y^{OC}_{L1} = 0$ as a unit point. This point corresponds to the point $Y^{OC}_{IN1} = th\gamma$ in Fig. 4.9.

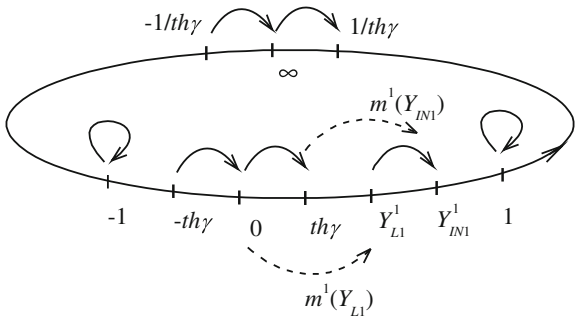

Fig. 4.10 Movement of the segment $Y_{L1}\ Y_{IN1}$ for different initial values Y_{L1}

Then

$$m^1(Y_{L1}) = (-1\ Y_{L1}^1\ 0\ 1) = \frac{1+Y_{L1}^1}{1-Y_{L1}^1},$$

$$m^1(Y_{IN1}) = (-1\ Y_{IN1}^1\ th\gamma\ 1) = \frac{1+Y_{IN1}^1}{1-Y_{IN1}^1} \div \frac{1+th\gamma}{1-th\gamma} = m^1(Y_{L1}).$$

These cross ratio are shown by dash arrows on the superposed axis in Fig. 4.10. In turn, we can consider the movement of point from the position Y_{L1} to position Y_{IN1}. This movement determines the segment $Y_{L1}\ Y_{IN1}$. The movement of this segment for different initial values Y_{L1} is shown by arrows in Fig. 4.10.

Then, the points ± 1 are fixed. It is possible to make the cross ratio for the points Y_{L1}, Y_{IN1} relatively the fixed points. This cross ratio determines the "length" of segment $Y_{L1}Y_{IN1}$ and has the view

$$m\,(Y_{L1}, Y_{IN1}) = (-1\ Y_{L1}\ Y_{IN1}\ 1).$$

It is known that the property of such a cross ratio; its value does not depend on running values Y_{L1}, Y_{IN1}. For simplification, we set $Y_{L1} = 0$, $Y_{IN1} = th\gamma$. Therefore, the cross ratio

$$m\,(Y_{L1}, Y_{IN1}) = \frac{1-th\gamma}{1+th\gamma} = K_{PM}.$$

It is seen that "length" of segment $Y_{L1}\ Y_{IN1}$ equals maximum efficiency of two-port.

Therefore, it turns out that the concept of maximum efficiency is already into this geometric interpretation, and it is not required to "think out" this definition.

Version 3

Transformation (4.19) is characterized by another invariant too. This expression for a symmetric two-port takes the form

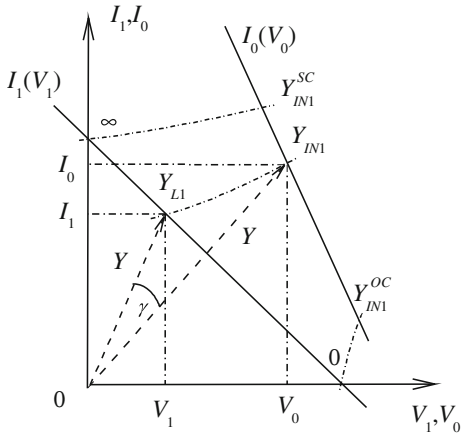

Fig. 4.11 Rotation of the radius-vector Y of constant length at the angle γ

$$\begin{bmatrix} V_0 \\ I_0\sqrt{\Delta_Y} \end{bmatrix} = \begin{bmatrix} ch\gamma & sh\gamma \\ sh\gamma & ch\gamma \end{bmatrix} \cdot \begin{bmatrix} V_1 \\ I_1\sqrt{\Delta_Y} \end{bmatrix}. \tag{4.38}$$

This transformation can be seen as rotation of radius-vector Y of constant length at angle γ in the pseudo-Euclidean plane I, V in Fig. 4.11.

The invariant is given by

$$(V_1)^2 - (I_1)^2\Delta_Y = (V_0)^2 - (I_0)^2\Delta_Y. \tag{4.39}$$

This value is the length of radius-vector Y. On the other hand, the trajectory of rotation is a hyperbola in the Euclidean plane.

Proposed interpretation corresponds to Lorenz's transformation for mechanics of relative motion [4]. In turn, expression (4.19) corresponds to the rule of addition of relativistic velocities.

4.2.3 Conformity of Cascaded Two-Ports

Let us now consider the cascade connection of two-ports *TP1* and *TP2* in Fig. 4.12. A variable conductivity Y_{L2} is the load of this connection.

At change of the load conductivity Y_{L2}, we get the family of load straight lines in Fig. 4.13. In this case, we have a projective transformation or mapping of load straight lines and conductivities $Y_{L2} \rightarrow Y_{L1} \rightarrow Y_{IN1}$ for various sections. This mapping is shown conditionally by dash-dot lines. According to (4.18), the resultant relationship $Y_{IN1}(Y_{L2})$ has the fractionally linear view.

In turn, the resultant matrix of a parameters is equal to product of the matrices for the first and second two-ports. Such a group property confirms projective transformations.

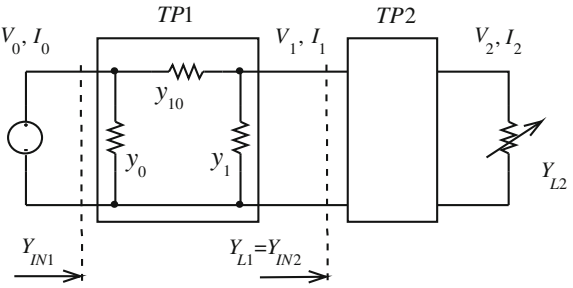

Fig. 4.12 Cascade connection of two-ports with a load conductivity

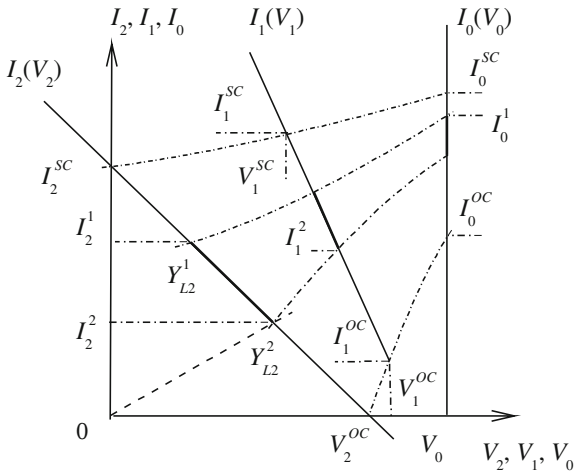

Fig. 4.13 Load straight lines for the cascade connection of two two-ports

Therefore, by (4.20) and (4.21), we constitute the cross ratio m_{L2}^1 for initial values of regime parameters relatively to the load Y_{L2}.

The conformity of all the parameters is given in Fig. 4.14.

Then, we get

$$
\begin{aligned}
m_{L2}^1 &= (Y_{L2}^{SC} \;\; Y_{L2}^1 \; Y_i \; Y_{L2}^{OC}) = \frac{Y_{L2}^1 - Y_{L2}^{SC}}{Y_{L2}^1 - Y_{L2}^{OC}} \div \frac{Y_i - Y_{L2}^{SC}}{Y_i - Y_{L2}^{OC}} = \frac{Y_i}{Y_{L2}^1}, \\
m_{L2}^1 &= (Y_{L1}^{SC} \;\; Y_{L1}^1 \; Y_{L1}^i \; Y_{L1}^{OC}) = \frac{Y_{L1}^1 - Y_{L1}^{SC}}{Y_{L1}^1 - Y_{L1}^{OC}} \div \frac{Y_{L1}^i - Y_{L1}^{SC}}{Y_{L1}^i - Y_{L1}^{OC}}, \\
m_{L2}^1 &= (Y_{IN1}^{SC} \;\; Y_{IN1}^1 \; Y_{IN1}^i \; Y_{IN1}^{OC}) = \frac{Y_{IN1}^1 - Y_{IN1}^{SC}}{Y_{IN1}^1 - Y_{IN1}^{OC}} \div \frac{Y_{IN1}^i - Y_{IN1}^{SC}}{Y_{IN1}^i - Y_{IN1}^{OC}} = \frac{Y_{IN1}^{SC} - Y_{IN1}^1}{Y_{IN1}^1 - Y_{IN1}^{OC}}.
\end{aligned}
\tag{4.40}
$$

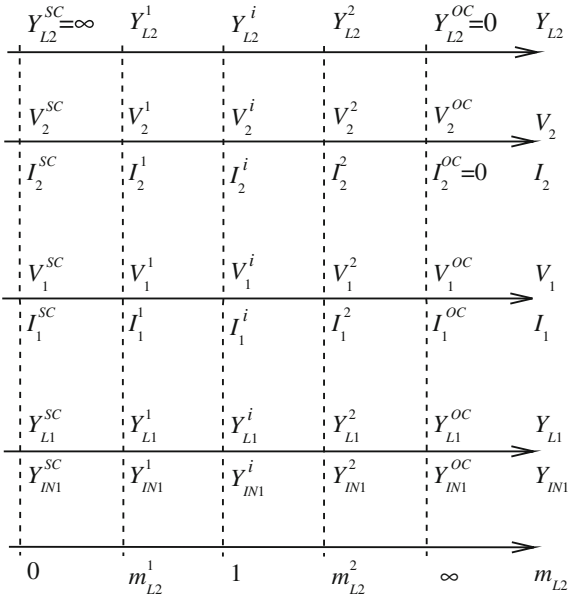

Fig. 4.14 Conformity of the regime parameters of cascaded two-ports

In the last expression,

$$Y_{IN1}^{i} = Y_{IN1}^{OC} + \frac{Y_{IN1}^{SC} - Y_{IN1}^{OC}}{2}.$$

Using (4.22)–(4.24), we may constitute the same cross ratio for all the currents and voltages. In particular, for the middle section with the parameters V_1, I_1

$$\begin{aligned} m_{L2}^{1} &= (\, V_1^{SC}\ V_1^{1}\ V_1^{i}\ V_1^{OC}) \\ &= \frac{V_1^{1} - V_1^{SC}}{V_1^{1} - V_1^{OC}} \div \frac{V_1^{i} - V_1^{SC}}{V_1^{i} - V_1^{OC}} = \frac{V_1^{1} - V_1^{SC}}{V_1^{OC} - V_1^{1}} \\ &= (\, I_1^{SC}\ I_1^{1}\ I_1^{i}\ I_1^{OC}) = \frac{I_1^{1} - I_1^{SC}}{I_1^{1} - I_1^{OC}} \div \frac{I_1^{i} - I_1^{SC}}{I_1^{i} - I_1^{OC}} = \frac{I_1^{SC} - I_1^{1}}{I_1^{1} - I_1^{OC}}, \end{aligned} \tag{4.41}$$

where

$$V_1^{i} = V_1^{OC} + \frac{V_1^{SC} - V_1^{OC}}{2}, \quad I_1^{i} = I_1^{OC} + \frac{I_1^{SC} - I_1^{OC}}{2}.$$

We consider the load change $Y_{L2}^{1} \to Y_{L2}^{2}$. This change defines the segments $Y_{L2}^{2}\, Y_{L2}^{1}$, $Y_{L1}^{2}\, Y_{L1}^{1}$, and $Y_{IN1}^{2}\, Y_{IN1}^{1}$. The cross ratio defines the same "length" of these segments

$$
\begin{aligned}
m_{L2}^{21} &= (Y_{L2}^{SC}\ \ Y_{L2}^{2}\ Y_{L2}^{1}\ Y_{L2}^{OC}) = \frac{Y_{L2}^{2}-Y_{L2}^{SC}}{Y_{L2}^{2}-Y_{L2}^{OC}} \div \frac{Y_{L2}^{1}-Y_{L2}^{SC}}{Y_{L2}^{1}-Y_{L2}^{OC}} = \frac{Y_{L2}^{1}}{Y_{L2}^{2}} \\
&= (Y_{L1}^{SC}\ \ Y_{L1}^{2}\ Y_{L1}^{1}\ Y_{L1}^{OC}) = \frac{Y_{L1}^{2}-Y_{L1}^{SC}}{Y_{L1}^{2}-Y_{L1}^{OC}} \div \frac{Y_{L1}^{1}-Y_{L1}^{SC}}{Y_{L1}^{1}-Y_{L1}^{OC}} \\
&= (Y_{IN1}^{SC}\ \ Y_{IN1}^{2}\ Y_{IN1}^{1}\ Y_{IN1}^{OC}) = \frac{Y_{IN1}^{2}-Y_{IN1}^{SC}}{Y_{IN1}^{2}-Y_{IN1}^{OC}} \div \frac{Y_{IN1}^{1}-Y_{IN1}^{SC}}{Y_{IN1}^{1}-Y_{IN1}^{OC}}.
\end{aligned}
\tag{4.42}
$$

Using (4.27)–(4.29), we may constitute the same cross ratio for all the currents and voltages. In particular, for the middle section with the parameters V_1, I_1, we get

$$
\begin{aligned}
m_{L2}^{21} &= (V_1^{SC}\ \ V_1^{2}\ V_1^{1}\ V_1^{OC}) = \frac{V_1^{2}-V_1^{SC}}{V_1^{2}-V_1^{OC}} \div \frac{V_1^{1}-V_1^{SC}}{V_1^{1}-V_1^{OC}} \\
&= (I_1^{SC}\ \ I_1^{2}\ I_1^{1}\ I_1^{OC}) = \frac{I_1^{2}-I_1^{SC}}{I_1^{2}-I_1^{OC}} \div \frac{I_1^{1}-I_1^{SC}}{I_1^{1}-I_1^{OC}}.
\end{aligned}
\tag{4.43}
$$

Using (4.42), we get the subsequent conductivity

$$
Y_{L1}^{2} = \frac{Y_{L1}^{SC} + N_{L1}^{1} Y_{L1}^{OC} m_{L2}^{21}}{1 + N_{L1}^{1} m_{L2}^{21}}, \quad N_{L1}^{1} = \frac{Y_{L1}^{SC} - Y_{L1}^{1}}{Y_{L1}^{1} - Y_{L1}^{OC}}. \tag{4.44}
$$

Similar to (4.33), the subsequent values

$$
V_1^{2} = \frac{V_1^{SC} + V_1^{OC} m_{L2}^{21} m_{L2}^{1}}{1 + m_{L2}^{21} m_{L2}^{1}}, \quad I_1^{2} = \frac{I_1^{SC} + I_1^{OC} m_{L2}^{21} m_{L2}^{1}}{1 + m_{L2}^{21} m_{L2}^{1}}. \tag{4.45}
$$

Proceeding from such a geometrical interpretation, it is possible to give the following added definition [8] of regimes to Chap. 2

- Invariance of regimes and their changes for all sections of circuit.

These invariant relationships of a cascaded circuit define the original "*conformity principle of regimes*".

Therefore, the definition of regime by cross ratios (4.40)–(4.43) removes the indeterminateness in the choice of possible relative expressions for all parameters and sections of circuit.

Example Let us consider a circuit with given elements in Fig. 4.15.

The first two-port has the following Y parameters

$$
Y_{10} = y_{10} = 4, Y_{00} = y_0 + y_{10} = 5, Y_{11} = y_1 + y_{10} = 6.4, \Delta_Y = Y_{00}Y_{11} - (Y_{10})^2 = 16, \sqrt{\Delta_Y} = 4.
$$

Equations (4.14) and (4.18)

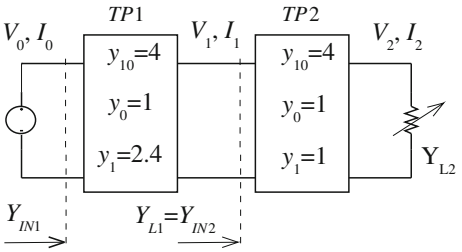

Fig. 4.15 Example of the cascaded circuit with the load conductivity

$$\begin{bmatrix} V_0 \\ I_0 \end{bmatrix} = \begin{bmatrix} a_{11} & a_{12} \\ a_{21} & a_{22} \end{bmatrix} \cdot \begin{bmatrix} V_1 \\ I_1 \end{bmatrix} = \begin{bmatrix} 1.6 & 0.25 \\ 4 & 1.25 \end{bmatrix} \cdot \begin{bmatrix} V_1 \\ I_1 \end{bmatrix},$$
$$Y_{IN1} = \frac{I_0}{V_0} = \frac{a_{22}Y_{L1} + a_{21}}{a_{12}Y_{L1} + a_{11}} = \frac{1.25 \cdot Y_{L1} + 4}{0.25 \cdot Y_{L1} + 1.6}.$$

Inverse expression (4.15)

$$\begin{bmatrix} V_1 \\ I_1 \end{bmatrix} = \begin{bmatrix} 1.25 & -0.25 \\ -4 & 1.6 \end{bmatrix} \cdot \begin{bmatrix} V_0 \\ I_0 \end{bmatrix} \tag{4.46}$$

For the second two-port

$$\begin{bmatrix} V_1 \\ I_1 \end{bmatrix} = \begin{bmatrix} 1.25 & 0.25 \\ 2.25 & 1.25 \end{bmatrix} \cdot \begin{bmatrix} V_2 \\ I_2 \end{bmatrix},$$
$$\begin{bmatrix} V_2 \\ I_2 \end{bmatrix} = \begin{bmatrix} 1.25 & -0.25 \\ -2.25 & 1.25 \end{bmatrix} \cdot \begin{bmatrix} V_1 \\ I_1 \end{bmatrix}, \tag{4.47}$$
$$Y_{IN2} = Y_{L1} = \frac{I_1}{V_1} = \frac{1.25 \cdot Y_{L2} + 2.25}{0.25 \cdot Y_{L2} + 1.25}.$$

The resultant transformations of the output–input

$$\begin{bmatrix} V_0 \\ I_0 \end{bmatrix} = \begin{bmatrix} 1.6 & 0.25 \\ 4 & 1.25 \end{bmatrix} \cdot \begin{bmatrix} 1.25 & 0.25 \\ 2.25 & 1.25 \end{bmatrix} \cdot \begin{bmatrix} V_2 \\ I_2 \end{bmatrix} = \begin{bmatrix} 2.5625 & 0.7125 \\ 7.8125 & 2.5625 \end{bmatrix} \cdot \begin{bmatrix} V_2 \\ I_2 \end{bmatrix},$$
$$Y_{IN1} = \frac{2.5625 \cdot Y_{L2} + 7.8125}{0.7125 \cdot Y_{L2} + 2.5625}. \tag{4.48}$$

Let the initial and subsequent load conductivities be given as

$$Y_{L2}^1 = 10.43, \quad Y_{L2}^2 = 1.08.$$

Using (4.48), we get

$$Y_{IN1}^1 = 3.456, \quad Y_{IN1}^2 = 3.175.$$
$$I_0^1 = Y_{IN1}^1 V_0 = 34.56, \quad I_0^2 = Y_{IN1}^2 V_0 = 31.75.$$

By (4.46), we obtain

$$V_1^1 = 3.86, \quad I_1^1 = 15.3, \quad Y_{L1}^1 = 15.3 \div 3.86 = 3.963;$$
$$V_1^2 = 4.562, \quad I_1^2 = 10.8, \quad Y_{L1}^2 = 10.8 \div 4.562 = 2.367.$$

Now, by (4.47)

$$V_2^1 = 1, \quad I_2^1 = 10.43, \quad Y_{L1}^1 = 10.43;$$
$$V_2^2 = 3, \quad I_1^2 = 3.241, \quad Y_{L1}^2 = 1.08.$$

The calculated regime parameters are shown in Fig. 4.16.
Initial regime cross ratio (4.40)

$$m_{L2}^1 = (Y_{L2}^{SC} \ \ Y_{L2}^1 \ Y_i \ Y_{L2}^{OC}) = \frac{10.43 - \infty}{10.43 - 0} \div \frac{3.597 - \infty}{3.597 - 0} = \frac{3.597}{10.43} = 0.344,$$
$$m_{L2}^1 = (Y_{L1}^{SC} \ \ Y_{L1}^1 \ Y_{L1}^i \ Y_{L1}^{OC}) = \frac{3.964 - 5}{3.964 - 1.8} \div \frac{3.138 - 5}{3.138 - 1.8} = 0.344,$$
$$m_{L2}^1 = (Y_{IN1}^{SC} \ \ Y_{IN1}^1 \ Y_{IN1}^i \ Y_{IN1}^{OC})$$
$$= \frac{3.456 - 3.596}{3.456 - 3.049} \div \frac{3.323 - 3.596}{3.323 - 3.049} = 0.344 \div 1 = 0.344.$$

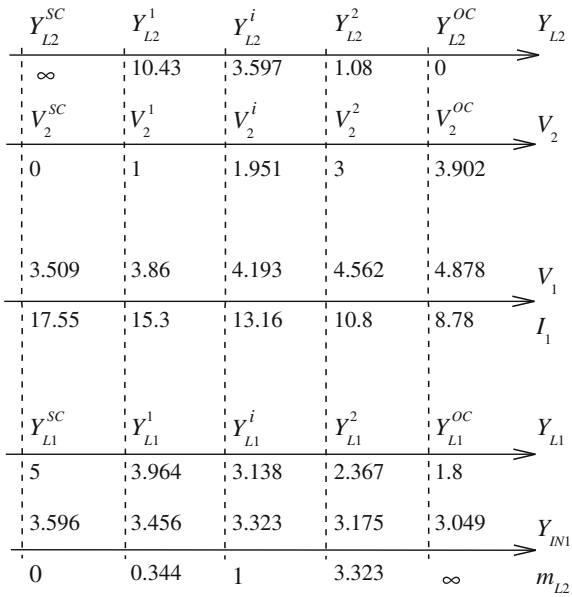

Fig. 4.16 Conformity of the calculated regime parameters

Cross ratio (4.41) for the middle section

$$m_{L2}^1 = (V_1^{SC}\ V_1^1\ V_1^i\ V_1^{OC}) = \frac{V_1^1 - V_1^{SC}}{V_1^{OC} - V_1^1} = \frac{3.86 - 3.509}{4.878 - 3.86} = 0.344,$$
$$m_{L2}^1 = (I_1^{SC}\ I_1^1\ I_1^i\ I_1^{OC}) = \frac{I_1^{SC} - I_1^1}{I_1^1 - I_1^{OC}} = \frac{17.55 - 15.3}{15.3 - 8.78} = 0.344.$$

Regime change (4.42) for the conductivities

$$m_{L2}^{21} = (Y_{L2}^{SC}\ Y_{L2}^2\ Y_{L2}^1\ Y_{L2}^{OC}) = \frac{Y_{L2}^1}{Y_{L1}^2} = \frac{10.43}{1.08} = 9.66,$$
$$m_{L2}^{21} = (Y_{L1}^{SC}\ Y_{L1}^2\ Y_{L1}^1\ Y_{L1}^{OC}) = \frac{Y_{L1}^2 - Y_{L1}^{SC}}{Y_{L1}^2 - Y_{L1}^{OC}} \div \frac{Y_{L1}^1 - Y_{L1}^{SC}}{Y_{L1}^1 - Y_{L1}^{OC}}$$
$$= \frac{2.367 - 5}{2.367 - 1.8} \div \frac{3.964 - 5}{3.964 - 1.8} = 4.64 \div 0.478 = 9.66,$$
$$m_{L2}^{21} = (Y_{IN1}^{SC}\ Y_{IN1}^2\ Y_{IN1}^1\ Y_{IN1}^{OC}) = \frac{Y_{IN1}^2 - Y_{IN1}^{SC}}{Y_{IN1}^2 - Y_{IN1}^{OC}} \div \frac{Y_{IN1}^1 - Y_{IN1}^{SC}}{Y_{IN1}^1 - Y_{IN1}^{OC}}$$
$$= \frac{3.175 - 3.596}{3.175 - 3.049} \div \frac{3.456 - 3.596}{3.456 - 3.049} = 3.323 \div 0.344 = 9.66.$$

Regime change (4.43) for the middle section

$$m_{L2}^{21} = (V_1^{SC}\ V_1^2\ V_1^1\ V_1^{OC}) = \frac{V_1^2 - V_1^{SC}}{V_1^2 - V_1^{OC}} \div \frac{V_1^1 - V_1^{SC}}{V_1^1 - V_1^{OC}}$$
$$= \frac{4.562 - 3.509}{4.562 - 4.878} \div \frac{3.86 - 3.509}{3.86 - 4.878} = 3.323 \div 0.344 = 9.66,$$
$$m_{L2}^{21} = (I_1^{SC}\ I_1^2\ I_1^1\ I_1^{OC}) = \frac{I_1^2 - I_1^{SC}}{I_1^2 - I_1^{OC}} \div \frac{I_1^1 - I_1^{SC}}{I_1^1 - I_1^{OC}}$$
$$= \frac{10.8 - 17.55}{10.8 - 8.78} \div \frac{15.3 - 17.55}{15.3 - 8.78} = 9.66.$$

The subsequent regime value

$$m_{L2}^2 = m_{L2}^{21} m_{L2}^1 = 9.66 \cdot 0.344 = 3.323.$$

We are checking the subsequent conductivity Y_{L1} by (4.44)

$$Y_{L1}^2 = \frac{Y_{L1}^{SC} + N_{L1}^1 Y_{L1}^{OC} m_{L2}^{21}}{1 + N_{L1}^1 m_{L2}^{21}} = \frac{5 + 0.478 \cdot 1.8 \cdot 9.66}{1 + 0.478 \cdot 9.66} = 2.367,$$
$$N_{L1}^1 = \frac{Y_1^{SC} - Y_{L1}^1}{Y_{L1}^1 - Y_1^{OC}} = 0.478.$$

The check of the subsequent values V_1, I_1 by (4.45)

$$V_1^2 = \frac{V_1^{SC} + V_1^{OC} m_{L2}^{21} m_{L2}^1}{1 + m_{L2}^{21} m_{L2}^1} = \frac{3.509 + 4.878 \cdot 3.323}{1 + 3.323} = \frac{19.72}{4.323} = 4.56,$$

$$I_1^2 = \frac{I_1^{SC} + I_1^{OC} m_{L2}^{21} m_{L2}^1}{1 + m_{L2}^{21} m_{L2}^1} = \frac{17.55 + 8.78 \cdot 3.323}{1 + 3.323} = 10.8.$$

4.3 Use of Invariant Properties for the Transfer of Measuring Signals

Different sensors of physical values are used for monitoring of technical or natural objects. For these, usually remote devices, it is necessary to transmit the measuring signals, for example, over wire lines. Usually, digital signals are used for this transmission. But such disadvantages as low noise stability, complicated and expensive equipment, separate wire lines of power supply and communication take place in digital systems. Therefore, researches and elaborations of easy-to-use systems for transmitting signals are important.

Invariant properties of two-port networks allow transmitting the measuring signals, using even the joint or combined wire line for communication and power supply [5, 12]. As it was shown, the value of affine and cross ratio does not depend on two-port network (wire line) parameters, accuracy of measuring devices, and influence of noises. The parameters of this communication wire line, for example, joint with a power supply line, are defined by both own parameters and current consumed by other devices.

4.3.1 Transfer of Signals over an Unstable Two-Port

Let us consider the transfer of signals for the following simple examples. More complex case of transmitting over a joint wire line for communication and power supply is presented in [10].

Example 1 The value of cross ratio m_{L1} is accepted as a transmitted analog signal V_S; that is, $V_S = m_{L1}$. The structure of the appliance, designed to this transfer, is shown in Fig. 4.17a.

In a short time $t_1, t_2, \ldots t_5$, when the parameters of this circuit do not change, the four samples of load conductivity are transmitting by connecting the respective conductivities $Y_{L1}^{SC}, Y_{L1}^1, Y_{L1}^i, Y_{L1}^{OC}$. The connection is realized by a multichannel switching and multi-output generator *Gen* with a pulse period T_K. The conductivity Y_{L1}^1 is the signal or information sample. Therefore, its value $Y_{L1}^1(V_S)$ is calculated by a unit F for the running signal value V_S.

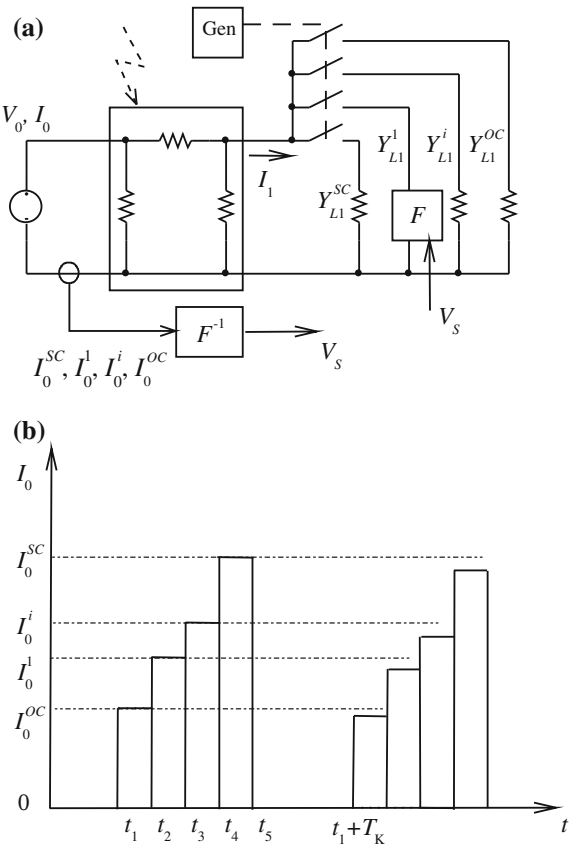

Fig. 4.17 **a** System of an accurate transmission of signal by conductivities, **b** diagram of the input current

Let us give expression of cross ratio (4.20). In general case

$$m^1_{L1} = (Y^{SC}_{L1}\ Y^1_{L1}\ Y^i_{L1}\ Y^{OC}_{L1}) = \frac{Y^1_{L1} - Y^{SC}_{L1}}{Y^1_{L1} - Y^{OC}_{L1}} \div \frac{Y^i_{L1} - Y^{SC}_{L1}}{Y^i_{L1} - Y^{OC}_{L1}} = V_S.$$

From this we find, similar to (4.44), the value

$$Y^1_{L1} = \frac{Y^{SC}_{L1} + V_S N^i_{L1} Y^{OC}_{L1}}{1 + V_S N^i_{L1}} = F(V_S), \quad N^i_{L1} = \frac{Y^{SC}_{L1} - Y^i_{L1}}{Y^i_{L1} - Y^{OC}_{L1}}.$$

In particular case

$$m^1_{L1} = (\infty\ Y^1_{L1}\ Y^i_{L1}\ 0) = \frac{Y^i_{L1}}{Y^1_{L1}} = V_S, \quad Y^1_{L1} = \frac{Y^i_{L1}}{V_S}.$$

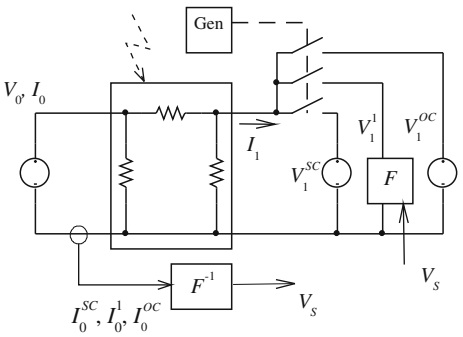

Fig. 4.18 System of an accurate transmission of signal by voltage sources

At the input of the circuit, the cross ratio or the signal is calculated by a unit F^{-1} similar to (4.24). For this purpose, the measured input currents $I_0^{SC}, I_0^1, I_0^i, I_0^{OC}$, shown in Fig. 4.17b, are used; that is,

$$V_S = m_{L1}^1 = (I_0^{SC}\ I_0^1\ I_0^i\ I_0^{OC}) = \frac{I_0^1 - I_0^{SC}}{I_0^1 - I_0^{OC}} \div \frac{I_0^i - I_0^{SC}}{I_0^i - I_0^{OC}} = F^{-1}(I_0^1).$$

The structure of this expression shows that measuring errors of currents mutually are reduced. The process of connection and calculation is repeated every period T_K. If during this time the parameters of two-port network changed, the values of input currents changed too (for example, the currents decreased in Fig. 4.17b). But the cross ratio value remains the same.

Example 2 The value of affine ratio n_1 is accepted as a transmitted analog signal V_S; that is, $V_S = n_1$. The structure of the appliance is shown in Fig. 4.18.

In a short time, the three samples of load voltages are transmitted by connecting the respective voltage sources $V_1^{OC}, V_1^1, V_1^{SC}$. The voltage V_1^1 is the information sample. Therefore, its value $V_1^1(V_S)$ is calculated by a unit F for the running signal value V_S.

We use expression of affine ratio (2.6) or (4.5)

$$n_1^1 = \frac{V_1^{OC} - V_1^1}{V_1^{OC} - V_1^{SC}} = V_S.$$

From this,

$$V_1^1 = V_1^{OC} - V_S(V_1^{OC} - V_1^{SC}) = F(V_S).$$

A unit F^{-1} calculates affine ratio (4.5) or the signal

$$V_S = n_1^1 = (I_0^1\ I_0^{OC}\ I_0^{SC}) = \frac{I_0^1 - I_0^{OC}}{I_0^{SC} - I_0^{OC}} = F^{-1}(I_0^1).$$

The structure of this expression shows that measuring errors of currents mutually are reduced. The process of connection and calculation is repeated by period T_K.

Also, we may use affine ratio (2.7)

$$V_S = \frac{V_1^{OC} - V_1^1}{V_1^1 - V_1^{SC}} = \frac{I_0^1 - I_0^{OC}}{I_0^{SC} - I_0^1}.$$

Then, the information sample

$$V_1^1 = \frac{V_1^{OC} + V_S V_1^{SC}}{V_S + 1}.$$

4.3.2 Conductivity Measurement by an Unstable Two-Port

Let us consider the circuit in Fig. 4.19. The action of this appliance is similar to the system in Fig. 4.17.

We need to calculate the conductivity value Y_{L1}^1 of a resistive sensor by input currents. The given conductivities $Y_{L1}^{SC}, Y_{L1}^i, Y_{L1}^{OC}$ are reference conductivities.

Using the known cross ratio

$$m_{L1}^1 = (Y_{L1}^{SC}\ \ Y_{L1}^1\ Y_{L1}^i\ Y_{L1}^{OC}) = \frac{Y_{L1}^1 - Y_{L1}^{SC}}{Y_{L1}^1 - Y_{L1}^{OC}} \div \frac{Y_{L1}^i - Y_{L1}^{SC}}{Y_{L1}^i - Y_{L1}^{OC}},$$

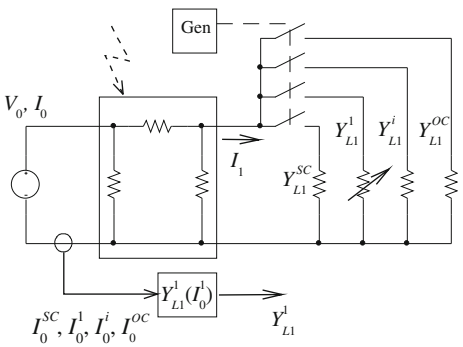

Fig. 4.19 System of accurate measurement of conductivity

we find the value

$$Y_{L1}^1 = \frac{Y_{L1}^{SC} + N_{L1}^i Y_{L1}^{OC} m_{L1}^1}{1 + N_{L1}^i m_{L1}^1} = Y_{L1}^1(m_{L1}^1), \quad N_{L1}^i = \frac{Y_{L1}^{SC} - Y_{L1}^i}{Y_{L1}^i - Y_{L1}^{OC}}.$$

On the other hand, the cross ratio, by the input currents $I_0^{SC}, I_0^1, I_0^i, I_0^{OC}$, has the view

$$\begin{aligned} m_{L1}^1 &= (I_0^{SC}\ I_0^1\ I_0^i\ I_0^{OC}) \\ &= \frac{I_0^1 - I_0^{SC}}{I_0^1 - I_0^{OC}} \div \frac{I_0^i - I_0^{SC}}{I_0^i - I_0^{OC}} = m_{L1}^1(I_0). \end{aligned}$$

Using this expression, we obtain the value $Y_{L1}^1(I_0)$.

4.4 Deviation from the Maximum Efficiency of a Two-Port

We use the results of Sects. 1.5.1 and 2.3. Let us consider a more complex case of a quadratic curve, as the efficiency of a two-port in accordance with expression (1.34)

$$K_P = K_G \frac{1 - K_G}{A - K_G}. \tag{4.49}$$

This expression represents a hyperbola in Fig. 4.20 for all area of load changes. The positive load consumes energy; the maximum power transfer ratio (1.33)

$$K_P^+ = (\sqrt{A} - \sqrt{A-1})^2. \tag{4.50}$$

Then, the corresponding voltage transfer ratio

$$K_G^+ = A - \sqrt{A(A-1)}. \tag{4.51}$$

In turn, the negative load returns energy and we get the corresponding maximum values

$$K_P^- = (\sqrt{A} + \sqrt{A-1})^2, \quad K_G^- = A + \sqrt{A(A-1)}. \tag{4.52}$$

Next, we must determine all the characteristic points [6, 11]. Obviously, there are points $B_1, 0, K_P^-, 1, A_1, K_P^+$ by Fig. 4.20b. These points correspond to points $T = \infty, 0, K_G^-, 1, A, K_G^+$ of the axis K_G.

It is possible to take up the points $0, 1$ as the base points and the point K_G^- as a unit point. But visibly, the other characteristic points have to be defined relatively to these basic points and not depend on the parameter A of comparable two-ports.

Therefore, we must, at first, define the possible systems of all the characteristic points. To do this, we will study a regime symmetry of efficiency using the regime symmetry for the load power of Sect. 2.3.

4.4.1 Regime Symmetry for the Input Terminals

In Fig. 4.20b, the pole S and polar TA_1 determine the mapping or symmetry of the region of power delivery by the voltage source V_0 (above of the polar) on the region of power consumption of this voltage source (below of the polar). The point K_P^+ passes into the point K_P^-. Points B_1, A_1 are the fixed base points and $K_G(B_1) = \infty$, $K_G(A_1) = A$. A hyperbola point is assigned by the hyperbolic rotation of radius-vector $R_S S$.

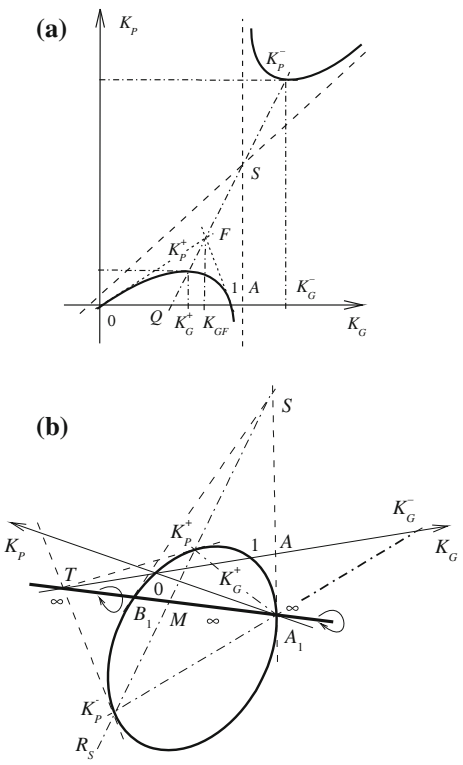

Fig. 4.20 **a** Efficiency of a two-port for load changes into the Cartesian coordinates, **b** this efficiency is as closed curve in projective coordinates

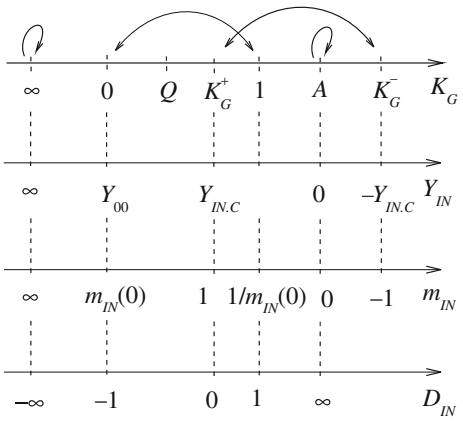

Fig. 4.21 Mutual mapping of the characteristic points and the correspondence of input values

In turn, the pole T and polar SM determine the mapping or symmetry of the hyperbola relatively to the straight line $K_P^+ K_P^-$ or to the points of maximum efficiency.

For the pole T, the following correspondences take place.

We believe harmonic conjugate points $T, 0, Q, 1$ onto the line TQ or the axis K_G. Therefore, these points correspond to the points $K_G(T) = \infty, 0$, $K_G(Q) = 0.5, 1$. The mutual mapping of the points $0, 1$ relatively to Q is shown by arrow in Fig. 4.21.

Similarly, for the pole S, the following correspondences take place.

We believe harmonic conjugate points S, K_P^+, M, K_P^-, which correspond to the points A, K_G^+, ∞, K_G^- of the axis K_G. The mutual mapping of the points K_G^+, K_G^- relatively to A, ∞ is shown by arrow in Fig. 4.21.

Let us use the points A, ∞ as the base points and K_G^+ as a unit point. Therefore, a running regime point is expressed by cross ratio

$$\begin{aligned} m_{IN} &= (\infty\ K_G^+\ K_G\ A) = \frac{A - K_G}{\sqrt{A(A-1)}} \\ &= (\infty\ Y_{IN.C}\ Y_{IN}\ 0) = \frac{Y_{IN}}{Y_{IN.C}}. \end{aligned} \tag{4.53}$$

This value is the deviation of K_G from the point K_G^+. The correspondence of the values K_G, Y_{IN}, m_{IN} is shown in Fig. 4.21.

Now, it is necessary to check the cross ratios for the points 0, 1

$$m_{IN}(0) = \sqrt{\frac{A}{A-1}} = \frac{Y_{00}}{Y_{IN.C}}, \quad m_{IN}(1) = \sqrt{\frac{A-1}{A}} = \frac{1}{m_{IN}(0)}. \tag{4.54}$$

The modules of these values are equal to each other if we use the hyperbolic metric

$$H_{IN}(0) = H_{IN}(1) = Ln[m_{IN}(0)].$$

Then, expression (4.53) becomes

$$H_{IN} = Ln[m_{IN}].$$

Therefore, we may introduce the normalized distance or relative deviation from the matched regime

$$D_{IN} = \frac{H_{IN}}{H_{IN}(0)} = \frac{Ln[m_{IN}]}{Ln[m_{IN}(0)]}. \tag{4.55}$$

The inverse expression

$$m_{IN} = [m_{IN}(0)]^{D_{IN}}$$

The expansion of this formula by (4.53) and (4.54) gives

$$\frac{A - K_G}{A - K_G^+} = \left(\frac{A}{A-1}\right)^{D_{IN}/2}, \quad \frac{Y_{IN}}{Y_{IN.C}} = \left(\frac{Y_{00}}{Y_{IN.C}}\right)^{D_{IN}}. \tag{4.56}$$

The first member of these equations is the relative deviation but this deviation is determined by a value D_{IN} and by parameters of a circuit (the second member).

If it is necessary to set any equal deviation by K_G for different circuits, we get

$$K_G = A - \sqrt{A(A-1)}\left(\frac{A}{A-1}\right)^{D_{IN}/2}. \tag{4.57}$$

4.4.2 Regime Symmetry for the Output or Load

In Fig. 4.22, the pole F and polar TQ, as the axis K_G, determine the mapping or symmetry of the region of power consumption by the load (above of the polar) on

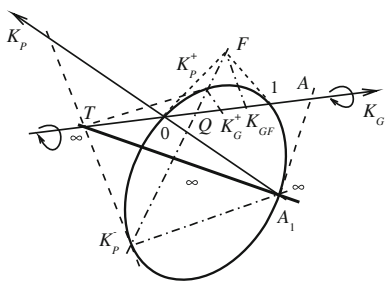

Fig. 4.22 Symmetry of the efficiency relatively to the axis K_G

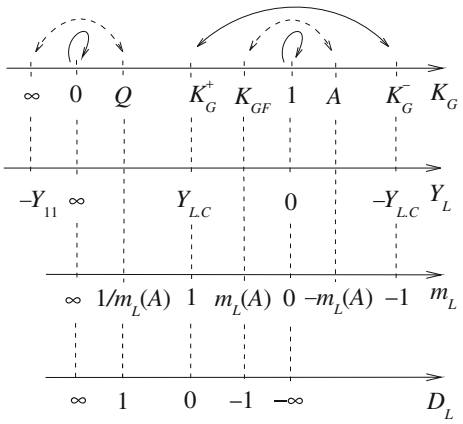

Fig. 4.23 Mutual mapping of the characteristic points and the correspondence of load values

the region of power return of this load (below of the polar). The point K_P^+ passes into the point K_P^-. The Points 0, 1 are the fixed base points.

In turn, the pole T and polar FQ are a complementary system and determine the mapping or symmetry of the hyperbola relatively to the straight line $K_P^+ K_P^-$ or to the points of maximum efficiency.

For the pole T, the following correspondences take place.

We believe harmonic conjugate points $T, 0, Q, 1$ onto the line TQ. The mutual mapping of the points $T = \infty, Q$ relatively to the points 0, 1 is shown by dash arrow in Fig. 4.23.

Similarly, for the pole F, the following correspondences take place.

We believe harmonic conjugate points F, K_P^+, Q, K_P^-, which correspond to the points $K_{GF}, K_G^+, 0.5, K_G^-$ of the axis K_G. The mutual mapping of the points K_G^+, K_G^- relatively to $0.5, K_{GF} = A/(2A-1)$ is shown by arrow in Fig. 4.23.

Let us use the point K_G^+ as a unit point. Therefore, a running regime point is expressed by cross ratio

$$\begin{aligned} m_L &= (0\ K_G^-\ K_G\ 1) = \frac{1-K_G}{K_G}\sqrt{\frac{A}{A-1}} \\ &= (\infty\ Y_{L.C}\ Y_L\ 0) = \frac{Y_L}{Y_{L.C}}. \end{aligned} \tag{4.58}$$

The correspondence of the values K_G, Y_L, m_L is shown in Fig. 4.23.

Now, it is necessary to check the cross ratio for the rest characteristic points, the points ∞, A

$$m_L(\infty) = -\sqrt{\frac{A}{A-1}} = -\frac{Y_{11}}{Y_{L.C}}, \quad m_L(A) = -\sqrt{\frac{A-1}{A}} = \frac{1}{m_L(\infty)}. \tag{4.59}$$

The negative values show that these points disposed into "external" area of the base points. We map these points into "internal" area and obtain the harmonic conjugate points $0.5, K_G(F)$ shown by dash arrows.

Similarly to (4.54) and (4.55), we may at once write the following expressions for deviation D_L relatively to the load

$$\frac{1-K_G}{K_G}\sqrt{\frac{A}{A-1}} = \left(\frac{A}{A-1}\right)^{D_L/2}, \quad \frac{Y_L}{Y_{L.C}} = \left(\frac{Y_{11}}{Y_{L.C}}\right)^{D_L}. \tag{4.60}$$

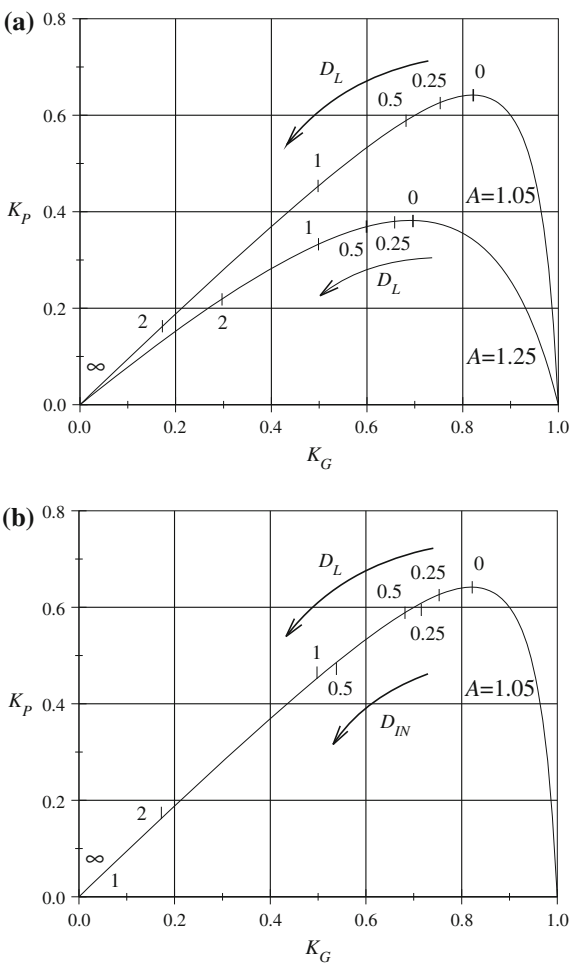

Fig. 4.24 **a** Deviation for two hyperboles relatively to the load, **b** comparison of deviations relatively to the load and input of one two-port

If it is necessary to set any equal deviation by K_G for different circuits, we get

$$K_G = \frac{1}{1 + \sqrt{\frac{A-1}{A}}\left(\frac{A}{A-1}\right)^{D_L/2}}. \tag{4.61}$$

As an example, the calibration of the hyperboles for two parameters A by deviation D_L of (4.61) is given in Fig. 4.24a. The comparison of calibration by D_{IN} of (4.57) and D_L is shown in Fig. 4.24b.

4.5 Effectiveness of Modular Connections

4.5.1 Complementary Knowledge About a Two-Port

At first, we develop the results of Sect. 4.4. Using Eq. (4.13), we pass on to the input and output power of a two-port

$$\begin{aligned} P_0 &= I_0 V_0 = Y_{00}(V_0)^2 - Y_{10} V_0 V_1 \\ P_1 &= I_1 V_1 = Y_{10} V_0 V_1 - Y_{11}(V_1)^2. \end{aligned} \tag{4.62}$$

The maximum input power at *SC* output, when $V_1 = 0$,

$$P_{0M} = Y_{00}(V_0)^2. \tag{4.63}$$

Then, the output current

$$I_1^{SC} = Y_{10} V_0.$$

We will use the Thévenin equivalent generator parameters. The maximum output voltage at *OC* output, when $I_1 = 0$,

$$V_1^{OC} = \frac{Y_{10}}{Y_{11}} V_0.$$

The maximum output power of the Thévenin equivalent generator

$$P_{GM} = V_1^{OC} I_1^{SC} = \frac{(Y_{10})^2}{Y_{11}} (V_0)^2. \tag{4.64}$$

In turn, the known value, as the effectiveness parameter,

$$A = ch^2\gamma = \frac{P_{0M}}{P_{GM}}. \tag{4.65}$$

Taking into account expressions (4.62)–(4.65), we obtain the following equation

$$\frac{P_1}{P_{0M}} = \left(1 - \frac{P_0}{P_{0M}}\right) - A\left(1 - \frac{P_0}{P_{0M}}\right)^2.$$

It is possible to consider $P_{0M} = 1$. Therefore,

$$P_1 = (1 - P_0) - A(1 - P_0)^2. \tag{4.66}$$

As it was told, expression (4.49) represents the hyperbola in Fig. 4.20 with the center S. This center coordinate corresponds to the value

$$K_{PS} = 2A - 1. \tag{4.67}$$

Using (4.50) and (4.52), we get the following equalities

$$K_P^+ = K_{PS} - 2\sqrt{A(A-1)}, \quad K_P^- = K_{PS} + 2\sqrt{A(A-1)}. \tag{4.68}$$

Therefore,

$$K_P^+ + K_P^- = 2K_{PS}.$$

4.5.2 *Parallel Connection of Two Converters*

Let us consider two regulable converters or voltage regulators $VR1, VR2$ with a common load R_1 in Fig. 4.25a. Two-ports $TP1, TP2$ with the corresponding effectiveness parameters A_1, A_2 are losses of these regulators are shown in Fig. 4.25b.

Taking into account the designations of the input and output powers, we form the following system of the equations

$$P_0 = P_{01} + P_{02}$$
$$P_1 = P_{11} + P_{12}.$$

We may believe that the corresponding maximum input powers are equal to $P_{01M} = P_{02M} = 1$.

Then, using (4.66), the efficiency of this modular connection takes the view

$$K_P = \frac{P_1}{P_0} = \frac{(1 - P_{01}) - A_1(1 - P_{01})^2 + (1 - P_{02}) - A_2(1 - P_{02})^2}{P_{01} + P_{02}}. \tag{4.69}$$

This equation $K_P(P_{01}, P_{02})$ represents a two-sheeted hyperboloid with the center S. Therefore, for this surface, we get characteristic regime curves besides characteristic regime points [7]. The center coordinate corresponds to the value

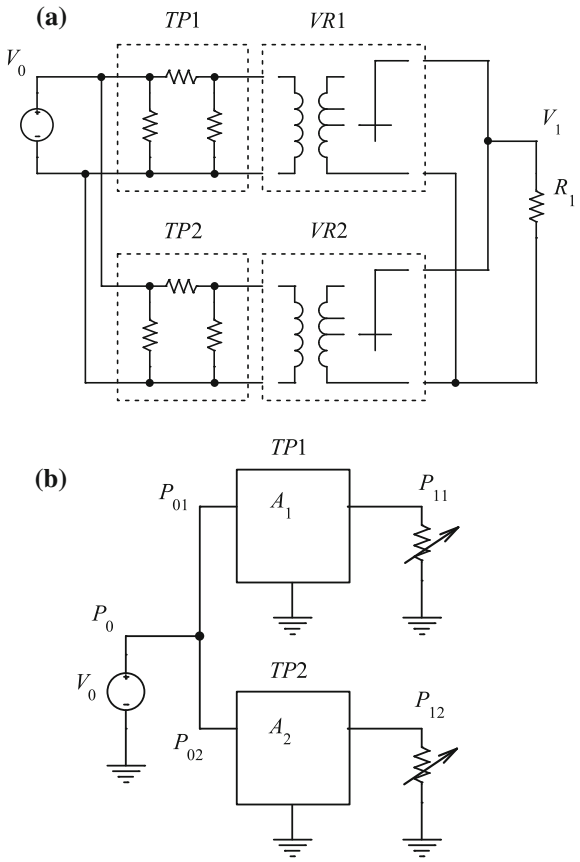

Fig. 4.25 **a** Parallel connection of two regulable converters with losses, **b** its equivalent circuit

$$K_{PS} = \frac{4A_1A_2}{A_1 + A_2} - 1. \tag{4.70}$$

Similarly to (4.67), we may introduce the value

$$A = \frac{2A_1A_2}{A_1 + A_2}. \tag{4.71}$$

This value determines the total effectiveness parameter of the given modular connection. In turn, equalities (4.68) take place, where the values K_P^+, K_P^- are the total maximum efficiency.

We must note that expression (4.71), as the parallel connection of two resistances R_1, R_2, corresponds to the harmonic conjugacy of four points or three

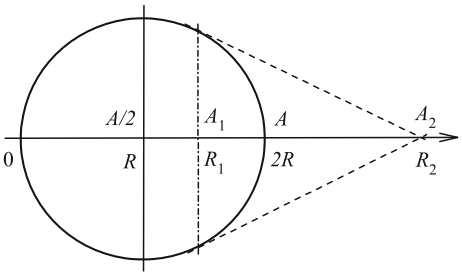

Fig. 4.26 Interpretation of four harmonic conjugate points $0, R_1, 2R, R_2$ and $0, A_1, A, A_2$

segments. Let us consider this property in details with the aid of Fig. 4.26. The points A_1, A_2 are harmonic conjugate relatively to the base points $0, A$. Also, the points R_1, R_2 are harmonic conjugate relatively to the base points 0, $2R$.

Therefore, we write the following cross ratio

$$(0\ \ A_1\ A_2\ A) = \frac{A_1 - 0}{A_1 - A} \div \frac{A_2 - 0}{A_2 - A} = -1.$$

Next, we obtain that

$$\frac{A_1}{A_1 - A} = \frac{-A_2}{A_2 - A}.$$

From here, expression (4.71) follows.

Analogously, we have

$$(0\ \ R_1\ R_2\ 2R) = \frac{R_1 - 0}{R_1 - 2R} \div \frac{R_2 - 0}{R_2 - 2R} = -1.$$

Further,

$$\frac{R_1}{R_1 - 2R} = \frac{-R_2}{R_2 - 2R}.$$

From here, the known formula follows

$$R = \frac{R_1 R_2}{R_1 + R_2}.$$

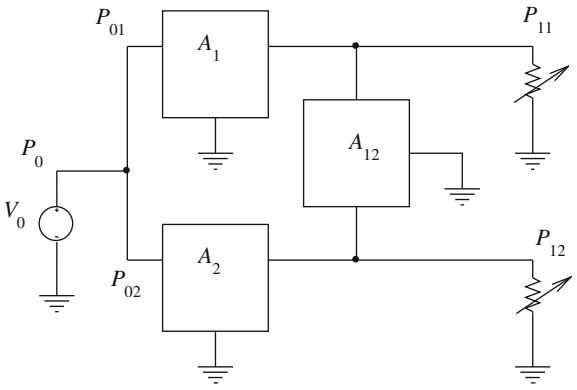

Fig. 4.27 An intermediate two-port A_{12} determines the interaction of the two two-ports A_1, A_2

4.5.3 Connection of Two-Ports with the Interaction

Other variant of modular connection of two two-ports is presented in Fig. 4.27. Besides the initial two-ports with the effectiveness parameters A_1, A_2, there is an intermediate two-port with a parameter A_{12}. Therefore, the interaction between the initial two-ports takes place [8].

In this case, a more general expression than (4.69) for the efficiency follows

$$K_P = \frac{P_1}{P_0} = \frac{b_1 - A_1(b_1)^2 + b_2 - A_2(b_2)^2 + 2Ab_1b_2}{2 - b_1 - b_2},$$

where $b_1 = 1 - P_{01}, b_2 = 1 - P_{02}$.

This equation represents a two-sheeted hyperboloid with the center S too. The center coordinate corresponds to the value

$$K_{PS} = 4\frac{A_1A_2 - (A_{12})^2}{A_1 + A_2 + 2A_{12}} - 1.$$

Similar to (4.71), we may introduce the value

$$A = 2\frac{A_1A_2 - (A_{12})^2}{A_1 + A_2 + 2A_{12}}. \tag{4.72}$$

Value (4.72) determines the total effectiveness parameter of the given module connection.

We may also introduce the values

$$\bar{A}_1 = \frac{A_1A_2 - (A_{12})^2}{A_2 + A_{12}}, \quad \bar{A}_2 = \frac{A_1A_2 - (A_{12})^2}{A_1 + A_{12}}.$$

These values determine the effectiveness parameters for every output terminal. Therefore, expression (4.71) carries out too

$$A = \frac{2\bar{A}_1\bar{A}_2}{\bar{A}_1 + \bar{A}_2}.$$

4.6 Effectiveness Indices of a Two-Port with Variable Losses

4.6.1 Problems of Energy Indices

Usually, the efficiency is used for evaluation of the power supply system effectiveness. But, there are some problems shown in [11].

For example, the efficiency value still tells nothing about the effectiveness of an appliance. Therefore, this efficiency value is compared or confronted with the load power or some reference regime. But, such proposed indices are insufficient to compare the effectiveness of diverse systems or at change in system parameters.

After all, each power supply is characterized by the power opportunities too; for example, maximum powers, currents and so on. Therefore, normalized regime parameters are used. But, for example, the normalized load power does not give information on the regime effectiveness.

4.6.2 Influence of Losses on the Load Power

We rewrite expression (4.66) for the normalized values; that is,

$$P_1(P_0) = (1 - P_0) - A(1 - P_0)^2. \tag{4.73}$$

Let us consider the dependences $P_1(P_0)$ for various losses or effectiveness parameters A in Fig. 4.28a. These dependences represent a bunch of parabolas passing through the common point $P_0^{SC} = 1$, $P_1 = 0$ corresponds to *SC* regime. At *OC* regime, we have the powers

$$P_1 = 0, \quad P_0^{OC} = th^2\gamma = \frac{A-1}{A}.$$

We note the parabolas with the characteristic effectiveness parameters A. If $A = 1$, then the power $P_0^{OC} = 0$. If $A < 1$, our curve gets into the second quadrant and the two-port, as an active circuit, gives energy. The singular case corresponds to $A = 0$; we get the tangential straight line and so called the "idealized" two-port.

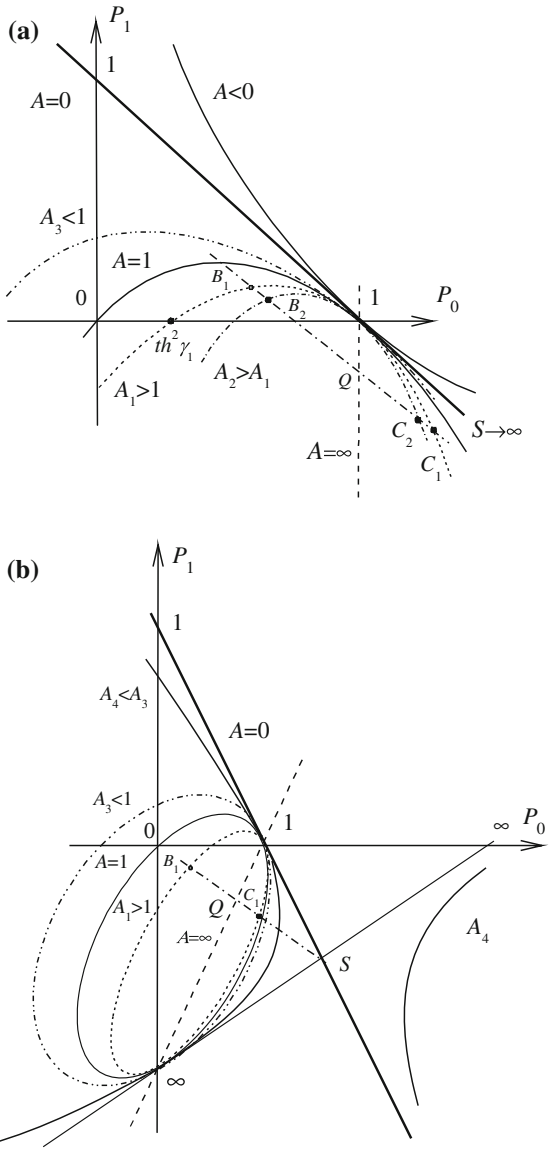

Fig. 4.28 Load power via the input power for various parameters A. **a** Cartesian coordinates, **b** projective coordinates

One more case corresponds to $A = \infty$; the parabola degenerates to the straight line $P_0 = 1$. In turn, the load returns power for the region $P_1 < 0$.

Change of losses

Let us consider the projective coordinates in Fig. 4.28b. The bunch of our parabolas represents the bunch of ellipses passing through the other common point $P_1 = \infty$.

The tangential infinitely remote straight line corresponds to this point $P_1 = \infty$ and the point $P_0 = \infty$.

So, we have the two tangential straight lines, which intersect into a point S. The point S is called a pole; the straight line, corresponding to $A = \infty$, is a polar.

These pole and polar determine the symmetry or mapping of points of ellipses of the region $P_0 > 1$ onto the region $P_0 < 1$. In this case, we have the symmetry of the points C_1, B_1 relatively to the fixed or base points Q, S. Analogously, the symmetry of the points C_2, B_2 takes place.

Thus, these symmetrical points and base points are the harmonic conjugate points. Similar to (4.72), we get

$$\frac{C_1 - Q}{C_1 - S} \div \frac{B_1 - Q}{B_1 - S} = \frac{C_2 - Q}{C_2 - S} \div \frac{B_2 - Q}{B_2 - S} = -1.$$

From here

$$\frac{C_2 - Q}{C_2 - S} \div \frac{C_1 - Q}{C_1 - S} = \frac{B_2 - Q}{B_2 - S} \div \frac{B_1 - Q}{B_1 - S}.$$

The obtained relationships are the cross ratios of the comparable pairs C_1, C_2 and B_1, B_2 relatively to the common base points Q, S; that is,

$$(Q\ C_2\ C_1\ S) = \frac{C_2 - Q}{C_2 - S} \div \frac{C_1 - Q}{C_1 - S} = m^{21}_{AP1} = (Q\ B_2\ B_1\ S).$$

We may consider this value m^{21}_{AP1} as a value of the effectiveness parameter change.

Let us map, for example, the points B_1, B_2, Q, S onto the axis P_0. Then

$$m^{21}_{AP1} = (Q\ B_2\ B_1\ S) = (P_0(Q)\ P_0(B_2)\ P_0(B_1)\ P_0(S)). \tag{4.74}$$

If we have executed all the calculation, the final expression follows [11]

$$m^{21}_{AP1} = \sqrt{\frac{A_1}{A_2}} = \frac{ch\gamma_1}{ch\gamma_2}. \tag{4.75}$$

Change of load power

Let us consider a given value of the power P_0 in Fig. 4.29a. This vertical straight line intersects all the parabolas with the characteristic effectiveness parameters $A = 0$, $A = 1$, $A = \infty$ and a running value A_1. So, we get the corresponding load powers $P_1(0)$, P^1_1, $P_1(1)$, $P_1(\infty)$ in Fig. 4.29b.

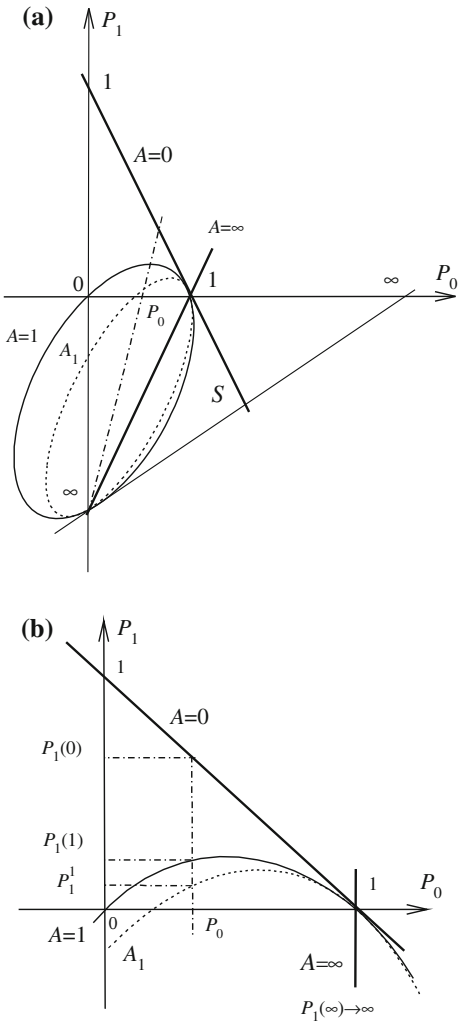

Fig. 4.29 Load power changes for a given value of the input power. **a** Projective coordinates, **b** Cartesian coordinates

Next, we may form the following cross ratio

$$m_{P1}^1 = (P_1(0)\ P_1^1\ P_1(1)\ P_1(\infty)). \tag{4.76}$$

According to (4.73),

$P_1^1 = (1 - P_0) - A_1(1 - P_0)^2, P_1(1) = P_0(1 - P_0), P_1(0) = (1 - P_0), P_1(\infty) = \infty.$

Therefore,

$$m_{P1}^{1} = \frac{P_1^1 - (1 - P_0)}{P_0(1 - P_0) - (1 - P_0)} = A_1.$$

Analogously, for the value A_2, we get the load power P_1^2 and

$$m_{P1}^{2} = \frac{P_1^2 - (1 - P_0)}{P_0(1 - P_0) - (1 - P_0)} = A_2.$$

Therefore, the load power change has the view

$$m_{P1}^{21} = m_{P1}^{2} \div m_{P1}^{1} = \frac{\frac{P_1^2}{1-P_0} - 1}{\frac{P_1^1}{1-P_0} - 1} = \frac{A_2}{A_1}. \tag{4.77}$$

So, there is a strong reason to introduce a specific index in the form

$$\frac{P_1}{1 - P_0} = \frac{P_1}{P_0^{SC} - P_0}. \tag{4.78}$$

The denominator, as the value $P_0^{SC} - P_0$, shows the load degree of a two-port. Therefore, this index gives more information about a running regime than simply normalized load power.

4.6.3 *Influence of Losses on the Efficiency*

Using (4.73), we get the following efficiency expression

$$K_P(P_0) = \frac{P_1}{P_0} = \frac{1 - P_0}{P_0} - A\frac{(1 - P_0)^2}{P_0}. \tag{4.79}$$

Let us consider the dependences $K_P(P_0)$ for various effectiveness parameters A in Fig. 4.30a.

These dependences represent a bunch of hyperbolas passing through the common point $P_0^{SC} = 1$, $P_1 = 0$ corresponds to *SC* regime. At *OC* regime we have

$$K_P = 0, \quad P_0^{OC} = th^2\gamma = \frac{A - 1}{A}.$$

Let us note the hyperbolas with the characteristic effectiveness parameters A. If $A = 1$, then the power $P_0^{OC} = 0$. In this case, the hyperbola degenerates into two

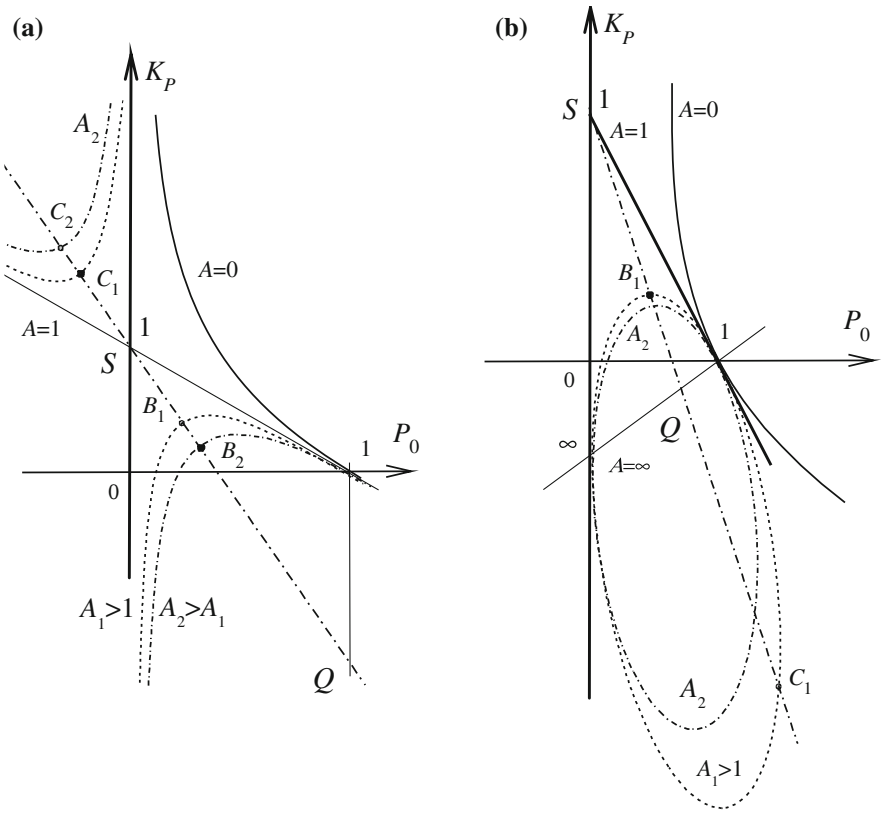

Fig. 4.30 Efficiency via the input power for various parameters A. **a** Cartesian coordinates, **b** projective coordinates

straight lines, which determine the point S of intersection; the corresponding efficiency $K_P = 1$. If $A = 0$, we obtain the hyperbola too.

Change of losses

Let us consider the projective coordinates in Fig. 4.30b. The bunch of our hyperbolas represents the bunch of ellipses passing through the other common point $K_P = \infty$. The tangential straight lines correspond to this point $K_P = \infty$ and the point $P_0^{SC} = 1$. Therefore, for $A = \infty$, the hyperbola degenerates into the infinitely remote straight line ∞.

The above point S is the pole too; the straight line, corresponding to $A = \infty$, is the polar. In this case, we have the symmetry of the points C_1, B_1 relatively to the infinitely remote straight line ∞ or the base points Q, S. Analogously, the symmetry of the points C_2, B_2 takes place.

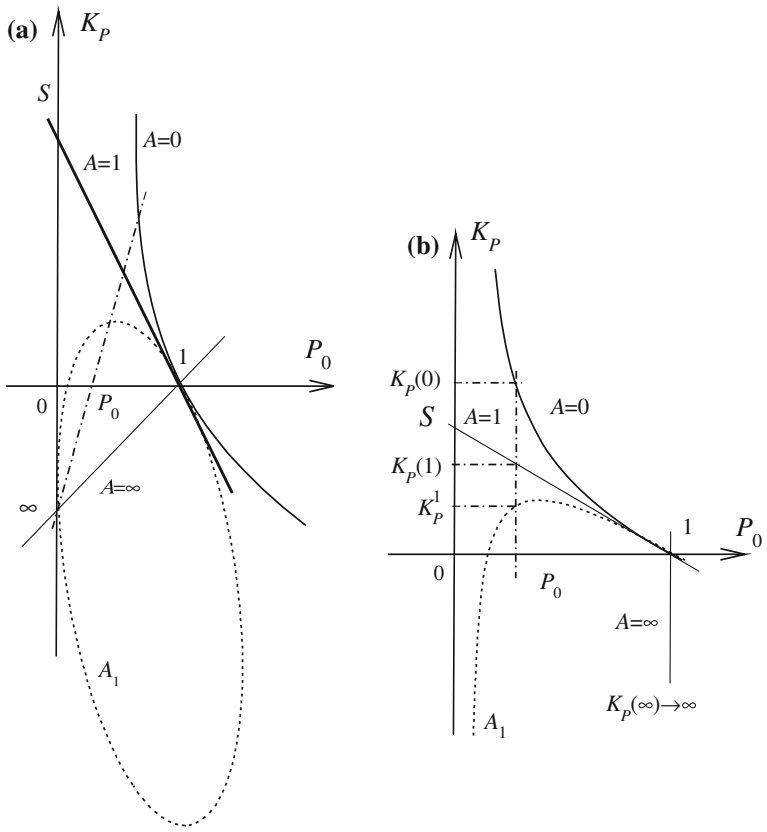

Fig. 4.31 Efficiency changes for a given value of the input power. **a** Projective coordinates, **b** Cartesian coordinates

Similar to (4.74), we may get at once an expression for the effectiveness parameter change

$$m_{AKP}^{21} = (S\ B_1\ B_2\ Q) = (0\ \ P_0(B_1)\ \ P_0(B_2)\ \ 1) = \frac{sh\gamma_1}{sh\gamma_2}. \tag{4.80}$$

The obtained expression differs from (4.75). From here, it follows that the form of losses change is determined by the initial dependences (4.73) and (4.79).

Change of efficiency

Let us consider a given value of the power P_0 in Fig. 4.31a. This vertical straight line intersects all the hyperbolas with the characteristic effectiveness parameters $A = 0$, $A = 1$, $A = \infty$ and a running value A_1. So, we get the corresponding efficiency $K_P(0)$, K_p^1, $K_P(1)$, $K_P(\infty)$ in Fig. 4.31b.

Next, we may form the following cross ratio for the value A_1,

$$m^1_{KP} = (K_P(0)\ K^1_P\ K_P(1)\ K_P(\infty)).$$

According to (4.79)

$$K_P(1) = (1 - P_0), \quad K_P(0) = \frac{1 - P_0}{P_0}, \quad K_P(\infty) = \infty.$$

Analogously, for the value A_2, we get the value m^2_{KP}.
Similar to (4.77), the efficiency change has the view

$$m^{21}_{KP} = m^2_{KP} \div m^1_{KP} = ((1 - P_0) \quad K^2_P \quad K^1_P \quad \infty)$$
$$= \frac{\frac{K^2_P}{1-P_0} - 1}{\frac{K^1_P}{1-P_0} - 1} = \frac{1 - A_2}{1 - A_1} = \frac{sh^2\gamma_2}{sh^2\gamma_1}.$$

So, there is a strong reason to introduce a specific index in the form

$$\frac{K_P}{1 - P_0}.$$

Therefore, this index gives more information about a running regime than the simply efficiency.

References

1. Alexander, C.K., Sadiku, M.N.O.: Fundamentals of Electric Circuits, 5th edn. McGraw-Hill, New York (2009)
2. Irwin, J.D., Nelms, R.M.: Basic Engineering Circuit Analysis, 10th edn. Wiley, Hoboken (2011)
3. Kagan, V.F.: Osnovania geometrii, Chasti II (Geometry Basics. Part II). Gostekhizdat, Moskva (1956)
4. Kittel, C.K., Knight, W.D., Ruderman, M.A.: Mechanics. Berkeley Physics Course, vol. 1. McGraw-Hill, New York (1962)
5. Penin, A.: Projectively—affine properties of resistive two-ports with a variable load. Tehnicheskaia elektrodinamika **2**, 37–41 (1991)
6. Penin, A.: Definition of deviation from the matching regime for two-port circuit. Electrichestvo **4**, 32–40 (1994)
7. Penin, A.: The relative regime of four-port connected in parallel: geometrical approach. Electrichestvo **2**, 49–57 (1997)
8. Penin, A.: Fractionally linear relations in the problems of analysis of resistive circuits with variable parameters. Electrichestvo **11**, 32–44 (1999)
9. Penin, A.: The invariant properties of two-port circuits. World Acad. Sci. Eng. Technol. **3**(4), 893–899 (2009). http://www.waset.org/publications/5517. Accessed 30 Nov 2014
10. Penin, A., Sidorenko, A.: Method for signal transmission through the direct current line. MD Patent 536, 12 Dec 2011

11. Penin, A.: Definition of normalized energy efficiency indices of resistive two-port networks. Probl. Reg. Energ. **2**(22), 20–37 (2013). http://journal.ie.asm.md/assets/files/m71_2_246.pdf. Accessed 30 Nov 2015
12. Penin, A., Sidorenko, A.: Transmission of measuring signals and power supply of remote sensors. In: Bonca, J., Kruchinin, S. (eds.) Nanotechnology in the Security Systems. NATO Science for Peace and Security Series C: Environmental Security, pp. 267–281. Springer, Dordrecht (2014)

Chapter 5
Paralleling of Limited Capacity Voltage Sources

5.1 Introduction

The paralleling of lower power voltage sources (converter modules) offers the well-known advantages over a single, high-power source. The base problem of such a power supply system is the load-current sharing among the paralleled modules. Various approaches of current distribution are known [3]. In the simplest droop method equalizing resistors are used [4, 5, 11], including lossless passive elements [10]. Usually, the equality of module parameters is provided; that is, open circuit voltages and internal resistances. Therefore, the distribution of currents means the equality of these currents.

On the other hand, scatter of module parameters, possible cases of use of primary voltage sources with different capacity determines the non-uniformity distribution of currents.

Therefore, it is natural to understand the uniform loading of sources in the relative sense when the actual loading corresponds to the capacity of the source. The analysis of this power supply system by the method of projective geometry has led to introduction of some concepts for the quantitative representation of operating regimes [6–8].

5.2 Initial Relationships

Let us consider voltage sources V_1, V_2 presented in Fig. 5.1. Resistances R_{i1}, R_{i2} are internal resistances of these voltage sources; equalizing resistors R_{e1}, R_{e2} provide the distribution of currents for a given load resistance R_0.

A. Penin, *Analysis of Electrical Circuits with Variable Load Regime Parameters*,
Power Systems, DOI 10.1007/978-3-319-28451-4_5

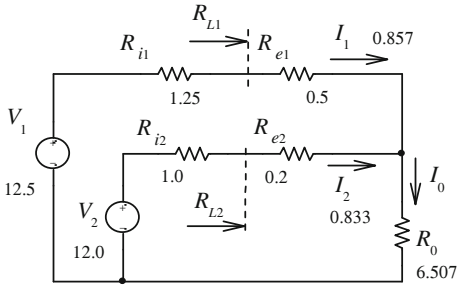

Fig. 5.1 Paralleling of voltage sources

A circuit in Fig. 5.1 is described by the following system of equations:

$$\begin{cases} V_1 = (R_{i1} + R_{e1})I_1 + V_0 \\ V_2 = (R_{i2} + R_{e2})I_2 + V_0 \\ V_0 = R_0 I_0 = R_0(I_1 + I_2). \end{cases} \tag{5.1}$$

The possible normalized parameters of a load regime (or source loading) of the first voltage source look like

$$m_1 = \frac{R_{L1}}{R_{i1}}, \quad J_1 = \frac{I_1}{I_{M1}}. \tag{5.2}$$

Here, the maximum current of the voltage source corresponds to its short circuit current

$$I_{M1} = \frac{V_1}{R_{i1}}. \tag{5.3}$$

Also, such relationships can be rewritten as

$$\frac{R_{L1} - R_{i1}}{R_{L1} + R_{i1}}, \quad \frac{I_{M1} - I_1}{I_{M1} + I_1}, \quad \frac{I_{M1}}{I_1},$$

and so on.

These expressions are used in different areas of electrical engineering, radio engineering, and power. Let us note that all these equations represent fractionally linear expressions and can be interpreted as projective transformations which possess an invariant. Therefore, all the above-mentioned expressions are equivalent. Further we will use expressions (5.2).

Since

$$R_{L1} = \frac{V_1 - R_{i1}I_1}{I_1} = \frac{V_1}{I_1} - R_{i1},$$

then

$$m_1 = \frac{R_{L1}}{R_{i1}} = \frac{V_1}{R_{i1} I_1} - 1 = \frac{I_{M1}}{I_1} - 1 = \frac{1}{J_1} - 1. \tag{5.4}$$

From here, we get the inverse expression

$$I_1 = \frac{I_{M1}}{m_1 + 1}. \tag{5.5}$$

Similar consideration can be done for the second source

$$m_2 = \frac{R_{L2}}{R_{i2}} = \frac{I_{M2}}{I_2} - 1 = \frac{1}{J_2} - 1, \quad J_2 = \frac{I_2}{I_{M2}},\ I_{M2} = \frac{V_2}{R_{i2}}, \tag{5.6}$$

$$I_2 = \frac{I_{M2}}{m_2 + 1}. \tag{5.7}$$

5.3 Influence of the Load Value on the Current Distribution

5.3.1 Analysis of Paralleling Voltage Sources

Let us write an expression, which associates parameters of source loading, in the form $m_2(m_1)$. From (5.1) it follows:

$$V_1 - V_2 = (R_{i1} + R_{e1}) I_1 - (R_{i2} + R_{e2}) I_2.$$

So, by (5.5) and (5.7)

$$I_1 = \frac{I_{M1}}{m_1 + 1} = \frac{V_1}{(m_1 + 1) R_{i1}}, \quad I_2 = \frac{V_2}{(m_2 + 1) R_{i2}},$$

then

$$V_1 - V_2 = (R_{i1} + R_{e1}) \frac{V_1}{(m_1 + 1) R_{i1}} - (R_{i2} + R_{e2}) \frac{V_2}{(m_2 + 1) R_{i2}}.$$

From here, we obtain finally

$$m_2 = \frac{-a m_1 + (d - a + 1)}{m_1 - d}, \tag{5.8}$$

where

$$a = \frac{V_1}{V_1 - V_2} + \frac{V_2}{V_1 - V_2}\frac{R_{e2}}{R_{i2}}, \quad d = \frac{V_2}{V_1 - V_2} + \frac{V_1}{V_1 - V_2}\frac{R_{e1}}{R_{i1}},$$
$$a - d + 1 = \frac{V_1}{V_1 - V_2}\frac{R_{e1}}{R_{i1}} - \frac{V_2}{V_1 - V_2}\frac{R_{e2}}{R_{i2}}. \tag{5.9}$$

We write now an expression, which associates parameters of source loading, in the form $J_2(J_1)$. So

$$J_1 = \frac{I_{M1}}{(m_1 + 1)I_{M1}} = \frac{1}{m_1 + 1}, \quad J_2 = \frac{I_{M2}}{(m_2 + 1)I_{M2}} = \frac{1}{m_2 + 1}.$$

Using (5.7), we get finally

$$J_2 = \frac{d+1}{a-1}J_1 - \frac{1}{a-1}. \tag{5.10}$$

The plots of dependences (5.8) and (5.10) are presented in Fig. 5.2.

Expression (5.8) corresponds to a hyperbole, and (5.10) corresponds to a straight line. The desirable operating regime corresponds to straight lines on these plots; that is, $m_2 = m_1$, $J_2 = J_1$. The crossing of this straight line with the hyperbole plot gives the two points $m^{(1)}$, $m^{(2)}$ of the equal loading of sources. The working area, when load consumes energy, corresponds to the first point $m^{(1)}$. The second point corresponds to the condition when the voltage sources relatively equally consume energy. Let us determine the points $m^{(1)}$, $m^{(2)}$. In this case, expression (5.8) leads to the quadratic equation

$$m^2 - (d - a)m - (d - a + 1) = 0.$$

Its solution gives the two roots

$$m^{(1)} = d - a + 1, \quad m^{(2)} = -1. \tag{5.11}$$

These roots correspond to points of (5.10)

$$J^{(1)} = \frac{1}{d - a + 2}, \quad J^{(2)} = \infty. \tag{5.12}$$

For the second point $J^{(2)}$, the currents $I_2, I_1 \to \infty$. Though this case physically is not feasible, but its mathematical description allows introducing some necessary characteristics of a circuit.

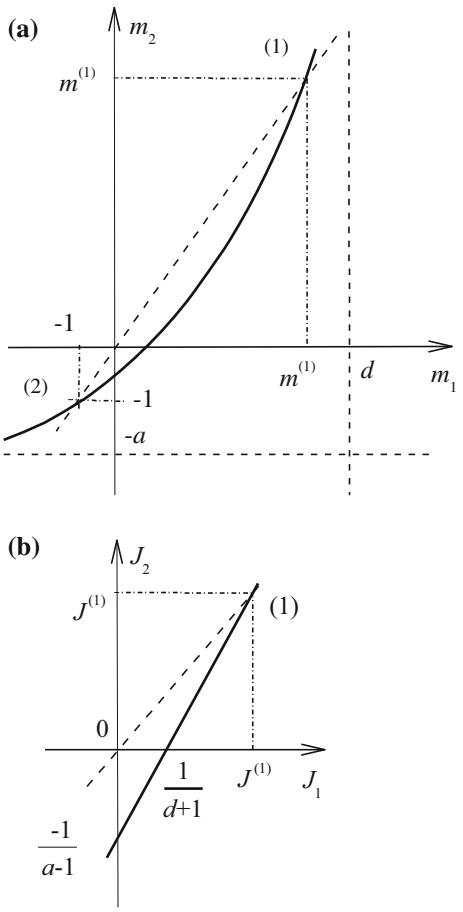

Fig. 5.2 **a** Correlated changes of source loading parameters as a hyperbole. **b** Correlated changes of source loading parameters as a straight line

5.3.2 *Introduction of Two Concepts*

The points of equal loading are the fixed points of the projective transformation $m_1 \rightarrow m_2,\ J_1 \rightarrow J_2$ [1, 2], as it is shown in Fig. 5.3.

Let us consider in detail this geometrical interpretation of transformation (5.8) for different initial values of the quantities m_1, m_2 at loading change. These quantities

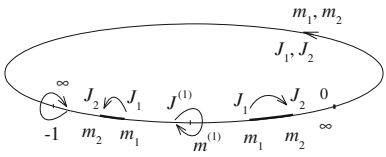

Fig. 5.3 Display of the projective transformation of points $m_1 \rightarrow m_2, J_1 \rightarrow J_2$

define a line segment, its length (in the usual sense of Euclidean geometry) or degree of difference of source loading is decreased at its approach to the fixed points. It is obvious that this length for the different circuits will be various.

Thus, *it is possible to enter two concepts; the first of them defines a circuit: how much the loadings of sources can differ. The second concept defines deviations of actual loadings from the fixed point in the relative form.*

In this case, it is possible to compare running regimes of the different circuits.

For introduction of such characteristics we use a number of concepts of projective geometry, applied in Chap. 2. We constitute the following cross-ratio:

$$(m^{(2)}\ m_2\ m_1\ m^{(1)}) = \frac{m_2 - m^{(2)}}{m_2 - m^{(1)}} \div \frac{m_1 - m^{(2)}}{m_1 - m^{(1)}}, \tag{5.13}$$

where the points $m^{(2)},\ m^{(1)}$ are the base ones. Also, it is known that the cross-ratio, concerning the fixed points, does not depend on running points m_1, m_2. Therefore, we accept $m_1 = \infty$ for simplification of calculations.So, by (5.8)

$$m_2(\infty) = \frac{-a \cdot \infty + (d - a + 1)}{\infty - d} = -a,$$

then

$$\begin{aligned}(m^{(2)}\ m_2(\infty)\ \infty\ m^{(1)}) &= \frac{m_2(\infty) - m^{(2)}}{m_2(\infty) - m^{(1)}} \\ &= \frac{-a - (-1)}{-a - (d - a + 1)} = \frac{a - 1}{d + 1} = K_L.\end{aligned} \tag{5.14}$$

Using the values a and d by (5.9), we get

$$K_L = \frac{V_2}{V_1} \frac{1 + R_{e2}/R_{i2}}{1 + R_{e1}/R_{i1}}. \tag{5.15}$$

The obtained expression is defined by circuit parameters only. This expression characterizes the ability of a circuit to equal loading of sources that corresponds to the first entered concept. We name this expression as the *non-uniformity loading factor* K_L.

Obviously, if $m_2 \to m_1$, then $K_L \to 1$ for a given circuit. In general, the factor $K_L \neq 1$. Equation (5.13), taking into account (5.14), allows expressing the dependence $m_2(m_1)$ using only the two parameters of a circuit, such as $m^{(1)}$ and K_L.

Let us represent (5.13) as

$$K_L = \frac{m_2 + 1}{m_2 - m^{(1)}} \div \frac{m_1 + 1}{m_1 - m^{(1)}}. \tag{5.16}$$

From here, we get the value

$$m_2 = \frac{-\frac{1+K_L m^{(1)}}{1-K_L} m_1 + m^{(1)}}{m_1 - \frac{K_L + m^{(1)}}{1-K_L}} = \frac{-(1+K_L m^{(1)})m_1 + (1-K_L)m^{(1)}}{(1-K_L)m_1 - (K_L + m^{(1)})}. \tag{5.17}$$

Dependence (5.17) for different values of K_L is presented in Fig. 5.4. The bunch of hyperboles is obtained for $K_L \neq 1$. In turn, if $K_L = 1$, these hyperboles degenerate into the straight line $m_2 = m_1$.

Let us analyze expression (5.15). We consider $V_1 = V_2$.

Then

$$K_L = \frac{1 + R_{e2}/R_{i2}}{1 + R_{e1}/R_{i1}}.$$

The condition $K_L = 1$ leads to the equality

$$\frac{R_{e2}}{R_{i2}} = \frac{R_{e1}}{R_{i1}}.$$

Therefore, it is quite possible to put $R_{e2} = R_{e1} = 0$. Thus, if voltage sources have identical open circuit voltages, they are equally loaded, and it is independent on their capacity.

Generally, expression (5.14) allows comparing the factors of non-uniformity of loading of different circuits; to determine the values of equalizing resistors for necessary value of this factor.

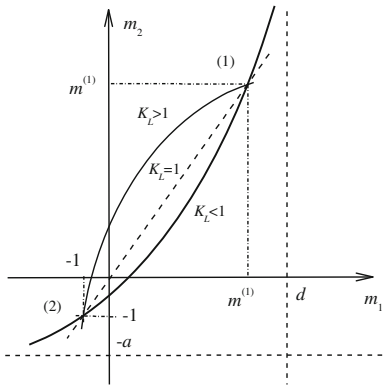

Fig. 5.4 Bunch of hyperboles for different K_L

5.3.3 Comparison of a Loading Regime of Different Circuits

At first, let us obtain the normalized representation of the dependence $m_2(m_1)$. For this purpose, we will consider the cross-ratios for the quantities (or variables) m_1 and m_2, using their conformity, according to transformation (5.8). Therefore, the cross-ratios are equal among themselves

$$(-1\ \ m_1\ \ m^{(1)}\ \ d) = (-1\ m_2\ \ m^{(1)}\ \ \infty),$$

where, according to (5.17),

$$d = \frac{K_L + m^{(1)}}{1 - K_L}.$$

The cross-ratio is the relative expression and gives necessary normalizing of variables. Therefore, any variety of relative expressions for variables m_1 and m_2 is excluded.

Let us present each cross-ratio as

$$\begin{aligned}(-1\ \ m_1\ \ m^{(1)}\ \ d) &= \frac{m_1+1}{m_1 - \frac{K_L+m^{(1)}}{1-K_L}} \div \frac{m^{(1)}+1}{m^{(1)} - \frac{K_L+m^{(1)}}{1-K_L}} \\ &= \frac{m_1+1}{m_1 - \frac{K_L+m^{(1)}}{1-K_L}} \cdot \frac{-K_L}{1-K_L},\end{aligned}$$

$$(-1\ \ m_2\ \ m^{(1)}\ \ \infty) = \frac{m_2+1}{m_2-\infty} \div \frac{m^{(1)}+1}{m^{(1)}-\infty} = \frac{m_2+1}{m^{(1)}+1}.$$

Therefore, we have the equation

$$\frac{m_2+1}{m^{(1)}+1} = \frac{m_1+1}{m_1 - \frac{K_L+m^{(1)}}{1-K_L}} \cdot \frac{-K_L}{1-K_L}.$$

The first member of this expression represents the normalized value and prompts how to write the similar value in the second member.

Therefore,

$$\frac{m_2+1}{m^{(1)}+1} = \frac{-\frac{K_L}{1-K_L}\frac{m_1+1}{m^{(1)}+1}}{\frac{m_1+1}{m^{(1)}+1} - \frac{1}{1-K_L}}. \tag{5.18}$$

Similarly, we have by (5.10), (5.12) and (5.14)

$$\frac{J_2}{J^{(1)}} = \frac{d+1}{a-1}\frac{J_1}{J^{(1)}} - \frac{d-a+2}{a-1} = \frac{J_1}{J^{(1)}K_L} - \frac{1-K_L}{K_L}. \tag{5.19}$$

It should be noted that expressions (5.18) and (5.19) set certainly deviation of running parameters of loading from the equal loading regime by the normalized values. But, it is not enough for comparison of deviations for circuits with different parameters K_L. As an example of the most simple relation (5.19), we will show, why it turns out.

Let us consider two circuits with the different parameters $K_L, \tilde{K}_L$, but with the identical value $J^{(1)} = 1$. The characteristics of circuits are presented in Fig. 5.5.

Loading regimes may be considered identical if conformity of the characteristic regime points takes place (are shown by arrows in Fig. 5.5) at change of the load. It follows from the similarity principle [9]. Then, a projective transformation takes place and it is set by the center at the point 0 and by three pairs of the characteristic regime points A, B, D, and $\tilde{A}, \tilde{B}, \tilde{D}$. The points $D, \tilde{D}$ coincide among themselves and correspond to the fixed point $J^{(1)}$. The point of running regime C should correspond to the point $\tilde{C}$. For such a projective transformation, the cross-ratio is carried out

$$(A\ C\ D\ B) = (\tilde{A}\ \tilde{C}\ \tilde{D}\ \tilde{B}).$$

Here, the points A, B and $\tilde{A}, \tilde{B}$ are the base points, and points $D, \tilde{D}$ are unit ones. Therefore, this cross-ratio can be accepted as the equal deviation of the running points $C, \tilde{C}$ from unit points.

Further, we map the points A, C, D, B onto the axis of current J_1. Then, we obtain the deviation for the first source

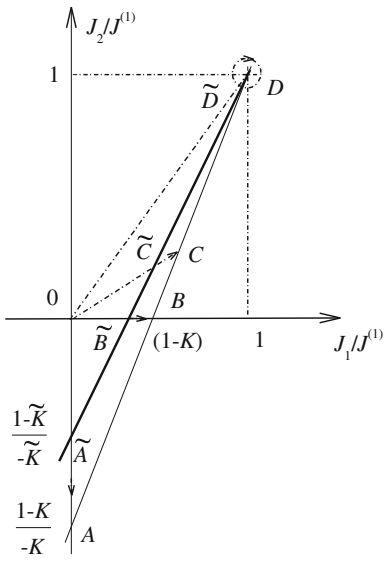

Fig. 5.5 Comparison of the loading regime of two different circuits

$$\begin{aligned}\Delta_1 &= (\,0\;\; J_1\;\; J^{(1)}\;\; (1-K_L)J^{(1)}\,)\\ &= \frac{J_1-0}{J_1-(1-K_L)J^{(1)}} \div \frac{J^{(1)}-0}{J^{(1)}-(1-K_L)J^{(1)}} = \frac{J_1}{J_1-(1-K_L)J^{(1)}}K_L.\end{aligned} \tag{5.20}$$

To compare deviations of sources among themselves, it is necessary to express the deviation for the second source in the same base points. Therefore, we obtain at once

$$\Delta_2 = (\,0\;\; J_2\;\; J^{(1)}\;\; (1-K_L)J^{(1)}\,) = \frac{J_2}{J_2-(1-K_L)J^{(1)}}K_L.$$

Thus, *the deviations include parameters of a circuit and are not simply the normalized values* $J_1/J^{(1)}$, $J_2/J^{(1)}$.

We can represent the deviations in the other form

$$\Delta_1 = \left(0\;\; J_1\;\; J^{(1)}\;\; \tfrac{1}{d+1}\right) = \frac{J_1}{J_1-\frac{1}{d+1}}\frac{a-1}{d+1} = \frac{(a-1)J_1}{(d+1)J_1-1}. \tag{5.21}$$

$$\Delta_2 = \left(0\;\; J_2\;\; J^{(1)}\;\; \tfrac{1}{d+1}\right) = \frac{(a-1)J_2}{(d+1)J_2-1}. \tag{5.22}$$

Taking into account conformity (5.4) and (5.6) between various definitions of parameters of loading regime, the deviations are expressed in the invariant form through the corresponding cross-ratio for the variables m_1, m_2

$$\begin{aligned}\Delta_1 &= \left(0\;\; J_1\;\; J^{(1)}\;\; \tfrac{1}{d+1}\right) = (\,\infty\; m_1\; m^{(1)}\; d\,) = \frac{m^{(1)}-d}{m_1-d} = \frac{1-a}{m_1-d},\\ \Delta_2 &= \left(0\;\; J_2\;\; J^{(1)}\;\; \tfrac{1}{d+1}\right) = \frac{1-a}{m_2-d}.\end{aligned} \tag{5.23}$$

The values of deviations for the characteristic points and running points are presented in Fig. 5.6.

In particular, the deviation $\Delta^{(2)}$ for the second fixed point, $m^{(2)} = -1$, is equal to the parameter K_L; that is,

$$\Delta^{(2)} = \frac{a-1}{d+1} = K_L. \tag{5.24}$$

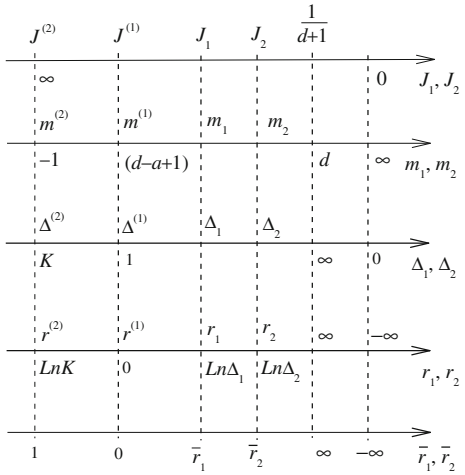

Fig. 5.6 Deviations for the characteristic and running points

It turns out that such a deviation depends on a circuit parameter. We can exclude this dependence as follows. We introduce the hyperbolic metrics or distances

$$r_1 = Ln\,\Delta_1, \quad r_2 = Ln\,\Delta_2. \tag{5.25}$$

The values of these distances are shown in Fig. 5.6.

In particular,

$$r^{(1)} = Ln\,\Delta^{(1)} = 0, \quad r^{(2)} = Ln\,\Delta^{(2)} = Ln\,K_L. \tag{5.26}$$

Only one nonzero and finite value of the distance $r^{(2)}$ is obtained. Therefore, we can use this value as the scale and introduce the normalized values

$$\bar{r}_1 = \frac{r_1}{r^{(2)}} = \frac{Ln\,\Delta_1}{Ln\,K_L}, \quad \bar{r}_2 = \frac{r_2}{r^{(2)}} = \frac{Ln\,\Delta_2}{Ln\,K_L}. \tag{5.27}$$

Example 1 We use the specific elements in Fig. 5.1. Maximum currents of sources (5.3)

$$I_{M1} = 10, \quad I_{M2} = 12.$$

Parameters of loading regimes (5.2) and (5.6)

$$m_1 = 10.66,\ J_1 = 0.0857; \quad m_2 = 13.4,\ J_2 = 0.0694.$$

Source loading regimes (5.8) and (5.10)

$$m_2 = \frac{-29.8m_1 + 5.2}{m_1 - 34}, \quad J_2 = 1.215J_1 - 0.0347.$$

First fixed points (5.11) and (5.12),

$$m^{(1)} = 5.2, \quad J^{(1)} = 0.1613.$$

Non-uniformity loading factor (5.14), $K_L = 0.8228$.
Deviations (5.23)

$$\Delta_1 = 1.2343, \quad \Delta_2 = 1.3986.$$

Hyperbolic distances (5.25)

$$r_1 = 0.2105, \quad r_2 = 0.3354.$$

Scale (5.26), $r^{(2)} = Ln\,0.8228 = -0.195$.
Normalized distances (5.27)

$$\bar{r}_1 = \frac{0.2105}{-0.195} = -1.0795, \quad \bar{r}_2 = \frac{0.3354}{-0.195} = -1.72.$$

All these values are presented in Fig. 5.7.

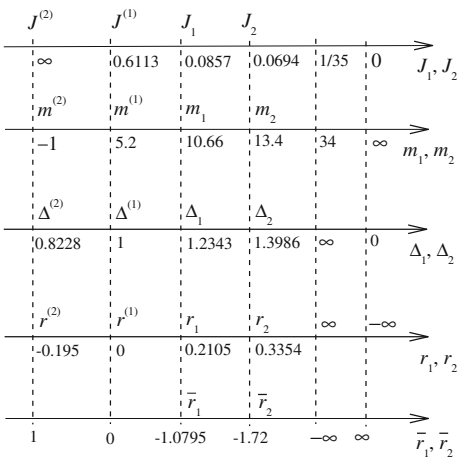

Fig. 5.7 Example of the deviations for the characteristic and running points

5.4 Influence of the Equalizing Resistance on the Current Distribution

5.4.1 Analysis of Paralleling Voltage Sources

Let us write expressions which associate parameters of source loadings in the form $m_2(m_1)$ and $J_2(J_1)$ with the variable equalizing resistor R_{e1} for a given load. From (5.1), (5.5) and (5.7) it follows:

$$V_2 = \frac{V_1}{(m_1+1)R_{i1}}R_0 + \frac{V_2}{(m_2+1)R_{i2}}(R_{i2}+R_{e2}+R_0).$$

Then, we obtain

$$m_2(m_1) = \frac{\alpha m_1 + (\delta+\alpha+1)}{m_1-\delta}, \tag{5.28}$$

where

$$\begin{aligned} \alpha &= \frac{R_{e2}+R_0}{R_{i2}}, \quad \delta = \frac{V_1}{V_2}\frac{R_0}{R_{i1}} - 1, \\ \alpha+\delta+1 &= \frac{R_{e2}+R_0}{R_{i2}} + \frac{V_1}{V_2}\frac{R_0}{R_{i1}}. \end{aligned} \tag{5.29}$$

Also, similarly to (5.10), we get

$$J_2(J_1) = -\frac{\delta+1}{\alpha+1}J_1 + \frac{1}{\alpha+1}, \tag{5.30}$$

The plots of dependences (5.28) and (5.30) are presented in Fig. 5.8. Expression (5.28) corresponds to a hyperbole and (5.30) corresponds to a straight line. The desirable operating regime corresponds to straight lines on these plots; that is, $m_2 = m_1, J_2 = J_1$. The crossing of this straight line with the hyperbole gives the two points $m^{(1)}$, $m^{(2)}$ of the equal loading of sources. The working area when load consumes energy corresponds to the first point $m^{(1)}$. The second point corresponds to the condition when the voltage sources relatively equally consume energy.

Let us find the fixed points $m^{(1)}$, $m^{(2)}$. In this case, expression (5.28) leads to the quadratic equation

$$m^2 - (\delta+\alpha)m - (\delta+\alpha+1) = 0.$$

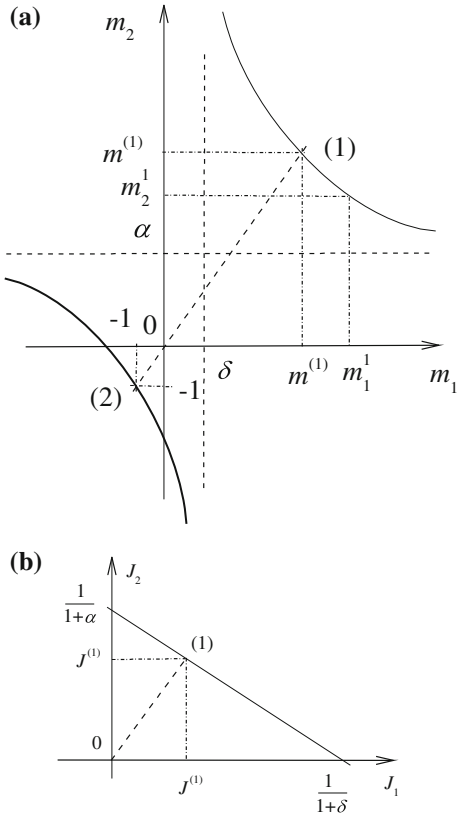

Fig. 5.8 **a** Correlated changes of source loading parameters as a hyperbole. **b** Correlated changes of source loading parameters as a straight line

Its solution gives the two roots

$$m^{(1)} = \delta + \alpha + 1, \quad m^{(2)} = -1. \tag{5.31}$$

These roots correspond to points of (5.30)

$$J^{(1)} = \frac{1}{\delta + \alpha + 2}, \quad J^{(2)} = \infty. \tag{5.32}$$

For the second $J^{(2)}$ point, the currents $I_2, I_1 \to \infty$.

5.4.2 *Introduction of Two Concepts*

The points of equal loading are fixed points of the projective transformations, for example, of points $m_1^1 \to m_2^1, m_1^2 \to m_2^2$, and $J_1^1 \to J_2^1, J_1^2 \to J_2^2$, shown in Fig. 5.9.

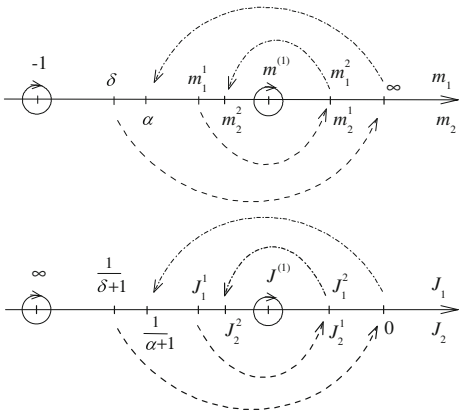

Fig. 5.9 Display of the projective transformations of points $m_1 \to m_2, J_1 \to J_2$

These transformations are another kind than those for variable load case (5.8) and (5.10).

Similarly, *it is possible to introduce two concepts; one of them defines a circuit: how much the source loadings can differ. The second concept defines deviations of actual loadings from the fixed point in the relative form.*

For introduction of such characteristics, we use also cross-ratio (5.13)

$$(m^{(2)}\ m_2\ m_1\ m^{(1)}) = \frac{m_2 - m^{(2)}}{m_2 - m^{(1)}} \div \frac{m_1 - m^{(2)}}{m_1 - m^{(1)}}.$$

We accept $m_1 = \infty$. So, by (5.28), $m_2(\infty) = \alpha$.

Then

$$(m^{(2)}\ m_2(\infty)\ \infty\ m^{(1)}) = \frac{m_2(\infty) - m^{(2)}}{m_2(\infty) - m^{(1)}} = -\frac{\alpha+1}{\delta+1} = K. \tag{5.33}$$

Using (5.29), we get

$$K = -\frac{V_2}{V_1}\frac{R_{i1}}{R_{i2}}\left(1 + \frac{R_{i2} + R_{e2}}{R_0}\right) < 0. \tag{5.34}$$

The obtained expression is only defined by circuit parameters and characterizes ability of a circuit to equal loading of sources that corresponds to the first introduced concept. We name this expression as the *non-uniformity loading factor K*.

The negative value of K shows that points m_1, m_2 are located on different sides from the fixed point $m^{(1)}$, as it is shown in Fig. 5.8a. For example, $m_1^1 > m^{(1)}, m_2^1 < m^{(1)}$. For the variable load case, these points are located on the one side from the fixed point and similar factor $K_L > 0$ by (5.15).

Similarly to (5.16), we have

$$K = \frac{m_2 + 1}{m_2 - m^{(1)}} \div \frac{m_1 + 1}{m_1 - m^{(1)}}. \tag{5.35}$$

From here

$$\begin{aligned} m_2 &= \frac{-\frac{1+Km^{(1)}}{1-K} m_1 + m^{(1)}}{m_1 - \frac{K+m^{(1)}}{1-K}} \\ &= \frac{-(1+Km^{(1)})m_1 + (1-K)m^{(1)}}{(1-K)m_1 - (K+m^{(1)})}, \end{aligned} \tag{5.36}$$

Therefore, $\delta = \frac{K+m^{(1)}}{1-K}$.

Dependence (5.36) for different values of K is presented in Fig. 5.10. We obtain the bunch of hyperboles with the common point (1).

If $K = K_2 = -1$, then

$$m_2 = \frac{\frac{m^{(1)}-1}{2} m_1 + m^{(1)}}{m_1 - \frac{m^{(1)}-1}{2}} = \frac{\delta m_1 + m^{(1)}}{m_1 - \delta}, \ \alpha = \delta.$$

The points m_1, m_2 are symmetric points concerning $m^{(1)}$ and carry the special name in projective geometry as harmonic conjugate points shown in Fig. 5.11. In particular, the point $m_1 = \delta$ corresponds to the point $m_2 = \infty$ and vice versa. Also, the center S_2 will be on the straight line of equal loading. The cross-ratio for harmonic conjugate points

$$(m^{(2)} \ m_1 \ m_2 \ m^{(1)}) = -1.$$

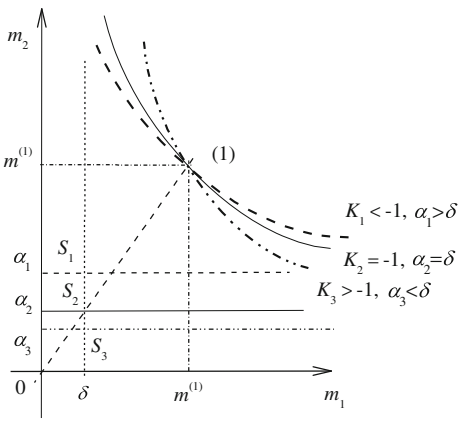

Fig. 5.10 Bunch of hyperboles for different K

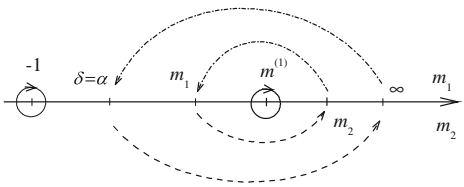

Fig. 5.11 Display of harmonic conjugate points $m_1 \to m_2, m_2 \to m_1$

5.4.3 *Comparison of a Loading Regime of Different Circuits*

Let us obtain the normalized representation of the dependence $m_2(m_1)$. For this purpose, we consider the cross-ratios for the variables m_1 and m_2, using their conformity, according to transformation (5.28). Therefore, the cross-ratios are equal among themselves

$$(-1 \;\; m_1 \;\; m^{(1)} \;\; \delta) = (-1 \;\; m_2 \;\; m^{(1)} \;\; \infty).$$

Therefore, similarly to (5.18) and (5.19), we get the same expressions at once

$$\frac{m_2+1}{m^{(1)}+1} = \frac{-\frac{K}{1-K}\frac{m_1+1}{m^{(1)}+1}}{\frac{m_1+1}{m^{(1)}+1} - \frac{1}{1-K}}. \tag{5.37}$$

$$\frac{J_2}{J^{(1)}} = \frac{J_1}{J^{(1)}K} - \frac{1-K}{K}. \tag{5.38}$$

It should be noted, that expressions (5.37) and (5.38) set certainly deviation of running parameters of loading from the equal loading regime by the normalized values. But it is not enough for comparison of deviations for circuits with different parameters K. As an example of the most simple relation (5.38), we will show, why it turns out.

Let us consider two circuits with the different parameters $K, \tilde{K}$, but with the identical value $J^{(1)} = 1$. The characteristics of circuits are presented in Fig. 5.12; we are reminding $K < 0$.

As it was noted above, the loading regimes may be considered identical if conformity of the characteristic regime points takes place (are shown by arrows) at change of the load. Then, a projective transformation takes place and it is set by the center at the point 0 and by three pairs of the characteristic regime points A, B, D, and $\tilde{A}, \tilde{B}, \tilde{D}$. The points $D, \tilde{D}$ coincide among themselves and correspond to the fixed point $J^{(1)}$. The point of running regime C corresponds to the point $\tilde{C}$. For such a projective transformation, the cross-ratio is carried out

$$(A \; C \; D \; B) = (\tilde{A} \; \tilde{C} \; \tilde{D} \; \tilde{B}).$$

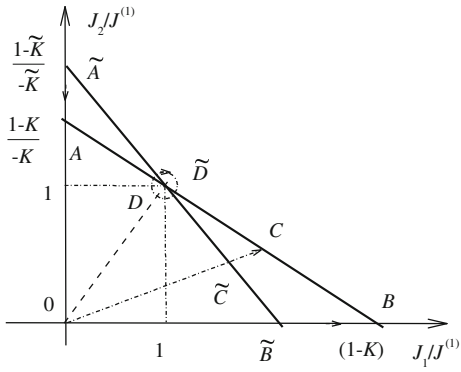

Fig. 5.12 Comparison of the loading regime of two different circuits

Therefore, this cross-ratio can be accepted as the equal deviation of the running points C, $\underline{C}$ from unit points. Further, we map the points A, C, D, B onto the axis of currents J_1. Then, similarly to (5.20), we obtain the deviations for the first and second sources at once

$$\Delta_1 = (\,0\;\; J_1\;\; J^{(1)}\;\; (1-K)J^{(1)}\,) = \frac{J_1}{J_1 - (1-K)J^{(1)}}K, \tag{5.39}$$

$$\Delta_2 = (\,0\;\; J_2\;\; J^{(1)}\;\; (1-K)J^{(1)}\,) = \frac{J_2}{J_2 - (1-K)J^{(1)}}K. \tag{5.40}$$

Thus, *the deviations include the parameters of a circuit and are not simply the normalized values* $J_1/J^{(1)}, J_2/J^{(1)}$.

With the aim to show the presented reasons for introduction of such deviations, we will consider the special case $K = -1$. Then, expressions (5.38) and (5.39) became

$$J_2/J^{(1)} = 2 - J_1/J^{(1)}, \quad \Delta_1 = \frac{J_1/J^{(1)}}{2 - J_1/J^{(1)}} = \frac{2 - J_2/J^{(1)}}{J_2/J^{(1)}} = \frac{1}{\Delta_2}. \tag{5.41}$$

Thus, deviations look like usual proportions and normalized values.

Similarly to (5.21) and (5.22), we can represent the deviations in the other form

$$\Delta_1 = \left(0\;\; J_1\;\; J^{(1)}\;\; \tfrac{1}{\delta+1}\right) = \frac{J_1}{J_1 - \frac{1}{\delta+1}}\frac{-\alpha-1}{\delta+1}. \tag{5.42}$$

$$\Delta_2 = \left(0\;\; J_2\;\; J^{(1)}\;\; \tfrac{1}{\delta+1}\right) = \frac{J_2}{J_2 - \frac{1}{\delta+1}}\frac{-\alpha-1}{\delta+1}. \tag{5.43}$$

Similarly to (5.23), the deviations are expressed in the invariant form through the cross-ratio for the variables m_1, m_2

$$\begin{aligned}\Delta_1 &= \left(0\ J_1\ J^{(1)}\ \tfrac{1}{\delta+1}\right) = (\infty\ m_1\ m^{(1)}\ \delta) = \frac{1+\alpha}{m_1-\delta},\\ \Delta_2 &= \left(0\ J_2\ J^{(1)}\ \tfrac{1}{\delta+1}\right) = \frac{1+\alpha}{m_2-\delta}.\end{aligned} \tag{5.44}$$

In particular, for the second fixed point $m^{(2)} = -1$, the deviation $\Delta^{(2)} = K$.

We can also use hyperbolic metric (5.25)

$$r_1 = Ln\,\Delta_1,\ r_2 = Ln\,\Delta_2. \tag{5.45}$$

Then, by (5.26) we get

$$r^{(1)} = Ln\,\Delta^{(1)} = 0.$$

Since the value $\Delta^{(2)} = K < 0$, we cannot use expression $r^{(2)} = Ln\,\Delta^{(2)}$ directly. Therefore, at first, we find the harmonic conjugate point $\hat{m}^{(2)}$ for the point $m^{(2)}$ by the following condition:

$$(\infty\ \hat{m}^{(2)}\ m^{(2)}\ \delta) = \frac{m^{(2)}-\delta}{\hat{m}^{(2)}-\delta} = \frac{-1-\delta}{\hat{m}^{(2)}-\delta} = -1. \tag{5.46}$$

Then, we get

$$\hat{m}^{(2)} = 1 + 2\delta.$$

Next, using (5.44), we find

$$\hat{\Delta}^{(2)} = \frac{1+\alpha}{\hat{m}^{(2)}-\delta} = \frac{1+\alpha}{1+\delta} = -K.$$

This value is also obtained from the similar condition to (5.46)

$$(0\ \hat{\Delta}^{(2)}\ \Delta^{(2)}\ \infty) = \frac{\hat{\Delta}^{(2)}}{\Delta^{(2)}} = -1.$$

Finally, we get

$$r^{(2)} = Ln\,(-K). \tag{5.47}$$

Using this value as the scale similar to (5.27), we have at once the same normalized expressions

$$\bar{r}_1 = \frac{r_1}{r^{(2)}}, \quad \bar{r}_2 = \frac{r_2}{r^{(2)}}. \tag{5.48}$$

The values of deviations for the characteristic points and running points are presented in Fig. 5.13.

If $K = -1$, then $\Delta^{(2)} = -1$. Using (5.41), we get $r_1 = -r_2$. In this case, there is no need to use the scale, because $\hat{\Delta}^{(2)} = 1 = \Delta^{(1)}$. From here, the physical sense of value $K = -1$ follows: *deviations of sources are equal by quantity, but are opposite by a sign (for the entire equalizing resistor values that can be useful for practice).*

For this case, the deviations for the characteristic and running points are presented in Fig. 5.14.

Example 2 We consider the circuit in Fig. 5.1 and rewrite the required date of Example 1.

Maximum currents of sources (5.3)

$$I_{M1} = 10, \quad I_{M2} = 12.$$

Parameters of loading regime (5.2), (5.6)

$$m_1 = 10.66, \quad J_1 = 0.0857, \; m_2 = 13.4, \quad J_2 = 0.0694.$$

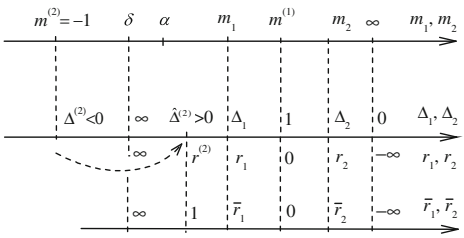

Fig. 5.13 Deviations of the characteristic and running points for $K \neq -1$

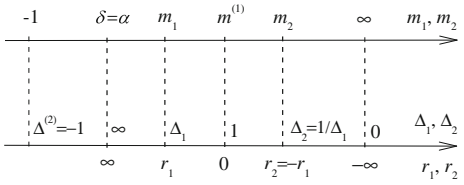

Fig. 5.14 Deviations of the characteristic and running points for $K = -1$

Further, we pass on to our example.
Source loading regimes (5.28) and (5.30)

$$m_2 = \frac{6.707m_1 + 12.13}{m_1 - 4.422}, \quad J_2 = -0.703J_1 + 0.13.$$

First fixed points (5.31) and (5.32)

$$m^{(1)} = 12.13, \quad J^{(1)} = 0.0761.$$

Non-uniformity loading factor (5.33), $K = -1.421$.
Deviations (5.44)

$$\Delta_1 = 1.235, \quad \Delta_2 = 0.858 = 1/1.165.$$

Hyperbolic distances (5.45)

$$r_1 = Ln\,\Delta_1 = 0.211, \quad r_2 = Ln\,\Delta_2 = -0.1526.$$

The deviation for the second source turns out less than for the first one.
Scale (5.47)

$$r^{(2)} = Ln\,1.421 = 0.351.$$

Normalized distances (5.48)

$$\bar{r}_1 = \frac{0.211}{0.351} = 0.601, \; \bar{r}_2 = \frac{-0.1526}{0.351} = -0.4347.$$

All these values are shown in Fig. 5.15.

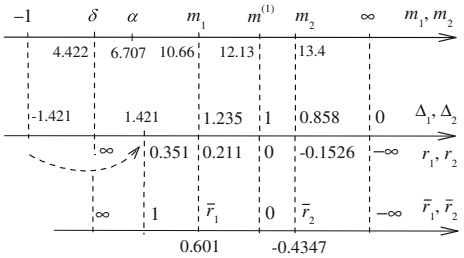

Fig. 5.15 Example of the deviations by equalizing resistance

Example 3 The case of a symmetrical circuit, $K = -1, \breve{\alpha} = \breve{\delta}$. We consider the initial circuit in Fig. 5.1 with the fixed points $m^{(1)} = 12.13, J^{(1)} = 0.0761$. Let us determine the elements $\breve{R}_{i1}$, $\breve{R}_{i2}$ of this symmetrical circuit.

Using (5.31) and (5.29), we get

$$\breve{\delta} = \frac{m^{(1)} - 1}{2} = 5.5647 = \frac{V_1 R_0}{V_2 R_{i1}} - 1, \quad \breve{\alpha} = \frac{R_{e2} + R_0}{R_{i2}}.$$

From here

$$R_{i1} = \frac{V_1}{V_2} \frac{2R_0}{m^{(1)} + 1} = 1.0325, \quad R_{i2} = 2\frac{R_{e2} + R_0}{m^{(1)} - 1} = 1.2052.$$

where R_0, R_{e2}, V_1, and V_2 are equal to the given initial values. Then, maximum currents of sources (5.3)

$$I_{M1} = 12.1065, \quad I_{M2} = 9.9563.$$

Let the deviation be $\Delta_1 = 1.235$ and, by (5.41), $\Delta_2 = 1/\Delta_1 = 0.8097$. Then, by (5.44),

$$m_1 = \delta + \frac{\delta + 1}{\Delta_1} = 10.8825, \quad m_2 = \delta + \frac{\delta + 1}{\Delta_2} = 13.67.$$

Normalized currents (5.4) and (5.6)

$$J_1 = \frac{1}{m_1 + 1} = 0.0841, \quad J_2 = \frac{1}{m_2 + 1} = 0.0682.$$

References

1. Frank, J.A.: Schaum's outline of theory and problems of projective geometry. McGraw–Hill, New York (1967)
2. Glagolev, N.A.: Proektivnaia geometria. (Projective geometry). Nauka, Moskva (1963)
3. Huang, Y., Tse, C.K.: Circuit theoretic classification of parallel connected DC–DC Converters. IEEE Trans. Circuits Syst. I Regul. Pap. **54**(5), 1099–1108 (2007)
4. Irving, B.T., Jovanović, M.M.: Analysis, design, and performance evaluation of droop current-sharing method. In: The 15th Annual IEEE Applied Power Electronics Conference (2000) http://www.deltartp.com/dpel/dpelconferencepapers/06_3.pdf. Accessed 30 Nov 2014
5. Kim, J.W., Choi, H.S., Cho, B.H.: A novel droop method for converter parallel operation. IEEE Trans. Power Electron. **17**(1), 25–32 (2002) http://pearlx.snu.ac.kr/Publication/IEEE0202.pdf. Accessed 30 Nov 2014
6. Penin, A.: Projectively–geometric approach to parallel connection of electric energy sources. Tehnicheskaia elektrodinamika **1**, 37–44 (1992)

7. Penin, A.: Analysis of paralleling limited capacity voltage sources by projective geometry method. Sci. World J. (2014). doi:10.1155/2014/359893
8. Penin, A., Sidorenko, A.: Investigation of the effect of an equalizing resistor on the paralleling voltage sources by projective geometry. Moldavian J. Phys. Sci. **11**(1–2), 124–131 (2012) http://sfm.asm.md/moldphys/2012/vol11/n12/ins_14_penin.pdf Accessed 30 Nov 2014
9. Venikov, V.A.: Theory of similarity and simulation: with applications to problems in electrical power engineering. Macdonald, London (1969)
10. Villarejo, J.A., De Jodar, E., Soto, F., Jimenez, J.: Multistage high power factor rectifier with passive lossless current sharing. In: The 7th WSEAS International Conference on Circuits, Systems, Electronics, Control and Signal Processing (CSECS'08) (2008)
11. Wang, J.B.: Primary droop current–sharing control of the parallel DC/DC converters system considering output cable resistance. Adv. Power Electron. (2011). doi:10.1155/2011/713250, http://www.hindawi.com/journals/ape/2011/713250/

Part II
Multi-port Circuits. Projective Coordinates of a Point on the Plane and Space

Chapter 6
Operating Regimes of an Active Multi-port

6.1 Active Two-Port. Affine and Projective Coordinates on the Plane

6.1.1 Affine Coordinates

Let us give necessary relationships for an active two-port network in Fig. 6.1 with changeable load voltage sources V_1, V_2.

Taking into account the specified directions of the load currents, this network is described by the following system of Y parameters equations [1, 5]:

$$\begin{bmatrix} I_1 \\ I_2 \end{bmatrix} = \begin{bmatrix} -Y_{11} & Y_{12} \\ Y_{12} & -Y_{22} \end{bmatrix} \cdot \begin{bmatrix} V_1 \\ V_2 \end{bmatrix} + \begin{bmatrix} I_1^{SC,SC} \\ I_2^{SC,SC} \end{bmatrix}, \tag{6.1}$$

where $I_1^{SC,SC}$, $I_2^{SC,SC}$ are the short circuit SC currents of both loads.

The inverse expression is

$$\begin{bmatrix} V_1 \\ \\ V_2 \end{bmatrix} = \begin{bmatrix} \frac{Y_{22}}{\Delta_Y} & \frac{Y_{12}}{\Delta_Y} \\ \frac{Y_{12}}{\Delta_Y} & \frac{Y_{11}}{\Delta_Y} \end{bmatrix} \cdot \begin{bmatrix} I_1^{\mathrm{SC,SC}} - I_1 \\ \\ I_2^{\mathrm{SC,SC}} - I_2 \end{bmatrix}. \tag{6.2}$$

From here, we obtain

$$I_2 - I_2^{SC,SC} = -\frac{Y_{22}}{Y_{12}}(I_1 - I_1^{SC,SC}) - \frac{\Delta_Y}{Y_{12}} V_1, \tag{6.3}$$

$$I_2 - I_2^{SC,SC} = -\frac{Y_{12}}{Y_{11}}(I_1 - I_1^{SC,SC}) - \frac{\Delta_Y}{Y_{11}} V_2. \tag{6.4}$$

A. Penin, *Analysis of Electrical Circuits with Variable Load Regime Parameters*, Power Systems, DOI 10.1007/978-3-319-28451-4_6

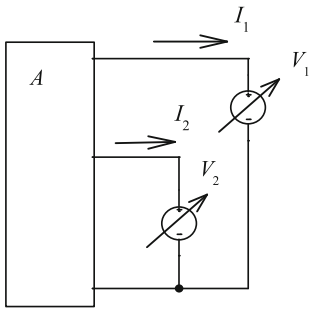

Fig. 6.1 Active two-ports with changeable load voltage sources

Equation (6.3) determines a family of parallel load straight lines with a parameter V_1. Similarly, Eq. (6.4) determines a family of parallel load straight lines with a parameter V_2. These load straight lines are shown in Fig. 6.2 for characteristic regimes (as the short circuit $V_1^{SC} = 0,\ V_2^{SC} = 0$ and open circuit $V_1^{OC},\ V_2^{OC}$) and a running regime$V_1^1,\ V_2^1$.

We consider that the load currents define the rectangular Cartesian system of coordinates $(I_1 0_I I_2)$. Then, the load voltages correspond to the affine coordinates $(V_1 0_V V_2)$ [2, 6].

The axis V_1 equation is defined by expression (6.4) as $V_2 = 0$:

$$I_2 - I_2^{SC,SC} = -\frac{Y_{12}}{Y_{11}}(I_1 - I_1^{SC,SC}). \tag{6.5}$$

This straight line passes through the point (SC, SC) with the coordinates $I_1^{SC,SC},\ I_2^{SC,SC}$ or the point 0_V. The value Y_{12}/Y_{11} corresponds to a slope angle. Similarly, the axis V_2 equation is defined by expression (6.3) as $V_1 = 0$:

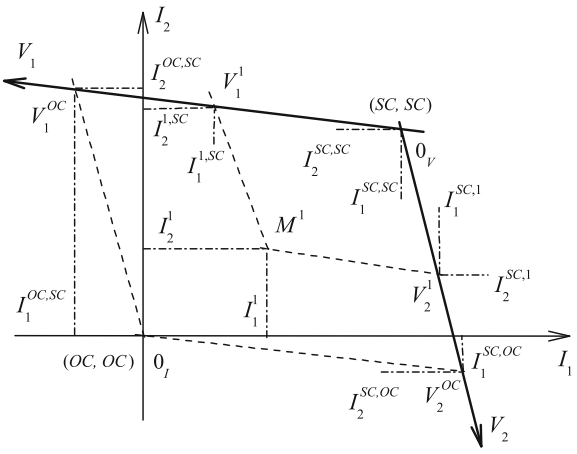

Fig. 6.2 Systems of Cartesian coordinates $(I_1 0_I I_2)$ and affine coordinates $(V_1 0_V V_2)$

$$I_2 - I_2^{SC,SC} = -\frac{Y_{22}}{Y_{12}}(I_1 - I_1^{SC,SC}). \tag{6.6}$$

The open circuit regime of both loads corresponds to the point (OC, OC) with the coordinates $I_1^{OC,OC} = 0,\ I_2^{OC,OC} = 0$ or the point 0_I.

Using (6.2), we get

$$V_1^{OC} = \frac{Y_{22}}{\Delta_Y} I_1^{SC,SC} + \frac{Y_{12}}{\Delta_Y} I_2^{SC,SC}, \tag{6.7}$$

$$V_2^{OC} = \frac{Y_{12}}{\Delta_Y} I_1^{SC,SC} + \frac{Y_{11}}{\Delta_Y} I_2^{SC,SC}. \tag{6.8}$$

We must map the point (OC, OC) onto the coordinate axes $V_1,\ V_2$ by parallel lines to these axes.

Then, the coordinates or components $I_1^{OC,SC},\ I_2^{OC,SC}$ correspond to the point V_1^{OC} on the axis V_1. Using (6.7) and (6.1) as $V_2 = 0$, we get

$$I_1^{OC,SC} = -Y_{11} V_1^{OC} + I_1^{SC,SC} = \left(1 - \frac{Y_{11} Y_{22}}{\Delta_Y}\right) I_1^{SC,SC} - \frac{Y_{11} Y_{12}}{\Delta_Y} I_2^{SC,SC}, \tag{6.9}$$

$$I_2^{OC,SC} = Y_{12} V_1^{OC} + I_2^{SC,SC} = \frac{Y_{12} Y_{22}}{\Delta_Y} I_1^{SC,SC} + \frac{Y_{11} Y_{22}}{\Delta_Y} I_2^{SC,SC}. \tag{6.10}$$

In turn, the coordinates $I_1^{SC,OC},\ I_2^{SC,OC}$ correspond to the point V_2^{OC} on the axis V_2. Using (6.8) and (6.1) as $V_1 = 0$, we obtain

$$I_1^{SC,OC} = Y_{12} V_2^{OC} + I_1^{SC,SC} = \left(1 + \frac{Y_{12}^2}{\Delta_Y}\right) I_1^{SC,SC} + \frac{Y_{11} Y_{12}}{\Delta_Y} I_2^{SC,SC}, \tag{6.11}$$

$$I_2^{SC,OC} = -Y_{22} V_2^{OC} + I_2^{SC,SC} = -\frac{Y_{12} Y_{22}}{\Delta_Y} I_1^{SC,SC} - \left(1 + \frac{Y_{11} Y_{22}}{\Delta_Y}\right) I_2^{SC,SC}. \tag{6.12}$$

Let an initial regime be given by values $V_1^1,\ V_2^1$ or by a point M^1. Then, the coordinates $I_1^{1,SC},\ I_2^{1,SC}$ define the point V_1^1 on the axis V_1. Using (6.1) as $V_2 = 0$, we have

$$I_1^{1,SC} = -Y_{11} V_1^1 + I_1^{SC,SC}, \tag{6.13}$$

$$I_2^{1,SC} = Y_{12} V_1^1 + I_2^{SC,SC}. \tag{6.14}$$

In turn, the coordinates $I_1^{SC,1},\ I_2^{SC,1}$ define the point V_2^1 on the axis V_2.
Using (6.1) as $V_1 = 0$,

$$I_1^{SC,1} = Y_{12} V_2^1 + I_1^{SC,SC}, \tag{6.15}$$

$$I_2^{SC,1} = -Y_{22} V_2^1 + I_2^{SC,SC}. \tag{6.16}$$

Let us introduce the normalized coordinates for the point M^1 of this running regime. The point (OC, OC) is the scale one for the coordinates $V_1\ 0_V\ V_2$. Then, the normalized coordinates have the view

$$n_1^1 = \frac{V_1^1 - 0_V}{V_1^{OC} - 0_V} = \frac{V_1^1}{V_1^{OC}}, \tag{6.17}$$

$$n_2^1 = \frac{V_2^1 - 0_V}{V_2^{OC} - 0_V} = \frac{V_2^1}{V_2^{OC}}. \tag{6.18}$$

Also, it is possible to represent the normalized coordinates by the components of current

$$n_1^1 = \frac{I_1^{1,SC} - I_1^{SC,SC}}{I_1^{OC,SC} - I_1^{SC,SC}} = \frac{I_2^{1,SC} - I_2^{SC,SC}}{I_2^{OC,SC} - I_2^{SC,SC}}, \tag{6.19}$$

$$n_2^1 = \frac{I_1^{SC,1} - I_1^{SC,SC}}{I_1^{SC,OC} - I_1^{SC,SC}} = \frac{I_2^{SC,1} - I_2^{SC,SC}}{I_2^{SC,OC} - I_2^{SC,SC}}. \tag{6.20}$$

The obtained expressions are similar to expressions (2.6) and (2.9). Also, we may obtain the other affine ratio similar to (2.7).

The presented approach will be used for analysis of input–output transformations of a circuit with two inputs and two outputs.

Example 1 We consider the following circuit with given parameters in Fig. 6.3. System of Eq. (6.1) has the view

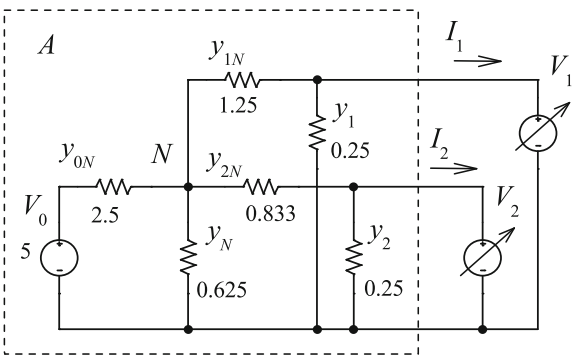

Fig. 6.3 Example of the circuit with two load voltage sources

$$\begin{bmatrix} I_1 \\ I_2 \end{bmatrix} = \begin{bmatrix} -Y_{11} & Y_{12} \\ Y_{12} & -Y_{22} \end{bmatrix} \cdot \begin{bmatrix} V_1 \\ V_2 \end{bmatrix} + \begin{bmatrix} I_1^{SC,SC} \\ I_2^{SC,SC} \end{bmatrix} = \begin{bmatrix} -1.2 & 0.2 \\ 0.2 & -0.95 \end{bmatrix} \cdot \begin{bmatrix} V_1 \\ V_2 \end{bmatrix} + \begin{bmatrix} 3 \\ 2 \end{bmatrix}.$$

Therefore, Y parameters are the following values:

$$Y_{11} = y_1 + y_{1N} - \frac{y_{1N}^2}{y_\Sigma} = 1.2, \quad y_\Sigma = y_{0N} + y_N + y_{1N} + y_{2N} = 5.208,$$
$$Y_{12} = y_{2N}\frac{y_{1N}}{y_\Sigma} = 0.2, \quad Y_{22} = y_2 + y_{2N} - \frac{y_{2N}^2}{y_\Sigma} = 0.95.$$

The SC currents of both loads are

$$I_1^{SC,SC} = Y_{10}V_0 = y_{0N}\frac{y_{1N}}{y_\Sigma}V_0 = 0.6 \cdot 5 = 3,$$
$$I_2^{SC,SC} = Y_{20}V_0 = y_{0N}\frac{y_{2N}}{y_\Sigma}V_0 = 0.4 \cdot 5 = 2.$$

The inverse expression (6.2) is

$$\begin{bmatrix} V_1 \\ V_2 \end{bmatrix} = \frac{1}{\Delta_Y} \cdot \begin{bmatrix} Y_{22} & Y_{12} \\ Y_{12} & Y_{11} \end{bmatrix} \cdot \begin{bmatrix} I_1^{SC,SC} - I_1 \\ I_2^{SC,SC} - I_2 \end{bmatrix} = \frac{1}{1.1} \cdot \begin{bmatrix} 0.95 & 0.2 \\ 0.2 & 1.2 \end{bmatrix} \cdot \begin{bmatrix} 3 - I_1 \\ 2 - I_2 \end{bmatrix}.$$

Equation (6.5) of the axis V_1 is

$$I_2 = -\frac{Y_{12}}{Y_{11}}(I_1 - I_1^{SC,SC}) + I_2^{SC,SC} = -\frac{1}{6}(I_1 - 3) + 2 = -\frac{1}{6}I_1 + 2.5.$$

Equation (6.6) of the axis V_2 is as follows:

$$I_2 = -\frac{Y_{22}}{Y_{12}}(I_1 - I_1^{SC,SC}) + I_2^{SC,SC} = -4.75I_1 + 16.25.$$

The obtained coordinates $V_1 0_V V_2$ are shown in Fig. 6.4.

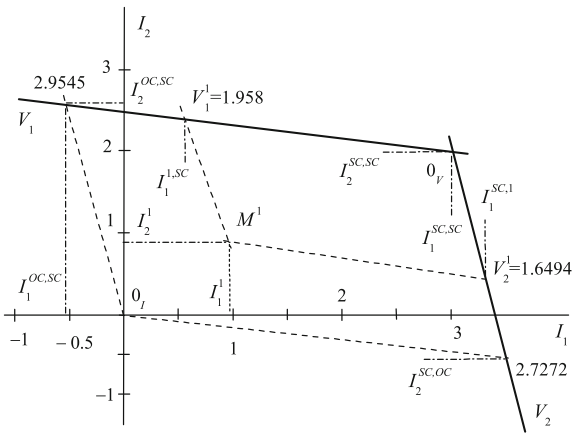

Fig. 6.4 Example of the affine coordinates $V_1 0_V V_2$

Open circuit voltages are (6.7) and (6.8)

$$V_1^{OC} = \frac{Y_{22}}{\Delta_Y} I_1^{SC,SC} + \frac{Y_{12}}{\Delta_Y} I_2^{SC,SC} = \frac{0.95}{1.1} 3 + \frac{0.2}{1.1} 2 = 2.9545,$$
$$V_2^{OC} = \frac{Y_{12}}{\Delta_Y} I_1^{SC,SC} + \frac{Y_{11}}{\Delta_Y} I_2^{SC,SC} = \frac{0.2}{1.1} 3 + \frac{1.2}{1.1} 2 = 2.7272.$$

Currents (6.9) and (6.10) are given as

$$I_1^{OC,SC} = -Y_{11} V_1^{OC} + I_1^{SC,SC} = -1.2 \cdot 2.9545 + 3 = -0.5454,$$
$$I_2^{OC,SC} = Y_{12} V_1^{OC} + I_2^{SC,SC} = 0.2 \cdot 2.9545 + 2 = 2.5909.$$

Currents (6.11) and (6.12) are given as

$$I_1^{SC,OC} = Y_{12} V_2^{OC} + I_1^{SC,SC} = 0.2 \cdot 2.7272 + 3 = 3.5454,$$
$$I_2^{SC,OC} = -Y_{22} V_2^{OC} + I_2^{SC,SC} = -0.95 \cdot 2.7272 + 2 = -0.5909.$$

Let the initial regime be given as follows:

$$V_1^1 = 1.958,\ V_2^1 = 1.6494.$$

Currents (6.1) are

$$I_1^1 = -Y_{11} V_1^1 + Y_{12} V_2^1 + I_1^{SC,SC} = -1.2 \cdot 1.958 + 0.2 \cdot 1.6494 + 3 = 0.979,$$
$$I_2^1 = Y_{12} V_1^1 - Y_{22} V_2^1 + I_2^{SC,SC} = 0.2 \cdot 1.958 - 0.95 \cdot 1.6494 + 2 = 0.8247.$$

Currents (6.13) and (6.14) are

$$I_1^{1,SC} = -Y_{11}V_1^1 + I_1^{SC,SC} = -1.2 \cdot 1.958 + 3 = 0.6504,$$
$$I_2^{1,SC} = Y_{12}V_1^1 + I_2^{SC,SC} = 0.2 \cdot 1.958 + 2 = 2.3916.$$

Currents (6.15) and (6.16) are given as

$$I_1^{SC,1} = Y_{12}V_2^1 + I_1^{SC,SC} = 0.2 \cdot 1.6494 + 3 = 3.3298,$$
$$I_2^{SC,1} = -Y_{22}V_2^1 + I_2^{SC,SC} = -0.95 \cdot 1.6494 + 2 = 0.433.$$

Normalized expressions (6.17) and (6.18) are

$$n_1^1 = \frac{V_1^1}{V_1^{OC}} = \frac{1.958}{2.9545} = 0.6627, \quad n_2^1 = \frac{V_2^1}{V_2^{OC}} = \frac{1.6494}{2.7272} = 0.6047.$$

We are checking normalized coordinates (6.19) and (6.20) as

$$n_1^1 = \frac{I_1^{1,SC} - I_1^{SC,SC}}{I_1^{OC,SC} - I_1^{SC,SC}} = \frac{I_2^{1,SC} - I_2^{SC,SC}}{I_2^{OC,SC} - I_2^{SC,SC}}$$
$$= \frac{0.6504 - 3}{-0.5454 - 3} = \frac{2.3916 - 2}{2.5909 - 2} = 0.6627,$$
$$n_2^1 = \frac{I_1^{SC,1} - I_1^{SC,SC}}{I_1^{SC,OC} - I_1^{SC,SC}} = \frac{I_2^{SC,1} - I_2^{SC,SC}}{I_2^{SC,OC} - I_2^{SC,SC}}$$
$$= \frac{3.3298 - 3}{3.5454 - 3} = \frac{0.433 - 2}{-0.5909 - 2} = 0.6047.$$

6.1.2 *Particular Case of a Two-Port. Introduction of the Projective Plane*

Now, let us introduce the projective plane. For this purpose, we consider the most simple active circuit, which contains two load conductivities Y_{L1}, Y_{L2} in Fig. 6.5a.

If an internal resistance of voltage source V_0 is equal to zero, the independent change of load currents takes place at the independent change of the load conductivities. The point M of running regime can be set by the values of load conductivities $M(Y_{L1}, Y_{L2})$ or by load currents $M(I_{L1}, I_{L2})$.

The family of load straight lines (there are parallel lines) coincides, for example, with the rectangular Cartesian coordinates in the Euclidean plane in Fig. 6.5a. Then, the calibrations of the coordinate axes, by the values of currents and conductivities, coincide. It is obvious that the circuit does not possess the own scales. Therefore, it is possible to express the regime only by the absolute or actual values of currents or conductivities.

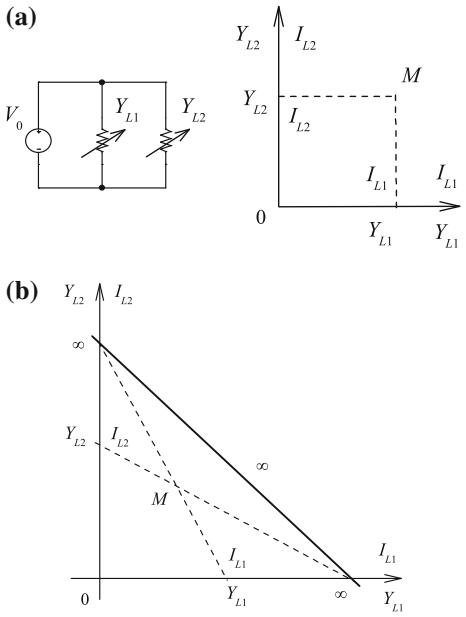

Fig. 6.5 **a** Simple active circuit and its load straight lines in the Cartesian coordinates. **b** This load straight lines in the projective coordinates

We can represent the obtained family of load straight lines in the projective plane [7, 10]. In this case, the infinitely large currents and conductivities (infinitely remote points) are located in a finite domain in Fig. 6.5b and form the line of infinity ∞. Therefore, the load straight lines represent two bunches of straight lines with the centers in these infinitely remote points.

Now, the internal resistance R_i of the voltage source V_0 accepts a finite value in Fig. 6.6. In this case, the dependent change of load currents takes place. There are two bunches of load straight lines; the bunch centers are defined by the *SC* current I_M. Then, the straight line of the maximum current I_M passes across these centers. This straight line is similar to the line of infinity ∞.

The obtained "deformed" coordinate grid defines the projective plane. The axes of coordinates can be calibrated by the values of corresponding currents or conductivities of the loads. In this case, there is an internal scale, that is, the value of conductivity $Y_i = 1/R_i$ or the current I_M.

It is possible to accept that the load conductivities are equal, for example, to the internal conductivity Y_i and define the point M_i of characteristic regime.

The projective coordinates are uniquely set by four points; there are three points of the reference triangle $G_1 0 G_2$ and scale point M_i [3, 4].

The point M of running regime can be set by the values of load conductivities (non-uniform coordinates) $M(Y_{L1}, Y_{L2})$ or by the load currents (homogeneous coordinates) $M(I_{L1}, I_{L2}, V_L)$. The sense of homogeneous coordinates consists that they are proportional to the length of perpendiculars from a point to the sides of reference triangle. The homogeneous coordinates are used for uncertainty elimination, when the point is on the line of infinity ∞. The presence of the fourth

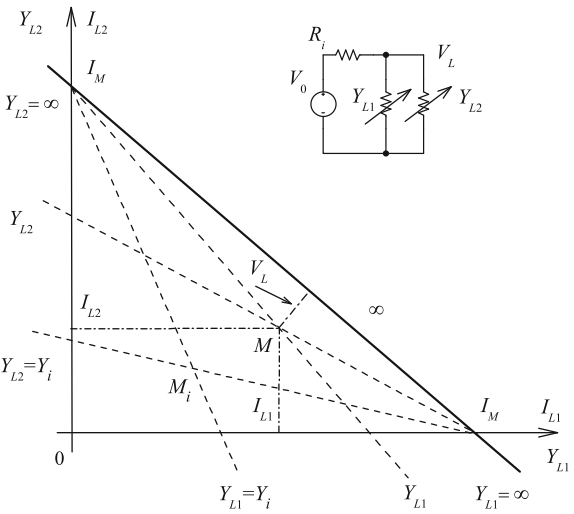

Fig. 6.6 Active circuit with the internal resistance of voltage source and its load straight lines in the projective coordinates

(characteristic) point allows to introduce the cross-ratios m_{L1}, m_{L2} and to set the regime in the relative form.

6.1.3 General Case of a Two-Port. Projective Coordinates

Let us give necessary relationships for an active two-port network in Fig. 6.7 with changeable load conductivities Y_{L1}, Y_{L2} [9, 11]. Taking into account the specified directions of the load currents, these active two-ports are described by (6.1)

$$\begin{bmatrix} I_1 \\ I_2 \end{bmatrix} = \begin{bmatrix} -Y_{11} & Y_{12} \\ Y_{12} & -Y_{22} \end{bmatrix} \cdot \begin{bmatrix} V_1 \\ V_2 \end{bmatrix} + \begin{bmatrix} I_1^{SC} \\ I_2^{SC} \end{bmatrix}, \tag{6.21}$$

where I_1^{SC}, I_2^{SC} are *SC* currents of both loads.

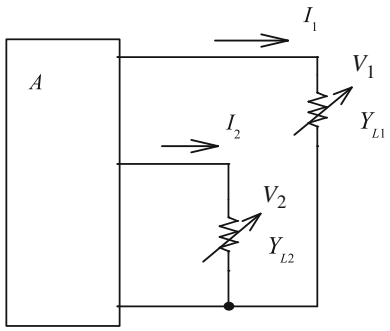

Fig. 6.7 Active two-port network with changeable load conductivities Y_{L1}, Y_{L2}

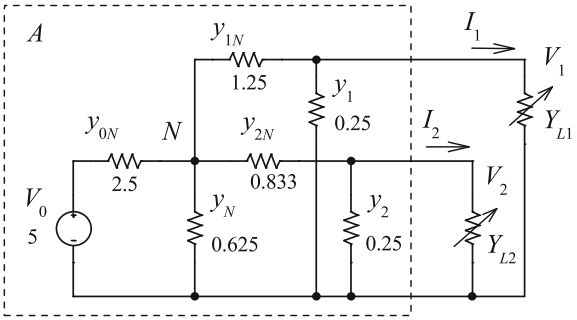

Fig. 6.8 Example of the circuit with two load conductivities

Next, we use the circuit of Example 1. In our case, this circuit is shown in Fig. 6.8. For convenience, we rewrite Y parameters

$$
\begin{aligned}
&Y_{11} = y_1 + y_{1N} - \frac{y_{1N}^2}{y_\Sigma}, \quad y_\Sigma = y_{0N} + y_N + y_{1N} + y_{2N},\\
&Y_{12} = y_{2N}\frac{y_{1N}}{y_\Sigma}, \quad Y_{22} = y_2 + y_{2N} - \frac{y_{2N}^2}{y_\Sigma}.\\
&I_1^{SC} = Y_{10}V_0 = y_{0N}\frac{y_{1N}}{y_\Sigma}V_0, \quad I_2^{SC} = Y_{20}V_0 = y_{0N}\frac{y_{2N}}{y_\Sigma}V_0.
\end{aligned}
\tag{6.22}
$$

Taking into account the voltages $V_1 = I_1/Y_{L1}$, $V_2 = I_2/Y_{L2}$, the equations of two bunches of straight lines with parameters Y_{L1}, Y_{L2} are obtained from system (6.21):

$$
\begin{aligned}
V_0(Y_{20}Y_{12} + Y_{10}Y_{22}) - Y_{12}I_2 &= I_1\left(Y_{22} + \frac{\Delta_Y}{Y_{L1}}\right),\\
V_0(Y_{10}Y_{12} + Y_{20}Y_{11}) - Y_{12}I_1 &= I_2\left(Y_{11} + \frac{\Delta_Y}{Y_{L2}}\right).
\end{aligned}
\tag{6.23}
$$

Bunches of these straight lines are presented in Fig. 6.9. The bunch center, a point G_2, corresponds to the straight lines with the parameter Y_{L1}. We would remind that bunch center corresponds to such a regime of the load Y_{L1} which does not depend on its values. It is carried out for the current and voltage $I_1 = 0$, $V_1 = 0$ at the expense of the second load Y_{L2} parameters.

Then, the center G_2 parameters will be as follows:

$$
\begin{aligned}
V_2^{G2} &= -\frac{1}{Y_{12}}I_1^{SC},\\
I_2^{G2} &= \frac{Y_{22}}{Y_{12}}I_1^{SC} + I_2^{SC} = V_0\, y_{0N}\left(1 + \frac{y_2}{y_{2N}}\right),
\end{aligned}
\tag{6.24}
$$

$$Y_{L2}^{G2} = \frac{I_{L2}^{G2}}{V_{L2}^{G2}} = -(y_2 + y_{2N}). \tag{6.25}$$

The center G_1 parameters are expressed similarly:

$$V_1^{G1} = -\frac{1}{Y_{12}} I_2^{SC},$$

$$I_1^{G1} = \frac{Y_{11}}{Y_{12}} I_2^{SC} + I_1^{SC} = V_0\, y_{0N}\left(1 + \frac{y_1}{y_{1N}}\right), \tag{6.26}$$

$$Y_{L1}^{G1} = \frac{I_{L1}^{G1}}{V_{L1}^{G1}} = -(y_1 + y_{1N}). \tag{6.27}$$

We accept that the center coordinates define the characteristic regimes.

Another kind of characteristic regime is the short-circuit regime of both loads ($Y_{L1} = \infty$, $Y_{L2} = \infty$) presented by the point SC in Fig. 6.9. The open-circuit regime of both loads is also the characteristic regime and corresponds to the origin of coordinates, the point 0.

So, the reference triangle $G_1\,0\,G_2$ and a unit point SC define the projective coordinates.

In turn, Fig. 6.10 demonstrates the axes V_1, V_2 of the familiar affine coordinates.

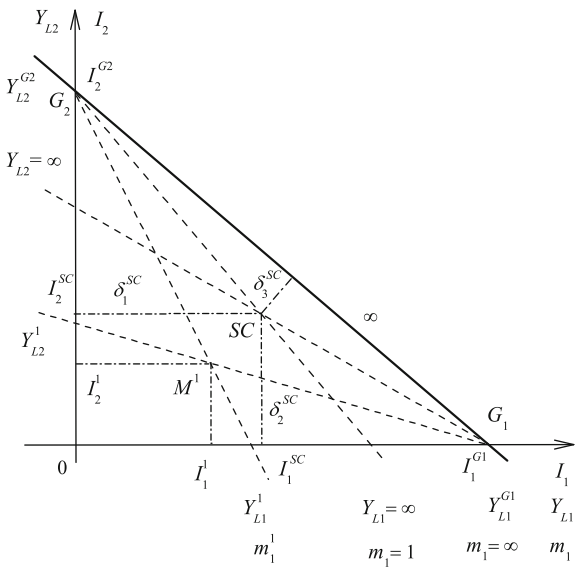

Fig. 6.9 Two bunches of straight lines with parameters Y_{L1}, Y_{L2}

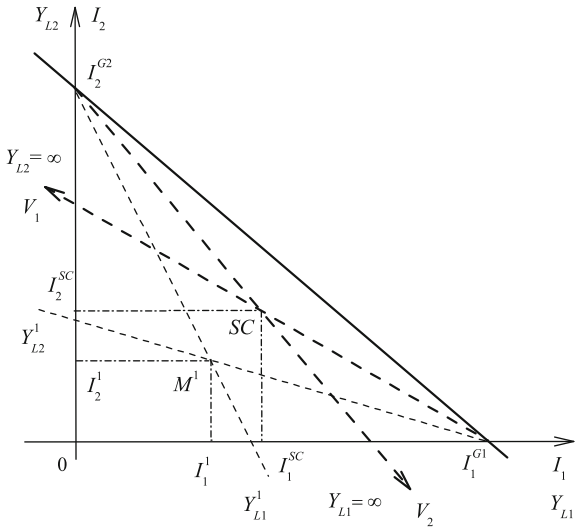

Fig. 6.10 Axes V_1, V_2 form the affine coordinates

Let an initial or running regime be corresponded to a point M^1 which is set by conductivities Y_{L1}^1, Y_{L2}^1 and currents I_1^1, I_2^1. Also, this point is defined by the projective non-uniform m_1^1, m_2^1 and homogeneous $\xi_1^1, \xi_2^1, \xi_3^1$ coordinates.

The point 0 is the origin of projective coordinates and the straight line $G_1\,G_2$ is the line of infinity ∞.

The non-uniform projective coordinate m_1^1 is set by the cross-ratio of four points similar to (2.24):

$$m_1^1 = (0\ Y_{L1}^1\ \infty\ Y_{L1}^{G1}) = \frac{Y_{L1}^1}{Y_{L1}^1 - Y_{L1}^{G1}} \div \frac{\infty - 0}{\infty - Y_{L1}^{G1}} = \frac{Y_{L1}^1}{Y_{L1}^1 - Y_{L1}^{G1}}. \tag{6.28}$$

There, the points $Y_{L1} = 0$, $Y_{L1}^1 = Y_{L1}^{G1}$ correspond to the base values. The point $Y_{L1} = \infty$ is a unit point. Also, the values of m_1 are shown in Fig. 6.9. For the point $Y_{L1}^1 = Y_{L1}^{G1}$, the projective coordinate $m_1 = \infty$ defines the sense of the line of infinity $G_1\,G_2$.

The projective coordinate m_2^1 is expressed by the same way

$$m_2^1 = (0\ Y_{L2}^1\ \infty\ Y_{L2}^{G2}) = \frac{Y_{L2}^1}{Y_{L2}^1 - Y_{L2}^{G2}}. \tag{6.29}$$

The homogeneous projective coordinates ξ_1, ξ_2, ξ_3 set the non-uniform coordinates as follows:

$$\frac{\xi_1}{\xi_3} = \frac{\rho\xi_1}{\rho\xi_3} = m_1, \quad \frac{\xi_2}{\xi_3} = \frac{\rho\xi_2}{\rho\xi_3} = m_2, \tag{6.30}$$

where ρ is a proportionality factor.

In turn, the homogeneous coordinates are defined by the ratio of the distances for points M^1, SC to the sides of reference triangle

$$\rho\xi_1^1 = \frac{\delta_1^1}{\delta_1^{SC}} = \frac{I_1^1}{I_1^{SC}}, \quad \rho\xi_2^1 = \frac{\delta_2^1}{\delta_2^{SC}} = \frac{I_2^1}{I_2^{SC}}, \quad \rho\xi_3^1 = \frac{\delta_3^1}{\delta_3^{SC}}. \tag{6.31}$$

For finding the distances $\delta_3^1, \delta_3^{SC}$ to the straight line $G_1\,G_2$, the following equation of this straight line is used:

$$\frac{I_1}{I_1^{G1}} + \frac{I_2}{I_2^{G2}} - 1 = 0. \tag{6.32}$$

Then, the distance is given as

$$\delta_3^{SC} = \frac{1}{\mu_3}\left(\frac{I_1^{SC}}{I_1^{G1}} + \frac{I_2^{SC}}{I_2^{G2}} - 1\right), \quad \mu_3 = \sqrt{\frac{1}{\left(I_1^{G1}\right)^2} + \frac{1}{\left(I_2^{G2}\right)^2}},$$

where μ_3 is a normalizing factor.

Further, we use these expressions in the form

$$\left(\frac{I_1^{SC}}{I_1^{G1}} + \frac{I_2^{SC}}{I_2^{G2}} - 1\right) = \mu_3\delta_3^{SC}, \tag{6.33}$$

$$\left(\frac{I_1^1}{I_1^{G1}} + \frac{I_2^1}{I_2^{G2}} - 1\right) = \mu_3\delta_3^1. \tag{6.34}$$

Then, by (6.31), the homogeneous coordinates have the view

$$\begin{aligned}
\rho\,\xi_1^1 &= \frac{I_1^1}{I_1^{SC}}, \\
\rho\,\xi_2^1 &= \frac{I_2^1}{I_2^{SC}}, \\
\rho\,\xi_3^1 &= \frac{I_1^1}{I_1^{G1}\mu_3\delta_3^{SC}} + \frac{I_2^1}{I_2^{G2}\mu_3\delta_3^{SC}} - \frac{1}{\mu_3\delta_3^{SC}}.
\end{aligned} \tag{6.35}$$

It allows presenting system of Eq. (6.35) in the matrix form:

$$\begin{bmatrix} \rho\,\xi_1 \\ \rho\,\xi_2 \\ \rho\,\xi_3 \end{bmatrix} = \begin{bmatrix} \frac{1}{I_1^{SC}} & 0 & 0 \\ 0 & \frac{1}{I_2^{SC}} & 0 \\ \frac{1}{I_1^{G1}\mu_3\delta_3^{SC}} & \frac{1}{I_2^{G2}\mu_3\delta_3^{SC}} & \frac{-1}{\mu_3\delta_3^{SC}} \end{bmatrix} \cdot \begin{bmatrix} I_1 \\ I_2 \\ 1 \end{bmatrix} = [\mathbf{C}] \cdot [\mathbf{I}]. \tag{6.36}$$

We do not use the superscripts "1" and "2" for currents. In this equation, the values $(I_1, I_2, 1)$ are the homogeneous Cartesian coordinates.

The inverse transformation is

$$\begin{bmatrix} \rho I_1 \\ \rho I_2 \\ \\ \rho 1 \end{bmatrix} = \begin{bmatrix} I_1^{SC} & 0 & 0 \\ 0 & I_2^{SC} & 0 \\ \frac{I_1^{SC}}{I_1^{G1}} & \frac{I_2^{SC}}{I_2^{G2}} & -\mu_3\delta_3^{SC} \end{bmatrix} \cdot \begin{bmatrix} \xi_1 \\ \xi_2 \\ \\ \xi_3 \end{bmatrix} = [\mathbf{C}]^{-1} \cdot [\xi]. \tag{6.37}$$

From here, we pass to the non-uniform Cartesian coordinates or currents as

$$\begin{aligned} I_1 &= \frac{\rho I_1}{\rho 1} = \frac{I_1^{SC} m_1}{\frac{I_1^{SC}}{I_1^{G1}} m_1 + \frac{I_2^{SC}}{I_2^{G2}} m_2 - \mu_3 \delta_3^{SC}}, \\ I_2 &= \frac{\rho I_2}{\rho 1} = \frac{I_2^{SC} m_2}{\frac{I_1^{SC}}{I_1^{G1}} m_1 + \frac{I_2^{SC}}{I_2^{G2}} m_2 - \mu_3 \delta_3^{SC}}. \end{aligned} \tag{6.38}$$

Thus, for preset values of the conductivities Y_{L1}, Y_{L2}, we find the coordinates m_1, m_2; transformation (6.38) allows finding the currents I_1, I_2.

It is possible to represent system of Eq. (6.38) by the normalized or relative form:

$$\begin{aligned} \frac{I_1}{I_1^{G1}} &= \frac{\frac{I_1^{SC}}{I_1^{G1}} m_1}{\frac{I_1^{SC}}{I_1^{G1}} m_1 + \frac{I_2^{SC}}{I_2^{G2}} m_2 - \frac{I_1^{SC}}{I_1^{G1}} - \frac{I_2^{SC}}{I_2^{G2}} + 1} \\ &= \frac{\frac{I_1^{SC}}{I_1^{G2}} m_1}{\frac{I_1^{SC}}{I_1^{G1}} (m_1 - 1) + \frac{I_2^{SC}}{I_2^{G2}} (m_2 - 1) + 1}. \\ \frac{I_2}{I_2^{G2}} &= \frac{\frac{I_2^{SC}}{I_2^{G2}} m_2}{\frac{I_1^{SC}}{I_1^{G1}} (m_1 - 1) + \frac{I_2^{SC}}{I_2^{G2}} (m_2 - 1) + 1}. \end{aligned} \tag{6.39}$$

From this system of equations, it is possible to obtain the equations of two bunches of straight lines, corresponding to (6.23):

$$\begin{aligned} 1 - \frac{I_2}{I_2^{G2}} &= \frac{I_1}{I_1^{G1}} \left[1 - \frac{1}{m_1} \left(1 - \frac{1 - I_2^{SC}/I_2^{G2}}{I_1^{SC}/I_1^{G1}} \right) \right], \\ 1 - \frac{I_1}{I_1^{G1}} &= \frac{I_2}{I_2^{G2}} \left[1 - \frac{1}{m_2} \left(1 - \frac{1 - I_1^{SC}/I_1^{G1}}{I_2^{SC}/I_2^{G2}} \right) \right]. \end{aligned} \tag{6.40}$$

Also, system of Eq. (6.39) allows obtaining in the relative form the equations of load characteristics $I_1(V_1, V_2),\ I_2(V_1, V_2)$ which correspond to Eq. (6.21). For this purpose, we express the non-uniform coordinates $m_1,\ m_2$ by currents and voltages:

$$m_1 = \frac{Y_{L1}}{Y_{L1} - Y_{L1}^{G1}} = \frac{I_1/V_1}{(I_1/V_1) - I_1^{G1}/V_1^{G1}} = \frac{I_1/I_1^{G1}}{(I_1/I_1^{G1}) - V_1/V_1^{G1}},$$
$$m_2 = \frac{I_2/I_2^{G2}}{(I_2/I_2^{G2}) - V_2/V_2^{G2}}.$$

Substituting these values in system (6.39), we obtain the required equations $I_1(V_1, V_2),\ I_2(V_1, V_2)$, excluding the currents $I_2,\ I_1$ accordingly:

$$\begin{aligned} \frac{I_1}{I_1^{G1}} &= \left(1 - \frac{I_1^{SC}}{I_1^{G1}}\right)\frac{V_1}{V_1^{G1}} - \frac{I_1^{SC}}{I_1^{G1}}\frac{V_2}{V_2^{G2}} + \frac{I_1^{SC}}{I_1^{G1}}, \\ \frac{I_2}{I_2^{G2}} &= -\frac{I_2^{SC}}{I_2^{G2}}\frac{V_1}{V_1^{G1}} + \left(1 - \frac{I_2^{SC}}{I_2^{G2}}\right)\frac{V_2}{V_2^{G2}} + \frac{I_2^{SC}}{I_2^{G2}}. \end{aligned} \tag{6.41}$$

The obtained system of equations represents the purely relative expressions. Therefore, such values, as

$$\left(1 - \frac{I_1^{SC}}{I_1^{G1}}\right), \frac{I_1^{SC}}{I_1^{G1}}, \frac{I_2^{SC}}{I_2^{G2}}, \left(1 - \frac{I_2^{SC}}{I_2^{G2}}\right),$$

represent the « normalized » Y parameters.

Let us pass to the absolute values of regime parameters in system (6.41):

$$\begin{aligned} I_1 &= \left(I_1^{G1} - I_1^{SC}\right)\frac{V_1}{V_1^{G1}} - I_1^{SC}\frac{V_2}{V_2^{G2}} + I_1^{SC}, \\ I_2 &= -I_2^{SC}\frac{V_1}{V_1^{G1}} + \left(I_2^{G2} - I_2^{SC}\right)\frac{V_2}{V_2^{G2}} + I_2^{SC}. \end{aligned} \tag{6.42}$$

From this, it follows that Y parameters are expressed by the parameters of characteristic regimes:

$$\begin{aligned} -Y_{11} &= \frac{I_1^{G2} - I_1^{SC}}{V_1^{G1}}, \\ -Y_{22} &= \frac{I_2^{G1} - I_2^{SC}}{V_2^{G2}}, \\ Y_{12} &= -\frac{I_1^{SC}}{V_2^{G2}} = -\frac{I_2^{SC}}{V_1^{G1}}. \end{aligned} \tag{6.43}$$

Systems of Eqs. (6.39) and (6.40) are important relationships, as represent the purely relative expressions. It allows defining, at first, the coordinates m_1, m_2 (as relative values) for different load conductivities, and then, the normalized currents.

Also, as (6.41), these expressions allow estimating at once a qualitative state of such a circuit; how much a running regime is close to the characteristic values. Then, the currents I_1^{G2}, I_2^{G1} represent the scales. In this sense, initial systems of Eqs. (6.21) and (6.22), containing the actual or absolute values of Y parameters, currents and voltages, are uninformative, because they do not give a direct representation about the qualitative characteristics of a circuit.

In addition, it is possible to notice that it is difficult to obtain directly the relative expressions of type (6.39)–(6.43) from systems of Eqs. (6.21) and (6.22). In this sense, the geometrical interpretation allows to solve this problem easily.

Example 2 We use the date of Example 1.

Equation (6.21) is given as

$$\begin{pmatrix} I_1 \\ I_2 \end{pmatrix} = \begin{pmatrix} -1.2 & 0.2 \\ 0.2 & -0.95 \end{pmatrix} \cdot \begin{pmatrix} V_1 \\ V_2 \end{pmatrix} + \begin{pmatrix} 3 \\ 2 \end{pmatrix}.$$

Bunch centers (6.24)–(6.27) are as follows:

$$I_1^{G1} = 15,\ V_1^{G1} = -10, Y_{L1}^{G1} = -1.5;$$
$$I_2^{G2} = 16.25,\ V_2^{G2} = -15, Y_{L2}^{G2} = -1.0833$$

Let the actual parameters of the running regime be given:

$$Y_{L1}^1 = 0.5, \quad Y_{L2}^1 = 0.5, \quad I_1^1 = 0.979, \quad I_2^1 = 0.8247.$$

Non-uniform projective coordinates (6.28) and (6.29) are

$$m_1^1 = 0.25, \quad m_2^1 = 0.3158.$$

The distances are

$$\mu_3 \delta_3^{SC} = -0.677, \quad \mu_3 \delta_3^1 = -0.8839, \quad \mu_3 = 0.0907.$$

Homogeneous coordinates (6.31) are

$$\rho\, \xi_1^1 = 0.979/3 = 0.3264, \quad \rho\, \xi_2^1 = 0.8247/2 = 0.4123,$$
$$\rho\, \xi_3^1 = 0.8839/0.677 = 1.3057.$$

Let us check up the non-uniform coordinates

$$m_1^1 = 0.3264/1.3057 = 0.25, \quad m_2^1 = 0.4123/1.3057 = 0.3158.$$

Matrix of transformation (6.36) is

$$[\mathbf{C}] = \begin{bmatrix} \frac{1}{3} & 0 & 0 \\ 0 & \frac{1}{2} & 0 \\ -\frac{1}{15 \cdot 0.677} & -\frac{1}{16.25 \cdot 0.677} & \frac{1}{0.677} \end{bmatrix}.$$

Matrix of inverse transformation (6.37) is

$$[\mathbf{C}]^{-1} = \begin{bmatrix} 3 & 0 & 0 \\ 0 & 2 & 0 \\ \frac{3}{15} & \frac{2}{16.25} & 0.677 \end{bmatrix}.$$

Let us check up the values of currents and Y parameters:

$$I_1^1 = \frac{3 \cdot 0.25}{\frac{3}{15} \cdot 0.25 + \frac{2}{16.25} \cdot 0.3158 + 0.677} = \frac{0.75}{0.7658} = 0.979,$$
$$I_2^1 = \frac{2 \cdot 0.3159}{0.7658} = 0.825;$$
$$-Y_{11} = \frac{15-3}{-10} = -1.2, \; -Y_{22} = \frac{16.25-2}{-15} = -0.95,$$
$$Y_{12} = \frac{3}{15} = \frac{2}{10} = 0.2.$$

6.2 Projective Coordinates in Space

6.2.1 Particular Case of a Multi-port

The popularized power supply system is shown in Fig. 6.11. Three and more loads are connected to a common supply voltage source V_0 or common node N by own circuits (two-port $TP1$, $TP2$ and so on). The interference of loads is observed because of the internal circuits by y_{0N}, y_N of the voltage source.

Let us use the above approach for an active two-port network with changeable conductivities of loads.

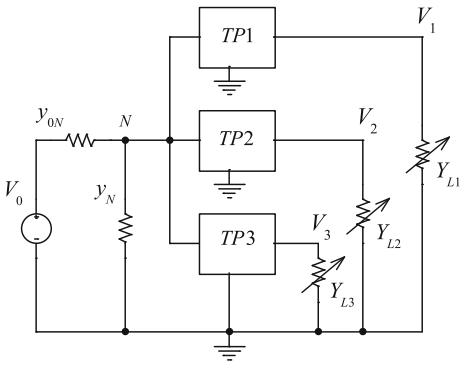

Fig. 6.11 Power supply system with a common voltage source

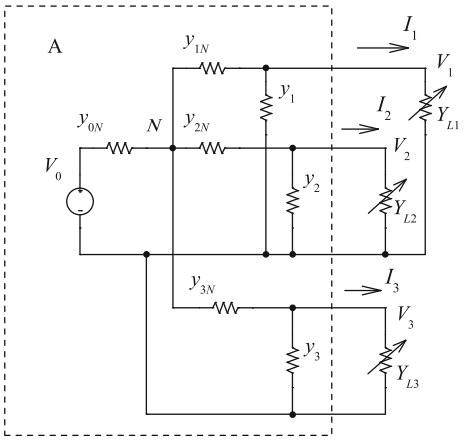

Fig. 6.12 Active multi-port with three loads

We now consider the concrete active multi-port network in Fig. 6.12. Similar to (6.21), this network is described by the following system of equations [8, 11]:

$$\begin{bmatrix} I_1 \\ I_2 \\ I_3 \end{bmatrix} = \begin{bmatrix} -Y_{11} & Y_{12} & Y_{13} \\ Y_{12} & -Y_{22} & Y_{23} \\ Y_{13} & Y_{23} & -Y_{33} \end{bmatrix} \cdot \begin{bmatrix} V_1 \\ V_2 \\ V_3 \end{bmatrix} + \begin{bmatrix} I_1^{SC} \\ I_2^{SC} \\ I_3^{SC} \end{bmatrix}, \tag{6.44}$$

where

$$Y_{11} = y_1 + y_{1N} - \frac{y_{1N}^2}{y_\Sigma}, \quad y_\Sigma = y_{0N} + y_{1N} + y_{2N} + y_{3N},$$

$$Y_{12} = y_{2N}\frac{y_{1N}}{y_\Sigma}, Y_{13} = y_{3N}\frac{y_{1N}}{y_\Sigma}, \quad Y_{22} = y_2 + y_{2N} - \frac{y_{2N}^2}{y_\Sigma},$$

$$Y_{23} = y_{3N}\frac{y_{2N}}{y_\Sigma}, \quad Y_{33} = y_3 + y_{3N} - \frac{y_{3N}^2}{y_\Sigma}.$$

The short-circuit *SC* currents of all the loads are

$$I_1^{SC} = Y_{10}V_0 = y_{0N}\frac{y_{1N}}{y_\Sigma}V_0, \quad I_2^{SC} = Y_{20}V_0 = y_{0N}\frac{y_{2N}}{y_\Sigma}V_0,$$
$$I_3^{SC} = Y_{30}V_0 = y_{0N}\frac{y_{3N}}{y_\Sigma}V_0.$$

Taking into account the voltages $V_1 = I_1/Y_{L1}$, $V_2 = I_2/Y_{L2}$, $V_3 = I_2/Y_{L3}$, the equations of three bunches of planes are obtained from system of Eq. (6.44) similar to Eq. (6.23) and the bunches of straight lines of the active two-port in Fig. 6.9. The intersection of the planes of one bunch among themselves defines a bunch axis. The equation of the axis of the bunch Y_{L1} corresponds to the condition $I_1 = 0$, $V_1 = 0$. Therefore, this axis is located into the plane I_2, I_3, as it is shown in Fig. 6.13.

The point of intersection with the current axis I_2 is defined by

$$I_2^{G2} = V_0\, y_{0N}\left(1 + \frac{y_2}{y_{2N}}\right) \tag{6.45}$$

that corresponds to the voltage and conductivity of the second load

$$V_2^{G2} = -\frac{Y_{10}}{Y_{12}}V_0 = -\frac{y_{0N}}{y_{2N}}V_0, \quad Y_{L2}^{G2} = -(y_{2N} + y_2).$$

The point of intersection with the current axis I_3 defines the third load:

$$I_3^{G3} = V_0\, y_{0N}\left(1 + \frac{y_3}{y_{3N}}\right), \quad V_3^{G3} = -\frac{y_{0N}}{y_{3N}}V_0, \quad Y_{L3}^{G3} = -(y_{3N} + y_3). \tag{6.46}$$

Similarly, the axis of the bunch Y_{L2} corresponds to the condition $I_2 = 0$ and is located in the plane I_1, I_3. The point of intersection with the current axis I_1 defines the first load

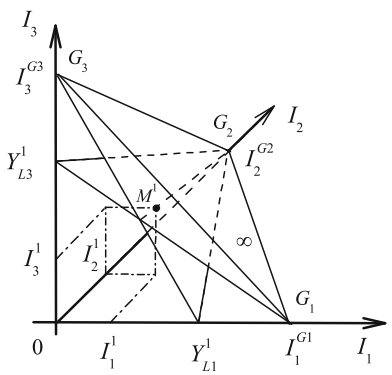

Fig. 6.13 Two bunches of the planes with parameters Y_{L1}, Y_{L3}

$$I_1^{G1} = V_0\, y_{0N}\left(1 + \frac{y_1}{y_{1N}}\right), \quad V_1^{G1} = -\frac{y_{0N}}{y_{1N}} V_0, \quad Y_{L1}^{G1} = -(y_{1N} + y_1). \tag{6.47}$$

The characteristic regime is the short circuit of the loads $Y_{L1} = \infty$, $Y_{L2} = \infty, Y_{L3} = \infty$. The open circuit of the loads is also characteristic and corresponds to the origin of coordinates, the point 0 in Fig. 6.13.

Also, we accept the plane, which passes through three points $I_1^{G1}, I_2^{G2}, I_3^{G3}$ on the axes of coordinates, as the plane of infinity ∞. This plane and three coordinate planes $I_1 = 0$, $I_2 = 0$, $I_3 = 0$ form the coordinate tetrahedron $0\,G_1G_2G_3$.

Let an initial or running regime be corresponded to a point M^1 which is set by conductivities $Y_{L1}^1, Y_{L2}^1, Y_{L3}^1$ and currents I_1^1, I_2^1, I_3^1. Also, this point is defined by the projective non-uniform coordinates m_1^1, m_2^1, m_3^1 and homogeneous $\xi_1^1, \xi_2^1, \xi_3^1, \xi_4^1$ coordinates, which are set by the coordinate tetrahedron $0\,G_1G_2G_3$ and a unit point SC. Then, the homogeneous coordinates are defined as the ratio of the distances for points M^1, SC to the planes of coordinate tetrahedron

$$\rho\xi_1^1 = \frac{I_1^1}{I_1^{SC}}, \quad \rho\xi_2^1 = \frac{I_2^1}{I_2^{SC}}, \quad \rho\xi_3^1 = \frac{I_3^1}{I_3^{SC}}, \quad \rho\xi_4^1 = \frac{\delta_4^1}{\delta_4^{SC}}. \tag{6.48}$$

The distances are

$$\delta_4^1 = \frac{1}{\mu_4}\left(\frac{I_1^1}{I_1^{G1}} + \frac{I_2^1}{I_2^{G2}} + \frac{I_3^1}{I_3^{G2}} - 1\right), \quad \delta_4^{SC} = \frac{1}{\mu_4}\left(\frac{I_1^{SC}}{I_1^{G1}} + \frac{I_2^{SC}}{I_2^{G2}} + \frac{I_3^{SC}}{I_3^{G2}} - 1\right),$$

$$\mu_4 = \sqrt{\frac{1}{\left(I_1^{G1}\right)^2} + \frac{1}{\left(I_2^{G2}\right)^2} + \frac{1}{\left(I_3^{G3}\right)^2}},$$

where μ_4 is a normalizing factor.

The non-uniform projective coordinate m_1^1 is set by the familiar cross-ratio:

$$m_1^1 = (0\ Y_{L1}^1\ \infty\ Y_{L1}^{G1}) = \frac{Y_{L1}^1}{Y_{L1}^1 - Y_{L1}^{G1}} \div \frac{\infty - 0}{\infty - Y_{L1}^{G1}} = \frac{Y_{L1}^1}{Y_{L1}^1 - Y_{L1}^{G1}}. \tag{6.49}$$

There, the points $Y_{L1} = 0$, $Y_{L1}^1 = Y_{L1}^{G1}$ correspond to the base values. The point $Y_{L1} = \infty$ is a unit point. For the point $Y_{L1}^1 = Y_{L1}^{G1}$, the coordinate $m_1 = \infty$

defines the sense of the line of infinity $G_1\,G_2$. The cross-ratio for m_2^1, m_3^1 is expressed similarly. Therefore, we get the plane $G_1G_2G_3$ of infinity ∞.

Also, the homogeneous projective coordinates ξ_1, ξ_2, ξ_3 set the non-uniform coordinates as follows:

$$\frac{\xi_1}{\xi_4} = \frac{\rho\xi_1}{\rho\xi_4} = m_1, \quad \frac{\xi_2}{\xi_4} = \frac{\rho\xi_2}{\rho\xi_4} = m_2, \quad \frac{\xi_3}{\xi_4} = \frac{\rho\xi_3}{\rho\xi_4} = m_3. \tag{6.50}$$

where ρ is a proportionality factor.

Homogeneous projective coordinates (6.48) have the matrix form

$$[\rho\,\xi] = [\mathbf{C}] \cdot [\mathbf{I}], \tag{6.51}$$

where

$$[\rho\xi] = \begin{bmatrix} \rho\xi_1 \\ \rho\xi_2 \\ \rho\xi_3 \\ \rho\xi_4 \end{bmatrix}, \; [\mathbf{I}] = \begin{bmatrix} I_1 \\ I_2 \\ I_3 \\ 1 \end{bmatrix},$$

$$[\mathbf{C}] = \begin{bmatrix} \frac{1}{I_1^{SC}} & 0 & 0 & 0 \\ 0 & \frac{1}{I_2^{SC}} & 0 & 0 \\ 0 & 0 & \frac{1}{I_3^{SC}} & 0 \\ \frac{1}{I_1^{G1}\mu_4\delta_4^{SC}} & \frac{1}{I_2^{G2}\mu_4\delta_4^{SC}} & \frac{1}{I_3^{G3}\mu_4\delta_4^{SC}} & -\frac{1}{\mu_4\delta_4^{SC}} \end{bmatrix}.$$

The inverse transformation is

$$\begin{gathered} [\rho\,\mathbf{I}] = [\mathbf{C}]^{-1} \cdot [\xi], \\ [\mathbf{C}]^{-1} = \begin{bmatrix} I_1^{SC} & 0 & 0 & 0 \\ 0 & I_2^{SC} & 0 & 0 \\ 0 & 0 & I_3^{SC} & 0 \\ \frac{I_1^{SC}}{I_1^{G1}} & \frac{I_2^{SC}}{I_2^{G2}} & \frac{I_3^{SC}}{I_3^{G3}} & -\mu_4\delta_4^{SC} \end{bmatrix}. \end{gathered} \tag{6.52}$$

From here, we find the currents

$$\begin{aligned} I_1 &= \frac{\rho I_1}{\rho 1} = \frac{I_1^{SC} m_1}{\frac{I_1^{SC}}{I_1^{G1}} m_1 + \frac{I_2^{SC}}{I_2^{G2}} m_2 + \frac{I_3^{SC}}{I_3^{G3}} m_3 - \mu_4\delta_4^{SC}}, \\ I_2 &= \frac{\rho I_2}{\rho 1}, \; I_3 = \frac{\rho I_3}{\rho 1}. \end{aligned} \tag{6.53}$$

Then, the normalized expressions for currents are

$$\frac{I_1}{I_1^{G1}} = \frac{\frac{I_1^{SC}}{I_1^{G1}} m_1}{(m_1, m_2, m_3)}, \quad \frac{I_2}{I_2^{G2}} = \frac{\frac{I_2^{SC}}{I_2^{G2}} m_2}{(m_1, m_2, m_3)}, \quad \frac{I_3}{I_3^{G3}} = \frac{\frac{I_3^{SC}}{I_3^{G3}} m_3}{(m_1, m_2, m_3)}, \tag{6.54}$$

where

$$\frac{1}{(m_1, m_2, m_3)} = \frac{1}{\frac{I_1^{SC}}{I_1^{G1}}(m_1 - 1) + \frac{I_2^{SC}}{I_2^{G2}}(m_2 - 1) + \frac{I_3^{SC}}{I_3^{G3}}(m_3 - 1) + 1}.$$

Also, system of Eq. (6.54) allows obtaining in the relative form the equations of load characteristics which correspond to Eq. (6.44). For this purpose, we express the non-uniform coordinates m_1, m_2, m_3 by the currents and voltages

$$m_1 = \frac{Y_{L1}}{Y_{L1} - Y_{L1}^{G1}} = \frac{I_1/I_1^{G1}}{(I_1/I_1^{G1}) - V_1/V_1^{G1}},$$
$$m_2 = \frac{I_2/I_2^{G2}}{(I_2/I_2^{G2}) - V_2/V_2^{G2}}, \quad m_3 = \frac{I_3/I_3^{G3}}{(I_3/I_3^{G3}) - V_3/V_3^{G3}}.$$

Having substituted these values in system (6.54), we obtain the required equations:

$$\begin{aligned}
\frac{I_1}{I_1^{G1}} &= \left(1 - \frac{I_1^{SC}}{I_1^{G1}}\right)\frac{V_1}{V_1^{G1}} - \frac{I_1^{SC}}{I_1^{G1}}\frac{V_2}{V_2^{G2}} - \frac{I_1^{SC}}{I_1^{G1}}\frac{V_3}{V_3^{G3}} + \frac{I_1^{SC}}{I_1^{G1}}, \\
\frac{I_2}{I_2^{G2}} &= -\frac{I_2^{SC}}{I_2^{G2}}\frac{V_1}{V_1^{G1}} + \left(1 - \frac{I_2^{SC}}{I_2^{G2}}\right)\frac{V_2}{V_2^{G2}} - \frac{I_2^{SC}}{I_2^{G2}}\frac{V_3}{V_3^{G3}} + \frac{I_2^{SC}}{I_2^{G2}}, \\
\frac{I_3}{I_3^{G3}} &= -\frac{I_3^{SC}}{I_3^{G3}}\frac{V_1}{V_1^{G1}} - \frac{I_3^{SC}}{I_3^{G3}}\frac{V_2}{V_2^{G2}} + \left(1 - \frac{I_3^{SC}}{I_3^{G3}}\right)\frac{V_3}{V_3^{G3}} + \frac{I_3^{SC}}{I_3^{G3}}.
\end{aligned} \tag{6.55}$$

The obtained equations represent the purely relative expressions. The currents $I_1^{G1}, I_2^{G2}, I_3^{G3}$ are the scales. It is obvious that relative expressions (6.55) are generalized to any number of loads by the formal way. If we use the absolute values of the regime parameters of Eq. (6.54), then Y parameters are expressed by the parameters of the characteristic regimes.

Example 3 We consider the circuit with given parameters in Fig. 6.14.

System of Eq. (6.44) is

$$\begin{bmatrix} I_1 \\ I_2 \\ I_3 \end{bmatrix} = \begin{bmatrix} -1.236 & 0.17 & 0.282 \\ 0.17 & -0.966 & 0.188 \\ 0.282 & 0.188 & 1.283 \end{bmatrix} \cdot \begin{bmatrix} V_1 \\ V_2 \\ V_3 \end{bmatrix} + \begin{bmatrix} 2.641 \\ 1.761 \\ 2.817 \end{bmatrix}.$$

Bunch centers (6.45)–(6.47) are

$$I_2^{G2} = 16.25, \quad Y_{L2}^{G2} = -1.0833; \quad I_3^{G3} = 14.844, Y_{L3}^{G3} = -1.583;$$
$$I_1^{G1} = 15, \; Y_{L1}^{G1} = -1.5.$$

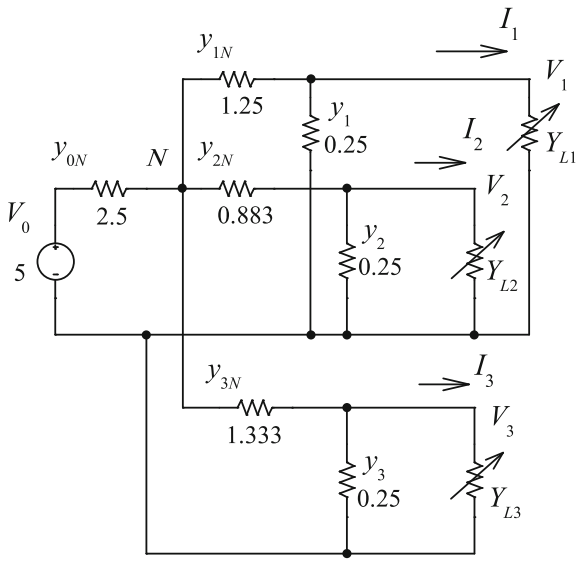

Fig. 6.14 Example of the circuit with three loads

Let the actual parameters of running regime be given

$$Y_{L1}^1 = 0.5, \quad Y_{L2}^1 = 0.5, \quad Y_{L3}^1 = 1;$$
$$I_1^1 = 0.974, \quad I_2^1 = 0.82, \quad I_3^1 = 1.61.$$

Non-uniform projective coordinates (6.49) are

$$m_1^1 = 0.25, \quad m_2^1 = 0.316, \quad m_3^1 = 0.387.$$

The distances are

$$\mu_4 \delta_4^{SC} = -0.526, \quad \mu_4 \delta_4^1 = -0.776, \quad \mu_4 = 0.0907.$$

The homogeneous coordinates (6.48) are

$$\rho\, \xi_1^1 = 0.974/2.641 = 0.369, \quad \rho\, \xi_2^1 = 0.466,$$
$$\rho\, \xi_3^1 = 0.571, \quad \rho\, \xi_4^1 = 1.476.$$

Matrix of transformation (6.52) is

$$[\mathbf{C}]^{-1} = \begin{bmatrix} 2.641 & 0 & 0 & 0 \\ 0 & 1.761 & 0 & 0 \\ 0 & 0 & 2.817 & 0 \\ 0.176 & 0.108 & 0.19 & 0.526 \end{bmatrix}.$$

Let us check current (6.53)

$$I_1^1 = \frac{2.641 \cdot 0.25}{0.176 \cdot 0.25 + 0.108 \cdot 0.316 + 0.19 \cdot 0.387 + 0.526} = \frac{0.66}{0.67} = 0.974.$$

6.2.2 General Case of a Multi-port. The Balanced Networks

Let us consider the general case of an active multi-port, for example, with three load conductivities Y_{L1}, Y_{L2}, and Y_{L3} in Fig. 6.15 [13–15]. The circuit is also described by system of Eq. (6.44).

Therefore, the equations of three bunches of planes are obtained in the form

$$(I_1, I_2, I_3, Y_{L1}) = 0, \quad (I_1, I_2, I_3, Y_{L2}) = 0, \quad (I_1, I_2, I_3, Y_{L3}) = 0.$$

The equation of the axis of the bunch Y_{L1} corresponds to the condition $I_1 = 0$, $V_1 = 0$ and to equation $(I_2, I_3) = 0$. Therefore, this axis is located in the plane I_2, I_3 in Fig. 6.16a.

The points $I_2(Y_{L1})$, $I_3(Y_{L1})$ are the points of intersection with corresponding axis. Similarly, we obtain the points $I_1(Y_{L2})$, $I_3(Y_{L2})$ of intersection of the bunch axis Y_{L2} and the points $I_1(Y_{L3})$, $I_2(Y_{L3})$ of intersection of the bunch axis Y_{L3}.

On the other hand, the projective system of coordinates has to represent the tetrahedron $0\,G_1G_2G_3$ in Fig. 6.16b. In this case, we accept the plane, which passes through three base points I_1^{G1}, I_2^{G2}, and I_3^{G3} on the axes of coordinates, as the plane of infinity ∞. Therefore, the next conditions have to be satisfied

$$I_1(Y_{L2}) = I_1(Y_{L3}) = I_1^{G1}, \quad I_2(Y_{L1}) = I_2(Y_{L3}) = I_2^{G2},$$
$$I_3(Y_{L1}) = I_3(Y_{L2}) = I_3^{G3}.$$

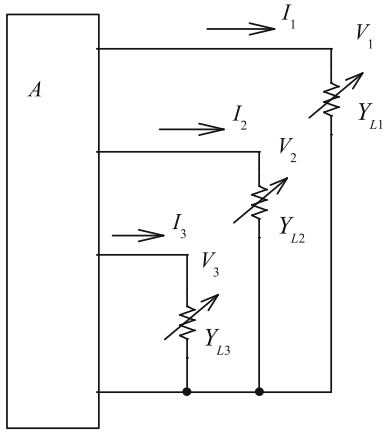

Fig. 6.15 Example of an active multi-port

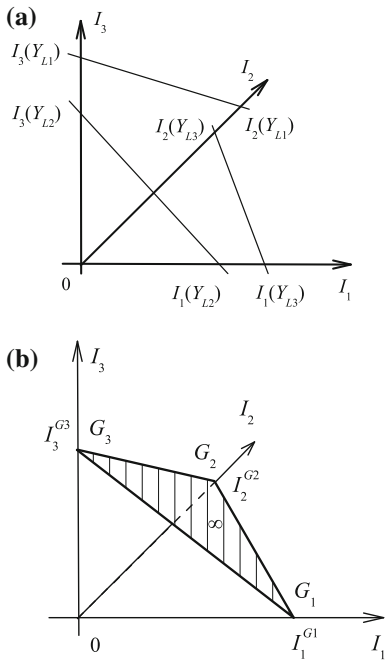

Fig. 6.16 **a** Points of intersection do not coincide among themselves. **b** Points of intersection coincide among themselves and form the plane of infinity ∞

We must determine requirements for Y parameters. Let us consider the base point or base values

$$I_1 = I_1^{G1}, \quad V_1 = V_1^{G1}.$$

Then,

$$I_2 = 0,\ V_2 = 0, \quad I_3 = 0, \quad V_3 = 0.$$

Using Eq. (6.44), we get

$$\begin{cases} I_1^{G1} = -Y_{11}V_1^{G1} + I_1^{SC} \\ 0 = Y_{12}V_1^{G1} + I_2^{SC} \\ 0 = Y_{13}V_1^{G1} + I_3^{SC}. \end{cases} \tag{6.56}$$

From here, the requirements have the view

$$-V_1^{G1} = \frac{I_2^{SC}}{Y_{12}} = \frac{I_3^{SC}}{Y_{13}}. \tag{6.57}$$

Similarly, we consider

$$I_2 = I_2^{G2}, \quad V_2 = V_2^{G2}.$$

Then,

$$\begin{cases} 0 = Y_{12}V_2^{G2} + I_1^{SC} \\ I_2^{G2} = -Y_{22}V_2^{G2} + I_2^{SC} \\ 0 = Y_{23}V_2^{G2} + I_3^{SC}, \end{cases} \quad -V_2^{G2} = \frac{I_1^{SC}}{Y_{12}} = \frac{I_3^{SC}}{Y_{23}}. \tag{6.58}$$

And we consider

$$I_3 = I_3^{G3}, \quad V_3 = V_3^{G3}.$$

$$\begin{cases} 0 = Y_{13}V_3^{G3} + I_1^{SC} \\ 0 = Y_{23}V_3^{G3} + I_2^{SC} \\ I_3^{G3} = -Y_{33}V_3^{G3} + I_3^{SC}, \end{cases} \quad -V_3^{G3} = \frac{I_1^{SC}}{Y_{13}} = \frac{I_2^{SC}}{Y_{23}}. \tag{6.59}$$

Obtained requirements or base points (6.56)–(6.59) are formally generalized for a larger number of loads.

For clarity, let us view the concrete network in Fig. 6.17. This circuit represents a multi-terminal or distributed network with three loads and $N - 4$ voltage sources. The voltage sources are connected to each of the loads. Therefore, internal conductivities $y_{44}, \ldots, y_{NN}$ of these voltage sources determine a mutual influence of the loads.

We consider the case

$$I_1 = I_1^{G1}, \quad V_1 = V_1^{G1}.$$

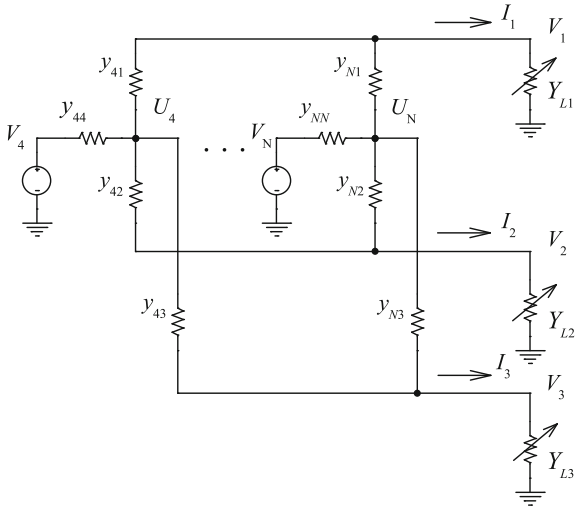

Fig. 6.17 Example of a multi-terminal network

Then, the equalities $U_4 = 0, \ldots, U_N = 0$ are the particular cases of the requirements $I_2 = 0, V_2 = 0, I_3 = 0, V_3 = 0$. Therefore, Eq. (6.56) reduces to the equalities

$$I_1^{G1} = I_4^{SC} + \cdots + I_N^{SC} = y_{44}V_4 + \cdots + y_{NN}V_N, \quad -V_1^{G1} = \frac{I_4^{SC}}{y_{41}} = \cdots = \frac{I_N^{SC}}{y_{N1}}.$$

Similar expressions are obtained for the rest loads.

One more circuit important for practice is presented in Fig. 6.18. There is a distributed network or active:multi-port, for example, with three pairs of voltage sources and loads, that is, a six-port.

Now, we obtain conditions (6.56)–(6.59) with the aid of Fig. 6.19. Let the first load voltage be $V_1 = -V_1^{G1}$.

For the others, we consider

$$V_2 = 0, I_2 = 0; \quad V_3 = 0, I_3 = 0.$$

This condition gives the following relationship:

$$U_a^{G1} = \frac{I_5^{SC}}{y_{ab}} = \frac{I_6^{SC}}{y_{ac}}. \tag{6.60}$$

In turn, the currents are

$$I_5^{SC} = y_{5b}V_5, \; I_6^{SC} = y_{6c}V_6. \tag{6.61}$$

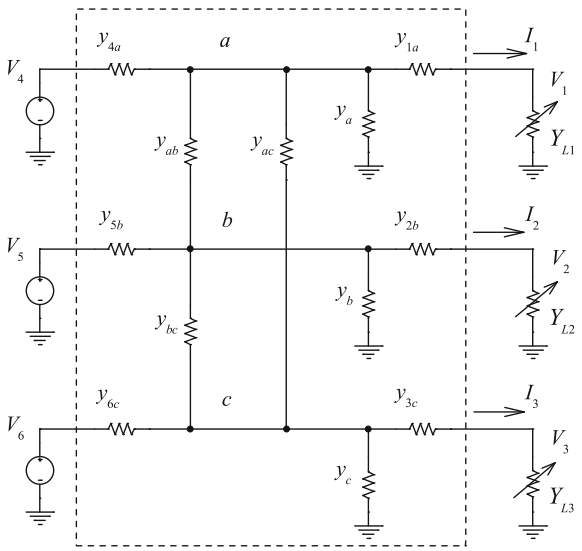

Fig. 6.18 Example of a multi-port or distributed network

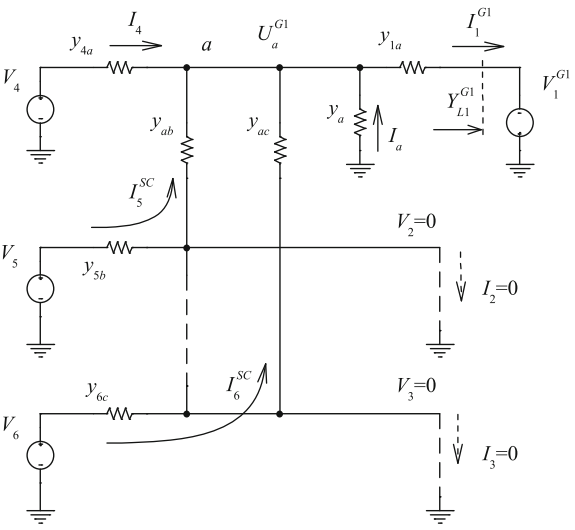

Fig. 6.19 Equivalent circuit of the multi-port for calculation the base values I_1^{G1}, V_1^{G1}

Therefore, we get

$$\frac{y_{5b}}{y_{ab}} V_5 = \frac{y_{6c}}{y_{ac}} V_6.$$

We determine the base values as

$$V_1^{G1} = U_a^{G1} + \frac{I_1^{G1}}{y_{1a}}, \quad I_1^{G1} = I_4 + I_5^{SC} + I_6^{SC} + I_a, \quad Y_{L1}^{G1} = \frac{I_1^{G1}}{V_1^{G1}}, \tag{6.62}$$

where

$$I_4 = (V_4 + U_a^{G1}) y_{4a}, \quad I_a = y_a U_a^{G1}. \tag{6.63}$$

Let the second load voltage be $V_2 = -V_2^{G2}$. For the others, we consider

$$V_1 = 0,\, I_1 = 0; \quad V_3 = 0, I_3 = 0.$$

This condition gives the following relationship:

$$U_b^{G2} = \frac{I_4^{SC}}{y_{ab}} = \frac{I_6^{SC}}{y_{bc}},$$

In turn, the current is

$$I_4^{SC} = y_{4a} V_4.$$

Therefore, we get

$$\frac{y_{4a}}{y_{ab}} V_4 = \frac{y_{6c}}{y_{bc}} V_6. \tag{6.64}$$

From here, we determine the base values

$$V_2^{G2} = U_b^{G2} + \frac{I_2^{G2}}{y_{2b}}, \quad I_2^{G2} = I_4^{SC} + I_5 + I_6^{SC} + I_b, \quad Y_{L2}^{G2} = \frac{I_2^{G2}}{V_2^{G2}}, \tag{6.65}$$

where

$$I_5 = (V_5 + U_b^{G2}) y_{5b}, \quad I_b = y_b U_b^{G2}.$$

Let the third load voltage be $V_3 = -V_3^{G3}$ and

$$V_1 = 0, I_1 = 0; \quad V_2 = 0, I_2 = 0.$$

Therefore,

$$U_c^{G3} = \frac{I_4^{SC}}{y_{ac}} = \frac{I_5^{SC}}{y_{bc}}.$$

From here,

$$\frac{y_{4a}}{y_{ac}} V_4 = \frac{y_{5b}}{y_{bc}} V_5. \tag{6.66}$$

The base values are

$$V_3^{G3} = U_c^{G3} + \frac{I_3^{G3}}{y_{3c}}, \quad I_3^{G3} = I_4^{SC} + I_5^{SC} + I_6 + I_c, \quad Y_{L3}^{G3} = \frac{I_3^{G3}}{V_3^{G3}}, \tag{6.67}$$

where

$$I_6 = (V_6 + U_c^{G3}) y_{6c}, \quad I_c = y_c U_c^{G3}.$$

Usually, the voltage sources of distributed power supply system have equal voltage values and different output powers. Let the voltage source V_5 and load Y_{L2} be the most powerful elements. Therefore, the values of conductivities $y_{5b}, y_{bc}, y_{ab}, y_{4a}$ can be given independently, for example, based on the power effectiveness of distributed network or current sharing among paralleled voltage sources.

Then, relative to these conductivities, using (6.64) and (6.66), we get the values of the rest conductivities

$$y_{6c} = \frac{y_{bc}}{y_{ab}} y_{4a}, \quad y_{ac} = \frac{y_{bc}}{y_{5b}} y_{4a} = \frac{y_{ab}}{y_{5b}} y_{6c}. \tag{6.68}$$

We will identify this distributed network *as balanced network for output terminals*.

The obtained conductivity values do not limit especially the functional possibility of such circuits but allow simplifying essential calculation of currents.

Let a running regime be corresponded to a point M^1, which is set by conductivities Y^1_{L1}, Y^1_{L2}, Y^1_{L3}. Therefore, we may use Fig. 6.13 and relationships (6.48), (6.49), (6.52), and (6.53) for finding the load currents I^1_1, I^1_2, I^1_3.

Also, we may represent (6.53) in the other form:

$$\begin{aligned}
I^1_1 &= \frac{I^{SC}_1 m^1_1}{\frac{I^{SC}_1}{I^{G1}_1} m^1_1 + \frac{I^{SC}_2}{I^{G2}_2} m^1_2 + \frac{I^{SC}_3}{I^{G3}_3} m^1_3 - \left(\frac{I^{SC}_1}{I^{G1}_1} + \frac{I^{SC}_2}{I^{G2}_2} + \frac{I^{SC}_3}{I^{G2}_3} - 1\right)} \\
&= \frac{I^{SC}_1 m^1_1}{\frac{I^{SC}_1}{I^{G1}_1}(m^1_1 - 1) + \frac{I^{SC}_2}{I^{G2}_2}(m^1_2 - 1) + \frac{I^{SC}_3}{I^{G3}_3}(m^1_3 - 1) + 1}, \\
I^1_2 &= \frac{\rho I^1_2}{\rho 1} = \frac{I^{SC}_2 m^1_2}{\frac{I^{SC}_1}{I^{G1}_1}(m^1_1 - 1) + \frac{I^{SC}_2}{I^{G2}_2}(m^1_2 - 1) + \frac{I^{SC}_3}{I^{G3}_3}(m^1_3 - 1) + 1}, \\
I^1_3 &= \frac{\rho I^1_3}{\rho 1} = \frac{I^{SC}_3 m^1_3}{\frac{I^{SC}_1}{I^{G1}_1}(m^1_1 - 1) + \frac{I^{SC}_2}{I^{G2}_2}(m^1_2 - 1) + \frac{I^{SC}_3}{I^{G3}_3}(m^1_3 - 1) + 1}.
\end{aligned} \tag{6.69}$$

Therefore,

$$\begin{aligned}
[\rho \mathbf{I}^1] &= \begin{bmatrix} \rho I^1_1 \\ \rho I^1_2 \\ \rho I^1_3 \\ \rho 1 \end{bmatrix} = [\mathbf{J^1}] \cdot \begin{bmatrix} I^{\mathrm{SC}}_1 \\ I^{\mathrm{SC}}_2 \\ I^{\mathrm{SC}}_3 \\ 1 \end{bmatrix} = [\mathbf{J^1}] \cdot [\mathbf{I^{SC}}], \\
[\mathbf{J^1}] &= \begin{bmatrix} m^1_1 & 0 & 0 & 0 \\ 0 & m^1_2 & 0 & 0 \\ 0 & 0 & m^1_3 & 0 \\ \frac{1}{I^{G1}_1}(m^1_1 - 1) & \frac{1}{I^{G2}_2}(m^1_2 - 1) & \frac{1}{I^{G3}_3}(m^1_3 - 1) & 1 \end{bmatrix}.
\end{aligned} \tag{6.70}$$

It is possible to view this expression as a recalculation formula of currents at respective change of loads from the *SC* regime to the initial regime M^1. The values m^1_1, m^1_2, m^1_3 are the parameters of such a projective transformation.

Example 4 We consider the network in Fig. 6.18. Let the voltages be $V_4 = V_5 = V_6 = 5$, the conductivities be $y_{5b} = 1/2.5$, $y_{bc} = 1/6$, $y_{ab} = 1/4$, $y_{4a} = 1/5$, $y_a = y_b = y_c = 1/20$, and $y_{1a} = y_{2b} = y_{3c} = 1$.

Using (6.68), we get conductivity $y_{6c} = 1/7.5$ and $y_{ac} = 1/12$.

We calculate *SC* output or load currents

$$I_1^{SC} = 0.8629, \quad I_2^{SC} = 1.246, \quad I_3^{SC} = 0.6601.$$

Voltage source or input *SC* currents (6.61) are $I_5^{SC} = 2$, $I_6^{SC} = 0.666$ and current is $I_4^{SC} = 1$.

In turn, voltage value (6.60) is $U_a^{G1} = 8$.

Currents (6.63) are $I_4 = 13/5 = 2.6$, $I_a = 8/20 = 0.4$.

Bunch centers (6.62), (6.65), and (6.67) are

$$\begin{aligned} &I_1^{G1} = 5.666, \quad V_1^{G1} = -13.666, \quad Y_{L1}^{G1} = -0.4146; \\ &I_2^{G2} = 5.466, \quad V_2^{G2} = -9.466, \quad Y_{L2}^{G2} = -0.5774; \\ &I_3^{G3} = 5.866, \quad V_3^{G3} = -17.866, \quad Y_{L3}^{G3} = -0.3283. \end{aligned}$$

The initial regimes are

$$\begin{aligned} &Y_{L1}^1 = 0.2, \quad Y_{L2}^1 = 0.25, \quad Y_{L3}^1 = 0.1666; \\ &I_1^1 = 0.4232, \quad I_2^1 = 0.5673, \quad I_3^1 = 0.3350. \end{aligned}$$

Non-uniform projective coordinates (6.49) are

$$m_1^1 = 0.3254, \quad m_2^1 = 0.3022, \quad m_3^1 = 0.3366$$

The distances are

$$\mu_4 \delta_4^1 = -0.7644, \quad \mu_4 \delta_4^{SC} = -0.5073.$$

Homogeneous coordinates (6.48) are

$$\begin{aligned} &\rho\xi_1^1 = 0.4232/0.8629 = 0.4904, \ \rho\xi_2^1 = 0.4553, \\ &\rho\xi_3^1 = 0.5075, \ \rho\xi_4^1 = 1.5069. \end{aligned}$$

Let us check non-uniform projective coordinates (6.50) as

$$\begin{aligned} &m_1^1 = \frac{0.4904}{1.5069} = 0.3254, \quad m_2^1 = \frac{0.4553}{1.5069} = 0.3022, \\ &m_3^1 = \frac{0.5075}{1.5069} = 0.3367. \end{aligned}$$

Inverse matrix (6.52) is

$$[\mathbf{C}]^{-1} = \begin{bmatrix} 0.8629 & 0 & 0 & 0 \\ 0 & 1.246 & 0 & 0 \\ 0 & 0 & 0.6601 & 0 \\ 0.1523 & 0.2279 & 0.1125 & 0.5073 \end{bmatrix}.$$

We check currents (6.53) as

$$I_1^1 = \frac{0.8629 \cdot 0.3254}{0.1523 \cdot 0.3254 + 0.2279 \cdot 0.3022 + 0.1125 \cdot 0.3367 + 0.5073} = \frac{0.2808}{0.6636} = 0.4232,$$

$$I_2^1 = \frac{1.246 \cdot 0.3022}{0.6636} = 0.5673, \quad I_3^1 = \frac{0.6601 \cdot 0.3367}{0.6636} = 0.335.$$

Transformation (6.70) is as follows:

$$\begin{bmatrix} \rho I_1^1 \\ \rho I_2^1 \\ \rho I_3^1 \\ \rho 1 \end{bmatrix} = \begin{bmatrix} 0.3254 & 0 & 0 & 0 \\ 0 & 0.3022 & 0 & 0 \\ 0 & 0 & 0.3367 & 0 \\ -0.1191 & -0.1277 & -0.1131 & 1 \end{bmatrix} \cdot \begin{bmatrix} I_1^{SC} \\ I_2^{SC} \\ I_3^{SC} \\ 1 \end{bmatrix}.$$

Then, we may check currents (6.69) as

$$I_1^1 = \frac{0.3254 \cdot 0.8629}{-0.1191 \cdot 0.8629 - 0.1277 \cdot 1.246 - 0.1131 \cdot 0.6601 + 1} = \frac{0.2808}{0.6636} = 0.4232,$$

$$I_2^1 = \frac{0.3022 \cdot 1.246}{0.6636} = 0.5673, \quad I_3^1 = \frac{0.3367 \cdot 0.6601}{0.6636} = 0.335.$$

6.3 Projective Coordinates of an Active Two-Port with Stabilization of Load Voltages

The popularized power supply system is shown in Fig. 6.20. The low-dropout linear regulators can be used as voltage stabilizers.

There are important features of such a circuit, that is, the interference of load currents on the voltage stabilizers regimes takes place; the *SC* regime has no physical sense and cannot be accepted as the characteristic regime.

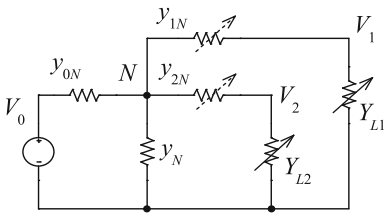

Fig. 6.20 Active two-port network with stabilization of load voltages

This brings up the problem for the choice of characteristic regimes, justification of the normalized expressions for parameters and equations of circuit, and comparison of regimes between the loads in a given circuit [12].

Let us introduce the projective coordinates using the results of Sect. 6.1.3.

Using Eqs. (6.21)–(6.23), we get the following system of equations:

$$\begin{aligned} I_1 \frac{y_{0N} + y_N + y_{1N}}{y_{1N}} &= y_{0N} V_0 - V_1 (y_{0N} + y_N) - I_2, \\ I_2 \frac{y_{0N} + y_N + y_{2N}}{y_{2N}} &= y_{0N} V_0 - V_2 (y_{0N} + y_N) - I_1. \end{aligned} \tag{6.71}$$

These equations define two bunches of the straight lines $(I_1, I_2, y_{1N}) = 0$, $(I_1, I_2, y_{2N}) = 0$, with parameters y_{1N}, y_{2N}. These bunches are presented in Fig. 6.21. The bunch center G_2 corresponds to the straight lines with parameter y_{1N}. Physically, the bunch center corresponds to such a characteristic regime of the load

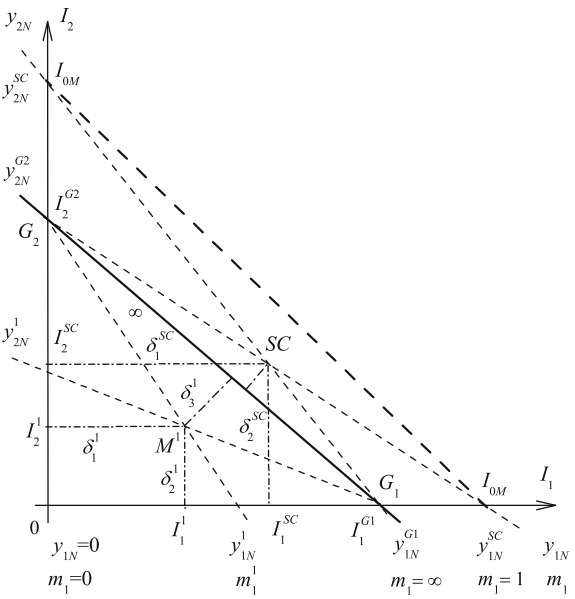

Fig. 6.21 Two bunches of straight lines with parameters y_{1N}, y_{2N}

Y_{L1} which does not depend on y_{1N}. It is carried out for the current $I_1 = 0$ at the expense of the second load current I_2^{G2}. In this case, the voltage is $V_N = V_1$. Using the first equation of system (6.71), we obtain the characteristic value of the second load current

$$I_2^{G2} = y_{0N}V_0 - V_1(y_{0N} + y_N). \tag{6.72}$$

The characteristic value of the first load current, which defines the bunch center G_1 of the straight lines with parameter y_{2N}, is expressed similarly

$$I_1^{G1} = y_{0N}V_0 - V_2(y_{0N} + y_N). \tag{6.73}$$

In this case, the current is given as $I_2 = 0$, and voltage as $V_N = V_2$.

Using the first equation of system (6.71) and current (6.73), we find the characteristic value of the first regulator

$$\begin{aligned} y_{1N}^{G1} &= I_1^{G1}\frac{y_{0N} + y_N}{y_{0N}V_0 - V_1(y_{0N} + y_N) - I_1^{G1}} \\ &= I_1^{G1}\frac{y_{0N} + y_N}{I_2^{G2} - I_1^{G1}} = \frac{I_1^{G1}}{V_2 - V_1}. \end{aligned} \tag{6.74}$$

Similarly, the characteristic value of the second regulator is

$$y_{2N}^{G2} = I_2^{G2}\frac{y_{0N} + y_N}{I_1^{G1} - I_2^{G2}} = \frac{I_2^{G2}}{V_1 - V_2}. \tag{6.75}$$

Let an initial regime corresponds to a point M^1 which is set by loads $Y_{L1}^1,\ Y_{L2}^1$ or currents $I_1^1 = Y_{L1}^1 V_1,\ I_2^1 = Y_{L2}^1 V_2$. The corresponding values of regulator conductivities are defined by system (6.71). However, using (6.72) and (6.73), we obtain the more convenient relationships as

$$y_{1N}^1 = I_1^1\frac{y_{0N} + y_N}{I_2^{G2} - (I_1^1 + I_2^1)}, \quad y_{2N}^1 = I_2^1\frac{y_{0N} + y_N}{I_1^{G1} - (I_1^1 + I_2^1)}. \tag{6.76}$$

Also, this point M^1 is defined by the projective nonuniform $m_1^1,\ m_2^1$ and homogeneous $\xi_1^1, \xi_2^1, \xi_3^1$ coordinates which are set by the reference triangle $G_1 0\ G_2$ and a unit point. The point 0 is the origin of coordinates and the straight line $G_1\ G_2$ is the line of infinity ∞. As a unit point, we must also choose some characteristic regime using the condition of stability of the voltages $V_1,\ V_2$. As mentioned above, the *SC* load current regime is not such one. However, the *SC* current regime of the voltage source, when $V_N = 0$, allows finding such a characteristic regime. In this case, the *SC* current of V_0 is

$$I_{0M} = y_{0N} V_0 = I_1 + I_2.$$

This expression corresponds to an equation of straight line. In Fig. 6.21, this line intersects the coordinate axes in the points $I_1 = I_{0M}$, $I_2 = I_{0M}$. The straight lines with the parameters y_{1N}^{SC}, y_{2N}^{SC} correspond to these points.

Let us determine the values y_{1N}^{SC}, y_{2N}^{SC}. We assume the current $I_2 = 0$ for the first and $I_1 = 0$ for the second equation of (6.71). Then, the values are

$$y_{1N}^{SC} = -y_{0N} V_0 / V_1, \quad y_{2N}^{SC} = -y_{0N} V_0 / V_2. \tag{6.77}$$

Now, using (6.77) and Eq. (6.71), we can define the load currents

$$\begin{aligned} I_1^{SC} &= V_1 \frac{I_1^{G1}}{V_2 + V_1 I_1^{G1} / I_{0M}}, \\ I_2^{SC} &= V_2 \frac{I_2^{G2}}{V_1 + V_2 I_2^{G2} / I_{0M}}. \end{aligned} \tag{6.78}$$

These currents correspond to the point SC as a unit point in Fig. 6.21.

Let us now return to the determination of projective coordinates for the running regime point. The nonuniform projective coordinate m_1^1 is set by cross-ratio (6.28). In our case, we have

$$m_1^1 = (0\ y_{1N}^1\ y_{1N}^{SC}\ y_{1N}^{G1}) = \frac{y_{1N}^1 - 0}{y_{1N}^1 - y_{1N}^{G1}} \div \frac{y_{1N}^{SC} - 0}{y_{1N}^{SC} - y_{1N}^{G1}}. \tag{6.79}$$

The points $y_{1N} = 0,\ y_{1N} = y_{1N}^{G1}$ correspond to the base points. The point y_{1N}^{SC} is a unit one. The values of m_1 are shown in Fig. 6.21. The nonuniform projective coordinate m_2^1 is expressed similarly

$$m_2^1 = (0\ y_{2N}^1\ y_{2N}^{SC}\ y_{2N}^{G2}\ ) = \frac{y_{2N}^1}{y_{2N}^1 - y_{2N}^{G2}} \div \frac{y_{2N}^{SC}}{y_{2N}^{SC} - y_{2N}^{G2}}. \tag{6.80}$$

These expressions demonstrate the conductivities $y_{1N},\ y_{2N}$ in the relative form.

The homogeneous projective coordinates ξ_1, ξ_2, ξ_3 set the nonuniform coordinates by (6.30). For convenience, we rewrite (6.30) and all the required formulas

$$\frac{\rho\xi_1}{\rho\xi_3} = m_1, \quad \frac{\rho\xi_2}{\rho\xi_3} = m_2. \tag{6.81}$$

Homogeneous coordinates (6.36) are

$$\begin{bmatrix} \rho\,\xi_1 \\ \rho\,\xi_2 \\ \rho\,\xi_3 \end{bmatrix} = \begin{bmatrix} \frac{1}{I_1^{SC}} & 0 & 0 \\ 0 & \frac{1}{I_2^{SC}} & 0 \\ \frac{1}{I_1^{G1}\mu_3\delta_3^{SC}} & \frac{1}{I_2^{G2}\mu_3\delta_3^{SC}} & \frac{-1}{\mu_3\delta_3^{SC}} \end{bmatrix} \cdot \begin{bmatrix} I_1 \\ I_2 \\ 1 \end{bmatrix} = [\mathbf{C}] \cdot [\mathbf{I}]. \tag{6.82}$$

Inverse transformation (6.37) is

$$\begin{bmatrix} \rho_I\, I_1 \\ \rho_I\, I_2 \\ \rho_I\, 1 \end{bmatrix} = \begin{bmatrix} I_1^{SC} & 0 & 0 \\ 0 & I_2^{SC} & 0 \\ \frac{I_1^{SC}}{I_1^{G1}} & \frac{I_2^{SC}}{I_2^{G2}} & -\mu_3\delta_3^{SC} \end{bmatrix} \cdot \begin{bmatrix} \xi_1 \\ \xi_2 \\ \xi_3 \end{bmatrix} = [\mathbf{C}]^{-1} \cdot [\xi]. \tag{6.83}$$

From here, we pass to currents (6.38) as

$$\begin{aligned} I_1 &= \frac{\rho_I I_1}{\rho_I 1} = \frac{I_1^{SC} m_1}{\frac{I_1^{SC}}{I_1^{G1}} m_1 + \frac{I_2^{SC}}{I_2^{G2}} m_2 - \mu_3\delta_3^{SC}}, \\ I_2 &= \frac{\rho_I I_2}{\rho_I 1} = \frac{I_2^{SC} m_2}{\frac{I_1^{SC}}{I_1^{G1}} m_1 + \frac{I_2^{SC}}{I_2^{G2}} m_2 - \mu_3\delta_3^{SC}}. \end{aligned} \tag{6.84}$$

Therefore, it is possible to consider that nonuniform and homogeneous projective coordinates reasonably represent a running regime of circuit by the relative form.

Next, we must obtain the inverse formulas to (6.84) for the calculation of parameters m_1^1, m_2^1 by the load currents. These inverse formulas are obtained at once by the following method. From (6.81) we get

$$\xi_1 = \xi_3 m_1,\ \xi_2 = \xi_3 m_2.$$

Substituting in (6.82), we have

$$\begin{bmatrix} \rho\,\xi_3 m_1 \\ \rho\,\xi_3 m_2 \\ \rho\,\xi_3 \end{bmatrix} = \begin{bmatrix} \frac{1}{I_1^{SC}} & 0 & 0 \\ 0 & \frac{1}{I_2^{SC}} & 0 \\ \frac{1}{I_1^{G1}\mu_3\delta_3^{SC}} & \frac{1}{I_2^{G2}\mu_3\delta_3^{SC}} & \frac{-1}{\mu_3\delta_3^{SC}} \end{bmatrix} \cdot \begin{bmatrix} I_1 \\ I_2 \\ 1 \end{bmatrix} = [\mathbf{C}] \cdot [\mathbf{I}]. \tag{6.85}$$

From here

$$m_1 = \frac{\rho\xi_3 m_1}{\rho\xi_3} = \frac{\dfrac{I_1}{I_1^{SC}}\mu_3\delta_3^{SC}}{\dfrac{I_1}{I_1^{G1}} + \dfrac{I_2}{I_2^{G2}} - 1}, \quad m_2 = \frac{\rho\xi_3 m_2}{\rho\xi_3} = \frac{\dfrac{I_2}{I_2^{SC}}\mu_3\delta_3^{SC}}{\dfrac{I_1}{I_1^{G1}} + \dfrac{I_2}{I_2^{G2}} - 1}. \tag{6.86}$$

Using (6.79), we get

$$y_{1N}^1 = \frac{m_1^1 y_{1N}^{G1}}{m_1^1 + \dfrac{y_{1N}^{G1}}{y_{1N}^{SC}} - 1}, \quad y_{2N}^1 = \frac{m_2^1 y_{2N}^{G2}}{m_2^1 + \dfrac{y_{2N}^{G2}}{y_{2N}^{SC}} - 1}. \tag{6.87}$$

Example 5 Let our circuit be given as the follows:

$$V_0 = 5, \quad y_{0N} = 2.5, \quad y_N = 0.625, \quad V_1 = 2, \quad V_2 = 3.$$

For the first load, characteristic currents (6.73) and (6.78) are

$$I_1^{G1} = 3.125, \quad I_1^{SC} = 1.785,$$

and conductivities (6.74) and (6.77) are

$$y_{1N}^{G1} = 3.125, \quad y_{1N}^{SC} = -6.25.$$

For the second load,

$$I_2^{G2} = 6.25, \quad I_2^{SC} = 5.357, \quad y_{2N}^{G2} = -6.25, \quad y_{2N}^{SC} = -4.166.$$

Let the initial currents be equal to $I_1^1 = 1, \quad I_2^1 = 1.$
Then, regulator conductivities (6.76) are

$$y_{1N}^1 = 0.735, \quad y_{2N}^1 = 2.777.$$

Nonuniform projective coordinates (6.79) and (6.80) are

$$m_1^1 = -0.461, \quad m_2^1 = -0.154.$$

The negative values mean that the point M_1 and a unit point SC are on the different sides from the infinitely remote straight line G_1G_2.
Distances (6.34) and (6.33) are

$$\mu_3\delta_3^1 = \left(\frac{1}{3.125} + \frac{1}{6.25} - 1\right) = -0.52,$$
$$\mu_3\delta_3^{SC} = \left(\frac{1.785}{3.125} + \frac{5.357}{6.25} - 1\right) = 0.428.$$

Homogeneous coordinates (6.35) are

$$\rho\xi_1^1 = \frac{1}{1.785}, \quad \rho\xi_2^1 = \frac{1}{5.357} = 0.186, \quad \rho\xi_3^1 = \frac{-0.52}{0.428}.$$

Matrix of transformation (6.82) is

$$[\mathbf{C}] = \begin{bmatrix} \frac{1}{1.785} & 0 & 0 \\ 0 & \frac{1}{5.357} & 0 \\ \frac{1}{3.125 \cdot 0.428} & \frac{1}{6.25 \cdot 0.428} & -\frac{1}{0.428} \end{bmatrix}.$$

Matrix of inverse transformation (6.83) is

$$[\mathbf{C}]^{-1} = \begin{bmatrix} 1.785 & 0 & 0 \\ 0 & 5.357 & 0 \\ \frac{1.785}{3.125} & \frac{5.357}{6.25} & -0.428 \end{bmatrix}.$$

Let us check up currents (6.84)

$$I_1^1 = \frac{-1.785 \cdot 0.461}{-\frac{1.785}{3.125} \cdot 0.461 - \frac{5.357}{6.25} \cdot 0.153 - 0.428} = \frac{-0.82}{-0.82} = 1,$$
$$I_2^1 = \frac{-5.357 \cdot 0.153}{-0.82} = 1.$$

We check parameters (6.86) as

$$m_1^1 = \frac{\frac{1}{1.785}0.428}{\frac{1}{3.125} + \frac{1}{6.25} - 1} = \frac{0.2397}{-0.52} = -0.461,$$
$$m_2^1 = \frac{\frac{1}{5.357}0.428}{\frac{1}{3.125} + \frac{1}{6.25} - 1} = \frac{0.07989}{-0.52} = -0.154.$$

References

1. Alexander, C.K., Sadiku, M.N.O.: Fundamentals of Electric Circuits, 5th edn. McGraw–Hill, New York (2009)
2. Bennett, M.K.: Affine and Projective Geometry. Wiley, Hoboken (2011)
3. Frank, J.A.: Schaum's Outline of Theory and Problems of Projective Geometry. McGraw–Hill, New York (1967)
4. Glagolev, N.A.: Proektivnaia Geometria. (Projective geometry). Nauka, Moskva (1963)
5. Irwin, J.D., Nelms, R.M.: Basic Engineering Circuit Analysis, 10th edn. Wiley, Hoboken (2011)
6. Penin, A.: Projective equivalency of operating regimes for two-ports. Electrichestvo **8**, 47–54 (1993)
7. Penin, A.: Fractionally linear relations in the problems of analysis of resistive circuits with variable parameters. Electrichestvo **11**, 32–44 (1999)
8. Penin, A.: Normalized representation of the equations of active multi-port net works on the basis of projective geometry. Moldavian J. Phys. Sci. **10**(3–4), 350–357 (2011). http://sfm.asm.md/moldphys/2011/vol10/n3-4/index.html. Accessed 30 Nov 2014
9. Penin, A.: Recalculating the load currents of an active multiport with variable parameters on the basis of projective geometry. Electrichestvo **10**, 66–73 (2012)
10. Penin, A.: Projective geometry method in the theory of electric circuits with variable parameters of elements. Int. J. Electron. Commun. Electr. Eng. **3**(2), 18–34 (2013). https://sites.google.com/site/ijeceejournal/volume-3-issue-2. Accessed 30 Nov 2014
11. Penin, A.: Recalculation of the loads current of active multiport networks on the basis of projective geometry. J. Circuits Syst. Comput. **22**(05), 1350031 (13 pages) (2013) doi: 10.1142/S021812661350031X. http://www.worldscientific.com/doi/abs/10.1142/S021812661350031X. Accessed 30 Nov 2014
12. Penin, A.: Comparison of regimes of active two-port networks with stabilization of load voltages. Inter. J. Electron. Commun. Electr. Eng. **3**(6), 1–18 (2013). https://sites.google.com/site/ijeceejournal/
13. Penin, A., Sidorenko, A.: Balanced multi-port electric network and its projective coordinates. Moldavian J. Phys. Sci. **14**(1–2), 102−112 (2015)
14. Penin, A., Sidorenko, A.: Sistemul distribuit de alimentare cu energie. MD Patent application S20150047, 2015
15. Penin, A., Sidorenko, A., Donu, S.: Metodă de transmitere a trei semnale prin linia de comunicaţie cu patru fire. MD Patent application S20150082, 2015

Chapter 7
Recalculation of Load Currents of Active Multi-ports

7.1 Recalculation of Currents for the Case of Load Changes

7.1.1 Active Two-Port

Let us continue with the matter we began in Sect. 6.1.3. Let a subsequent regime correspond to a point M^2 with conductivities $Y^2_{L1},\ Y^2_{L2}$ and currents $I^2_1,\ I^2_2$ of loads. The non-uniform coordinates are defined similarly to (6.28) and (6.29)

$$m^2_1 = \frac{Y^2_{L1}}{Y^2_{L1} - Y^{G1}_{L1}}, \quad m^2_2 = \frac{Y^2_{L2}}{Y^2_{L2} - Y^{G2}_{L2}}.$$

Therefore, the regime change m^{21}_1 is naturally expressed by the cross-ratio [3]

$$\begin{aligned} m^{21}_1 &= (0\ Y^2_{L1}\ Y^1_{L1}\ Y^{G1}_{L1}) = \frac{Y^2_{L1} - 0}{Y^2_{L1} - Y^{G1}_{L1}} \div \frac{Y^1_{L1} - 0}{Y^1_{L1} - Y^{G1}_{L1}} = m^2_1 \div m^1_1, \\ m^{21}_2 &= (0\ Y^2_{L2}\ Y^1_{L2}\ Y^{G2}_{L2}) = m^2_2 \div m^1_2. \end{aligned} \tag{7.1}$$

Using (6.31) and (6.34), we define the homogeneous coordinates of the point M^2

$$\rho\,\xi^2_1 = \frac{I^2_1}{I^{SC}_1},\ \rho\,\xi^2_2 = \frac{I^2_2}{I^{SC}_2},\ \rho\,\xi^2_3 = \frac{\delta^2_3}{\delta^{SC}_3},\ \mu_3\delta^2_3 = \left(\frac{I^2_1}{I^{G1}_1} + \frac{I^2_2}{I^{G1}_2} - 1\right).$$

A. Penin, *Analysis of Electrical Circuits with Variable Load Regime Parameters*, Power Systems, DOI 10.1007/978-3-319-28451-4_7

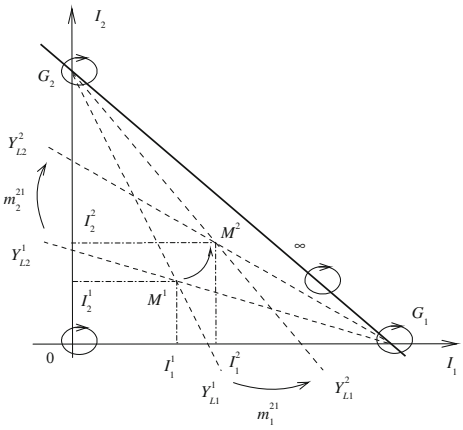

Fig. 7.1 Regime change at the expense of change of the load conductivities

The corresponding regime change is shown by arrows in Fig. 7.1. Using transformations (6.28), we obtain the subsequent currents

$$I_1^2 = \frac{I_1^{SC} m_1^2}{\frac{I_1^{SC}}{I_1^{G1}} m_1^2 + \frac{I_2^{SC}}{I_2^{G2}} m_2^2 - \mu_3 \delta_3^{SC}}, \quad I_2^2 = \frac{I_2^{SC} m_2^2}{\frac{I_1^{SC}}{I_1^{G1}} m_1^2 + \frac{I_2^{SC}}{I_2^{G2}} m_2^2 - \mu_3 \delta_3^{SC}}.$$

Taking into account (7.1), we present the non-uniform coordinates m_1^2, m_2^2 as

$$m_1^2 = m_1^{21} \frac{\xi_1^1}{\xi_3^1}, \quad m_2^2 = m_2^{21} \frac{\xi_2^1}{\xi_3^1}.$$

Therefore, the currents

$$I_1^2 = \frac{(I_1^{SC} m_1^{21}) \frac{\xi_1^1}{\xi_3^1}}{\left(\frac{I_1^{SC}}{I_1^{G1}} m_1^{21}\right) \frac{\xi_1^1}{\xi_3^1} + \left(\frac{I_2^{SC}}{I_2^{G2}} m_2^{21}\right) \frac{\xi_2^1}{\xi_3^1} - \mu_3 \delta_3^{SC}},$$

$$I_2^2 = \frac{(I_2^{SC} m_2^{21}) \frac{\xi_2^1}{\xi_3^1}}{\left(\frac{I_1^{SC}}{I_1^{G1}} m_1^{21}\right) \frac{\xi_1^1}{\xi_3^1} + \left(\frac{I_2^{SC}}{I_2^{G2}} m_2^{21}\right) \frac{\xi_2^1}{\xi_3^1} - \mu_3 \delta_3^{SC}}.$$

Then, by (6.37), we get transformation

$$\rho[\mathbf{I}^2] = [\mathbf{C}^{21}]^{-1} \cdot [\xi^1],$$

where the matrix

$$[C^{21}]^{-1} = \begin{bmatrix} I_1^{SC} m_1^{21} & 0 & 0 \\ 0 & I_2^{SC} m_2^{21} & 0 \\ \frac{I_1^{SC}}{I_1^{G1}} m_1^{21} & \frac{I_2^{SC}}{I_2^{G2}} m_2^{21} & -\mu_3 \delta_3^{SC} \end{bmatrix}.$$

Using (6.36), we obtain the resultant transformation as the multiplication of the two matrixes

$$\rho[\mathbf{I}^2] = [\mathbf{C}^{21}]^{-1} \cdot [\mathbf{C}] \cdot [\mathbf{I}^1] = [\mathbf{J}^{21}] \cdot [\mathbf{I}^1], \tag{7.2}$$

where the matrix

$$[J^{21}] = \begin{bmatrix} m_1^{21} & 0 & 0 \\ 0 & m_2^{21} & 0 \\ \frac{1}{I_1^{G1}}(m_1^{21} - 1) & \frac{1}{I_2^{G2}}(m_2^{21} - 1) & 1 \end{bmatrix}.$$

From here, we pass to the required currents

$$\begin{aligned} I_1^2 &= \frac{\rho\, I_1^2}{\rho\, 1} = \frac{I_1^1 m_1^{21}}{\frac{I_1^1}{I_1^{G1}}(m_1^{21} - 1) + \frac{I_2^1}{I_2^{G2}}(m_2^{21} - 1) + 1}, \\ I_2^2 &= \frac{\rho\, I_2^2}{\rho\, 1} = \frac{I_2^1 m_2^{21}}{\frac{I_1^1}{I_1^{G1}}(m_1^{21} - 1) + \frac{I_2^1}{I_2^{G2}}(m_2^{21} - 1) + 1}. \end{aligned} \tag{7.3}$$

The obtained relationships carry out the recalculation of currents at a respective change of load conductivities. These relations are the projective transformations and possess group properties. The performance of the group properties is advantage of projective transformations.

Let the regime be changed once again; we have changes m_1^{32}, m_2^{32}. Then, the final regime value is expressed as follows:

$$m_1^3 = m_1^{32} \cdot\ m_1^2 = m_1^{32} \cdot m_1^{21} \cdot m_1^1 = m_1^{31} \cdot m_1^1,\ m_2^3 = m_2^{31} \cdot m_2^1.$$

Using (7.2), we obtain the resultant transformation

$$\rho[\mathbf{I}^3] = [\mathbf{J}^{32}] \cdot [\mathbf{I}^2] = [\mathbf{J}^{32}] \cdot [\mathbf{J}^{21}] \cdot [\mathbf{I}^1] = [\mathbf{J}^{31}] \cdot [\mathbf{I}^1],$$

where the matrices

$$[J^{32}] = \begin{bmatrix} m_1^{32} & 0 & 0 \\ 0 & m_2^{32} & 0 \\ \frac{m_1^{32}-1}{I_1^{G1}} & \frac{m_2^{32}-1}{I_2^{G2}} & 1 \end{bmatrix}, \quad [J^{31}] = \begin{bmatrix} m_1^{31} & 0 & 0 \\ 0 & m_2^{31} & 0 \\ \frac{m_1^{31}-1}{I_1^{G1}} & \frac{m_2^{31}-1}{I_2^{G2}} & 1 \end{bmatrix}.$$

Projective transformation (7.2) or (7.3) with parameters $m_1^{21},\ m_2^{21}$ translates any initial points of the plane $I_1,\ I_2$ into a new position shown in Fig. 7.1. The fixed points and fixed straight lines are shown too.

Example 1 We continue Example 2 of Sect. 6.1.3 and rewrite the parameters of an initial regime

$$Y_{L1}^1 = 0.5,\ Y_{L2}^1 = 0.5, I_1^1 = 0.979,\ I_2^1 = 0.8247;$$
$$m_1^1 = 0.25, m_2^1 = 0.3158.$$

Let the parameters of a subsequent regime be given as

$$Y_{L1}^2 = 1,\ Y_{L2}^2 = 2,\ I_1^2 = 1.434,\ I_2^2 = 1.5504.$$

The non-uniform coordinates

$$m_1^2 = 0.4,\ m_2^2 = 0.6486.$$

Regime change (7.1)

$$m_1^{21} = 0.4 \div 0.25 = 1.6, \quad m_2^{21} = 0.6486 \div 0.3158 = 2.0538.$$

Transformation (7.2)

$$\begin{bmatrix} \rho I_1^2 \\ \rho I_2^2 \\ \rho 1 \end{bmatrix} = \begin{bmatrix} 1.6 & 0 & 0 \\ 0 & 2.0538 & 0 \\ 0.04 & 0.0648 & 1 \end{bmatrix} \cdot \begin{bmatrix} I_1^1 \\ I_2^1 \\ 1 \end{bmatrix}.$$

Subsequent currents (7.3)

$$I_1^2 = \frac{\rho I_1^2}{\rho 1} = \frac{1.6 \cdot 0.979}{0.04 \cdot 0.979 + 0.0648 \cdot 0.825 + 1} = \frac{1.5664}{1.0926} = 1.4335,$$
$$I_2^2 = \frac{\rho I_2^2}{\rho 1} = \frac{2.0538 \cdot 0.825}{1.0926} = 1.5507.$$

Once again we notice that the offered formulas of recalculation are especially convenient, when the fixed values m_1^{21}, m_2^{21} are used for any values of initial currents.

7.1.2 Active Three-Port

We continue Sect. 6.2. Let a subsequent regime correspond to a point M^2 with conductivities $Y_{L1}^2,\ Y_{L2}^2, Y_{L3}^2$ and currents $I_1^2,\ I_2^2, I_3^2$ of loads.

The non-uniform coordinates

$$m_1^2 = \frac{Y_{L1}^2}{Y_{L1}^2 - Y_{L1}^{G1}}, \quad m_2^2 = \frac{Y_{L2}^2}{Y_{L2}^2 - Y_{L2}^{G2}}, \quad m_3^2 = \frac{Y_{L3}^2}{Y_{L3}^2 - Y_{L3}^{G3}}.$$

The regime change

$$m_1^{21} = m_1^2 \div m_1^1, \quad m_2^{21} = m_2^2 \div m_2^1, \quad m_3^{21} = m_3^2 \div m_3^1 \tag{7.4}$$

We define the coordinates of the point M^2 similarly to (6.48). The distance

$$\delta_4^2 = \frac{1}{\mu_4}\left(\frac{I_1^2}{I_1^{G1}} + \frac{I_2^2}{I_2^{G2}} + \frac{I_3^2}{I_3^{G2}} - 1\right).$$

Then

$$\rho\,\xi_1^2 = \frac{I_1^2}{I_1^{SC}}, \quad \rho\,\xi_2^2 = \frac{I_2^2}{I_2^{SC}}, \quad \rho\,\xi_3^2 = \frac{I_3^2}{I_3^{SC}}, \quad \rho\,\xi_4^2 = \frac{\delta_4^2}{\delta_4^{SC}}.$$

Repeating a mental step for the plane, we obtain the required transformation similarly to (7.2) and matrix

$$[\mathbf{J^{21}}] = \begin{bmatrix} m_1^{21} & 0 & 0 & 0 \\ 0 & m_2^{21} & 0 & 0 \\ 0 & 0 & m_3^{21} & 0 \\ \frac{m_1^{21}-1}{I_1^{G1}} & \frac{m_2^{21}-1}{I_2^{G2}} & \frac{m_3^{21}-1}{I_3^{G3}} & 1 \end{bmatrix}. \tag{7.5}$$

From here, we pass to the required currents

$$\begin{aligned} I_1^2 &= \frac{\rho I_1^2}{\rho 1} = \frac{I_1^1 m_1^{21}}{\frac{I_1^1}{I_1^{G1}}(m_1^{21}-1) + \frac{I_2^1}{I_2^{G2}}(m_2^{21}-1) + \frac{I_3^1}{I_3^{G3}}(m_3^{21}-1) + 1}, \\ I_2^2 &= \frac{\rho I_2^2}{\rho 1} = \frac{I_2^1 m_2^{21}}{\frac{I_1^1}{I_1^{G1}}(m_1^{21}-1) + \frac{I_2^1}{I_2^{G2}}(m_2^{21}-1) + \frac{I_3^1}{I_3^{G3}}(m_3^{21}-1) + 1}, \\ I_3^2 &= \frac{\rho I_3^2}{\rho 1} = \frac{I_3^1 m_3^{21}}{\frac{I_1^1}{I_1^{G1}}(m_1^{21}-1) + \frac{I_2^1}{I_2^{G2}}(m_2^{21}-1) + \frac{I_3^1}{I_3^{G3}}(m_3^{21}-1) + 1}. \end{aligned} \tag{7.6}$$

These relationships are directly generalized for any number of loads.

Special case
Only the load conductivity Y_{L3} is changed. The matrix

$$[\mathbf{J}^{21}] = \begin{bmatrix} 1 & 0 & 0 & 0 \\ 0 & 1 & 0 & 0 \\ 0 & 0 & m_3^{21} & 0 \\ 0 & 0 & \frac{m_3^{21}-1}{I_3^{03}} & 1 \end{bmatrix}.$$

Example 2 We continue Example 3 of Sect. 6.2 and rewrite the initial regime parameters

$$\begin{aligned} Y_{L1}^1 = 0.5,\ Y_{L2}^1 = 0.5,\ Y_{L3}^1 = 1; \\ I_1^1 = 0.974,\ I_2^1 = 0.82,\ I_3^1 = 1.61; \\ m_1^1 = 0.25, m_2^1 = 0.316, m_3^1 = 0.387. \end{aligned}$$

The subsequent regime parameters

$$\begin{aligned} Y_{L1}^2 = 1,\ \ Y_{L2}^2 = 2,\ \ Y_{L3}^2 = 20; \\ I_1^2 = 1.254,\ \ I_2^2 = 1.356,\ \ I_3^2 = 3.1. \end{aligned}$$

The non-uniform coordinates

$$m_1^2 = 0.4, \quad m_2^2 = 0.6486, \quad m_3^2 = 0.9266.$$

Regime change (7.4)

$$\begin{aligned} m_1^{21} = 0.4 \div 0.25 = 1.6, \quad m_2^{21} = 0.6486 \div 0.3158 = 2.0538, \\ m_3^{21} = 0.9266 \div 0.387 = 2.3948. \end{aligned}$$

Matrix (7.5)

$$[\mathbf{J}^{21}] = \begin{bmatrix} 1.6 & 0 & 0 & 0 \\ 0 & 2.0538 & 0 & 0 \\ 0 & 0 & 2.394 & 0 \\ 0.04 & 0.0648 & 0.0939 & 1 \end{bmatrix}.$$

We check up subsequent currents (7.6)

$$\begin{aligned} I_1^2 = \frac{1.6 \cdot 0.974}{0.04 \cdot 0.974 + 0.0648 \cdot 0.82 + 0.09396 \cdot 1.61 + 1} = \frac{1.5592}{1.2433} = 1.254, \\ I_2^2 = \frac{2.0538 \cdot 0.82}{1.2433} = 1.356, \quad I_3^2 = \frac{2.3394 \cdot 1.61}{1.2433} = 3.1. \end{aligned}$$

7.2 Recalculation of Currents for the Case of Changes of Circuit Parameters

We consider the concrete circuit (see Sect. 6.1.3) in Fig. 7.2.

The above results allow investigating the influence of a lateral conductivity y_N and longitudinal conductivity y_{0N} on load currents [2]

7.2.1 Change of Lateral Conductivity

Let the conductivity value y_N be changed, $y_N \to \bar{y}_N$. Corresponding changes of an initial point $M \to \bar{M}$ and short circuit point $SC \to \overline{SC}$ are shown in Fig. 7.3. On the other hand, the coordinates of the points G_1, G_2 by (6.26) and (6.24) do not depend on the value y_N. Therefore, a straight line $G_1\ G_2$ is the fixed line. The point 0, as the open circuit regime, does not depend on this element too.

According to Fig. 7.1, the influence of this conductivity y_N can be interpreted as a projective transformation in the plane I_1, I_2. This transformation, as similar to

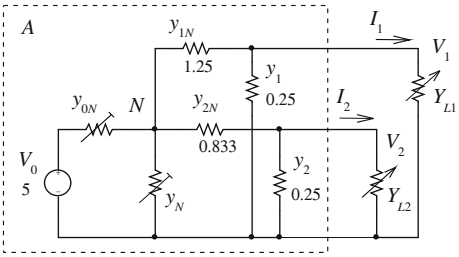

Fig. 7.2 Example of a circuit with variable conductivities of voltage source

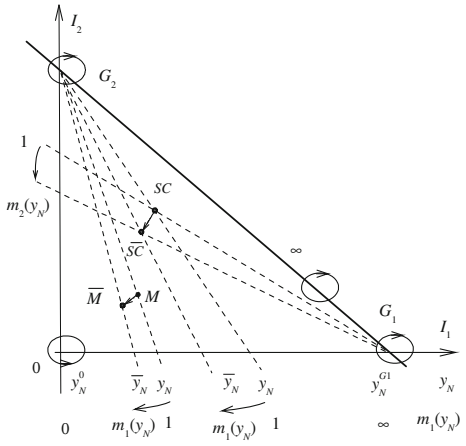

Fig. 7.3 Regime change at the expense of conductivity $y_N \to \bar{y}_N$

(7.2) and (7.3), can recalculate the initial currents I_1, I_2 of the point M to the subsequent currents $\bar{I}_1$, $\bar{I}_2$ of the point $\bar{M}$.

The point M has the homogeneous coordinates ξ_1, ξ_2, ξ_3, which are set by reference triangle $G_1\,0\,G_2$ and a unit point SC. On the other hand, the fixed reference triangle $G_1\,0\,G_2$ and a new unit point $S\overline{C}$ form a subsequent system of projective coordinates. Therefore, the point $\bar{M}$ has the same homogeneous coordinates $\bar{\xi}_1, \bar{\xi}_2, \bar{\xi}_3$; that is,

$$[\bar{\rho}\bar{\xi}] = [\xi].$$

Using (6.36), we may write

$$[\bar{\rho}\bar{\xi}] = [\bar{\mathbf{C}}] \cdot [\bar{\mathbf{I}}], \quad [\rho\xi] = [\mathbf{C}] \cdot [\mathbf{I}].$$

The desired transformation is the multiplication of matrices

$$[\rho\bar{I}] = [\bar{\mathbf{C}}]^{-1} \cdot [\mathbf{C}] \cdot [\mathbf{I}] = [\mathbf{J}] \cdot [\mathbf{I}];$$

the matrix $[\bar{\mathbf{C}}]^{-1}$ has view (6.37).

Therefore, the resultant matrix

$$[\mathbf{J}] = \begin{bmatrix} J_{11} & 0 & 0 \\ 0 & J_{22} & 0 \\ J_{31} & J_{32} & J_{33} \end{bmatrix}, \tag{7.7}$$

where its elements

$$J_{11} = \frac{\bar{I}_1^{SC}}{I_1^{SC}}, \quad J_{22} = \frac{\bar{I}_2^{SC}}{I_2^{SC}}, \quad J_{33} = \frac{\bar{\delta}_3^{SC}}{\delta_3^{SC}},$$

$$J_{31} = \frac{\bar{\delta}_3^{SC}}{\delta_3^{SC} I_1^{G1}} \left(\frac{\bar{I}_1^{SC}}{I_1^{SC}} \frac{\delta_3^{SC}}{\bar{\delta}_3^{SC}} - 1 \right),$$

$$J_{32} = \frac{\bar{\delta}_3^{SC}}{\delta_3^{SC} I_2^{G2}} \left(\frac{\bar{I}_2^{SC}}{I_2^{SC}} \frac{\delta_3^{SC}}{\bar{\delta}_3^{SC}} - 1 \right).$$

Dividing all these elements by J_{33}, we obtain the resultant matrix in the form

$$[J] = \begin{bmatrix} \frac{\bar{I}_1^{SC}}{I_1^{SC}} \frac{\delta_3^{SC}}{\bar{\delta}_3^{SC}} & 0 & 0 \\ 0 & \frac{\bar{I}_2^{SC}}{I_2^{SC}} \frac{\delta_3^{SC}}{\bar{\delta}_3^{SC}} & 0 \\ \frac{\frac{\bar{I}_1^{SC}}{I_1^{SC}} \frac{\delta_3^{SC}}{\bar{\delta}_3^{SC}} - 1}{I_1^{G1}} & \frac{\frac{\bar{I}_2^{SC}}{I_2^{SC}} \frac{\delta_3^{SC}}{\bar{\delta}_3^{SC}} - 1}{I_2^{G2}} & 1 \end{bmatrix}.$$

In this case, the factor ρ contains the value J_{33}.

We may introduce transformation parameters

$$m_1(y_N) = \frac{\bar{I}_1^{SC}}{I_1^{SC}} \frac{\delta_3^{SC}}{\bar{\delta}_3^{SC}}, \quad m_2(y_N) = \frac{\bar{I}_2^{SC}}{I_2^{SC}} \frac{\delta_3^{SC}}{\bar{\delta}_3^{SC}}. \tag{7.8}$$

Because the conductivity y_N has an equal effect on the load currents, these parameters are equal to each other; that is, $m_1(y_N) = m_2(y_N) = m_N$.

Finally, we obtain the above desired transformation

$$\begin{bmatrix} \rho\bar{I}_1 \\ \rho\bar{I}_2 \\ \rho 1 \end{bmatrix} = \begin{bmatrix} m_N & 0 & 0 \\ 0 & m_N & 0 \\ \frac{m_N-1}{I_1^{G1}} & \frac{m_N-1}{I_2^{G2}} & 1 \end{bmatrix} \cdot \begin{bmatrix} I_1 \\ I_2 \\ 1 \end{bmatrix}. \tag{7.9}$$

From here, we pass to the required currents

$$\begin{aligned} \bar{I}_1 &= \frac{I_1 m_N}{\frac{I_1}{I_1^{G1}}(m_N - 1) + \frac{I_2}{I_2^{G2}}(m_N - 1) + 1}, \\ \bar{I}_2 &= \frac{I_2 m_N}{\frac{I_1}{I_1^{G1}}(m_N - 1) + \frac{I_2}{I_2^{G2}}(m_N - 1) + 1}. \end{aligned} \tag{7.10}$$

The obtained relationships carry out the recalculation of currents at the respective change of conductivity y_N in the form of parameter m_N. Transformation (7.9) is a projective transformation and possesses group properties.

Let us formulate the value m_N by the initial and subsequent currents I_1^1, $\bar{I}_1^1$. To do this, we use expression (7.10) for the current I_1 as $I_2 = 0$.

Then

$$\bar{I}_1 = \frac{I_1 m_N}{\frac{I_1}{I_1^{G1}}(m_N - 1) + 1}. \tag{7.11}$$

From here, we obtain expression

$$m_N = \frac{\bar{I}_1 - 0}{\bar{I}_1 - I_1^{G1}} \div \frac{I_1 - 0}{I_1 - I_1^{G1}}.$$

It is possible to consider this expression as the cross-ratio for points $I_1, \bar{I}_1$ relatively to the base points $I_1 = 0, \quad I_1 = I_1^{G1}$; that is,

$$m_N = \left(0 \quad \bar{I}_1 \quad I_1 \quad I_1^{G1}\right).$$

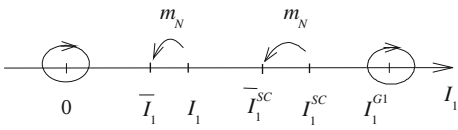

Fig. 7.4 Change of the current $I_1 \to \bar{I}_1$ at the change of y_N

The points $I_1 = 0, \quad I_1 = I_1^{G1}$ are fixed points and do not depend on the value y_N. Therefore, expression (7.11) is the transformation $I_1 \to \bar{I}_1$ with parameter m_N as it is shown in Fig. 7.4.

Therefore, the cross-ratio has the same value for the points $I_1^{SC}, \quad \bar{I}_1^{SC}$

$$\begin{aligned} m_N &= (0 \quad \bar{I}_1 \quad I_1 \quad I_1^{G1}) = (0 \quad \bar{I}_1^{SC} \quad I_1^{SC} \quad I_1^{G1}) \\ &= \frac{\bar{I}_1 - 0}{\bar{I}_1 - I_1^{G1}} \div \frac{I_1 - 0}{I_1 - I_1^{G1}} = \frac{\bar{I}_1^{SC} - 0}{\bar{I}_1^{SC} - I_1^{G1}} \div \frac{I_1^{SC} - 0}{I_1^{SC} - I_1^{G1}}. \end{aligned} \tag{7.12}$$

Now, let us formulate the value m_N by $y_N, \bar{y}_N$ and determine the sense of the parameter m_N.

Viewing expressions (6.28), we may consider expression (7.8) of m_N as a non-uniform coordinate

$$m_N = \frac{\bar{I}_1^{SC}}{I_1^{SC}} \frac{\delta_3^{SC}}{\bar{\delta}_3^{SC}} = \frac{\bar{I}_1^{SC}}{\bar{\delta}_3^{SC}} \div \frac{I_1^{SC}}{\delta_3^{SC}} = \bar{\xi}_3^1 \div \xi_3^1.$$

Hence, the value m_N is the cross-ratio of the initial SC and subsequent points $S\overline{C}$ shown in Fig. 7.3.

The base values of conductivity y_N are values y_N^0, y_N^{G1}. The value $y_N^0 = \infty$ determines the current $I_1 = 0$. The value y_N^{G1} presets the current $I_1 = I_1^{G1}$ as $I_2 = 0$.

Analysis of the circuit gives the following relationship for y_N^{G1}

$$-y_N^{G1} = y_{0N} + \frac{y_1 y_{1N}}{y_1 + y_{1N}} + \frac{y_2 y_{2N}}{y_2 + y_{2N}} = y_N^i. \tag{7.13}$$

The sense of value y_N^i will be explained below.

Therefore, the cross-ratio has the view

$$\begin{aligned} m_N &= (\infty \quad \bar{y}_N \quad y_N \quad -y_N^i) \\ &= \frac{\bar{y}_N - \infty}{\bar{y}_N + y_N^i} \div \frac{y_N - \infty}{y_N + y_N^i} = \frac{y_N + y_N^i}{\bar{y}_N + y_N^i}. \end{aligned} \tag{7.14}$$

Now, we formulate the value m_N by the $y_N, \bar{y}_N$ for the general case of currents I_1, I_2.

Using (6.21), we get *SC* currents

$$\bar{I}_1^{SC} = V_0 \bar{Y}_{10} = V_0 y_{0N} \frac{y_{1N}}{\bar{y}_\Sigma}, \quad I_1^{SC} = V_0 Y_{10} = V_0 y_{0N} \frac{y_{1N}}{y_\Sigma}.$$

Substituting these currents in (7.8), we obtain

$$\frac{\bar{I}_1^{SC}}{I_1^{SC}} = \frac{y_\Sigma}{\bar{y}_\Sigma} = \frac{y^{SER} + y_N}{y^{SER} + \bar{y}_N}, y^{SER} = y_{0N} + y_{1N} + y_{2N},$$
$$\frac{\bar{\delta}_3^{SC}}{\delta_3^{SC}} = \left(\frac{\bar{I}_1^{SC}}{I_1^{G1}} + \frac{\bar{I}_2^{SC}}{I_2^{G2}} - 1\right) \Big/ \left(\frac{I_1^{SC}}{I_1^{G1}} + \frac{I_2^{SC}}{I_2^{G2}} - 1\right)$$
$$= \frac{y^{SER} + y_N}{y^{SER} + \bar{y}_N} \cdot \frac{y_N^i + \bar{y}_N}{y_N^i + y_N}.$$

Finally, we have

$$m_N = \frac{\bar{I}_1^{SC}}{I_1^{SC}} \frac{\delta_3^{SC}}{\bar{\delta}_3^{SC}} = \frac{y_N + y_N^i}{\bar{y}_N + y_N^i}.$$

This expression is equal to (7.14).

So, the value m_N can be interpreted as a relative change of the conductivity y_N.

In turn, the value y_N^i is a scale for y_N. The correspondence of the values m_N, y_N is shown in Fig. 7.5.

Let us clarify the sense of the values y_N^i and $y_N^{G1} = -y_N^i$. The value y_N^i is the internal conductance of circuit relatively to terminals of disconnected conductivity y_N for the open circuit of loads, as it is shown in Fig. 7.6a.

In turn, if $y_N = -y_N^i$, the determinate of matrix Y parameters (6.21), $\Delta_Y = 0$. In this case, we have the current $I_1 = I_1^{G1}$ for the first given load Y_{L1}^1 and the disconnected second load, as it is shown in Fig. 7.6b. And vice versa, the current $I_2 = I_2^{G2}$ is preset for the second given load Y_{L2}^1 and the disconnected first load.

Example 3 We use the date of Example 1 for the initial regime

$$Y_{L1} = 0.5,\ Y_{L2} = 0.5,\ y_N = 0.625,\ I_1 = 0.979,\ I_2 = 0.8247,$$
$$I_1^{SC} = 3,\ I_2^{SC} = 2,\ \mu_3 \delta_3^{SC} = -0.677.$$

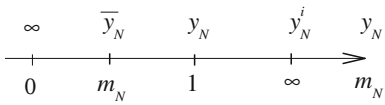

Fig. 7.5 Correspondence of the conductivity y_N and transformation parameter m_N

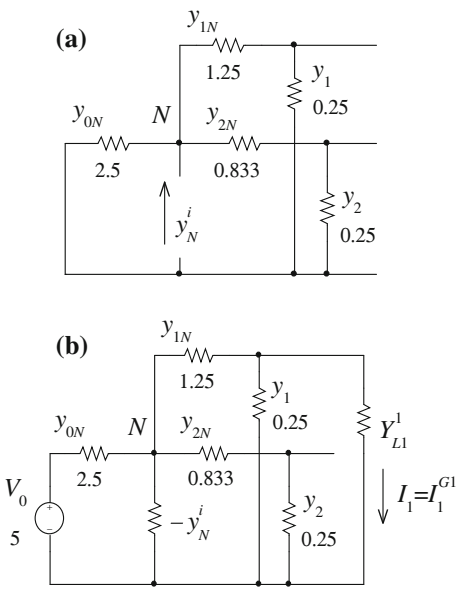

Fig. 7.6 **a** Internal conductance y_N^i of circuit. **b** Conductance $-y_N^i$ presets current I_1^{G1}

Let the subsequent regime parameters be given as

$$\bar{y}_N = 1.25, \quad \bar{I}_1^1 = 0.8465, \quad \bar{I}_2^1 = 0.713,$$
$$\bar{I}_1^{SC} = 2.679, \quad \bar{I}_2^{SC} = 1.785, \quad \mu_3 \bar{\delta}_3^{SC} = -0.7116.$$

Then, transformation parameter (7.8)

$$m_N = 0.8494.$$

Transformation (7.9)

$$\begin{bmatrix} \rho\bar{I}_1 \\ \rho\bar{I}_2 \\ \rho 1 \end{bmatrix} = \begin{bmatrix} 0.8494 & 0 & 0 \\ 0 & 0.8494 & 0 \\ -0.01 & -0.009262 & 1 \end{bmatrix} \cdot \begin{bmatrix} I_1 \\ I_2 \\ 1 \end{bmatrix}.$$

Subsequent currents (7.10)

$$\bar{I}_1 = \frac{0.8494 \cdot 0.979}{-0.01 \cdot 0.979 - 0.009262 \cdot 0.8247 + 1} = \frac{0.8315}{0.9825} = 0.8465,$$
$$\bar{I}_2 = \frac{0.8494 \cdot 0.8247}{0.9825} = 0.713.$$

Internal conductivity (7.13)

$$y_N^i = 2.5 + \frac{0.25 \cdot 1.25}{0.25 + 1.25} + \frac{0.25 \cdot 0.833}{0.25 + 0.833} = 2.9 \ .$$

We check transformation parameter (7.14)

$$m_N = \frac{y_N + y_N^i}{\bar{y}_N + y_N^i} = \frac{0.625 + 2.9}{1.25 + 2.9} = 0.8494 \ .$$

7.2.2 Change of Longitudinal Conductivity

We consider again the circuit in Fig. 7.2. Let the conductivity y_{0N} be changed, $y_{0N} \to \bar{y}_{0N}$. Corresponding changes of an initial point $M \to \bar{M}$ and short circuit point $SC \to \overline{SC}$ are shown in Fig. 7.7. Also, the coordinates of points G_1, G_2 by (6.24) and (6.26) are proportional to the value y_{0N}. Therefore, the subsequent straight line $\bar{G}_1\ \bar{G}_2$ is parallel to the initial line $G_1\ G_2$; the values Y_{L1}^{G1}, Y_{L2}^{G2} do not change.

Let us determine fixed points and lines as y_{0N} change. Naturally, the point 0 does not depend on this element. If the current across conductivity y_{0N} is equal to zero, a straight line $S_1\ S_2$ is the fixed line and we have the following equation of this line:

$$\frac{y_{1N}}{y_1 + y_{1N}} I_1 + \frac{y_{2N}}{y_2 + y_{2N}} I_2 + y_{0N}^i \cdot V_0 = 0.$$

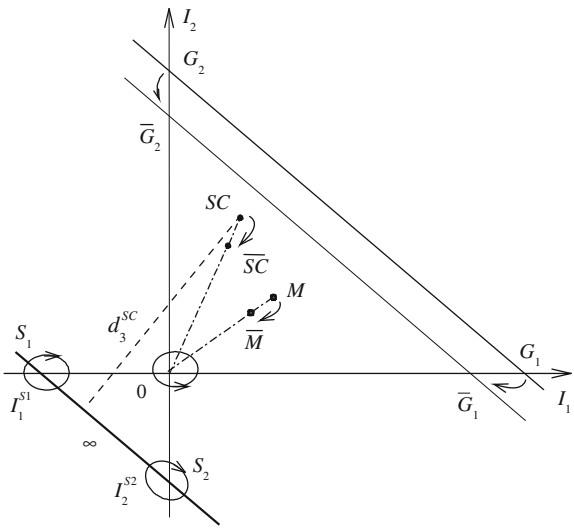

Fig. 7.7 Regime change at the expense of conductivity $y_{0N} \to \bar{y}_{0N}$

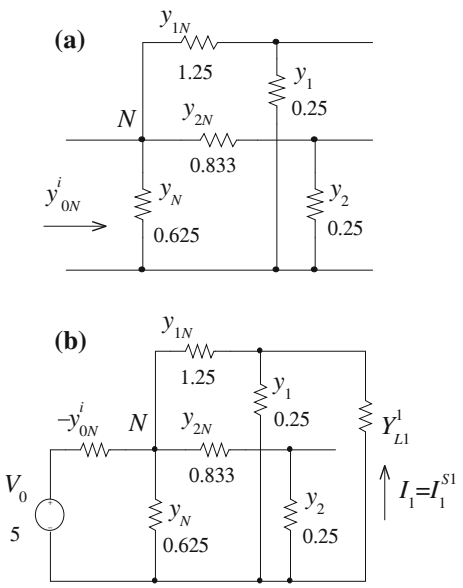

Fig. 7.8 **a** Internal conductivity y^i_{0N} of circuit. **b** Conductivity $-y^i_{0N}$ presets the current I_1^{S1}

The internal conductivity y^i_{0N} of the circuit relatively to terminals of conductivity y_{0N}, by Fig. 7.8a, has the value

$$y^i_{0N} = y_N + \frac{y_1 y_{1N}}{y_1 + y_{1N}} + \frac{y_2 y_{2N}}{y_2 + y_{2N}}. \tag{7.15}$$

The normalized view of the line $S_1\ S_2$ equation

$$\frac{I_1}{I_1^{S1}} + \frac{I_2}{I_2^{S2}} - 1 = 0,$$

where the points

$$I_1^{S1} = -y^i_{0N}\left(1 + \frac{y_1}{y_{1N}}\right)V_0, \quad I_2^{S2} = -y^i_{0N}\left(1 + \frac{y_2}{y_{2N}}\right)V_0 \tag{7.16}$$

In turn, if $y_{0N} = -y^i_{0N}$, the determinant $\Delta_Y = 0$. In this case, we have the load current $I_1 = I_1^{S1}$ for the first given load Y^1_{L1} and the disconnected second load, as it is shown in Fig. 7.8b. And vice versa, the current $I_2 = I_2^{S2}$ is preset for the second given load Y^1_{L2} and the disconnected first load.

Therefore, the influence of conductivity y_{0N} can be interpreted as a projective transformation in the plane $I_1,\ I_2$. In this case, we have the reference triangle $S_1\ 0\ S_2$ and a unit point SC, which form the initial system of projective coordinates.

Similarly to (6.36), we may determine the projective coordinates of the point M^1. The homogeneous coordinates

$$\rho\,\xi_1 = \frac{I_1}{I_1^{SC}}, \quad \rho\,\xi_2 = \frac{I_2}{I_2^{SC}}, \quad \rho\,\xi_3 = \frac{\delta_3}{\delta_3^{SC}}.$$

The distances δ_3, δ_3^{SC} to the straight line $S_1\,S_2$ have the view

$$\begin{aligned} \delta_3 &= \frac{1}{\mu_3}\left(\frac{I_1}{I_1^{S1}} + \frac{I_2}{I_2^{S2}} - 1\right), \\ \delta_3^{SC} &= \frac{1}{\mu_3}\left(\frac{I_1^{SC}}{I_1^{S1}} + \frac{I_2^{SC}}{I_2^{S2}} - 1\right). \end{aligned} \tag{7.17}$$

In turn, the non-uniform coordinates

$$m_1 = \frac{\rho\xi_1}{\rho\xi_3}, \quad m_2 = \frac{\rho\xi_2}{\rho\xi_3}.$$

For explanation, these non-uniform coordinates are represented in Fig. 7.9.

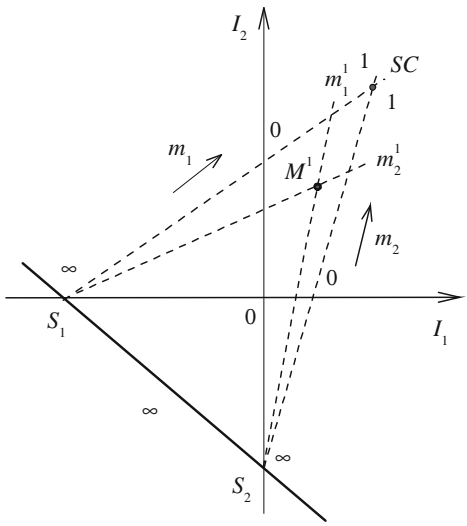

Fig. 7.9 View of the non-uniform coordinates

Transformation matrices (6.36) and (6.37)

$$[C] = \begin{bmatrix} \frac{1}{I_1^{SC}} & 0 & 0 \\ 0 & \frac{1}{I_2^{SC}} & 0 \\ \frac{1}{I_1^{S1}\mu_3\delta_3^{SC}} & \frac{1}{I_2^{S2}\mu_3\delta_3^{SC}} & -\frac{1}{\mu_3\delta_3^{SC}} \end{bmatrix},$$

$$[C]^{-1} = \begin{bmatrix} I_1^{SC} & 0 & 0 \\ 0 & I_2^{SC} & 0 \\ \frac{I_1^{SC}}{I_1^{S1}} & \frac{I_2^{SC}}{I_2^{S2}} & -\mu_3\delta_3^{SC} \end{bmatrix}.$$

On the other hand, the same reference triangle $S_1 0 S_2$ and a new unit point $S\overline{C}$ form the other system of projective coordinates and distance $\bar{\delta}_3^{SC}$.

Then, the required transformation is similar to (7.9)

$$\begin{bmatrix} \rho\bar{I}_1 \\ \rho\bar{I}_2 \\ \rho 1 \end{bmatrix} = \begin{bmatrix} m_1(y_{0N}) & 0 & 0 \\ 0 & m_2(y_{0N}) & 0 \\ \frac{m_1(y_{0N})-1}{I_1^{S1}} & \frac{m_2(y_{0N})-1}{I_2^{S2}} & 1 \end{bmatrix} \cdot \begin{bmatrix} I_1 \\ I_2 \\ 1 \end{bmatrix},$$

where transformation parameters

$$m_1(y_{0N}) = \frac{\bar{I}_1^{SC}}{I_1^{SC}}\frac{\delta_3^{SC}}{\bar{\delta}_3^{SC}}, \quad m_2(y_{0N}) = \frac{\bar{I}_2^{SC}}{I_2^{SC}}\frac{\delta_3^{SC}}{\bar{\delta}_3^{SC}}, \tag{7.18}$$

Because the conductivity y_{0N} has an equal effect on the load currents, these parameters are equal to each other; that is, $m_1(y_{0N}) = m_2(y_{0N}) = m_{0N}$.

Finally, we obtain

$$\begin{bmatrix} \rho\bar{I}_1 \\ \rho\bar{I}_2 \\ \rho 1 \end{bmatrix} = \begin{bmatrix} m_{0N} & 0 & 0 \\ 0 & m_{0N} & 0 \\ \frac{m_{0N}-1}{I_1^{S1}} & \frac{m_{0N}-1}{I_2^{S2}} & 1 \end{bmatrix} \cdot \begin{bmatrix} I_1 \\ I_2 \\ 1 \end{bmatrix}. \tag{7.19}$$

From here, we pass to the required subsequent currents

$$\begin{aligned} \bar{I}_1 &= \frac{I_1 m_{0N}}{\frac{I_1}{I_1^{S1}}(m_{0N}-1) + \frac{I_2}{I_2^{S2}}(m_{0N}-1) + 1}, \\ \bar{I}_2 &= \frac{I_2 m_{0N}}{\frac{I_1}{I_1^{S1}}(m_{0N}-1) + \frac{I_2}{I_2^{S2}}(m_{0N}-1) + 1}. \end{aligned} \tag{7.20}$$

Let us formulate the value m_{0N} by the initial and subsequent currents $I_1, \bar{I}_1$.

To do this, we use (7.20) for the current I_1 as $I_2 = 0$. Then, we get transformation

$$\bar{I}_1 = \frac{I_1 m_{0N}}{\frac{I_1}{I_1^{S1}}(m_{0N} - 1) + 1}. \tag{7.21}$$

The fixed points of this transformation are the points $I_1 = 0$, $I_1 = I_1^{S1}$ in Fig. 7.10.

Similarly to (7.12), it is possible to constitute the cross-ratio

$$m_{0N} = \left(0 \quad \bar{I}_1 \quad I_1 \quad I_1^{S1}\right) = \left(0 \quad \bar{I}_1^{SC} \quad I_1^{SC} \quad I_1^{S1}\right) = \left(0 \quad \bar{I}_1^{G1} \quad I_1^{G1} \quad I_1^{S1}\right).$$

Now, we formulate the value m_{0N} by y_{0N}, $\bar{y}_{0N}$ and determine the sense of this parameter m_{0N}. According to the above case, we get

$$m_{0N} = (0\ \bar{y}_{0N}\ y_{0N}\ -y_{0N}^i) = \frac{\bar{y}_{0N} - 0}{\bar{y}_{0N} + y_{0N}^i} \div \frac{y_{0N} - 0}{y_{0N} + y_{0N}^i}. \tag{7.22}$$

The value m_{0N} can be considered as a relative change of the conductivity y_{0N}.

In turn, the value y_{0N}^i is a scale for y_{0N}. The correspondence of values m_{0N} and y_{0N} is shown in Fig. 7.11.

Example 4 We use the date of Example 1 for the initial regime

$$y_{0N} = 2.5,\ I_1 = 0.979,\ \ I_2 = 0.8247,$$
$$I_1^{SC} = 3,\ \ I_2^{SC} = 2,\ \ \mu_3\delta_3^{SC} = -0.677.$$

Let the subsequent regime parameters be given as

$$\bar{y}_{0N} = 2, \quad \bar{I}_1 = 0.896, \quad \bar{I}_2 = 0.7545,$$
$$\bar{I}_1^{SC} = 2.6548, \quad \bar{I}_2^{SC} = 1.77, \quad \mu_3\bar{\delta}_3^{SC} = -1.6969.$$

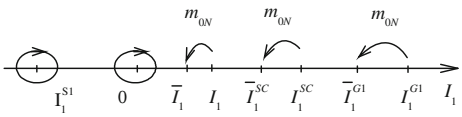

Fig. 7.10 Change of current at change of y_{0N}

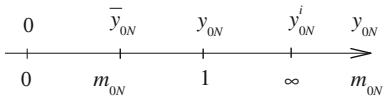

Fig. 7.11 Correspondence of the conductivity y_{0N} and parameter m_{0N}

Transformation parameter (7.18)

$$m_{0N} = 0.9323.$$

Transformation (7.9)

$$\begin{bmatrix} \rho\bar{I}_1 \\ \rho\bar{I}_2 \\ \rho 1 \end{bmatrix} = \begin{bmatrix} 0.9323 & 0 & 0 \\ 0 & 0.9323 & 0 \\ -0.011 & -0.01016 & 1 \end{bmatrix} \cdot \begin{bmatrix} I_1 \\ I_2 \\ 1 \end{bmatrix}.$$

Subsequent currents (7.20)

$$\bar{I}_1 = \frac{0.9323 \cdot 0.979}{0.011 \cdot 0.979 + 0.01016 \cdot 0.8247 + 1} = \frac{0.9127}{1.01914} = 0.896,$$
$$\bar{I}_2 = \frac{0.9323 \cdot 0.8247}{0.011 \cdot 0.979 + 0.01016 \cdot 0.8247 + 1} = \frac{0.7688}{1.01914} = 0.7545.$$

Internal conductivity (7.14)

$$y^i_{0N} = y_N + \frac{y_1 y_{1N}}{y_1 + y_{1N}} + \frac{y_2 y_{2N}}{y_2 + y_{2N}} = 0.625 + 0.4 = 1.025.$$

We check transformation parameter (7.22)

$$m_{0N} = \frac{\bar{y}_{0N}}{\bar{y}_{0N} + y^i_{0N}} \div \frac{y_{0N}}{y_{0N} + y^i_{0N}}$$
$$= \frac{2}{2 + 1.025} \div \frac{2.5}{2.5 + 1.025} = \frac{0.6611}{0.7092} = 0.9323.$$

7.3 Comparison of Regimes and Parameters of Active Two-Ports

Let two active two-ports be given with different parameters. Bunches of load straight lines and the conformity of points of characteristic and running regimes are presented in Fig. 7.12.

The problem is to find such values of conductivities and currents of loads of the second two-port (a point $\bar{M}$) that its relative regimes would be equal to regimes of the first two-port (a point M with preset values of conductivities Y_{L1}, Y_{L2} and currents I_1, I_2).

For this purpose, we consider systems of projective coordinates of these two-ports [1]. Such systems are set by the triangles of reference $G_1 0\, G_2$, $\bar{G}_1 0\, \bar{G}_2$ and unit points SC, $S\overline{C}$ respectively.

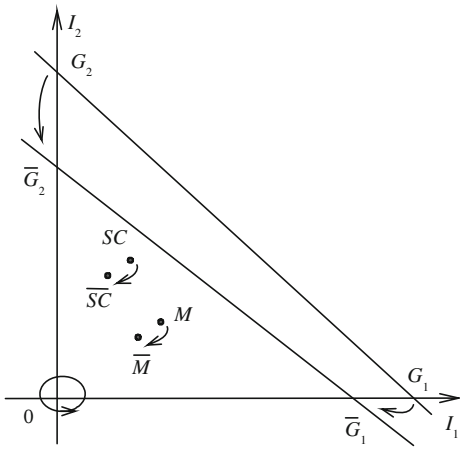

Fig. 7.12 Conformity of the characteristics of two active two-ports

Therefore, we have the equality of non-uniform coordinates by (6.28) for the load conductivities

$$m_1 = \frac{Y_{L1}}{Y_{L1} - Y_{L1}^{G1}} = \frac{\bar{Y}_{L1}}{\bar{Y}_{L1} - \bar{Y}_{L1}^{G1}}, \quad m_2 = \frac{Y_{L2}}{Y_{L2} - Y_{L2}^{G2}} = \frac{\bar{Y}_{L2}}{\bar{Y}_{L2} - \bar{Y}_{L2}^{G2}}. \tag{7.23}$$

From here, we get the formulas

$$\bar{Y}_{L1} = \bar{Y}_{L1}^{G1} \frac{m_1}{m_1 - 1}, \quad \bar{Y}_{L2} = \bar{Y}_{L2}^{G2} \frac{m_2}{m_2 - 1}. \tag{7.24}$$

Next, it is necessary to find a transformation which provides the recalculation of currents.

The conditions of equal regimes lead to the equality of homogeneous projective coordinates; that is,

$$[\bar{\rho}\bar{\xi}] = [\xi].$$

According to (6.36) for these two-ports, we get

$$[\rho\xi] = [\mathbf{C}] \cdot [\mathbf{I}], [\bar{\rho}\bar{\xi}] = [\bar{\mathbf{C}}] \cdot [\bar{\mathbf{I}}].$$

Therefore, we obtain the necessary transformation as

$$[\bar{\rho}\bar{I}] = [\bar{\mathbf{C}}]^{-1} \cdot [\mathbf{C}] \cdot [\mathbf{I}] = [\mathbf{J}] \cdot [\mathbf{I}], \tag{7.25}$$

where the matrixes

$$[\bar{C}]^{-1} = \begin{bmatrix} \bar{I}_1^{SC} & 0 & 0 \\ 0 & \bar{I}_2^{SC} & 0 \\ \frac{\bar{I}_1^{SC}}{\bar{I}_1^{G1}} & \frac{\bar{I}_2^{SC}}{\bar{I}_2^{G2}} & -\bar{\mu}_3\bar{\delta}_3^{SC} \end{bmatrix}, \tag{7.26}$$

$$[\mathbf{C}] = \begin{bmatrix} \frac{1}{I_1^{SC}} & 0 & 0 \\ 0 & \frac{1}{I_2^{SC}} & 0 \\ \frac{1}{I_1^{G1}\mu_3\delta_3^{SC}} & \frac{1}{I_2^{G2}\mu_3\delta_3^{SC}} & -\frac{1}{\mu_3\delta_3^{SC}} \end{bmatrix}. \tag{7.27}$$

Then, the matrix$[\mathbf{J}]$ has the form

$$[\mathbf{J}] = \begin{bmatrix} J_{11} & 0 & 0 \\ 0 & J_{22} & 0 \\ J_{31} & J_{33} & J_{33} \end{bmatrix}. \tag{7.28}$$

In turn, the matrix elements are

$$J_{11} = \frac{\bar{I}_1^{SC}}{I_1^{SC}},\ J_{22} = \frac{\bar{I}_2^{SC}}{I_2^{SC}},\ J_{33} = \frac{\bar{\mu}_3\bar{\delta}_3^{SC}}{\mu_3\delta_3^{SC}},$$
$$J_{31} = \frac{\bar{\mu}_3\bar{\delta}_3^{SC}}{I_1^{G1}\mu_3\delta_3^{SC}}\left(\frac{\bar{I}_1^{SC}I_1^{G1}}{I_1^{SC}\bar{I}_1^{G1}}\cdot\frac{\mu_3\delta_3^{SC}}{\bar{\mu}_3\bar{\delta}_3^{SC}} - 1\right),$$
$$J_{32} = \frac{\bar{\mu}_3\bar{\delta}_3^{SC}}{I_2^{G2}\mu_3\delta_3^{SC}}\left(\frac{\bar{I}_2^{SC}I_2^{G2}}{I_2^{SC}\bar{I}_2^{G2}}\cdot\frac{\mu_3\delta_3^{SC}}{\bar{\mu}_3\bar{\delta}_3^{SC}} - 1\right).$$

The form of these expressions shows that we may divide all the elements by J_{33} and introduce values

$$\bar{m}_1 = \frac{\bar{I}_1^{SC}}{I_1^{SC}}\frac{\mu_3\delta_3^{SC}}{\bar{\mu}_3\bar{\delta}_3^{SC}},\quad \bar{m}_2 = \frac{\bar{I}_2^{SC}}{I_2^{SC}}\frac{\mu_3\delta_3^{SC}}{\bar{\mu}_3\bar{\delta}_3^{SC}}. \tag{7.29}$$

These values state a quantitative estimation of the circuit distinctions.
Then, the required transformation becomes

$$\begin{bmatrix} \rho\bar{I}_1 \\ \rho\bar{I}_2 \\ \rho 1 \end{bmatrix} = \begin{bmatrix} \bar{m}_1 & 0 & 0 \\ 0 & \bar{m}_2 & 0 \\ \frac{1}{I_1^{G1}}\left(\frac{I_1^{G1}}{\bar{I}_1^{G1}}\bar{m}_1 - 1\right) & \frac{1}{I_2^{G2}}\left(\frac{I_2^{G2}}{\bar{I}_2^{G2}}\bar{m}_2 - 1\right) & 1 \end{bmatrix} \cdot \begin{bmatrix} I_1 \\ I_2 \\ 1 \end{bmatrix}. \tag{7.30}$$

In turn,

$$\begin{aligned}\bar{I}_1 &= \frac{I_1\bar{m}_1}{\frac{I_1}{I_1^{G1}}\left(\frac{I_1^{G1}}{\bar{I}_1^{G1}}\bar{m}_1 - 1\right) + \frac{I_2}{I_2^{G2}}\left(\frac{I_2^{G2}}{\bar{I}_2^{G2}}\bar{m}_2 - 1\right) + 1},\\ \bar{I}_2 &= \frac{I_2\bar{m}_2}{\frac{I_1}{I_1^{G1}}\left(\frac{I_1^{G1}}{\bar{I}_1^{G1}}\bar{m}_1 - 1\right) + \frac{I_2}{I_2^{G2}}\left(\frac{I_2^{G2}}{\bar{I}_2^{G2}}\bar{m}_2 - 1\right) + 1}.\end{aligned} \tag{7.31}$$

The structure of expressions (7.31) shows that it is possible to introduce the normalized values

$$\bar{m}_1^N = \bar{m}_1\frac{I_1^{G1}}{\bar{I}_1^{G1}}, \quad \bar{m}_2^N = \bar{m}_2\frac{I_2^{G2}}{\bar{I}_2^{G2}}.$$

Then, we obtain the normalized form of transformation (7.30)

$$\begin{bmatrix} \bar{\rho}\,\frac{\bar{I}_1}{\bar{I}_1^{G1}} \\ \bar{\rho}\,\frac{\bar{I}_2}{\bar{I}_2^{G2}} \\ \bar{\rho}\,\bar{1} \end{bmatrix} = \begin{bmatrix} \bar{m}_1^N & 0 & 0 \\ 0 & \bar{m}_2^N & 0 \\ \bar{m}_1^N - 1 & \bar{m}_2^N - 1 & 1 \end{bmatrix} \cdot \begin{bmatrix} \frac{I_1}{I_1^{G1}} \\ \frac{I_2}{I_2^{G2}} \\ 1 \end{bmatrix}. \tag{7.32}$$

The obtained transformations allow carrying out the recalculation of currents of the second two-port for any currents of the first two-port, using the preset values $\bar{m}_1, \bar{m}_2$ or $\bar{m}_1^N, \bar{m}_2^N$.

Example 5 We consider two circuits similar to the circuit in Fig. 6.8 and use some date of example 2 of Sect. 6.1.3.

Let the following different conductivities be given for these two-ports as

$$\begin{aligned} y_{1N} = 1.25 \rightarrow \bar{y}_{1N} = 0.8928,\\ y_{2N} = 0.8333 \rightarrow \bar{y}_{1N} = 0.5681. \end{aligned}$$

The bunch centers of the second two-port

$$\begin{aligned} \bar{I}_1^{G1} = 16,\ \bar{Y}_{L1}^{G1} = -1.1428;\\ \bar{I}_2^{G2} = 18,\ \bar{Y}_{L2}^{G2} = -0.8181. \end{aligned}$$

Let the relative regimes of these two-ports be equal to each other by (7.23)

$$m_1 = 0.25, \quad m_2 = 0.3158.$$

For the second circuit we find the following values.

Load conductivities (7.24)

$$\bar{Y}_{L1} = \bar{Y}_{L1}^{G1}\frac{m_1}{m_1 - 1} = 0.3809,$$
$$\bar{Y}_{L2} = \bar{Y}_{L2}^{G2}\frac{m_2}{m_2 - 1} = 0.3776.$$

SC currents

$$\bar{I}_1^{SC} = 2.434, \quad \bar{I}_2^{SC} = 1.549.$$

The distances

$$\bar{\mu}_3\bar{\delta}_3^{\mathrm{SC}} = -0.7618, \quad \bar{\mu}_3\bar{\delta}_3^{1} = -0.9211, \quad \bar{\mu}_3 = 0.08362.$$

Distinctions (7.29)

$$\bar{m}_1 = 0.721, \quad \bar{m}_2 = 0.6882.$$

Transformation (7.30)

$$\begin{bmatrix} \bar{\rho}\,\bar{I}_1 \\ \bar{\rho}\,\bar{I}_2 \\ \bar{\rho}1 \end{bmatrix} = \begin{bmatrix} 0.721 & 0 & 0 \\ 0 & 0.6882 & 0 \\ -0.0216 & -0.0233 & 0 \end{bmatrix} \cdot \begin{bmatrix} I_1 \\ I_2 \\ 1 \end{bmatrix}.$$

Currents (7.31)

$$\bar{I}_1 = \frac{0.721 \cdot 0.979}{-0.0216 \cdot 0.979 - 0.0233 \cdot 0.8247 + 1} = \frac{0.7058}{0.9596} = 0.7355,$$
$$\bar{I}_2 = \frac{0.6882 \cdot 0.8247}{0.9596} = 0.5915.$$

7.4 Comparison of Regime of Active Two-Ports with Linear Stabilizations of Load Voltages

We use the circuit in Fig. 6.20. For convenience, we redraw this circuit in Fig. 7.13.

Let us consider the two similar circuits with different values of element parameters and regime parameters. It is necessary to prove an approach to the comparison or recalculation of running regimes of such circuits. The characteristics of these comparable circuits are given in Fig. 7.14. The condition of regime comparison is the conformity of characteristic regimes as a projective transformation [4].

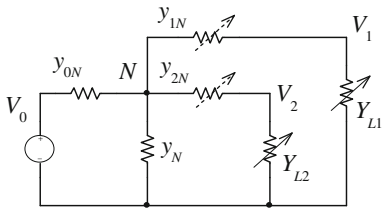

Fig. 7.13 Active two-port with stabilization of load voltages

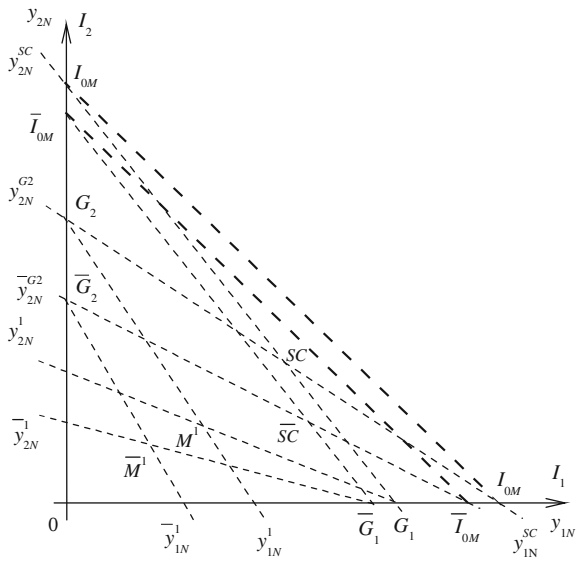

Fig. 7.14 Conformity of characteristics of similar circuits

Case of equal regimes

The running regimes of these circuits (a point M_1 corresponds to a point $\bar{M}_1$) will be equivalent or equal to each other if their non-uniform coordinates (6.79) and (6.80) are equal, and homogeneous projective coordinates (6.82) are proportional; that is,

$$m_1 = \bar{m}_1,\ m_2 = \bar{m}_2,\ [\rho\ \xi] = [\bar{\xi}]. \tag{7.33}$$

Using relationships (6.82) and (6.83), we find the required conformity of load currents

$$[\rho\,\bar{\mathbf{I}}] = [\bar{\mathbf{C}}]^{-1} \cdot [\bar{\xi}] = [\bar{\mathbf{C}}]^{-1} \cdot [\mathbf{C}] \cdot [\mathbf{I}] = [\mathbf{M}] \cdot [\mathbf{I}]. \tag{7.34}$$

The resulting matrix [**M**] has the view

$$[\mathbf{M}] = \begin{bmatrix} M_{11} & 0 & 0 \\ 0 & M_{22} & 0 \\ M_{31} & M_{32} & M_{33} \end{bmatrix}, \tag{7.35}$$

$$M_{11} = \frac{\bar{I}_1^{SC}}{I_1^{SC}}, \quad M_{22} = \frac{\bar{I}_2^{SC}}{I_2^{SC}}, \quad M_{33} = \frac{\bar{\mu}_3 \bar{\delta}_3^{SC}}{\mu_3 \delta_3^{SC}},$$
$$M_{31} = \frac{\bar{I}_1^{SC}}{\bar{I}_1^{G1}} \frac{1}{I_1^{SC}} - \frac{\bar{\mu}_3 \bar{\delta}_3^{SC}}{I_1^{G1} \mu_3 \delta_3^{SC}}, \quad M_{32} = \frac{\bar{I}_2^{SC}}{\bar{I}_2^{G2}} \frac{1}{I_2^{SC}} - \frac{\bar{\mu}_3 \bar{\delta}_3^{SC}}{I_2^{G2} \mu_3 \delta_3^{SC}}.$$

The similar condition for the conformity of regulator conductivities follows from (6.79) and (6.80). In particular, the conductivity $\bar{y}_{1N}$ is defined by the equality

$$\frac{y_{1N}^1}{y_{1N}^1 - y_{1N}^{G1}} \div \frac{y_{1N}^{SC}}{y_{1N}^{SC} - y_{1N}^{G1}} = \frac{\bar{y}_{1N}^1}{\bar{y}_{1N}^1 - \bar{y}_{1N}^{G1}} \div \frac{\bar{y}_{1N}^{SC}}{\bar{y}_{1N}^{SC} - \bar{y}_{1N}^{G1}}. \tag{7.36}$$

Case of not equal regimes

Let a subsequent regime of the second circuit be given by a point $\bar{M}_2$. The point M_2 of equal regime of the first circuit corresponds to this point $\bar{M}_2$.

Therefore, it is possible to consider the points M_1, M_2 of the first circuit as the change of its regime; that is, $M_1 \to M_2$. Then, the same change of regime will be for the second circuit, $\bar{M}_1 \to \bar{M}_2$. Therefore, this regime change defines the difference of regimes of comparable circuits, $M_1 \to \bar{M}_2$.

Let us validate an expression of regime change via the change of non-uniform projective coordinates. The non-uniform coordinate $\bar{m}_1^2$ of subsequent regime, the point $\bar{M}_2$, is given by (6.79)

$$\bar{m}_1^2 = (0\ \bar{y}_{1N}^2\ \bar{y}_{1N}^{SC}\ \bar{y}_{1N}^{G1}) = \frac{\bar{y}_{1N}^2}{\bar{y}_{1N}^2 - \bar{y}_{1N}^{G1}} \div \frac{\bar{y}_{1N}^{SC}}{\bar{y}_{1N}^{SC} - \bar{y}_{1N}^{G1}}.$$

The regime change are naturally expressed through the cross-ratio

$$\bar{m}_1^{21} = (0\ \bar{y}_{1N}^2\ \bar{y}_{1N}^1\ \bar{y}_{1N}^{G1}) = \frac{\bar{y}_{1N}^2}{\bar{y}_{1N}^2 - \bar{y}_{1N}^{G1}} \div \frac{\bar{y}_{1N}^1}{\bar{y}_{1N}^1 - \bar{y}_{1N}^{G1}} = \bar{m}_1^2 \div \bar{m}_1^1. \tag{7.37}$$

This change is also equal to the change of regime of the first circuit

$$\bar{m}_1^{21} = m_1^{21} = m_1^2 \div m_1^1.$$

Let us express these changes through load currents. Using (6.81) and (6.31), we obtain

$$m_1^{21} = \frac{I_1^2}{I_1^1}\frac{\mu_3\delta_3^1}{\mu_3\delta_3^2}, \quad m_2^{21} = \frac{I_2^2}{I_2^1}\frac{\mu_3\delta_3^1}{\mu_3\delta_3^2}. \tag{7.38}$$

Let the changes m_1^{21}, m_2^{21} and the initial equal regime, the points $M_1, \bar{M}_1$, be given.

At first, it is necessary to find load currents of these regime changes, the points $M_2, \bar{M}_2$. Similarly to (7.2), we have for the second circuit

$$\left[\rho\bar{\mathbf{I}}^2\right] = \left[\mathbf{J^{21}}\right] \cdot \left[\bar{\mathbf{I}}^{\mathbf{1}}\right], \tag{7.39}$$

The matrix

$$\left[\mathbf{J^{21}}\right] = \begin{bmatrix} m_1^{21} & 0 & 0 \\ 0 & m_2^{21} & 0 \\ \frac{1}{\bar{I}_1^{G1}}(m_1^{21}-1) & \frac{1}{\bar{I}_2^{G2}}(m_2^{21}-1) & 1 \end{bmatrix}.$$

From here, we pass to the required currents

$$\begin{aligned} \bar{I}_1^2 &= \frac{\bar{I}_1^1 m_1^{21}}{\frac{\bar{I}_1^1}{\bar{I}_1^{G1}}(m_1^{21}-1) + \frac{\bar{I}_2^1}{\bar{I}_2^{G2}}(m_2^{21}-1) + 1}, \\ \bar{I}_2^2 &= \frac{\bar{I}_2^1 m_2^{21}}{\frac{\bar{I}_1^1}{\bar{I}_1^{G1}}(m_1^{21}-1) + \frac{\bar{I}_2^1}{\bar{I}_2^{G2}}(m_2^{21}-1) + 1}. \end{aligned} \tag{7.40}$$

Similar relationships are obtained for the first circuit.

At last, we find the required expression of recalculation for comparable circuit currents, the conformity $M_1 \to \bar{M}_2$.

Using (7.39) and (7.34), we obtain

$$[\rho\bar{\mathbf{I}}^2] = [\mathbf{J^{21}}] \cdot [\bar{\mathbf{I}}^1] = [\mathbf{J^{21}}] \cdot [\mathbf{M}] \cdot [\mathbf{I^1}] = [\bar{\mathbf{J}}^{21}] \cdot [\mathbf{I^1}]. \tag{7.41}$$

The resultant matrix $[\bar{\mathbf{J}}^{21}]$ has the view

$$[\bar{\mathbf{J}}^{21}] = \begin{bmatrix} \bar{J}_{11} & 0 & 0 \\ 0 & \bar{J}_{22} & 0 \\ \bar{J}_{31} & \bar{J}_{32} & \bar{J}_{33} \end{bmatrix}, \tag{7.42}$$

where

$$\bar{J}_{11} = m_1^{21}\frac{\bar{I}_1^{SC}}{I_1^{SC}},\ \bar{J}_{22} = m_2^{21}\frac{\bar{I}_2^{SC}}{I_2^{SC}},\ \bar{J}_{33} = \frac{\bar{\mu}_3\bar{\delta}_3^{SC}}{\mu_3\delta_3^{SC}},$$
$$\bar{J}_{31} = m_1^{21}\frac{\bar{I}_1^{SC}}{\bar{I}_1^{G1}}\frac{1}{I_1^{SC}} - \frac{\bar{\mu}_3\bar{\delta}_3^{SC}}{I_1^{G1}\mu_3\delta_3^{SC}},$$
$$\bar{J}_{32} = m_2^{21}\frac{\bar{I}_2^{SC}}{\bar{I}_2^{G2}}\frac{1}{I_2^{SC}} - \frac{\bar{\mu}_3\bar{\delta}_3^{SC}}{I_2^{G2}\mu_3\delta_3^{SC}}.$$

From the obtained expressions, the procedure of regime comparison of two circuits follows. For this purpose, we consider an example.

Example We use the date of Example 5 for Sect. 6.3. The element parameters have the following values:

$$V_0 = 5\,,\ y_{0N} = 2.5\,,\ y_N = 0.625.$$

We have for the first circuit.

The characteristic values of currents and conductivities

$$I_1^{G1} = 3.125,\ \ y_{1N}^{G1} = 3.125,\ \ y_{1N}^{SC} = -6.25,\ \ I_1^{SC} = 1.785;$$
$$I_2^{G2} = 6.25,\ \ y_{2N}^{G2} = -6.25,\ \ y_{2N}^{SC} = -4.166,\ \ I_2^{SC} = 5.357.$$

The currents of the initial regime, point M_1

$$I_1^1 = 1,\ \ I_2^1 = 1.$$

The conductivities of the regulators

$$y_{1N}^1 = 0.735,\quad y_{2N}^1 = 2.777.$$

The non-uniform projective coordinates

$$m_1^1 = -0.461,\quad m_2^1 = -0.154.$$

The distances of the points M_1,SC to the straight line G_1G_2

$$\mu_3\delta_3^1 = -0.52,\quad \mu_3\delta_3^{SC} = 0.428.$$

We have for the second circuit.

The element parameters have the same values, except $\bar{y}_N = 0.25$.

The characteristic values of currents and conductivities

$$\bar{I}_1^{G1} = 4.25,\ \bar{y}_{1N}^{G1} = 4.25,\ \bar{y}_{1N}^{SC} = -6.25,\ \bar{I}_1^{SC} = 2.309;$$
$$\bar{I}_2^{G2} = 7,\ \bar{y}_{2N}^{G2} = -7,\ \bar{y}_{2N}^{\mathrm{SC}} = -4.166,\ \bar{I}_2^{SC} = 5.706.$$

The distance of point $S\overline{C}$ to straight line $\bar{G}_1\bar{G}_2$

$$\bar{\mu}_3\bar{\delta}_3^{SC} = 0.358.$$

Case of equal regimes

Elements of matrix (7.35)

$$M_{11} = \frac{2.309}{1.785} = 1.293, \quad M_{22} = \frac{5.706}{5.357} = 1.0652, \quad M_{33} = \frac{0.358}{0.428} = 0.836,$$
$$M_{31} = \frac{2.309}{4.25}\frac{1}{1.785} - \frac{0.358}{3.125 \cdot 0.428} = 0.0365,$$
$$M_{32} = \frac{5.706}{7}\frac{1}{5.357} - \frac{0.358}{6.25 \cdot 0.428} = 0.0183.$$

Currents (7.34)

$$\bar{I}_1^1 = \frac{M_{11}I_1^1}{M_{31}I_1^1 + M_{32}I_2^1 + M_{33}}$$
$$= \frac{1.293 \cdot 1}{0.0365 \cdot 1 + 0.0183 \cdot 1 + 0.836} = \frac{1.293}{0.89} = 1.4528,$$
$$\bar{I}_2^1 = \frac{M_{22}I_2^1}{M_{31}I_1^1 + M_{32}I_2^1 + M_{33}}$$
$$= \frac{1.0652 \cdot 1}{0.0365 \cdot 1 + 0.0183 \cdot 1 + 0.836} = \frac{1.0652}{0.89} = 1.194.$$

Conductivities of regulators (6.76)

$$\bar{y}_{1N}^1 = \bar{I}_1^1 \frac{y_{0N} + \bar{y}_N}{\bar{I}_2^{G2} - (\bar{I}_1^1 + \bar{I}_2^1)} = 1.45\frac{2.75}{7 - 2.646} = 0.916.$$
$$\bar{y}_{2N}^1 = \bar{I}_2^1 \frac{y_{0N} + \bar{y}_N}{\bar{I}_1^{G1} - (\bar{I}_1^1 + \bar{I}_2^1)} = 1.194\frac{2.75}{4.25 - 2.646} = 2.047.$$

Let us check up the equality of non-uniform coordinates (7.33).

Non-uniform coordinates (7.36)

$$\bar{m}_1^1 = \frac{0.916}{0.916 - 4.25} \div \frac{-6.25}{-6.25 - 4.25} = -0.274 \div 0.595 = -0.461 = m_1^1,$$
$$\bar{m}_2^1 = \frac{2.0475}{2.0475 + 7} \div \frac{-4.166}{-4.166 + 7} = 0.226 \div (-1.47) = -0.154 = m_2^1.$$

Case of not equal regimes

Let us consider the second circuit. We believe that the regime corresponds to the point $\bar{M}_2$. Let the currents be given as

$$\bar{I}_1^2 = 1.5, \quad \bar{I}_2^2 = 2,$$

Then, the conductivities

$$\bar{y}_{1N}^2 = 1.179, \quad \bar{y}_{2N}^2 = 7.333.$$

Regime change (7.37)

$$m_1^{21} = \frac{1.179}{1.179 - 4.25} \div \frac{0.916}{0.916 - 4.25} = 0.3839 \div 0.2749 = 1.396.$$

Similarly, we get

$$m_2^{21} = \frac{7.333}{7.333 + 7} \div \frac{2.0475}{2.0475 + 7} = 0.5116 \div 0.2263 = 2.261.$$

The currents of the second circuit by (7.40)

$$\bar{I}_1^2 = \frac{1.45 \cdot 1.397}{1.45 \cdot 0.0935 + 1.194 \cdot 0.18 + 1} = \frac{2.02}{1.35} = 1.5,$$
$$\bar{I}_2^2 = \frac{1.194 \cdot 2.261}{1.35} = 2.$$

Matrix (7.42)

$$[\bar{\mathbf{J}}^{21}] = \begin{bmatrix} 1.8073 & 0 & 0 \\ 0 & 2.4089 & 0 \\ 0.1574 & 0.2103 & 0.8368 \end{bmatrix}.$$

We check the currents of point $\bar{M}_2$ by (7.41)

$$\bar{I}_1^2 = \frac{1.8073 \cdot 1}{0.1574 \cdot 1 + 0.2103 \cdot 1 + 0.836} = \frac{1.8073}{1.2045} = 1.5,$$
$$\bar{I}_2^2 = \frac{2.4089}{1.2045} = 2.$$

References

1. Penin, A.: Normalized representation of the equations of active multiport networks on the basis of projective geometry. Moldavian J. Phys. Sci. **10**(3–4), 350–357 (2011). http://sfm.asm.md/moldphys/2011/vol10/n3-4/index.html Accessed 30 Nov 2014
2. Penin, A.: Recalculating the load currents of an active multiport with variable parameters on the basis of projective geometry. Electrichestvo **10**, 66–73 (2012)
3. Penin, A.: Recalculation of the loads current of active multiport networks on the basis of projective geometry. J. Circ. Syst. Comput. **22**(05), 1350031, 13 p. (2013). doi: 10.1142/S021812661350031X http://www.worldscientific.com/doi/abs/10.1142/S021812661350031X Accessed 30 Nov 2014
4. Penin, A.: Comparison of regimes of active two-port networks with stabilization of load voltages. Int. J. Electron. Commun. Electr. Eng. **3**(6), 1–18 (2013). https://sites.google.com/site/ijeceejournal/

Chapter 8
Passive Multi-port Circuits

8.1 Input-Output Conformity of Four-Ports as an Affine Transformation

We use the results of Sect. 6.1.1. Let us consider a four-port circuit with changeable load voltage sources in Fig. 8.1 and give necessary relationships $I_3(V_1, V_2), I_4(V_1, V_2)$ for this network.

Taking into account the specified directions of currents, this network is described by the following system of Y parameters equations

$$\begin{bmatrix} I_1 \\ I_2 \\ I_3 \\ I_4 \end{bmatrix} = \begin{bmatrix} -Y_{11} & Y_{12} & Y_{13} & Y_{14} \\ Y_{12} & -Y_{22} & Y_{23} & Y_{24} \\ -Y_{13} & -Y_{23} & Y_{33} & -Y_{34} \\ -Y_{14} & -Y_{24} & -Y_{34} & Y_{44} \end{bmatrix} \cdot \begin{bmatrix} V_1 \\ V_2 \\ V_3 \\ V_4 \end{bmatrix} = [\mathbf{Y}] \cdot [\mathbf{V}], \tag{8.1}$$

From here, we obtain

$$\begin{bmatrix} I_3 \\ I_4 \end{bmatrix} = \begin{bmatrix} -Y_{13} & -Y_{23} \\ -Y_{14} & -Y_{24} \end{bmatrix} \cdot \begin{bmatrix} V_1 \\ V_2 \end{bmatrix} + \begin{bmatrix} I_3^{SC,SC} \\ I_4^{SC,SC} \end{bmatrix}, \tag{8.2}$$

where SC currents of both loads

$$\begin{bmatrix} I_3^{SC,SC} \\ I_4^{SC,SC} \end{bmatrix} = \begin{bmatrix} Y_{33} & -Y_{34} \\ -Y_{34} & Y_{44} \end{bmatrix} \cdot \begin{bmatrix} V_3 \\ V_4 \end{bmatrix}. \tag{8.3}$$

A. Penin, *Analysis of Electrical Circuits with Variable Load Regime Parameters*, Power Systems, DOI 10.1007/978-3-319-28451-4_8

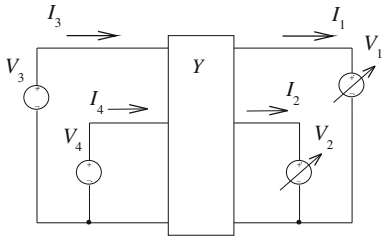

Fig. 8.1 Four-port with changeable load voltage sources V_1, V_2

The inverse expression of (8.2)

$$\begin{bmatrix} V_1 \\ V_2 \end{bmatrix} = \frac{1}{\Delta_Y^{34}} \begin{bmatrix} Y_{24} & -Y_{23} \\ -Y_{14} & Y_{13} \end{bmatrix} \cdot \begin{bmatrix} I_3^{SC,SC} - I_3 \\ I_4^{SC,SC} - I_4 \end{bmatrix}, \tag{8.4}$$

where determinant $\Delta_Y^{34} = Y_{13}Y_{24} - Y_{23}Y_{14}$.

Therefore, we get

$$I_4 - I_4^{SC,SC} = \frac{Y_{24}}{Y_{23}}(I_3 - I_3^{SC,SC}) + \frac{\Delta_Y^{34}}{Y_{23}} V_1, \tag{8.5}$$

$$I_4 - I_4^{SC,SC} = \frac{Y_{14}}{Y_{13}}(I_3 - I_3^{SC,SC}) - \frac{\Delta_Y^{34}}{Y_{13}} V_2. \tag{8.6}$$

Equation (8.5) determines a family of parallel load straight lines with a parameter V_1. Similarly, Eq. (8.6) determines a family of parallel load straight lines with parameter V_2. These load straight lines are shown in Fig. 8.2 for characteristic regimes (as the short circuit $V_1^S C = 0, V_2^S C = 0$ and open circuit V_1^{OC}, V_2^{OC}) and a running regime V_1^1, V_2^1.

We consider that the load currents define the rectangular Cartesian system of coordinates $(I_3 0_I I_4)$. Then, the load voltages correspond to the system of affine coordinates $(V_1 0_V V_2)$.

The equation of the axis V_1 is defined by the expression (8.6) as $V_2 = 0$

$$I_4 - I_4^{SC,SC} = \frac{Y_{14}}{Y_{13}}(I_3 - I_3^{SC,SC}). \tag{8.7}$$

This straight line passes through the point (SC, SC) or the point 0_V. The value Y_{14}/Y_{13} corresponds to a slope angle. The currents $I_3^{SC,SC}, I_4^{SC,SC}$ determine the point (SC, SC).

Similarly, the equation of the axis V_2 is defined by the expression (8.5) as $V_1 = 0$

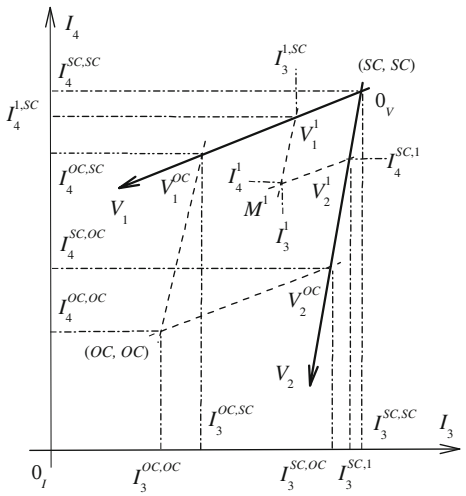

Fig. 8.2 Systems of Cartesian coordinates $(I_3 0_I I_4)$ and affine coordinates $(V_1 0_V V_2)$

$$I_4 - I_4^{SC,SC} = \frac{Y_{24}}{Y_{23}}(I_3 - I_3^{SC,SC}). \tag{8.8}$$

The open circuit regime of both loads corresponds to the point (OC, OC) or to point 0_I. Let us determine the voltages V_1^{OC}, V_2^{OC}. From (8.1), we get

$$\begin{bmatrix} I_1 \\ I_2 \end{bmatrix} = \begin{bmatrix} -Y_{11} & Y_{12} \\ Y_{12} & -Y_{22} \end{bmatrix} \cdot \begin{bmatrix} V_1 \\ V_2 \end{bmatrix} + \begin{bmatrix} I_1^{SC,SC} \\ I_2^{SC,SC} \end{bmatrix}, \tag{8.9}$$

where SC currents of both loads

$$\begin{bmatrix} I_1^{SC,SC} \\ I_2^{SC,SC} \end{bmatrix} = \begin{bmatrix} Y_{13} & Y_{14} \\ Y_{23} & Y_{24} \end{bmatrix} \cdot \begin{bmatrix} V_3 \\ V_4 \end{bmatrix}. \tag{8.10}$$

The inverse expression of (8.9)

$$\begin{bmatrix} V_1 \\ V_2 \end{bmatrix} = \frac{1}{\Delta_Y^{12}} \begin{bmatrix} Y_{22} & Y_{12} \\ Y_{12} & Y_{11} \end{bmatrix} \cdot \begin{bmatrix} I_1^{SC,SC} - I_1 \\ I_2^{SC,SC} - I_2 \end{bmatrix}, \tag{8.11}$$

where determinant $\Delta_Y^{12} = Y_{11}Y_{22} - (Y_{12})^2$.

Using (8.11), we get, similarly to (6.7) and (6.8), that

$$V_1^{OC} = \frac{Y_{22}}{\Delta_Y^{12}} I_1^{SC,SC} + \frac{Y_{12}}{\Delta_Y^{12}} I_2^{SC,SC}, \tag{8.12}$$

$$V_2^{OC} = \frac{Y_{12}}{\Delta_Y^{12}} I_1^{SC,SC} + \frac{Y_{11}}{\Delta_Y^{12}} I_2^{SC,SC}. \tag{8.13}$$

We determine now the currents $I_3^{OC,OC}, I_4^{OC,OC}$ by (8.2)

$$I_3^{\mathrm{OC,OC}} = -Y_{13} V_1^{OC} - Y_{23} V_2^{OC} + I_3^{\mathrm{SC,SC}}, \tag{8.14}$$

$$I_4^{OC,OC} = -Y_{14} V_1^{OC} - Y_{24} V_2^{OC} + I_4^{SC,SC}. \tag{8.15}$$

We must map the point (OC, OC) onto the axes V_1, V_2 by parallel lines to these axes. Then, the coordinates or components $I_3^{OC,SC}, I_4^{OC,SC}$ will correspond to the point V_1^{OC} on the axis V_1. Using (8.12) and (8.2) as $V_2 = 0$, we get

$$I_3^{OC,SC} = -Y_{13} V_1^{OC} + I_3^{SC,SC}, \tag{8.16}$$

$$I_4^{OC,SC} = -Y_{14} V_1^{OC} + I_4^{SC,SC}. \tag{8.17}$$

In turn, the coordinates $I_3^{SC,OC}, I_4^{SC,OC}$ correspond to the point V_2^{OC} on the axis V_2. Using (8.13) and (8.2) as $V_1 = 0$, we obtain

$$I_3^{SC,OC} = -Y_{23} V_2^{OC} + I_3^{\mathrm{SC,SC}}, \tag{8.18}$$

$$I_4^{SC,OC} = -Y_{24} V_2^{OC} + I_4^{\mathrm{SC,SC}}. \tag{8.19}$$

Let an initial regime be given by values V_1^1, V_2^1 or by a point M^1. Then, the coordinates $I_3^{1,SC}, I_4^{1,SC}$ define the point V_1^1 on the axis V_1. Using (8.2) as $V_2 = 0$, we have

$$I_3^{1,SC} = -Y_{13} V_1^1 + I_3^{\mathrm{SC,SC}}, \tag{8.20}$$

$$I_4^{1,SC} = -Y_{14} V_1^1 + I_4^{\mathrm{SC,SC}}. \tag{8.21}$$

In turn, the coordinates $I_3^{SC,1}, I_4^{SC,1}$ define the point V_2^1 on the axis V_2. Using (8.2) as $V_1 = 0$, we have

$$I_1^{SC,1} = -Y_{23} V_2^1 + I_3^{\mathrm{SC,SC}}, \tag{8.22}$$

$$I_4^{SC,1} = -Y_{24} V_2^1 + I_4^{\mathrm{SC,SC}}. \tag{8.23}$$

Let us introduce normalized coordinates for the point M^1. The point (OC, OC) is a length scale for the system of coordinates $V_1 0_V V_2$.

Then, similarly to (6.17)–(6.20), the normalized coordinates have the view

$$n_1^1 = \frac{V_1^1 - 0_V}{V_1^{OC} - 0_V} = \frac{V_1^1}{V_1^{OC}} = \frac{I_3^{1,SC} - I_3^{SC,SC}}{I_3^{OC,SC} - I_3^{SC,SC}}, \tag{8.24}$$

$$n_2^1 = \frac{V_2^1}{V_2^{OC}} = \frac{I_4^{SC,1} - I_4^{SC,SC}}{I_4^{SC,OC} - I_4^{SC,SC}}. \tag{8.25}$$

These normalized coordinates, as an affine ratio, are the invariants of affine transformation (8.2).

Similarly to (2.7), we get the other affine ratios in the form

$$N_1^1 = \frac{V_1^1}{V_1^{OC} - V_1^1} = \frac{I_3^{1,SC} - I_3^{SC,SC}}{I_3^{OC,SC} - I_3^{1,SC}}, \tag{8.26}$$

$$N_2^1 = \frac{V_2^1}{V_2^{OC} - V_2^1} = \frac{I_4^{SC,1} - I_4^{SC,SC}}{I_4^{SC,OC} - I_4^{SC,1}}. \tag{8.27}$$

The presented approach will be used for transmission of two measuring signals.

Example 1 We consider the following four-port circuit with given parameters in Fig. 8.3.

System of Eq. (8.1)

$$\begin{bmatrix} I_1 \\ I_2 \\ I_3 \\ I_4 \end{bmatrix} = \begin{bmatrix} -0.6813 & 0.1393 & 0.147 & 0.0464 \\ 0.1393 & -0.7727 & 0.087 & 0.159 \\ -0.147 & -0.087 & 0.3247 & -0.029 \\ -0.0464 & -0.159 & -0.029 & 0.2803 \end{bmatrix} \cdot \begin{bmatrix} V_1 \\ V_2 \\ V_3 \\ V_4 \end{bmatrix}.$$

Currents (8.3)

$$\begin{bmatrix} I_3^{SC,SC} \\ I_4^{SC,SC} \end{bmatrix} = \begin{bmatrix} 0.3247 & -0.029 \\ -0.029 & 0.2803 \end{bmatrix} \cdot \begin{bmatrix} 12 \\ 10 \end{bmatrix} = \begin{bmatrix} 3.6064 \\ 2.455 \end{bmatrix}.$$

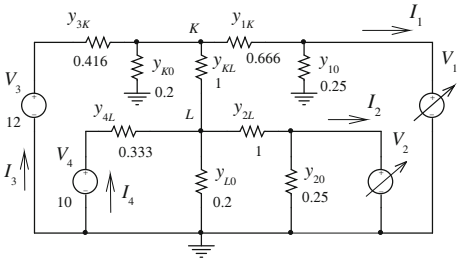

Fig. 8.3 Four-port represents two two-port networks connected by conductivity y_{KL}

System of Eq. (8.2)

$$\begin{bmatrix} I_3 \\ I_4 \end{bmatrix} = \begin{bmatrix} -0.147 & -0.087 \\ -0.0464 & -0.159 \end{bmatrix} \cdot \begin{bmatrix} V_1 \\ V_2 \end{bmatrix} + \begin{bmatrix} 3.6064 \\ 2.455 \end{bmatrix}.$$

The inverse expression

$$\begin{bmatrix} V_1 \\ V_2 \end{bmatrix} = \frac{1}{\Delta_Y^{34}} \begin{bmatrix} 0.159 & -0.087 \\ -0.0464 & 0.147 \end{bmatrix} \cdot \begin{bmatrix} 3.6064 - I_3 \\ 2.455 - I_4 \end{bmatrix},$$
$$\Delta_Y^{34} = 0.147 \cdot 0.159 - 0.087 \cdot 0.0464 = 0.01934.$$

Equation (8.7) of the axis V_1

$$I_4 - 2.455 = 0.3156 \cdot (I_3 - 3.6064).$$

Equation (8.8) of the axis V_2

$$I_4 - 2.455 = 1.8275 \cdot (I_3 - 3.6064).$$

The obtained system of coordinates is shown in Fig. 8.4.
SC currents (8.10) of both loads

$$\begin{bmatrix} I_1^{\mathrm{SC,SC}} \\ I_2^{\mathrm{SC,SC}} \end{bmatrix} = \begin{bmatrix} 0.147 & 0.0464 \\ 0.087 & 0.159 \end{bmatrix} \cdot \begin{bmatrix} 12 \\ 10 \end{bmatrix} = \begin{bmatrix} 2.228 \\ 2.634 \end{bmatrix}.$$

The voltages V_1^{OC}, V_2^{OC} by (8.12) and (8.13)

$$V_1^{OC} = \frac{0.7727}{0.507} 2.228 + \frac{0.1393}{0.507} 2.634 = 4.119,$$
$$V_2^{OC} = \frac{0.1393}{0.507} 2.228 + \frac{0.6813}{0.507} 2.634 = 4.1514;$$
$$\Delta_Y^{12} = 0.6813 \cdot 0.7727 - 0.1393^2 = 0.507.$$

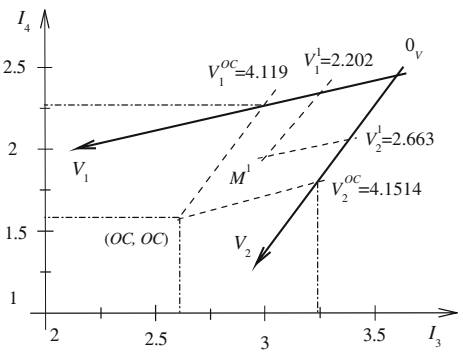

Fig. 8.4 Example of the Cartesian coordinates $(I_3 0_I I_4)$ and affine coordinates $(V_1 0_V V_2)$

The currents $I_3^{\mathrm{OC,OC}}, I_4^{\mathrm{OC,OC}}$ by (8.14) and (8.15)

$$I_3^{\mathrm{OC,OC}} = -0.147 \cdot 4.119 - 0.087 \cdot 4.1514 + 3.6064 = 2.6397,$$
$$I_4^{\mathrm{OC,OC}} = -0.0464 \cdot 4.119 - 0.159 \cdot 4.1514 + 2.455 = 1.6038.$$

The components $I_3^{OC,SC}, I_4^{OC,SC}$ by (8.16) and (8.17)

$$I_3^{OC,SC} = -0.147 \cdot 4.119 + 3.6064 = 3.0,$$
$$I_4^{OC,SC} = -0.0464 \cdot 4.119 + 2.455 = 2.263.$$

The components $I_3^{SC,OC}, I_4^{SC,OC}$ by (8.18) and (8.19)

$$I_3^{SC,OC} = -0.087 \cdot 4.1514 + 3.6064 = 3.2452$$
$$I_4^{SC,OC} = -0.159 \cdot 4.1514 + 2.455 = 1.795.$$

Let the initial regime, the point M^1, be given by voltages

$$V_1^1 = 2.202, \quad V_2^1 = 2.663.$$

Currents (8.2)

$$\begin{bmatrix} I_3^1 \\ I_4^1 \end{bmatrix} = \begin{bmatrix} -0.147 & -0.087 \\ -0.0464 & -0.159 \end{bmatrix} \cdot \begin{bmatrix} 2.202 \\ 2.663 \end{bmatrix} + \begin{bmatrix} 3.6064 \\ 2.455 \end{bmatrix} = \begin{bmatrix} 3.051 \\ 1.93 \end{bmatrix}.$$

The coordinates $I_3^{1,SC}, I_4^{1,SC}$ by (8.20) and (8.21)

$$I_3^{1,SC} = -0.147 \cdot 2.202 + 3.6064 = 3.2827,$$
$$I_4^{1,SC} = -0.0464 \cdot 2.202 + 2.455 = 2.3528.$$

The coordinates $I_3^{SC,1}, I_4^{SC,1}$ by (8.22) and (8.23)

$$I_1^{SC,1} = -0.087 \cdot 2.663 + 3.6064 = 3.3747,$$
$$I_4^{SC,1} = -0.159 \cdot 2.663 + 2.455 = 2.032.$$

Normalized coordinates (8.24) and (8.25)

$$n_1^1 = \frac{2.202}{4.119} = \frac{3.2827 - 3.6064}{3.0 - 3.6064} = 0.5346,$$
$$n_2^1 = \frac{2.663}{4.1514} = \frac{2.032 - 2.455}{1.795 - 2.455} = 0.6415.$$

Affine ratios (8.26) and (8.27)

$$N_1^1 = \frac{2.202}{4.119 - 2.202} = \frac{3.2827 - 3.6064}{3.0 - 3.2827} = 1.1446,$$
$$N_2^1 = \frac{2.663}{4.1514 - 2.663} = \frac{2.032 - 2.455}{1.795 - 2.032} = 1.789.$$

8.2 Input-Output Conformity of Four-Ports as a Projective Transformation

Now, we consider a four-port circuit in Fig. 8.5. Let us give necessary relationships between input currents and load conductivities [1]. This network is described by system of Eqs. (8.1). Also, we have that

$$V_1 = I_1/Y_{L1}, \quad V_2 = I_2/Y_{L2}.$$

8.2.1 Output of a Four-Port

The above circuit concerning loads represents an active two-port network. Therefore, we use the results of Sect. 6.1.3. As it was shown in Fig. 6.9, the family of straight lines $(I_1, I_2, Y_{L1}) = 0, (I_1, I_2, Y_{L2}) = 0$ at change of Y_{L1}, Y_{L2} is represented by two bunches of straight lines in the system of coordinates $(I_1 0 I_2)$. For convenience, we show this family in Fig. 8.6.

Next, we use the idea of projective coordinates of a running regime point. Let the initial or running regime corresponds to the point M^1, which is set by the values of the conductivities Y_{L1}^1, Y_{L2}^1 and currents I_1^1, I_2^1.

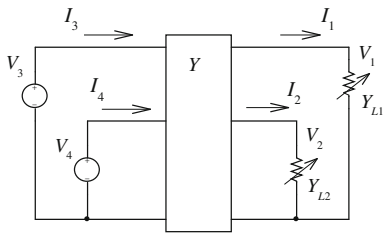

Fig. 8.5 Four-port with changeable load conductivities Y_{L1}, Y_{L2}

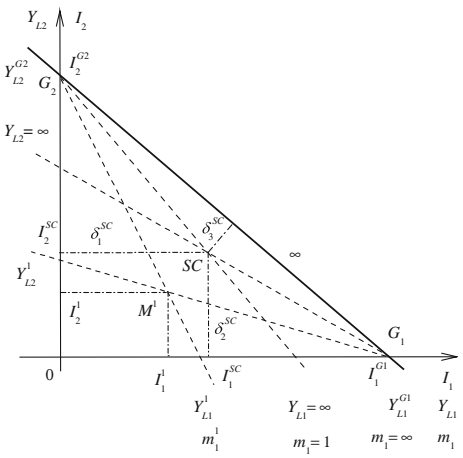

Fig. 8.6 Two bunches of load straight lines with the parameters Y_{L1}, Y_{L2}

In addition, this point is defined by projective non-uniform coordinates m_1^1, m_2^1 and homogeneous coordinates $\xi_1^1, \xi_2^1, \xi_3^1$ which are set by the reference triangle $G_1 0 G_2$ and a unit point SC.

We rewrite requirement relationships. Non-uniform projective coordinate (6.28) and (6.29)

$$m_1^1 = \frac{Y_{L1}^1}{Y_{L1}^1 - Y_{L1}^{G1}}, \quad m_2^1 = \frac{Y_{L2}^1}{Y_{L2}^1 - Y_{L2}^{G2}}. \tag{8.28}$$

In turn, homogeneous projective coordinates ξ_1, ξ_2, ξ_3 set the non-uniform coordinates by (6.30)

$$m_1 = \frac{\rho\xi_1}{\rho\xi_3}, \quad m_2 = \frac{\rho\xi_2}{\rho\xi_3}, \tag{8.29}$$

where ρ is a proportionality factor. Homogeneous coordinates (6.36) are defined by load currents

$$\begin{bmatrix} \rho\xi_1 \\ \rho\xi_2 \\ \rho\xi_3 \end{bmatrix} = \begin{bmatrix} \frac{1}{I_1^{SC}} & 0 & 0 \\ 0 & \frac{1}{I_2^{SC}} & 0 \\ \frac{1}{I_1^{G1}\mu_3\delta_3^{SC}} & \frac{1}{I_2^{G2}\mu_3\delta_3^{SC}} & \frac{-1}{\mu_3\delta_3^{SC}} \end{bmatrix} \cdot \begin{bmatrix} I_1 \\ I_2 \\ 1 \end{bmatrix} = [\mathbf{C}] \cdot \begin{bmatrix} I_1 \\ I_2 \\ 1 \end{bmatrix}, \tag{8.30}$$

where $\mu_3\delta_3^{SC} = \left(\frac{I_1^{SC}}{I_1^{G1}} + \frac{I_2^{SC}}{I_2^{G2}} - 1\right)$.

From here, the non-uniform coordinates assume the convenient form

$$m_1 = \frac{\frac{1}{I_1^{SC}} I_1}{\frac{I_1}{I_1^{G1}\mu_3\delta_3^{SC}} + \frac{I_2}{I_2^{G2}\mu_3\delta_3^{SC}} - \frac{1}{\mu_3\delta_3^{SC}}},$$
$$m_2 = \frac{\frac{1}{I_2^{SC}} I_2}{\frac{I_1}{I_1^{G1}\mu_3\delta_3^{SC}} + \frac{I_2}{I_2^{G2}\mu_3\delta_3^{SC}} - \frac{1}{\mu_3\delta_3^{SC}}}. \tag{8.31}$$

The inverse transformation of (8.30)

$$\begin{bmatrix} \rho I_1 \\ \rho I_2 \\ \\ \rho 1 \end{bmatrix} = \begin{bmatrix} I_1^{SC} & 0 & 0 \\ 0 & I_2^{SC} & 0 \\ \frac{I_1^{SC}}{I_1^{G1}} & \frac{I_2^{SC}}{I_2^{G2}} & -\mu_3\delta_3^{SC} \end{bmatrix} \cdot \begin{bmatrix} \xi_1 \\ \xi_2 \\ \\ \xi_3 \end{bmatrix} = [\mathbf{C}]^{-1} \cdot \begin{bmatrix} \xi_1 \\ \xi_2 \\ \xi_3 \end{bmatrix}, \tag{8.32}$$

Therefore, the currents

$$I_1 = \frac{\rho I_1}{\rho 1} = \frac{I_1^{SC} m_1}{\frac{I_1^{SC}}{I_1^{G1}} m_1 + \frac{I_2^{SC}}{I_2^{G2}} m_2 - \mu_3\delta_3^{SC}},$$
$$I_2 = \frac{I_2^{SC} m_2}{\frac{I_1^{SC}}{I_1^{G1}} m_1 + \frac{I_2^{SC}}{I_2^{G2}} m_2 - \mu_3\delta_3^{SC}}. \tag{8.33}$$

8.2.2 Input of a Four-Port

Let us consider the input currents (I_3, I_4) of our four-port. We may superpose the system of coordinates $(I_3\,0\,I_4)$ with the system of coordinates $(I_1\,0\,I_2)$ in Fig. 8.7.

Then, any point with coordinates (I_1, I_2) corresponds to a point with coordinates (I_3, I_4). In terms of geometry, a projective transformation takes place which transfers points of the plane (I_1, I_2) into points of the plane (I_3, I_4). Therefore, the reference triangle $G_1 0\, G_2$, point SC, and running regime point M^1 correspond to the triangle $\overline{G}_1 \overline{0}\, \overline{G}_2$, point $\overline{SC}$, and point $\overline{M}^1$, as it is shown by arrows in Fig. 8.7.

Next, the axes of currents I_1, I_2 correspond to the axes $\overline{I}_1, \overline{I}_2$. Also, two bunches of the straight lines $(I_1, I_2, Y_{L1}) = 0$, $(I_1, I_2, Y_{L2}) = 0$ correspond to two bunches of the lines $(I_3, I_4, Y_{L1}) = 0$, $(I_3, I_4, Y_{L2}) = 0$ with centers in the points $\overline{G}_2$, $\overline{G}_1$. Thus, the point $\overline{M}^1$ is set by other currents I_3^1, I_4^1. Also, this point is defined by projective non-uniform and homogeneous coordinates which are set by the reference triangle $\overline{G}_1 \overline{0}\, \overline{G}_2$ and a unit point $\overline{SC}$.

The property of projective transformations shows that the point $\overline{M}^1$ coordinates are equal to the point M^1 coordinates, as these points M^1, $\overline{M}^1$ are set by the same

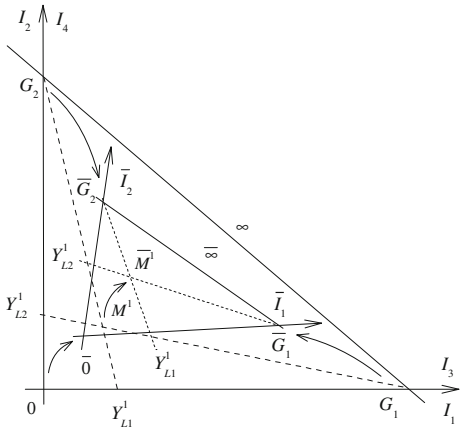

Fig. 8.7 Projective transformation of the plane (I_1, I_2) onto plane (I_3, I_4)

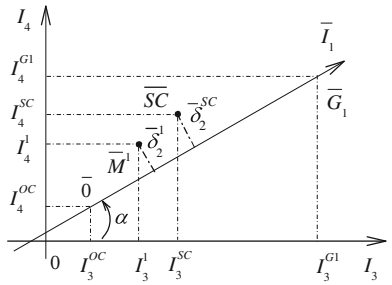

Fig. 8.8 Distances of points $\overline{M}^1$, $\overline{SC}$ to the axis $\overline{I}_1$

loads Y^1_{L1}, Y^1_{L2}. Therefore, this property gives required invariant relations between input and output currents.

For finding of the point $\overline{M}^1$ projective coordinates, it is necessary to obtain equations of sides of reference triangle. The normalized equation of the side $\overline{0}\,\overline{G}_1$ or axis $\overline{I}_1$ in Fig. 8.8 looks like

$$\frac{I_4}{I_4^{OC} - \overline{k}_1 I_3^{OC}} - \frac{\overline{k}_1 I_3}{I_4^{OC} - \overline{k}_1 I_3^{OC}} - 1 = 0, \quad \overline{k}_1 = tg\alpha_1 = \frac{I_4^{G1} - I_4^{OC}}{I_3^{G1} - I_3^{OC}},$$

where $\overline{k}_1$ is an angular coefficient or slope ratio.

Then, the point $\overline{M}^1$ distance $\overline{\delta}_2^1$ to the axis $\overline{I}_1$ is defined by expression

$$\overline{\mu}_2 \overline{\delta}_2^1 = \frac{I_4^1}{I_4^{OC} - \overline{k}_1 I_3^{OC}} - \frac{\overline{k}_1 I_3^1}{I_4^{OC} - \overline{k}_1 I_3^{OC}} - 1,$$

$$\overline{\mu}_2 = \sqrt{\left(\frac{1}{I_4^{OC} - \overline{k}_1 I_3^{OC}}\right)^2 + \left(\frac{\overline{k}_1}{I_4^{OC} - \overline{k}_1 I_3^{OC}}\right)^2},$$

where $\overline{\mu}_2$ is a normalizing factor.

The point $\overline{SC}$ distance $\overline{\delta}_2^{SC}$ to the axis $\overline{I}_1$ is

$$\overline{\mu}_2\overline{\delta}_2^{SC} = \frac{I_4^{SC}}{I_4^{OC} - \overline{k}_1 I_3^{OC}} - \frac{\overline{k}_1 I_3^{SC}}{I_4^{OC} - \overline{k}_1 I_3^{OC}} - 1.$$

Similarly, the axis $\overline{I}_2$ equation is

$$\frac{I_4}{\overline{k}_2 I_3^{OC} - I_4^{OC}} - \frac{\overline{k}_2 I_3}{\overline{k}_2 I_3^{OC} - I_4^{OC}} + 1 = 0,$$
$$\overline{k}_2 = tg\alpha_2 = \frac{I_4^{G2} - I_4^{OC}}{I_3^{G2} - I_3^{OC}}.$$

Then, the point $\overline{M}^1$ distance $\overline{\delta}_1^1$ to the axis $\overline{I}_2$ is

$$\overline{\mu}_1\overline{\delta}_1^1 = \frac{I_4^1}{\overline{k}_2 I_3^{OC} - I_4^{OC}} - \frac{\overline{k}_2 I_3^1}{\overline{k}_2 I_3^{OC} - I_4^{OC}} + 1,$$
$$\overline{\mu}_1 = \sqrt{\left(\frac{1}{\overline{k}_2 I_3^{OC} - I_4^{OC}}\right)^2 + \left(\frac{\overline{k}_2}{\overline{k}_2 I_3^{OC} - I_4^{OC}}\right)^2}.$$

The point $\overline{SC}$ distance $\overline{\delta}_1^{SC}$ to the axis $\overline{I}_2$ is

$$\overline{\mu}_1\overline{\delta}_1^{SC} = \frac{I_4^{SC}}{\overline{k}_2 I_3^{OC} - I_4^{OC}} - \frac{\overline{k}_2 I_3^{SC}}{\overline{k}_2 I_3^{OC} - I_4^{OC}} + 1.$$

Similarly, the infinitely remote straight line $\overline{\infty}$ equation is

$$\frac{I_4}{I_4^{G1} + \overline{k}_\infty I_3^{G1}} + \frac{\overline{k}_\infty I_3}{I_4^{G1} + \overline{k}_\infty I_3^{G1}} - 1 = 0,$$
$$\overline{k}_\infty = \frac{I_4^{G2} - I_4^{G1}}{I_3^{G1} - I_3^{G2}}.$$

The point $\overline{M}^1$ distance $\overline{\delta}_3^1$ to the line $\overline{\infty}$ is

$$\overline{\mu}_3\overline{\delta}_3^1 = \frac{I_4^1}{I_4^{G1} + \overline{k}_\infty I_3^{G1}} + \frac{\overline{k}_\infty I_3^1}{I_4^{G1} + \overline{k}_\infty I_3^{G1}} - 1,$$
$$\overline{\mu}_3 = \sqrt{\left(\frac{1}{I_4^{G1} + \overline{k}_\infty I_3^{G1}}\right)^2 + \left(\frac{\overline{k}_\infty}{I_4^{G1} + \overline{k}_\infty I_3^{G1}}\right)^2}.$$

The point $\overline{SC}$ distance $\overline{\delta}_3^{SC}$ to the line $\overline{\infty}$ is

$$\overline{\mu}_3\overline{\delta}_3^{SC} = \frac{I_4^{SC}}{I_4^{G1}+\overline{k}_\infty I_3^{G1}} + \frac{\overline{k}_\infty I_3^{SC}}{I_4^{G1}+\overline{k}_\infty I_3^{G1}} - 1.$$

The homogeneous projective coordinates are

$$\begin{aligned}
\rho\xi_1^1 &= \frac{\overline{\delta}_1^1}{\overline{\delta}_1^{SC}} = -\frac{\overline{k}_2}{(\overline{k}_2 I_3^{OC} - I_4^{OC})\overline{\mu}_1\overline{\delta}_1^{SC}} I_3^1 \\
&\quad + \frac{1}{(\overline{k}_2 I_3^{OC} - I_4^{OC})\overline{\mu}_1\overline{\delta}_1^{SC}} I_4^1 + \frac{1}{\overline{\mu}_1\overline{\delta}_1^{SC}}, \\
\rho\xi_2^1 &= \frac{\overline{\delta}_2^1}{\overline{\delta}_2^{SC}} = -\frac{\overline{k}_1}{(I_4^{OC} - \overline{k}_1 I_3^{OC})\overline{\mu}_2\overline{\delta}_2^{SC}} I_3^1 \\
&\quad + \frac{1}{(I_4^{OC} - \overline{k}_1 I_3^{OC})\overline{\mu}_2\overline{\delta}_2^{SC}} I_4^1 - \frac{1}{\overline{\mu}_2\overline{\delta}_2^{SC}}, \\
\rho\xi_3^1 &= \frac{\overline{\delta}_3^1}{\overline{\delta}_3^{SC}} = \frac{\overline{k}_\infty}{(I_4^{G1}+\overline{k}_\infty I_3^{G1})\overline{\mu}_3\overline{\delta}_3^{SC}} I_3^1 \\
&\quad + \frac{1}{(I_4^{G1}+\overline{k}_\infty I_3^{G1})\overline{\mu}_3\overline{\delta}_3^{SC}} I_4^1 - \frac{1}{\overline{\mu}_3\overline{\delta}_3^{SC}}.
\end{aligned}$$

The matrix form of these expressions

$$\begin{bmatrix} \rho\xi_1 \\ \\ \rho\xi_2 \\ \\ \rho\xi_3 \end{bmatrix} = [\overline{\mathbf{C}}] \cdot \begin{bmatrix} I_3 \\ \\ I_4 \\ \\ 1 \end{bmatrix} = \begin{bmatrix} -\overline{C}_{11} & \frac{\overline{C}_{11}}{\overline{k}_2} & \frac{1}{\overline{\mu}_1\overline{\delta}_1^{SC}} \\ -\overline{C}_{21} & \frac{\overline{C}_{21}}{\overline{k}_1} & -\frac{1}{\overline{\mu}_2\overline{\delta}_2^{SC}} \\ \overline{C}_{31} & \frac{\overline{C}_{31}}{\overline{k}_\infty} & -\frac{1}{\overline{\mu}_3\overline{\delta}_3^{SC}} \end{bmatrix} \cdot \begin{bmatrix} I_3 \\ \\ I_4 \\ \\ 1 \end{bmatrix}. \tag{8.34}$$

The constituents of this matrix

$$\overline{C}_{11} = \frac{\overline{k}_2}{(\overline{k}_2 I_3^{OC} - I_4^{OC})\overline{\mu}_1\overline{\delta}_1^{SC}}, \quad \overline{C}_{21} = \frac{\overline{k}_1}{(I_4^{OC} - \overline{k}_1 I_3^{OC})\overline{\mu}_2\overline{\delta}_2^{SC}}$$
$$\overline{C}_{31} = \frac{\overline{k}_\infty}{(I_4^{G1}+\overline{k}_\infty I_3^{G1})\overline{\mu}_3\overline{\delta}_3^{SC}}.$$

From here, the non-uniform coordinates have the form similar to (8.31)

$$
\begin{aligned}
m_1 &= \frac{-\overline{C}_{11} I_3 + \frac{\overline{C}_{11}}{\overline{k}_2} I_4 + \frac{1}{\overline{\mu}_1 \overline{\delta}_1^{SC}}}{\overline{C}_{31} I_3 + \frac{\overline{C}_{31}}{\overline{k}_\infty} I_4 - \frac{1}{\overline{\mu}_3 \overline{\delta}_3^{SC}}}, \\
m_2 &= \frac{-\overline{C}_{21} I_3 + \frac{\overline{C}_{21}}{\overline{k}_1} I_4 - \frac{1}{\overline{\mu}_2 \overline{\delta}_2^{SC}}}{\overline{C}_{31} I_3 + \frac{\overline{C}_{31}}{\overline{k}_\infty} I_4 - \frac{1}{\overline{\mu}_3 \overline{\delta}_3^{SC}}}.
\end{aligned}
\tag{8.35}
$$

The obtained expressions have the general appearance in comparison with (8.31) because of the non-orthogonal coordinates $\overline{I}_1 \overline{0} \overline{I}_2$.

In practice, characteristic values of input current, output currents (as vertexes of coordinate triangles), and loads are precalculated or preprogrammed by the calculation or testing of four-port network.

Further, using running values of input currents, we find or, more precisely, restore values of non-uniform coordinates (8.35) and values of given load conductivities according to the expressions $Y_{L1}(m_1), Y_{L2}(m_2)$. These expressions are inverse to expression (8.28).

Such a formulated algorithm represents a practical interest for transfer of two sensing signals via an unstable four-port network or a three-wire line; it is analogous to a signal transmission via a two-port network of Chap. 4.

The inverse transformation of (8.34)

$$
\begin{bmatrix} \rho I_3 \\ \rho I_4 \\ \rho 1 \end{bmatrix} = [\overline{\mathbf{C}}]^{-1} \cdot \begin{bmatrix} \xi_1 \\ \xi_2 \\ \xi_\infty \end{bmatrix} = \begin{bmatrix} \overline{C}_{11}^{-1} & \overline{C}_{12}^{-1} & \overline{C}_{13}^{-1} \\ \overline{C}_{11}^{-1} \frac{I_4^{G1}}{I_3^{G1}} & \overline{C}_{12}^{-1} \frac{I_4^{G2}}{I_3^{G2}} & \overline{C}_{13}^{-1} \frac{I_4^{OC}}{I_3^{OC}} \\ \overline{C}_{11}^{-1} \frac{1}{I_3^{G1}} & \overline{C}_{12}^{-1} \frac{1}{I_3^{G2}} & \overline{C}_{13}^{-1} \frac{1}{I_3^{OC}} \end{bmatrix} \cdot \begin{bmatrix} \xi_1 \\ \xi_2 \\ \xi_3 \end{bmatrix}. \tag{8.36}
$$

The constituents of this matrix

$$
\begin{aligned}
\overline{C}_{11}^{-1} &= \frac{\overline{k}_2 I_3^{OC} - I_4^{OC}}{(\overline{k}_1 - \overline{k}_2)(I_3^{OC} - I_3^{G1})} I_3^{G1} \overline{\mu}_1 \overline{\delta}_1^{SC}, \\
\overline{C}_{12}^{-1} &= -\frac{\overline{k}_1 I_3^{OC} - I_4^{OC}}{(\overline{k}_1 - \overline{k}_2)(I_3^{OC} - I_3^{G2})} I_3^{G2} \overline{\mu}_2 \overline{\delta}_2^{SC}, \\
\overline{C}_{13}^{-1} &= \frac{\overline{k}_\infty I_3^{G1} + I_4^{G1}}{(\overline{k}_1 + \overline{k}_\infty)(I_3^{OC} - I_3^{G1})} I_3^{OC} \overline{\mu}_3 \overline{\delta}_3^{SC}.
\end{aligned}
$$

Similarly to (8.33), we may pass to the currents

$$\begin{aligned} I_3 &= \frac{\overline{C}_{11}^{-1} m_1 + \overline{C}_{12}^{-1} m_2 + \overline{C}_{13}^{-1}}{\overline{C}_{11}^{-1} \frac{1}{I_3^{G1}} m_1 + \overline{C}_{12}^{-1} \frac{1}{I_3^{G2}} m_2 + \overline{C}_{13}^{-1} \frac{1}{I_3^{OC}}}, \\ I_4 &= \frac{\overline{C}_{11}^{-1} \frac{I_4^{G1}}{I_3^{G1}} m_1 + \overline{C}_{12}^{-1} \frac{I_4^{G2}}{I_3^{G2}} m_2 + \overline{C}_{13}^{-1} \frac{I_4^{OC}}{I_3^{OC}}}{\overline{C}_{11}^{-1} \frac{1}{I_3^{G1}} m_1 + \overline{C}_{12}^{-1} \frac{1}{I_3^{G2}} m_2 + \overline{C}_{13}^{-1} \frac{1}{I_3^{OC}}}. \end{aligned} \tag{8.37}$$

The obtained expressions have the general view in comparison with (8.33) because of non-orthogonal coordinates.

Convenience of expressions (8.35) and (8.37) consists in their identical form; we replace load conductivities by their non-uniform projective coordinates and currents are already non-uniform coordinates too.

8.2.3 Recalculation of Currents at Load Changes

Let a subsequent regime be corresponded to a point M^2 with loads Y_{L1}^2, Y_{L2}^2, non-uniform coordinates m_1^2, m_2^2, output currents I_1^2, I_2^2, and input currents I_3^2, I_4^2.

At first, using the result of Sect. 7.1.1, we rewrite subsequent currents I_1^2, I_2^2 (7.2)

$$\begin{bmatrix} \rho I_1^2 \\ \rho I_2^2 \\ \rho 1 \end{bmatrix} = [\mathbf{J}^{21}] \cdot \begin{bmatrix} I_1^1 \\ I_2^1 \\ 1 \end{bmatrix} = [\mathbf{C}^{21}]^{-1} \cdot [\mathbf{C}] \cdot \begin{bmatrix} I_1^1 \\ I_2^1 \\ 1 \end{bmatrix}. \tag{8.38}$$

The matrix

$$[\mathbf{J}^{21}] = \begin{bmatrix} J_{11}^{21} & 0 & 0 \\ 0 & J_{22}^{21} & 0 \\ J_{31}^{21} & J_{32}^{21} & 1 \end{bmatrix} = \begin{bmatrix} m_1^{21} & 0 & 0 \\ 0 & m_2^{21} & 0 \\ \frac{m_1^{21}-1}{I_1^{G1}} & \frac{m_2^{21}-1}{I_2^{G2}} & 1 \end{bmatrix}.$$

In turn, the matrix

$$[\mathbf{C}^{21}]^{-1} = [\mathbf{C}]^{-1} \cdot [\mathbf{M}^{21}],$$

where

$$[\mathbf{M}^{21}] = \begin{bmatrix} m_1^{21} & 0 & 0 \\ 0 & m_2^{21} & 0 \\ 0 & 0 & 1 \end{bmatrix}.$$

Here, we use the regime changes

$$m_1^{21} = m_1^2 \div m_1^1, \quad m_2^{21} = m_2^2 \div m_2^1. \tag{8.39}$$

These changes of the non-uniform coordinates are also true for the input currents. Therefore, it is possible at once to obtain similar relationships for the recalculation of the input currents.

$$\begin{bmatrix} \rho I_3^2 \\ \rho I_4^2 \\ \rho 1 \end{bmatrix} = [\overline{\mathbf{C}}]^{-1} \cdot [\mathbf{M}^{21}] \cdot [\overline{\mathbf{C}}] \cdot \begin{bmatrix} I_3^1 \\ I_4^1 \\ 1 \end{bmatrix} = [\overline{\mathbf{J}}^{21}] \cdot \begin{bmatrix} I_3^1 \\ I_4^1 \\ 1 \end{bmatrix}. \tag{8.40}$$

We calculate the matrix $[\overline{\mathbf{J}}^{21}]$. This matrix has the general view in comparison with (8.38)

$$[\overline{\mathbf{J}}^{21}] = \begin{bmatrix} \overline{J}_{11}^{21} & \overline{J}_{12}^{21} & \overline{J}_{13}^{21} \\ \overline{J}_{21}^{21} & \overline{J}_{22}^{21} & \overline{J}_{23}^{21} \\ \overline{J}_{31}^{21} & \overline{J}_{32}^{21} & \overline{J}_{33}^{21} \end{bmatrix}. \tag{8.41}$$

Using transformations (8.38) and (8.40), we find the subsequent currents

$$\begin{aligned} I_1^2 &= \frac{\rho I_1^2}{\rho 1} = \frac{m_1^{21} I_1^1}{\frac{m_1^{21}-1}{I_1^{G1}} I_1^1 + \frac{m_2^{21}-1}{I_2^{G2}} I_2^1 + 1}, \\ I_2^2 &= \frac{\rho I_2^2}{\rho 1} = \frac{m_2^{21} I_2^1}{\frac{m_1^{21}-1}{I_1^{G1}} I_1^1 + \frac{m_2^{21}-1}{I_2^{G2}} I_2^1 + 1}. \end{aligned} \tag{8.42}$$

$$\begin{aligned} I_3^2 &= \frac{\rho I_3^2}{\rho 1} = \frac{\overline{J}_{11}^{21} I_3^1 + \overline{J}_{12}^{21} I_4^1 + \overline{J}_{13}^{21}}{\overline{J}_{31}^{21} I_3^1 + \overline{J}_{32}^{21} I_4^1 + \overline{J}_{33}^{21}}, \\ I_4^2 &= \frac{\rho I_4^2}{\rho 1} = \frac{\overline{J}_{21}^{21} I_3^1 + \overline{J}_{22}^{21} I_4^1 + \overline{J}_{23}^{21}}{\overline{J}_{31}^{21} I_3^1 + \overline{J}_{32}^{21} I_4^1 + \overline{J}_{33}^{21}}. \end{aligned} \tag{8.43}$$

We note that the denominators of expressions (8.42) and (8.43) are equal to each other.

8.2.4 *Two Cascaded Four-Port Networks*

Let us consider cascaded four-port networks in Fig. 8.9. The first four-port is given by a matrix Y^{3-6} of Y parameters and the second four-port corresponds to a matrix Y^{1-4}.

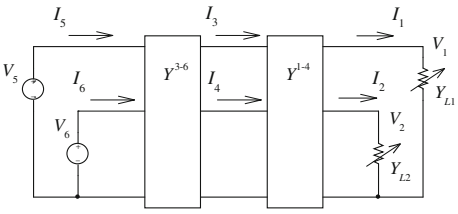

Fig. 8.9 Cascaded four-port networks

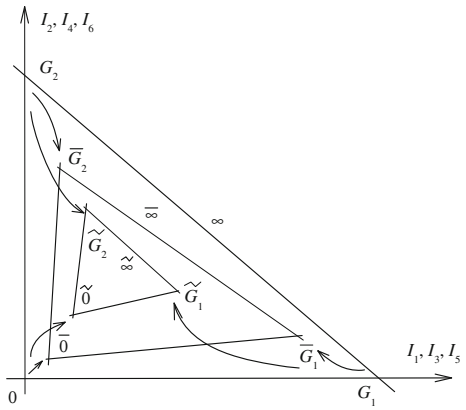

Fig. 8.10 Mapping of reference triangles

Similarly, we may superpose the system of coordinates $(I_5\,0\,I_6)$ with the systems of coordinates $(I_3\,0\,I_4)$, $(I_1\,0\,I_2)$ in Fig. 8.10.

Then, a projective transformation, which transfers points of the plane (I_1, I_2) into points of the plane (I_5, I_6), takes place. Therefore, the reference triangle $G_1 0 G_2$ corresponds to the triangle $\tilde{G}_1\tilde{0}\tilde{G}_2$. Also, a unit point SC, running regime point M^1 correspond to points $\tilde{\mathrm{S}}\tilde{\mathrm{C}}, \tilde{M}^1$. Moreover, two bunches of the straight lines $(I_1, I_2, Y_{L1}) = 0, (I_1, I_2, Y_{L2}) = 0$ correspond to two bunches of the lines $(I_5, I_6, Y_{L1}) = 0, (I_5, I_6, Y_{L2}) = 0$ with centers in the points $\tilde{G}_2, \tilde{G}_1$.

Also, the point $\tilde{M}^1$ is defined by projective non-uniform and homogeneous coordinates which are set by the reference triangle $\tilde{G}_1\tilde{0}\tilde{G}_2$ and a unit point $\tilde{\mathrm{S}}\tilde{\mathrm{C}}$. These projective coordinates of the point $\tilde{M}^1$ are equal to the projective coordinates of the points $M^1, \overline{M}^1$ according to the property of projective transformations. Thus, this property gives required invariant relationships between input and output currents of cascaded networks.

Projective coordinates of the point $\tilde{M}^1$ are obtained similarly to projective coordinates of the point $\overline{M}^1$. For this purpose, it is necessary to form equations of sides of the reference triangle $\tilde{G}_1\tilde{0}\tilde{G}_2$.

8.2.5 *Examples of Calculation*

Let the four-port be given in Fig. 8.11.

We use Example 1 and rewrite system of Eqs. (8.1)

$$[\mathbf{I}] = [\mathbf{Y}] \cdot [\mathbf{V}],$$

$$[\mathbf{Y}] = \begin{bmatrix} -0.6813 & 0.1393 & 0.147 & 0.0464 \\ 0.1393 & -0.7727 & 0.087 & 0.159 \\ -0.147 & -0.087 & 0.3247 & -0.029 \\ -0.0464 & -0.159 & -0.029 & 0.2803 \end{bmatrix}.$$

For the output of the four-port we have the next results

Short circuit currents (8.10)

$$I_1^{SC} = 2.228, \quad I_2^{SC} = 2.634.$$

System of Eq. (8.9)

$$\begin{bmatrix} I_1 \\ I_2 \end{bmatrix} = \begin{bmatrix} -Y_{11} & Y_{12} \\ Y_{12} & -Y_{22} \end{bmatrix} \cdot \begin{bmatrix} V_1 \\ V_2 \end{bmatrix} + \begin{bmatrix} I_1^{\mathrm{SC,SC}} \\ I_2^{\mathrm{SC,SC}} \end{bmatrix}$$

$$= \begin{bmatrix} -0.6813 & 0.1393 \\ 0.1393 & -0.7727 \end{bmatrix} \cdot \begin{bmatrix} V_1 \\ V_2 \end{bmatrix} + \begin{bmatrix} 2.228 \\ 2.634 \end{bmatrix}.$$

Parameters of bunch centers G_1, G_2 (6.26) and (6.24)

$$I_1^{G1} = \frac{Y_{11}}{Y_{12}} I_2^{\mathrm{SC,SS}} + I_1^{\mathrm{SC,SS}} = \frac{-0.6813}{0.1393} 2.634 + 2.228 = 15.11,$$

$$V_1^{G1} = -\frac{1}{Y_{12}} I_2^{\mathrm{SC,SS}} = -\frac{2.634}{0.1393} = -18.9, \quad Y_{L1}^{G1} = \frac{I_{L1}^{G1}}{V_{L1}^{G1}} = -0.8,$$

$$I_2^{G2} = \frac{Y_{22}}{Y_{12}} I_1^{\mathrm{SC,SS}} + I_2^{\mathrm{SC,SS}} = \frac{0.7727}{0.1393} 2.228 + 2.634 = 15,$$

$$V_2^{G2} = -\frac{1}{Y_{12}} I_1^{\mathrm{SC,SS}} = -\frac{2.228}{0.1393} = -16, \quad Y_{L2}^{G2} = \frac{I_{L2}^{G2}}{V_{L2}^{G2}} = -0.9375.$$

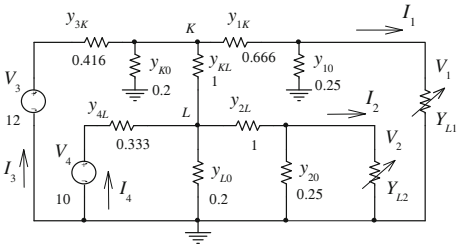

Fig. 8.11 Example of the four-port

Let the initial regime be given by

$$Y_{L1}^1 = 0.5, \quad I_1^1 = 1.101, \quad V_1^1 = 2.202;$$
$$Y_{L2}^1 = 0.333, \quad I_2^1 = 0.8868, \quad V_2^1 = 2.663.$$

Non-uniform projective coordinates (8.28)

$$m_1^1 = \frac{Y_{L1}^1}{Y_{L1}^1 - Y_{L1}^{G1}} = \frac{0.5}{0.5 + 0.8} = 0.3846,$$
$$m_2^1 = \frac{Y_{L2}^1}{Y_{L2}^1 - Y_{L2}^{G2}} = \frac{0.333}{0.333 + 0.9375} = 0.2622.$$

Matrix (8.30)

$$[\mathbf{C}] = \begin{bmatrix} \frac{1}{2.228} & 0 & 0 \\ 0 & \frac{1}{2.634} & 0 \\ \frac{-1}{15.11 \cdot 0.6769} & \frac{-1}{15 \cdot 0.6769} & \frac{1}{0.6769} \end{bmatrix},$$

For this matrix, the value

$$\mu_3 \delta_3^{SC} = \left(\frac{I_1^{SC}}{I_1^{G1}} + \frac{I_2^{SC}}{I_2^{G2}} - 1 \right) = \frac{2.228}{15.11} + \frac{2.634}{15} - 1 = -0.6769.$$

Homogeneous projective coordinates (8.30)

$$\rho\xi_1^1 = \frac{I_1^1}{I_1^{SC}} = \frac{1.101}{2.228} = 0.4942, \quad \rho\xi_2^1 = \frac{I_2^1}{I_2^{SC}} = \frac{0.8868}{2.634} = 0.3366,$$
$$\rho\xi_3^1 = \frac{-1.101}{15.11 \cdot 0.6769} + \frac{-0.8868}{15 \cdot 0.6769} + \frac{1}{0.6769}$$
$$= -0.1076 - 0.08734 + 1.4773 = 1.2823.$$

Let us check up the non-uniform projective coordinates

$$m_1^1 = \frac{\rho\xi_1}{\rho\xi_3} = \frac{0.4942}{1.2823} = 0.3846, \quad m_2^1 = \frac{\rho\xi_2}{\rho\xi_3} = \frac{0.3366}{1.2823} = 0.2622.$$

Inverse matrix (8.32)

$$[\mathbf{C}]^{-1} = \begin{bmatrix} 2.228 & 0 & 0 \\ 0 & 2.634 & 0 \\ 0.1474 & 0.1757 & 0.6769 \end{bmatrix}.$$

Currents (8.33)

$$I_1^1 = \frac{2.228 \cdot 0.3846}{0.1474 \cdot 0.3846 + 0.1757 \cdot 0.2622 + 0.6769} = \frac{0.86}{0.7797} = 1.101,$$
$$I_2^1 = \frac{2.634 \cdot 0.2622}{0.7797} = 0.8868.$$

For the input of the four-port we have the next results
The currents, corresponding to the short circuit,

$$I_3^{SC,SC} = 3.6064, \quad I_4^{SC,SC} = 2.455.$$

Using (8.2), we may find the bunch centers $\overline{G}_1, \overline{G}_2$. Then, we get the following systems of equations:

$$\begin{bmatrix} I_3^{G1} \\ I_4^{G1} \end{bmatrix} = \begin{bmatrix} -Y_{13} & -Y_{23} \\ -Y_{14} & -Y_{24} \end{bmatrix} \cdot \begin{bmatrix} V_1^{G1} \\ 0 \end{bmatrix} + \begin{bmatrix} I_3^{SC,SC} \\ I_4^{SC,SC} \end{bmatrix},$$
$$\begin{bmatrix} I_3^{G2} \\ I_4^{G2} \end{bmatrix} = \begin{bmatrix} -Y_{13} & -Y_{23} \\ -Y_{14} & -Y_{24} \end{bmatrix} \cdot \begin{bmatrix} 0 \\ V_2^{G2} \end{bmatrix} + \begin{bmatrix} I_3^{SC,SC} \\ I_4^{SC,SC} \end{bmatrix}.$$

Therefore,

$$I_3^{G1} = 0.147 \cdot 18.9 + 3.6064 = 6.4423,$$
$$I_4^{G1} = 0.0464 \cdot 18.9 + 2.455 = 3.333,$$
$$I_3^{G2} = 0.087 \cdot 16 + 3.6064 = 5,$$
$$I_4^{G2} = 0.159 \cdot 16 + 2.455 = 5.$$

The currents, corresponding to the open circuit,

$$I_3^{OC} = 2.6397, \quad I_4^{OC} = 1.6038.$$

The currents of the point $\overline{M}^1$ by (8.2)

$$I_3^1 = 3.051, \quad I_4^1 = 1.93.$$

The normalized equation of the axis $\overline{I}_1$

$$\overline{k}_1 = \frac{I_4^{G1} - I_4^{OC}}{I_3^{G1} - I_3^{OC}} = \frac{3.333 - 1.6038}{6.442 - 2.6397} = 0.4617,$$
$$\frac{I_4}{I_4^{OC} - \overline{k}_1 I_3^{OC}} - \frac{\overline{k}_1 I_3}{I_4^{OC} - \overline{k}_1 I_3^{OC}} - 1 = \frac{I_4}{0.3835} - \frac{I_3}{0.8305} - 1 = 0.$$

The point $\overline{M}^1$ distance to the axis $\overline{I}_1$

$$\overline{\mu}_2\overline{\delta}_2^1 = \frac{1.93}{0.3835} - \frac{3.051}{0.8305} - 1 = 0.3566,$$
$$\overline{\mu}_2 = \sqrt{\left(\frac{1}{0.3835}\right)^2 + \left(\frac{1}{0.8305}\right)^2} = 2.8721.$$

The point $\overline{SC}$ distance to the axis $\overline{I}_1$

$$\overline{\mu}_2\overline{\delta}_2^{SC} = \frac{2.455}{0.3835} - \frac{3.606}{0.8305} - 1 = 1.0576.$$

The normalized equation of the axis $\overline{I}_2$

$$\frac{I_4}{\overline{k}_2 I_3^{OC} - I_4^{OC}} - \frac{\overline{k}_2 I_3}{\overline{k}_2 I_3^{OC} - I_4^{OC}} + 1 = \frac{I_4}{2.1961} - \frac{I_3}{1.5258} + 1 = 0,$$
$$\overline{k}_2 = \frac{I_4^{G2} - I_4^{OC}}{I_3^{G2} - I_3^{OC}} = \frac{5 - 1.6038}{5 - 2.6397} = 1.4392.$$

The point $\overline{M}^1$ distance to the axis $\overline{I}_2$

$$\overline{\mu}_1\overline{\delta}_1^1 = \frac{1.93}{2.196} - \frac{3.051}{1.5258} + 1 = -0.1216,$$
$$\overline{\mu}_1 = \sqrt{\left(\frac{1}{2.1961}\right)^2 + \left(\frac{1}{1.5258}\right)^2} = 0.798.$$

The point $\overline{SC}$ distance to the axis $\overline{I}_2$

$$\overline{\mu}_1\overline{\delta}_1^{SC} = \frac{2.455}{2.1961} - \frac{3.606}{1.5258} + 1 = -0.2458.$$

The normalized equation of the infinitely remote line $\overline{\infty}$

$$\frac{I_4}{I_4^{G1} + \overline{k}_\infty I_3^{G1}} + \frac{\overline{k}_\infty I_3}{I_4^{G1} + \overline{k}_\infty I_3^{G1}} - 1 = \frac{I_4}{11} + \frac{I_3}{9.166} - 1 = 0,$$
$$\overline{k}_\infty = \frac{I_4^{G2} - I_4^{G1}}{I_3^{G1} - I_3^{G2}} = \frac{5 - 3.333}{6.442 - 5} = 1.2.$$

The point $\overline{M}^1$ distance to the line $\overline{\infty}$

$$\overline{\mu}_3\overline{\delta}_3^1 = \frac{1.93}{11} + \frac{3.051}{9.166} - 1 = -0.4918,$$
$$\overline{\mu}_3 = \sqrt{\left(\frac{1}{11}\right)^2 + \left(\frac{1}{9.166}\right)^2} = 0.142.$$

The point $\overline{SC}$ distance to the line $\overline{\infty}$

$$\overline{\mu}_3\overline{\delta}_3^{SC} = \frac{2.455}{11} + \frac{3.606}{9.166} - 1 = -0.3835.$$

The homogeneous projective coordinates have the same values

$$\rho\xi_1^1 = \frac{\overline{\delta}_1^1}{\overline{\delta}_1^{SC}} = \frac{0.1216}{0.2458} = 0.4942,$$

$$\rho\xi_2^1 = \frac{\overline{\delta}_2^1}{\overline{\delta}_2^{SC}} = \frac{0.3566}{1.057} = 0.3366,$$

$$\rho\xi_3^1 = \frac{\overline{\delta}_3^1}{\overline{\delta}_3^{SC}} = \frac{0.4918}{0.3835} = 1.2823.$$

Matrix (8.34)

$$[\overline{\mathbf{C}}] = \begin{bmatrix} \frac{1}{0.2458\cdot 1.5258} & \frac{1}{-0.2458\cdot 2.1961} & \frac{1}{-0.2458} \\ \frac{1}{-1.057\cdot 0.8305} & \frac{1}{1.057\cdot 0.3834} & \frac{1}{-1.057} \\ -\frac{1}{0.3835\cdot 9.166} & -\frac{1}{0.3835\cdot 11} & \frac{1}{0.3835} \end{bmatrix} = \begin{bmatrix} 2.666 & -1.852 & -4.067 \\ -1.1383 & 2.4653 & -0.9454 \\ -0.2844 & -0.237 & 2.607 \end{bmatrix}.$$

Let us carry out the requalification of non-uniform projective coordinate (8.35)

$$m_1^1 = \frac{2.666\cdot 3.051 - 1.8522\cdot 1.93 - 4.067}{-0.2844\cdot 3.051 - 0.237\cdot 1.93 + 2.607} = \frac{0.495}{1.282} = 0.3846.$$
$$m_2^1 = \frac{-1.1383\cdot 3.051 + 2.4653\cdot 1.93 - 0.9454}{-0.2844\cdot 3.051 - 0.237\cdot 1.93 + 2.607} = \frac{0.339}{1.282} = 0.2622.$$

The matrix of inverse transformation (8.36)

$$[\overline{\mathbf{C}}]^{-1} = \begin{bmatrix} 0.9422 & 0.8789 & 1.7868 \\ 0.4915 & 0.8791 & 1.0847 \\ 0.1474 & 0.1757 & 0.6768 \end{bmatrix}.$$

We check input currents (8.37)

$$I_3^1 = \frac{0.9422 \cdot 0.3846 + 0.8789 \cdot 0.2622 + 1.7868}{0.1474 \cdot 0.3846 + 0.1757 \cdot 0.2622 + 0.6768} = \frac{2.3796}{0.7796} = 3.051,$$
$$I_4^1 = \frac{0.4915 \cdot 0.3846 + 0.8791 \cdot 0.2622 + 1.0847}{0.7796} = \frac{1.5042}{0.7796} = 1.93.$$

For the recalculation of currents we have the next results
Let the subsequent regime, the point M^2, be given by

$$Y_{L1}^2 = 1, \quad I_1^2 = 1.459, \quad V_1^2 = 1.459;$$
$$Y_{L2}^2 = 1, \quad I_2^2 = 1.602, \quad V_2^2 = 1.602.$$

Non-uniform projective coordinates (8.28)

$$m_1^2 = \frac{1}{1 + 0.8} = 0.555, \quad m_2^2 = 0.516.$$

Currents (8.2)

$$I_3^2 = 3.253, \quad I_4^2 = 2.132.$$

Regime changes (8.39)

$$m_1^{21} = m_1^2 \div m_1^1 = 0.555 \div 0.3846 = 1.442,$$
$$m_2^{21} = m_2^2 \div m_2^1 = 0.516 \div 0.2622 = 1.968.$$

Matrix (8.38)

$$[\mathbf{J}^{21}] = \begin{bmatrix} 1.442 & 0 & 0 \\ 0 & 1.968 & 0 \\ 0.0292 & 0.0645 & 1 \end{bmatrix}.$$

We may check up recalculation formulas (8.42) for the output current I_1

$$I_1^2 = \frac{1.442 \cdot 1.101}{0.0292 \cdot 1.101 + 0.0645 \cdot 0.8868 + 1} = \frac{1.5876}{1.0893} = 1.459.$$

Matrix (8.41) for the input current I_3

$$[\overline{\mathbf{J}}^{21}] = \begin{bmatrix} 1.1463 & 1.3225 & -2.503 \\ \overline{J}_{21}^{21} & \overline{J}_{22}^{21} & \overline{J}_{23}^{21} \\ -0.01927 & 0.2982 & 0.5728 \end{bmatrix}.$$

We check up recalculation formula (8.43) for the current I_3

$$I_3^2 = \frac{1.1463 \cdot 3.051 + 1.3225 \cdot 1.93 - 2.503}{-0.01927 \cdot 3.051 + 0.2982 \cdot 1.93 + 0.5728} = \frac{3.545}{1.0893} = 3.253.$$

8.3 Transmission of Two Signals Over Three-Wire Line

We continue with the transfer of signals in Sect. 4.3.1. We consider three-wire communication line with losses. Therefore, the interference of transmitted signals takes place. Using the measured input currents of the line, we may restore these two signals. To do this, let us consider the following two examples.

8.3.1 Transmission by Using of Cross-Ratio

We may use non-uniform coordinates or cross-ratios (8.28) as transferable analog signals V_{S1}, V_{S2}. The corresponding appliance is shown in Fig. 8.12 [3].

We believe that the communication line is equivalent to the resistive four-port in Fig. 8.11. Then, for a short time, when parameters of the four-port do not change, five pairs of conductivities are connected to the output terminals of the line by turns. This connection is realized by the contact pairs 1, 2, 3, 4, 5 of two multichannel switches with a pulse generator *Gen*. The sets of five pairs of input and output currents of the line correspond to these pairs of conductivities, as it is shown in Table 8.1.

So, the non-uniform coordinates m_1, m_2 of the point $M(Y_{L1}, Y_{L2})$ are set by cross-ratios (8.28) of four points

$$m_1 = (Y_{L1}^{OC} Y_{L1} Y_{L1}^{SC} Y_{L1}^{G1}) = (0\, Y_{L1} \infty Y_{L1}^{G1}) = \frac{Y_{L1}}{Y_{L1} - Y_{L1}^{G1}},$$

$$m_2 = (Y_{L2}^{OC} Y_{L2} Y_{L2}^{SC} Y_{L2}^{G2}) = (0\, Y_{L2} \infty Y_{L2}^{G2}) = \frac{Y_{L2}}{Y_{L2} - Y_{L2}^{G2}}.$$

Since these cross-ratios m_1, m_2 are equal to the transferable signals V_{S1}, V_{S2}, then the information conductivities Y_{L1}, Y_{L2} are expressed by the formulas

$$Y_{L1} = \frac{Y_{L1}^{G1} V_{S1}}{V_{S1} - 1}, \quad Y_{L2} = \frac{Y_{L2}^{G2} V_{S2}}{V_{S2} - 1}. \tag{8.44}$$

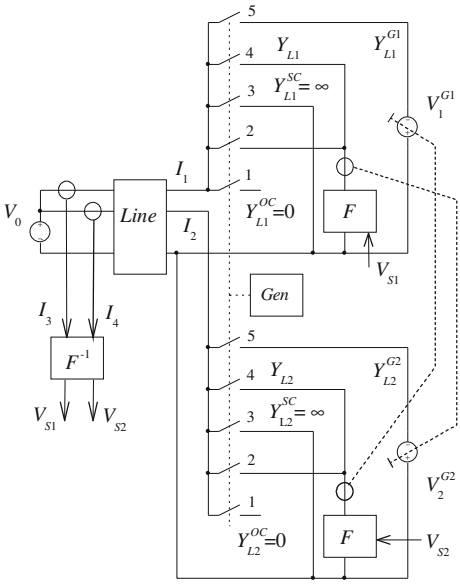

Fig. 8.12 System of transmission signals V_{S1}, V_{S2} by cross ratio

Table 8.1 Correspondence between output conductivities, input currents, and output currents

Number of set	Load conductivities		Output currents		Input currents	
1	$Y_{L1}=0$	$Y_{L2}=0$	$I_1=0$	$I_2=0$	I_3^{OC}	I_4^{OC}
2	Y_{L1}	Y_{L2}	I_1	I_2	I_3	I_4
3	$Y_{L1}=\infty$	$Y_{L2}=\infty$	I_1^{SC}	I_2^{SC}	I_3^{SC}	I_4^{SC}
4	Y_{L1}	Y_{L2}^{G2}	$I_1^{G2}=0$	I_2^{G2}	I_3^{G2}	I_4^{G2}
5	Y_{L1}^{G1}	Y_{L2}	I_1^{G1}	$I_2^{G1}=0$	I_3^{G1}	I_4^{G1}

The function unit F works according to these expressions. The information conductivities Y_{L1}, Y_{L2} may directly present measuring thermistors or resistive-strain sensors.

In turn, the inverse function unit F^{-1} calculates the transmitted signals V_{S1}, V_{S2} by formulas (8.35)

$$\begin{aligned} V_{S1} = m_1 &= \frac{-\overline{C}_{11}I_3 + \frac{\overline{C}_{11}}{\overline{k}_2}I_4 + \frac{1}{\overline{\delta}_1^{SC}}}{-\overline{C}_{31}I_3 + \frac{\overline{C}_{31}}{\overline{k}_\infty}I_4 - \frac{1}{\overline{\delta}_3^{SC}}}, \\ V_{S2} = m_2 &= \frac{-\overline{C}_{21}I_3 + \frac{\overline{C}_{21}}{\overline{k}_1}I_4 - \frac{1}{\overline{\delta}_2^{SC}}}{-\overline{C}_{31}I_3 + \frac{\overline{C}_{31}}{\overline{k}_\infty}I_4 - \frac{1}{\overline{\delta}_3^{SC}}}. \end{aligned} \tag{8.45}$$

So, it is possible to separate (or restore) two signals by only the input currents (five pairs of current values) of line. We note also that multiplicative and additive errors of the measurement of input conductivities are mutually reduced in expression (8.45). Therefore, such a communication line is subject to action of electromagnetic noises to a lesser degree.

8.3.2 Transmission by Using of Affine Ratio

Affine ratios (8.24) and (8.25) or (8.26) and (8.27) are accepted as transferable analog signals V_{S1}, V_{S2}. The corresponding appliance is shown in Fig. 8.13 [2]. Similarly, for a short time, four pairs of voltage sources are connected to the output terminals of the line by turns. This connection is realized by the contact pairs 1, 2, 3, 4 of two multichannel switches with a pulse generator *Gen*. The sets of four pairs of input and output currents of the line correspond to these pairs of voltages, as it is shown in Table 8.2. The voltages V_1^{SC}, V_2^{SC} are minimum values; in particular case, these values equal zero. The voltages V_1^{OC}, V_2^{OC} are maximum values; these values are greater than the information values $V_1,\ V_2$.

So, the normalized coordinates of the point $M(V_1, V_2)$ are set by affine ratios (8.24) and (8.25)

$$n_1 = \frac{V_1 - V_1^{SC}}{V_1^{OC} - V_1^{SC}}, \quad n_2 = \frac{V_2 - V_2^{SC}}{V_2^{OC} - V_2^{SC}}.$$

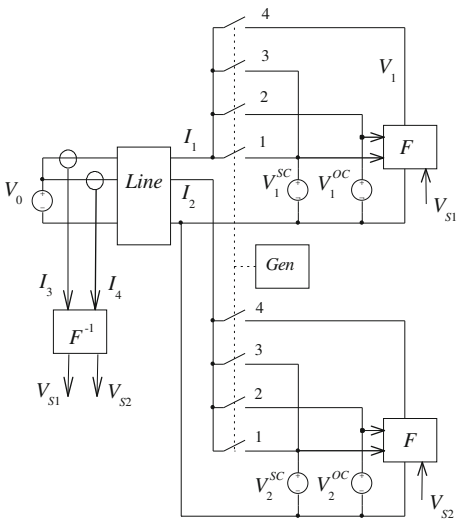

Fig. 8.13 System of transmission signals V_{S1}, V_{S2} by affine ratios

Table 8.2 Correspondence between load voltages and input currents

Number of set	Load voltages		Input currents	
1	V_1^{SC}	V_2^{SC}	$I_3^{\mathrm{SC,SC}}$	$I_4^{\mathrm{SC,SC}}$
2	V_1^{OC}	V_2^{SC}	$I_3^{OC,SC}$	$I_4^{OC,SC}$
3	V_1^{SC}	V_2^{OC}	$I_3^{SC,OC}$	$I_4^{SC,OC}$
4	V_1	V_2	I_3	I_4

Since these affine ratios n_1, n_2 are equal to transferable signals V_{S1}, V_{S2}, then the information voltages V_1, V_2 are expressed by the formulas

$$V_1 = V_1^{SC} - (V_1^{OC} - V_1^{SC})V_{S1}, \quad V_2 = V_2^{SC} - (V_2^{OC} - V_2^{SC})V_{S2}. \tag{8.46}$$

The function unit F works according to these expressions.

In turn, the inverse function unit F^{-1} calculates the transmitted signals V_{S1}, V_{S2} by formulas (8.24) and (8.25)

$$V_{S1} = \frac{I_3^{1,SC} - I_3^{\mathrm{SC,SC}}}{I_3^{OC,SC} - I_3^{\mathrm{SC,SC}}}, \quad V_{S2} = \frac{I_4^{1,SC} - I_4^{\mathrm{SC,SC}}}{I_4^{OC,SC} - I_4^{\mathrm{SC,SC}}}. \tag{8.47}$$

For other affine ratios (8.26) and (8.27), we get similarly to (8.46) that

$$V_1 = \frac{V_1^{SC} + V_{S1}V_1^{OC}}{1 - V_{S1}}, \quad V_2 = \frac{V_2^{SC} + V_{S2}V_2^{OC}}{1 - V_{S2}}. \tag{8.48}$$

The function unit F works according to these expressions. Also, the inverse function unit F^{-1} calculates the transmitted signals V_{S1}, V_{S2} by formulas

$$V_{S1} = \frac{I_3^{1,SC} - I_3^{\mathrm{SC,SC}}}{I_3^{OC,SC} - I_3^{1,SC}}, \quad V_{S2} = \frac{I_4^{SC,1} - I_4^{\mathrm{SC,SC}}}{I_4^{SC,OC} - I_4^{SC,1}}. \tag{8.49}$$

These two variants of use of affine ratios allow to separate (or restore) two signals by only the input currents (four pairs of current values) of line. We note also that multiplicative and additive errors of measurement of input conductivity values are mutually reduced in expressions (8.47) and (8.49).

8.4 Input-Output Conformity of a Balanced Six-Port

Let us continue with the matter we began in Sect. 6.2.2. We consider the currents I_4, I_5, I_6 of the voltage sources V_4, V_5, V_6 for the balanced network in Fig. 6.18.

Let us superpose the coordinate system (I_4, I_5, I_6) with the coordinate system (I_1, I_2, I_3) in Fig. 8.14. Then, any point with coordinates (I_1, I_2, I_3) corresponds to a

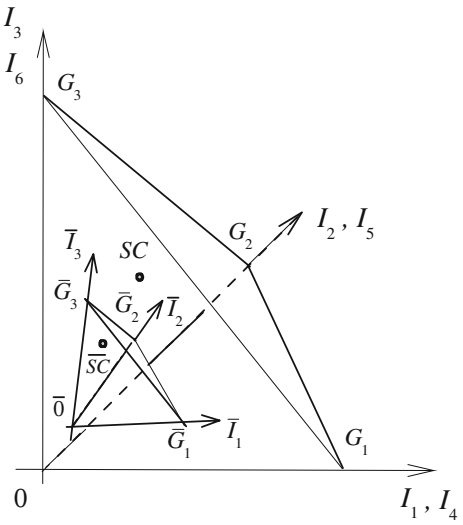

Fig. 8.14 Superposition of coordinate systems of output (I_1, I_2, I_3) and input (I_4, I_5, I_6) currents

point with coordinates (I_4, I_5, I_6). In particular, the running regime point M^1, a unit point SC and coordinate tetrahedron $0G_1G_2G_3$ correspond to the points $\overline{M}^1, \overline{SC}$ and $\overline{0G}_1\overline{G}_2\overline{G}_3$. These tetrahedrons are the generalization of the reference triangles for a plane in Fig. 8.7.

For convenience, the conformity of the output and input characteristic regime points is shown in Table 8.3.

Using Fig. 6.19, we determine the input current for the point $\overline{G}_1$. According to (6.61), the currents

$$I_5^{G1} = I_5^{SC}, \quad I_6^{G1} = I_6^{SC}. \tag{8.50}$$

In turn, according to (6.63), the current

$$I_4^{G1} = (V_4 + U_a^{G1}) y_{4a}. \tag{8.51}$$

Table 8.3 Output-input conformity of the six-port

Output				Input			
Points	I_1	I_2	I_3	Points	I_4	I_5	I_6
0	0	0	0	$\overline{0}$	I_4^{OC}	I_5^{OC}	I_6^{OC}
G_1	I_1^{G1}	0	0	$\overline{G}_1$	I_4^{G1}	I_5^{G1}	I_6^{G1}
G_2	0	I_2^{G2}	0	$\overline{G}_2$	I_4^{G2}	I_5^{G2}	I_6^{G2}
G_3	0	0	I_3^{G3}	$\overline{G}_3$	I_4^{G3}	I_5^{G3}	I_6^{G3}
SC	I_1^{SC}	I_2^{SC}	I_3^{SC}	$\overline{SC}$	I_4^{SC}	I_5^{SC}	I_6^{SC}

For the point $\overline{G}_2$, we get similarly

$$I_4^{G2} = I_4^{SC} = y_{4a}V_4, \quad I_6^{G2} = I_6^{SC} = I_6^{G1}, \quad I_5^{G2} = (V_5 + U_b^{G2})y_{5b}. \tag{8.52}$$

Likewise for the point $\overline{G}_3$, the currents

$$I_4^{G3} = I_4^{SC} = I_4^{G2}, \quad I_5^{G3} = I_5^{SC} = I_5^{G1}, \quad I_6^{G3} = (V_6 + U_c^{G3})y_{6c}. \tag{8.53}$$

It is known that projective coordinates of points M^1 and $\overline{M}^1$, concerning the own coordinate systems, are equal among themselves. Therefore, we must introduce the known coordinates $\xi_1^1, \xi_2^1, \xi_3^1, \xi_4^1$ of the point $\overline{M}^1$.

These homogeneous coordinates are defined as the ratio of the distances $\overline{\delta}_1^1, \overline{\delta}_2^1, \overline{\delta}_3^1, \overline{\delta}_4$ for the point $\overline{M}^1$ and distances $\overline{\delta}_1^{SC}, \overline{\delta}_2^{SC}, \overline{\delta}_3^{SC}, \overline{\delta}_4^{SC}$ for a unit point $\overline{SC}$ to the planes of the coordinate tetrahedron $\overline{0G}_1\overline{G}_2\overline{G}_3$.

At first, we get the equations of these planes.

The plane $\overline{0G}_1\overline{G}_2$ equation has the general view

$$A_{12}I_4 + B_{12}I_5 + C_{12}I_6 + D_{12} = 0.$$

Matrix determinants

$$\begin{aligned} A_{12} &= \begin{vmatrix} I_5^{OC} & I_6^{OC} & 1 \\ I_5^{G1} & I_6^{G1} & 1 \\ I_5^{G2} & I_6^{G2} & 1 \end{vmatrix}, \quad B_{12} = \begin{vmatrix} I_6^{OC} & I_4^{OC} & 1 \\ I_6^{G1} & I_4^{G1} & 1 \\ I_6^{G2} & I_4^{G2} & 1 \end{vmatrix}, \\ C_{12} &= \begin{vmatrix} I_4^{OC} & I_5^{OC} & 1 \\ I_4^{G1} & I_5^{G1} & 1 \\ I_4^{G2} & I_5^{G2} & 1 \end{vmatrix}, \quad D_{12} = \begin{vmatrix} I_4^{OC} & I_5^{OC} & I_6^{OC} \\ I_4^{G1} & I_5^{G1} & I_6^{G1} \\ I_4^{G2} & I_5^{G2} & I_6^{G2} \end{vmatrix}. \end{aligned} \tag{8.54}$$

We reduce A_{12}, B_{12} by expressions (8.50) and (8.52). Then

$$\begin{aligned} A_{12} &= \begin{vmatrix} I_5^{OC} & I_6^{OC} & 1 \\ I_5^{G1} & I_6^{SC} & 1 \\ I_5^{G2} & I_6^{SC} & 1 \end{vmatrix} = (I_5^{G2} - I_5^{G1})(I_6^{OC} - I_6^{SC}), \\ B_{12} &= \begin{vmatrix} I_6^{OC} & I_4^{OC} & 1 \\ I_6^{SC} & I_4^{G1} & 1 \\ I_6^{SC} & I_4^{G2} & 1 \end{vmatrix} = (I_4^{G1} - I_4^{G2})(I_6^{OC} - I_6^{SC}). \end{aligned}$$

Also, it turns out

$$I_5^{G2} - I_5^{G1} = \frac{y_{4a}}{y_{ab}} y_{5b}V_5, \quad I_4^{G1} - I_4^{G2} = \frac{y_{4a}}{y_{ab}} y_{5b}V_4.$$

If the voltage $V_4 = V_5$, then $A_{12} = B_{12}$.
The plane $\overline{0G}_2\overline{G}_3$ equation

$$A_{23}I_4 + B_{23}I_5 + C_{23}I_6 + D_{23} = 0.$$

Matrix determinants

$$\begin{aligned} A_{23} &= \begin{vmatrix} I_5^{OC} & I_6^{OC} & 1 \\ I_5^{G2} & I_6^{G2} & 1 \\ I_5^{G3} & I_6^{G3} & 1 \end{vmatrix}, \quad B_{23} = \begin{vmatrix} I_6^{OC} & I_4^{OC} & 1 \\ I_6^{G2} & I_4^{G2} & 1 \\ I_6^{G3} & I_4^{G3} & 1 \end{vmatrix}, \\ C_{23} &= \begin{vmatrix} I_4^{OC} & I_5^{OC} & 1 \\ I_4^{G2} & I_5^{G2} & 1 \\ I_4^{G3} & I_5^{G3} & 1 \end{vmatrix}, \quad D_{23} = \begin{vmatrix} I_4^{OC} & I_5^{OC} & I_6^{OC} \\ I_4^{G2} & I_5^{G2} & I_6^{G2} \\ I_4^{G3} & I_5^{G3} & I_6^{G3} \end{vmatrix}. \end{aligned} \tag{8.55}$$

If $V_5 = V_6$, then $B_{23} = C_{23}$.
The plane $\overline{0G}_1\overline{G}_3$ equation

$$A_{13}I_4 + B_{13}I_5 + C_{13}I_6 + D_{13} = 0.$$

Matrix determinants

$$\begin{aligned} A_{13} &= \begin{vmatrix} I_5^{OC} & I_6^{OC} & 1 \\ I_5^{G1} & I_6^{G1} & 1 \\ I_5^{G3} & I_6^{G3} & 1 \end{vmatrix}, \quad B_{13} = \begin{vmatrix} I_6^{OC} & I_4^{OC} & 1 \\ I_6^{G1} & I_4^{G1} & 1 \\ I_6^{G3} & I_4^{G3} & 1 \end{vmatrix}, \\ C_{13} &= \begin{vmatrix} I_4^{OC} & I_5^{OC} & 1 \\ I_4^{G1} & I_5^{G1} & 1 \\ I_4^{G3} & I_5^{G3} & 1 \end{vmatrix}, \quad D_{13} = \begin{vmatrix} I_4^{OC} & I_5^{OC} & I_6^{OC} \\ I_4^{G1} & I_5^{G1} & I_6^{G1} \\ I_4^{G3} & I_5^{G3} & I_6^{G3} \end{vmatrix}. \end{aligned} \tag{8.56}$$

If $V_4 = V_6$, then $A_{13} = C_{13}$.
For the plane $\overline{G}_1\overline{G}_2\overline{G}_3$, we have

$$\begin{aligned} &A_\infty I_4 + B_\infty I_5 + C_\infty I_6 + D_\infty = 0, \\ &A_\infty = \begin{vmatrix} I_5^{G1} & I_6^{OG1} & 1 \\ I_5^{G2} & I_6^{G2} & 1 \\ I_5^{G3} & I_6^{G3} & 1 \end{vmatrix}, \quad B_\infty = \begin{vmatrix} I_6^{G1} & I_4^{G1} & 1 \\ I_6^{G2} & I_4^{G2} & 1 \\ I_6^{G3} & I_4^{G3} & 1 \end{vmatrix}, \\ &C_\infty = \begin{vmatrix} I_4^{G1} & I_5^{G1} & 1 \\ I_4^{G2} & I_5^{G2} & 1 \\ I_4^{G3} & I_5^{G3} & 1 \end{vmatrix}, \quad D_\infty = \begin{vmatrix} I_4^{G1} & I_5^{G1} & I_6^{G1} \\ I_4^{G2} & I_5^{G2} & I_6^{G2} \\ I_4^{G3} & I_5^{G3} & I_6^{G3} \end{vmatrix}. \end{aligned} \tag{8.57}$$

If $V_4 = V_5 = V_6$, then $A_\infty = B_\infty = C_\infty$.
At last, we give expressions for the distances.
The distances $\overline{\delta}_1^1, \overline{\delta}_1^{SC}$ correspond to the plane $\overline{0G}_2\overline{G}_3$, therefore

$$\begin{aligned}\overline{\mu}_1\overline{\delta}_1^1 &= A_{23}I_4^1 + B_{23}I_5^1 + C_{23}I_6^1 + D_{23},\\ \overline{\mu}_1\overline{\delta}_1^{SC} &= A_{23}I_4^{SC} + B_{23}I_5^{SC} + C_{23}I_6^{SC} + D_{23}.\end{aligned}$$

The distances $\overline{\delta}_2^1, \overline{\delta}_2^{SC}$ correspond to $\overline{0G}_1\overline{G}_3$, then

$$\begin{aligned}\overline{\mu}_2\overline{\delta}_2^1 &= A_{13}I_4^1 + B_{13}I_5^1 + C_{13}I_6^1 + D_{13},\\ \overline{\mu}_2\overline{\delta}_2^{SC} &= A_{13}I_4^{SC} - B_{13}I_5^{SC} + C_{13}I_6^{SC} + D_{13}.\end{aligned}$$

The distances $\overline{\delta}_3^1, \overline{\delta}_3^{SC}$ match to $\overline{0G}_1\overline{G}_2$, in that case

$$\begin{aligned}\overline{\mu}_3\overline{\delta}_3^1 &= A_{12}I_4^1 + B_{12}I_5^1 + C_{12}I_6^1 + D_{12},\\ \overline{\mu}_3\overline{\delta}_3^{SC} &= A_{12}I_4^{SC} + B_{12}I_5^{SC} + C_{12}I_6^{SC} + D_{12}.\end{aligned}$$

Similarly, $\overline{\delta}_4^1, \overline{\delta}_4^{SC}$ correspond to $\overline{G}_1\overline{G}_2\overline{G}_3$ and

$$\begin{aligned}\overline{\mu}_4\overline{\delta}_4^1 &= A_\infty I_4^1 + B_\infty I_5^1 + C_\infty I_6^1 + D_\infty,\\ \overline{\mu}_4\overline{\delta}_4^{SC} &= A_\infty I_4^{SC} + B_\infty I_5^{SC} + C_\infty I_6^{SC} + D_\infty.\end{aligned}$$

Finally, the homogeneous coordinates $\xi_1^1, \xi_2^1, \xi_3^1, \xi_4^1$ have the view

$$\begin{aligned}\rho\xi_1^1 &= \frac{\overline{\mu}_1\overline{\delta}_1^1}{\overline{\mu}_1\overline{\delta}_1^{SC}} = \frac{A_{23}I_4^1 + B_{23}I_5^1 + C_{23}I_6^1 + D_{23}}{A_{23}I_4^{SC} + B_{23}I_5^{SC} + C_{23}I_6^{SC} + D_{23}}\\ &= \frac{A_{23}}{\overline{\mu}_1\overline{\delta}_1^{SC}}I_4^1 + \frac{B_{23}}{\overline{\mu}_1\overline{\delta}_1^{SC}}I_5^1 + \frac{C_{23}}{\overline{\mu}_1\overline{\delta}_1^{SC}}I_6^1 + \frac{D_{23}}{\overline{\mu}_1\overline{\delta}_1^{SC}},\\ \rho\xi_2^1 &= \frac{\overline{\mu}_2\overline{\delta}_2^1}{\overline{\mu}_2\overline{\delta}_2^{SC}} = \frac{A_{13}I_4^1 + B_{13}I_5^1 + C_{13}I_6^1 + D_{13}}{A_{13}I_4^{SC} + B_{13}I_5^{SC} + C_{13}I_6^{SC} + D_{13}}\\ &= \frac{A_{13}}{\overline{\mu}_2\overline{\delta}_2^{SC}}I_4^1 + \frac{B_{13}}{\overline{\mu}_2\overline{\delta}_2^{SC}}I_5^1 + \frac{C_{13}}{\overline{\mu}_2\overline{\delta}_2^{SC}}I_6^1 + \frac{D_{13}}{\overline{\mu}_2\overline{\delta}_2^{SC}},\\ \rho\xi_3^1 &= \frac{\overline{\mu}_3\overline{\delta}_3^1}{\overline{\mu}_3\overline{\delta}_3^{SC}} = \frac{A_{12}I_4^1 + B_{12}I_5^1 + C_{12}I_6^1 + D_{12}}{A_{12}I_4^{SC} + B_{12}I_5^{SC} + C_{12}I_6^{SC} + D_{12}}\\ &= \frac{A_{12}}{\overline{\mu}_3\overline{\delta}_3^{SC}}I_4^1 + \frac{B_{12}}{\overline{\mu}_3\overline{\delta}_3^{SC}}I_5^1 + \frac{C_{12}}{\overline{\mu}_3\overline{\delta}_3^{SC}}I_6^1 + \frac{D_{12}}{\overline{\mu}_3\overline{\delta}_3^{SC}},\\ \rho\xi_4^1 &= \frac{\overline{\mu}_4\overline{\delta}_4^1}{\overline{\mu}_4\overline{\delta}_4^{SC}} = \frac{A_\infty I_4^1 + B_\infty I_5^1 + C_\infty I_6^1 + D_\infty}{A_\infty I_4^{SC} + B_\infty I_5^{SC} + C_\infty I_6^{SC} + D_\infty}\\ &= \frac{A_\infty}{\overline{\mu}_4\overline{\delta}_4^{SC}}I_4^1 + \frac{B_\infty}{\overline{\mu}_4\overline{\delta}_4^{SC}}I_5^1 + \frac{C_\infty}{\overline{\mu}_4\overline{\delta}_4^{SC}}I_6^1 + \frac{D_\infty}{\overline{\mu}_4\overline{\delta}_4^{SC}}.\end{aligned}$$

The conformable matrix form

$$\begin{bmatrix} \rho\xi_1^1 \\ \rho\xi_2^1 \\ \rho\xi_3^1 \\ \rho\xi_4 \end{bmatrix} = [\overline{C}] \cdot \begin{bmatrix} I_4^1 \\ I_5^1 \\ I_6^1 \\ 1 \end{bmatrix},$$

$$[\overline{C}] = \begin{bmatrix} \dfrac{A_{23}}{\overline{\mu}_1\overline{\delta}_1^{SC}} & \dfrac{B_{23}}{\overline{\mu}_1\overline{\delta}_1^{SC}} & \dfrac{C_{23}}{\overline{\mu}_1\overline{\delta}_1^{SC}} & \dfrac{D_{23}}{\overline{\mu}_1\overline{\delta}_1^{SC}} \\ \dfrac{A_{13}}{\overline{\mu}_2\overline{\delta}_2^{SC}} & \dfrac{B_{13}}{\overline{\mu}_2\overline{\delta}_2^{SC}} & \dfrac{C_{13}}{\overline{\mu}_2\overline{\delta}_2^{SC}} & \dfrac{D_{13}}{\overline{\mu}_2\overline{\delta}_2^{SC}} \\ \dfrac{A_{12}}{\overline{\mu}_3\overline{\delta}_3^{SC}} & \dfrac{B_{12}}{\overline{\mu}_3\overline{\delta}_3^{SC}} & \dfrac{C_{12}}{\overline{\mu}_3\overline{\delta}_3^{SC}} & \dfrac{D_{12}}{\overline{\mu}_3\overline{\delta}_3^{SC}} \\ \dfrac{A_\infty}{\overline{\mu}_4\overline{\delta}_4^{SC}} & \dfrac{B_\infty}{\overline{\mu}_4\overline{\delta}_4^{SC}} & \dfrac{C_\infty}{\overline{\mu}_4\overline{\delta}_4^{SC}} & \dfrac{D_\infty}{\overline{\mu}_4\overline{\delta}_4^{SC}} \end{bmatrix}. \tag{8.58}$$

In turn, the non-uniform coordinates have the view

$$\begin{aligned} m_1^1 &= \frac{\rho\xi_1^1}{\rho\xi_4^1} = \frac{\overline{\mu}_4\overline{\delta}_4^{SC}}{\overline{\mu}_1\overline{\delta}_1^{SC}} \frac{A_{23}I_4^1 + B_{23}I_5^1 + C_{23}I_6^1 + D_{23}}{A_\infty I_4^1 + B_\infty I_5^1 + C_\infty I_6^1 + D_\infty}, \\ m_2^1 &= \frac{\rho\xi_2^1}{\rho\xi_4^1} = \frac{\overline{\mu}_4\overline{\delta}_4^{SC}}{\overline{\mu}_2\overline{\delta}_2^{SC}} \frac{A_{13}I_4^1 + B_{13}I_5^1 + C_{13}I_6^1 + D_{13}}{A_\infty I_4^1 + B_\infty I_5^1 + C_\infty I_6^1 + D_\infty}, \\ m_3^1 &= \frac{\rho\xi_3^1}{\rho\xi_4^1} = \frac{\overline{\mu}_4\overline{\delta}_4^{SC}}{\overline{\mu}_3\overline{\delta}_3^{SC}} \frac{A_{12}I_4^1 + B_{12}I_5^1 + C_{12}I_6^1 + D_{12}}{A_\infty I_4^1 + B_\infty I_5^1 + C_\infty I_6^1 + D_\infty}. \end{aligned} \tag{8.59}$$

So, we use only the input currents for (8.59). In practice, the characteristic values are obtained by calculation or testing the multi-port only by manipulations at the output terminals. It is technically more convenient than determination of all the Y parameter.

In turn, we obtain or restore the load conductivities

$$Y_{L1}^1 = \frac{Y_{L1}^{G1} m_1^1}{m_1^1 - 1}, \quad Y_{L2}^1 = \frac{Y_{L2}^{G2} m_2^1}{m_2^1 - 1}, \quad Y_{L3}^1 = \frac{Y_{L3}^{G3} m_3^1}{m_3^1 - 1}. \tag{8.60}$$

Table 8.4 Parameters of the coordinate tetrahedron

Regime points	Input currents		
	I_4	I_5	I_6
$\overline{0}$	$I_4^{OC} = 0.1793$	$I_5^{OC} = 0.2986$	$I_6^{OC} = 0.1382$
$\overline{G}_1$	$I_4^{G1} = 2.6$	$I_5^{G1} = 2.0$	$I_6^{G1} = 0.6666$
$\overline{G}_2$	$I_4^{G2} = 1.0$	$I_5^{G2} = 3.6$	$I_6^{G2} = 0.6666$
$\overline{G}_3$	$I_4^{G3} = 1.0$	$I_5^{G3} = 2.0$	$I_6^{G3} = 2.2666$
$\overline{SC}$	$I_4^{SC} = 0.8272$	$I_5^{SC} = 1.501$	$I_6^{SC} = 0.5786$

Example 2 We continue Example 4 of Sect. 6.2.2. The calculated values of the characteristic regime points are shown in Table 8.4.

Determinates (8.54)

$$A_{12} = \begin{vmatrix} 0.2986 & 0.1382 & 1 \\ 2.0 & 0.6666 & 1 \\ 3.6 & 0.6666 & 1 \end{vmatrix} = -0.8454,$$

$$B_{12} = \begin{vmatrix} 0.1382 & 0.1793 & 1 \\ 0.6666 & 2.6 & 1 \\ 0.6666 & 2.6 & 1 \end{vmatrix} = -0.8454,$$

$$C_{12} = \begin{vmatrix} 0.1793 & 0.2986 & 1 \\ 2.6 & 2.0 & 1 \\ 1.0 & 3.6 & 1 \end{vmatrix} = 6.5954,$$

$$D_{12} = \begin{vmatrix} 0.1793 & 0.2986 & 0.1382 \\ 2.6 & 2.0 & 0.6666 \\ 1.0 & 3.6 & 0.6666 \end{vmatrix} = -0.5079.$$

The plane $\overline{0G}_1\overline{G}_2$ equation

$$-0.8454I_4 - 0.8454I_5 + 6.5954I_6 - 0.5079 = 0.$$

Determinates (8.55)

$$A_{23} = \begin{vmatrix} 0.2986 & 0.1382 & 1 \\ 3.6 & 0.6666 & 1 \\ 2.0 & 2.2666 & 1 \end{vmatrix} = 6.1264,$$

$$B_{23} = \begin{vmatrix} 0.1382 & 0.1793 & 1 \\ 0.6666 & 1.0 & 1 \\ 2.2666 & 1.0 & 1 \end{vmatrix} = -1.3131,$$

$$C_{23} = \begin{vmatrix} 0.1793 & 0.2986 & 1 \\ 1.0 & 3.6 & 1 \\ 1.0 & 2.0 & 1 \end{vmatrix} = -1.3131,$$

$$D_{23} = \begin{vmatrix} 0.1793 & 0.2986 & 0.1382 \\ 1.0 & 3.6 & 0.6666 \\ 1.0 & 2.0 & 2.2666 \end{vmatrix} = -0.5253.$$

The plane $\overline{0G}_2\overline{G}_3$ equation

$$6.1264I_4 - 1.3131I_5 - 1.3131I_6 - 0.5253 = 0.$$

Determinates (8.56)

$$A_{13} = \begin{vmatrix} 0.2986 & 0.1382 & 1 \\ 2.0 & 0.6666 & 1 \\ 2.0 & 2.2666 & 1 \end{vmatrix} = 2.7222,$$

$$B_{13} = \begin{vmatrix} 0.1382 & 0.1793 & 1 \\ 0.6666 & 2.6 & 1 \\ 2.2666 & 1.0 & 1 \end{vmatrix} = -4.7186,$$

$$C_{13} = \begin{vmatrix} 0.1793 & 0.2986 & 1 \\ 2.6 & 2.0 & 1 \\ 1.0 & 2.0 & 1 \end{vmatrix} = 2.7222,$$

$$D_{13} = \begin{vmatrix} 0.1793 & 0.2986 & 0.1382 \\ 2.6 & 2.0 & 0.6666 \\ 1.0 & 2.0 & 2.2666 \end{vmatrix} = 0.5382.$$

The plane $\overline{0G}_1\overline{G}_3$ equation

$$2.7222I_4 - 4.7186I_5 + 2.7222I_6 + 0.5382 = 0.$$

Determinates (8.57)

$$A_\infty = \begin{vmatrix} 2.0 & 0.6666 & 1 \\ 3.6 & 0.6666 & 1 \\ 2.0 & 2.2666 & 1 \end{vmatrix} = 2.56, \quad B_\infty = \begin{vmatrix} 0.6666 & 2.6 & 1 \\ 0.6666 & 1 & 1 \\ 2.2666 & 1 & 1 \end{vmatrix} = 2.56,$$

$$C_\infty = \begin{vmatrix} 2.6 & 2.0 & 1 \\ 1 & 3.6 & 1 \\ 1 & 2.0 & 1 \end{vmatrix} = 2.56,$$

$$D_\infty = \begin{vmatrix} 2.6 & 2.0 & 0.6666 \\ 1 & 3.6 & 0.6666 \\ 1 & 2.0 & 2.2666 \end{vmatrix} = -13.4825.$$

The plane $\overline{G}_1 G_2 \overline{G}_3$ equation

$$2.56I_4 + 2.56I_5 + 2.56I_6 - 13.4825 = 0.$$

We rewrite the values of the initial regime

$$\begin{aligned} Y_{L1}^1 = 0.2, \quad Y_{L2}^1 = 0.25, \quad Y_{L3}^1 = 0.1666; \\ I_1^1 = 0.4232, \quad I_2^1 = 0.5673, \quad I_3^1 = 0.335; \\ I_4^1 = 0.4921, \quad I_5^1 = 0.8654, \quad I_6^1 = 0.354. \end{aligned}$$

The distances $\overline{\delta}_1^1, \overline{\delta}_1^{SC}$

$$\begin{aligned} \overline{\mu}_1 \overline{\delta}_1^1 &= 6.1264 \cdot 0.4921 - 1.3131 \cdot 0.8654 \\ &\quad - 1.3131 \cdot 0.354 - 0.5253 = 0.8883, \\ \overline{\mu}_1 \overline{\delta}_1^{SC} &= 6.1264 \cdot 0.8272 - 1.3131 \cdot 1.501 \\ &\quad - 1.3131 \cdot 0.5786 - 0.5253 = 1.8147. \end{aligned}$$

The distances $\overline{\delta}_2^1, \overline{\delta}_2^{SC}$

$$\begin{aligned} \overline{\mu}_2 \overline{\delta}_2^1 &= 2.7222 \cdot 0.4921 - 4.7186 \cdot 0.8654 \\ &\quad + 2.7222 \cdot 0.354 + 0.5382 = 1.242, \\ \overline{\mu}_2 \overline{\delta}_2^{SC} &= 2.7222 \cdot 0.8272 - 4.7186 \cdot 1.501 \\ &\quad + 2.7222 \cdot 0.5786 + 0.5382 = -2.7176. \end{aligned}$$

The distances $\overline{\delta}_3^1, \overline{\delta}_3^{SC}$

$$\begin{aligned} \overline{\mu}_3 \overline{\delta}_3^1 &= -0.8454 \cdot 0.4921 - 0.8454 \cdot 0.8654 \\ &\quad + 6.5954 \cdot 0.354 - 0.5079 = 0.6792, \\ \overline{\mu}_3 \overline{\delta}_3^{SC} &= -0.8454 \cdot 0.8272 - 0.8454 \cdot 1.501 \\ &\quad + 6.5954 \cdot 0.5786 - 0.5079 = 1.3399. \end{aligned}$$

The distances $\overline{\delta}_4^1, \overline{\delta}_4^{SC}$

$$\begin{aligned}\overline{\mu}_4\overline{\delta}_4^1 &= 2.56\cdot 0.4921 + 2.56\cdot 0.8654\\ &\quad + 2.56\cdot 0.354 - 13.4825 = -9.101,\\ \overline{\mu}_4\overline{\delta}_4^{SC} &= 2.56\cdot 0.8272 + 2.56\cdot 1.501\\ &\quad + 2.56\cdot 0.5786 - 13.4825 = -6.0411\ .\end{aligned}$$

The homogeneous coordinates

$$\begin{aligned}\rho\xi_1^1 &= \frac{\overline{\mu}_1\overline{\delta}_1^1}{\overline{\mu}_1\overline{\delta}_1^{SC}} = \frac{0.8883}{1.8147} = 0.4895\\ &= \frac{6.1264}{1.8147}I_4^1 - \frac{1.3131}{1.8147}I_5^1 - \frac{1.3131}{1.8147}I_6^1 - \frac{0.5253}{1.8147}\\ &= 3.376I_4^1 - 0.7236I_5^1 - 0.7236I_6^1 - 0.2895,\\ \rho\xi_2^1 &= \frac{\overline{\mu}_2\overline{\delta}_2^1}{\overline{\mu}_2\overline{\delta}_2^{SC}} = \frac{1.242}{2.7176} = 0.457\\ &= -\frac{2.7222}{2.7176}I_4^1 + \frac{4.7186}{2.7176}I_5^1 - \frac{2.7222}{2.7176}I_6^1 - \frac{0.5382}{2.7176}\\ &= -1.0017I_4^1 + 1.7363I_5^1 - 1.0017I_6^1 - 0.198,\\ \rho\xi_3^1 &= \frac{\overline{\mu}_3\overline{\delta}_3^1}{\overline{\mu}_3\overline{\delta}_3^{SC}} = \frac{0.6792}{1.3399} = 0.5069\\ &= -\frac{0.8454}{1.3399}I_4^1 - \frac{0.8454}{1.3399}I_5^1 + \frac{6.5954}{1.3399}I_6^1 - \frac{0.5079}{1.3399}\\ &= -0.6309I_4^1 - 0.6309I_5^1 + 4.9I_6^1 - 0.379,\\ \rho\xi_4^1 &= \frac{\overline{\mu}_4\overline{\delta}_4^1}{\overline{\mu}_4\overline{\delta}_4^{SC}} = \frac{9.101}{6.0411} = 1.5065\\ &= -\frac{2.56}{6.0411}I_4^1 - \frac{2.56}{6.0411}I_5^1 - \frac{2.56}{6.0411}I_6^1 + \frac{13.4825}{6.0411}\\ &= -0.4238I_4^1 - 0.4238I_5^1 - 0.4238I_6^1 + 2.2318.\end{aligned}$$

Matrix form (8.58)

$$\begin{pmatrix}\rho\xi_1\\ \rho\xi_2\\ \rho\xi_3\\ \rho\xi_4\end{pmatrix} = \begin{pmatrix}3.376 & -0.7236 & -0.7236 & -0.2895\\ -1.0017 & 1.7363 & -1.0017 & -0.198\\ -0.6309 & -0.6309 & 4.9 & -0.379\\ -0.4238 & -0.4238 & -0.4238 & 2.2318\end{pmatrix}\cdot\begin{pmatrix}I_4\\ I_5\\ I_6\\ 1\end{pmatrix}.$$

We check non-uniform coordinates (8.59)

$$m_1^1 = \frac{3.376 \cdot 0.4921 - 0.7236 \cdot 0.8654 - 0.7236 \cdot 0.354 - 0.2895}{-0.4238 \cdot 0.4921 - 0.4238 \cdot 0.8654 - 0.4238 \cdot 0.354 + 2.2318}$$
$$= \frac{0.4895}{1.5065} = 0.3254,$$
$$m_2^1 = \frac{-1.0017 \cdot 0.4921 + 1.7363 \cdot 0.8654 - 1.0017 \cdot 0.354 - 0.198}{1.5065}$$
$$= \frac{0.457}{1.5065} = 0.3022,$$
$$m_3^1 = \frac{-0.6309 \cdot 0.4921 - 0.6309 \cdot 0.8654 + 4.9 \cdot 0.354 - 0.379}{1.5065}$$
$$= \frac{0.5069}{1.5065} = 0.3367.$$

Load conductivities (8.60)

$$Y_{L1}^1 = \frac{-0.4146 \cdot 0.3254}{0.3254 - 1} = 0.2,$$
$$Y_{L2}^1 = \frac{-0.5775 \cdot 0.3022}{0.3022 - 1} = 0.25,$$
$$Y_{L3}^1 = \frac{-0.3284 \cdot 0.3367}{0.3367 - 1} = 0.1666.$$

References

1. Penin, A.: Invariant properties of cascaded six-pole networks. Int. J. Circuit Syst. Signal Process. **6**(5), 305–314 (2012)
2. Penin, A., Sidorenko, A.: Method for transmitting signals through the three- wire direct current line. MD Patent 692, 31 Oct (2013)
3. Penin, A., Sidorenko, A.: Transmission of measuring signals and power supply of remote sensors. In: Bonca, J., Kruchinin, S. (eds.) Nanotechnology in the Security Systems. NATO Science for Peace and Security Series C: Environmental Security, pp. 267–281. Springer Science + Business Media, Dordrecht (2014)

Chapter 9
Generalized Equivalent Circuit of a Multi-port

9.1 Generalized Equivalent of an Active Two-Port

9.1.1 Disadvantages of Known Equivalent

Let us consider, for example, a familiar active two-port network in Fig. 9.1 with changeable load conductivities Y_{L1}, Y_{L2}.

We rewrite the main relationships of Sect. 6.1.3. These active two-port is described by the system of equations

$$\begin{bmatrix} I_1 \\ I_2 \end{bmatrix} = \begin{bmatrix} -Y_{11} & Y_{12} \\ Y_{12} & -Y_{22} \end{bmatrix} \cdot \begin{bmatrix} V_1 \\ V_2 \end{bmatrix} + \begin{bmatrix} I_1^{SC} \\ I_2^{SC} \end{bmatrix}. \tag{9.1}$$

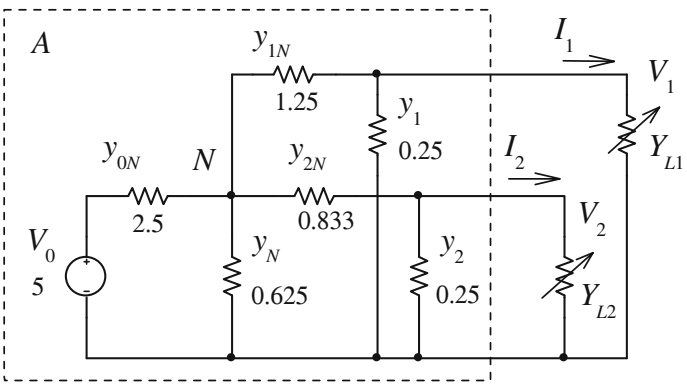

Fig. 9.1 Circuit with two load conductivities

A. Penin, *Analysis of Electrical Circuits with Variable Load Regime Parameters*, Power Systems, DOI 10.1007/978-3-319-28451-4_9

where Y parameters

$$Y_{11} = y_1 + y_{1N} - \frac{y_{1N}^2}{y_\Sigma}, \quad y_\Sigma = y_{0N} + y_N + y_{1N} + y_{2N},$$

$$Y_{12} = y_{2N}\frac{y_{1N}}{y_\Sigma}, \quad Y_{22} = y_2 + y_{2N} - \frac{y_{2N}^2}{y_\Sigma}.$$

The short circuit SC currents of both loads

$$I_1^{SC} = Y_{10}V_0 = y_{0N}\frac{y_{1N}}{y_\Sigma}V_0, \quad I_2^{SC} = Y_{20}V_0 = y_{0N}\frac{y_{2N}}{y_\Sigma}V_0. \tag{9.2}$$

Expression (9.1) shows that the active two-port represents a passive part, which is set by conductivities of Y parameters, and two sources of currents I_1^{SC}, I_2^{SC}, as it is illustrated in Fig. 9.2 [1].

We may notice that SC currents are set by parameters Y_{10}, Y_{20} which depend practically on all elements of this circuit except y_1, y_2.

Therefore, at a possible change, for example, of conductivity y_N, it is necessary to make the recalculation of these SC currents what is inconvenient. The conductivity y_N can be a part of a possible third load. In turn, the conductivity y_{1N} belongs more to the first load, but also influences on the SC current of the second load. And mutually, conductivity y_{2N} influences on the SC current of the first load.

All these features determine inconveniences for the evaluation of circuit characteristics, complicates regime calculations. In this sense, the parameters of the generalized equivalent generator, proposed in Chap. 3, do not depend on a chosen element of circuit.

9.1.2 Introduction of the Formal Variant of a Generalized Equivalent

We use results of Sect. 3.3. At first, let us consider the above two-port network concerning the load Y_{L1}. Therefore, this circuit will be an active two-pole with changeable element Y_{L2} in Fig. 9.3.

The family of load straight lines $I_1(V_1)$ is presented by expression (3.79)

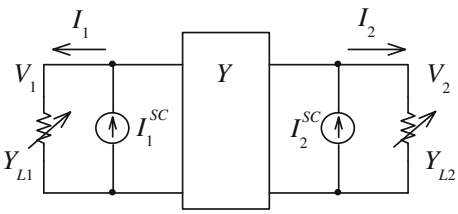

Fig. 9.2 Known equivalent circuit of an active two-port

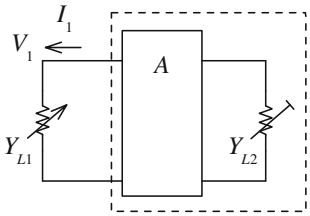

Fig. 9.3 An active two-pole with changeable element Y_{L2}

$$(I_1 - I_1^{G1}) = -Y_{i1}(V_1 + V_1^{G1}). \tag{9.3}$$

The internal conductivity

$$Y_{i1} = Y_{11} - \frac{(Y_{12})^2}{Y_{L2} + Y_{22}}. \tag{9.4}$$

The family of load straight lines shown in Fig. 9.4 represents a bunch of straight lines with familiar center G_1.

The bunch center coordinates correspond to expressions (3.77), (3.78), (3.80), or (6.26), (6.27). Therefore, we get

$$V_1^{G1} = -\frac{Y_{20}}{Y_{12}} V_0 = -\frac{y_{0N}}{y_{1N}} V_0, \quad I_1^{G1} = y_{0N}\left(1 + \frac{y_1}{y_{1N}}\right) V_0, \tag{9.5}$$

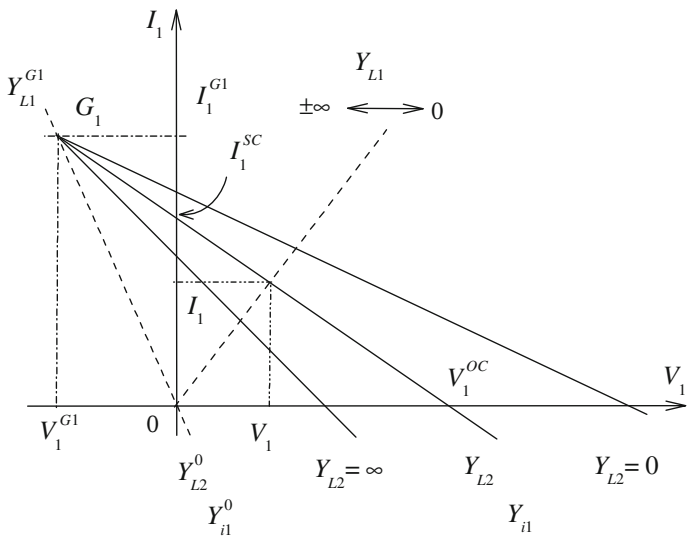

Fig. 9.4 Family of load straight lines with the parameter Y_{L2}

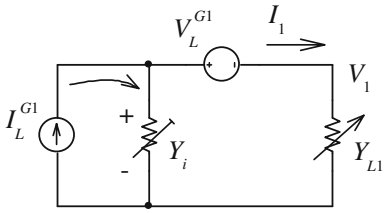

Fig. 9.5 Generalized equivalent generator to the load Y_{L1}

$$Y_{L1}^{G1} = \frac{I_1^{G1}}{V_1^{G1}} = -(y_1 + y_{1N}). \tag{9.6}$$

Let us convert expression (9.3) to the relative form

$$\frac{I_1}{I_1^{G1}} - 1 = -\frac{Y_{i1}}{Y_{L1}^{G1}}\left(\frac{V_1}{V_1^{G1}} + 1\right). \tag{9.7}$$

Thus, the values I_1^{G1}, Y_{L1}^{G1}, and V_1^{G1} are scales for corresponding values. Expressions (9.3) and (9.7) determine a generalized equivalent generator in Fig. 9.5.

We remind that the value $Y_{i1}^0 = -Y_{L1}^{G1}$ is the characteristic value for the conductivity Y_i. In this case, the conductivity Y_i voltage is equal and opposite to the source V_1^{G1} voltage. Therefore, $I_1 = 0$, $V_1 = 0$ for all conductivity Y_{L1} values.

Second, let us consider now the above two-port network concerning the load Y_{L2}. This circuit will be an active two-pole with changeable element Y_{L1} in Fig. 9.6 too.

Similar relationships are obtained for the second load Y_{L2}

$$(I_2 - I_2^{G2}) = -Y_{i2}(V_2 + V_2^{G2}), \quad Y_{i2} = Y_{22} - \frac{(Y_{12})^2}{Y_{L1} + Y_{11}}. \tag{9.8}$$

$$V_2^{G2} = -\frac{y_{0N}}{y_{2N}}V_0, \quad I_2^{G2} = y_{0N}\left(1 + \frac{y_2}{y_{2N}}\right)V_0, \quad Y_{L2}^{G2} = -(y_2 + y_{2N}). \tag{9.9}$$

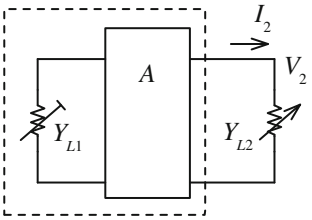

Fig. 9.6 An active two-pole with changeable element Y_{L1}

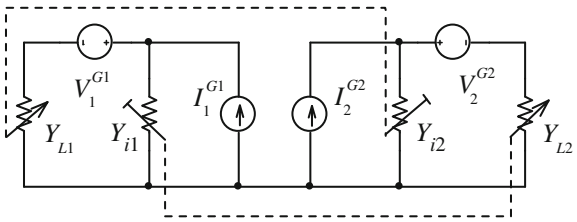

Fig. 9.7 Formal equivalent generator as the association of the two active two-poles

These expressions determine also the similar generalized equivalent generator.

Third, the common or formal scheme of the equivalent generator of our active two-port network may be constituted by Fig. 9.7 [2].

This scheme gives an evident representation about mutual influence of loads and allows carrying out regime calculations.

9.1.3 *Introduction of the Principal Variant of a Generalized Equivalent Circuit*

It is possible also to obtain one more scheme of the equivalent generator. This principal variant is demonstrated by Fig. 9.8 [2].

To prove that, we consider expression (6.43) for the first input conductivity

$$Y_{11} = \frac{I_1^{G1} - I_1^{SC}}{V_1^{G1}} = \frac{J_1}{U_1}.$$

This expression defines the input conductivity for the passive part of two-port network at the short circuit for the first load and short circuit for the second pair of terminals in Fig. 9.9a.

The similar relationship is for the second input conductivity

$$Y_{22} = \frac{I_2^{G2} - I_2^{SC}}{V_2^{G2}} = \frac{J_2}{U_2}.$$

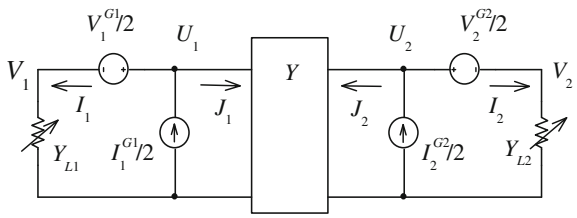

Fig. 9.8 Electrical scheme of the generalized equivalent generator of the active two-port

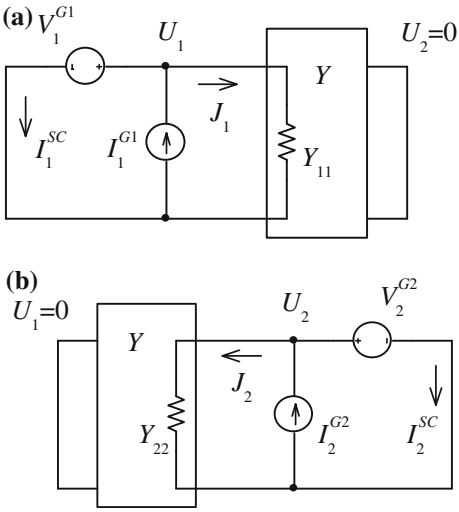

Fig. 9.9 **a** Definition of the first input conductivity of the passive part of two-port network, **b** definition of the second input conductivity

Analogously, we have the input conductivity for the passive part of two-port network at the short circuit for the second load and short circuit for the first pair of terminals in Fig. 9.9b.

The association of these two schemes leads to the above scheme in Fig. 9.8. Taking into account the superposition theorem, the values of all constituent sources of current and voltage are decreased twice. The calculation proves such a scheme for equivalent generator.

Next, we may obtain the system of equations which describes the proposed equivalent generator. Using the specified designations in Fig. 9.8, it is possible to write down

$$\begin{aligned} U_1 &= \frac{V_1^{G1}}{2} + V_1, \quad J_1 = \frac{I_1^{G1}}{2} - I_1, \\ U_2 &= \frac{V_2^{G2}}{2} + V_2, \quad J_2 = \frac{I_2^{G2}}{2} - I_2. \end{aligned} \tag{9.10}$$

The following relationships take place for the passive part of two-port network

$$\begin{aligned} J_1 &= Y_{11}U_1 - Y_{12}U_2 \\ J_2 &= -Y_{12}U_1 + Y_{22}U_2. \end{aligned} \tag{9.11}$$

Then, taking into account (9.10), the expression is obtained

$$I_1 = -Y_{11}V_1 + Y_{12}V_2 + \left(-Y_{11}\frac{V_1^{G1}}{2} + Y_{12}\frac{V_2^{G2}}{2} + \frac{I_1^{G1}}{2}\right). \tag{9.12}$$

Let us compare this form to expression (9.1). Then, the term in the brackets is equal to the *SC* current I_1^{SC}. In addition, the structure of this short circuit current for (9.12) demonstrates its components.

The component $Y_{11}V_1^{G1}/2$ corresponds to the own current of the two-port network and depends on its parameters.

The component $I_1^{G1}/2$ is defined by the constituent current source.

The component $Y_{12}V_2^{G2}/2$ corresponds to a mutual current on account of the constituent voltage source for the second pair of terminals.

The expression for the current I_2 is obtained similarly to (9.12)

$$I_2 = -Y_{22}V_2 + Y_{12}V_1 + \left(-Y_{22}\frac{V_2^{G2}}{2} + Y_{12}\frac{V_1^{G1}}{2} + \frac{I_2^{G2}}{2}\right). \tag{9.13}$$

The offered scheme of the equivalent generator is convenient at the modeling of an active two-port network.

The values of the constituent voltage and current sources of the generalized equivalent generator do not depend on the conductivity y_N in Fig. 9.1. This feature represents a practical interest. This conductivity may be a part of the third changeable load. Therefore, Y parameters of the passive part of two-port are only recalculated.

Besides, the bunch center parameters of one load do not depend on the conductivities entering into the circuit of other load. For example, the center G_1 is defined by the elements y_1, y_{1N} ,and does not depend on y_2, y_{2N}.

Therefore, such property of this equivalent generator simplifies analysis of a circuit.

Example 1 We use the date of Example 2, Sect. 6.1.3. For the running regime, expressions (9.10) have the values

$$U_1 = \frac{10}{2} + V_1 = 6.958, \quad J_1 = \frac{15}{2} - I_1 = 6.521,$$
$$U_2 = \frac{15}{2} + V_2 = 9.149, \quad J_2 = \frac{16.25}{2} - I_2 = 7.3.$$

We check relationships (9.11)

$$J_1 = Y_{11}U_1 - Y_{12}U_2 = 1.2 \cdot 6.958 - 0.2 \cdot 9.149 = 6.52,$$
$$J_2 = -Y_{12}U_1 + Y_{22}U_2 = -0.2 \cdot 6.958 + 0.95 \cdot 9.149 = 7.3.$$

SC currents (9.12), (9.13)

$$I_1^{SC} = -1.2 \cdot 5 + 0.2 \cdot 7.5 + 7.5 = 3,$$
$$I_2^{SC} = -0.95 \cdot 7.5 + 0.2 \cdot 5 + 8.125 = 2.$$

9.2 Generalized Equivalent of an Active Three-Port

Let us use the above approach for an active three-port network with changeable load conductivities in Fig. 9.10. We use now the results of Sect. 6.2. This network is described by the following system of equations

$$\begin{bmatrix} I_1 \\ I_2 \\ I_3 \end{bmatrix} = \begin{bmatrix} -Y_{11} & Y_{12} & Y_{13} \\ Y_{12} & -Y_{22} & Y_{23} \\ Y_{13} & Y_{23} & -Y_{33} \end{bmatrix} \cdot \begin{bmatrix} V_1 \\ V_2 \\ V_3 \end{bmatrix} + \begin{bmatrix} I_1^{SC} \\ I_2^{SC} \\ I_3^{SC} \end{bmatrix}. \tag{9.14}$$

Taking into account the voltages $V_1 = I_1/Y_{L1}$, $V_2 = I_2/Y_{L2}$, and $V_3 = I_2/Y_{L3}$, we get three bunches of planes. The intersection of planes of one bunch among themselves defines a bunch axis.

The point of intersection of this bunch axis with the axis I_1 is defined by (6.47)

$$I_1^{G1} = V_0 y_{0N}\left(1 + \frac{y_1}{y_{1N}}\right), \quad V_1^{G1} = -\frac{y_{0N}}{y_{1N}} V_0, \quad Y_{L1}^{G1} = -(y_{1N} + y_1). \tag{9.15}$$

This point gives the center G_1. Similarly, we get the center G_2 by (6.45)

$$I_2^{G2} = V_0\, y_{0N}\left(1 + \frac{y_2}{y_{2N}}\right), \quad V_2^{G2} = -\frac{y_{0N}}{y_{2N}} V_0, \quad Y_{L2}^{G2} = -(y_{2N} + y_2). \tag{9.16}$$

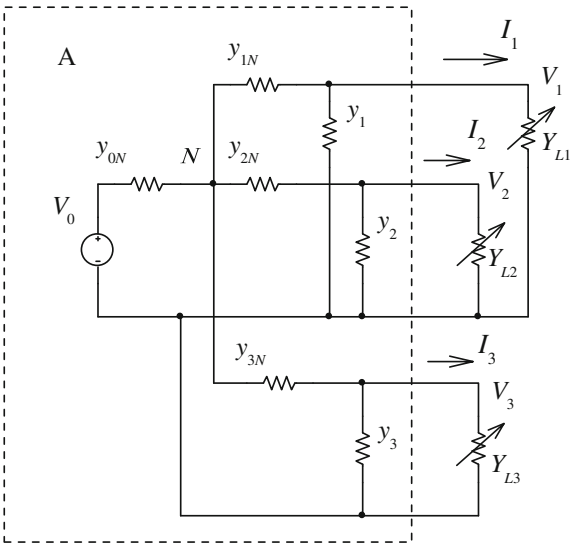

Fig. 9.10 Active multi-port with three loads

Also, the center G_3 by (6.46)

$$I_3^{G3} = V_0 y_{0N}\left(1 + \frac{y_3}{y_{3N}}\right), \quad V_3^{G3} = -\frac{y_{0N}}{y_{3N}} V_0, \quad Y_{L3}^{G3} = -(y_{3N} + y_3). \tag{9.17}$$

Using these parameters of the centers, we get form (6.55) of system (9.14)

$$\begin{aligned}
\frac{I_1}{I_1^{G1}} &= \frac{V_1}{V_1^{G1}}\left(1 - \frac{I_1^{SC}}{I_1^{G1}}\right) - \frac{I_1^{SC}}{I_1^{G1}}\frac{V_2}{V_2^{G2}} - \frac{I_1^{SC}}{I_1^{G1}}\frac{V_3}{V_3^{G3}} + \frac{I_1^{SC}}{I_1^{G1}}, \\
\frac{I_2}{I_2^{G2}} &= -\frac{I_2^{SC}}{I_2^{G2}}\frac{V_1}{V_1^{G1}} + \frac{V_2}{V_2^{G2}}\left(1 - \frac{I_2^{SC}}{I_2^{G2}}\right) - \frac{I_2^{SC}}{I_2^{G2}}\frac{V_3}{V_3^{G3}} + \frac{I_2^{SC}}{I_2^{G2}}, \\
\frac{I_3}{I_3^{G3}} &= -\frac{I_3^{SC}}{I_3^{G3}}\frac{V_1}{V_1^{G1}} - \frac{I_3^{SC}}{I_3^{G3}}\frac{V_2}{V_2^{G2}} + \frac{V_3}{V_3^{G3}}\left(1 - \frac{I_3^{SC}}{I_3^{G3}}\right) + \frac{I_3^{SC}}{I_3^{G3}}.
\end{aligned} \tag{9.18}$$

From here, we may express Y parameters

$$\begin{aligned}
Y_{11} &= \frac{I_1^{G1} - I_1^{SC}}{-V_1^{G1}}, \quad Y_{12} = \frac{I_1^{SC}}{-V_2^{G2}} = \frac{I_2^{SC}}{-V_1^{G1}}, \quad Y_{13} = \frac{I_1^{SC}}{-V_3^{G3}} = \frac{I_3^{SC}}{-V_1^{G1}}, \\
Y_{22} &= \frac{I_2^{G2} - I_2^{SC}}{-V_2^{G2}}, \quad Y_{23} = \frac{I_2^{SC}}{-V_3^{G3}} = \frac{I_3^{SC}}{-V_2^{G2}}, \quad Y_{33} = \frac{I_3^{G3} - I_3^{SC}}{-V_3^{G3}}.
\end{aligned} \tag{9.19}$$

Let us obtain the generalized equivalent generator similar to Fig. 9.8. For this purpose, we consider also expression (9.19) for the first conductivity

$$Y_{11} = \frac{I_1^{G1} - I_1^{SC}}{V_1^{G1}} = \frac{J_1}{U_1}.$$

This expression defines the input conductivity for the passive part of three-port network at the short circuit for the first load and short circuit for the second and third pairs of terminals in Fig. 9.11a.

The similar formulas for the second and third conductivities have the view

$$Y_{22} = \frac{I_2^{G2} - I_2^{SC}}{V_2^{G2}} = \frac{J_2}{U_2}, \quad Y_{33} = \frac{I_3^{G3} - I_3^{SC}}{V_3^{G3}} = \frac{J_3}{U_3}.$$

These relationships correspond to Fig. 9.11b, c.

The association of these three schemes leads to the scheme in Fig. 9.12. Taking into account the superposition theorem, the values of all constituent sources of current and voltage are decreased thrice [3]. The calculation proves such a scheme.

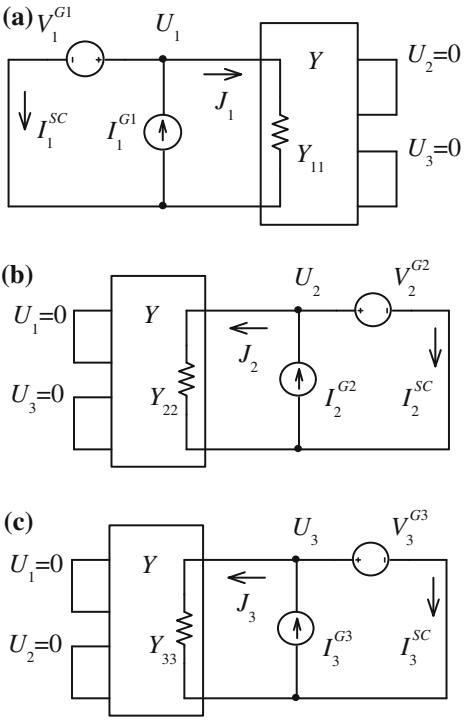

Fig. 9.11 **a** Definition of the first input conductivity of the passive part of three-port network, **b** definition of the second input conductivity, **c** definition of the third input conductivity

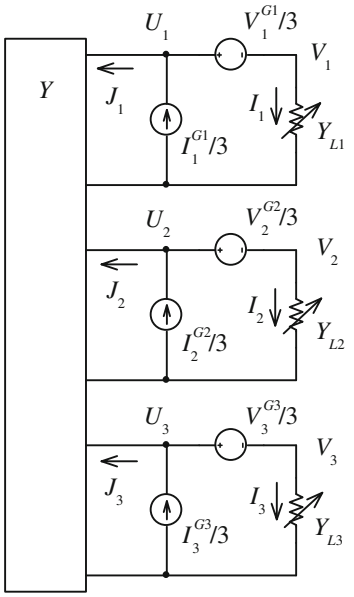

Fig. 9.12 Generalized equivalent generator of the active three-port

We obtain the system of equations which describes the proposed equivalent generator. Using the specified designations in Fig. 9.12, it is possible to write down

$$\begin{aligned} U_1 &= \frac{V_1^{G1}}{3} + V_1, \quad J_1 = \frac{I_1^{G1}}{3} - I_1, \\ U_2 &= \frac{V_2^{G2}}{3} + V_2, \quad J_2 = \frac{I_2^{G2}}{3} - I_2, \\ U_3 &= \frac{V_3^{G3}}{3} + V_3, \quad J_3 = \frac{I_3^{G3}}{3} - I_3. \end{aligned} \tag{9.20}$$

The following relationships take place for the passive part of three-port network

$$\begin{aligned} J_1 &= Y_{11}U_1 - Y_{12}U_2 - Y_{13}U_3, \\ J_2 &= -Y_{12}U_1 + Y_{22}U_2 - Y_{23}U_3, \\ J_3 &= -Y_{13}U_1 - Y_{23}U_2 + Y_{33}U_3. \end{aligned} \tag{9.21}$$

Then, taking into account (9.20), the current is obtained

$$\begin{aligned} I_1 = &-Y_{11}V_1 + Y_{12}V_2 + Y_{13}V_3 \\ &+ \left(-Y_{11}\frac{V_1^{G1}}{3} + Y_{12}\frac{V_2^{G2}}{3} + Y_{13}\frac{V_3^{G3}}{3} + \frac{I_1^{G1}}{3}\right). \end{aligned} \tag{9.22}$$

The term in the brackets is equal to the *SC* current I_1^{SC}. This term shows the components of this current.

The expressions for the currents I_2, I_3 are obtained similarly

$$\begin{aligned} I_2 = &Y_{12}V_1 - Y_{22}V_2 + Y_{23}V_3 \\ &+ \left(Y_{12}\frac{V_1^{G1}}{3} - Y_{22}\frac{V_2^{G2}}{3} + Y_{23}\frac{V_3^{G3}}{3} + \frac{I_2^{G2}}{3}\right), \end{aligned} \tag{9.23}$$

$$\begin{aligned} I_3 = &Y_{13}V_1 + Y_{23}V_2 - Y_{33}V_3 \\ &+ \left(Y_{13}\frac{V_1^{G1}}{3} + Y_{23}\frac{V_2^{G2}}{3} - Y_{33}\frac{V_3^{G3}}{3} + \frac{I_3^{G3}}{3}\right). \end{aligned} \tag{9.24}$$

The values of the constituent voltage and current sources of the generalized equivalent generator do not depend on the conductivity y_N in Fig. 9.10. It represents a practical interest. This conductivity can be a part of the fourth changeable load.

Besides, the bunch center parameters of one load do not depend on the conductivities entering into the circuit of other loads. For example, the center G_1 is defined by elements y_1, y_{1N} and does not depend from y_2, y_{2N}, and y_3, y_{3N}.

Example 2 We use the date of Example 3, Sect. 6.2. Expressions (9.20) give the values

$$U_1 = \frac{10}{3} + 1.948 = 5.28133, \quad J_1 = \frac{15}{3} - 0.974 = 4.026,$$
$$U_2 = \frac{15}{3} + 1.64 = 6.64, \quad J_2 = \frac{16.25}{3} - 0.82 = 4.596,$$
$$U_3 = \frac{9.377}{3} + 1.61 = 4.7356, \quad J_3 = \frac{14.844}{3} - 1.61 = 3.338.$$

We check relationships (9.21)

$$J_1 = 1.236 \cdot 5.2813 - 0.176 \cdot 6.64 - 0.282 \cdot 4.7356 = 4.026,$$
$$J_2 = -0.176 \cdot 5.2813 + 0.966 \cdot 6.64 - 0.188 \cdot 4.7356 = 4.596,$$
$$J_3 = -0.282 \cdot 5.2813 - 0.188 \cdot 6.64 + 1.283 \cdot 4.7356 = 3.338.$$

SC currents (9.22)–(9.24)

$$I_1^{SC} = \left(-1.236\frac{10}{3} + 0.176\frac{15}{3} + 0.282\frac{9.377}{3} + \frac{15}{3}\right) = 2.641,$$
$$I_2^{SC} = \left(0.176\frac{10}{3} - 0.966\frac{15}{3} + 0.188\frac{9.377}{3} + \frac{16.25}{3}\right) = 1.761,$$
$$I_3^{SC} = \left(0.282\frac{10}{3} + 0.188\frac{15}{3} - 1.283\frac{9.377}{3} + \frac{14.844}{3}\right) = 2.817.$$

References

1. Bessonov, L.A.: Teoreticheskie Osnovy Elektrotekhniki. Elektricheskie tsepi, Izd.9. (Basic Electrical Engineering Theory: Electric Circuits, 9th edn.). Vyshaia shkola, Moskva (1996)
2. Penin, A.: About the definition of parameters and regimes of active two-port networks with variable loads on the basis of projective geometry. WSEAS Trans. Circuits Syst. **10**(5), 157–172 (2011). http://www.worldses.org/journals/circuits/circuits-2011.htm. Accessed 30 Nov 2014
3. Penin, A.: Parameters and characteristics of the modified equivalent generator of an active multiport network. Elektrichestvo **5**, 32–39 (2012)

Part III
Circuits with Non-Linear Regulation Curves

Chapter 10
Regulation of Load Voltages

10.1 Base Model. Display of Conformal Geometry

In power supply systems with limited voltage source power, the restriction of load power, two-valued regulation characteristic, and interference of several loads is observed [15]. Distributed power supply systems, autonomous or hybrid power supply systems with solar cells, fuel elements, and accumulators may be examples of such systems [8].

At the present time, a digital control of voltage converters is used. One way of the digital control performance is a predictive technique. In one switching period, a duty cycle for the next switching cycle is calculated, based on a sensed or observed state and input/output information [2, 3].

Also, a feed-forward control method improves a load regulation dynamics of converter [1]. This method calculates the required duty ratio variation by a predicted load current.

Therefore, it is necessary to take into account an internal resistance of power supply, to carry out analysis of the load interference and obtain relationships for definition of regime parameters at the possible coordinated predictive control for preset load regimes. To simplify the solution of task and to reveal basic moments of this influence, it is expedient to consider static regulation characteristics and idealized models of voltage converters.

Anyway, we consider a power supply system with two regulated voltage converters (or voltage regulators $VR1$, $VR2$) and given loads R_1, R_2 in Fig. 10.1 [9–11, 13]. Generally, voltage converters with switched tapped secondary windings of transformers, multicell or multilevel voltage converters, pulse-width modulation PWM converters, and so on may be examples of these regulators.

The regulators define transformation ratios n_1, n_2

$$n_1 = \frac{V_1}{V}, \quad n_2 = \frac{V_2}{V}. \tag{10.1}$$

A. Penin, *Analysis of Electrical Circuits with Variable Load Regime Parameters*, Power Systems, DOI 10.1007/978-3-319-28451-4_10

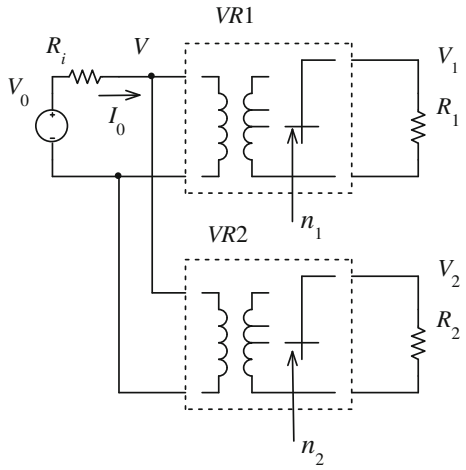

Fig. 10.1 Power supply system with regulation of load voltagesof load voltages

The interference of the regulators on the load voltages V_1, V_2 is observed because of an internal resistance R_i.

Let us obtain equations describing behavior of this circuit at change of the values n_1, n_2.

From (10.1) it is evident

$$V_1 = n_1 V, \quad V_2 = n_2 V.$$

The total load power

$$P_L = \frac{1}{R_1}(V_1)^2 + \frac{1}{R_2}(V_2)^2 = \left(\frac{1}{R_1}(n_1)^2 + \frac{1}{R_2}(n_2)^2\right)(V)^2.$$

On the other hand,

$$P_L = I_0 V = \frac{V_0 - V}{R_i} V.$$

Finally, we get the required equation

$$\frac{R_i}{R_1}(V_1)^2 + \frac{R_i}{R_2}(V_2)^2 + \left(V - \frac{V_0}{2}\right)^2 = \frac{(V_0)^2}{4}. \tag{10.2}$$

This expression represents a sphere by the coordinates V_1, V_2, V in Fig. 10.2. For simplification of drawing, the axes V_1, V_2 are superposed.

In turn, the variables n_1, n_2 are resulted by a stereographic projection of sphere's points from the pole 0, 0, 0 [14]. These variables define the conformal plane $n_1 n_2$ [4] the axes n_1, n_2 are superposed too.

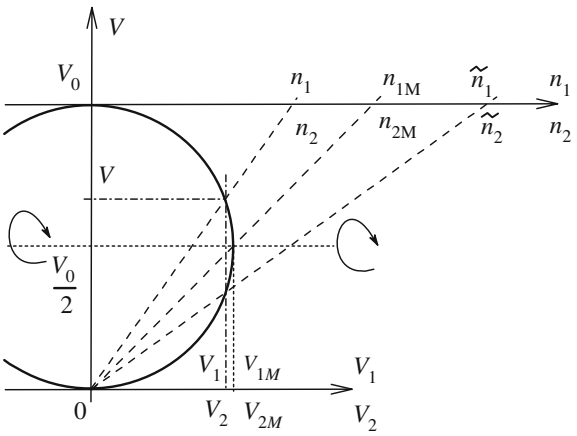

Fig. 10.2 Stereographic projection of sphere's points on a tangent plane n_1n_2

In the plane V_1, V_2 we have an area of voltage changes. This area is defined by the internal area of circle (ellipse) in Fig. 10.3a and corresponds to the sphere's equator. In this case $V = V_0 / 2$. Taking into account (10.2), we obtain the equation of this circle

$$\frac{R_i}{R_1}(V_1)^2 + \frac{R_i}{R_2}(V_2)^2 = \frac{(V_0)^2}{4}. \tag{10.3}$$

In the plane n_1n_2 this equation has the form

$$\frac{R_i}{R_1}(n_1)^2 + \frac{R_i}{R_2}(n_2)^2 = 1. \tag{10.4}$$

Then, we get the maximum load voltages

$$V_{1M} = \pm\frac{V_0}{2}\sqrt{\frac{R_1}{R_i}}, \quad V_{2M} = \pm\frac{V_0}{2}\sqrt{\frac{R_2}{R_i}}. \tag{10.5}$$

Similarly, the maximum transformation ratios

$$n_{1M} = \pm\sqrt{\frac{R_1}{R_i}}, \quad n_{2M} = \pm\sqrt{\frac{R_2}{R_i}}. \tag{10.6}$$

Let, for example, the first load voltage regime $V_1 = const$ (there is a line L_1 in Fig. 10.3a) be supported by n_1, n_2 changes. Then, a sphere's circular section L_1 and corresponding circle L_1 in the plane n_1n_2 (there is a line L_1 in Fig. 10.3b) turns out.

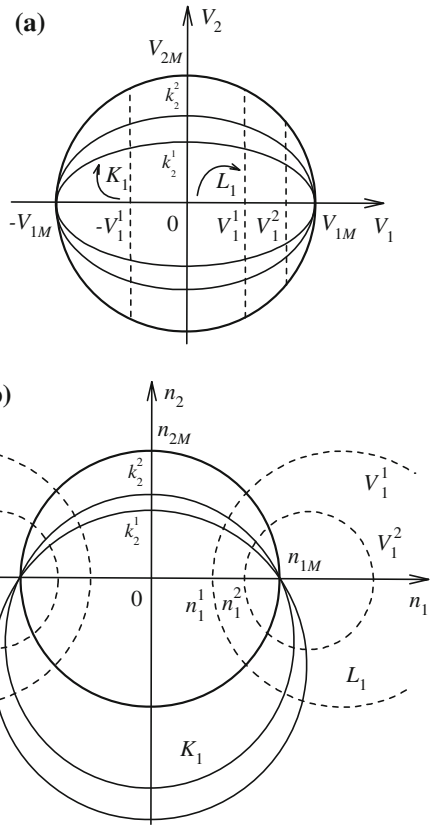

Fig. 10.3 **a** Lines L_1, K_1 of characteristic regimes in the plane V_1V_2. **b** The same lines in the conformal plane n_1n_2

Let us obtain the equation of this circle L_1.
From (10.1) it is evident

$$(V_1)^2 = (n_1)^2V^2, \quad (V_2)^2 = (n_2)^2V^2.$$

Then, by (10.2)

$$V = \frac{V_0}{1 + \frac{R_i}{R_1}(n_1)^2 + \frac{R_i}{R_2}(n_2)^2}. \tag{10.7}$$

Therefore, we have

$$V_1 = \frac{n_1V_0}{1 + \frac{R_i}{R_1}(n_1)^2 + \frac{R_i}{R_2}(n_2)^2}. \tag{10.8}$$

Thus, the equation of the circle L_1 has the view

$$\frac{R_i}{R_2}(n_2)^2 + \frac{R_i}{R_1}(n_1)^2 - n_1\frac{V_0}{V_1} + 1 = 0, \tag{10.9}$$

where the voltage V_1 is a parameter.

The points of intersection of the circle L_1 with the axis n_1 correspond to Eq. (10.9) as $n_2 = 0$. Then

$$(n_1)^2 - n_1\frac{R_1}{R_i}\frac{V_0}{V_1} + \frac{R_1}{R_i} = 0.$$

Roots $n_1, \tilde{n}_1$ of this equation are characterized by the inverse property

$$n_1 \cdot \tilde{n}_1 = \frac{R_1}{R_i} = (n_{1M})^2.$$

Therefore, in the plane n_1n_2, the two families of circles L_1 correspond to the parallel straight lines in the plane V_1V_2 for different values V_1. These two families of circles have the centers $\pm\, n_{1M}$. In turn, the values $\pm\, n_{1M}$ conform to maximum voltages $\pm\, V_{1M}$.

Such families of circles L_1 describe the regime $V_1 = const$ as the rotation group of sphere, as it is shown by arrows in Figs. 10.2 and 10.4.

This motion of points $n^1 \rightarrow n^2$ has the two fixed points $\pm\, n_{1M}$ and it is the elliptic projectivity in the form

$$n^2 = \frac{an^1 + b}{cn^1 + d}, \tag{10.10}$$

where coefficients a, b, c, d are parameters [5, 6]. The initial point $n^1 = n_1^1 + jn_2^1$ and subsequent point $n^2 = n_1^2 + jn_2^2$ are complex values.

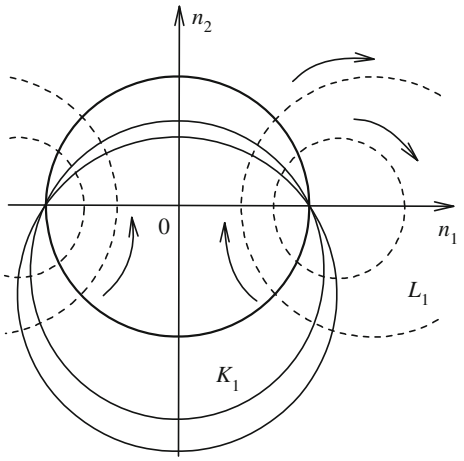

Fig. 10.4 Regime $V_1 = const$ as the rotation group of sphere

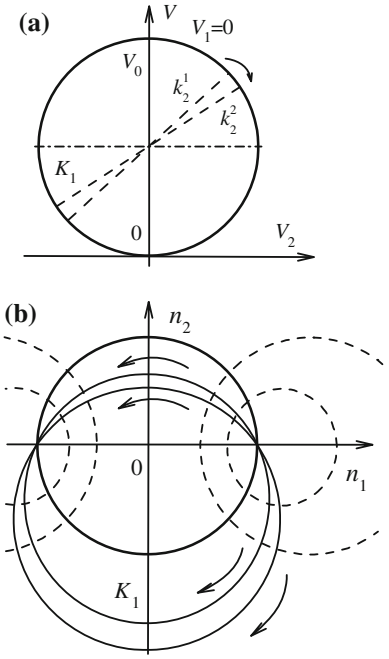

Fig. 10.5 **a** Rotation of the equatorial plane of sphere in the coordinate plane V, V_2 gives the circle family K_1. **b** Moving of points of the circles K_1 as a hyperbolic transformation

Let a set of initial points be situated on the sphere's equator for different values of V_1. Projective transformation (10.10) shifts each initial point along its circle L_1. In turn, all subsequent points constitute an arc of circle K_1 in Fig. 10.4. This circle K_1 is orthogonal to all circles of family L_1.

Let us consider this shift in detail. The rotation of the equatorial plane of sphere about its diameter, shown by arrows in Fig. 10.2, gives the circle family K_1 with parameters k_2^1, k_2^2, and so on in Fig. 10.3. This rotation by the coordinates $V\,V_2$ is shown in Fig. 10.5a.

In turn, in the plane V_1V_2, the projected circles k_2^1, k_2^2 give the family of ellipses K_1, as shown in Fig. 10.3a. Let us obtain the equation of this ellipse.

By Fig. 10.5a, we have

$$V_2 = k_2\left(V - \frac{V_0}{2}\right) = n_2 V, \tag{10.11}$$

where k_2 is an angular coefficient. Therefore

$$\left(V - \frac{V_0}{2}\right) = \frac{V_2}{k_2}.$$

Substituting this expression in (10.2), we get

$$\frac{R_i}{R_1}(V_1)^2 + \left(\frac{R_i}{R_2} + \frac{1}{(k_2)^2}\right)(V_2)^2 = \frac{(V_0)^2}{4}. \tag{10.12}$$

Next, we obtain the equation of corresponding circles in the plane n_1n_2. From (10.11) it follows that

$$\frac{V_0}{V} = 2\frac{k_2 - n_2}{k_2}.$$

Using (10.7), we get the required equation of circle K_1

$$\frac{R_i}{R_2}(n_2)^2 + \frac{R_i}{R_1}(n_1)^2 + 2\frac{n_2}{k_2} - 1 = 0. \tag{10.13}$$

This expression corresponds to (10.4) as $k_2 = \infty$. The moving of points of the circles K_1 is shown by arrows in Fig. 10.5b. Such moving, as a hyperbolic transformation with the two fixed points $\pm n_{1M}$, has form (10.10) too.

10.2 Using of Hyperbolic Geometry Model

At the increase of the values n_1, n_2 on some step of switching cycle, a running point may pass over the equator and the voltage V_2 is going down that is inadmissible. Therefore, it is better to use such groups of transformations or movements of points in the plane n_1n_2, when it is impossible to move out the running point over the circle or equator of sphere. So, we must decrease the next values n_1, n_2 by some rule.

In this sense, we come to hyperbolic geometry [7]. There is Poincare's model in the plane n_1, n_2 shown in Fig. 10.6. The corresponding circle carries the name of absolute and defines an infinitely remote border. The equation of absolute conforms to (10.4).

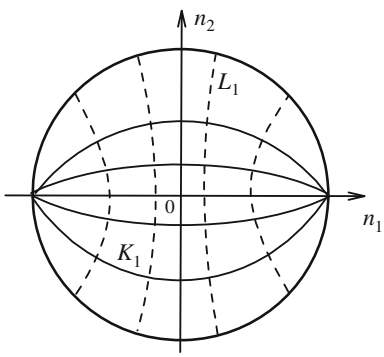

Fig. 10.6 Poincare's model of hyperbolic geometry

The arcs of circles L_1 are "straight lines" of this model. In turn, the arcs of circles K_1 are the lines too. The distance between these lines is constant. The straight lines L_1 are orthogonal to these equidistant lines K_1.

In turn, the Beltrami– Klein model is the other hyperbolic geometry model in the plane V_1V_2 in Fig. 10.3a. The lines L_1, K_1 of this model have the same sense.

Now, we may obtain required expressions or rules of regime parameters and their changes.

10.2.1 Case of One Load

At first, we consider our power supply system with one load, as $n_2 = 0$, $V_2 = 0$.

Using (10.8), we get the regulation characteristic equation

$$V_1 = \frac{n_1 V_0}{1 + \frac{R_i}{R_1}(n_1)^2}.$$

For example, this regulation characteristic is shown in Fig. 10.7a as $R_i = R_1$.

Let us consider transformation (10.10). In the given case, this expression is a projective transformation for the real variable n_1. The regime change goes only on the axes V_1, n_1 as it is illustrated by arrows. Points n_1^1, n_1^2 of initial and subsequent regime form a segment $n_1^1 n_1^2$. The moving of this segment for different initial points and the conformity of variables n_1, V_1 is shown in Fig. 10.7b.

It is obvious that the Euclidean length of segment $n_1^1 n_1^2$ is being decreased, while this segment approaches to the fixed points $\pm\, n_{1M}$ of the absolute.

We know that a projective transformation has an invariant in the form of cross-ratio for four points. In the given case, there are these two fixed points (as the base points), point n_1^1 of initial regime, and point n_1^2 of subsequent one.

Then, the cross-ratio m_n^{21}, which corresponds to the regime change, has the form [12]

$$m_n^{21} = (-n_{1M}\ \ n_1^2\ \ n_1^1\ \ n_{1M}) = \frac{n_1^2 + n_{1M}}{n_{1M} - n_1^2} \div \frac{n_1^1 + n_{1M}}{n_{1M} - n_1^1}. \tag{10.14}$$

The value of this cross-ratio is constant for different initial points, as it is shown in Fig. 10.7b.

It is also possible to constitute the cross-ratio m_n^1 for the initial or running regime n_1^1 relatively to the origin of coordinate $n_1 = 0$; that is,

$$m_n^1 = (-n_{1M}\ \ n_1^1\ \ 0\ \ n_{1M}) = \frac{n_1^1 + n_{1M}}{n_{1M} - n_1^1}. \tag{10.15}$$

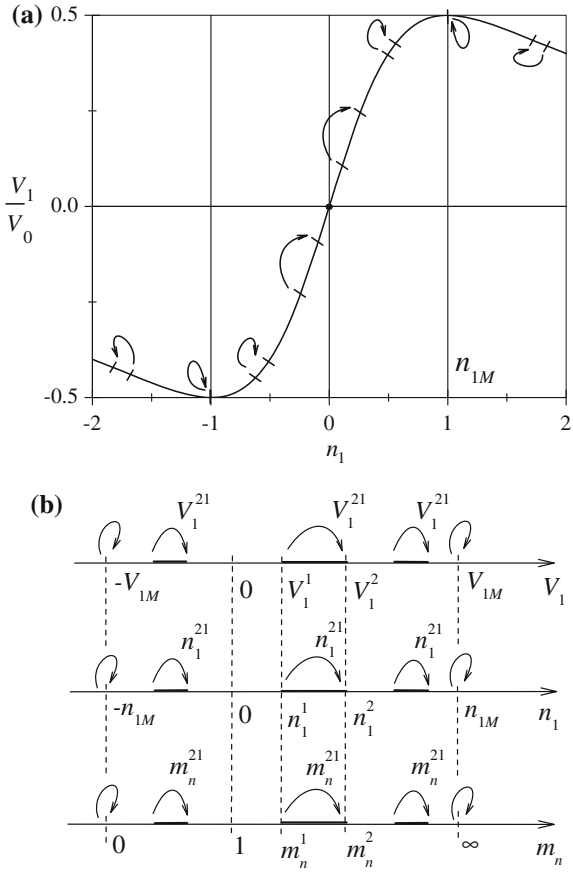

Fig. 10.7 **a** Regulation characteristic. **b** Moving of a segment for different initial points

The conformity of the values n_1^1, m_n^1 is shown in Fig. 10.7b too.

The value m_n^1 determines the non-uniform projective coordinate of the value n_1^1. Hence, the point $n_1 = 0$ is a unite point.

In the same way, the cross-ratio for the subsequent regime n_1^2

$$m_n^2 = (-n_{1M}\ \ n_1^2\ \ 0\ \ n_{1M}) = \frac{n_1^2 + n_{1M}}{n_{1M} - n_1^2}. \tag{10.16}$$

Obviously, a group property is executed; a subsequent regime value is equals to initial regime value multiplied by regime change value.

Let us obtain transformation (10.10) for our case. To do this, using normalized values

$$\bar{n}_1^2 = \frac{n_1^2}{n_{1M}}, \quad \bar{n}_1^1 = \frac{n_1^1}{n_{1M}},$$

we get (10.14) in the form

$$m_n^{21} = (-1 \;\; \bar{n}_1^2 \;\; \bar{n}_1^1 \;\; 1) = \frac{\bar{n}_1^2 + 1}{1 - \bar{n}_1^2} \div \frac{\bar{n}_1^1 + 1}{1 - \bar{n}_1^1}. \tag{10.17}$$

Then, the subsequent value

$$\bar{n}_1^2 = \frac{\bar{n}_1^1 + (m_n^{21} - 1)/(m_n^{21} + 1)}{1 + \bar{n}_1^1 (m_n^{21} - 1)/(m_n^{21} + 1)}. \tag{10.18}$$

We may introduce a value

$$n_1^{21} = \frac{m_n^{21} - 1}{m_n^{21} + 1}. \tag{10.19}$$

Finally, we obtain

$$\bar{n}_1^2 = \frac{\bar{n}_1^1 + n_1^{21}}{1 + \bar{n}_1^1 n_1^{21}}. \tag{10.20}$$

There is a required property of this transformation. If the initial value $\bar{n}_1^1 = 1$, then the subsequent value $\bar{n}_1^2 = 1$ for various values n_1^{21}.

In turn,

$$n_1^{21} = \frac{\bar{n}_1^2 - \bar{n}_1^1}{1 - \bar{n}_1^2 \bar{n}_1^1}. \tag{10.21}$$

So, *there is a strong reason to introduce the transformation ratio change as* n_1^{21}.

Let us now consider the variable V_1. Then, the cross-ratio m_V for the initial regime V_1^1 and subsequent regime V_1^2 has the form

$$m_V^1 = (-V_{1M} \;\; V_1^1 \;\; 0 \;\; V_{1M}) = \frac{V_1^1 + V_{1M}}{V_{1M} - V_1^1}, \quad m_V^2 = \frac{V_1^2 + V_{1M}}{V_{1M} - V_1^2}. \tag{10.22}$$

The following equality takes place:

$$m_V = (m_n)^2. \tag{10.23}$$

This expression leads to identical values if we use the hyperbolic metric to determine a regime value

$$S = Ln\, m_V = 2Ln\, m_n. \tag{10.24}$$

Using normalized values

$$\bar{V}_1^2 = \frac{V_1^2}{V_{1M}}, \quad \bar{V}_1^1 = \frac{V_1^1}{V_{1M}},$$

we get (10.8) in the form

$$\bar{V}_1 = \frac{2\bar{n}_1}{1 + (\bar{n}_1)^2}. \tag{10.25}$$

Similarly to (10.20) and (10.21), it follows that

$$\bar{V}_1^2 = \frac{\bar{V}_1^1 + V_1^{21}}{1 + \bar{V}_1^1 V_1^{21}}, \tag{10.26}$$

$$V_1^{21} = \frac{\bar{V}_1^2 - \bar{V}_1^1}{1 - \bar{V}_1^2 \bar{V}_1^1}. \tag{10.27}$$

Thus, *there is a strong reason to introduce the value of voltage change as* V_1^{21}.

The validity of such definition for the changes n_1^{21} and V_1^{21} is confirmed by expression (10.25); that is,

$$V_1^{21} = \frac{2n_1^{21}}{1 + (n_1^{21})^2}. \tag{10.28}$$

Therefore, *a concrete kind of circuit and character of regime determines system parameters.*

Hence, arbitrary expressions are excluded.

10.2.2 Case of Two Loads

Moving of points in the plane $\bar{n}_1\bar{n}_2$

Let us consider the kinds of points move in the plane $\bar{n}_1\bar{n}_2$ with the aid of Fig. 10.6. The arcs of lines L_1, K_1 are virtual trajectories of regime changes. In turn, points of initial and subsequent regimes are labeled on these lines, as it is shown in Fig. 10.8.

The family of lines L_1 corresponds to the voltages or parameters V_1^1, V_1^2, and so on. These lines intersect the lines K_1 with parameters k_2^1, k_2^2, and so on.

As the result, we have the sets of points on the lines L_1. For example, there are points C_{1n}, D_{1n} for the line with V_1^1 parameter.

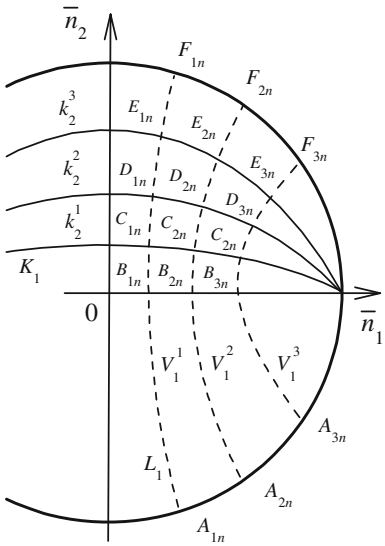

Fig. 10.8 Lines L_1, K_1 as virtual trajectories of regime change

System of Eqs. (10.9) and (10.13)

$$\begin{cases} \dfrac{R_i}{R_2}(n_2)^2 + \dfrac{R_i}{R_1}(n_1)^2 - n_1\dfrac{V_0}{V_1} + 1 = 0 \\ \dfrac{R_i}{R_2}(n_2)^2 + \dfrac{R_i}{R_1}(n_1)^2 + 2\dfrac{n_2}{k_2} - 1 = 0\,. \end{cases}$$

determines coordinates of these points.

This system gives the quadratic equation for n_1

$$\left[\left(k_2\frac{V_0}{2V_1}\right)^2\frac{R_i}{R_2} + \frac{R_i}{R_1}\right](n_1)^2 - \frac{V_0}{V_1}\left[(k_2)^2\frac{R_i}{R_2} + 1\right]n_1 + \left[(k_2)^2\frac{R_i}{R_2} + 1\right] = 0. \tag{10.29}$$

In turn,

$$n_2 = k_2\left(1 - n_1\frac{V_0}{2V_1}\right). \tag{10.30}$$

Further, we must determine the coordinates of points A_1, F_1 with the aid of Eqs. (10.4) and (10.9)

$$\begin{cases} \frac{R_i}{R_2}(n_2)^2 + \frac{R_i}{R_1}(n_1)^2 - n_1\frac{V_0}{V_1} + 1 = 0 \\ \frac{R_i}{R_2}(n_2)^2 + \frac{R_i}{R_1}(n_1)^2 - 1 = 0. \end{cases}$$

Then

$$n_1 = 2\frac{V_1}{V_0}, \quad n_2 = \pm\sqrt{\frac{R_2}{R_i} - \frac{R_2}{R_1}\left(2\frac{V_1}{V_0}\right)^2}. \tag{10.31}$$

Moving of points along the line L_1

Let us constitute the cross-ratio m_{nL1}^{21} that corresponds to the regime change; that is, points C_{1n}, D_{1n} of line L_1 and line K_1 with parameters k_2^1, k_2^2.

Then

$$m_{nL1}^{21} = (A_{1n}\ D_{1n}\ C_{1n}\ F_{1n}) = \frac{D_{1n} - A_{1n}}{D_{1n} - F_{1n}} \div \frac{C_{1n} - A_{1n}}{C_{1n} - F_{1n}}. \tag{10.32}$$

The coordinates of the points A_{1n}, C_{1n}, D_{1n}, F_{1n} are defined by normalized complex values

$$\bar{n}^{A1} = \bar{n}_1^{A1} + j\bar{n}_2^{A1}, \quad \bar{n}^{C1} = \bar{n}_1^{C1} + j\bar{n}_2^{C1},$$
$$\bar{n}^{D1} = \bar{n}_1^{D1} + j\bar{n}_2^{D1}, \quad \bar{n}^{F1} = \bar{n}_1^{F1} + j\bar{n}_2^{F1}.$$

In particular, the coordinates of A_1, F_1, are conjugate complex values

$$\bar{n}_1^{A1} = \bar{n}_1^{F1}, \quad j\bar{n}_2^{A1} = -j\bar{n}_2^{F1},$$

where $\bar{n}_1^{F1} = \bar{V}_1^1$, $(\bar{n}_1^{F1})^2 + (\bar{n}_2^{F1})^2 = 1$.

Then, the cross-ratio has the form

$$m_{nL1}^{21} = (\bar{n}^{A1}\,\bar{n}^{D1}\,\bar{n}^{C1}\,\bar{n}^{F1}) = \frac{\bar{n}^{D1} - \bar{n}^{A1}}{\bar{n}^{D1} - \bar{n}^{F1}} \div \frac{\bar{n}^{C1} - \bar{n}^{A1}}{\bar{n}^{C1} - \bar{n}^{F1}}. \tag{10.33}$$

The result of calculation shows that this cross-ratio is a real value. The cross-ratio m_{nL1}^{21} corresponds to the points C_{2n}, D_{2n} and so on.

Let us determine transformation (10.10) for the line L_1 with parameter V_1^1. Using (10.33), we get the subsequent value

$$\bar{n}^{D1} = \frac{\left[\bar{n}_1^{F1} + j\bar{n}_2^{F1}(1 + m_{nL1}^{21})/(m_{nL1}^{21} - 1)\right]\bar{n}^{C1} - 1}{\bar{n}^{C1} - \left[\bar{n}_1^{F1} - j\bar{n}_2^{F1}(1 + m_{nL1}^{21})/(m_{nL1}^{21} - 1)\right]}, \tag{10.34}$$

where $\bar{n}^{C1}$ is the initial value.

In particular, when the initial and subsequent value situated on the axis $\bar{n}_2$, this expression has the form

$$\bar{n}_2^{D1} = \frac{\bar{n}_2^{C1} + (1 + m_{nL1}^{21})/(m_{nL1}^{21} - 1)}{1 + \bar{n}_2^{C1}(1 + m_{nL1}^{21})/(m_{nL1}^{21} - 1)}.$$

This transformation conforms to (10.18) of one load.

Moving of points along the line K_1

Similarly, we have the sets of points on the lines K_1. For example, there are points C_{1n}, C_{2n} for the line with k_2^1 parameter.

Let us constitute the cross-ratio m_{nK1}^{21} that corresponds to the regime change; that is, points C_{1n}, C_{2n}

$$m_{nK1}^{21} = (-1 \;\; C_{2n} \;\; C_{1n} \;\; 1) = \frac{C_{2n} + 1}{C_{2n} - 1} \div \frac{C_{1n} + 1}{C_{1n} - 1}. \tag{10.35}$$

The coordinate of C_{2n} is defined by normalized complex value

$$\bar{n}^{C2} = \bar{n}_1^{C2} + j\bar{n}_2^{C2}.$$

Then, the cross-ratio has the form

$$m_{nK1}^{21} = (-1 \;\; \bar{n}^{C2} \;\; \bar{n}^{C1} \;\; 1) = \frac{\bar{n}^{C2} + 1}{1 - \bar{n}^{C2}} \div \frac{\bar{n}^{C1} + 1}{1 - \bar{n}^{C1}}. \tag{10.36}$$

The result of calculation shows that this cross-ratio is a real value. The cross-ratio m_{nK1}^{21} corresponds to points, D_{1n}, D_{2n} and so on.

Let us determine transformation (10.10) for line K_1. Using (10.18) and (10.19), we get the subsequent value

$$\bar{n}^{C2} = \frac{\bar{n}^{C1} + n_{K1}^{21}}{1 + \bar{n}^{C1} n_{K1}^{21}}, \tag{10.37}$$

where the real value

$$n_{K1}^{21} = \frac{m_{nK1}^{21} - 1}{m_{nK1}^{21} + 1} \tag{10.38}$$

determinates the transformation ratio change.

Moving of points in the plane $\bar{V}_1\,\bar{V}_2$

Points of initial and subsequent regimes are labeled on the lines L_1, K_1 as it is shown in Fig. 10.9.

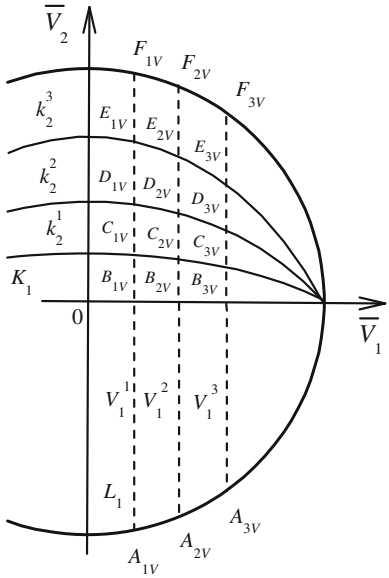

Fig. 10.9 Lines L_1, K_1 as virtual trajectories of regime changes

Moving of points along the line L_1

Similarly to (10.32), let us constitute the cross-ratio

$$m_{VL1}^{21} = (A_{1V}\ D_{1V}\ C_{1V}\ F_{1V}) = \frac{D_{1V} - A_{1V}}{D_{1V} - F_{1V}} \div \frac{C_{1V} - A_{1V}}{C_{1V} - F_{1V}}. \tag{10.39}$$

The coordinates of the points A_{1V}, D_{1V}, C_{1V}, F_{1V} are defined by normalized complex values

$$\begin{aligned} \bar{V}^{A1} &= \bar{V}_1^1 + j\bar{V}_2^{A1}, \quad \bar{V}^{D1} = \bar{V}_1^1 + j\bar{V}_2^{D1}, \\ \bar{V}^{C1} &= \bar{V}_1^1 + j\bar{V}_2^{C1}, \quad \bar{V}^{F1} = \bar{V}_1^1 + j\bar{V}_2^{F1}. \end{aligned} \tag{10.40}$$

In particular, the coordinates of A_{1V}, F_{1V} are conjugate complex values

$$\bar{V}_2^{A1} = -j\bar{V}_2^{F1}.$$

Then, cross-ratio (10.39) has the form

$$m_{VL1}^{21} = \frac{\bar{V}_2^{D1} + \bar{V}_2^{F1}}{\bar{V}_2^{D1} - \bar{V}_2^{F1}} \div \frac{\bar{V}_2^{C1} + \bar{V}_2^{F1}}{\bar{V}_2^{C1} - \bar{V}_2^{F1}} = \frac{\frac{\bar{V}_2^{D1}}{\bar{V}_2^{F1}} + 1}{\frac{\bar{V}_2^{D1}}{\bar{V}_2^{F1}} - 1} \div \frac{\frac{\bar{V}_2^{C1}}{\bar{V}_2^{F1}} + 1}{\frac{\bar{V}_2^{C1}}{\bar{V}_2^{F1}} - 1}. \tag{10.41}$$

The result of calculation shows that equality (10.23) takes place

$$m_{VL1}^{21} = (m_{nL1}^{21})^2. \tag{10.42}$$

Let us determine transformation (10.10) for line L_1 with parameter V_1^1. Using (10.41), (10.36) and (10.37), we get the subsequent value

$$\frac{\bar{V}_2^{D1}}{\bar{V}_2^{F1}} = \frac{\frac{\bar{V}_2^{C1}}{\bar{V}_2^{F1}} + V_{L1}^{21}}{1 + \frac{\bar{V}_2^{C1}}{\bar{V}_2^{F1}} V_{L1}^{21}}, \tag{10.43}$$

where the value

$$V_{L1}^{21} = \frac{m_{VL1}^{21} - 1}{m_{VL1}^{21} + 1} = \frac{\frac{\bar{V}_2^{D1}}{\bar{V}_2^{F1}} - \frac{\bar{V}_2^{C1}}{\bar{V}_2^{F1}}}{1 - \frac{\bar{V}_2^{D1}}{\bar{V}_2^{F1}} \frac{\bar{V}_2^{C1}}{\bar{V}_2^{F1}}} \tag{10.44}$$

determinates the voltage change for $\bar{V}_2$.

Moving of points along the line K_1

Similarly to (10.36) let us constitute the cross-ratio

$$m_{VK1}^{21} = (-1 \;\; \bar{V}_1^2 \;\; \bar{V}_1^1 \;\; 1). \tag{10.45}$$

The result of calculation shows that equality (10.23) and (10.42) takes place

$$m_{VK1}^{21} = (m_{nK1}^{21})^2.$$

Let us determine the transformation which similar to (10.26) for voltage $\bar{V}_1$. Then

$$\bar{V}_1^2 = \frac{\bar{V}_1^1 + V_{K1}^{21}}{1 + \bar{V}_1^1 V_{K1}^{21}}, \tag{10.46}$$

where the value

$$V_{K1}^{21} = \frac{m_{VK1}^{21} - 1}{m_{VK1}^{21} + 1} = \frac{\bar{V}_1^2 - \bar{V}_1^1}{1 - \bar{V}_1^2 \bar{V}_1^1} \tag{10.47}$$

determinates the voltage change for $\bar{V}_1$.

Now, let us determine the transformation for voltage $\bar{V}_2$. To do this, we use ellipse Eq. (10.12) for normalized values

$$(V_1)^2 + \left(1 + \frac{R_2}{R_i}\frac{1}{(k_2)^2}\right)(V_2)^2 = 1. \tag{10.48}$$

Substituting the coordinates $(\bar{V}_1^1,\ \bar{V}_2^1)$, $(\bar{V}_1^2,\ \bar{V}_2^2)$ of the initial C_{1V} and subsequent C_{2V} points into (10.48), we get the system of equation

$$\begin{cases} (\bar{V}_1^1)^2 + \left(1 + \dfrac{R_2}{R_i}\dfrac{1}{(k_2)^2}\right)(\bar{V}_2^1)^2 = 1 \\ (\bar{V}_1^2)^2 + \left(1 + \dfrac{R_2}{R_i}\dfrac{1}{(k_2)^2}\right)(\bar{V}_2^2)^2 = 1. \end{cases}$$

Using (10.46), we obtain the equation for $\bar{V}_2^2$

$$\left(\frac{\bar{V}_1^1 + V_{K1}^{21}}{1 + \bar{V}_1^1 V_{K1}^{21}}\right)^2 + (\bar{V}_2^2)^2 \frac{1 - (\bar{V}_1^1)^2}{(\bar{V}_2^1)^2} = 1.$$

This equation gives the required subsequent voltage

$$\bar{V}_2^2 = \frac{\bar{V}_2^1}{1 + \bar{V}_1^1 V_{K1}^{21}}\sqrt{1 - (V_{K1}^{21})^2}. \tag{10.49}$$

Obtained expressions (10.46) and (10.49), as transformation groups, define a parallel shift or sliding along the axis $\bar{V}_1$; that is, $C_{1V} \rightarrow C_{2V} \rightarrow C_{3V}$ and so on, step by step. The parameter V_{K1}^{21} is the value of this shift. In this case, we have a priority control of the load voltage $\bar{V}_1$. The parallel shift is one of the known three types of movement in the hyperbolic plane.

The obtained expressions may be generalized for three or more loads.

10.3 Example

Consider the circuit in Fig. 10.1. Let the parameters be given as follows:

$$V_0 = 5, \quad R_i = 1, \quad R_1 = 1.25, \quad R_2 = 2.$$

Expression (10.2) of sphere

$$0.8(V_1)^2 + 0.5(V_2)^2 + (V - 2.5)^2 = 6.25.$$

Equations (10.3) and (10.4) of absolute

$$0.8(V_1)^2 + 0.5(V_2)^2 = 6.25,$$
$$0.8(n_1)^2 + 0.5(n_2)^2 = 1.$$

Maximum load voltages (10.5)

$$V_{1M} = \pm 2.5\sqrt{1.25} = 2.795, \quad V_{2M} = \pm 2.5\sqrt{2} = 3.5353.$$

Maximum transformation ratios (10.6)

$$n_{1M} = \pm\sqrt{1.25} = 1.118, \quad n_{2M} = \pm\sqrt{2} = 1.4142.$$

Equation (10.9) of circle L_1

$$0.5(n_2)^2 + 0.8(n_1)^2 - n_1\frac{5}{V_1} + 1 = 0.$$

Equations (10.12) and (10.13) of ellipse and circle K_1

$$0.8(V_1)^2 + \left(0.5 + \frac{1}{(k_2)^2}\right)(V_2)^2 = 6.25,$$
$$0.5(n_2)^2 + 0.8(n_1)^2 + 2\frac{n_2}{k_2} - 1 = 0.$$

10.3.1 Case of One Load

Let the initial and subsequent load voltage be equal to

$$V_1^1 = 1, \quad V_1^2 = 2.5.$$

Then, the corresponding transformation ratios

$$n_1^1 = 0.2068, \quad n_1^2 = 0.6909.$$

Cross-ratio (10.14) of regime change

$$m_n^{21} = \frac{0.6909 + 1.118}{0.6909 - 1.118} \div \frac{0.2068 + 1.118}{0.2068 - 1.118} = 2.913.$$

Cross-ratio (10.15) for the initial regime by n_1^1

$$m_n^1 = \frac{0.2068 + 1.118}{1.118 - 0.2068} = 1.4539.$$

Cross-ratio (10.16) for subsequent regime by n_1^2

$$m_n^2 = \frac{0.6909 + 1.118}{1.118 - 0.6909} = 4.2353 = 2.913 \cdot 1.4539.$$

The normalized transformation ratios

$$\bar{n}_1^2 = \frac{0.6909}{1.118} = 0.618, \quad \bar{n}_1^1 = \frac{0.2068}{1.118} = 0.185.$$

Transformation ratio change (10.19)

$$n_1^{21} = \frac{2.913 - 1}{2.913 + 1} = 0.4888.$$

Projective transformation (10.20) for subsequent value

$$\bar{n}_1^2 = \frac{0.185 + 0.4888}{1 + 0.185 \cdot 0.4888} = 0.618.$$

The next subsequent value $\bar{n}_1^3$ relatively to $\bar{n}_1^2$

$$\bar{n}_1^3 = \frac{\bar{n}_1^2 + 0.4888}{1 + \bar{n}_1^2 \cdot 0.4888} = \frac{0.618 + 0.4888}{1 + 0.618 \cdot 0.4888} = 0.85.$$

and so on.

We see that actual values of the transformation ratio changes are decreasing at each time.

Cross-ratio (10.22) for initial and subsequent regimes by voltages V_1^1, V_1^2

$$m_V^1 = \frac{1 + 2.795}{2.795 - 1} = 2.1142, \quad m_V^2 = \frac{2.5 + 2.795}{2.795 - 2.5} = 17.949.$$

Equality (10.23)

$$m_V^1 = 2.1142 = 1.4539^2, \quad m_V^2 = 17.949 = 4.2353^2.$$

Hyperbolic metric (10.24)

$$S^1 = Ln\,2.1142 = 2Ln\,1.4539 = 0.7486,$$
$$S^2 = Ln\,17.949 = 2Ln\,4.2353 = 2.8875.$$

The normalized voltage values

$$\bar{V}_1^2 = \frac{2.5}{2.795} = 0.8944, \quad \bar{V}_1^1 = \frac{1}{2.795} = 0.3577.$$

Voltage change (10.27)

$$V_1^{21} = \frac{0.8944 - 0.3577}{1 - 0.8944 \cdot 0.3577} = 0.7892.$$

We check expression (10.28)

$$V_1^{21} = \frac{2 \cdot 0.4888}{1 + 0.4888^2} = 0.7892.$$

10.3.2 Case of Two Loads

Plane $\bar{n}_1\bar{n}_2$

Let the load voltages be equal to $V_1^1 = 1$, $V_1^2 = 2.5$, and parameters $k_2^1 = 1$, $k_2^2 = 2$.

The point C_{1n} corresponds to the values $V_1^1 = 1$, $k_2^1 = 1$. Then, Eq. (10.29) has the view

$$\left[\left(\frac{5}{2_1}\right)^2 0.5 + 0.8\right](n_1)^2 - 5(0.5+1)n_1 + (0.5+1) = 0.$$

From here, $n_1^{C1} = 0.2269$.

In accordance with (10.30)

$$n_2^{C1} = (1 - 2.5 \cdot 0.2269) = 0.4326.$$

Similarly, we calculate the coordinates of the point D_{1n}, which corresponds to the values $V_1^1 = 1$, $k_2^2 = 2$.

Table 10.1 Coordinates of four points A_{1n}, C_{1n}, D_{1n}, F_{1n} in the plane $\bar{n}_1\bar{n}_2$

	n_1	n_2	$\bar{n}_1$	$\bar{n}_2$
A_{1n}	0.4	−1.3206	0.3578	−0.9338
C_{1n}	0.2269	0.4326	0.203	0.3059
D_{1n}	0.26	0.7	0.2323	0.4954
F_{1n}	0.4	1.3206	0.3578	0.9338

The coordinates of the point F_{1n} by (10.31)

$$n_1^{F1} = 0.4, \quad n_2^{F1} = \pm\sqrt{2 - \frac{2}{1.25}0.4^2} = \pm 1.3206.$$

The coordinates of all these points are presented in Table 10.1.

Moving of points along the line L_1

Cross-ratio (10.32)

$$m_{nL1}^{21} = \frac{(0.2323 + j0.4954) - (0.4 - j0.9338)}{(0.2323 + j0.4954) - (0.4 + j0.9338)} \div \frac{(0.203 + j0.3059) - (0.4 - j0.9338)}{(0.203 + j0.3059) - (0.4 + j0.9338)} = 1.6282.$$

We obtain the same cross-ratio for the points C_{2n}, D_{2n} with the voltage V_1^2. The coordinates of all required points are presented in Table 10.2.
Using (10.34), we define

$$\frac{1 + m_{nL1}^{21}}{m_{nL1}^{21} - 1} = \frac{1 + 1.6282}{1.6282 - 1} = 4.1837.$$

Then, the subsequent value

$$\bar{n}^{D1} = \frac{(0.203 + j0.3059) \cdot (0.3578 + j0.9338 \cdot 4.1837) - 1}{(0.203 + j0.3059) - (0.3578 - j0.9338 \cdot 4.1837)} = 0.2323 + j0.4953.$$

Table 10.2 Coordinates of four points A_{2n}, C_{2n}, D_{2n}, F_{2n} in the plane $\bar{n}_1\bar{n}_2$

	n_1	n_2	$\bar{n}_1$	$\bar{n}_2$
A_{2n}	1.0	−0.6324	0.8944	−0.4472
C_{2n}	0.7325	0.2674	0.6552	0.1891
D_{2n}	0.7948	0.4104	0.71088	0.2902
F_{2n}	1.0	0.6324	0.8944	0.4472

Moving of points along the line K_1

Cross-ratio (10.35) or (10.36)

$$m_{nK1}^{21} = \frac{(0.6552 + j0.1891) + 1}{(0.6552 + j0.1891) - 1} \div \frac{(0.203 + j0.3059) + 1}{(0.203 + j0.3059) - 1} = 2.9135.$$

Transformation ratio change (10.38)

$$n_{K1}^{21} = \frac{2.9135 - 1}{2.9135 + 1} = 0.4889.$$

Subsequent value (10.37)

$$\bar{n}^{C2} = \frac{(0.203 + j0.3059) + 0.4889}{1 + (0.203 + j0.3059) \cdot 0.4889} = 0.6552 + j0.1891.$$

Plane $\bar{V}_1\,\bar{V}_2$

Moving of points along the line L_1

The coordinates of required points for the voltage $\bar{V}_1^1 = 0.3577$ are given in Table 10.3.

Cross-ratio (10.41)

$$m_{VL1}^{21} = \frac{0.7624 + 0.9338}{0.7624 - 0.9338} \div \frac{0.5391 + 0.9338}{0.5391 - 0.9338} = 2.6519.$$

Equality (10.42)

$$2.6519 = 1.6282^2.$$

Voltage change (10.44)

$$V_{L1}^{21} = \frac{2.6519 - 1}{2.6519 + 1} = 0.4523.$$

Table 10.3 Coordinates of four points A_{1V}, C_{1V}, D_{1V}, F_{1V} in the plane $\bar{V}_1\,\bar{V}_2$ for the given $\bar{V}_1^1 = 0.3577$

	n_1	n_2	V_2	$\bar{V}_2$
A_{1V}	0.4	−1.3206	−3.3015	−0.9338
C_{1V}	0.2269	0.4326	1.906	0.5391
D_{1V}	0.26	0.7	2.6956	0.7624
F_{1V}	0.4	1.3206	3.3015	0.9338

Subsequent value (10.43)

$$\frac{\bar{V}_2^{D1}}{\bar{V}_2^{F1}} = \frac{\frac{0.5391}{0.9338} + 0.4523}{1 + \frac{0.5391}{0.9338} 0.4523} = 0.8164.$$

Moving of points along the line K_1

Cross-ratio (10.45) for the voltages $\bar{V}_1^1 = 0.3577$, $\bar{V}_1^2 = 0.8944$

$$m_{VK1}^{21} = \frac{0.8944 + 1}{0.8944 - 1} \div \frac{0.3577 + 1}{0.3577 - 1} = 8.4867.$$

Let us check the equality $m_{VK1}^{21} = (m_{nK1}^{21})^2$. Then

$$8.4867 = 2.9135^2.$$

Voltage change (10.47)

$$V_{K1}^{21} = \frac{8.4867 - 1}{1 + 8.4867} = 0.7892.$$

Subsequent value (10.46)

$$\bar{V}_1^2 = \frac{0.3577 + 0.7892}{1 + 0.3577 \cdot 0.7892} = 0.8944.$$

Now, we use points of the line L_1 for the voltage $\bar{V}_1^2 = 0.8944$. The coordinates of required points are given in Table 10.4.

We check expression (10.49) for the points C_{1V}, C_{2V}, which correspond to voltages $\bar{V}_2^{C1}$, $\bar{V}_2^{C2}$,

$$\bar{V}_2^{C2} = \frac{\bar{V}_2^{C1}}{1 + \bar{V}_1^1 V_{K1}^{21}} \sqrt{1 - (V_{K1}^{21})^2}$$
$$= \frac{0.5391}{1 + 0.3577 \cdot 0.7892} \sqrt{1 - 0.7892^2} = 0.2582.$$

Table 10.4 Coordinates of four points A_{2V}, C_{2V}, D_{2V}, F_{2V} in the plane $\bar{V}_1\,\bar{V}_2$ for the given $\bar{V}_1^2 = 0.8944$

	n_1	n_2	V_2	$\bar{V}_2$
A_{2V}	1.0	−0.6324	−1.5811	−0.4472
C_{2V}	0.27325	0.2674	0.9128	0.2582
D_{2V}	0.7948	0.4104	1.2909	0.3651
F_{2V}	1.0	0.6324	1.5811	0.4472

In turn, expression (10.49) for the points D_{1V}, D_{2V}

$$\bar{V}_2^{D2} = \frac{\bar{V}_2^{D1}}{1 + \bar{V}_1^1 V_{K1}^{21}} \sqrt{1 - (V_{K1}^{21})^2}$$
$$= \frac{0.7624}{1 + 0.3577 \cdot 0.7892} \sqrt{1 - 0.7892^2} = 0.3651.$$

We see that the results of this calculation coincide with the data of Table 10.4.

References

1. Chae, S., Hyun, B., Agarwal, P., Kim, W., Cho, B.: Digital predictive feed-forward controller for a DC–DC converter in plasma display panel. IEEE Trans. Power Electron. **23**(2), 627–634 (2008)
2. Chattopadhyay, S., Das, S.: A digital current-mode control technique for DC–DC converters. IEEE Trans. Power Electron. **21**(6), 1718–1726 (2006)
3. Chen, J., Prodic, A., Erickson, R.W., Maksimovic, D.: Predictive digital current programmed control. IEEE Trans. Power Electron. **18**(1), 411–419 (2003)
4. Conformal geometry. Encyclopedia Wikipedia. http://en.wikipedia.org/wiki/Conformal_geometry (2014). Accessed 30 Nov 2014
5. Frank, J.A.: Schaum's Outline of Theory and Problems of Projective Geometry. McGraw–Hill, New York (1967)
6. Glagolev, N.A.: Proektivnaia geometria. (Projective geometry). Nauka, Moskva (1963)
7. Hyperbolic geometry. Encyclopedia Wikipedia. http://en.wikipedia.org/wiki/Hyperbolic_geometry (2014). Accessed 30 Nov 2014
8. Lui, X., Wang, P., Loh, P.: A Hybrid AC/ DC micro grid and its coordination control. IEEE Trans. Smart Grid **2**(2), 278–286 (2011)
9. Penin, A.: Geometrical properties of regulated voltage converters at limited capacity voltage sources. Tehnicheskaia elektrodinamika **3**, 61–64 (1991)
10. Penin, A.: Fractionally linear relations in the problems of analysis of resistive circuits with variable parameters. Electrichestvo **11**, 32–44 (1999)
11. Penin, A.: Analysis of regimes of voltage regulators with limited capacity voltage sources. Geometrical approach. WSEAS Trans. Circuits Syst. **12**(1), 12 (2013). http://www.wseas.org/wseas/cms.action?id=6933. Accessed 30 Nov 2014
12. Penin, A.: Projective geometry method in the theory of electric circuits with variable parameters of elements. Int. J. Electron. Commun. Electr. Eng. **3**(2), 18–34 (2013) https://sites.google.com/site/ijeceejournal/volume-3-issue-2. Accessed 30 Nov 2014
13. Penin, A.: Non-Euclidean geometry and regulated characteristics of limited capacity power supply. J. Electr. Eng. **2**(4), 175–186 (2014)
14. Stereographic projection. Encyclopedia Wikipedia. http://en.wikipedia.org/wiki/Stereographic_projection (2014). Accessed 30 Nov 2014
15. Yehia, D.M., Yokomizu, Y., Iioka, D., Matsumura, T.: Delivaraible-power dependence on distribution-line resistance and number of loads in low-voltage DC distribution system. IEEJ Trans. Electr. Electron. Eng. **7**(1), 23–30 (2012)

Chapter 11
Stabilization of Load Voltages

11.1 Analysis of Load Voltage Stabilization Regimes

We use the same power supply system with two idealized voltage regulators $VR1, VR2$, and load resistances R_1, R_2 in Fig. 11.1 [5, 6]. The regulators define the transformation ratios $n_1 = V_1/V_2$, $n_2 = V_2/V$; an internal resistance R_i determines the interference of the voltage regulators on load regimes.

For convenience, we rewrite Eq. (10.2)

$$\frac{R_i}{R_1}(V_1)^2 + \frac{R_i}{R_2}(V_2)^2 + \left(V - \frac{V_0}{2}\right)^2 = \frac{(V_0)^2}{4}. \tag{11.1}$$

11.1.1 Case of One Load

In this case, the transformation ratio $n_2 = 0$. Then,

$$\frac{R_i}{R_1}(V_1)^2 + \left(V - \frac{V_0}{2}\right)^2 = \frac{(V_0)^2}{4}. \tag{11.2}$$

For different load values (R_1^1, R_1^2 and so on), this expression represents a bunch of circles (ellipses) by the coordinates V_1, V in Fig. 11.2.

Let the stabilized load voltage $V_1 = V_{1=}$ be given [7]. Then, the vertical line with the coordinate $V_{1=}$ intersects the bunch of circles in two points.

At the same time, the transformation ratio n_1 is resulted by a stereographic projection of circle's points from the pole 0,0. Therefore, the load resistance R_1^1 corresponds to the variable n_1^1; R_1^2 corresponds to n_1^2 and so on.

A. Penin, *Analysis of Electrical Circuits with Variable Load Regime Parameters*,
Power Systems, DOI 10.1007/978-3-319-28451-4_11

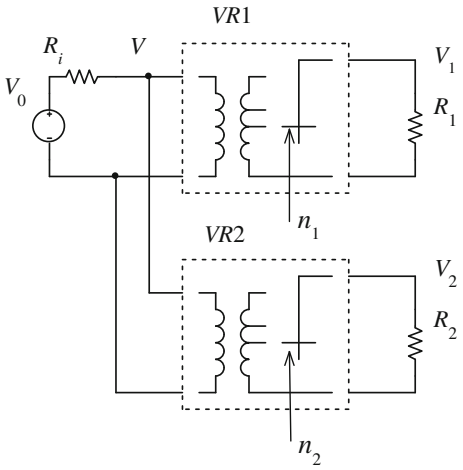

Fig. 11.1 Power supply system with two voltage regulators $VR1, VR2$, and loads R_1, R_2

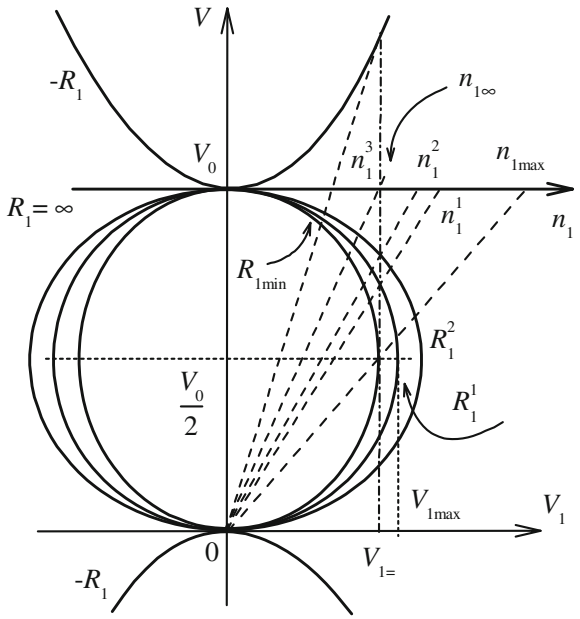

Fig. 11.2 Stereographic projection of bunch of ellipses on a tangent line n_1

For a minimum value $R_{1\min}$ of the load resistance, the circle is tangent to the vertical line $V_{1=}$. In this case, $V = V_0/2$. Using (11.2), we get the condition

$$\frac{R_i}{R_{1\min}}(V_{1=})^2 = \frac{(V_0)^2}{4}.$$

Then, the minimum load resistance value

$$R_{1\min} = 4R_i \frac{(V_{1=})^2}{(V_0)^2}. \tag{11.3}$$

The respective maximum allowable transformation ratio

$$n_{1\max} = 2\frac{V_{1=}}{V_0}. \tag{11.4}$$

The operating area of all the circles must be above the diameters of these circles; that is, $V \geq V_0/2$. Therefore, we use the upper point of the intersection.

In turn, on some step of switching period at increase of the parameter n_1, a running point may pass over the diameter that is inadmissible. Therefore, it is better to use such groups of transformations or movements of points along the line n_1 when it is impossible to move out the running point over the diameter. So, we must decrease the next values n_1 by some rule. In this sense, we come to hyperbolic geometry.

11.1.2 Use of Hyperbolic Geometry

Let us consider the dependence $R_1(n_1, V_{1=})$, where the voltage $V_{1=}$ is a parameter. Similarly to (10.15) and (10.17), we must validate the definition of regime and its changes and find the invariants of regime parameters. To do this, we consider such a characteristic regime as $R_1 = \infty$. In this case, the ellipse degenerates into the two straight lines, $V = 0$, $V = V_0$.

Then, for the voltage $V = V_0$, the transformation ratio

$$n_{1\infty} = \frac{V_{1=}}{V_0}. \tag{11.5}$$

However, the question arises about the range $0 < n_1 < n_{1\infty}$ of this transformation ratio. According to Fig. 11.2, this range corresponds to negative load values $-R_1$ and expression (11.2) determines a hyperbola. In this case, the load gives energy back and the voltage source V_0 consumes this energy as it is shown in Fig. 11.3.

In this regard, we consider a physical realization of such a power source, as a negative resistance. For this purpose, we remind something of the electric circuit theory by examples of two circuits in Fig. 11.4.

Let a voltage source V_1 be connected to a resistance R_1 for the left-hand circuit. Then, the negative resistance $-R_1$ and the drain current I_1 correspond to this voltage source.

We consider Fig. 11.3 again. Then, it is possible to connect up the voltage source V_1 instead of the resistance $-R_1$. At the same time, the input resistance of this

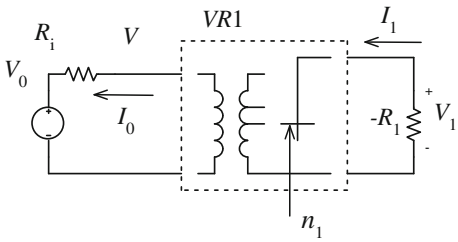

Fig. 11.3 Negative load $-R_1$ gives energy back

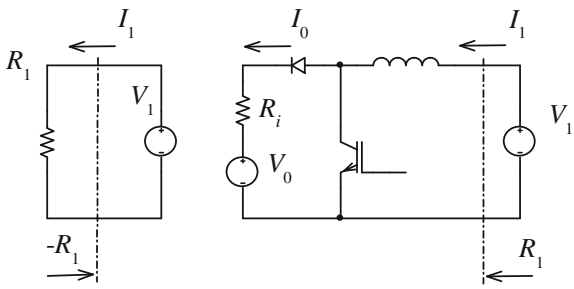

Fig. 11.4 Negative resistance $-R_1$ corresponds to a voltage source V_1 and its practical realization by *PWM* boost converter

circuit must be equal to the constant value R_1 at the voltage V_1 change. This condition is satisfied due to the variable value n_1. We obtain so-called a loss-free resistance [8]. The example of another such a circuit is the right-hand circuit in Fig. 11.4 as a high-power-factor boost rectifier [4].

Taking into account the value $n_1 = V_{1=}/V$ and Eq. (11.2), we obtain

$$V_{1=} = \frac{n_1 V_0}{1 + \frac{R_i}{R_1}(n_1)^2}. \tag{11.6}$$

Thus, the required relationship $n_1(R_1)$ and its inverse $R_1(n_1)$ is obtained

$$(n_1)^2 - n_1 \frac{V_0}{V_{1=}} \frac{R_1}{R_i} + \frac{R_1}{R_i} = 0, \quad \frac{R_1}{R_i} = \frac{(n_1)^2}{n_1 \frac{V_0}{V_{1=}} - 1}. \tag{11.7}$$

In turn, the dependence $R_1(n_1)$ determines a hyperbola in Fig. 11.5.

We have a single-valued mapping of hyperbola points onto the axis n_1. This projective transformation preserves a cross ratio of four points. Similarly to (10.15), let us constitute the cross ratio m_n^1 for the points 0, n_1^1, $n_{1\infty}$, $n_{1\max}$; that is,

$$m_n^1 = (0\ n_1^1\ n_{1\infty}\ n_{1\max}) = \frac{n_1^1 - 0}{n_1^1 - n_{1\max}} \div \frac{n_{1\infty} - 0}{n_{1\infty} - n_{1\max}}, \tag{11.8}$$

where the points $0, n_{1\max}$ are base ones and $n_{1\infty}$ is a unit point.

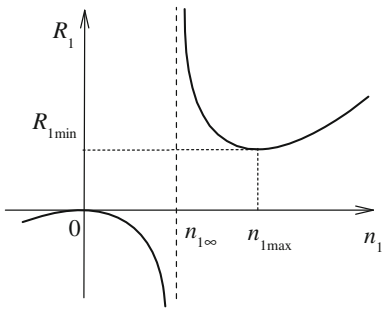

Fig. 11.5 Dependence $R_1(n_1)$

Using (11.4) and (11.5), we get

$$m_n^1 = \begin{pmatrix} 0 & n_1^1 & \dfrac{V_{1=}}{V_0} & 2\dfrac{V_{1=}}{V_0} \end{pmatrix} = \frac{n_1^1}{2\frac{V_{1=}}{V_0} - n_1^1} = \frac{n_1^1}{n_{1\max} - n_1^1}. \tag{11.9}$$

The conformity of the points n_1^1, m_n^1 is shown in Fig. 11.6. In this case, the value m_n^1 is a non-homogeneous coordinate of n_1^1.

Further, the cross ratio m_n^{21}, which corresponds to the regime change $n_1^1 \to n_1^2$, has the form

$$m_n^{21} = (0 \;\; n_1^2 \;\; n_1^1 \;\; n_{1\max}) = \frac{n_1^2(n_1^1 - n_{1\max})}{n_1^1(n_1^2 - n_{1\max})}. \tag{11.10}$$

Using the normalized values

$$\bar{n}_1^2 = \frac{n_1^2}{n_{1\max}}, \quad \bar{n}_1^1 \frac{n_1^1}{n_{1\max}},$$

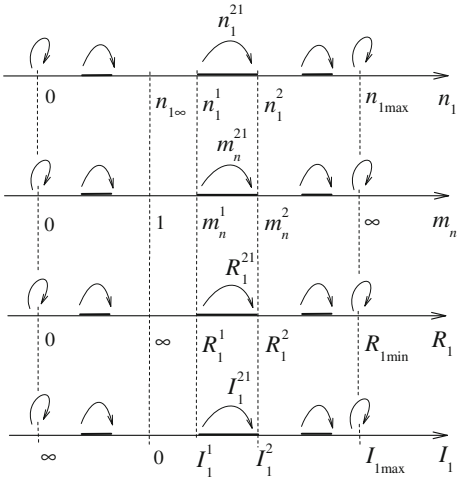

Fig. 11.6 Conformity of different regime parameters

we get the regime change (segment $\bar{n}_1^2\ \bar{n}_1^1$) or cross ratio (11.10) in the view

$$m_n^{21} = (0\ \bar{n}_1^2\ \bar{n}_1^1\ 1) = \frac{\bar{n}_1^2(\bar{n}_1^1 - 1)}{\bar{n}_1^1(\bar{n}_1^2 - 1)}. \tag{11.11}$$

Similarly to (10.19), we may obtain the analogous expression for the change n_1^{21} of the transformation ratio so that the following relationships are performed

$$n_1^{21} = \frac{m_n^{21} - 1}{m_n^{21} + 1}, \quad m_n^{21} = \frac{n_1^{21} + 1}{1 - n_1^{21}}. \tag{11.12}$$

For this purpose, we make the substitution of variables so that to use ready expressions (10.19). Therefore, we introduce the value

$$\tilde{n}_1 = 2\bar{n}_1 - 1 \tag{11.13}$$

This simple conformity of variables is shown in Fig. 11.7.

According to (10.21),

$$\tilde{n}_1^{21} = \frac{\tilde{n}_1^2 - \tilde{n}_1^1}{1 - \tilde{n}_1^2\tilde{n}_1^1}.$$

Using substitution of variables (11.13), we get

$$\tilde{n}_1^{21} = \frac{\bar{n}_1^2 - \bar{n}_1^1}{\bar{n}_1^2 + \bar{n}_1^1 - 2\bar{n}_1^2\bar{n}_1^1} = n_1^{21}. \tag{11.14}$$

In this expression, the changes of the variables are equal to among themselves; that is, $\tilde{n}_1^{21} = n_1^{21}$.

There is a following foundation for this equality. Linear expression (11.13) preserves a cross ratio and, consequently, the regime change m_n^{21}. On the other hand, the change of the transformation ratio n_1^{21} is expressed by regime change (11.12).

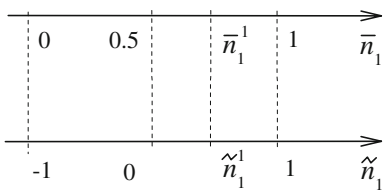

Fig. 11.7 Conformity of the normalized transformation ratio $\bar{n}_1$ and a new variable $\tilde{n}_1$

Using (11.14), we obtain the subsequent transformation ratio

$$\bar{n}_1^2 = \frac{\bar{n}_1^1(1+n_1^{21})}{1+n_1^{21}(2\bar{n}_1^1-1)}. \tag{11.15}$$

There is a group transformation. Moreover, if the initial value $\bar{n}_1^1 = 1$, then the subsequent value $\bar{n}_1^2 = 1$ regardless of the value n_1^{21}. Therefore, such movement of point corresponds to hyperbolic geometry.

Similarly to the above, let us consider the cross ratio for the load resistance R_1. Using the dependence $R_1(n_1)$ in Fig. 11.5, we demonstrate the conformity of the variables R_1, n_1 by Fig. 11.6. The cross ratio for the initial point R_1^1 relatively to the base points $0, R_{1\min}$, and a unit point $R_1 = \infty$ has the form

$$m_R^1 = (0\ R_1^1\ \infty\ R_{1\min}) = \frac{R_1^1 - 0}{R_1^1 - R_{1\min}} = \frac{1}{1 - 4\frac{R_i}{R_1^1}\frac{(V_{1=})^2}{(V_0)^2}}. \tag{11.16}$$

Expression (11.16) equals the corresponding cross ratio for the conductance $Y_1 = 1/R_1$ and the load current $I_1 = U_{1=}/R_1$. Also, the following equality takes place

$$m_R = (m_n)^2. \tag{11.17}$$

This expression leads to identical values if we use the hyperbolic metric to determine a regime value or distance

$$S = Ln\, m_R = 2Ln\, m_n. \tag{11.18}$$

The base points $0, R_{1\min}$ correspond to the infinitely large distance.

Similarly to (11.10), the cross ratio m_R^{21}, which corresponds to the regime change $R_1^1 \to R_1^2$, has the view

$$m_R^{21} = (0\ R_1^2\ R_1^1\ R_{1\min}) = \frac{R_1^2(R_1^1 - R_{1\min})}{R_1^1(R_1^2 - R_{1\min})}. \tag{11.19}$$

We may introduce the change R_1^{21} of the load resistance by the following expression

$$m_R^{21} = \frac{1+R_1^{21}}{1-R_1^{21}}. \tag{11.20}$$

Further, we use the normalized values

$$\bar{R}_1^2 = \frac{R_1^2}{R_{1\min}}, \quad \bar{R}_1^1 = \frac{R_1^1}{R_{1\min}}.$$

Similarly to (11.14), we get

$$R_1^{21} = \frac{\bar{R}_1^2 - \bar{R}_1^1}{\bar{R}_1^2 + \bar{R}_1^1 - 2\bar{R}_1^2\bar{R}_1^1}. \tag{11.21}$$

Then, *there is a strong reason to introduce the value of load resistance change as* R_1^{21} *and the value of transformation ratio change as* n_1^{21}.

The validity of such definitions for changes is confirmed by the following expression similar to initial expression (11.6); that is,

$$R_1^{21} = \frac{2n_1^{21}}{1 + (n_1^{21})^2}. \tag{11.22}$$

Using (2.21), we obtain the subsequent value R_1^2 of the load resistance

$$\bar{R}_1^2 = \frac{\bar{R}_1^1(1 + R_1^{21})}{1 + R_1^{21}(2\bar{R}_1^1 - 1)}. \tag{11.23}$$

As well as (11.15), if the initial value $\bar{R}_1^1 = 1$, then the subsequent value $\bar{R}_1^2 = 1$ regardless of the value R_1^{21}.

Thus, *a concrete kind of a circuit and character of regime imposes the requirements to definition of already system parameters*.

Therefore, arbitrary and formal expressions for regime parameters are excluded.

Example Let the circuit parameters be given as follows

$$V_0 = 5, \quad R_i = 1, \quad V_{1=} = 2.5.$$

The initial and subsequent value of the load resistance

$$R_1^1 = 2.0, \quad R_1^2 = 1.25.$$

Minimum load resistance (11.3)

$$R_{1\min} = 4R_i \frac{(V_{1=})^2}{(V_0)^2} = 1.$$

Maximum transformation ratio (11.4)

$$n_{1\max} = 2\frac{V_{1=}}{V_0} = 1.$$

Transformation ratio (11.5)

$$n_{1\infty} = \frac{V_{1=}}{V_0} = 0.5.$$

The values of the transformation ratio by quadratic Eq. (11.7)

$$n_1^1 = 0.585, \quad n_1^2 = 0.691.$$

The normalized values are equal to these transformation ratios.
Cross ratio (11.8) for the initial regime

$$m_n^1 = (0 \ n_1^1 \ n_{1\infty} \ n_{1\max}) = \frac{0.585}{1 - 0.585} = 1.41.$$

Cross ratio (11.10) for the regime change

$$m_n^{21} = (0 \ n_1^1 \ n_{1\max}) = \frac{n_1^2(n_1^1 - n_{1\max})}{n_1^1(n_1^2 - n_{1\max})} = \frac{2.236}{1.41} = 1.581.$$

Change (11.14) of the transformation ratio

$$n_1^{21} = \frac{\bar{n}_1^2 - \bar{n}_1^1}{\bar{n}_1^2 + \bar{n}_1^1 - 2\bar{n}_1^1\bar{n}_1^2} = \frac{0.106}{0.467} = 0.226.$$

Now, we consider the cross ratio for the load resistance R_1.
Cross ratio (11.16) for the initial regime

$$m_R^1 = (0 \ R_1^1 \ \infty \ R_{1\min}) = \frac{1}{1 - 4\frac{R_i(V_{1=})^2}{R_1^1(V_0)^2}} = \frac{1}{1 - 4\frac{6.25}{2 \cdot 25}} = 2.0.$$

Let us check equality (11.17); that is,

$$m_R^1 = (m_n^1)^2 = 1.41^2 = 2.0.$$

Cross ratio (11.19) for the regime change

$$m_R^{21} = (0 \ R_1^2 \ R_1^1 \ R_{1\min}) = \frac{R_1^2(R_1^1 - R_{1\min})}{R_1^1(R_1^2 - R_{1\min})} = 2.5.$$

The equality

$$m_R^{21} = (m_n^{21})^2 = 1.581^2 = 2.5.$$

Change (11.21) of the load resistance

$$R_1^{21} = \frac{\bar{R}_1^2 - \bar{R}_1^1}{\bar{R}_1^2 + \bar{R}_1^1 - 2\bar{R}_1^1\bar{R}_1^2} = 0.429.$$

Equality (11.22)

$$R_1^{21} = \frac{2n_1^{21}}{1 + (n_1^{21})^2} = \frac{2 \cdot 0.226}{1 + 0.051} = 0.429.$$

11.1.3 Case of Two Loads

Let us now consider a circuit with two loads in Fig. 11.1. The variation of one of these loads leads to a mutual change of stabilization regimes for both loads. Therefore, it is necessary to change the transformation ratios n_1, n_2 in some coordination for the stabilization of $V_{1=}, V_{2=}$. We will obtain the required relationships.

We rewrite Eq. (11.1)

$$\frac{R_i}{R_1}(V_{1=})^2 + \frac{R_i}{R_2}(V_{2=})^2 + \left(V - \frac{V_0}{2}\right)^2 = \frac{(V_0)^2}{4}. \tag{11.24}$$

By definition,

$$n_1 = \frac{V_{1=}}{V}, \quad n_2 = \frac{V_{2=}}{V}. \tag{11.25}$$

Using (11.6), (11.24) and (11.25), we get the system of equations

$$\begin{cases} V_{1=} = \frac{n_1 V_0}{1 + \frac{R_i}{R_1}(n_1)^2 + \frac{R_i}{R_2}(n_2)^2} \\ V_{2=} = \frac{n_2 V_0}{1 + \frac{R_i}{R_1}(n_1)^2 + \frac{R_i}{R_2}(n_2)^2}. \end{cases} \tag{11.26}$$

It follows that

$$\begin{cases} \frac{R_i}{R_1}(n_1)^2 + \frac{R_i}{R_2}(n_2)^2 - \frac{n_1 V_0}{V_{1=}} + 1 = 0 \\ \frac{R_i}{R_1}(n_1)^2 + \frac{R_i}{R_2}(n_2)^2 - \frac{n_2 V_0}{V_{2=}} + 1 = 0. \end{cases} \tag{11.27}$$

By definition (11.25)

$$n_2 = n_1 \frac{V_{2=}}{V_{1=}}. \tag{11.28}$$

Substituting this expression in the first equation of system (11.27), we get

$$(n_1)^2 R_i \left[\frac{1}{R_1} + \frac{1}{R_2} \left(\frac{V_{2=}}{V_{1=}} \right)^2 \right] - \frac{n_1 V_0}{V_{1=}} + 1 = 0. \tag{11.29}$$

The expression in the square brackets is the total resistance (conductance) of both loads relatively to the first load; that is,

$$\frac{1}{R_T} = \frac{1}{R_1} + \frac{1}{R_2} \left(\frac{V_{2=}}{V_{1=}} \right)^2 = Y_T. \tag{11.30}$$

If, for example, the load voltages are equal to among themselves, $V_{2=} = V_{1=}$, then these loads are connected in parallel and

$$\frac{1}{R_T} = \frac{1}{R_1} + \frac{1}{R_2} = Y_T.$$

Finally, we get the expression

$$(n_1)^2 \frac{R_i}{R_T} - \frac{n_1 V_0}{V_{1=}} + 1 = 0. \tag{11.31}$$

This expression corresponds to (11.7) and the dependence $R_T(n_1)$ coincides with Fig. 11.5.

Therefore, for given load resistances, we determine:

- total resistance (11.30);
- transformation ratio n_1 as the solution of (11.31);
- value n_1 by (11.28) or by the second equation of (11.27).

Also, we must check stability conditions (11.3), (11.4). In this case, these conditions have the form

$$\begin{cases} R_{T\min} = 4R_i \frac{(V_{1=})^2}{(V_0)^2} \\ n_{1\max} = 2\frac{V_{1=}}{V_0}, \quad n_{2\max} = 2\frac{V_{2=}}{V_0}. \end{cases} \tag{11.32}$$

Further, it is possible to use the above idea of hyperbolic geometry in the case of one load.

11.2 Given Voltage for the First Variable Load and Voltage Regulation of the Second Given Load

We consider again the circuit shown in Fig. 11.1. Let the first load voltage $V_{1=}$ be stabilized. But for all that, the first load resistance may be both positive $R_1 > 0$ and negative $R_1 < 0$. Also, the second constant load resistance is positive $R_2 > 0$.

For example, the circuit in Fig. 11.8 corresponds to the positive load $R_1 > 0$ and *PWM* regulators in Fig. 11.9a conform to the negative load $R_1 < 0$.

We rewrite Eq. (11.1)

$$\frac{R_i}{R_1}(V_1)^2 + \frac{R_i}{R_2}(V_2)^2 + \left(V - \frac{V_0}{2}\right)^2 = \frac{(V_0)^2}{4},$$

which correspond to a surface with a parameter R_1 in the coordinates V_1, V_2, V_3.

If $R_1 > 0$, this expression represents a sphere (ellipsoid) similarly to the circle in Fig. 11.2. The both loads consume energy; the voltage source V_0 gives energy.

If $R_1 < 0$, we get a one-sheeted hyperboloid in Fig. 11.9b [3]. The first load, as a constant voltage source $V_{1=}$, gives energy. In addition, the voltage source V_0, as energy storage, may consume and give back energy. The corresponding direction of the current I_0 determines these regimes.

For different values R_1, our expression represents a bunch of spheres or hyperboloids. If $R_1 = \infty$, as the open circuit regime, the corresponding surface degenerates into a cylinder.

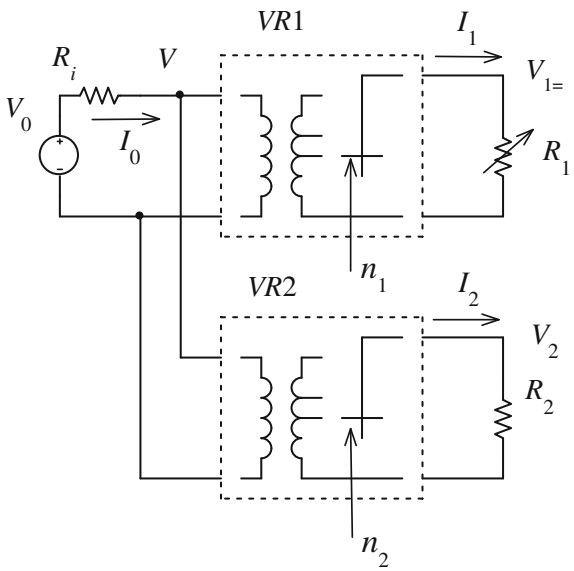

Fig. 11.8 Power supply system with the invariable voltage $V_{1=}$ and given load R_2

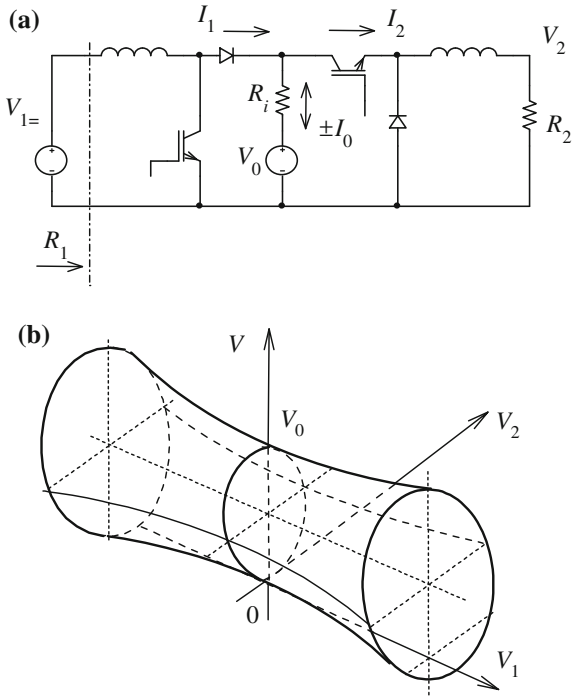

Fig. 11.9 **a** Power supply system with resistance $-R_1$. **b** Its geometric model

Let us now return to given operating regime; that is,

$$V_1 = V_{1=}, \quad R_2 = \text{const}.$$

For realization of this regime, it is necessary to change the transformation ratios n_1, n_2 in some coordination. Let us obtain the required relationships.

So, the plane with the parameter $V_{1=}$ intersects the bunch of spheres and hyperboloids. As the result of this section, the bunch of circles in coordinates V_2, V is obtained, as it is shown in Fig. 11.10.

In this case, our expression has the form

$$\frac{R_i}{R_2}(V_2)^2 + \left(V - \frac{V_0}{2}\right)^2 = \frac{(V_0)^2}{4} - \frac{R_i}{R_1}(V_{1=})^2. \tag{11.33}$$

The second member of this equation is a radius of circle for the given value R_1.

It is possible to consider the voltage V_2 change as the radius-vector rotation. This rotation determines a point movement along the straight line $V_{1=}$ in coordinates V_1, V in Fig. 11.11. This figure at $V_2 = 0$ is analogous to Fig. 11.2.

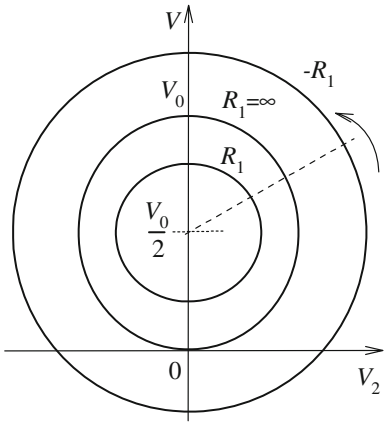

Fig. 11.10 Bunch of circles for different R_1 as $V_{1=}$

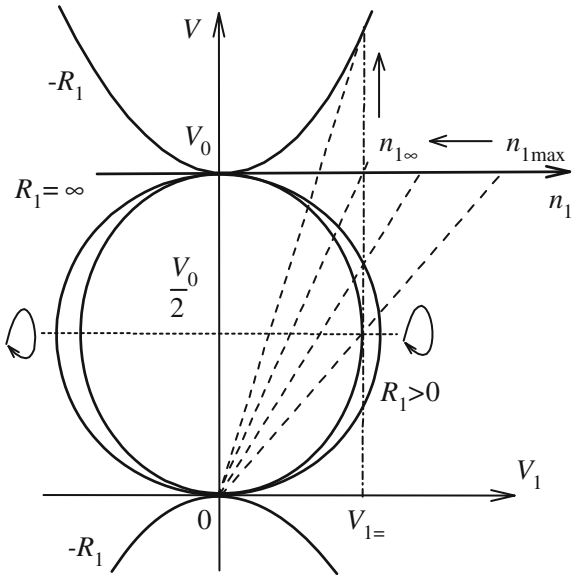

Fig. 11.11 Bunch of curves at $V_2 = 0$ and a point moving along lines $V_{1=}$

In the general case of the variable V_2, we get the surfaces, which rotate around the diameter $V = V_0/2$, as it is shown by closed arrows. Also, the transformation ratios n_1, n_2 are resulted by the familiar stereographic projection of sphere's points on the tangent plane or conformal plane. The axes n_1, n_2 are superposed in Fig. 11.11.

Further, we use the first equation of system (11.27)

$$\frac{R_i}{R_1}(n_1)^2 + \frac{R_i}{R_2}(n_2)^2 - \frac{n_1 V_0}{V_{1=}} + 1 = 0. \tag{11.34}$$

This equation circumscribes trajectories for different values R_1, as it is shown in Fig. 11.12. These trajectories are characteristic lines for the conformal plane.

If $R_1 > 0$, the bunch of circles with parameters R_1^1, R_1^2 is obtained.

For $R_1 = \infty$, Eq. (11.34) corresponds to a parabola; that is,

$$\frac{R_i}{R_2}(n_2)^2 - \frac{n_1 V_0}{V_{1=}} + 1 = 0. \tag{11.35}$$

The case $R_1 < 0$ conforms to a hyperbola. For the limit values $R_1 = 0$ and $n_1 = 0$, the hyperbola degenerates and coincides with the axis n_2.

The radius-vector rotation in the plane V_2V determines the analogous rotation in the plane n_1n_2 with the center $n_{1\max}$. This center corresponds to the minimum load resistance $R_{1\min}$.

Let us find these values $n_{1\max}$, $R_{1\min}$. We assume $n_2 = 0$ in expression (11.34). Then, we get the quadratic equation

$$\frac{R_i}{R_1}(n_1)^2 - \frac{n_1 V_0}{V_{1=}} + 1 = 0. \tag{11.36}$$

The roots coincide for

$$R_1 = R_{1\min} = 4R_i \frac{(V_{1=})^2}{(V_0)^2}.$$

Using (11.36), we get

$$n_{1\max} = 2\frac{V_{1=}}{V_0},$$

These values equal (11.3) and (11.4) for one load.

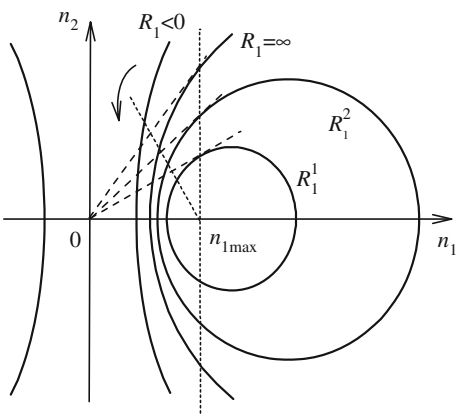

Fig. 11.12 Trajectories for different values R_1 as $V_{1=}$

Next, we display the voltage V_2 value for the trajectories in Fig. 11.12. Using definition (11.25), we obtain

$$V_2 = V_{1=}\frac{n_2}{n_1}.$$

Therefore, the voltage V_2 is directly proportional to the voltage $V_{1=}$ as constant value n_2/n_1; that is, we have a straight line, which intersects the bunch of circles with the parameter R_1 in two points. Then, the tangent lines to the circles (curves) determine the points of the maximum voltage $V_{2\max}$, the voltage $V = V_0/2$.

In this case, we get

$$V_{2\max} = \frac{V_0}{2}\sqrt{\frac{R_2}{R_i}}\sqrt{1-\frac{R_{1\min}}{R_1}}, \quad n_{2\max} = \sqrt{\frac{R_2}{R_i}}\sqrt{1-\frac{R_{1\min}}{R_1}}. \tag{11.37}$$

It is interestingly to note that all these tangent lines to the curves correspond to the value $n_{1\max}$. Therefore, the operating area of the transformation ratio is limited by the value $n_1 \le n_{1\max}$. So, we must decrease the next value n_1, for the next regulator switching period, by some rule. In this sense, we come to hyperbolic geometry.

11.2.1 Use of Hyperbolic Geometry

We may suppose that the straight line $n_{1\max}$ in the plane $n_2\, n_1$ is the infinitely remote line. Therefore, geometry of the half plane $n_2, n_1 \le n_{1\max}$ in Fig. 11.12 and of normalized half plane $\bar{n}_2\, \bar{n}_1 \le 1$ in Fig. 11.13 corresponds to Poincare's model of hyperbolic geometry. This Poincare's model is also demonstrated by projective coordinates g_2, g_1 for the left-hand figure and by these Cartesian coordinates for the right-hand figure in Fig. 11.13 for the half plane $g_2, g_1 \ge 0$.

For Poincare's model of hyperbolic geometry, the half-rounds with the given resistance R_1 intersect the axes g_2 orthogonally. Let us introduce this geometry. To do this, it is necessary to change the variables $n_2(g_1, g_2), n_1(g_1, g_2)$ so that all curves of the plane $n_2\, n_1$ would be converted into circles of the plane $g_2\, g_1$.

Further, we use the normalized values

$$\bar{n}_1 = \frac{n_1}{n_{1\max}}, \quad \bar{n}_2 = \frac{n_2}{n_{2ref}}.$$

As the scale value $n_{2\mathrm{ref}}$, we may use a circle with some characteristic value of the parameter R_1. The resistance value $R_1 = \infty$ may be such a characteristic value. Using (11.35) and the value $n_{1\max}$, we get

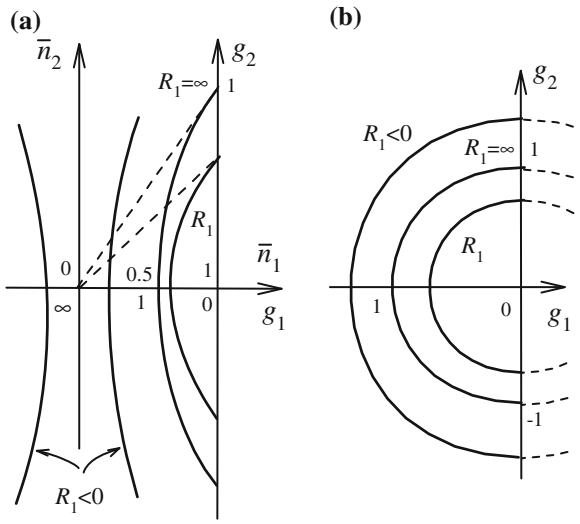

Fig. 11.13 **a** Poincare's model of hyperbolic geometry for superposed half planes $\bar{n}_2, \bar{n}_1 \leq 1$ and $g_2, g_1 \geq 0$. **b** Half plane for orthogonal coordinates g_2, g_1

$$n_{2\text{ref}} = \sqrt{\frac{R_2}{R_i}}. \tag{11.38}$$

It is possible to represent expression (11.34) in the normalized form

$$\frac{R_{1\min}}{R_1}(\bar{n}_1)^2 + (\bar{n}_2)^2 - 2\bar{n}_1 + 1 = 0. \tag{11.39}$$

The required change of variables has the view [1]

$$\bar{n}_1 = \frac{1}{1+g_1}, \quad \bar{n}_2 = \frac{g_2}{1+g_1}. \tag{11.40}$$

Let us check the offered expressions. In this case, Eq. (11.39) transforms into the equation of circle; that is,

$$(g_1)^2 + (g_2)^2 = 1 - \frac{R_{1\min}}{R_1} = (r_1)^2. \tag{11.41}$$

The second member of this equation is a radius squared for the given R_1. We may term the variables g_1, g_2 as hyperbolic transformation ratios.

This geometric model allows to use a cross ratio for the determination of regimes and their change.

11.2.2 Regime Change for the First Given Load Resistance

For clarity, let us consider the half-rounds with the parameter R_1^1 in Fig. 11.14.

Let points C_{1g}, D_{1g} be points of an initial and subsequent regime. Then, the cross ratio, which corresponds to the regime change $C_{1g} \to D_{1g}$, has the form similar to (11.10); that is,

$$m_g^{DC} = (A_{1g}\ D_{1g}\ C_{1g}\ F_{1g}) = \frac{D_{1g} - A_{1g}}{D_{1g} - F_{1g}} \div \frac{C_{1g} - A_{1g}}{C_{1g} - F_{1g}}. \tag{11.42}$$

The points A_{1g}, F_{1g} are the base points.

The coordinates of all the points $A_{1g}, D_{1g}, C_{1g}, F_{1g}$ are given by complex numbers as follows

$$g^{A1} = g_2^{A1} + j0, \quad g^{D1} = g_2^{D1} + jg_1^{D1},$$

$$g^{C1} = g_2^{C1} + jg_1^{C1}, \quad g^{F1} = g_2^{F1} + j0.$$

In particular, radius of half-rounds (11.41) defines the coordinates g_2^{A1}, g_2^{F1} as the follows

$$g_2^{A1} = -r_1, \quad g_2^{F1} = r_1.$$

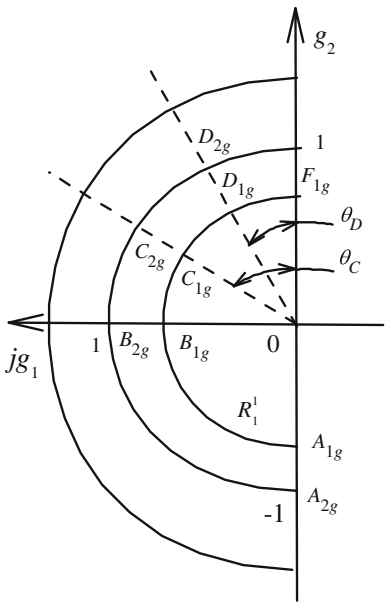

Fig. 11.14 Regime change for Poincare's model of hyperbolic geometry

For Poincare's model of hyperbolic geometry by Fig. 11.14, cross ratio (11.42) looks like [2]

$$m_g^{DC} = \frac{tg\theta_C}{tg\theta_D} = \frac{r_1 - g_2^{C1}}{g_1^{C1}} \div \frac{r_1 - g_2^{D1}}{g_1^{D1}}. \tag{11.43}$$

Using (11.41), we get

$$\left(m_g^{DC}\right)^2 = \frac{r_1 - g_2^{C1}}{r_1 + g_2^{C1}} \div \frac{r_1 - g_2^{D1}}{r_1 + g_2^{D1}}. \tag{11.44}$$

This expression gives the subsequent value

$$\frac{g_2^{D1}}{r_1} = \frac{\frac{g_2^{C1}}{r_1} + g_2^{DC}}{1 + \frac{g_2^{C1}}{r_1} g_2^{DC}}, \tag{11.45}$$

where the hyperbolic transformation ratio change is introduced as

$$g_2^{DC} = \frac{\left(m_g^{DC}\right)^2 - 1}{\left(m_g^{DC}\right)^2 + 1}. \tag{11.46}$$

This change corresponds to the points C_{2g}, D_{2g} of the half-rounds with parameter R_1^2 and so on.

We may obtain an expression for the subsequent value of the transformation ratios n_1, n_2. To do this, it is necessary to apply to (11.45) the inverse change of variables relatively to (11.40); that is,

$$g_1 = \frac{1 - \bar{n}_1}{\bar{n}_1}, \quad g_2 = \frac{\bar{n}_2}{\bar{n}_1}. \tag{11.47}$$

But complicated formulas are obtained. Therefore, using (11.40), we may directly calculate the subsequent value of transformation ratios n_1, n_2.

Let us now compare the half-rounds in the plane $g_2\, g_1$ with the half-rounds in the plane V_2, V in Fig. 11.15.

The points A_{1V}, F_{1V} are the base points. The points C_{1V}, D_{1V} correspond to the initial and subsequent regime. It is possible to conclude that the half plane $V_2, V \geq V_0/2$ is also hyperbolic geometry model.

Therefore, similarly to (11.44), the regime change has the view

$$\begin{aligned} m_V^{DC} &= (-V_{2\max}\ \ V_2^{D1}\ \ V_2^{C1}\ \ V_{2\max}) \\ &= \frac{V_2^{D1} + V_{2\max}}{V_2^{D1} - V_{2\max}} \div \frac{V_2^{C1} + V_{2\max}}{V_2^{C1} - V_{2\max}}. \end{aligned} \tag{11.48}$$

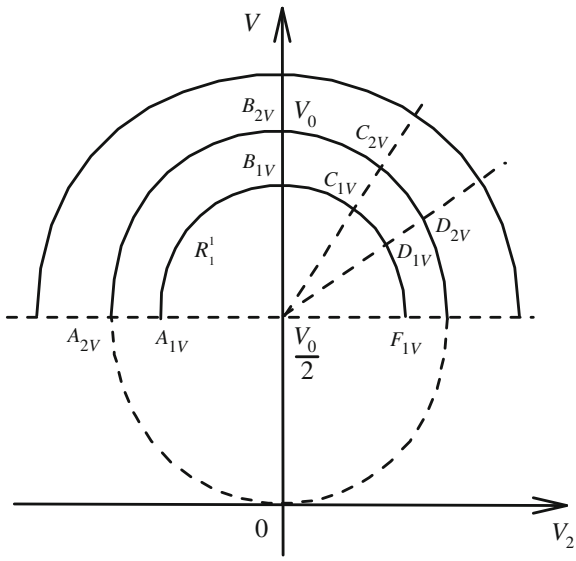

Fig. 11.15 Regime change for hyperbolic geometry in the half plane $V_2, V \geq V_0/2$

Also, the following equality takes place

$$m_V^{DC} = \left(m_g^{DC}\right)^2.$$

Using (11.48), we obtain the subsequent voltage

$$\frac{V_2^{D1}}{V_{2\max}} = \frac{\frac{V_2^{C1}}{V_{2\max}} + V_2^{DC}}{1 + \frac{V_2^{C1}}{V_{2\max}} V_2^{DC}}, \tag{11.49}$$

where the voltage change is introduced as

$$V_2^{DC} = \frac{m_V^{DC} - 1}{m_V^{DC} + 1} = g_2^{DC}. \tag{11.50}$$

It now follows that

$$\frac{V_2^{D1}}{V_{2\max}} = \frac{g_2^{D1}}{r_1}. \tag{11.51}$$

The obtained expressions may be generalized for three or more loads.

11.2.3 Example

Let the circuit parameters be given as follows

$$V_0 = 5, \quad R_i = 1, \quad R_2 = 2, \quad V_{1=} = 2.5, \quad R_{1\min} = 1, \quad n_{1\max} = 1.$$

Scale value (11.38), $n_{2\text{ref}} = 1.414$.

The initial regime, the point C_1, is set by the first load resistance $R_1^1 = 1.25$ and the second load voltage $V_2^{C1} = 0.707$.

Using (11.24), we get

$$V = \begin{cases} 3.5 \\ 1.5 \end{cases}.$$

Further, we use the voltage value $V^{C1} = 3.5$ because this value is greater than $V_0/2 = 2.5$.

Maximum values (11.37)

$$V_{2\max} = \frac{5}{2}\sqrt{2}\sqrt{1 - \frac{1}{1.25}} = 2.5\sqrt{2}\sqrt{0.2} = 1.581,$$
$$n_{2\max} = \sqrt{2}\sqrt{0.2} = 0.6324.$$

Radius (11.41), $r_1 = \sqrt{0.2} = 0.447$.

Transformation ratios (11.25)

$$n_1^{C1} = \frac{2.5}{3.5} = 0.714, \quad n_2^{C1} = \frac{0.707}{3.5} = 0.202.$$

The normalized transformation ratios

$$\bar{n}_1^{C1} = 0.714, \quad \bar{n}_2^{C1} = \frac{0.202}{1.414} = 0.143.$$

Hyperbolic transformation ratios (11.47)

$$g_1^{C1} = \frac{1 - 0.714}{0.714} = 0.4, \quad g_2^{C1} = \frac{0.143}{0.714} = 0.2.$$

We check expression (11.41)

$$0.4^2 + 0.2^2 = 0.2.$$

Further, we are verifying the regime change for the given load resistance R_1.

Let the subsequent regime, the point D_1, be given by the second load voltage $V_2^{D1} = 1.414$ and voltage $V^{D1} = 3$.

Therefore,

$$\bar{n}_1^{D1} = \frac{2.5}{3} = 0.833, \quad \bar{n}_2^{D1} = \frac{1.414}{3 \cdot 1.414} = 0.333,$$
$$g_1^{D1} = \frac{1 - 0.833}{0.833} = 0.2, \quad g_2^{D1} = \frac{0.333}{0.833} = 0.4.$$

Regime changes (11.43), (11.44)

$$m_g^{DC} = \frac{\sqrt{0.2} - 0.2}{0.4} \div \frac{\sqrt{0.2} - 0.4}{0.2} = 2.618.$$
$$\left(m_g^{DC}\right)^2 = \frac{\sqrt{0.2} - 0.2}{\sqrt{0.2} + 0.2} \div \frac{\sqrt{0.2} - 0.4}{\sqrt{0.2} + 0.4} = 6.8528 = 2.618^2.$$

Transformation ratio change (11.46)

$$g_2^{DC} = \frac{6.8528 - 1}{6.8528 + 1} = 0.7453.$$

Subsequent value (11.45)

$$\frac{g_2^{D1}}{r_1} = \frac{\frac{0.2}{\sqrt{0.2}} + 0.7453}{1 + \frac{0.2}{\sqrt{0.2}} \cdot 0.7453} = 0.8944 = \frac{0.4}{\sqrt{0.2}}.$$

Regime change (11.48)

$$m_V^{DC} = \frac{1.414 + 1.581}{1.414 - 1.581} \div \frac{0.707 + 1.581}{0.707 - 1.581} = 6.8528 = (2.618)^2.$$

Equality (11.51)

$$\frac{1.414}{1.581} = \frac{0.4}{0.4472} = 0.8944.$$

References

1. Glagolev, N.A.: Proektivnaia geometria. (projective geometry). Nauka, Moskva (1963)
2. Kagan, V.F.: Osnovania geometrii, Chasti II. (Geometry basics. Part II). Gostekhizdat, Moskva (1956)
3. Korn, G.A., Korn, T.M.: Mathematical handbook for scientists and engineers. MacGraw–Hill, New York (1968)
4. Maksimovic, D., Jang, Y., Erickson, R.W.: Nonlinear-carrier control for high—power—factor boost rectifiers. IEEE Trans. Power Electron. **11**(4), 578–584 (1996)

5. Penin, A.: Analysis of regime of voltage regulators with limited capacity voltage sources. Geometrical approach. WSEAS Trans. Circuits Syst. **12**(1), 12 (2013). http://www.wseas.org/wseas/cms.action?id=6933 Accessed 30 Nov 2014
6. Penin, A.: Non-Euclidean geometry and regulated characteristics of limited capacity power supply. J. Electr. Eng. **2**(4), 175–186 (2014)
7. Penin, A.: Non–Euclidean geometrical transformation groups in the electric circuit theory with stabilization and regulation of load voltages. Int. J. Circuits Syst. Sign. Process. **8**, 182–194 (2014). http://www.naun.org/cms.action?id=7621 Accessed 30 Nov 2014
8. Singer, S., Erickson, R.W.: Power–source element and its properties. IEE Proceedings–Circuits, Devices and Systems. **141**(3), 220–226 (1994). http://ecee.colorado.edu/~rwe/papers/IEE94.pdf

Chapter 12
Pulse-Width Modulation Regulators

12.1 Introduction

As it was noted in Chap. 10, into power supply systems with limited capacity voltage sources, the limitation of load voltage is appeared. Renewable power supply with solar array, fuel cell, and rechargeable battery may be the example of one's [4]. The output voltage of these sources changes over a wide range. In such systems it is convenient to apply the pulse-width modulation *PWM* boost and buck–boost regulators or converters which can step up or step down the input voltage [2, 10], but these regulators have a nonlinear regulation curve or characteristic. Therefore, the problem of linearization is appeared [9].

The linearization methods are proposed for idealized, without losses buck–boost regulators [3, 5].

Also, the real boost and buck–boost converters have the two-valued regulation characteristic. In this case, the up-slope direction or the forward branch of its regulation characteristic is used and the down movement of the operating point on the back branch is restrained.

Therefore, it is necessary to correctly determine the regime parameters of the converter relatively to the maximum permissible load voltage and control pulse width. It will allow estimating, for example, reserves of the control voltage and load voltage, to use this data for a direct digital or predictive control, and to carry out some kind of the linearization of the regulation characteristic in a wide range of load voltage changes.

12.2 Regulation Characteristic of Boost Converter

Let us consider a *PWM* boost voltage converter with a given load resistance R_L in Fig. 12.1 [8].

A. Penin, *Analysis of Electrical Circuits with Variable Load Regime Parameters*,
Power Systems, DOI 10.1007/978-3-319-28451-4_12

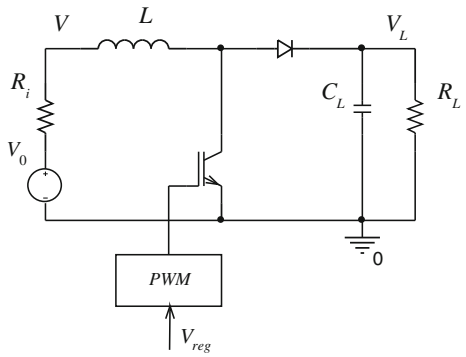

Fig. 12.1 Boost voltage converter

We know the expression of the static regulation characteristic for the continuous current mode of the choke L with the loss resistance R_i [1]

$$V_L = V_0 \frac{1-D}{(1-D)^2 + \frac{R_i}{R_L}} = V_0 \frac{\frac{1}{1-D}}{1 + \frac{(\sigma)^2}{(1-D)^2}}, \tag{12.1}$$

where $D \leq 1$ is a relative pulse width and σ is a relative loss. For convenience, let the converter be given by the following parameters:

$$V_0 = 25, \quad \sigma = 0.08.$$

Then, characteristic (12.1) has the view of Fig. 12.2.

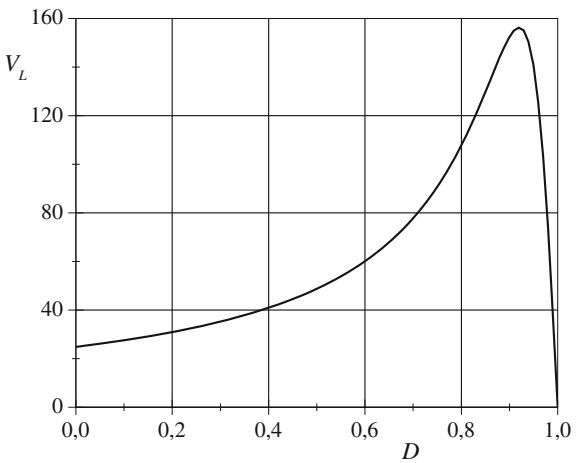

Fig. 12.2 Example of regulation characteristic via the pulse width

We may introduce a value

$$n = \frac{1}{1-D} \geq 1. \tag{12.2}$$

This value is the inverse relative pause width or the transformation ratio of the idealized boost converter

$$n = \frac{V_L}{V}. \tag{12.3}$$

Thus, we obtain that

$$V_L = V_0 \frac{n}{1+(\sigma n)^2}. \tag{12.4}$$

This equation corresponds to regulation characteristic (10.8) for power supply system with one load of Sect. 10.2.1. Therefore, we may use the results of this section directly. Regulation characteristic (12.4) for our example is given in Fig. 12.3.

Expression of ellipse (10.2) obtains the general form

$$(\sigma)^2 (V_L)^2 + (V)^2 - V_0 V = 0. \tag{12.5}$$

The plot of this ellipse is given in Fig. 12.4.

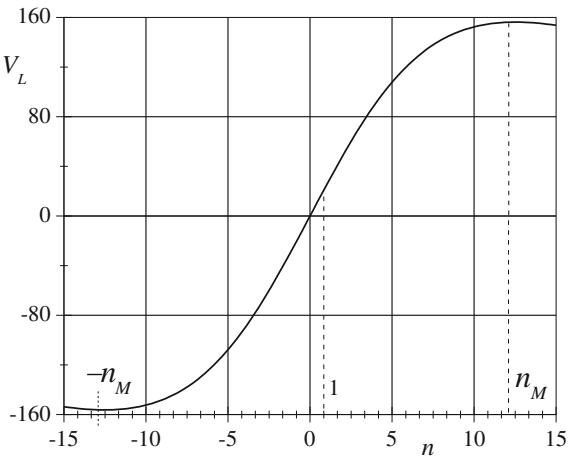

Fig. 12.3 Example of regulation characteristic via the transformation ratio

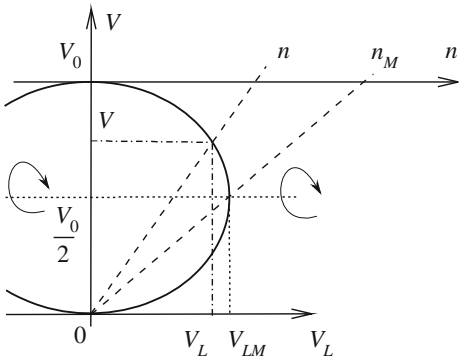

Fig. 12.4 Geometrical model of the regulation characteristic of the boost converter

The variable n turns out at the expense of a stereographic projection too. Therefore, the maximum values

$$V_{LM} = \pm\frac{V_0}{2\sigma} = \pm 156.25, \quad n_M = \pm\frac{1}{\sigma} = \pm 12.5. \tag{12.6}$$

coincide with (10.5) and (10.6).

We note that the real working area $n \geq 1$, but the whole area from $-n_M$ to $+n_M$ allows using the above results.

We consider that a regime change or load voltage regulation is defined by a group hyperbolic transformation, which consecutively, step by step, translates an initial point V_L^1 into a subsequent point V_L^2 and so on.

The conformity of the characteristic points and running points of different variables is shown in Fig. 12.5.

Such transformation possesses a familiar invariant; it is a cross ratio of four points. We determine necessary points of characteristic regimes. There are two points of the maximum voltage: $\pm V_{LM}$. Also, there is a unit or starting point, when

$$V_{L0} = \frac{V_0}{1+(\sigma)^2}, \quad n = 1, \quad D = 0. \tag{12.7}$$

For the initial values n^1, V_L^1, the corresponding cross ratios are

$$m_n^1 = \left(-\frac{1}{\sigma} \;\; n^1 \;\; 1 \;\; \frac{1}{\sigma}\right) = \frac{\frac{1}{\sigma}+n^1}{\frac{1}{\sigma}-n^1}\cdot\frac{1-\sigma}{1+\sigma}, \tag{12.8}$$

$$\begin{aligned} m_v^1 &= \left(-\frac{V_0}{2\sigma} \;\; V_L^1 \;\; \frac{V_0}{1+\sigma^2} \;\; \frac{V_0}{2\sigma}\right) \\ &= \frac{\frac{V_0}{2\sigma}+V_L^1}{\frac{V_0}{2\sigma}-V_L^1}\cdot\frac{(1-\sigma)^2}{(1+\sigma)^2} = (m_n^1)^2. \end{aligned} \tag{12.9}$$

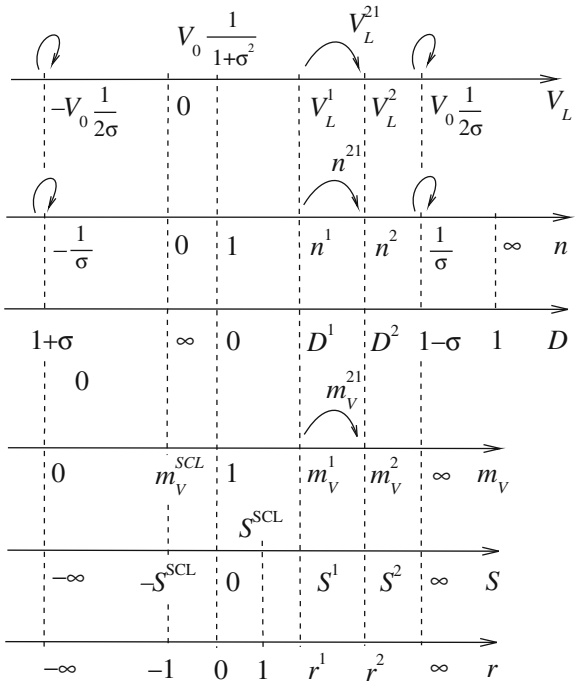

Fig. 12.5 Regime change as a group transformation and conformity of the characteristic and running points of the variables V_L, n, D

By definition (12.2), the values D and n are connected among themselves by the fractionally linear expression

$$D = \frac{n-1}{n}.$$

Then, it is possible at once to express cross ratio (12.8) by the value D

$$\begin{aligned} m_D^1 = m_n^1 &= \left((1+\sigma)\ D^1\ 0\ (1+\sigma)\right) \\ &= \frac{(1+\sigma)-D^1}{(1-\sigma)-D^1} \cdot \frac{1-\sigma}{1+\sigma}. \end{aligned} \tag{12.10}$$

Expressions (12.8) and (12.9) lead to identical values if we take the logarithm

$$S^1 = Ln\, m_v^1 = 2Ln\, m_n^1.$$

Then, the hyperbolic distance

$$S^1 = Ln \frac{\frac{V_0}{2\sigma} + V_L^1}{\frac{V_0}{2\sigma} - V_L^1} + 2Ln \frac{1-\sigma}{1+\sigma} = Ln \frac{\frac{V_0}{2\sigma} + V_L^1}{\frac{V_0}{2\sigma} - V_L^1} - 2Ln \frac{1+\sigma}{1-\sigma}.$$

In particular, for a unit point, this hyperbolic distance is equal to zero.

Besides the considered three points of the characteristic regimes, there is still a fourth one, the scale points $V = 0, n = 0, D = \infty$. This scale point should be considered too. The cross ratio and hyperbolic distance for the scale point are

$$m_V^{SCL} = \left(\frac{1-\sigma}{1+\sigma}\right)^2 < 1, \quad Ln\, m_V^{SCL} = 2Ln\frac{1-\sigma}{1+\sigma} < 0.$$

The corresponding hyperbolic distance will be positive for inverse value of the cross ratio:

$$S^{SCL} = 2Ln\frac{1+\sigma}{1-\sigma} > 0.$$

Further, it is natural to introduce the normalized hyperbolic distance for a running regime (the index « 1 » is lowered), using the obtained scale

$$r = \frac{S}{S^{SCL}} = Ln\frac{\frac{V_0}{2\sigma} + V_L}{\frac{V_0}{2\sigma} - V_L} \cdot \frac{1}{2Ln\frac{1+\sigma}{1-\sigma}} - 1. \tag{12.11}$$

Thus, the normalized distance considers all the characteristic points. In turn, the inverse expression is

$$V_L = \frac{V_0}{2\sigma}\frac{\left(\frac{1+\sigma}{1-\sigma}\right)^{2(r+1)} - 1}{\left(\frac{1+\sigma}{1-\sigma}\right)^{2(r+1)} + 1}. \tag{12.12}$$

For a regime change $n^1 \to n^2$, we have

$$m_n^{21} = (-\frac{1}{\sigma} \;\; n^2 \;\; n^1 \;\; \frac{1}{\sigma}) = \frac{\frac{1}{\sigma} + n^2}{\frac{1}{\sigma} - n^2} \div \frac{\frac{1}{\sigma} + n^1}{\frac{1}{\sigma} - n^1} = \frac{\frac{1}{\sigma} + \frac{n^2 - n^1}{1-(\sigma)^2 n^2 n^1}}{\frac{1}{\sigma} - \frac{n^2 - n^1}{1-(\sigma)^2 n^2 n^1}}.$$

It is possible to introduce, similar to (10.21), the transformation ratio change as

$$n^{21} = \frac{n^2 - n^1}{1 - (\sigma)^2 n^2 n^1}. \tag{12.13}$$

Then,

$$m_n^{21} = \frac{\frac{1}{\sigma} + n^{21}}{\frac{1}{\sigma} - n^{21}}. \tag{12.14}$$

The subsequent value of the transformation ratio is

$$n^2 = \frac{n^1 + n^{21}}{1 + (\sigma)^2 n^1 n^{21}}. \tag{12.15}$$

Similarly, for the voltage change $V_L^1 \to V_L^2$, it is possible to write down at once

$$\begin{aligned} m_V^{21} &= \frac{\frac{V_0}{2\sigma} + V_L^{21}}{\frac{V_0}{2\sigma} - V_L^{21}}, \\ V_L^{21} &= \frac{V_L^2 - V_L^1}{1 - 4(\sigma)^2 \frac{V_L^2 V_L^1}{(V_0)^2}}, \qquad V_L^2 = \frac{V_L^{21} + V_L^1}{1 + 4(\sigma)^2 \frac{V_L^{21} V_L^1}{(V_0)^2}}. \end{aligned} \tag{12.16}$$

Let us suppose the change m_D^{21}. Using (12.10), we have

$$m_D^{21} = m_D^2 \div m_D^1 = \frac{(1+\sigma) - D^2}{(1-\sigma) - D^2} \div \frac{(1+\sigma) - D^1}{(1-\sigma) - D^1} = \frac{1 - \sigma D^{21}}{1 + \sigma D^{21}},$$

where the change is

$$D^{21} = \frac{D^1 - D^2}{1 - \sigma^2 + D^1 D^2 - (D^1 + D^2)}, \quad n^{21} = D^{21}. \tag{12.17}$$

Thus, the mutually coordinated system of all the regime parameters turns out.

We will consider the linearization of the regulation characteristic of a converter in Fig. 12.6 [6]

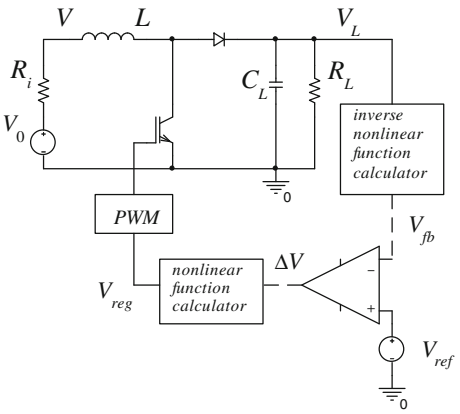

Fig. 12.6 Boost converter with linearization function calculators of the control voltage ΔV and feedback voltage V_{fb}

Let us express D and n via r similar to (12.12). Then

$$D = 1 - \sigma \frac{\left(\frac{1+\sigma}{1-\sigma}\right)^{r+1} + 1}{\left(\frac{1+\sigma}{1-\sigma}\right)^{r+1} - 1}, \quad n = \frac{1}{\sigma} \frac{\left(\frac{1+\sigma}{1-\sigma}\right)^{r+1} - 1}{\left(\frac{1+\sigma}{1-\sigma}\right)^{r+1} + 1}. \tag{12.18}$$

It turns out that the value r is equally expressed by D and V_L. It is possible to interpret this equality as the linearization of the dependence $V_L(D)$.

Further, it is possible to accept that the value D is equal to the regulating voltage V_{reg} for PWM. We believe that the input voltage ΔV of a nonlinear function calculator (introduced before PWM) is the hyperbolic distance r.

Therefore, we obtain, by (12.18), that

$$V_{reg} = 1 - \sigma \frac{\left(\frac{1+\sigma}{1-\sigma}\right)^{\Delta V+1} + 1}{\left(\frac{1+\sigma}{1-\sigma}\right)^{\Delta V+1} - 1}. \tag{12.19}$$

The plot of the function $V_{reg}(\Delta V)$ is given in Fig. 12.7.

Additionally, expressing r via V_L by an inverse nonlinear function calculator according to (12.11), we obtain a value close to the voltage ΔV, that is, the feedback voltage V_{fb} in Fig. 12.8. Therefore, we rewrite expression (12.11)

$$V_{fb} = Ln \frac{\frac{V_0}{2\sigma} + V_L}{\frac{V_0}{2\sigma} - V_L} \frac{1}{2Ln\frac{1+\sigma}{1-\sigma}} - 1. \tag{12.20}$$

So, we obtain that V_{fb} is equal to ΔV. If to use a feedback closed loop (shown by the dashed line in Fig. 12.6), the output voltage of the error amplifier will be the voltage ΔV. ORCAD model of this converter is proposed by [8].

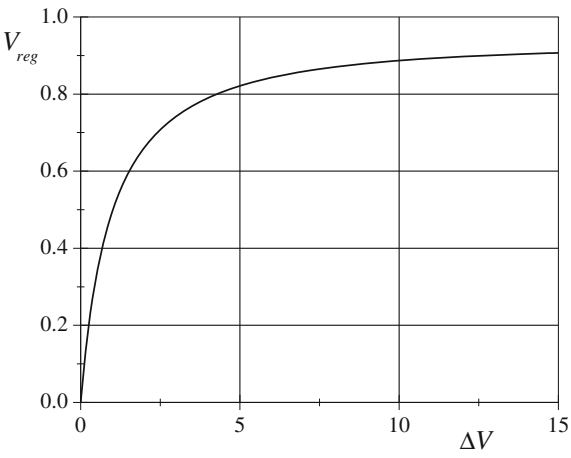

Fig. 12.7 Nonlinear characteristic of the function calculator

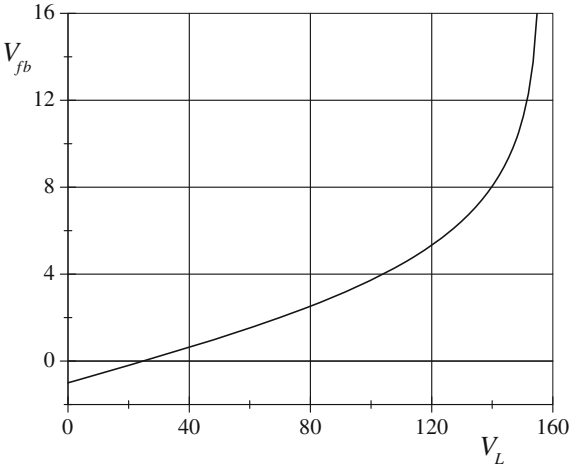

Fig. 12.8 Nonlinear characteristic of the inverse function calculator

Examples We use the above converter parameters as $V_0 = 25$, $\sigma = 0.08$.

The characteristic values of all the regime parameters are as follows:

$$V_{LM} = \pm\frac{V_0}{2\sigma} = \pm 156.25, \quad n_M = \pm\frac{1}{\sigma} = \pm 12.5,$$
$$D_M = \frac{n_M - 1}{n_M} = 1 - \sigma = 0.92.$$

Example 1 Let $V_L^1 = 48.49$ be the initial regime. We must define the normalized distance for this regime.

For $n = 1$, we have a unit value

$$V_L = 25\frac{1}{1 + 0.08^2} = 24.841.$$

All these values are shown in Fig. 12.9.

Cross ratio of initial regime (12.9) is

$$m_V^1 = \frac{156.25 + 48.49}{156.25 - 48.49} \cdot (0.852)^2 = 1.378.$$

Then,

$$m_n^1 = \sqrt{m_V^1} = \sqrt{1.378} = 1.174.$$

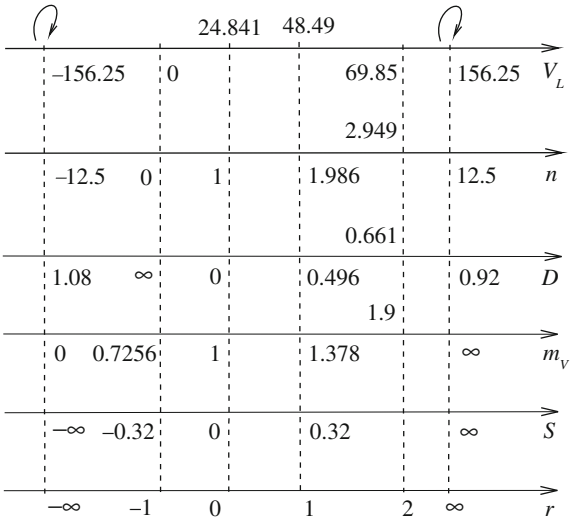

Fig. 12.9 Example of a regime change and conformity of points of the variables V_L, n, D

The corresponding value n^1 may be calculated from the inverse formula to (12.8)

$$n^1 = \frac{1}{\sigma} \cdot \frac{\frac{1+\sigma}{1-\sigma} m_n^1 - 1}{\frac{1+\sigma}{1-\sigma} m_n^1 + 1} = 1.986.$$

In turn,

$$D^1 = 0.496, \quad S_V^1 = Ln\, 1.378 = 0.320.$$

The cross ratio and distance for the scale point are

$$m_V^{SCL} = \left(\frac{1-\sigma}{1+\sigma}\right)^2 = 0.725, \quad S^{SCL} = 2Ln\frac{1+\sigma}{1-\sigma} = 0.320.$$

Then, normalized distance (12.11) is

$$r^1 = \frac{S^1}{S^{SCL}} = 1.$$

Example 2 The regime has changed on the value $r^{21} = 1$. It is necessary to define its actual regime parameters.

The distance for this regime is

$$r_1^2 = r_1^1 + r_1^{21} = 2.$$

Then, subsequent voltage (12.12) is

$$V_L^2 = 156.25 \cdot \frac{1.174^{2(2+1)} - 1}{1.174^{2(2+1)} + 1} = 156.25 \cdot \frac{2.618 - 1}{2.618 + 1} = 69.85.$$

In turn, voltage change (12.16) is given as

$$V_L^{21} = \frac{69.85 - 48.49}{1 - 4 \cdot 0.0064 \frac{69.85 \cdot 48.49}{25^2}} = 24.841.$$

On the other hand, as the change V_L^{21} is equal to a unit value, the change is $n^{21} = 1$ by (12.7).

Then, by (12.15), we get the subsequent values

$$n^2 = \frac{1.986 + 1}{1 + 0.0064 \cdot 1.986 \cdot 1} = 2.949, \quad D^2 = 0.661.$$

The values V_L, D, n for the further steps are shown in Fig. 12.9.

It is visible that *each time the actual voltage change is reduced and cannot reach the maximum value*.

Example 3 Let the regime with the initial value $V_L^1 = 48.49$ be changed to the value $V_L^{N+1} = 69.85$ by small steps consistently. In turn, the consecutive reduction of the change step reduces undesirable transients.

Let the number of steps be $N = 5$. It is necessary to find the values V_L^i, n^i on the each step i.

We find the hyperbolic distance r^{61} corresponding to the initial (the zero step) regime and final (the fifth step) regime. According to Example 2, this distance is as follows: $r^{61} = 1$.

For these five steps, the regime change (as a hyperbolic distance) equals $\Delta r = 0.2$.

The value (or length) of the first step is

$$r^2 = r^1 + r^{21} = 1 + 0.2 = 1.2.$$

The first step is V_L^2 according to (12.12) and n^2 by (12.18) are given as

$$V_L^2 = 156.25 \frac{1.174^{2 \cdot 2.2} - 1}{1.174^{2 \cdot 2.2} + 1} = 52.96,$$
$$n^2 = \frac{1}{0.08} \frac{1.174^{2.2} - 1}{1.174^{2.2} + 1} = 2.183.$$

The voltage change on the first step according to (12.16) is

$$V_L^{21} = \frac{52.963 - 48.49}{1 - 4 \cdot 0.0064 \frac{52.963 \cdot 48.49}{25^2}} = 5.$$

The changes on the following steps are also equal to this value.
The transformer ratio change on the first step according to (12.13) is

$$n^{21} = \frac{2.183 - 1.986}{1 - 0.0064 \cdot 2.183 \cdot 1.986} = 0.202.$$

For subsequent steps, the values n, V_L are obtained via the recurrent relationships (12.15), (12.16), since the changes on the following steps keep their values

$$n^3 = \frac{2.183 + 0.2029}{1 + 0.0064 \cdot 2.183 \cdot 0.2029} = 2.379,$$
$$V_L^3 = \frac{52.963 + 5}{1 + 4 \cdot 0.0064 \frac{52.963 \cdot 5}{25^2}} = 57.34,$$
$$n^4 = 2.574, \quad n^5 = 2.768, \quad n^6 = 2.96,$$
$$V_L^4 = 61.617, \quad V_L^5 = 65.78, \quad V_L^6 = 69.84.$$

It is visible, as such actual changes of the values n,V_L are decreased.

12.3 Regulation Characteristic of Buck–Boost Converter

12.3.1 Buck–Boost Converter with an Idealized Choke

Let us consider a *PWM* buck–boost converter with a given load resistance R_L in Fig. 12.10.

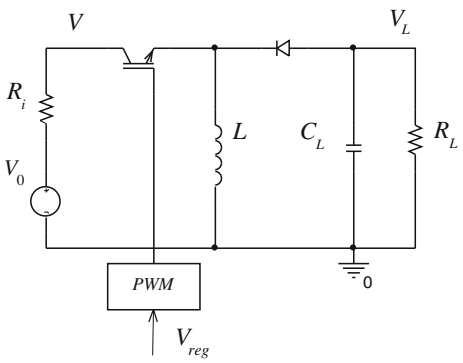

Fig. 12.10 Buck–boost converter with an idealized choke

The static regulation characteristic of the idealized converter for the continuous current of the choke L has the well-known view:

$$V_L = V\frac{D}{1-D}.$$

If we take into account an internal resistance R_i, the regulation characteristic is given by

$$V_L = V_0\frac{D(1-D)}{(1-D)^2 + \frac{R_i}{R_L}(D)^2} = V_0\frac{\frac{D}{1-D}}{1+(\sigma)^2\left(\frac{D}{1-D}\right)^2}. \tag{12.21}$$

For convenience, we use the same converter parameters. Then, characteristic (12.21) has the view of Fig. 12.11.

Similar to (12.2), we introduce the same value

$$n = \frac{1}{1-D} \geq 1.$$

Then

$$V_L = V_0\frac{n-1}{1+(n-1)^2(\sigma)^2}.$$

This expression is close to (12.4). Therefore, we may introduce the value

$$n_{con} = n - 1 = \frac{1}{1-D} - 1 = \frac{D}{1-D} = \frac{V_L}{V}. \tag{12.22}$$

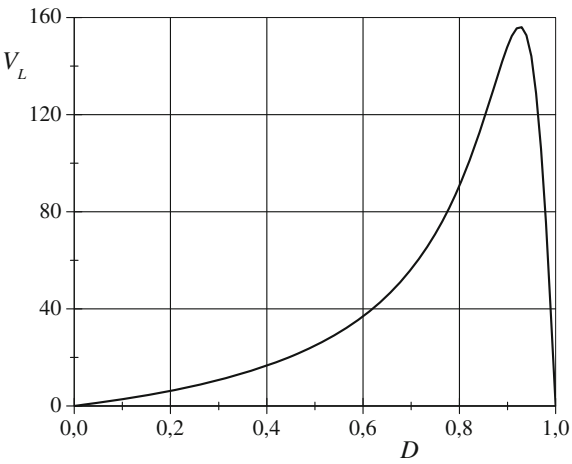

Fig. 12.11 Example of regulation characteristic via the pulse width

This value, at that $n_{con} \geq 0$, is the transformation ratio of the idealized converter itself.

Finally, we obtain

$$V_L = V_0 \frac{n_{con}}{1 + (\sigma n_{con})^2}. \tag{12.23}$$

This equation corresponds to (12.4). Thus, we may use the above results. Regulation characteristic (12.23) is given in Fig. 12.12. The working area involves the zero points n_{con},V_L.

Next, we may use ellipse Eq. (12.5) at once

$$\sigma^2 (V_L)^2 + (V)^2 - VV_0 = 0.$$

The plot of this ellipse is given in Fig. 12.13.

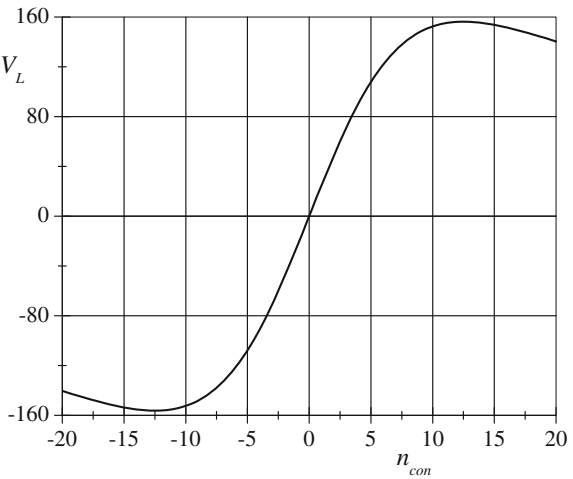

Fig. 12.12 Example of regulation characteristic via the converter transformation ratio

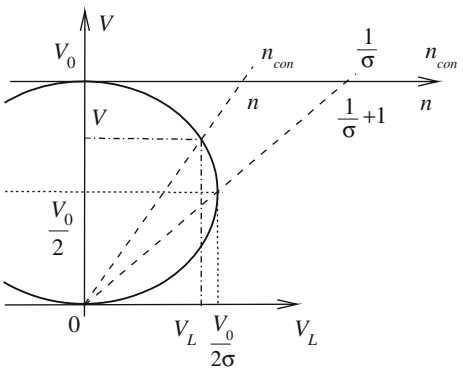

Fig. 12.13 Geometrical model of the regulation characteristic of the buck–boost converter

The values n_{con}, n turn out at the expense of a stereographic projection too. The maximum values are

$$V_{LM} = \pm\frac{V_0}{2\sigma}, \quad n_{conM} = \pm\frac{1}{\sigma}. \tag{12.24}$$

The regime change or load voltage regulation is defined by a group hyperbolic transformation, which consecutively, step by step, translates an initial point V_L^1 to a subsequent point V_L^2 and so on. The conformity of the characteristic points and running points of various variables is shown in Fig. 12.14.

Also, we will use a cross ratio of four points. For that, let us determine necessary points of characteristic regimes. There are two points of the maximum voltage and a unit or starting point

$$V_L = 0, \quad n_{\text{con}} = 0, \quad n = 1, \quad D = 0.$$

As it is visible, this case of a unit point differs from above case (12.7).

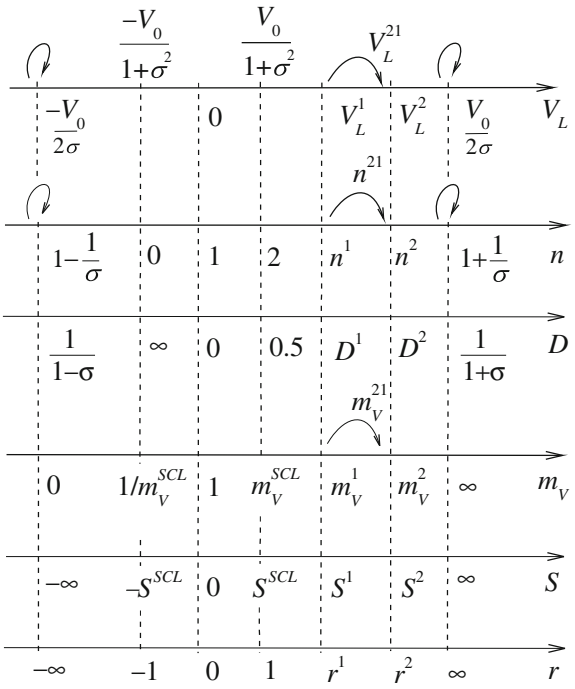

Fig. 12.14 Regime change as a group transformation and conformity of the characteristic and running points of the variables V_L, n, D

For the initial values n^1_{con}, n^1, V^1_L, the corresponding cross ratios are similar to (12.8), (12.9)

$$m^1_n = (-\frac{1}{\sigma}\ \ n^1_{con}\ \ 0\ \ \frac{1}{\sigma}) = \left(\left(1-\frac{1}{\sigma}\right)\ n^1\ \ 1\ \ \left(1+\frac{1}{\sigma}\right)\right)$$
$$= \frac{\frac{1}{\sigma}+n^1_{con}}{\frac{1}{\sigma}-n^1_{con}} = \frac{n^1-\left(1-\frac{1}{\sigma}\right)}{\left(1+\frac{1}{\sigma}\right)-n^1}, \tag{12.25}$$

$$m^1_V = \left(-\frac{V_0}{2\sigma}\ \ V^1_L\ \ 0\ \ \frac{V_0}{2\sigma}\right) = \frac{\frac{V_0}{2\sigma}+V^1_L}{\frac{V_0}{2\sigma}-V^1_L} = (m^1_n)^2. \tag{12.26}$$

Because the values D, n are connected among themselves by the fractionally linear expression, it is possible to express cross ratio (12.25) via the value D

$$m^1_D = m^1_n = \left(-\frac{1}{\sigma-1}\ \ D^1\ \ 0\ \ \frac{1}{\sigma+1}\right) = \frac{\frac{1}{\sigma-1}+D^1}{\frac{1}{\sigma+1}-D^1}\cdot\frac{\sigma-1}{\sigma+1}. \tag{12.27}$$

Expressions (12.25) and (12.26) lead also to identical values if we take the logarithm

$$S^1 = Ln\, m^1_V = Ln\ m^1_n, \quad S^1 = Ln\frac{\frac{V_0}{2\sigma}+V_L}{\frac{V_0}{2\sigma}-V_L}.$$

In particular, for a unit point, this distance is equal to zero.

Besides the considered three points of the characteristic regimes, there is still a fourth one, the scale point:

$$n_{con} = 1, \quad V_L = \frac{V_0}{1+(\sigma)^2}, \quad n = 2, \quad D = 0.5.$$

This scale point should be considered too. The cross ratio and hyperbolic distance for the scale point are as follows:

$$m^{SCL}_V = \left(-\frac{V_0}{2\sigma}\ \ \frac{V_0}{1+(\sigma)^2}\ \ 0\ \ \frac{V_0}{2\sigma}\right) = \frac{(1+\sigma)^2}{(1-\sigma)^2},$$
$$S^{SCL} = Ln\ m^{SCL}_V = 2Ln\frac{1+\sigma}{1-\sigma}. \tag{12.28}$$

Also, we will note that as such a characteristic fourth point, it is possible to accept the symmetric point, that is,

$$n_{con} = -1, \quad V_L = \frac{-V_0}{1+(\sigma)^2}, \quad n = 0, \quad D = \infty.$$

This point is also specified in Fig. 12.14. In this case, the cross ratio will be the inverse value to the above received value, but the hyperbolic distance will be identical in the absolute value.

Further, it is natural to introduce the normalized hyperbolic distance for the running regime (the index "1" is lowered), using the obtained scale

$$r = \frac{S}{S^{SCL}} = Ln\frac{\frac{V_0}{2\sigma} + V_L}{\frac{V_0}{2\sigma} - V_L} \div 2Ln\frac{1+\sigma}{1-\sigma}. \tag{12.29}$$

Thus, the normalized distance considers all the characteristic points.

In turn, the inverse expression is

$$V_L = \frac{V_0}{2\sigma}\frac{\left(\frac{1+\sigma}{1-\sigma}\right)^{2r} - 1}{\left(\frac{1+\sigma}{1-\sigma}\right)^{2r} + 1}. \tag{12.30}$$

For a regime change, $n^1_{con} \to n^2_{con}$, we have

$$m^{21}_n = \begin{pmatrix} -\frac{1}{\sigma} & n^2_{con} & n^1_{con} & \frac{1}{\sigma} \end{pmatrix}$$

$$= \frac{\frac{1}{\sigma} + n^2_{con}}{\frac{1}{\sigma} - n^2_{con}} \div \frac{\frac{1}{\sigma} + n^1_{con}}{\frac{1}{\sigma} - n^1_{con}} = \frac{\frac{1}{\sigma} + \frac{n^2_{con} - n^1_{con}}{1-(\sigma)^2 n^2_{con} n^1_{con}}}{\frac{1}{\sigma} - \frac{n^2_{con} - n^1_{con}}{1-(\sigma)^2 n^2_{con} n^1_{con}}}.$$

It is possible to introduce, similarly to (12.13), the transformation ratio change

$$n^{21} = \frac{n^2_{con} - n^1_{con}}{1 - (\sigma)^2 n^2_{con} n^1_{con}} = \frac{(n^2 - 1) - (n^1 - 1)}{1 - (\sigma)^2 (n^2 - 1)(n^1 - 1)}.$$

Then

$$m^{21}_n = \frac{\frac{1}{\sigma} + n^{21}}{\frac{1}{\sigma} - n^{21}}. \tag{12.31}$$

The subsequent value

$$n^2_{con} = \frac{n^1_{con} + n^{21}}{1 + (\sigma)^2 n^1_{con} n^{21}}. \tag{12.32}$$

Similarly, for the voltage change, $V_L^1 \to V_L^2$, it is possible to write down at once

$$\begin{aligned} m_V^{21} &= \frac{\frac{V_0}{2\sigma} + V_L^{21}}{\frac{V_0}{2\sigma} - V_L^{21}}, \\ V_L^{21} &= \frac{V_L^2 - V_L^1}{1 - 4(\sigma)^2 \frac{V_L^2 V_L^1}{(V_0)^2}}, \quad V_L^2 = \frac{V_L^{21} + V_L^1}{1 + 4(\sigma)^2 \frac{V_L^{21} V_L^1}{(V_0)^2}}. \end{aligned} \tag{12.33}$$

Let us consider the change m_D^{21}. Using (12.27), we have

$$m_D^{21} = m_D^2 \div m_D^1 = \frac{\frac{1}{\sigma-1} + D^2}{\frac{1}{\sigma+1} - D^2} \div \frac{\frac{1}{\sigma-1} + D^1}{\frac{1}{\sigma+1} - D^1}, \tag{12.34}$$

where the change

$$\begin{aligned} D^{21} = n^{21} &= \frac{\frac{D^2}{1-D^2} - \frac{D^1}{1-D^1}}{1 - (\sigma)^2 \frac{D^2}{1-D^2} \frac{D^1}{1-D^1}} \\ &= \frac{D^2 - D^1}{1 - (D^2 + D^1) + D^2 D^1 (1 - (\sigma)^2)}. \end{aligned} \tag{12.35}$$

Thus, the mutually coordinated system of all the regime parameters turns out.

Similar to Fig. 12.6 and relationships (12.18)–(12.20), we can use the linearization of the regulation characteristic.

For that, we give, similar to (12.30), the expression for the nonlinear function calculator as

$$V_{reg} = D = \frac{\left(\frac{1+\sigma}{1-\sigma}\right)^r - 1}{(1+\sigma)\left(\frac{1+\sigma}{1-\sigma}\right)^r - (1-\sigma)}. \tag{12.36}$$

In turn, we rewrite (12.29) for variable as

$$V_{fb} = Ln \frac{\frac{V_0}{2\sigma} + V_L}{\frac{V_0}{2\sigma} - V_L} \div 2Ln \frac{1+\sigma}{1-\sigma}. \tag{12.37}$$

12.3.2 Buck–Boost Converter with Losses of Choke

Let us consider a buck–boost converter with an idealized voltage source V_0 in Fig. 12.15 [7].

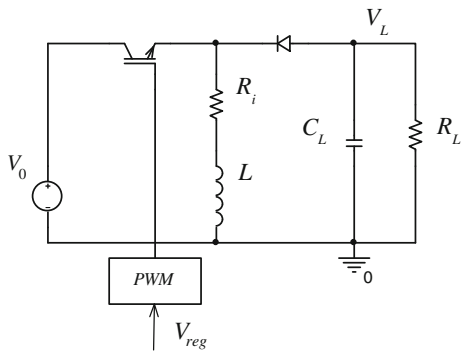

Fig. 12.15 Buck–boost converter with a loss resistance of choke

Taking into account a loss resistance R of choke L, the regulation characteristic is set by well-known expressions

$$V_L = V_0 \frac{D(1-D)}{(1-D)^2 + (\sigma)^2} = V_0 \frac{n-1}{1+(\sigma n)^2}, \tag{12.38}$$

The plots of these dependences are close to Figs. 12.11 and 12.12.

Similar to (12.22), let us introduce the variable V so that

$$\frac{V_L}{V} = n - 1. \tag{12.39}$$

Then, we obtain the general equation of ellipse as

$$(\sigma)^2 V_L^2 + (1+\sigma^2)(V)^2 + 2(\sigma)^2 V_L V - V_0 V = 0. \tag{12.40}$$

The plot of this ellipse is shown in Fig. 12.16. The value n turns out at the expense of a stereographic projection.

Let us obtain the characteristic values, using the data of the previous example. So, we give the ready formulas for the maximum values

$$V_{LM} = \frac{V_0}{2\sigma(\sigma \pm \sqrt{1+\sigma^2})} = \frac{V_0}{2\sigma^2 n_M}$$
$$= \frac{25}{2 \cdot 0.08(0.08 \pm 1.0032)} = \begin{cases} +144.2 = V_{LM}^+ \\ -169.24 = V_{LM}^- \end{cases},$$
$$n_M = \frac{\sigma + \sqrt{1+\sigma^2}}{\sigma} = \begin{cases} +13.54 = n_M^+ \\ -11.54 = n_M^- \end{cases}.$$

We accept the points $V_L = 0, n = 1$ as a unit points, and $V_L = -25, n = 0$ as the scale points.

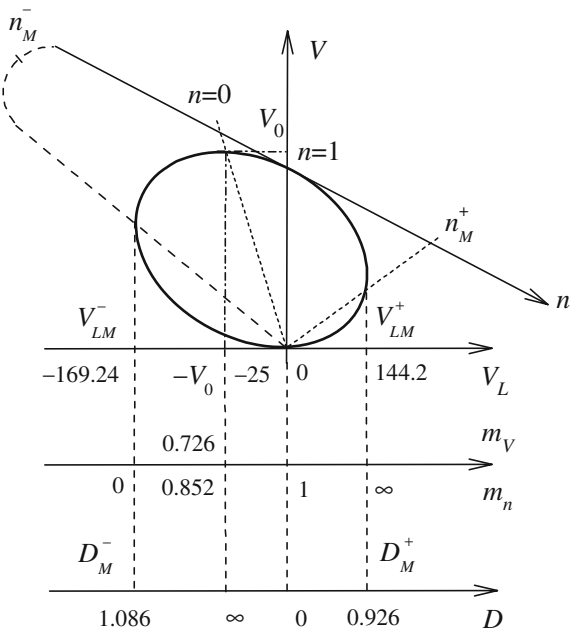

Fig. 12.16 Geometrical model of the regulation characteristic of the buck–boost converter with the loss resistance of choke and conformity of the points V_L, n, D

Then, the cross ratios for the initial regime are

$$m_V^1 = (V_{LM}^- \;\; V_L^1 \;\; 0 \;\; V_{LM}^+) = \frac{V_L^1 - V_{LM}^-}{V_L^1 - V_{LM}^+} \cdot \frac{V_{LM}^+}{V_{LM}^-},$$
$$m_n^1 = (n_M^- \;\; n^1 \;\; 1 \;\; n_M^+) = \frac{n^1 - n_M^-}{n^1 - n_M^+} \cdot \frac{1 - n_M^+}{1 - n_M^-}.$$

The cross ratios for the scale points are

$$m_V^{SCL} = \frac{-V_0 - V_{LM}^-}{-V_0 - V_{LM}^+} \cdot \frac{V_{LM}^+}{V_{LM}^-} = 0.726,$$
$$m_n^{SCL} = \frac{n_M^-}{n_M^+} \cdot \frac{1 - n_M^+}{1 - n_M^-} = 0.852.$$

All the above relationships are applicable further.

Also, we may use the linearization of the regulation characteristic. For this, we give the required expression for the nonlinear function calculator

$$V_{reg} = D = 1 + \sigma^2 - \sigma\sqrt{1+\sigma^2}\,\frac{\left(\frac{1+\sigma/\sqrt{1+\sigma^2}}{1-\sigma/\sqrt{1+\sigma^2}}\right)^{2r+1} + 1}{\left(\frac{1+\sigma/\sqrt{1+\sigma^2}}{1-\sigma/\sqrt{1+\sigma^2}}\right)^{2r+1} - 1} \tag{12.41}$$

and for the inverse nonlinear function calculator

$$V_{fb} = r = Ln\frac{\frac{V_0}{2\sigma} - V_L(\sigma - \sqrt{1+\sigma^2})}{\frac{V_0}{2\sigma} - V_L(\sigma + \sqrt{1+\sigma^2})} \div Ln\frac{1+2\sigma(\sigma+\sqrt{1+\sigma^2})}{1+2\sigma(\sigma-\sqrt{1+\sigma^2})}. \tag{12.42}$$

References

1. Erickson, R.W., Maksimovic, D.: Fundamentals of Power Electronics. Springer, Berlin (2001)
2. Iskender, I., Genc, N.: Design and analysis of a novel zero–voltage-transition interleaved boost converter for renewable power applications. Int. J. Electron. **97**(9), 1051–1070 (2010)
3. Lo, Y.K., Chen, J.T., Lin, C.Y., Ou, S.Y.: Improved control-to-output characteristics of a PWM buck-boost converter. Int. J. Circuit Theory Appl. **39**(2), 203–209 (2011)
4. Lui, X., Wang, P., Loh, P.: A Hybrid AC/ DC micro grid and its coordination control. IEEE Trans. Smart Grid **2**(2), 278–286 (2011)
5. Michal, V., Premont, C.H., Pillonet, G.: Switched DC/DC boost power stage with linear control-to-output conversion ratio, based on the ramp-modulated PWM generator. European patent EP 2482433 A2, 1 Aug 2012
6. Penin, A.: Method of regulating the voltage with step-up and inverting pulse converters. MD Patent 4067, 26 Aug 2008
7. Penin, A.: Regimes analysis of the voltage pulse regulators on the basic of the invariance property of the control characteristics. Probl. Reg. Energ. **1** (2009)
8. Penin, A.: Analysis of regimes of voltage regulators with limited capacity voltage sources. Geometrical approach. WSEAS Trans. Circuits Systems. **12**(1), 12 (2013) http://www.wseas.org/wseas/cms.action?id=6933. Accessed 30 Nov 2014
9. Sira– Ramirez, H., Rios-Bolivar, M.: Sliding mode control of dc–to–dc power converters via extended linearization. IEEE Trans. Circuits Syst.—1. Fundam. Theory Appl. **41**(10), 652–660 (1994)
10. Sundareswaran, K., Devi, V., Nadeem, S.K., Sreedevi, V.T., Palani, S.: Buck–boost converter feedback controller design via evolutionary search. Int. J. Electron. **97**(11), 1317–1327 (2010)

Part IV
Circuits with Non-Linear Load Characteristics

Chapter 13
Power-Source and Power-Load Elements

13.1 Introduction

In the electric circuit theory, the concepts of power-source and power-load elements are developed on the basis of generalization of results in power processing systems [1–4, 8]. Analysis of a power supply system, which contains a power-load element, shows the two-valued voltage of a limited capacity voltage source. But for all that, the volt-ampere characteristic of this power-load element has one-valued representation. On the other hand, taking into account the losses of real power-source and power-load elements, we get the two-valued volt-ampere characteristic of these elements [6]. Also, the influence of supply line losses onto the power-load element has practical importance [5, 7].

Therefore, it is desirable reasonably to determine the regime parameters of the power-source and power-load element using the single-valued area of their characteristics; that is, to present the regime parameters in the relative form.

13.2 Two-Valued Regime of a Regulated Converter. The Concept of a Power-Source and Power-Load Element

Let us consider the simplest power supply system with a voltage regulator (stabilizer) *VR* and given load resistance R_1 in Fig. 13.1. The load power

$$P = \frac{(V_{1=})^2}{R_1} = IV, \quad \text{or} \quad I = P/V$$

represents a hyperbola in Fig. 13.2.

A. Penin, *Analysis of Electrical Circuits with Variable Load Regime Parameters*,
Power Systems, DOI 10.1007/978-3-319-28451-4_13

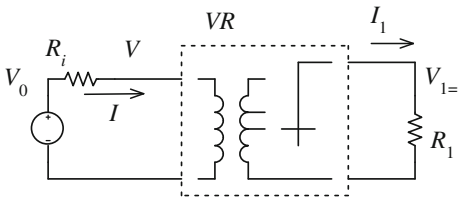

Fig. 13.1 Power supply system with a given load power

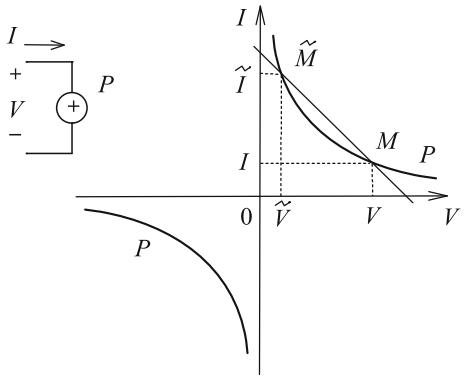

Fig. 13.2 Power-load element P and its hyperbolic characteristic

So, we have a power-load element P for different values of voltage V and current I. In turn, the voltage source characteristic

$$I = \frac{V_0}{R_i} - \frac{V}{R_i}, \tag{13.1}$$

as a straight line, intersects the hyperbola into two points M, $\tilde{M}$.

Using load power characteristic $I = P/V$, we get the quadratic equation

$$\frac{V_0 V}{R_i} - \frac{(V)^2}{R_i} = P. \tag{13.2}$$

Therefore, we have the corresponding two roots

$$V = \frac{V_0}{2}\left(1 + \sqrt{1 - \frac{4PR_i}{(V_0)^2}}\right), \quad \tilde{V} = \frac{V_0}{2}\left(1 - \sqrt{1 - \frac{4PR_i}{(V_0)^2}}\right). \tag{13.3}$$

On the contrary, we may say about a power-source element, which gives a constant power into a variable load in Fig. 13.3.

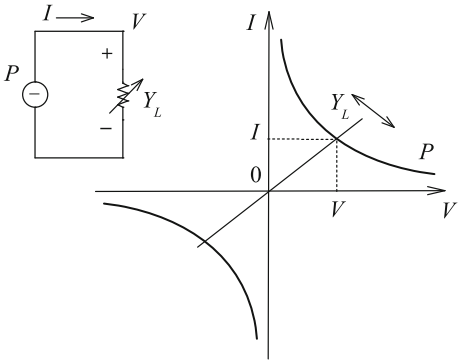

Fig. 13.3 Power-source element P and its hyperbolic characteristic

Note

The offered graphic representation of both power-load $+P$ and power-source $-P$ elements corresponds by analogy to a voltage source and source of current.

Further, we will consider power-load elements using the results [5, 6].

13.3 Influence of Voltage Source Parameters and Power-Load Element onto a Power Supply Regime

13.3.1 Ideal Voltage Source

The power-load element P with an ideal voltage source V_0 is represented in Fig. 13.4. A volt-ampere characteristic of P is the known hyperbola $I = P/V$.

In turn, a volt-ampere characteristic of V_0 represents a vertical line with the coordinate $V = V_0$. A point of intersection (I, V_0) of this line and hyperbola determines a single or one-valued regime of this circuit.

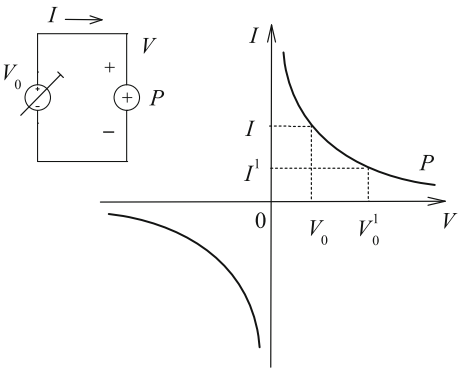

Fig. 13.4 Power-load element and an ideal voltage source

For a different voltage source value V_0^1, a new point (I^1, V_0^1) will be the energy equivalent point to the initial point (I, V_0) because this circuit does not possess the own or internal scales, which can specify the qualitative characteristics of an operating regime. It is true for the infinite large values $I = \infty, V = \infty$ of our ideal circuit. Therefore, regimes of different comparable circuits are equivalent always.

13.3.2 Voltage of a Power Supply with Limited Capacity

Let us consider the simplest power supply system in Fig. 13.5. For different voltage source values (V_0^1, V_0^2, and so on), we get the voltage source characteristic as parallel lines. These lines intersect the hyperbola into pairs of points M_1, $\tilde{M}_1$; M_2, $\tilde{M}_2$, and so on. The arrows show the conformity of these points. Also, the characteristic points M^+, M^- correspond to the tangent lines $\pm V_{0M}$. The closed arrows illustrate these fixed points. For the fixed points, from (13.3), when $V = \tilde{V} = V_0/2$, the following condition takes place

$$1 - \frac{4PR_i}{(V_0)^2} = 0.$$

Therefore, we get the allowable minimum voltage source values

$$V_{0M} = \pm 2\sqrt{PR_i}. \tag{13.4}$$

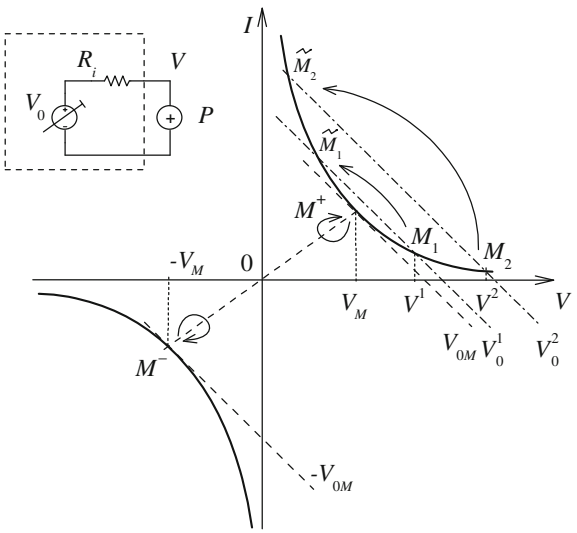

Fig. 13.5 Characteristics of a power-load element with different values of a voltage source

The corresponding power-load element voltages

$$V_M = \pm\sqrt{PR_i}. \tag{13.5}$$

We must prove the single-valued area of the power-load element characteristic.

To do this, we consider the characteristics of the power-load element in the projective coordinates in Fig. 13.6. The parallel lines of the voltage source characteristics are intersected into point S onto the infinitely remote line ∞. This point S is a pole and the straight line M^+M^- is a polar. Therefore, we get some symmetry or mapping of the "lower" part of our curve onto the "upper" part. The points M^+, M^- are the fixed or base points. So, the obtained single-valued area involves the characteristic points $V_M, \infty, -V_M$.

Now, using the conformity of the voltages V, V_0, we may represent the regime parameters in the relative form.

From (13.2), we get

$$V_0 = \frac{R_i P}{V} + V. \tag{13.6}$$

This dependence determines a hyperbola in Fig. 13.7. Therefore, the single-valued mapping of the hyperbola points onto the axis V takes place.

Let us constitute the cross-ratio m_V^1 for the initial point V^1

$$m_V^1 = \left(V_M \;\; V^1 \;\; \infty \;\; -V_M\right) = \frac{V^1 - V_M}{V^1 + V_M}, \tag{13.7}$$

where the points $V_M = \frac{V_{0M}}{2}$, $-V_M = -\frac{V_{0M}}{2}$ are base ones and $V = \infty$ is a unit point. The conformity of the points V^1, m_V^1 is shown in Fig. 13.8.

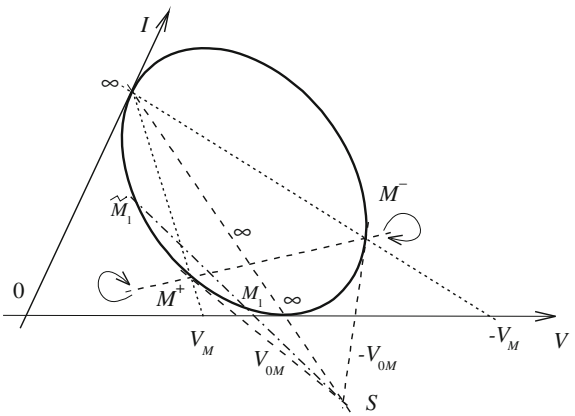

Fig. 13.6 Characteristics of the power-load element in the projective coordinates

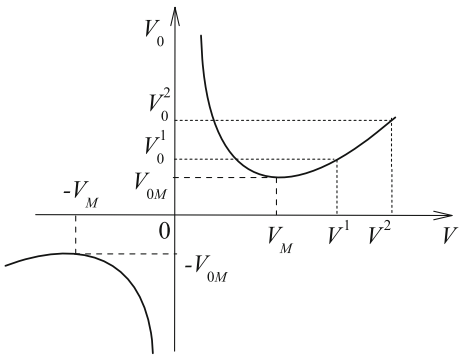

Fig. 13.7 Dependence $V_0(V)$ for a given load power

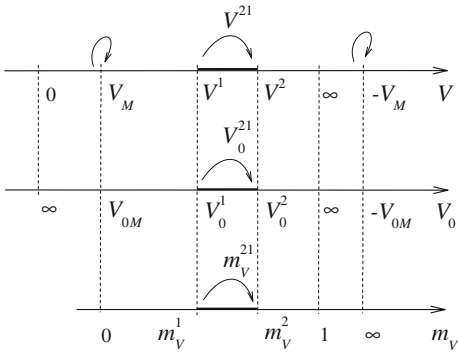

Fig. 13.8 Conformity of different regime parameters

Further, the cross-ratio m_V^{21}, which corresponds to a regime change $V^1 \to V^2$, has the form

$$m_V^{21} = \left(\frac{V_{0M}}{2} \;\; V^2 \;\; V^1 \;\; -\frac{V_{0M}}{2}\right) = \frac{V^2 - \frac{V_{0M}}{2}}{V^2 + \frac{V_{0M}}{2}} \div \frac{V^1 - \frac{V_{0M}}{2}}{V^1 + \frac{V_{0M}}{2}}. \tag{13.8}$$

Using the normalized values

$$\bar{V}^2 = 2\frac{V^2}{V_{0M}} > 1, \quad \bar{V}^1 = 2\frac{V^1}{V_{0M}} > 1,$$

we get regime change (13.8) as

$$m_V^{21} = \left(1 \;\; \bar{V}^2 \;\; \bar{V}^1 \;\; -1\right) = \frac{\bar{V}^2 - 1}{\bar{V}^2 + 1} \div \frac{\bar{V}^1 - 1}{\bar{V}^1 + 1}. \tag{13.9}$$

This expression we rewrite in the view

$$m_V^{21} = \frac{\bar{V}^2 - 1}{\bar{V}^2 + 1} \cdot \frac{\bar{V}^1 + 1}{\bar{V}^1 - 1} = \frac{\frac{\bar{V}^2\bar{V}^1 - 1}{\bar{V}^2 - \bar{V}^1} + 1}{\frac{\bar{V}^2\bar{V}^1 - 1}{\bar{V}^2 - \bar{V}^1} - 1}. \tag{13.10}$$

Then, we introduce the voltage change V^{21} expression

$$V^{21} = \frac{\bar{V}^2\bar{V}^1 - 1}{\bar{V}^2 - \bar{V}^1}. \tag{13.11}$$

So, the following relationships are performed

$$m_V^{21} = \frac{V^{21} + 1}{V^{21} - 1}, \quad V^{21} = \frac{m_V^{21} - 1}{m_V^{21} + 1}. \tag{13.12}$$

Using (13.11), we obtain the subsequent voltage

$$\bar{V}^2 = \frac{V^{21}\bar{V}^1 - 1}{V^{21} - \bar{V}^1}. \tag{13.13}$$

There is a group transformation. Moreover, if the initial value $\bar{V}^1 = 1$, then the subsequent value $\bar{V}^2 = 1$ regardless of the value V^{21}.

Similarly to the above, let us consider the cross-ratio m_0^1 for the voltage V_0 using the conformity of the variables by Fig. 13.8 for the single-valued area. This cross-ratio has the form

$$m_0^1 = \left(V_{0M}\ \ V_0^1\ \ \infty\ \ -V_{0M}\right) = \frac{V_0^1 - V_{0M}}{V_0^1 + V_{0M}}. \tag{13.14}$$

Also, the following equality takes place

$$m_0^1 = (m_V^1)^2. \tag{13.15}$$

We may use the hyperbolic metric to determine a regime value or distance

$$H^1 = Ln\, m_0^1 = 2Ln\, m_V^1. \tag{13.16}$$

The base points $V_0, -V_0$ and points $V_M, -V_M$, as the limit points, correspond to the infinitely large distance. Therefore, this limit regime has a clear physical sense.

Similarly to (13.8), the cross-ratio m_0^{21}, which corresponds to a voltage source regime change $V_0^1 \to V_0^2$, has the view

$$m_0^{21} = \left(V_{0M}\ \ V_0^2\ \ V_0^1\ \ -V_{0M}\right) = \frac{V_0^2 - V_{0M}}{V_0^2 + V_{0M}} \div \frac{V_0^1 - V_{0M}}{V_0^1 + V_{0M}}. \tag{13.17}$$

Using the normalized values

$$\bar{V}_0^2 = \frac{V_0^2}{V_{0M}} > 1, \quad \bar{V}_0^1 = \frac{V_0^1}{V_{0M}} > 1,$$

we get the regime change in the view

$$m_0^{21} = \left(1 \;\; \bar{V}_0^2 \;\; \bar{V}_0^1 \;\; -1\right) = \frac{\bar{V}_0^2 - 1}{\bar{V}_0^2 + 1} \div \frac{V_0^1 - 1}{V_0^1 + 1}. \tag{13.18}$$

This expression we rewrite in the view

$$m_0^{21} = \frac{\bar{V}_0^2 - 1}{\bar{V}_0^2 + 1} \cdot \frac{\bar{V}_0^1 + 1}{\bar{V}_0^1 - 1} = \frac{\frac{\bar{V}_0^2 \bar{V}_0^1 - 1}{\bar{V}_0^2 - \bar{V}_0^1} + 1}{\frac{\bar{V}_0^2 \bar{V}_0^1 - 1}{\bar{V}_0^2 - \bar{V}_0^1} - 1}. \tag{13.19}$$

Similarly to (13.11), we introduce the analogous expression for the voltage source change V_0^{21}

$$V_0^{21} = \frac{\bar{V}_0^2 \bar{V}_0^1 - 1}{\bar{V}_0^2 - \bar{V}_0^1}. \tag{13.20}$$

Then, the following relationships are performed

$$m_0^{21} = \frac{V_0^{21} + 1}{V_0^{21} - 1}, \quad V_0^{21} = \frac{m_0^{21} - 1}{m_0^{21} + 1}. \tag{13.21}$$

Using (13.20), we obtain the subsequent voltage

$$\bar{V}_0^2 = \frac{V_0^{21} \bar{V}_0^1 - 1}{V_0^{21} - \bar{V}_0^1}. \tag{13.22}$$

Then, *there is a strong reason to introduce a voltage source change as* V_0^{21} *and a voltage change of power-load element as* V^{21}.

The validity of such definitions for the changes is confirmed by the following expression similar to initial expression (13.6); that is,

$$2V_0^{21} = \frac{1}{V^{21}} + V^{21}.$$

Example Let the circuit parameters be given as $V_0 = 5$, $R_i = 2$, $P = 3$.

Power-load voltages (13.3)

$$V = \frac{5}{2}\left[1 \pm \sqrt{1 - \frac{4 \cdot 3 \cdot 2}{5^2}}\right] = \frac{5}{2}\frac{5 \pm 1}{5} = \begin{cases} 3 = V \\ 2 = \tilde{V} \end{cases}.$$

Voltages (13.5), $V_M = \pm\sqrt{PR_i} = \pm\sqrt{3 \cdot 2} = \pm\sqrt{6}$.
Cross-ratio (13.7) for the initial regime $V^1 = 3$

$$m_V^1 = \frac{3 - \sqrt{6}}{3 + \sqrt{6}} = \frac{0.5505}{5.4494} = 0.10102.$$

Let the subsequent regime be given by $V_0^2 = 8$.
Then, subsequent power-load voltages (13.3) equals to $V^2 = 7.1623$.
Regime change cross-ratio (13.8)

$$m_V^{21} = \frac{V^2 - \frac{V_{0M}}{2}}{V^2 + \frac{V_{0M}}{2}} \div \frac{V^1 - \frac{V_{0M}}{2}}{V^1 + \frac{V_{0M}}{2}} = 0.4903 \div 0.10102 = 4.8536.$$

The normalized values

$$\bar{V}^2 = \frac{7.1623}{\sqrt{6}} = 2.924, \quad \bar{V}^1 = \frac{3}{\sqrt{6}} = 1.2247.$$

Voltage change (13.11)

$$V^{21} = \frac{2.924 \cdot 1.2247 - 1}{2.924 - 1.2247} = 1.519.$$

We check expression (13.12)

$$m_V^{21} = \frac{1.519 + 1}{1.519 - 1} = 4.8536.$$

Let us check subsequent voltage (13.13)

$$\bar{V}^2 = \frac{1.519 \cdot 1.2247 - 1}{1.519 - 1.2247} = \frac{0.8604}{0.2942} = 2.924.$$

Now, we consider the cross-ratio for the source voltage V_0.
Initial regime cross-ratio (13.14)

$$m_0^1 = \frac{5 - 2\sqrt{6}}{5 + 2\sqrt{6}} = \frac{0.101}{9.9} = 0.0102.$$

Equality (13.15), $0.0102 = 0.10102^2$.

Distance (13.16)

$$H^1 = Ln\,0.0102 = 2Ln\,0.10102 = -4.5848.$$

Voltage source regime change (13.17)

$$m_0^{21} = \frac{8-2\sqrt{6}}{8+2\sqrt{6}} \div 0.0102 = 0.2404 \div 0.0102 = 23.5578.$$

The normalized values

$$\bar{V}_0^2 = \frac{8}{2\sqrt{6}} = 1.633, \quad \bar{V}_0^1 = \frac{V_0^1}{V_{0M}} = \frac{5}{2\sqrt{6}} = 1.021.$$

Voltage source change (13.20)

$$V_0^{21} = \frac{1.633 \cdot 1.021 - 1}{1.633 - 1.021} = \frac{0.6666}{0.6124} = 1.0887.$$

We check expression (13.21)

$$m_0^{21} = \frac{V_0^{21}+1}{V_0^{21}-1} = \frac{1.0887+1}{1.0887-1} = 23.5578.$$

Let us check subsequent voltage (13.22)

$$\bar{V}_0^2 = \frac{V_0^{21}\bar{V}_0^1 - 1}{V_0^{21} - \bar{V}_0^1} = \frac{1.0887 \cdot 1.021 - 1}{1.0887 - 1.021} = \frac{0.1111}{0.068} = 1.633.$$

13.3.3 Internal Resistance of a Voltage Source

Let us consider the circuit with a variable internal resistance in Fig. 13.9. For its different values, we get the voltage source characteristics as a bunch of straight lines. The bunch center S conforms to the voltage V_0.

For example, the line R_i^1 intersects the hyperbola into points M_1, $\tilde{M}_1$. The arrow shows the conformity of these points. Also, the characteristic point M^+ corresponds to the first tangent lines SM^+ for R_{iM}. For this value R_{iM}, from (13.3), as $V = \tilde{V} = V_0/2$, we get

$$R_{iM} = \frac{(V_0)^2}{4P}, \quad V_M = \frac{V_0}{2}. \tag{13.23}$$

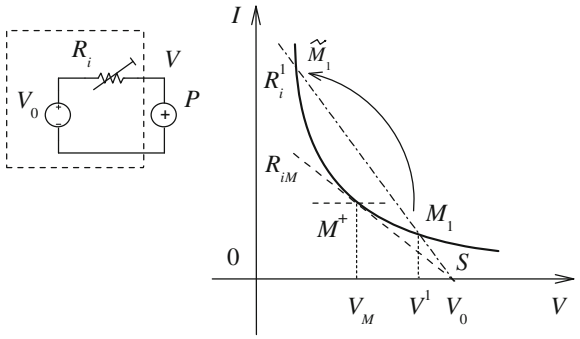

Fig. 13.9 Characteristics of a power-load element with different values of an internal resistance

We must prove the single-valued area of the power-load element characteristic. To do this, we consider the characteristics of the power-load element in the projective coordinates in Fig. 13.10.

Using the bunch center, the point S, we may draw the second tangent lines SM^-. The point M^- corresponds to the infinitely remote point ∞. This point S is the pole and the straight line M^+M^- is the polar.

Therefore, we get mapping of the "lower" part of our curve onto the "upper" part. The points M^+, M^- are the fixed or base points. So, the obtained single-valued area involves the characteristic points V_M, V_0, ∞.

Now, using the conformity of the values V, R_i, we may represent the regime parameters in the relative form.

From (13.2), we get

$$R_i = \frac{V_0 V}{P} - \frac{(V)^2}{P}. \tag{13.24}$$

This dependence $R_i(V)$ determines a parabola in Fig. 13.11.

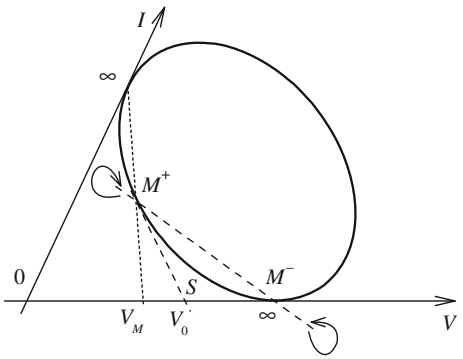

Fig. 13.10 Characteristics of the power-load element in the projective coordinates

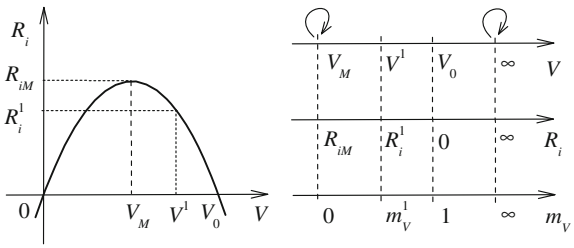

Fig. 13.11 Dependence $R_i(V)$ for a given load power and conformity of different regime parameters

Therefore, the single-valued mapping of the parabola points onto the axis V takes place.

Using expression (13.7), we may constitute the cross-ratio m_V^1 for the initial point V^1; that is,

$$m_V^1 = \left(V_M \;\; V^1 \;\; V_0 \;\; \infty\right) = \frac{V^1 - V_M}{V_0 - V_M} = \frac{V^1 - V_0/2}{V_0/2}. \tag{13.25}$$

The points $V_M = \frac{V_{0M}}{2}$, $V = \infty$ are base ones and V_0 is a unit point. The conformity of the points V^1, m_V^1 is shown in Fig. 13.11.

Similarly to the above, let us consider the cross-ratio m_i^1 for the resistance R_i using the conformity of the variables by Fig. 13.11 for the single-valued area. This cross-ratio has the form

$$m_i^1 = \left(R_{iM} \;\; R_i^1 \;\; 0 \;\; \infty\right) = \frac{R_{tiM} - R_i^1}{R_{iM}}. \tag{13.26}$$

Also, the following equality takes place

$$m_i^1 = (m_V^1)^2. \tag{13.27}$$

13.3.4 Power of a Power-Load Element

Let us consider the circuit with a variable power of power-load element P in Fig. 13.12.

For its different values, we get the load power characteristic as a bunch of hyperbolas. The voltage source characteristic is the known straight line.

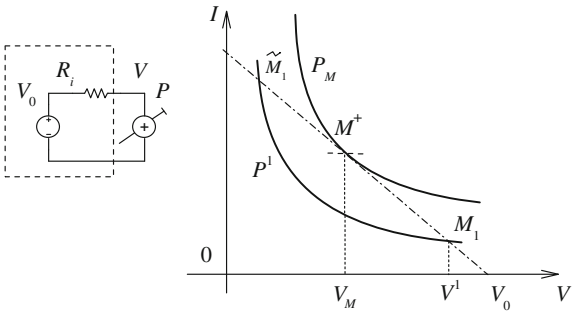

Fig. 13.12 Characteristics of a power-load element with different values of its power

For example, this line intersects the hyperbola P^1 into points M_1, $\tilde{M}_1$. Also, the characteristic point M^+ corresponds to the tangent hyperbola P_M. From (13.23), we get

$$P_M = \frac{(V_0)^2}{4R_i}, \quad V_M = \frac{V_0}{2}. \tag{13.28}$$

We must prove the single-valued area of the power-load element characteristic. To do this, we may use expression (13.24). In this case, we get the similar form

$$P = \frac{V_0 V}{R_i} - \frac{(V)^2}{R_i}. \tag{13.29}$$

This dependence $P(V)$ determines a parabola in Fig. 13.13. Therefore, the single-valued mapping of the parabola points onto the axis V takes place, which coincides with Fig. 13.11.

So, we may use the same cross-ratio (13.25) for the initial point V^1 at once

$$m_V^1 = \left(V_M \;\; V^1 \;\; V_0 \;\; \infty\right) = \frac{V^1 - V_0/2}{V_0/2}. \tag{13.30}$$

The conformity of the points V^1, m_V^1 is shown in Fig. 13.13.

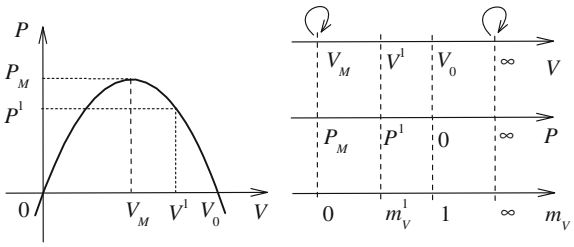

Fig. 13.13 Dependence $P(V)$ for a given voltage source and conformity of different regime parameters

Similarly to the above, let us consider the cross-ratio m_P^1 for the power P^1 using the conformity of the variables by Fig. 13.13 for the single-valued area. This cross-ratio has the form

$$m_P^1 = \left(P_M \;\; P^1 \;\; 0 \;\; \infty\right) = \frac{P_M - P^1}{P_M}. \tag{13.31}$$

Also, the following equality takes place

$$m_P^1 = (m_V^1)^2. \tag{13.32}$$

13.4 Power-Load Element with Losses

13.4.1 Series Loss Resistance

Let the power-load element contain a series loss resistance R_0 in Fig. 13.14. We must obtain equations of the superposed characteristics of the voltage source and the power-load element. The known power-load characteristic has the view

$$V(I) = P/I.$$

Using (13.1), we obtain the following expression for the current

$$I = \frac{V_0}{R_0} - \frac{V}{R_0} = \frac{V_0}{R_0} - \frac{P}{IR_0}.$$

From here,

$$V_0(I) = \frac{P}{I} + IR_0. \tag{13.33}$$

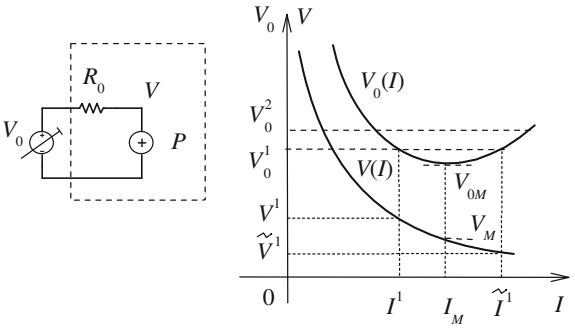

Fig. 13.14 Variable voltage source, power-load element with a series loss resistance and their characteristics

Evidently, this equation contains the sum of the hyperbola and straight line.

For different voltage source values (V_0^1, V_0^2 and so on), we get the voltage source characteristic as parallel horizontal lines. The pairs of the currents I^1, $\tilde{I}^1$, and voltages V^1, $\tilde{V}^1$ correspond to the given source voltage V_0^1. Therefore, the volt-ampere characteristic $V_0(I)$ of this voltage source is the two-valued one.

From (13.33), we get

$$V_0(V) = \frac{PR_0}{V} + V.$$

Obviously, this expression coincides with (13.6) and corresponds to Fig. 13.7. Therefore, all expressions (13.7)–(13.22) remain in force.

13.4.2 Two-Port Loss Circuit

Let the losses be given by a two-port in Fig. 13.15.

Let us obtain an equation of the volt-ampere characteristic$V_0(I_0)$. We rewrite expression (1.27) of a two-port

$$\begin{bmatrix} I_0 \\ I_1 \end{bmatrix} = \begin{bmatrix} Y_{00} - Y_{10} \\ Y_{10} - Y_{11} \end{bmatrix} \cdot \begin{bmatrix} V_0 \\ V_1 \end{bmatrix},$$

where Y parameters

$$Y_{00} = y_{10} + y_0, \quad Y_{11} = y_{10} + y_1, \quad Y_{10} = y_{10}.$$

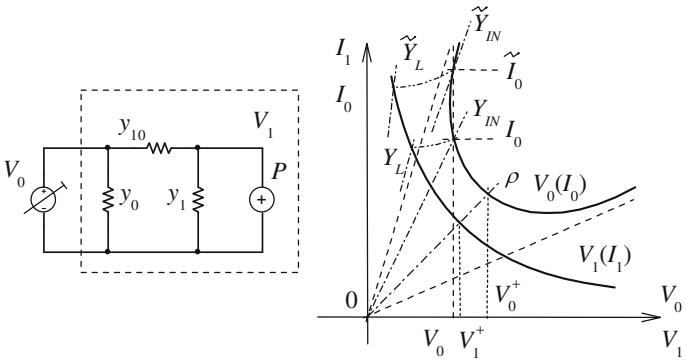

Fig. 13.15 Variable voltage source, power-load element with loss two-port and their characteristics

The matrix determinant

$$\Delta_Y = Y_{00}Y_{11} - (Y_{10})^2.$$

Further, we will consider the bilateral two-port with $Y_{00} = Y_{11}$. Next, we use the transmission parameters. In this case, expression (1.30) has the view

$$\begin{bmatrix} V_0 \\ \dfrac{I_0}{\rho} \end{bmatrix} = \begin{bmatrix} ch\gamma & sh\gamma \\ shy & ch\gamma \end{bmatrix} \cdot \begin{bmatrix} V_1 \\ \dfrac{I_1}{\rho} \end{bmatrix}, \tag{13.34}$$

$$ch^2\gamma = \frac{Y_{00}Y_{11}}{(Y_{10})^2}, \quad sh^2\gamma = \frac{\Delta_Y}{(Y_{10})^2},$$

γ is the attenuation coefficient, $\rho = \sqrt{\Delta_Y}$ is the characteristic admittance.

Admittance transformation (1.31)

$$Y_{IN} = \frac{Y_{00}Y_L + \Delta_Y}{Y_{11} + Y_L}, \quad \frac{Y_{IN}}{\rho} = \frac{\frac{Y_L}{\rho} + th\gamma}{1 + \frac{Y_L}{\rho} th\gamma}, \tag{13.35}$$

where load conductivity $Y_L = I_1/V_1$.

The inverse expression of (13.34) is

$$\begin{bmatrix} V_1 \\ \dfrac{I_1}{\rho} \end{bmatrix} = \begin{bmatrix} ch\gamma & -sh\gamma \\ -shy & ch\gamma \end{bmatrix} \cdot \begin{bmatrix} V_0 \\ \dfrac{I_0}{\rho} \end{bmatrix}.$$

From here, we find the power of the power-load element

$$\begin{aligned} V_1 \frac{I_1}{\rho} = \frac{P_1}{\rho} &= (V_0\, ch\gamma - \frac{I_0}{\rho} sh\gamma) \cdot (-V_0\, sh\gamma + \frac{I_0}{\rho} ch\gamma) \\ &= -\left[(V_0)^2 + \frac{(I_0)^2}{\rho^2}\right] sh\gamma \cdot ch\gamma + V_0 \frac{I_0}{\rho} [(ch\gamma)^2 + (sh\gamma)^2]. \end{aligned}$$

Finally, we obtain

$$(V_0)^2\rho + \frac{(I_0)^2}{\rho} - V_0 I_0 \frac{(ch\gamma)^2 + (sh\gamma)^2}{sh\gamma \cdot ch\gamma} + \frac{P_1}{sh\gamma \cdot ch\gamma} = 0. \tag{13.36}$$

For a given power P_1, this dependence $V_0 = (I_0)$ determines a hyperbola in Fig. 13.15.

The equations of the asymptotes to this hyperbola has the view

$$V_0 = \frac{I_0}{\rho} th\gamma, \quad V_0 = \frac{I_0}{\rho \cdot th\gamma} \text{ or}$$
$$I_0 = \frac{\rho V_0}{th\gamma}, \quad I_0 = \rho V_0 \cdot th\gamma.$$

The pairs of input conductivities Y_{IN}, $\tilde{Y}_{IN}$, and the pairs of currents I_0, $\tilde{I}_0$ correspond to a given source voltage V_0 that determines the above two-valued volt-ampere characteristic $V_0(I_0)$. In that sense, the value Y_{IN} defines the single-valued regime.

The maximum efficiency value K_P^+ and the minimum input power value $P_{0\,MIN}$ corresponds to the admittance matching $Y_L = Y_{IN} = \rho$; that is,

$$K_P^+ = (ch\gamma - sh\gamma)^2, \quad P_{0\,MIN} = P_1/K_P^+ . \tag{13.37}$$

The corresponding voltages of the maximum efficiency

$$V_1^+ = \sqrt{\frac{P_1}{\rho}}, \quad V_0^+ = \sqrt{\frac{P_{0\,MIN}}{\rho}}. \tag{13.38}$$

For different voltage source values, we get the voltage source characteristic as parallel vertical lines in Fig. 13.16. These lines intersect the hyperbola into pairs of points, for example, the points M_1, $\tilde{M}_1$ by the voltage V_0^1. The arrow shows the conformity of these points. Also, the characteristic points M^+, M^- correspond to the tangent lines $\pm V_{0M}$. The closed arrows illustrate these fixed points.

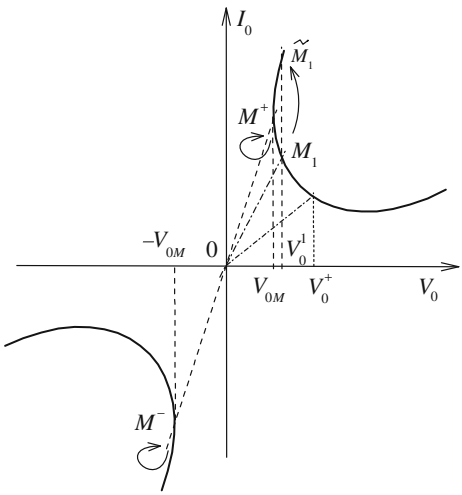

Fig. 13.16 Two-valued regime of a variable voltage source

To finding the fixed points, we obtain the following expression from (13.34)

$$V_0 = V_1 ch\gamma + \frac{I_1}{\rho} sh\gamma = V_1 ch\gamma + \frac{P_1}{\rho V_1} sh\gamma.$$

This expression is similar to (13.6) and Fig. 13.7. We suppose the derivation equals zero; that is,

$$\frac{dV_0}{dV_1} = ch\gamma - \frac{P_1}{\rho (V_1)^2} sh\gamma = 0.$$

From here, we obtain

$$V_{1M} = \pm\sqrt{\frac{P_1}{\rho} th\gamma}. \tag{13.39}$$

Therefore, we get the allowable minimum voltage source values

$$V_{0M} = \pm 2\,(ch\gamma)\sqrt{\frac{P_1}{\rho} th\gamma} = \pm 2 V_{1M}\, ch\gamma. \tag{13.40}$$

We must show the single-valued area of the voltage source characteristic. To do this, we consider this characteristic in the projective coordinates in Fig. 13.17.

The parallel tangent lines $\pm V_{0M}$ intersect at the point S as the infinitely remote point ∞ onto the axis I_0. This point S is the pole and the straight line M^+M^- is the polar.

Therefore, we get mapping of the "lower" part of our curve onto the "upper" part. The points M^+, M^- are the fixed or base points. So, the obtained single-valued area involves the characteristic points $V_{0M}, \infty, -V_{0M}$ and point V_0^+ too.

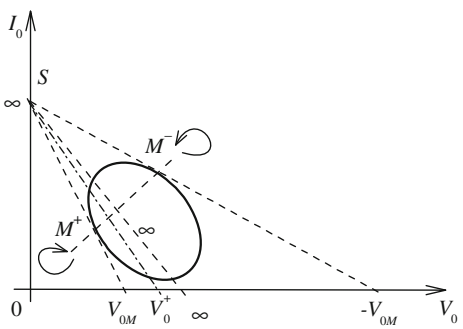

Fig. 13.17 Characteristic of the variable voltage source in the projective coordinates

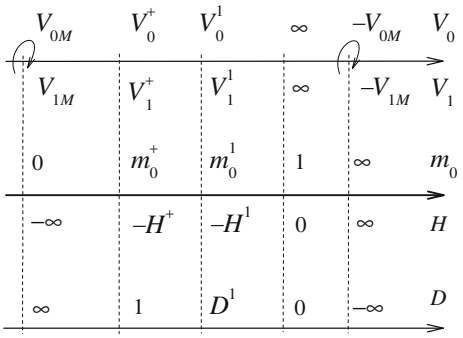

Fig. 13.18 Conformity of different regime parameters

Further, we may use all expressions (13.7), (13.8), (13.14)–(13.17). The conformity of all the points is shown in Fig. 13.18.

But, we must take into account the characteristic points for K_P^+; that is, the voltages V_1^+, V_0^+.

Let us consider the cross-ratio m_V^+ for the voltage V_1^+ similarly to (13.7)

$$m_V^+ = \left(V_M \;\; V_1^+ \;\; \infty \;\; -V_M\right) = \frac{V_1^+ - V_M}{V_1^+ + V_M}. \tag{13.41}$$

Similarly to (13.14), we consider the cross-ratio m_0^+ for the voltage V_0^+

$$m_0^+ = \left(V_{0M} \;\; V_0^+ \;\; \infty \;\; -V_{0M}\right) = \frac{V_0^+ - V_{0M}}{V_0^+ + V_{0M}}. \tag{13.42}$$

We use also hyperbolic metric (13.16)

$$H^+ = Ln\, m_0^+ = 2\, Ln\, m_V^+. \tag{13.43}$$

Further, we may introduce the normalized distance or relative deviation from the matched regime

$$D^1 = \frac{H^1}{H^+} = \frac{Ln\, m_0^1}{Ln\, m_0^+} = \frac{Ln\, m_V^1}{Ln\, m_V^+}. \tag{13.44}$$

In this case, the value H^+ is a scale value. The conformity of D^1 is presented in Fig. 13.13 too.

Example Let the circuit in Fig. 13.15 be given by the following parameters

$$Y_{10} = \sqrt{5} = 2.2361, \quad Y_{00} = Y_{11} = y_0 + y_{10} = \sqrt{5.25} = 2.2913, \quad P_1 = 8.$$

Using (13.34), we get

$$\Delta_Y = Y_{00}Y_{11} - (Y_{10})^2 = 5.25 - 5 = 0.25,$$
$$ch\gamma = \sqrt{1.05} = 1.0247, \quad sh\gamma = \sqrt{0.05} = 0.2236,$$
$$th\gamma = 0.2182, \quad \rho = \sqrt{\Delta_Y} = \sqrt{0.25} = 0.5.$$

According to (13.37)

$$K_P^+ = (1.0247 - 0.2236)^2 = 0.6417,$$
$$P_{0\,MIN} = P_1/K_P^+ = 8/0.6417 = 12.466.$$

Maximum efficiency voltages (13.38)

$$V_1^+ = \sqrt{\frac{P_1}{\rho}} = \sqrt{\frac{8}{0.5} = 4}, \quad V_0^+ = \sqrt{\frac{P_{0\,MIN}}{\rho}} = \sqrt{\frac{12.466}{0.5}} = 4.9932.$$

Minimum voltages (13.39) and (13.40)

$$V_{1M} = \pm\sqrt{\frac{P_1}{\rho}th\gamma} = \pm\sqrt{\frac{8}{0.5}0.2182} = \pm 1.8685,$$
$$V_{0M} = \pm 2V_{1M}\,ch\gamma = \pm 2 \cdot 1.8685 \cdot 1.0247 = \pm 3.8293.$$

Let the initial regime point be given as

$$V_1^1 = 8, \quad I_1^1 = P_1/V_1^1 = 1.$$

Using (13.34), we get

$$V_0^1 = 8.6448, \quad I_0^1 = 1.9191.$$

Cross-ratios (13.7) and (13.14)

$$m_V^1 = \frac{V_1^1 - V_{1M}}{V_1^1 + V_{1M}} = \frac{8 - 1.8685}{8 + 1.8685} = 0.6213,$$
$$m_0^1 = \frac{V_0^1 - V_{0M}}{V_0^1 + V_{0M}} = \frac{8.6448 - 3.8293}{8.6448 + 3.8293} = 0.386 = 0.6213^2.$$

Hyperbolic metric (13.16)

$$H^1 = Ln\, m_0^1 = Ln\, 0.386 = -0.9519.$$

Cross-ratio (13.42) and its hyperbolic metric (13.33)

$$m_0^+ = \frac{V_0^+ - V_{0M}}{V_0^+ + V_{0M}} = \frac{4.9932 - 3.8293}{4.9932 + 3.8293} = 0.1319,$$
$$H^+ = Ln\, m_0^+ = Ln\, 0.1319 = -2.0257.$$

Relative deviation from the matched regime (13.44)

$$D^1 = \frac{-H^1}{-H^+} = \frac{-0.9519}{-2.0257} = 0.4699.$$

13.5 Power Supply Line with Losses

Let the power-load element be connected to a voltage source V_0 via T network in Fig. 13.19.

For different resistance r_0 values, we get the voltage source characteristic as a bunch of straight lines in Fig. 13.20. These load straight lines intersect at a point G. For example, the line r_0^1 intersects the hyperbola into points M_1, $\tilde{M}_1$. The arrow shows the conformity of these points.

The characteristic point M^+ corresponds to the first tangent line GM^+ for r_0^+.

Also, the characteristic point M^- corresponds to the second tangent line GM^- for r_0^-. The closed arrows illustrate these fixed points.

We must prove the single-valued area of the power-load element characteristic. To do this, we consider the characteristics of the power-load element in the projective coordinates in Fig. 13.21.

Therefore, the point G is the pole and the straight line M^+M^- is the polar. Then, we get some symmetry or mapping of the "lower" part of our curve onto the "upper" part. The points M^+, M^- are the base points.

So, the obtained single-valued area involves the characteristic points $V_{1M}^+, \infty, V_{1M}^-$. We must determine all the characteristic values for voltage V_1 and resistance r_0.

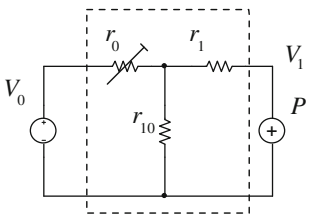

Fig. 13.19 Supply line with a variable series resistance

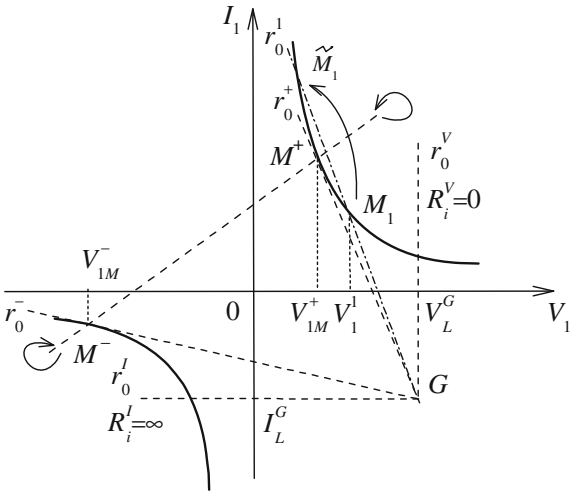

Fig. 13.20 Characteristics of a power-load element with a variable series resistance of supply line

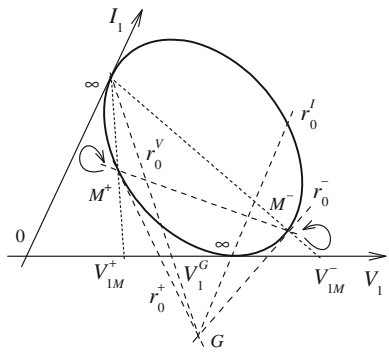

Fig. 13.21 Characteristics of the power-load element in the projective coordinates

As it was shown above, the load straight lines intersect at the point G, which has coordinates I_L^G, V_L^G. Physically, it means that regime parameters do not depend on the value r_0; that is, the current across this element is equal to zero at the expense of the load voltage.

Therefore, it is convenience to use the generalized Thévenin/Helmholtz equivalent generator of our network shown in Fig. 13.22. Then, the parameters of this generator are the following values

$$-I_L^G = \frac{V_0}{r_{10}}, \tag{13.45}$$

$$V_L^G = \frac{r_1 + r_{10}}{r_{10}} V_0. \tag{13.46}$$

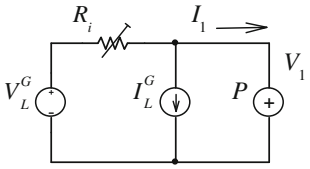

Fig. 13.22 Equivalent circuit for the power-load element with the supply line

The internal resistance

$$R_i = r_1 + \frac{r_0 r_{10}}{r_0 + r_{10}}. \tag{13.47}$$

In turn,

$$r_0 = \frac{r_{10}(R_i - r_1)}{r_{10} - (R_i - r_1)}. \tag{13.48}$$

The resistances R_i, r_0 have the following characteristic values

$$R_i^V = 0, \quad r_0^V = -\frac{r_{10} \cdot r_1}{r_{10} + r_1}, \tag{13.49}$$

$$R_i^I = \infty, \quad r_0^I = -r_{10}. \tag{13.50}$$

Thus, an equation of straight line, passing through the point G, has the form

$$I_1 = \frac{V_L^G - V_1}{R_i} - I_L^G. \tag{13.51}$$

From here, we find the power-load

$$P = V_1 I_1 = V_1 \frac{V_L^G - V_1}{R_i} - V_1 I_L^G. \tag{13.52}$$

Then, we get

$$R_i = V_1 \frac{V_L^G - V_1}{P + V_1 I_L^G}. \tag{13.53}$$

This dependence $R_i(V_1)$ determines a hyperbola in Fig. 13.23.

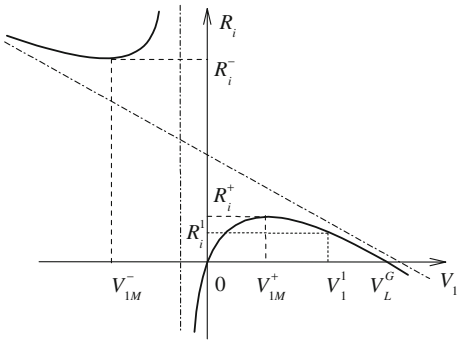

Fig. 13.23 Dependence $R_i(V_1)$ for a given load power

Let us obtain the extreme values R_i^+, R_i^- and the corresponding values V_{1M}^+, V_{1M}^-. We suppose that

$$\frac{\mathrm{d}R_i}{\mathrm{d}V_1} = \frac{V_L^G - 2V_1}{P + V_1 I_L^G} - \frac{(V_L^G - V_1)V_1 I_L^G}{(P + V_1 I_L^G)^2} = 0.$$

The solution of this equation gives the two roots

$$V_{1M}^+ = P\frac{-1 + \sqrt{1 + V_L^G I_L^G / P}}{I_L^G}, \quad V_{1M}^- = P\frac{-1 - \sqrt{1 + V_L^G I_L^G / P}}{I_L^G}. \tag{13.54}$$

Substituting (13.54) in (13.53), we get R_i^+, R_i^-. Using (13.48), we obtain r_0^+, r_0^-. The conformity of the points V_1, R_i, r_0 is shown in Fig. 13.24.

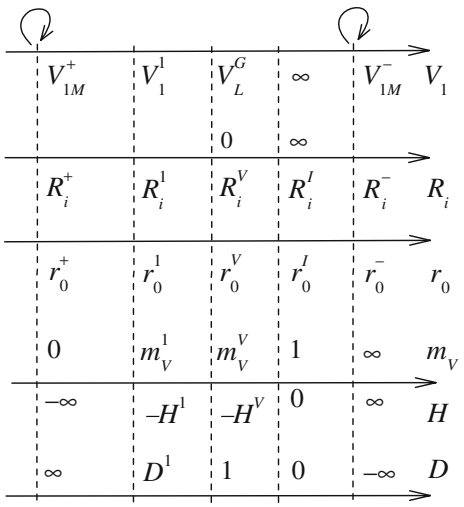

Fig. 13.24 Conformity of different regime parameters

Let us constitute the cross-ratio m_V^1 for the initial point V_1^1; that is,

$$m_V^1 = \left(V_{1M}^+ \;\; V_1^1 \;\; \infty \;\; V_{1M}^-\right) = \frac{V_1^1 - V_{1M}^+}{V_1^1 + V_{1M}^-}, \tag{13.55}$$

where the points V_{1M}^+, V_{1M}^- are base ones and $V_1 = \infty$ is a unit point. The m_V values are shown in Fig. 13.24.

Similarly to the above, let us consider the cross-ratio m_i^1 for the resistance R_i^1 using the conformity of the variables by Fig. 13.24 for the single-valued area. This cross-ratio has the form

$$m_i^1 = \left(R_i^+ \;\; R_i^1 \;\; \infty \;\; R_i^-\right) = \frac{R_i^1 - R_i^+}{R_i^1 - R_i^-}. \tag{13.56}$$

Next, let us consider the cross-ratio m_0^1 for the resistance r_0^1 using the conformity of the variables by Fig. 13.24. This cross-ratio has the form

$$m_0^1 = \left(r_0^+ \;\; r_0^1 \;\; r_0^I \;\; r_0^-\right) = \frac{r_0^1 - r_0^+}{r_0^1 - r_0^-} \div \frac{r_0^I - r_0^+}{r_0^I - r_0^-}. \tag{13.57}$$

Also, the following equality takes place

$$m_i^1 = m_0^1 = (m_V^1)^2. \tag{13.58}$$

We use hyperbolic metric (13.16)

$$H^1 = Ln\, m_i^1 = Ln\, m_0^1 = 2Ln\, m_V^1. \tag{13.59}$$

Further, we must support the characteristic points V_L^G, R_i^V, r_0^V. Then

$$\begin{aligned} m_V^V &= \left(V_{1M}^+ \;\; V_L^G \;\; \infty \;\; V_{1M}^-\right) = \frac{V_L^G - V_{1M}^+}{V_L^G + V_{1M}^-}, \\ m_i^V &= \left(R_i^+ \;\; R_i^V \;\; \infty \;\; R_i^-\right) = \frac{R_i^V - R_i^+}{R_i^V - R_i^-} = \frac{R_i^+}{R_i^-}, \\ m_0^V &= \left(r_0^+ \;\; r_0^V \;\; r_0^I \;\; r_0^-\right) = \frac{r_0^V - r_0^+}{r_0^V - r_0^-} \div \frac{r_0^I - r_0^+}{r_0^I - r_0^-}. \end{aligned} \tag{13.60}$$

Hyperbolic metric (13.16)

$$H^V = Ln\, m_i^V = Ln\, m_0^V = 2Ln\, m_V^V. \tag{13.61}$$

Further, we may introduce the normalized distance

$$D^1 = \frac{H^1}{H^V}. \tag{13.62}$$

In this case, the value H^V is a scale value. The conformity of D^1 is presented in Fig. 13.24 too.

Similarly, we may consider the other variable resistances of this line.

Example Let the circuit in Fig. 13.19 be given by the following parameters

$$V_0 = 10, \quad r_{10} = 5, \quad r_1 = 1, \; P_1 = 3.$$

Parameters (13.45) and (13.46) of the generalized generator

$$-I_L^G = \frac{10}{5} = 2, \quad V_L^G = \frac{1+5}{5}10 = 12.$$

Characteristic values (13.49) and (13.50)

$$R_i^V = 0, \quad r_0^V = -\frac{5 \cdot 1}{5+1} = -0.8333, \quad R_i^I = \infty, \; r_0^I = -5.$$

Extreme voltage values (13.54)

$$V_{1M}^+ = 3\frac{-1+\sqrt{1+\frac{12\cdot 2}{3}}}{2} = 3, \quad V_{1M}^- = 3\frac{-1-3}{2} = -6.$$

Substituting these values in (13.53), we get the corresponding extreme values

$$R_i^+ = V_{1M}^+ \frac{V_L^G - V_{1M}^+}{P + V_{1M}^+ I_L^G} = 3\frac{12-3}{3+3\cdot 2} = 3, \quad R_i^- = -6\frac{12+6}{3-6\cdot 2} = 12.$$

Using (13.48), we obtain

$$r_0^+ = \frac{r_{10}(R_i^+ - r_1)}{r_{10} - (R_i^+ - r_1)} = \frac{5(3-1)}{5-(3-1)} = 3.3333,$$
$$r_0^- = \frac{r_{10}(R_i^- - r_1)}{r_{10} - (R_i^- - r_1)} = \frac{5(12-1)}{5-(12-1)} = -9.1666.$$

Let the initial regime point be given as

$$P = 3, \quad V_1^1 = 4, \quad r_0^1 = 3.0882.$$

Using (13.42), we get

$$R_i^1 = r_1 + \frac{r_0^1 r_{10}}{r_0^1 + r_{10}} = 2.909.$$

Cross-ratios (13.55)–(13.57)

$$\begin{aligned}
m_V^1 &= \frac{V_1^1 - V_{1M}^+}{V_1^1 + V_{1M}^-} = \frac{4-3}{4+6} = 0.1,\\
m_i^1 &= \frac{R_i^1 - R_i^+}{R_i^1 - R_i^-} = \frac{2.909-3}{2.909-12} = 0.01 = 0.1^2,\\
m_0^1 &= \frac{r_0^1 - r_0^+}{r_0^1 - r_0^-} \div \frac{r_0^J - r_0^+}{r_0^J - r_0^-}\\
&= \frac{3.0882 - 3.3333}{3.0882 + 9.1666} \div \frac{-5 - 3.3333}{-5 + 9.1666} = 0.02 \div 2 = 0.01.
\end{aligned}$$

Hyperbolic metric (13.59)

$$H^1 = Ln\,0.01 = 2Ln\,0.1 = -4.6052.$$

For the characteristic points V_L^G, R_i^V, r_0^V, cross-ratios (13.60)

$$\begin{aligned}
m_V^V &= \frac{V_L^G - V_{1M}^+}{V_L^G + V_{1M}^-} = \frac{12-3}{12+6} = 0.5,\\
m_i^V &= \frac{R_i^+}{R_i^-} = \frac{3}{12} = 0.25 = 0.5^2,\\
m_0^V &= \frac{r_0^V - r_0^+}{r_0^V - r_0^-} \div \frac{r_0^J - r_0^+}{r_0^J - r_0^-}\\
&= \frac{-0.8333 - 3.3333}{-0.8333 + 9.1666} \div \frac{-5 - 3.3333}{-5 + 9.1666} = 0.25.
\end{aligned}$$

Hyperbolic metric (13.61)

$$H^V = Ln\,0.25 = 2Ln\,0.5 = -1.3863.$$

Normalized distance (13.62)

$$D^1 = \frac{-4.6052}{-1.3863} = 3.3219.$$

References

1. Cid-Pastor, A., Martinez-Salamero, L., El Aroudi, A., Giral, R., Calvente, J., Leyva, R.: Synthesis of loss-free resistors based on sliding-mode control and its applications in power processing. Contr. Eng. Pract. **21**(5), 689–699 (2013)
2. Emadi, A., Khaligh, A., Rivetta, C.H., Williamson, G.: Constant power loads and negative impedance instability in automotive systems: definition, modeling, stability, and control of power electronic converters and motor drives. IEEE Trans. Veh. Technol. **55**(4), 1112–1125 (2006)
3. Griffo, A., Wang, J., Howe, D.: Large signal stability analysis of DC power systems with constant power loads. In: Vehicle Power and Propulsion Conference 2008. VPPC'08. IEEE, 1–6 (2008)
4. Maksimovic, D., Jang, Y., Erickson, R.W.: Nonlinear-carrier control for high– power– factor boost rectifiers. IEEE Trans. Power Electron. **11**(4), 578–584 (1996)
5. Penin, A.: Analysis of regime changes of constant power–load. Elektrichestvo **12**, 43–49 (2008)
6. Penin, A.: Constant power sources and its properties. Elektrichestvo **4**, 60–65 (2010)
7. Sergeev, B., Romash, A., Nagovitsyn, V., Kurchenkova, N.: Analysis of electric circuit with constant power–load. Elektrichestvo **6**, 16–22 (2002)
8. Singer, S., Erickson, R.W.: Power–source element and its properties. IEEE Proc. Circ. Devices Syst. **141**(3), 220–226 (1994)

Chapter 14
Quasi-resonant Voltage Converter with Self-limitation of Load Current. Similarity of Load Characteristics of Some Electronic Devices

14.1 Load Curve of an Active Two-Pole with Self-limitation of the Current

In the above Part I, we have considered active two-poles with the load straight lines. In turn, there are active two-poles with self-limitation of the output current, which are characterized by nonlinear load curves [13]. So-called the zero-current switching load resonant converters have these load curves [9]. The typical form of this load curve is represented by a convex line 1 in Fig. 14.1. In the first quadrant, the active two-pole gives energy; the corresponding regime is changed from the short circuit SC to the open circuit OC. Thus, depending on degree of convexity, curve 1 can alter from line 2 to line 3.

In the second and fourth quadrants, the active two-pole consumes energy, but there is limitation of the current even for the high load voltage.

Examples of load quasi-resonant converters

Example 1 It is known the load-resonant converters, for example, with the zero-current switching [3, 9]. These converters regulate their output by changing of a switching period T_S. Let us consider *DC* resonant converter with given elements in Fig. 14.2. It has self-limitation of the output current if the switching period $T_S \geq 2T_r$; the value $T_r \cong 2\pi\sqrt{L_r(C_{r1} + C_{r2})}$ is the own oscillation or resonance period.

Let us suppose *ORCAD* simulation for $T_S = 32\ \mu S$, $T_r = 16\ \mu S$ [15]. The load curve for the first quadrant is almost rectangular and represents two obvious areas. Area 1 corresponds to a voltage source; the load voltage depends on its current a little. Area 2 corresponds to the start of the current limitation and determines the maximum load power point P_M. Areas 3, 4 correspond to a current source. In particular, point 4 defines *SC* regime. So, the limitation of the load current takes place.

A. Penin, *Analysis of Electrical Circuits with Variable Load Regime Parameters*, Power Systems, DOI 10.1007/978-3-319-28451-4_14

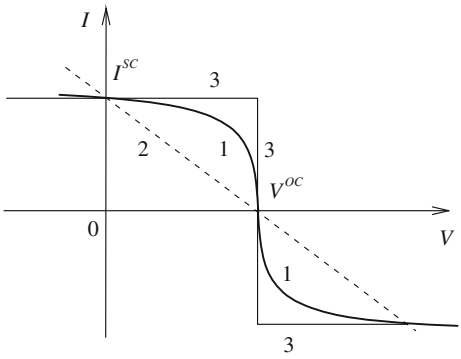

Fig. 14.1 Typical load lines of an active two-poles. *1* Convex. *2* Linear. *3* Rectangular

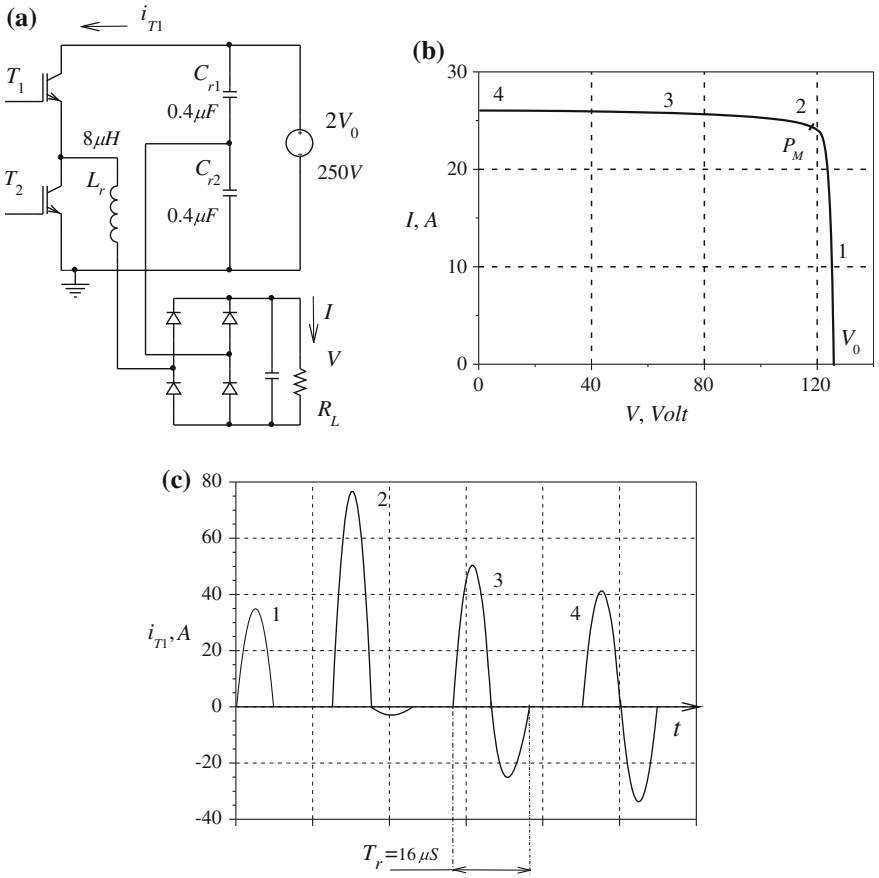

Fig. 14.2 Known quasi-resonant converter. **a** Electric circuit. **b** Load curve with characteristic areas by numbers *1–4*. **c** Superposed current pulses of one transistor for these characteristic areas

The current pulses for these characteristic areas explain the line convex and its horizontal part. The forward pulse amplitude 1 is determined by a light load, which changes from *OC* to the maximum load power. The maximum amplitude corresponds to a point P_M and equals about 80 A. Area 3 determines the overload regime for a heavy load, the forward amplitude is decreased, and the reverse pulse appears. For *SC* regime, the reverse amplitude is equal to the forward amplitude 4 if we do not consider losses. We note that the total amplitude of forward and reverse pulses does not change for areas 2–4 and equals about 80 A.

Example 2 The proposed *DC* resonant converter in Fig. 14.3 with given elements has the natural self-limitation of the output current [14]. The switching period $T_S \geq T_r$; the value $T_r \cong 2\pi\sqrt{L_{r1}C_r} = 43$ μS is the own oscillation period.

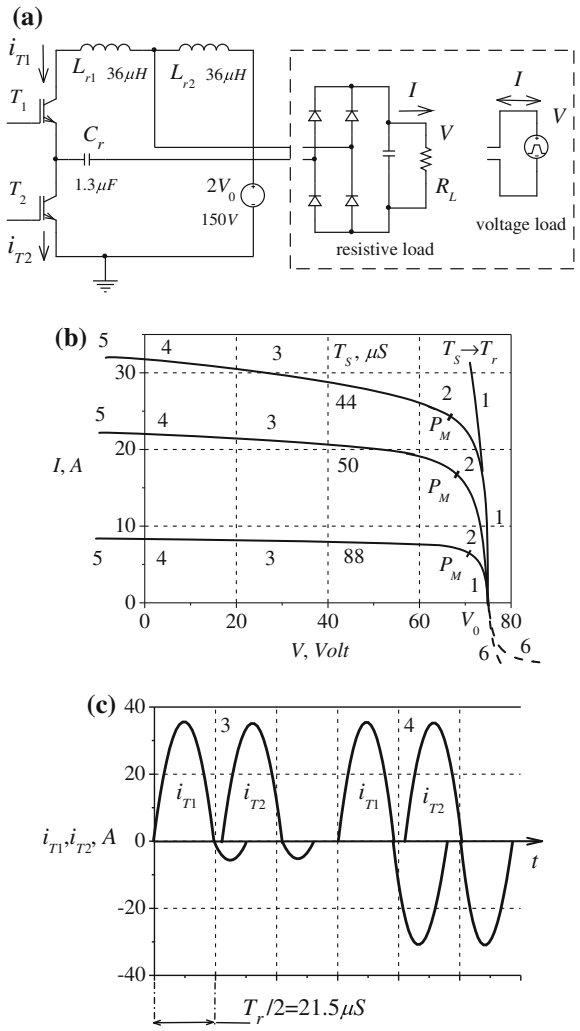

Fig. 14.3 Proposed quasi-resonant converter. **a** Electric circuit. **b** Load curve with characteristic areas by numbers *1–6*. **c** Current pulses of both transistors for characteristic areas *3*, *4*

Let us consider *ORCAD* simulation, for the first quadrant, of the load curves (a resistive load) with the different switching period T_S [15]. The period $T_S = 44\ \mu S$ is the minimum working value and $T_s = 88\ \mu S$ is the doubled period.

Area 1 for all the curves corresponds to a voltage source too. Area 2 corresponds to the start of the current limitation and determines the maximum load power point P_M. Area 3 in the form of an inclined line corresponds to the further current limitation up to *SC* point 4.

The current pulses for the characteristic areas 3, 4 explain the load line convex and its inclined part. Area 3 determines the overload regime for a heavy load; the forward amplitude does not decrease but the short reverse pulse appears.

For *SC* regime, the reverse pulse extends and its amplitude equals to the forward current amplitude.

In the general case, for construction of the load line in all the quadrants, it is necessary to use an alternating voltage source of variable amplitude and corresponding frequency as a load. Therefore, in the second and fourth quadrants, the converter transfers power from this voltage load to the own voltage source $2V_0$. In this case, there is a limitation of the current even for the high load voltage too. It is clear for areas 5, 6. In particular, for area 5, the reverse pulse amplitude is being increased more than the forward current amplitude. In turn, the forward current is absent for area 6 and the converter is simply a rectifier.

Further, we note that the load curve for the first quadrant is almost rectangular for the doubled period $T_S = 88\ \mu S$ too. On the contrary, if the period $T_S \rightarrow T_r$, *SC* current rises and the load line aspire to a straight line.

The represented load characteristics allow carrying out the analysis and justifying an equivalent generator or circuit of such an active two-pole with self-limitation of output current.

In addition, similarity of characteristics of such a quasi-resonant converter and characteristics of different nonlinear elements as transistors, solar cells, and so on attracts attention.

14.2 Equivalent Generator of an Active Two-Pole with Self-limitation of Current

Such points of the characteristic regimes as *SC* and *OC* are suggesting the possibility of using an equivalent generator with a nonlinear internal resistance R_{i1} in Fig. 14.4 [13]. The voltage source V^{OC} and *SC* current I_1^{SC} determines the corresponding value of the internal resistance

$$R_{i1}^{SC} = \frac{V_0^{OC}}{I_1^{SC}}.$$

Then, it is necessary to determine the dependence of the internal resistance on the voltage. Therefore, it is worth noting three regions of the above represented characteristics.

For the first region, when $T_S \geq 2T_r$, after the point P_M until SC point and further in the area $V \leq 0$, the current is increasing a little. Therefore, the equivalent generator characteristic is similar to a current source.

The third region, when $T_S \rightarrow T_r$, corresponds to resonance, the characteristic has the linear form. Therefore, SC current is defined by a small loss resistance. Thus, the equivalent generator is a voltage source.

For the second region, when $T_r < T_S \leq 2T_S$, there is an intermediate case; that is, the equivalent generator type changes from a voltage source to current source.

Therefore, the characteristic changes from a curve similar to vertical line to a curve similar to horizontal line.

The first region of characteristics

Let us consider one curve of the load characteristics. To establish the dependence of the internal resistance on the voltage, we define the resistance value $R_{i1}(V)$ for the actual simulated data of the current and voltage and build a plot of this relationship in Fig. 14.5; that is, line 1.

A strictly linear dependence, which defines the minimum resistance value R_{i1}^{OC}, attracts our attention. This value corresponds to the voltage V^{OC}.

Further, we will define the load resistance $R_L(P_M)$ for the maximum load power P_M according to the actual data. It turned out that this value is close to the internal resistance value (as for the known equivalent circuit) but for SC regime

$$R_L(P_M) = R_{i1}^{SC}. \tag{14.1}$$

Accepting the linear dependence of line 1, it is possible to obtain an approximation expression of a load characteristic and analytically to check condition (14.1). It will be the weighty logical justification of the above equivalent generator.

For obviousness, lines 2, 3 show different dependences of $R_{i1}(V)$ in Fig. 14.5 too. If the resistance $R_{i1}(V)$ is not dependent on the voltage (the straight line 2), we get a voltage source with this internal resistance and a usually linear load characteristic in Fig. 14.1; that is, line 2. If the resistance $R_{i1}(V)$ goes through the point V^{OC}

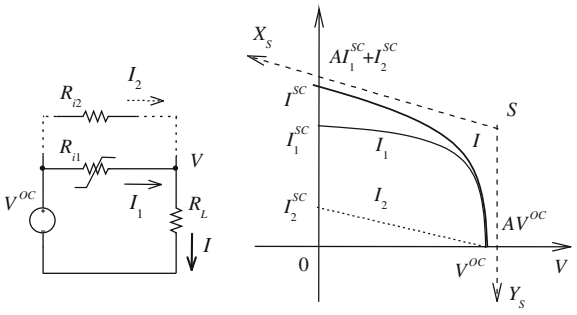

Fig. 14.4 Equivalent generator and its load characteristic

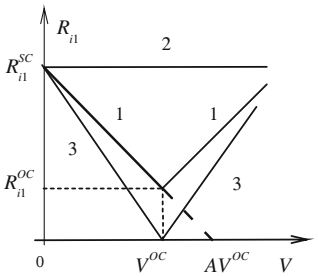

Fig. 14.5 Internal resistance dependence of the typical active two-pole. *1* With self-limitation of the load current. *2* Real voltage source. *3* Ideal current source

(the straight line 3), we have a current source with the rectangular characteristic in Fig. 14.1; that is, line 3.

Then, the given case represents the intermediate version, when the straight line 1 passes through the point (AV^{OC}, 0). Line 1 equation has the following appearance for the work area, $V \le V^{OC}$,

$$R_{i1} = \frac{1}{I_1^{SC}}\left(V^{OC} - \frac{V}{A}\right). \tag{14.2}$$

On the other hand, we obtain from the equivalent circuit that

$$R_{i1} = \frac{V^{OC} - V}{I_1}. \tag{14.3}$$

Eliminating value R_{i1}, we get a load curve equation

$$I_1(V) = I_1^{SC} A \frac{1 - V}{A - V}. \tag{14.4}$$

Here and further, the value V is a normalized voltage by the value V^{OC}.

Expression (14.4) defines a hyperbole. The parameter A determines degree of convexity of curve 1 in Fig. 14.1 for the working area $V \le V^{OC}$. If $A \to \infty$, this curve degenerates into a straight line in Fig. 14.1; that is, line 2. If $A = 1$, we get a rectangular characteristic; the hyperbola merges with its asymptotes (Fig. 14.1; lines 3).

The load power has the view

$$\frac{P}{P_G^{SC}} = AV\frac{1 - V}{A - V}, \tag{14.5}$$

where P_G^{SC} is the maximum power of the equivalent generator for *SC* regime. This expression determines a hyperbola and is similar to efficiency expression (4.49). Therefore, we may use the known results.

The maximum load power

$$\frac{P_M^+}{P_G^{SC}} = A\left(\sqrt{A} - \sqrt{A-1}\right)^2. \tag{14.6}$$

The corresponding load voltage

$$V(P_M^+) = A - \sqrt{A(A-1)} = V_M^+. \tag{14.7}$$

From here, we may find the value A.

If $A \to \infty$, hyperbola (14.5) transforms to known parabola (2.49). If to express the load resistance $R_L = V/I_1$ via voltage $V = V_M^+$ by (14.4), condition (14.1) is confirmed.

Similarly, we may get the load curve equation for the working area $V \geq V^{OC}$.

The second region of characteristics

Area 3 of characteristics becomes more linear with a greater inclination if $T_S \to T_r$. Therefore, the characteristics have the linearly hyperbolic form.

Then, we may make an assumption about the introduction of a linear resistor R_{i2} in the equivalent circuit in Fig. 14.4. The resistor value R_{i2} is specified by the period T_S. A physical support of this element R_{i2} is that, in the third area, its value is so small that the load current is set by this resistance in a greater extent.

Let us obtain an approximation expression of the load characteristic for this case.

Under the equivalent generator, taking into account (14.3) and (14.4), the load current is given as the sum of the following hyperbolic and linear components:

$$I(V) = I_1(V) + I_2(V) = I_1^{SC} A \frac{1-V}{A-V} + I_2^{SC}(1-V), \tag{14.8}$$

where *SC* current for the linear component

$$I_2^{SC} = \frac{V^{OC}}{R_{i2}}. \tag{14.9}$$

Expression (14.8) defines a hyperbola with a center S and asymptotes SX_S, SY_S in Fig. 14.4 for $I_1^{SC} = 1$. In practice, for a given resultant curve $I(V)$, we must find the following settings as I_1^{SC}, A, and I_2^{SC}. To do this, the system of three Eq. (14.8) for three pairs of points (I^1, V^1), (I^2, V^2), and (I^3, V^3) is being solved.

14.3 Deviation from the Maximum Load Power Point

The maximum load power corresponds to different load voltage values depending on the parameter A or proportions between the hyperbolic and linear component of the currents. For clarity, this voltage coordinate can accept values from (14.7) for the hyperbolic characteristic up to the value for the straight line one; that is, $1 \geq V_M^+ \geq 0.5$. Therefore, likewise to Sect. 4.4, the similar problem arises for scales and relative expressions of the above deviation.

To do this, we consider regime symmetries of load characteristic (14.8) for a given value of A in Fig. 14.6. Let the load be changed from SC to OC regime. We pass to the projective coordinates, which is determined by a center F similarly to Figs. 2.24 and 4.22. The point F is formed due to the intersection of the tangential lines or asymptotes FX_F, FY_F at the fixed or base points I^{SC}, V^{OC}. In this case, a point on the hyperbola is assigned as the rotation of radius vector $R_F F$ from the initial point P_M^+ to a running point or load R_1.

Therefore, the pole F and polar TQ (which passes through the points I^{SC}, V^{OC}) determine the mapping or symmetry of the region of power consumption by the load on the region of power return; that is, $P \rightarrow -P$.

In turn, the pole T and polar FQ, as a complementary system, determine the mapping or symmetry of the running points R_1, R_2 relatively to the maximum power point P_M^+. The point T is formed due to the intersection of the tangential line TP_M^+ and the known line TQ. In this case, the point on the hyperbola is assigned as the rotation of radius vector $R_T T$ from the base point P_M^+ to the running point or load R_1.

Further, we will consider the concrete example of the load characteristic in Fig. 14.3b. For $T_S = 44\ \mu S$, the following settings, as $I_1^{SC} = 24.33$, $A = 1.016$, and $I_2^{SC} = 9.805$ are obtained.

Equation (14.8), for all the normalized currents by $I_1^{SC} = 24.33$, has the view

$$I(V) = 1.016\frac{1-V}{1.016-V} + 0.403(1-V). \tag{14.10}$$

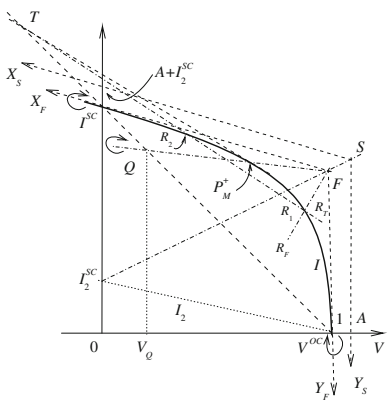

Fig. 14.6 Symmetry of the load characteristic relatively to the maximum power point P_M^+

The maximum load power coordinates equal $V_M^+ = 0.86$, $I_M^+ = 0.968$. The point F coordinates have the form

$$V_F = \frac{A}{2A-1} = 0.9845, \quad I_F = \frac{A}{2A-1} + I_2^{SC}\frac{A-1}{2A-1} = 0.99.$$

To find the point T coordinates, we use the following equations of the straight lines TQ and TP_M^+ accordingly:

$$\begin{cases} I(V) = -(1+I_2^{SC})V + (1+I_2^{SC}) = -1.403V + 1.403 \\ I(V) = V\,tg\alpha + (I_M^+ - V_M^+\,tg\alpha) = -1.071V + 1.889, \end{cases} \tag{14.11}$$

where the value

$$tg\alpha = \frac{dI}{dV} = -A\frac{A-1}{(A-V)^2} - I_2^{SC} = -1.071$$

determines the slope angle for the tangential line TP_M^+. The solution of these equations gives $V_T = -1.464$, $I_T = 3.457$.

Similarly, we find the point Q coordinates using the equations of the straight lines TQ and FP_M^+ accordingly

$$\begin{cases} I(V) = -(1+I_2^{SC})V + (1+I_2^{SC}) = -1.403V + 1.403 \\ I(V) = V\,tg\beta + (I_F - V_F\,tg\beta) = 0.176V + 0.816, \end{cases}$$

where the value

$$tg\beta = \frac{I_F - I_M^+}{V_F - V_M^+} = 0.176$$

determines the slope angle for the line FP_M^+. The solution of these equations gives $V_Q = 0.371$.

Let us map the harmonic conjugate points T, I^{SC}, Q, V^{OC} of the polar TQ onto the axis V in Fig. 14.7. These points correspond to the points V_T, 0, V_Q, 1 accordingly.

The mutual mapping of the points V_T, V_Q relatively to 0, 1 is shown by arrows. For these harmonic conjugate points, the cross-ratio equals −1; that is,

$$(0\ \ V_T\ \ V_Q\ \ 1) = (0\ \ -1.464\ \ 0.371\ \ 1) = \frac{-1.464-0}{-1.464-1} \div \frac{0.371-0}{0.371-1} = -1.$$

Similarly, let us map the harmonic conjugate points Q, P_M^+, F, P_M^- of the polar FQ onto the axis V. These points correspond to the points V_Q, V_M^+, V_F, V_M^- accordingly.

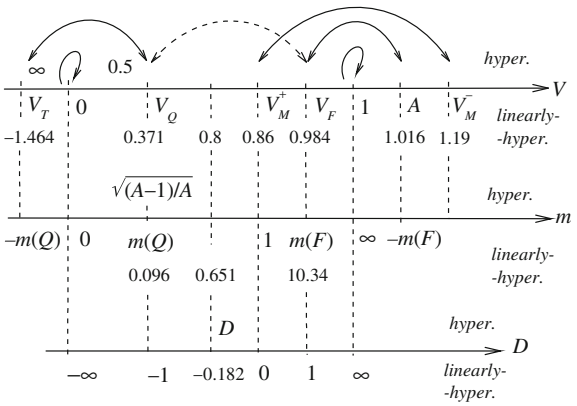

Fig. 14.7 Mutual mapping of the characteristic points and its correspondence for the voltage, cross-ratio, and distance for the hyperbolic and linearly hyperbolic cases

The mutual mapping of the points V_F, V_Q relatively to V_M^+, V_M^- is shown by arrows. The point $V_M^- = 1.19$ is a point of intersection of the hyperbola second branch and the line FQ; in Fig. 14.6 it is not shown.

As it is, we get the two conjugate systems of poles and polar lines. Now, it is necessary to find the common fixed or base points for these conjugate systems.

We note, that the points 0, 1 and V_M^+, V_M^- are the harmonic conjugate points shown by arrows. Therefore, we may choose the points 0, 1 as the base ones. Now, it is necessary to check the cross ratios for each points V_F, V_Q, using a unit point V_M^+; that is,

$$m(Q) = (0 \;\; V_Q \;\; V_M^+ \;\; 1) = (0 \;\; 0.371 \;\; 0.86 \;\; 1) = 0.096,$$
$$m(F) = (0 \;\; V_F \;\; V_M^+ \;\; 1) = (0 \;\; 0.9845 \;\; 0.86 \;\; 1) = 10.34 = \frac{1}{m(Q)} = \frac{1}{0.096}.$$

Also, we check the cross ratios for the rest characteristic points V_T, $V = A$

$$m(T) = (0 \;\; V_T \;\; V_M^+ \;\; 1) = (0 \;\; -1.464 \;\; 0.86 \;\; 1) = -0.096 = -m(Q),$$
$$m(A) = (0 \;\; A \;\; V_M^+ \;\; 1) = (0 \;\; 1.016 \;\; 0.86 \;\; 1) = -10.33 = -m(F) = -\frac{1}{m(Q)}.$$

Therefore, we may accept the value $m(Q)$ as a scale value. So, all the characteristic points are evaluated via this scale, as it is shown by the axis m in Fig. 14.7.

So, a running regime point V (for example, $V = 0.8$) is expressed by the following cross-ratio:

$$\begin{aligned} m(V) = (0 \;\; V \;\; V_M^+ \;\; 1) &= \frac{V}{V-1} \div \frac{V_M^+}{V_M^+ - 1} \\ &= \frac{0.8}{0.8-1} \div \frac{0.86}{0.86-1} = 4 \div 6.142 = 0.651. \end{aligned} \tag{14.12}$$

The corresponding hyperbolic distance from the maximum load power point

$$H(V) = Ln[m(V)] = -0.428.$$

Similarly, the scale hyperbolic distance

$$H(Q) = -Ln[m(Q)] = -Ln\ 0.096\ = 2.343 = Ln[m(F)] = Ln\ 10.33.$$

Then, the normalized distance or relative deviation from the maximum load power point

$$D = \frac{H(V)}{H(Q)} = -0.182.$$

The inverse expression

$$m(V) = [m(Q)]^D.$$

If the value D be given, we find the actual value V using (14.12) and the known value $m(Q)$.

Similar expressions are being obtained for the fourth quadrant.

Particular case

If $T \to \infty$, we get the hyperbolic load characteristic. Then, the fundamental expressions obtain the view

$$\begin{aligned} m(Q) &= (0\ \ V_Q\ \ V_M^+\ \ 1) = (0\ \ 0.5\ \ A - \sqrt{A(A-1)}\ \ 1) = \sqrt{\frac{A-1}{A}}, \\ m = m(V) &= (0\ \ V\ \ V_M^+\ \ 1) = \frac{V}{1-V}\sqrt{\frac{A-1}{A}} = m_0(V)\sqrt{\frac{A-1}{A}}, \end{aligned} \tag{14.13}$$

The scale hyperbolic distance

$$H(0.5) = Ln[m(0.5)].$$

The inverse expression

$$\begin{aligned} m(V) &= [m(0.5)]^D, \text{ or} \\ m_0(V) &= \frac{V}{1-V} = \left(\frac{A-1}{A}\right)^{(D-1)/2}. \end{aligned} \tag{14.14}$$

If it is necessary to set any equal deviation D for different A, we find $m_0(V)$ using the second member of (14.14) and then, we get the value V by (14.13). The corresponding mapping of V, m is shown in Fig. 14.7 too.

14.4 Symmetrical Load Characteristic for the Full Area of the Load Voltage Variation

Let us return to Fig. 14.5. Two lines 1 for the corresponding areas $V \le V^{OC}$, $V \ge V^{OC}$ we are replacing by one hyperbola 2 shown in Fig. 14.8a. In this case, initial Eq. (14.2) obtain the following view

$$\left(\frac{R_i}{R_i^{OC}}\right)^2 - \frac{1}{A^2}\left(\frac{V_i}{V^{OC}}\right)^2 = \left(\frac{r_i^{OC}}{R_i^{OC}}\right)^2 = r^2, \tag{14.15}$$

where $V_i = V^{OC} - V$ is the internal resistance voltage and a value $r_i^{OC} \ge R_i^{OC}$. Hereinafter, the subscript "1" for R_{i1} and I_{i1} is not used.

From here, using the equivalent circuit in Fig. 14.4, we obtain the normalized load characteristic equation

$$\frac{I(V_i)}{AI^{SC}} = \frac{V_i/rAV^{OC}}{\sqrt{A^2r^2 + \left(V_i/rAV^{OC}\right)^2}}. \tag{14.16}$$

The plot of this expression has the typical view in Fig. 14.8b.

If to introduce the coordinate system $I_D\,0_{GS}\,V_{GS}$, this curve is close to the typical transfer characteristic $I_D(V_{GS})$ of *MOSFET* transistors and its approximation by a hyperbolic tangent [6]. The values I_D^C, V_{GS}^C correspond to the cusp of this curve.

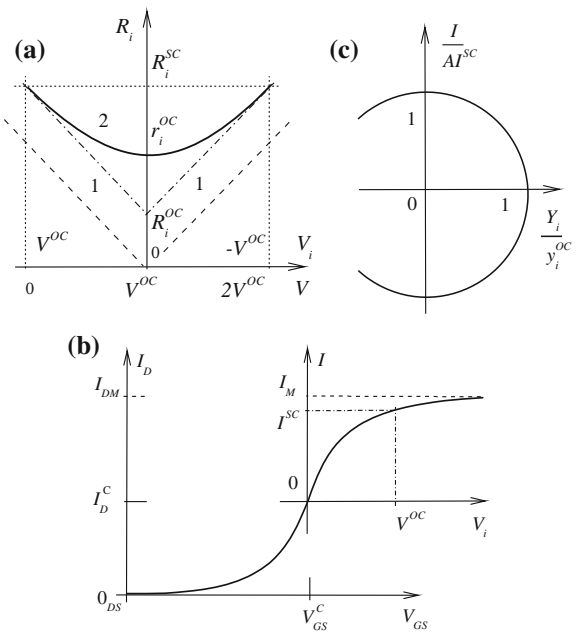

Fig. 14.8 Symmetrical load characteristic. **a** Internal resistance via its voltage. **b** Current of the internal resistance via its voltage and transfer characteristic. **c** Current via internal conductivity

Also, it is possible to note that expression (14.16) is the particular case of Rapp's model of a solid-state microwave power amplifier [8, 19].

If to express the current I through the internal conductivity $Y_i = 1/R_i$, $y_i^{OC} = 1/r_i^{OC}$, the circle equation turns out

$$\left(\frac{Y_i}{y_i^{OC}}\right)^2 + \left(\frac{I}{AI^{SC}}\right)^2 = 1. \tag{14.17}$$

The plot of this circle is shown in Fig. 14.8c.

14.5 Asymmetrical Load Characteristics

We may introduce asymmetrical characteristics of a common view too. For example, a transfer characteristic of *MOSFET* transistor may considerably be differing from a symmetric curve.

Case 1

We consider a new position of the known hyperbola in Fig. 14.9a.

Let the asymptotes $0y$, $0x$ form a rectangular coordinate system $y0x$, which turned on an angle α concerning the initial system $R_i\ 0\ V_i$. Therefore, the equation of the hyperbola has the view

$$y = k/x. \tag{14.18}$$

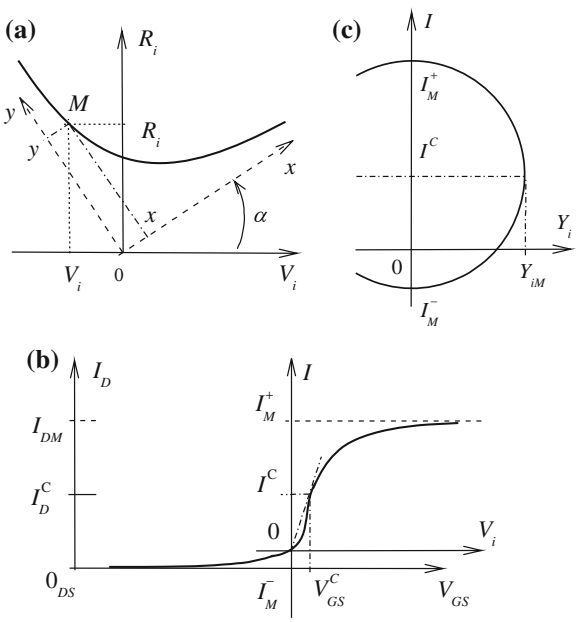

Fig. 14.9 Asymmetrical load characteristic. **a** Internal resistance via its voltage. **b** Current of the internal resistance via its voltage and transfer characteristic. **c** Current via the internal conductivity

On the other hand, for the coordinates of point M, the following orthogonal transformation is known [10]

$$\begin{bmatrix} x \\ y \end{bmatrix} = \begin{bmatrix} \cos\alpha & \sin\lambda \\ -\sin\alpha & \cos\alpha \end{bmatrix} \cdot \begin{bmatrix} V_i \\ R_i \end{bmatrix}. \tag{14.19}$$

Then, expression (14.18) obtains the view

$$\cos\alpha \cdot \sin\alpha \cdot R_i^2 + \left(\cos^2\alpha - \sin^2\alpha\right) R_i V_i - \cos\alpha \cdot \sin\alpha \cdot V_i^2 - k = 0.$$

This view corresponds to the quadratic form [10]

$$a_{11} R_i^2 + 2a_{12} R_i V_i + a_{22} V_i^2 + a_{33} = 0. \tag{14.20}$$

Hereinafter, dimensions of the values are not used.

Using transformation of the variable R_i by I, we get a quadratic equation

$$I^2 + 2\frac{a_{12} V_i^2}{a_{22} V_i^2 + a_{33}} I + \frac{a_{11} V_i^2}{a_{22} V_i^2 + a_{33}} = 0. \tag{14.21}$$

The plot of this expression has the typical view in Fig. 14.9b with different values of the maximum currents I_M^+, I_M^-.

If to express the current I through the internal conductivity Y_i, the general circle equation turns out

$$a_{11} + 2a_{12} I + a_{22} I^2 + a_{33} Y_i^2 = 0.$$

From here, we get the explicit circle equation

$$\frac{k}{\cos\alpha \cdot \sin\alpha} Y_i^2 + \left(I - I^C\right)^2 = \left(1 + I^C\right)^2, \tag{14.22}$$

where

$$I^C = \frac{\cos^2\alpha - \sin^2\alpha}{2\cos\alpha \cdot \sin\alpha} = \frac{1}{2}\left(\frac{1}{tg\alpha} - tg\alpha\right).$$

The plot of this circle is shown in Fig. 14.9c.

The maximum currents I_M^+, I_M^- correspond to $Y_i = 0$. Therefore,

$$I_M^+ = 1/tg\alpha, \quad I_M^- = -tg\alpha.$$

In turn, the current I^C conforms to the center of the segment $I_M^+ I_M^-$ and determines the maximum value Y_{iM}.

If asymmetrical curve (14.21) is used for approximation of the transfer characteristic $I_D(V_{GS})$ of *MOSFET* transistor, it is necessary, in the initial coordinate system $I_D 0_{GS}\ V_{GS}$, to restore the coordinate system $I\ 0\ V_i$. To do this, we may use the following property of the tangent line into the cusp I_D^C, V_{GS}^C of the asymmetrical characteristic; this line passes through the origin of the coordinate system $I\ 0\ V_i$. This property follows from circle (14.22).

We note, if $\alpha = 45^0$, the above symmetrical curve is realized. In our case, expression (14.21) contains two parameters as k, α, which realize comprehensive facilities for approximation.

We get still more facilities, if to use a nonrectangular coordinate system. Then, similar expression (14.21) will contain three parameters.

Case 2

We may consider the known hyperbola $R_i(V_i)$ in Fig. 14.10a and rewrite Eq. (14.18) for the coordinate system $y0x$

$$y = k/x. \tag{14.23}$$

On the other hand, for the coordinates of point M, the following transformation takes place:

$$\begin{bmatrix} x \\ y \end{bmatrix} = \begin{bmatrix} 1/\cos\alpha & 0 \\ -tg\alpha & 1 \end{bmatrix} \cdot \begin{bmatrix} V_i \\ R_i \end{bmatrix}.$$

Then, expression (14.23) obtains the view

$$R_i = V_i \cdot tg\alpha + \frac{k \cdot \cos\alpha}{V_i}. \tag{14.24}$$

Using transformation of the variable R_i by Y_i and I, we get the two equations

$$Y_i = \frac{V_i}{V_i^2 \cdot tg\alpha + k \cdot \cos\alpha}, \quad I = \frac{V_i^2}{V_i^2 \cdot tg\alpha + k \cdot \cos\alpha}. \tag{14.25}$$

The maximum values

$$Y_{iM} = \frac{1}{2\sqrt{k \cdot \sin\alpha}}, \quad V_{iM} = \sqrt{\frac{k \cdot \cos\alpha}{tg\alpha}} = \frac{1}{2Y_{iM} \cdot tg\alpha}.$$

From here, we get

$$tg\alpha = \frac{1}{2Y_{iM}V_i}, \quad k \cdot \cos\alpha = \frac{V_{iM}}{2Y_{iM}}.$$

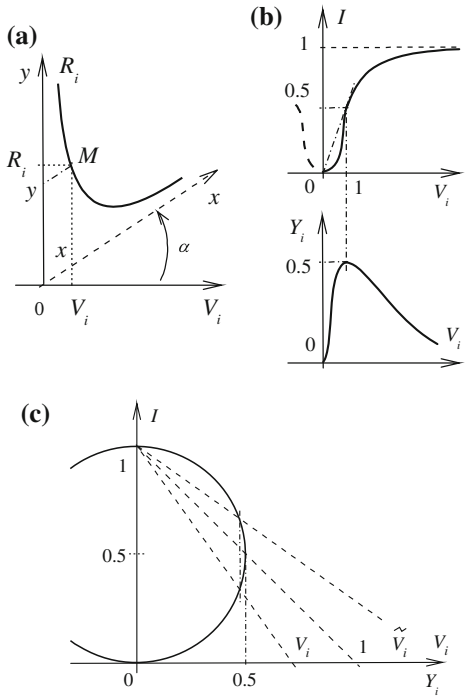

Fig. 14.10 Asymmetrical load characteristic. **a** Internal resistance via its voltage. b Current and internal conductivity via its voltage. **c** Current via internal conductivity and its stereographic projection onto the voltage axis

Then, expressions (14.25) obtain the relative form

$$\frac{Y_i}{Y_{iM}} = \frac{2\,V_i/V_{iM}}{(V_i/V_{iM})^2 + 1}, \quad \frac{I}{I_M} = \frac{(V_i/V_{iM})^2}{(V_i/V_{iM})^2 + 1},$$

where $I_M = 2I(Y_{iM}) = 2Y_{iM}\,V_{iM}$. The plots of these curves are shown in Fig. 14.10b for the normalized values Y_i, V_i, I.

If to express the current I through the internal conductivity Y_i, the explicit circle equation turns out

$$\left(\frac{Y_i}{2Y_{iM}}\right)^2 + \left(\frac{I}{I_M} - \frac{1}{2}\right)^2 = \frac{1}{4}.$$

The plot of this circle is shown in Fig. 14.10c for the normalized values. In turn, the voltages V_i, $\tilde{V}_i$ are resulted by the known stereographic projection.

The considered dependences are similar to the regulation characteristic of the above voltage regulators in Chap.10 that gives a certain physical meaning to the parameters of the approximation curves.

Also, these dependences coincide with Saleh's models of a modulation characteristic for traveling-wave tube [11, 21].

So, we have obtained a whole class of curves and convenient approximation expressions for characteristics of different electronic devices.

14.6 Linearly Hyperbolic Approximation of a Solar Cell Characteristic

14.6.1 Approximation Problem

For the analysis and calculation of power supply systems based on solar cell generators, a mathematical model of solar cell is needed [20]. The traditional exponent model requires iterative numerical calculation methods. Therefore, it might be valuable to use simpler models that allow carrying out the direct or analytical computations [2, 4, 5, 7].

Other directions use formal approximation. In particular, the quadratic fractional expression of the model allows calculating the maximum load power point by a quadratic equation [1]. But, a resistive load leads to a cubic equation that complicates the calculations in real time of working regime; that is, the load current and voltage.

More convenient a linearly hyperbolic model is similar to Eq. (14.8). The calculation with a resistance load leads to a quadratic equation [16].

Also, this model makes it possible to soundly determine deviation from the maximum load power point and to compare the effectiveness of different solar cells. The fact is that in photovoltaic power systems the maximum power point tracker *MPPT* is used extensively, for example [12]. Usually, solar array is a set of solar cell modules connected in parallel and in series. Then, it is possible to use either a common or individual *MPPT* for each module.

In the case of the common *MPPT*, the differences in the module parameters will appear. This leads to the deviation of the module regime within a large range from its maximum load power point, although, as a whole, the array works under these conditions.

If the individual *MPPT* is used, then this device can be turned on only in the case of sufficiently great regime deviations.

14.6.2 Formal Linearly Hyperbolic Approximation

Let us consider the calculated load curves in Fig. 14.11 according [1].

Numbers 1–3 denote the typical areas similar to Fig. 14.3b. Area 1 for all the curves, as inclined lines, corresponds to a voltage source with a relatively high internal resistance. Area 2 corresponds to the start of the current limitation and

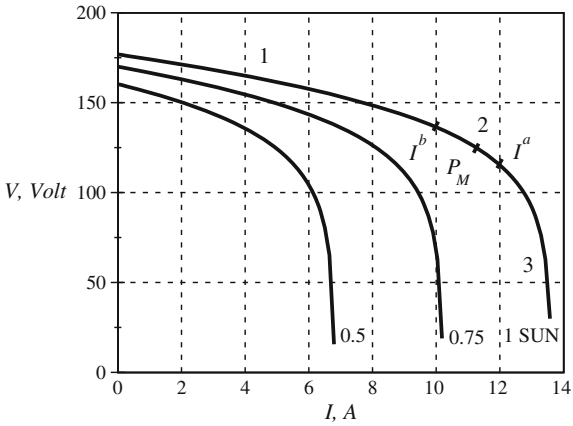

Fig. 14.11 Example of the typical solar cell load curves with different values of insulation and characteristic areas shown by number

determines the maximum load power point P_M. Then, area 3 corresponds to a current source with nearly horizontal straight line.

Hence, the "inverse" similarity follows with the curves in Fig. 14.3b; that is, the inclined area 1 in Fig. 14.11 corresponds to area 3 in Fig. 14.3b. Then, using Fig. 14.4, it is possible to draw up a dual equivalent generator in Fig. 14.12.

The current generator I^{SC} and the internal nonlinear conductivity Y_{i1} define a hyperbolic component, and the linear conductance Y_{i2} defines a linear component of the load voltage. We may write the equation immediately, using expression (14.8) and changing formally currents I by voltages V and resistances by conductivities

$$V(I) = V_1(I) + V_2(I) = V_1^{OC} A \frac{1 - I/I^{SC}}{A - I/I^{SC}} + V_2^{OC}(1 - I/I^{SC}), \qquad (14.26)$$

where OC voltage for the hyperbolic component is $V_1^{OC} = I^{SC}/Y_{i1}^{OC}$, andfor the linear component is $V_2^{OC} = I^{SC}/Y_{i2}$.

Similarly to Fig. 14.5, we may propose the nonlinear conductivity Y_{i1} dependence on the load current I in Fig. 14.13 for the dual active two-pole.

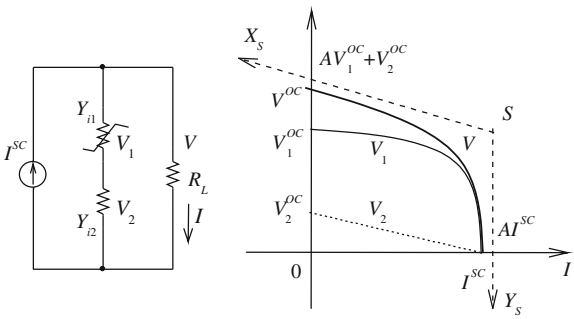

Fig. 14.12 Equivalent generator of a solar cell and its load characteristic

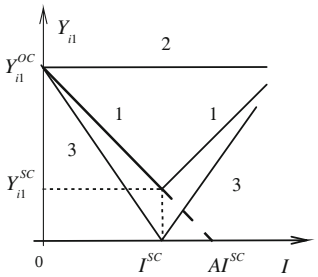

Fig. 14.13 Internal conductivity dependence on the load current of the typical active two-port. *1* With self-limitation of the load voltage. *2* Real current source. *3* Ideal voltage source

For the given curves in Fig. 14.11, it is need to find the settings A, V_1^{OC}, and V_2^{OC} using SC, OC points and two points a, b points and two points a, b, which are on the each side near to the maximum load power point (a working area) with I^a, V^a and I^b, V^b coordinates.

Let us give the necessary design parameters

$$A = \frac{\alpha I^a}{\alpha - \beta}, \quad \alpha = \frac{I^b}{I^a - I^b},$$
$$\beta = \frac{\frac{V^b}{1-I^b} - V^{OC}}{\beta_{12}}, \quad \beta_{12} = \frac{V^a}{1 - I^a} - \frac{V^b}{1 - I^b},$$
$$V_1^{OC} = \frac{1}{A}\frac{\beta_{12}}{\frac{1}{A-i^a} - \frac{1}{A-i^b}}, \quad V_2^{OC} = V^{OC} - V_1^{OC}.$$

The currents I^a, I^b are normalized by the current I^{SC}.

Proposed expression (14.26) allows the direct calculation of the current I at the given load resistance R_L. In this case, the load voltage $V = R_L I$.

Substituting this expression in (14.26), we get the requirement equation

$$I^2 - \left(AI^{SC} + \frac{AV_1^{OC} + V_2^{OC}}{R_L + V_2^{OC}/I^{SC}}\right)I + AI^{SC}\frac{V_1^{OC} + V_2^{OC}}{R_L + V_2^{OC}/I^{SC}} = 0. \tag{14.27}$$

The maximum power point parameters are found from the cubic equation

$$2I^3 - (1 + 3A + Au)I^2 + 2A(1 + Au)I - A^2u = 0,$$

where $u = 1 + V_1^{OC}/V_2^{OC}$.

Example At first, we use the traditional characteristic of a solar cell [1]

$$V = -R_S I + \frac{mkT}{q} Ln \frac{I_{ph} - I + I_0}{I_0}, \tag{14.28}$$

where R_S is the series resistance of the cell, the values m, k, T, q are the diode factor, Boltzmann constant, temperature, electron charge correspondingly; the values I_{ph}, I_0 are the photocurrent and reverse saturation current.

For the given values, this expression takes the view

$$V = -0.9I + \frac{1}{0.042} Ln \frac{13.615 - I + 0.0081}{0.0081}. \tag{14.29}$$

From here, V^{OC} = 176, I^{SC} = 13.608.

In turn, the maximum load power parameters have the following values

$$P_M = I_M V_M = 11.32 \cdot 123.6 = 1400, \quad R_{LM} = V_M / I_M = 10.92.$$

Next, we consider proposed expression (14.26).

Then OC voltage, V_1^{OC} + V_2^{OC} = 176.

Let I^a = 12, V^a = 114.76, I^b = 10, V^b = 135.58.

Then,

$$\alpha = \frac{10}{12 - 10} = 5, \quad \beta_{12} = \frac{114.76}{1 - 0.881} - \frac{135.58}{1 - 0.734} = 459.8,$$

$$\beta = \frac{\frac{135.58}{1-0.734} - 176}{459.8} = 0.7293, \quad A = \frac{0.881 \cdot 5}{5 - 0.7293} = 1.0324,$$

$$V_1^{OC} = \frac{1}{1.0324} \cdot \frac{459.81}{\frac{1}{1.0324-0.881} - \frac{1}{1.0324-0.7293}} = 134.7$$

$$V_2^{OC} = V^{OC} - V_1^{OC} = 41.3.$$

Finally, we get the approximation expression

$$V(I) = 139.06 \frac{1 - \frac{I}{13.608}}{1.0324 - \frac{I}{13.608}} + 41.3 \left(1 - \frac{I}{13.608}\right). \tag{14.30}$$

The curves $V(I)$ under expressions (14.29), (14.30) are shown in Fig. 14.14.

Examination of these curves shows that proposed model simulates a solar cell characteristic well for practical tasks. The found errors of the working area (for example, from I^b to I^a) are less than 2 %.

In turn, the curves of the power $P = IV$ are shown in Fig. 14.15.

Then, if R = 10.92, we get from (14.27)

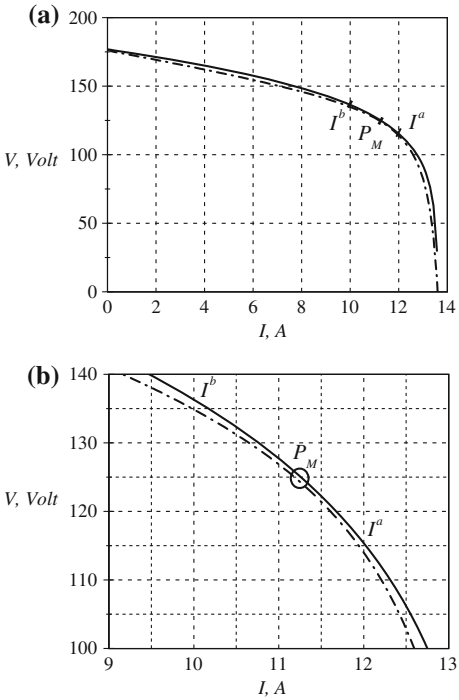

Fig. 14.14 Comparison between the proposed (*dash-dot line*) and traditional (*solid line*) model of volt-ampere characteristics: **a** Full scale. **b** Working area is near to the maximum power point

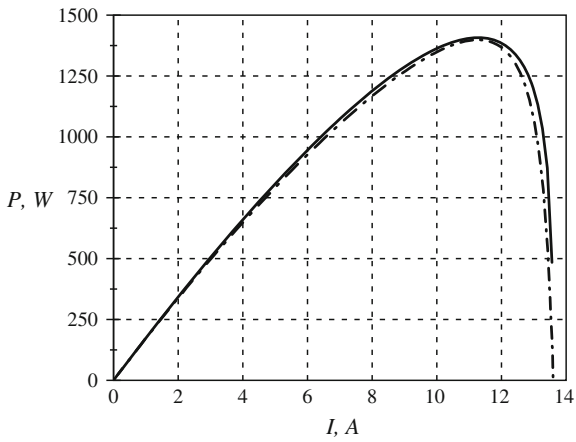

Fig. 14.15 Comparison between the proposed (*dash-dot line*) and traditional (*solid line*) model of power volt characteristics

$$I^2 - 26.97I + 177.2 = 0.$$

The solution gives I_M = 11.33. Using (14.30), we are finding V_M = 123.36. Therefore, this power is equal to 1398 and coincides with the maximum load power.

About of Validation of the Linearly Hyperbolic Approximation
As it was shown above, the model parameters are calculated for the concrete curve (with the appropriate level of insolation) from two points near the maximum load power point. But, the calculated values depend on coordinates of these points that complicate the finding the parameters on photocurrent levels. Therefore, there is a problem of a physical validation of linearly hyperbolic approximation.

An empirical approximation is presented in [18]. This approximation is based on a possible hyperbolic dependence of *p–n* junction current for its large value.

Deviation from Maximum Load Power Point
The considered results make it possible to soundly determine deviation from the maximum load power regime and to compare the effectiveness of different solar cells [17]. To do this, we may use the corresponding expressions of Sect. 14.3.

References

1. Akbaba, M., Alattavi, M.: A new model for *I-V* characteristic of solar cell generators and its applications. Solar Energy Mater. Solar Cells **37**, 123–132 (1995)
2. Alghuwainem, S.: A close-form solution for the maximum-power operating point of a solar cell array. Solar Energy Mater. Solar Cells **46**(3), 249–257 (1997)
3. Ang, S., Oliva, A.: Power-switching converters, 2nd ed., Taylor & Francis Group (2005)
4. Cubas, J., Pindado, S., Victoria, M.: On the analytical approach for modeling photovoltaic systems behavior. J. Power Sources **247**, 467–474 (2014)
5. Das, A.: Analytical derivation of explicit J-V model of a solar cell from physics based implicit model. Sol. Energy **86**(1), 26–30 (2012)
6. Diakov, V.P., Maximchuk, A.A., Remnev, A.M., Smerdov, V.Y.: Entsiklopedia ustroistv na polevyh transistorah (Encyclopedia of equipments on field transistors). Solon-R, Moskva (2002)
7. El Tayyan, A.: An approach to extract the parameters of solar cells from their illuminated I-V curves using the Lambert W function. Turkish J. Phys. **39**(1), 1–15 (2015)
8. Eltholth, A., Mekhail, A., Elshirbini, A., Dessouki, M., Abdelfattah, A.: A new- trend model-based to solve the peak power problems in OFDM systems. Model. Simul. Eng. **2008**, 5 (2008)
9. Hui, S.R., Chung, H.: Resonant and soft-switching converters. In: Power Electronics Hand book, pp. 405–449. Elsevier Inc. (2006)
10. Korn, G.A., Korn, T.M.: Mathematical Handbook for Scientists and Engineers. MacGraw–Hill, New York (1968)
11. Lee, B.M., de Figueiredo, R.J.: Adaptive predistorters for linearization of high-power am plifiers in OFDM wireless communications. Circ. Syst. Signal Proc. **25**(1), 59–80 (2006)
12. Ma, J., Man, K., Zhang, N., Guan, S., Wong, P., Lim, E., Lei, C.: Improving power-conversion efficiency via a hybrid MPPT approach for photovoltaic systems. Elektronika ir Elektrotechnika **19**(7), 57–60 (2013)
13. Penin, A.: The voltage-current characteristics of an active two-pole with self-limitation of current. Elektrichestvo **7**, 54–60 (2008)
14. Penin, A., Semionov, A.: Method of regulated resonance DC-DC voltage conversion. Europ. patent EP 1 504 517 B1. 05 Nov 2008
15. Penin, A.: A quasi-resonance voltage converter with improved parameters. Elektrichestvo **2**, 58–64 (2009)

16. Penin, A., Sidorenko, A.: A convenient model for IV characteristic of a solar cell generator as an active two-pole with self-limitation of current. World Acad. Sci. Eng. Technol. **3**(4), 905–909 (2009)
17. Penin, A., Sidorenko, A.: Determination of deviation from the maximum power regime of a photovoltaic module. Moldavian J. Phys. Sci. **9**(2), 191–198 (2010)
18. Penin, A.: An empirical validation of the linear-hyperbolic approximation of the IV characteristic of a solar cell generator. World Acad. Sci. Eng. Technol. **5**(3), 1363–1368 (2011)
19. Rapp, C.: Effects of HPA-Nonlinearity on a 4-DPSK/OFDM-signal for a digital sound broadcasting system. In: In ESA, Second European Conference on Satellite Communications (ECSC-2) pp. 179–184 (SEE N92-15210 06-32), vol. 1, pp. 179-184 (1991)
20. Rekioua, D., Matagne, E.: Optimization of Photovoltaic Power System. Modelization, Simulation and Control. Spriger, London (2012)
21. Saleh, A.: Frequency-independent and frequency-dependent nonlinear models of TWT amplifiers. IEEE Trans. Comm. **29**(11), 1715–1720 (1981)

Conclusions

In this book, the features of an electric circuit with changeable operating regimes are considered. The reader will agree that for such a circuit it is important to determine the parameters of the running regime in the normalized form using the characteristic parameter values as scales, to receive the equivalent of this circuit.

But there are two problems.

On the one hand, the actual regime parameters of the load resistance, current, voltage result in various values of the corresponding normalized quantities. The hands-on experience as if agrees with that.

On the other hand, interference of loads or any resistance on the load regime leads to change of scales.

The offered approach to interpretation of regime changes as projective transformation allowed connecting regime parameters in one system and to consider these changes through an invariant value in the form of the cross ratio of four points. The reader will agree that the adequate mathematical model of regime behavior turned out and we obtain the basis for research of such circuits and introduction of necessary concepts. Naturally, the presented results are only the beginning of researches. In particular, it is possible to apply such approach to alternating current circuits.

If we look more widely, it is possible to speak about representation of "flowed" processes of the different physical nature, using known electromechanical analogy. Also, the presented approach is being applied for a long time in other scientific domains, as mechanics, biology, and so on; for example, it is possible to see the following publications:

1. Vaseashta, A.K., Penin, A., Sidorenko, A.: On the analogy of non-euclidean geometry of human body with electrical networks. Int. J. Electr. Comput. Eng. **4**(3). 378–388 (2014)
2. Stakhov, A.P.: The mathematics of harmony: From Euclid to contemporary mathematics and computer science. Series on knots and everything, vol. 22, World Scientific Publishing Co. Pte. Ltd. (2009)

A. Penin, *Analysis of Electrical Circuits with Variable Load Regime Parameters*,
Power Systems, DOI 10.1007/978-3-319-28451-4

Index

A. Penin, *Analysis of Electrical Circuits with Variable Load Regime Parameters*, Power Systems, DOI 10.1007/978-3-319-28451-4